Virchows Arch [Pathol Anat] (1982) 395:1–9

Virchows Archiv A

Original Articles

Alpha-1-Antitrypsin in Malakoplakia *

Francesco Callea, Boudewijn Van Damme, Valeer J. Desmet
Laboratorium voor Cyto- en Histochemie, Departement Medische Navorsing, Katholieke Universiteit Leuven, Leuven, Belgium

Summary. Macrophages in malakoplakia contain large amounts of immunoreactive alpha-1-antitrypsin (AAT). The amount of AAT remains unchanged during the morphogenetic stages of the pathological process (early, granulomatous, fibrosing phases), and does not correlate with the number or the presence of Michaelis-Gutmann (M.G.) bodies.

Macrophages from other pathological processes, closely resembling malakoplakia cells but without M.G. bodies, did not contain AAT, except for a few macrophages in tuberculosis and xanthogranulomatous pyelonephritis.

Whatever the source and the pathogenic role of AAT in malakoplakia, its presence in all macrophages seems to be specific for this disease. Immunohistochemical staining for AAT is therefore proposed as a useful test for an early and accurate differential diagnosis of malakoplakia.

Key words: Malakoplakia – Macrophages – Alpha-1-antitrypsin – Michaelis-Gutmann bodies – Immunohistochemistry

Malakoplakia is a granulomatous inflammatory process, characterized by the accumulation of large mononuclear cells with abundant cytoplasm called "von Hansemann histiocytes" (Lou and Teplitz 1974). These cells contain a variety of PAS positive diastase-resistant intracytoplasmic inclusions, and the so called Michaelis-Gutmann (M.G.) bodies (Michaelis-Gutmann 1902) which are considered to be the diagnostic hallmark of malakoplakia (Lou and Teplitz 1974). Smith (1965) described the morphogenesis of malakoplakia as consisting of 3 phases (early, classic or granulomatous and fibrosing or healing phases). The disease was initially observed in association with chronic infections of the urinary

Offprint requests to: Francesco Callea, Laboratorium voor Cyto- en Histochemie K.U.L., Minderbroederstraat 12, B-3000 Leuven – Belgium

* Part of this work has been presented at the VIIIth European Congress of Pathology, Helsinki, Sept. 1981

0340-1227/82/0395/0001/$01.80

tract (Smith 1965), but other locations (Stanton and Maxted 1981) or systemic distribution (Mc Clure et al. 1981) and even an aggressive behaviour (Lewin et al. 1974) are now recognized. The pathogenesis remains unknown. Ultrastructural (Lewin et al. 1974; Lou and Teplitz 1974) and biochemical-enzymatic studies, suggest a basic macrophage abnormality, probably at the phagolysosomal level (Abdou 1977; Biggar et al. 1981), resulting in an inability to digest phagocytosed products.

We have found that all malakoplakia cells contain large amounts of immunoreactive alpha-1-antitrypsin (AAT) and that this is characteristic for malakoplakia, and probably for malakoplakia only.

Material and Methods

The material for this study comprised two groups of lesions:

1. Four Malakoplakia Cases

Three occurred in the bladder (two endoscopic biopsies, one partial cystectomy), the fourth in the kidney (nephrectomy). All cases were selected on the base of the presence of typical M.G. bodies.

2. Control

As control specimens, 9 biopsies from xanthogranulomatous pyelonephritis, 2 from ceroid granuloma of the gall-bladder and 2 from intestinal Whipple's disease were selected, because of the macroscopical or histological similarity (Takahashi et al. 1976; Lewin et al. 1974) and/or supposed pathogenetic analogy (Kelly and Murad 1981). In addition a further subgroup of chronic inflammatory processes occurring in the urinary tract was examined, comprising 5 cases of chronic interstitial nephritis, 4 of tuberculosis, 3 of chronic cystitis, and 1 bladder in the prune belly syndrome with xanthogranulomatous histological features.

Tissue specimens from all cases were fixed in Bouin's fluid or 10% formalin. Paraffin sections were stained with H.E., PAS without and with diastase digestion.

Immunohistochemical Techniques

For the demonstration of AAT, an indirect immunofluorescence technique as previously described (Ray and Desmet 1975) and a peroxidase-antiperoxidase (PAP) technique according to Taylor (Taylor 1978) were applied. Both trypsinized and non trypsinized 4 micron sections were processed. Endogenous peroxidase activity was blocked with methanol containing 0,3% H202. Anti-AAT rabbit antiserum was purchased from Beringwerke. This was applied at dilution 1:1,280. Swine anti rabbit IgG antiserum and the PAP complex were obtained from Dako and were used at dilutions of 1:40 and 1:100 respectively. Additional sections from all cases were stained for Lysozyme by the same PAP technique. Anti-Lysozyme antiserum was obtained from Dako and used at the dilution of 1:2,500. Substitution of non immune rabbit serum for the antisera and slides treated with diaminobenzidine alone served as controls. Sections were counterstained with haematoxylin.

Results

1. Malakoplakia Cases

The nephrectomy specimen and one of the three bladder lesions presented a tumor-like appearance; one endoscopic biopsy appeared to be multiple yellow mucosal patches in vivo. Analogous appearences, with additional features of an infiltrating process, were described by the endoscopist in the fourth case.

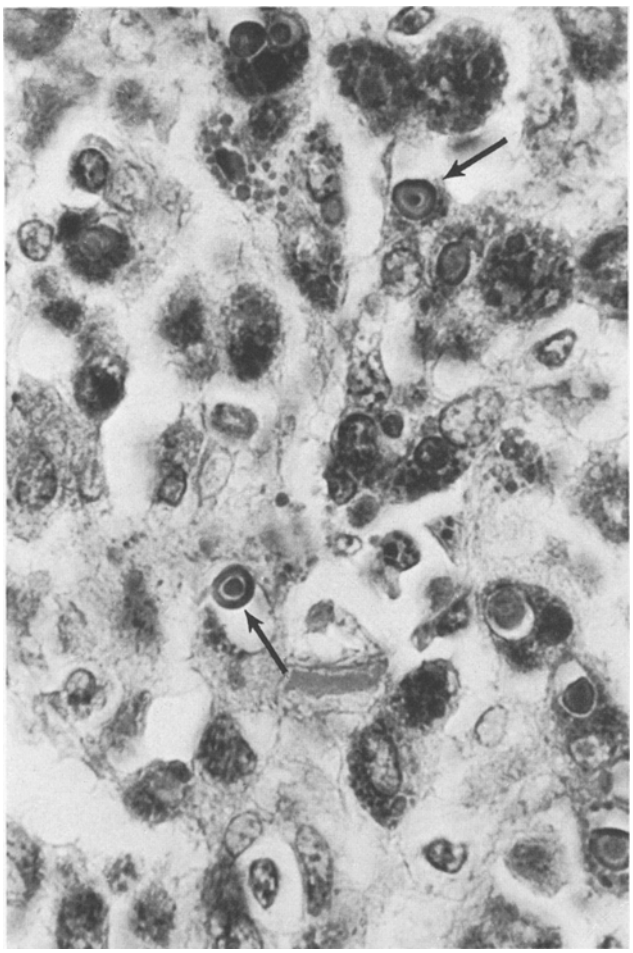

Fig. 1. Renal malakoplakia. Numerous intracellular and extracellular Michaelis-Gutmann bodies (→) and goups of macrophages filled with PAS positive inclusions. PAS after diastase × 1,200

On routine histological examination all cases were characterized by the presence of large mononuclear cells with eosinophilic inclusions. These stained positively with PAS with and without diastase. In all cases, Michaelis-Gutmann bodies were easily recognized as round, weakly basophilic, concentrically laminated cytoplasmic and extracellular bodies (Fig. 1).

The M.G. bodies were extremely numerous in the granulomatous phase of the process, less numerous in the healing phase and very rare in the early stage (bladder endoscopic biopsy).

The malakoplakia cells were organized in vast confluent masses in three out of four cases and appeared as small intramucosal clusters in one endoscopic bladder biopsy.

An extension of sheets of malakoplakia cells to the perirenal and perivesical tissue was observed in the two surgical specimens. In the remaining endoscopic biopsy, macrophages were found within the muscle layer.

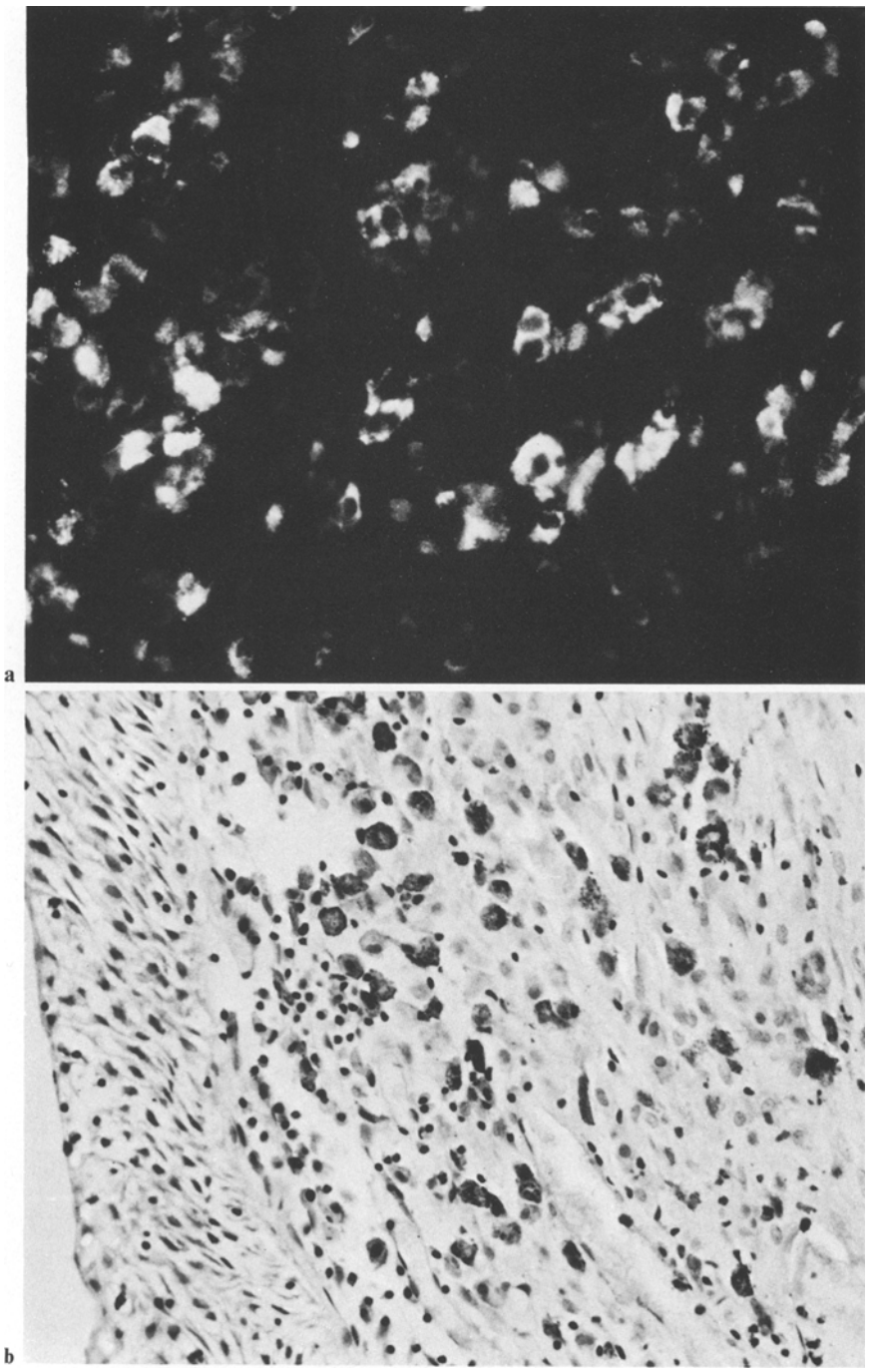

Fig. 2. Early phase in a bladder malakoplakia case. Intramucosal macrophages positively stained for AAT. **a** Immunofluorescence ×280, **b** PAP ×280

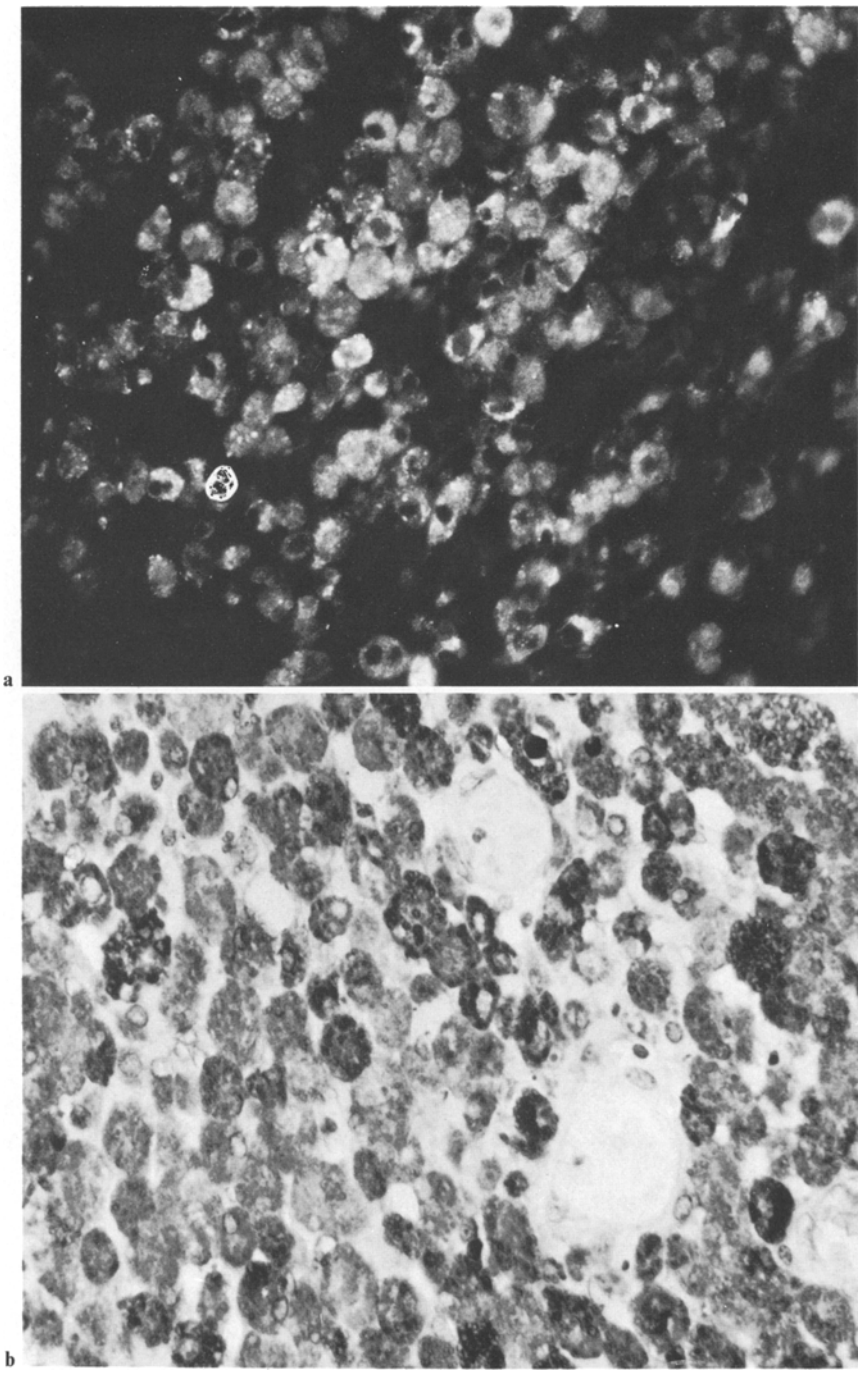

Fig. 3. Granulomatous phase in a bladder malakoplakia case. Closely packed macrophages, all positively stained for AAT. **a** Immunofluorescence ×280, **b** PAP ×450

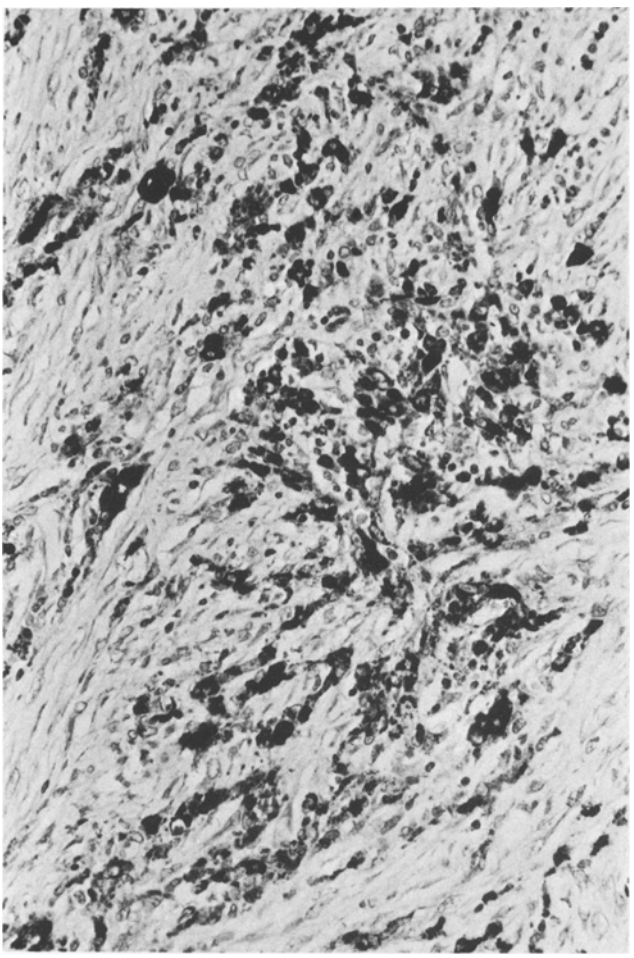

Fig. 4. Fibrosing phase in a bladder malakoplakia case. Macrophages strongly positive for AAT among fibroblast and collagen fibre bands. PAP × 120

Polymorphs, plasma cells and lymphocytes were present in variable amount, fibroblast-like cells were prominent in areas with fibrosing appearence, mast cells were rarely seen. All malakoplakia cells were positive for AAT on both immunofluorescence and PAP stain. The positivity remained unchanged during the three stages of the process (Fig. 2a–b, 3a–b, 4) and did not correlate with the number or the presence of M.G. bodies.

The reaction was granular-globular (Fig. 5) and very strong in character. The small sized M.G. bodies were positive for AAT, but when they became larger, only a peripheral ring-like positivity was observed, which, sometimes was very strong (Fig. 5).

In the two surgical specimens, it was a common finding to observe polymorphs within large macrophages. Both cells stained positively for AAT (Fig. 6).

Lysozyme staining was positive in a vast majority of macrophages in all cases. The staining pattern was finely granular rather than globular.

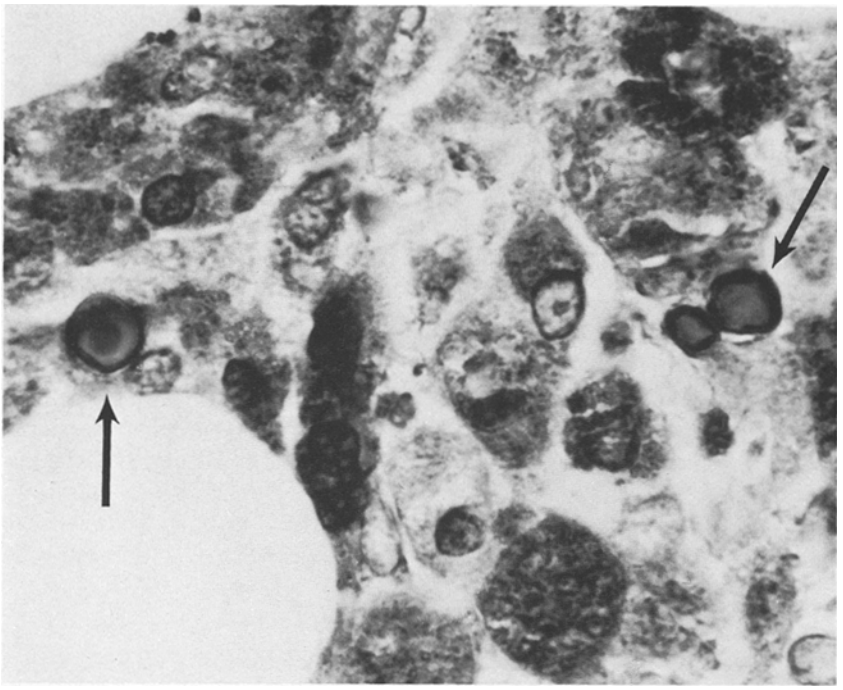

Fig. 5. Renal malakoplakia case. AAT positivity is granular-globular and very strong in character. M.G. bodies show immunoreactive peripheral rim (→) PAP ×1,450

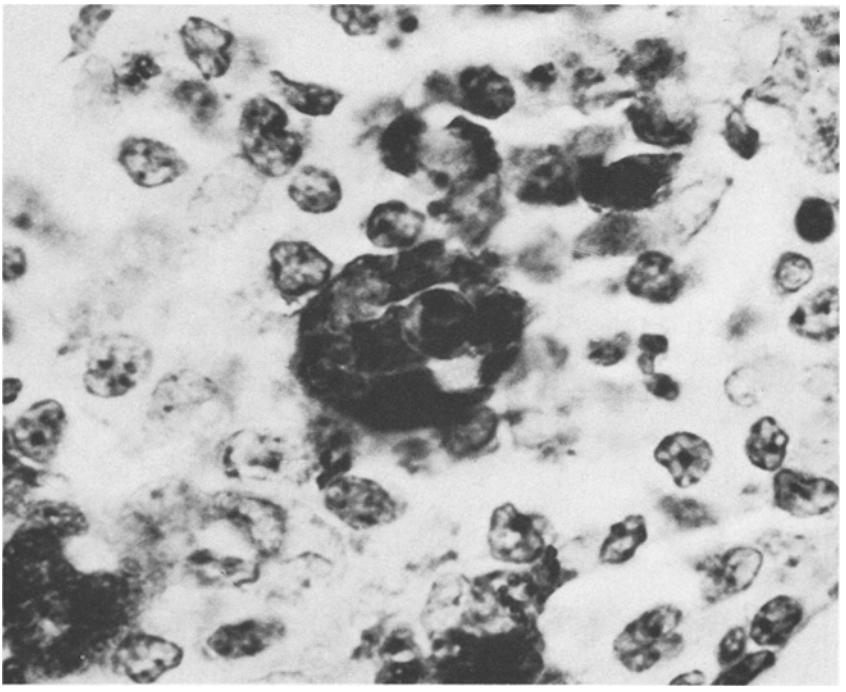

Fig. 6. Renal malakoplakia case. A polymorphonuclear leucocyte within a large macrophage. Both cell are positively stained for AAT. PAP ×1,600

2. Controls

In control cases, the macrophages looking like malakoplakia cells (xanthogranulomatous pyelonephritis, Whipple's disease, ceroid granuloma of the gall bladder), were negative on AAT staining. In the tuberculosis and in two of the xanthogranulomatous specimens with foci of necrosis, the cellular debris, degenerating polymorphs and a few macrophages were positive on AAT staining. In areas distant from necrosis and in other cases solitary positive macrophages were rarely detected.

The foamy histiocytes, specific for xanthogranulomatous pyelonephritis (Kelly and Murad 1981) were always negative, except in one case in which a few histiocytes showed a single coarse reactive globule. A few epithelioid and giant cells of Langhans type showed a very weak diffuse cytoplasmic positivity. Polymorphs and mast cells were positive for AAT both in malakoplakia and in controls. In the control cases, phagocytosis of polymorphs was only observed in xanthogranulomatous pyelonephritis. Positive granular and globular staining for lysozyme occurred in macrophages, polymorphs and mast cells of all control cases.

Discussion

M.G. bodies represent, thus far, the only histological marker for the diagnosis of malakoplakia. However, it should be emphasized that in the early phase, M.G. bodies may not be seen (Dionne et al. 1975) and that in the end stage, only occasional bodies may be found (Smith 1965). Therefore, such structures are not necessary for the diagnosis (Nation 1956; Stanton and Maxted 1981). We have found that all macrophages in renal and bladder malakoplakia cases, contain large amounts of immunoreactive AAT, in a granular-globular pattern. In contrast, macrophages, otherwise closely resembling the von Hansemann cells but without M.G. bodies, occurring in diverse pathological conditions, did not contain AAT. The only exception to this was a few macrophages in tuberculosis and xanthogranulomatous pyelonephritis. Lysozyme, which is a good marker of benign reactive macrophages in tissue sections (Isaacson et al. 1981) was positive in both malakoplakia and control cases.

AAT has been previously identified in pulmonary macrophages (Cohen 1973) and, quite recently, in other tissue macrophages, such as those of the liver, spleen and lymph node (Isaacson). In contrast, spleen and lymphnode macrophages were found to be negative for AAT by others (Motoi et al. 1980; Papaimitriou et al. 1980). Polymorphs, mast cells, a few epithelioid and giant cell of Langhans type were positively stained for AAT. These findings have already been reported (Benitez-Bribiesca and Frere-Horta 1978; Motoi et al. 1980).

The finding of AAT in malakoplakia cells raises the question about its pathogenetic significance. AAT may be synthetised by macrophages, since monocytes in colture have been shown to produce AAT (Wilson et al. 1980). Alternatively, ingested breakdown products of AAT containing cells (polymorphs, platelets, mast cells) could account for the presence of AAT within the malakoplakia cells. Whatever its source, the excess of intracellular AAT, which is a protease inhibitor, may be responsible for the defective digestion of phagocytosed materi-

al, including bacteria (Lou and Teplitz 1974). Even if the pathogenetic role of AAT in malakoplakia remains obscure, its presence in all macrophages seems to be a specific finding in this disease.

We therefore propose immunohistochemical staining for AAT as a useful test for an early and accurate differential diagnosis of malakoplakia. This may be particularly valuable when dealing with small endoscopic biopsies in which, owing to sampling error or to the stage of the lesion, M.G. bodies may not be present or difficult to detect.

Acknowledgments. The authors thank Mrs. B. Tips-Smets for technical assistance, Mr. M. Roosel eers for preparing photographs, Miss C. Vuylsteke for typing the manuscript.

References

Abdou NI, Napombejara C, Sagawa A, Regland C, Stechschulte DJ, Nilson U, Gourley W, Watanabe I, Undsey NJ, Allen MS (1977) Malakoplakia: evidence for monocyte lysosomal abnormality correctable by cholinergic agonist in vitro and in vivo. N Engl J Med 297:1413

Benitez-Bribiesca L, Frere-Horta R (1978) Immunofluorescent localisation of alpha-I-antitrypsin in human polymorphonuclear leucocytes. Life Sci 21:99–104

Biggar DW, Keating A, Bear RA (1981) Malakoplakia: evidence for an acquired disease secondary to immunosuppression. Transplantation 31:109–112

Cohen AB (1973) Interrelationships between the human alveolar macrophage and alpha-I-antitrypsin. J Clin Invest 52:2793–2799

Dionne GP, Bovill EG, Seemayer TA (1975) New fine structural observations in testicular malakoplakia: role of the Sertoli cell. Urology 5:828

Isaacson P, Dones GB, Millward-Sadler GH, Judd MA, Payne S (1981) Alpha-I-antitrypsin in human macrophages. J Clin Pathol 34:982–990

Kelly DR, Murad TM (1981) Megalocytic interstitial nephritis, xanthogranulomatous pyelonephritis and malakoplakia. Am J Clin Pathol 75:333–344

Lewin KJ, Harrel GS, Lee AS, Crowley LG (1974) Malakoplakia. An electron microscopic study: demonstration of bacilliform organisms in malakoplakic macrophages. Gastroenterology 66:28

Lou TY, Teplitz C (1974) Malakoplakia: pathogenesis and ultrastructural morphogenesis. A problem of altered macrophage (phagolysosomal) response Hum Pathol 5:191

Mc Clure J, Cameron CHS, Garret R (1981) The ultrastructural features of malakoplakia. J Pathol 134:13–26

Michaelis I, Gutmann C (1902) Ueber Eischlusse in blasentumoren. Z Klin Med 47:208

Motoi M, Stein H, Lennert K (1980) Demonstration of lysozime, alpha-I-antichymotrypsin, alpha-I-antitrypsin, albumin and transferrin with the immunoperoxidase method in lymph node cells. Virch Arch B Cell Path 35:73–82

Nation EF (1956) Malakoplakia of the urinary tract. J Urol 76:576

Ray MB, Desmet VJ (1975) Immunofluorescent detection of alpha-I-antitrypsin in paraffin embedded liver tissue. J Clin Pathol 28:717–721

Smith BH (1965) Malakoplakia of the urinary tract: a study of 24 cases. Am J Clin Pathol 43:409

Stanton MJ, Maxted W (1981) Malakoplakia: a study of the literature and current concepts of pathogenesis, diagnosis and treatment. J Urol 125:139–146

Takahashi K, Oka K, Hazokazi H, Kojima M (1976) Ceroid-like histiocytic granuloma of gall bladder – a previously undescribed lesion – Acta Pathol Jpn 26:25–46

Taylor CR (1978) Immunoperoxidase techniques. Practical and theoretical aspects. Arch Pathol Lab Med 102:113–121

Wilson GB, Walker GH, Watkins JR, Wolroch D (1980) Determination of subpopulations of leucocytes involved in the synthesis of alpha-I-antitrypsin in vitro. Proc Soc Exp Biol Med 164:105–114

Accepted December 29, 1981

Virchows Arch [Pathol Anat] (1982) 395:11–43

Virchows Archiv A

Development of Malignant Lymphoma in Myoepithelial Sialadenitis (Sjögren's Syndrome)*

U. Schmid[1]**, Dagmar Helbron[2]***, and K. Lennert[2]

[1] Institut für Pathologie, Kantonsspital, CH-9007 St. Gallen, Switzerland
[2] Institut für Pathologie, Klinikum der Christian-Albrechts-Universität, Hospitalstrasse 42, D-2300 Kiel, Federal Republic of Germany

Summary. Forty-five cases of myoepithelial sialadenitis (MESA) were investigated histologically, immunologically, and clinically. Two patients with clinical evidence of Sjögren's syndrome were also included in the study, though salivary gland biopsies showing MESA were not available. A total of 16 patients had Sjögren's syndrome or another type of autoimmune disease. In 42 cases of MESA, so-called proliferation areas composed of immunoblasts and lymphoplasmacytoid cells were found. The proliferation areas were small and circumscribed in 16 cases, and extensive and confluent in 26 cases. All the confluent proliferation areas analyzed with the immunoperoxidase (PAP) method showed a monotypic immunoglobulin pattern (predominantly IgM/κ). Extrasalivary malignant lymphoma with the same histologic and immunohistologic features as the confluent proliferation areas was found in 14 patients. Thus, this type of MESA is called "manifest malignant lymphoma". The tumor was classified as LP immunocytoma in 23 patients, and as LP immunocytoma transforming into immunoblastic lymphoma in three patients. One patient developed nodal B-immunoblastic lymphoma. The term "early lymphoma" is suggested for MESA with circumscribed proliferation areas showing a monotypic immunoglobulin pattern (usually IgM/κ), because extrasalivary malignant lymphoma developed later in four of the patients with this type of MESA. The two patients with only clinical evidence of Sjögren's syndrome also showed extrasalivary malignant lymphoma (LP immunocytoma in one case and immunoblastic lymphoma in the other).

There is a close histogenetic relation between MESA with or without autoimmune disease and certain malignant non-Hodgkin's lymphomas of B type, namely, LP immunocytoma and B-immunoblastic lymphoma. The interval

Offprints requests to: K. Lennert at the above address

* Dedicated to Professor Dr. G. Seifert, Hamburg, on the occasion of his 60th birthday

** Supported by the Schweizerischer Nationalfonds
*** Supported by the Kind-Philipp-Stiftung

0340-1227/82/0395/0011/$06.60

between the appearance of salivary gland enlargement and the diagnosis of malignant lymphoma varied from 1.5 to 12 years. Generalization of malignant lymphoma led to death in 11 cases.

Key words: Myoepithelial sialadenitis – Sjögren's syndrome – Non-Hodgkin's lymphoma – LP immunocytoma – Immunoblastic lymphoma

Introduction

There is much interest in lymphoproliferative disorders arising in patients with immunologic disturbances, especially those in the group of autoimmune diseases. The latter include lupus erythematosus, Hashimoto's disease (immunothyroiditis), and Sjögren's syndrome (Talal et al. 1967; Repetto et al. 1974; Bolognini and Riva 1975; Green et al. 1978; Banks et al. 1979; Lennert et al. 1979; Maurer et al. 1979; Schwarze and Papadimitriou 1980). In patients with Sjögren's syndrome, the risk of development of a malignant lymphoma is 43.8 times greater than in a comparable normal population (Kassan et al. 1978). Autoimmune phenomena may also appear secondarily, however, in patients with malignant lymphoma (Miller 1976).

Sjögren's syndrome is a particularly interesting type of autoimmune disease, because the lymphoproliferative disorders observed in this syndrome may belong to any part of the spectrum (ranging from prelymphomas to morphologically and clinically recognizable malignant lymphomas) (Anderson and Talal 1971). The malignant lymphomas arising within and outside the salivary glands are chiefly non-Hodgkin's lymphomas of B-cell type that show production and sometimes also secretion of immunoglobulin (Ig). Heckmayr et al. (1976) reviewed the literature up to 1976 and found, together with their own cases, a total of 20 patients with malignant lymphoma in the salivary glands and 25 patients with malignant lymphoma outside the salivary glands in Sjögren's syndrome. The tumors included 9 lymphocytic lymphomas (including "germinoblastomas" or "lymphosarcomas"), 2 lymphohistiocytic lymphomas, 1 lymphoplasmacytoid immunocytoma, 16 reticulum cell sarcomas (or immunoblastic lymphomas), 11 cases of Waldenström's disease, 5 cases of Hodgkin's disease, and 1 unclassifiable lymphoma. The literature also contains descriptions of a thymoma (Pinkus and Dekker 1970), a myeloma secreting free λ chains (Shearn et al. 1975), a lymphocytic lymphoma arising in a patient treated with Dilantin (Lapes et al. 1976), and a "Lennert's lymphoma" (Sebahoun et al. 1977). Colby and Dorfman (1979) did not find a preference for a particular type of lymphoma in a group of 14 patients with non-Hodgkin's lymphoma associated with myoepithelial sialadenitis (MESA). We do not know of any reports of a T-cell lymphoma in a salivary gland with MESA.

On histologic examination, Sjögren's syndrome shows MESA, which used to be known as a benign lymphoepithelial lesion or Mikulicz's disease (Godwin 1952). Seifert and Donath (1976) considered this lesion to be a prototype of an autoimmune disease of the salivary gland. It may also occur without the clinical picture of Sjögren's syndrome, and malignant lymphomas are frequently

seen in such cases as well (Pinkus and Dekker 1970; Azzopardi and Evans 1971; Batsakis et al. 1975; Lapes et al. 1976).

The identification and especially the early recognition of malignant lymphomas in MESA have often presented us with unsolvable problems. Thus, the goal of the present investigation was to develop criteria that would enable the definite and early recognition of malignant lymphomas in MESA and allow us to distinguish them from reactive lesions. These criteria are based on the results of systematic histologic and cytologic studies, immunohistologic analyses (using the PAP method), and examinations of clinical data and follow-up reports on 45 patients with MESA. These could be compared with biopsies from 25 patients without immunosialadenitis who showed primary malignant lymphoma of the salivary gland or surrounding tissue (Schmid et al. 1982).

Materials and Methods

Biopsies from 45 patients with MESA were examined. They had been sent to the Lymph Node Registry in Kiel for diagnosis between 1965 and 1980, and included at least one salivary gland biopsy from each patient, more than one salivary gland biopsy from each of 6 patients, lymph node biopsies from 20 patients, and extranodal biopsies from 7 patients. Two other patients with clinical evidence of Sjögren's syndrome and malignant lymphoma of extrasalivary lymph nodes were also included in the study, even though salivary gland biopsies were not available for examination.

In some cases, the sections had been prepared elsewhere and no other material was available. In all other cases, 3–4 μm thick sections were cut from formalin-fixed and paraffin-embedded tissue and stained with hematoxylin and eosin, Giemsa, periodic acid Schiff (PAS), and silver impregnation (Gomori). In a few cases, AS-D-chloroacetate esterase and Congo red stainings were also performed. The imprints available in 5 cases were stained by Pappenheim (May-Grünwald-Giemsa). When enough imprints were available, additional cytochemical stainings were performed (acid nonspecific esterase, alkaline phosphatase, acid phosphatase, and PAS).

Paraffin sections from 36 cases could be analyzed for cytoplasmic immunoglobulin (CIg) by the peroxidase-antiperoxidase (PAP) method of Sternberger et al. (1970). We used the modification of Mepham et al. (1979). After blocking of endogenous peroxidase in methanol/H_2O_2 (20–30 min), the dewaxed sections were pretreated with fresh 0.1% solution of trypsin in 0.1% $CaCl_2$ (pH 7.8) at 37 °C for 20–30 min. After two washes in PBS buffer (pH 7.4) for 10 min each, the sections were treated with normal sheep serum (diluted 1:5) for 10 min. Antisera were then applied in the following order: specific rabbit antisera (IgA, IgM, and albumin were diluted 1:200; IgG, κ, and λ, 1:300; and lysozyme and J chains, 1:100), swine anti-rabbit IgG serum (diluted 1:50), and rabbit PAP complex (diluted 1:100). Each incubation lasted 30 min and was followed by washing in PBS buffer (pH 7.4). Peroxidase reactivity was demonstrated with 3,3-diaminobenzidine tetrahydrochloride (Walter, Kiel, FRG) according to Graham and Karnovsky (1966). The sections were then counterstained with hemalum and covered. The specific antisera against human IgA, IgG, IgM, κ, λ, albumin, and lysozyme, the swine anti-rabbit IgG, and the PAP complex were purchased from Dako (Copenhagen, Denmark). The specific anti-J chain serum (RAHu/J) was obtained from Nordic Immunology (Leuven, Belgium). The specificity of the commercial antisera is tested in the immunologic laboratory of the Institute of Pathology in Kiel by immunostaining tumors with a known CIg pattern (plasmacytoma, lymphoplasmacytoid immunocytoma).

The non-Hodgkin's lymphomas were diagnosed according to the Kiel classification (Lennert et al. 1975; Lennert 1978).

Clinical data were collected by sending questionnaires to the patients' physicians or hospitals. In some cases, we had access to the hospital records. We are grateful to all the clinicians who provided us with data.

Results

I. Histologic Findings

1. Salivary Glands (Table 1)

A total of 53 salivary gland biopsies from 45 patients were examined. The biopsies included 41 from the parotid gland and 12 from the submandibular gland. There were no biopsies of sublingual glands or lips.

All biopsies revealed circumscribed or diffuse, dense lymphoid cell infiltrates in the salivary gland tissue. The acini were largely destroyed, and there were islands of myoepithelial cells in the salivary ducts. In 28 patients (62%), the islands contained focal deposits of hyaline. In 42 patients (93%), the islands were surrounded by lymphocytes with abundant pale cytoplasm and markedly polymorphic nuclei, which often showed multiple indentations; sometimes these cells were somewhat similar to nuclei of granulocytes (Figs. 1 and 11), but staining with chloroacetate esterase excluded this possibility. In 37 patients (82%), cells of the same appearance were also found within the myoepithelial complexes; these infiltrates sometimes resembled the Pautrier's pseudoabscesses seen in mycosis fungoides. In 16 patients (36%), usually circumscribed infiltrates of such lymphocytes were seen near venules.

Two of the three available imprints of salivary glands showed a large number of large lymphocytes with pale cytoplasm and irregularly shaped nuclei. In all three cases, there were many lymphocytes with focal acid nonspecific esterase activity and a few lymphocytes with focal acid phosphatase activity.

The lymphocyte infiltrates in the salivary ducts were loosely arranged, and the cells resembled T lymphocytes because of their polymorphic nuclei. In con-

Table 1. Histologic findings in myoepithelial sialadenitis ($n=45$)

	n	%
Myoepithelial complexes	45	100
Myoepithelial complexes with hyaline deposits	28	62
Polymorphonuclear lymphocytes		
around myoepithelial complexes	42	93
within myoepithelial complexes	37	82
in perivascular areas	16	36
Proliferation areas		
none	3	7
circumscribed	16	35
confluent	26	58
PAS-positive globules		
intracytoplasmic	23	51
intranuclear	18	40
Giant cells resembling Sternberg-Reed cells	26	58
Germinal centers	38	84
Epithelioid cells	22	49
Epithelioid venules increased in number	25	56
Reticulin fibers increased in number	34	76

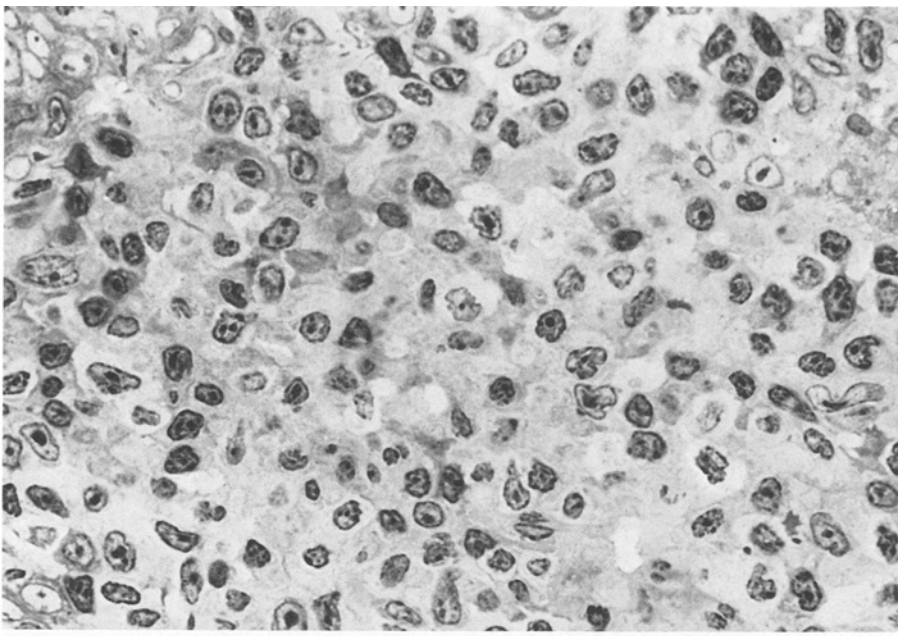

1

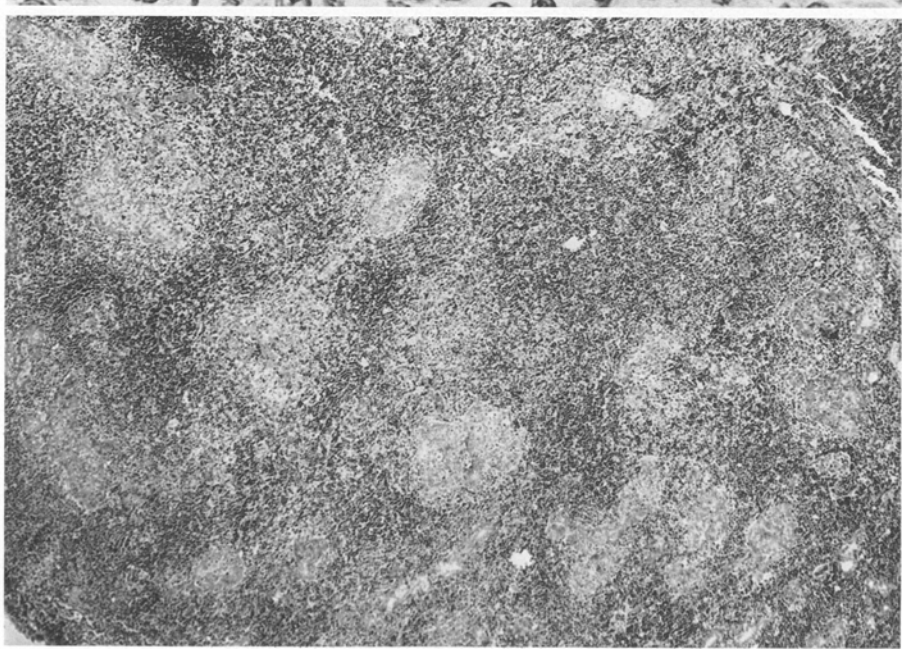

2

Fig. 1. Polymorphonuclear lymphocytes (T lymphocytes?) within a myoepithelial complex. Methylene blue. × 882

Fig. 2. Myoepithelial sialadenitis with several myoepithelial complexes. Circumscribed, pale-looking proliferation areas are seen between the complexes. Giemsa. × 56

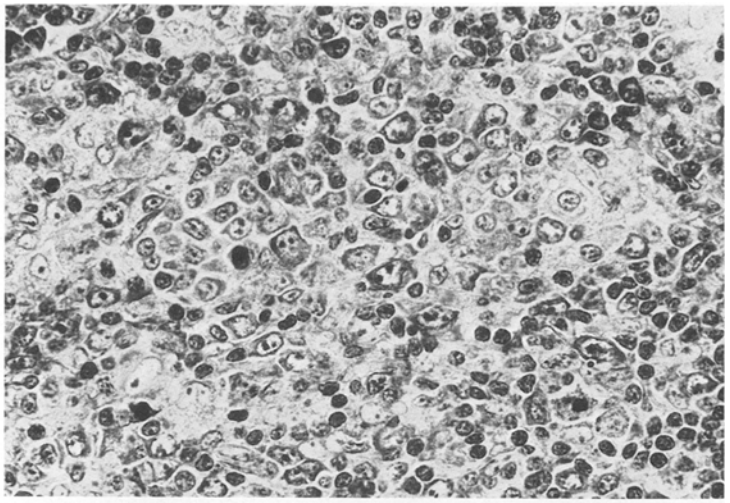

3

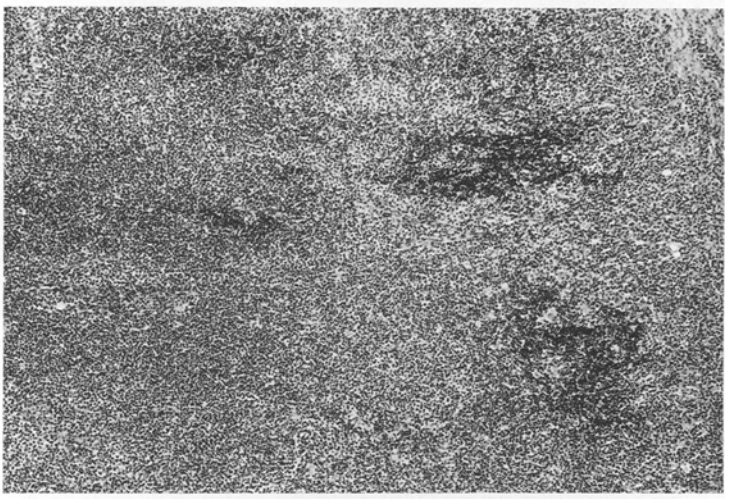

4

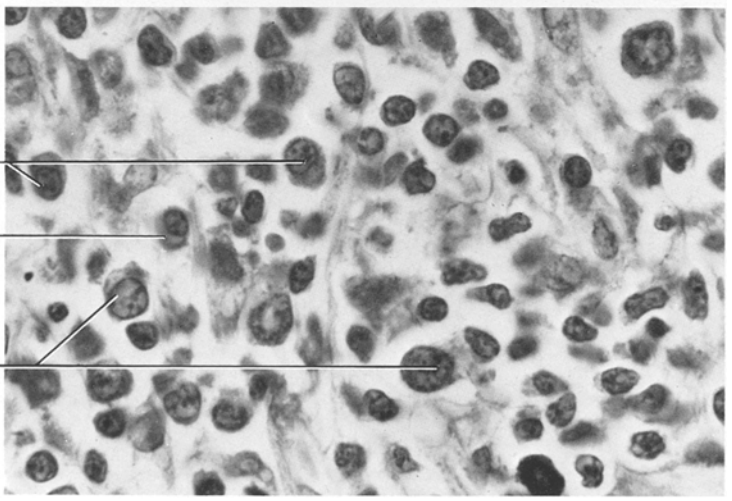

5

trast, the lymphocytes in the areas between the ducts (previously salivary gland parenchyma) were densely packed and were probably mostly B lymphocytes.

Within the dense lymphocyte infiltrates there were usually small or quite large foci of a mixture of cells, which always included immunoblasts. We chose to call these foci "proliferation areas", especially because they often showed mitotic activity. Based on the presence (or absence) and the size of the proliferation areas, three types of MESA could be distinguished:

1. MESA without Proliferation Areas. This type showed dense, deep blue (Giemsa staining), homogeneous infiltration of the salivary gland tissue by small lymphocytes, which usually had round nuclei. There were hardly any immunoblasts and no plasmacytoid cells. Typical plasma cells, however, were sometimes found. Only three cases (7%) showed this histologic picture.

2. MESA with Small, Circumscribed Proliferation Areas. In this type, circumscribed areas were evident within the dense infiltrates of small lymphocytes. These areas looked pale with Giemsa staining and often contained only a few cells (Fig. 2), mostly immunoblasts and lymphoplasmacytoid cells (Fig. 3). Mitotic activity was sometimes considerable, especiallly among the immunoblasts; some atypical mitotic figures were found. The immunoblasts and lymphoplasmacytoid cells were interspersed with a few typical plasma cells. Sixteen cases (35%) showed this histologic picture.

3. MESA with Extensive, Confluent Proliferation Areas. This type showed extensive, confluent proliferation areas that looked pale with Giemsa staining and were composed of the same cells as were the foci of the second type, although there was often a larger number of lymphoplasmacytoid cells (Figs. 4 and 5). The dense component of small lymphocytes was frequently reduced to only a few islands and was completely missing in two biopsies. This third group contained 26 patients (58%).

In MESA of types 2 and 3, PAS-positive intracytoplasmic globules were found in lymphoplasmacytoid cells of 23 patients (51%) and intranuclear globules in lymphoplasmacytoid cells of 18 patients (40%) (see Table 7). A remarkable finding in 26 patients (58%) were large cells resembling mononuclear Hodgkin cells and Sternberg-Reed cells within the proliferation areas (Fig. 6). Salivary gland biopsies from three patients showed not only MESA with confluent proliferation areas, but also non-Hodgkin's lymphoma of immunoblastic type (Fig. 7).

Examination of multiple salivary gland biopsies from three patients revealed a significant enlargement of the proliferation areas during the course of the

Fig. 3. Circumscribed proliferation area with many immunoblasts and lymphoplasmacytoid cells. Giemsa. ×556

Fig. 4. Myoepithelial sialadenitis with confluent, pale-looking proliferation areas and only a few dark-looking islands of small lymphocytes. Hematoxylin and eosin. ×56

Fig. 5. Confluent proliferation area composed of large plasmacytoid cells (*pc*), plasmablasts (*pb*), and small and medium-sized lymphocytes. One normal plasma cell (*npc*). Giemsa. ×822

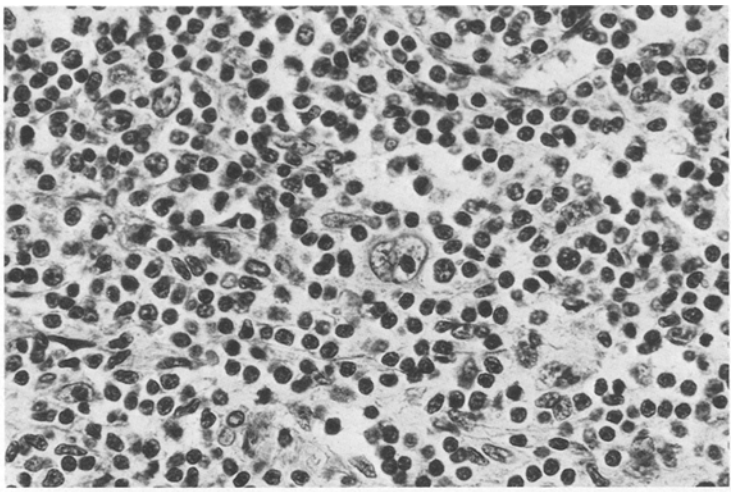

6

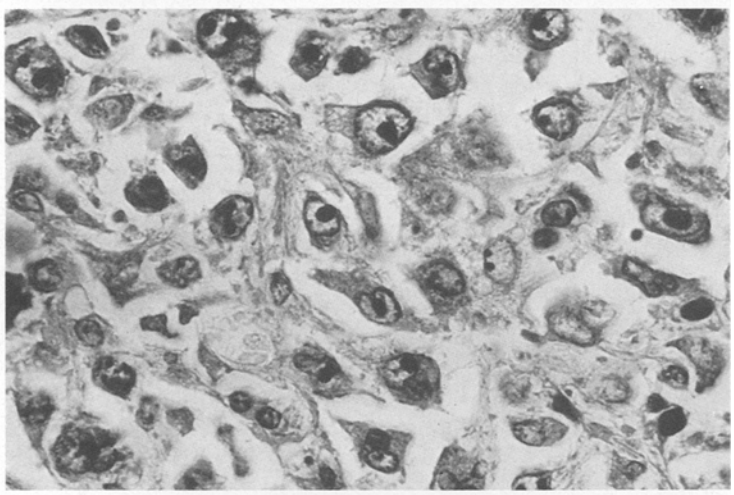

7

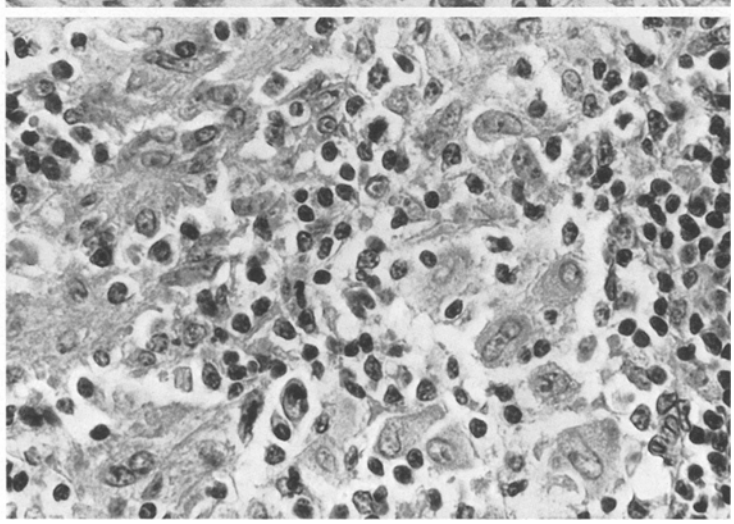

8

Table 2. Histologic findings in lymph nodes of 20 patients with myoepithelial sialadenitis (MESA)

Type of MESA	Lymph node lesion					
	Reactive	Circumscribed proliferation areas	Malignant lymphoma			
			Lymphoplasmacytoid immunocytoma	Polymorphic immunocytoma	Polymorphic immunocytoma with transformation into immunoblastic lymphoma	Immunoblastic lymphoma
Without proliferation areas	1	–	–	–	–	–
Circumscribed proliferation areas	3	1[a]	–	1	1	–
Confluent proliferation areas	1	–	7 (9)[b]	2 (5)[b]	2 (5)[b]	1

[a] Two later lymph node biopsies from this patient showed first lymphoplasmacytoid immunocytoma and then polymorphic immunocytoma transforming into immunoblastic lymphoma

[b] A total of 28 lymph nodes were examined, because multiple biopsies were available from some patients. The number in parentheses is the number of nodes showing the respective picture

disease (the interval between biopsies was 5–11 months). In one patient, circumscribed proliferation areas turned into confluent ones.

Active germinal centers were a relatively constant finding, as they were seen in 38 cases (84%). Epithelioid cells were found remarkably often, namely in 22 patients (49%); they were disseminated or arranged in small foci, usually near the proliferation areas (Fig. 8).

Another notable finding was a slight to moderate increase in the number of epithelioid venules in 25 patients (56%). An increase in the number of reticulin fibers, frequently confined to the proliferation areas, was found in 34 patients (76%).

Three biopsies showed foci of lymphoid cells with pale cytoplasm. Some of these foci resembled the so-called immature sinus histiocytosis of lymph nodes.

2. Lymph Nodes (Table 2)

A total of 28 lymph nodes from 20 patients with MESA and two lymph nodes from two patients with Sjögren's syndrome, but without histologically document-

Fig. 6. Multinucleate giant cell resembling a Sternberg-Reed cell in a confluent proliferation area. Hematoxylin and eosin. ×556

Fig. 7. Immunoblastic lymphoma with plasmablastic differentiation in a salivary gland involved by myoepithelial sialadenitis with confluent proliferation areas. Giemsa. ×882

Fig. 8. Epithelioid cells near a confluent proliferation area. Hematoxylin and eosin. ×560

ed MESA, were examined. There were 21 cervical, 4 supraclavicular, 2 axillary, and 3 inguinal lymph nodes. Multiple lymph node biopsies from the same patient usually showed the same histologic picture and thus will not be described separately. The lymph node findings will be presented here in relation to the different types of MESA.

a) Lymph Node Lesions Associated with MESA without Proliferation Areas. The one available lymph node biopsy from only 1 of the 3 patients in this group revealed reactive changes without proliferation areas.

b) Lymph Node Lesions Associated with MESA with Circumscribed Proliferation Areas. Lymph node biopsies from 6 of the 16 patients in this group were examined. Three of the lymph nodes showed reactive changes like those of the node in group *a*. In the fourth lymph node, the architecture was preserved and there were typical secondary follicles, but circumscribed proliferation areas were found in the pulp. The cellular composition of these proliferation areas was the same as that of the proliferation areas seen in the MESA examined at the same time. Additional lymph nodes were removed from the same patient 5 and 52 months later; these biopsies revealed first lymphoplasmacytoid immunocytoma and later the picture of polymorphic immunocytoma transforming into immunoblastic lymphoma. In the last two cases, lymph node biopsies were examined 1 or 4 years after the salivary gland biopsies. These lymph nodes showed infiltration by polymorphic immunocytoma, in one case with transformation into immunoblastic lymphoma. The tumor involved chiefly the pulp; lymph follicles were partially preserved.

c) Lymph Node Lesions Associated with MESA with Confluent Proliferation Areas. A total of 21 lymph node biopsies from 13 of the 26 patients in this group were examined. In 8 cases, the first lymph node biopsies were obtained at the same time as the first salivary gland biopsy, and in 5 cases, 14–66 months after the first salivary gland biopsy. Only one lymph node showed reactive changes. In all other lymph node biopsies, the histologic pictures were found to be about the same, and the lesions were largely identical with those seen in the salivary glands. On the basis of our previous experience, however, the lymph node lesions could be identified clearly as malignant lymphomas. The infiltration was diffuse in 4 cases; in the other 8 patients, the lymph nodes were only partially infiltrated, with the tumor infiltrates often confined to the pulp, and some lymph follicles were intact (Fig. 9).

Fig. 9. Lymph node infiltrated by pale-looking cells of LP immunocytoma. There are a few small lymph follicles. Hematoxylin and eosin. ×35

Fig. 10. Lymph node with polymorphic immunocytoma, which contains not only lymphoplasmacytoid cells and immunoblasts, but also plasmablasts and centrocytes. Giemsa. ×882

Fig. 11. Myoepithelial complex (*ME*) surrounded by J chain-positive lymphoplasmacytoid cells (*J*). Polymorphonuclear lymphocytes (*pol. Ly*) within the myoepithelial complex are negative. Immunostaining for J chains. ×220

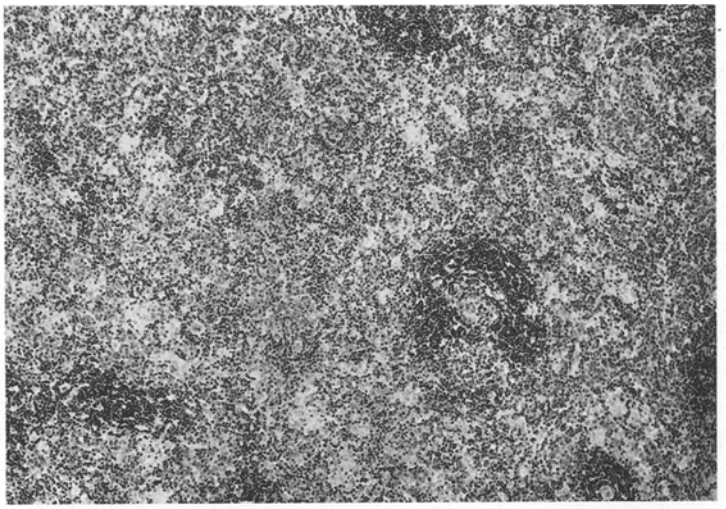

9

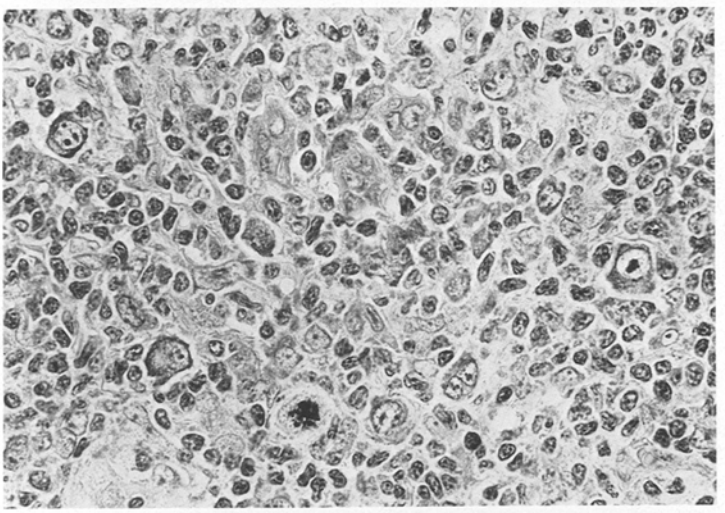

10

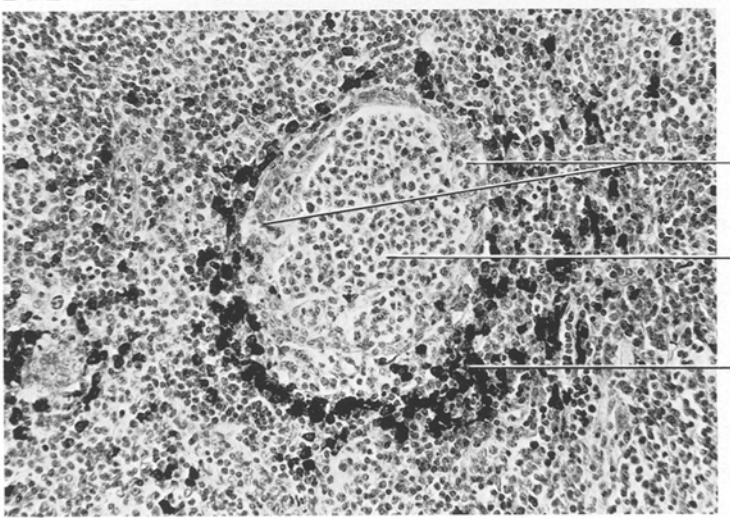

11

Only two types of non-Hodgkin's lymphoma were diagnosed: LP immunocytoma and immunoblastic lymphoma. Lymph nodes from 7 patients showed the lymphoplasmacytoid subtype of immunocytoma and 2 showed the polymorphic subtype (Fig. 10). There were 2 cases in which polymorphic immunocytoma was transforming into immunoblastic lymphoma. One tumor was a purely immunoblastic lymphoma. In 2 cases, a second lymph node biopsy was examined 5 or 33 months after the first. One of these patients showed transformation of lymphoplasmacytoid immunocytoma into the polymorphic subtype. The other patient showed transformation of lymphoplasmacytoid immunocytoma into polymorphic immunocytoma with immunoblastic lymphoma.

The content of epithelioid cells and "Sternberg-Reed cells" in the lymph nodes was largely identical with that of the respective salivary glands. This was not true for the polymorphonuclear lymphocytes (T lymphocytes?) demonstrated in MESA. Such cells were found in perivascular areas in lymph nodes from only four patients with malignant lymphoma. In addition, lymphomatous lymph nodes from three patients showed bands of lymphocytes with pale cytoplasm, which resembled the picture of so-called immature sinus histiocytosis.

d) Extrasalivary Nodal Malignant Lymphomas in Sjögren's Syndrome. Lymph nodes from 2 patients with clinical evidence of Sjögren's syndrome, but without histologically verified MESA, were also included in the present study. In one case, a cervical lymph node biopsy revealed polymorphic immunocytoma. In the other case, an inguinal lymph node biopsy showed immunoblastic lymphoma with plasmacytic differentiation.

3. Extrasalivary and Extranodal Findings Associated with MESA

Two patients with MESA (one with circumscribed proliferation areas and the other with confluent ones) showed focal infiltration of the bone marrow by a low-grade malignant non-Hodgkin's lymphoma. In another patient with MESA with confluent proliferation areas, polymorphic immunocytoma, which transformed into immunoblastic lymphoma, developed in the soft tissue of a lower leg 10 months after the salivary gland biopsy. One patient with circumscribed proliferation areas in the salivary gland showed benign lymphoma of the skin after 7 months. A skin biopsy from another patient with similar changes in the salivary gland revealed allergic vasculitis. Puncture material from liver and spleen was examined in one case of MESA with circumscribed proliferation areas, and bone marrow puncture material was examined in one case of MESA with confluent proliferation areas; these specimens were found to be free of tumor infiltration.

II. Immunohistologic Findings

1. Salivary Glands (Tables 3–5)

Salivary gland biopsies from 34 patients were available for immunohistologic investigation. The immunologic results were closely correlated with the histologic findings and will therefore be presented in relation to the three types of MESA.

Table 3. Immunohistologic findings in myoepithelial sialadinitis (MESA)

Type of MESA	CIg[a] pattern of proliferation areas			CIg pattern of germinal centers		
	n[b]	Polytypic	Monotypic	n[b]	Polytypic	Tending to be monotypic
Without proliferation areas	3	–	–	3	3	0
Circumscribed proliferation areas	13	4	9	12	7	5
Confluent proliferation areas	18	0	18	14	8	6

[a] CIg = cytoplasmic immunoglobulin
[b] n = number of cases analyzed with the PAP method

Table 4. Monotypic cytoplasmic immunoglobulin (CIg), J chain, and albumin staining patterns in myoepithelial sialadenitis (MESA) with circumscribed or confluent proliferation areas ($n = 27$)

	MESA with circumscribed proliferation areas	MESA with confluent proliferation areas
CIg		
IgM/κ	8	13
IgM/λ	–	1
IgM/–	1	–
–/κ	–	2
IgG/κ	–	1
IgA/λ	–	1
J chains[a]	3	5
Albumin	–	–

[a] Only 19 cases could be stained for J chains

In all types of immunosialadenitis, cytoplasmic immunoglobulin (CIg) could not be demonstrated in the polymorphonuclear lymphocytes located around or within the myoepithelial complexes and in perivascular areas. In particular, there were no J chains in such cells (Fig. 11). The polymorphonuclear lymphocytes in the salivary ducts were interspersed, however, with occasional typical reactive plasma cells.

The immunohistologic results presented below were obtained on albumin-negative cells. This excludes the possibility of secondary uptake of Ig.

a) MESA Without Proliferation Areas. Within the lymphocytic infiltrates in the three salivary gland biopsies in this group there were many plasma cells with a polytypic pattern of κ and λ chains, IgA, IgG, and IgM. The heavy chains

Table 5. Comparative ratio of number of immunoblasts (IB) to number of lymphoplasmacytoid cells (LPC) with monotypic immunoglobulin patterns in myoepithelial sialadenitis (MESA)

Type of MESA	*n*	IB > LPC	IB ≅ LPC	IB < LPC
Circumscribed proliferation areas	9	5	3	1
Confluent proliferation areas	18	3	2	13

showed a slight predominance of IgG. The germinal centers also contained κ- and λ-positive cells.

b) MESA with Circumscribed Proliferation Areas. In 8 of the 13 biopsies in this group, the proliferation areas contained immunoblasts and plasmacytoid cells with monotypic staining for IgM/κ (Figs. 12 and 13). In another case, we could demonstrate only IgM and no light chains. Three of the 7 cases analyzed for J chains showed a positive reaction. The ratio of immunoblasts to lymphoplasmacytoid cells was about 1:1 in 3 biopsies; immunoblasts predominated in 5 biopsies, and lymphoplasmacytoid cells predominated in one biopsy. Germinal centers were seen in 8 biopsies; in 5 of these biopsies, they showed a predominance of the CIg chains demonstrated in the corresponding proliferation areas with a monotypic pattern. Between the proliferation areas, but still within the lymphocytic infiltrates, there were a few reactive plasma cells with a polytypic CIg pattern.

The proliferation areas in the other four biopsies in this group contained a few immunoblasts with a polytypic CIg pattern of κ and λ chains, IgA, IgG, and IgM (slight predominance of IgG). The germinal centers in these four biopsies also showed a polytypic pattern. Plasma cells lying between the proliferation areas had a polytypic CIg pattern (the heavy chain class was frequently IgG) and were clearly increased in number when compared with the cases showing monotypic proliferation areas.

c) MESA with Confluent Proliferation Areas. The salivary gland biopsies from all 18 patients in this group revealed proliferation areas with a monotypic CIg pattern (Figs. 14 and 15): IgM/κ in 13, IgM/λ in one, $-/\kappa$ in two, IgG/κ in one, and IgA/λ in one. Five of the 12 biopsies stained for J chains showed a positive reaction.

The ratio of immunoblasts to plasmacytoid cells was about 1:1 in 2 cases. Immunoblasts predominated in 3 cases, and lymphoplasmacytoid cells predominated in 13 cases.

Fig. 12. Circumscribed proliferation area with a monotypic immunoglobulin pattern. Immunostaining for κ. ×140

Fig. 13. Circumscribed proliferation area (same as Fig. 12) with many lymphoplasmacytoid cells and a monotypic immunoglobulin pattern. Immunostaining for κ. ×882

Fig. 14. Myoepithelial sialadenitis with confluent proliferation areas showing a monotypic immunoglobulin pattern, and one myoepithelial complex. Immunostaining for κ. ×56

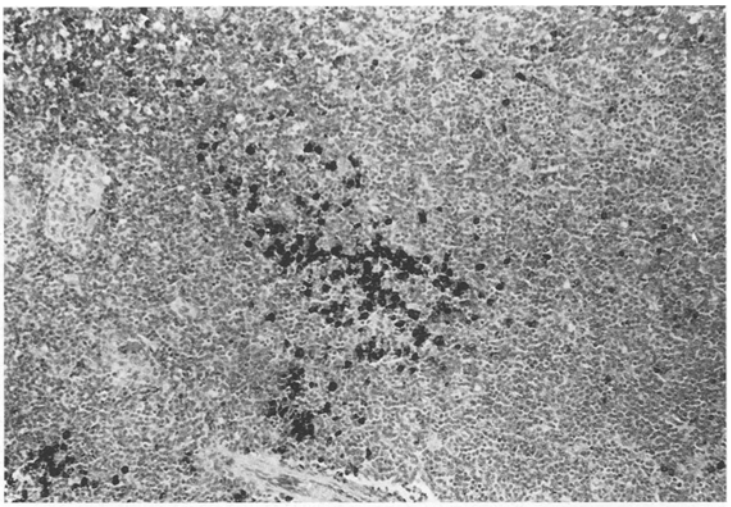

12

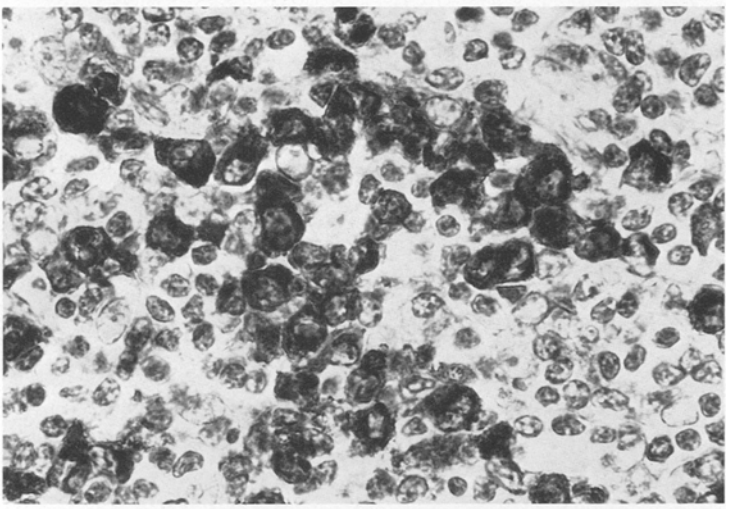

13

14

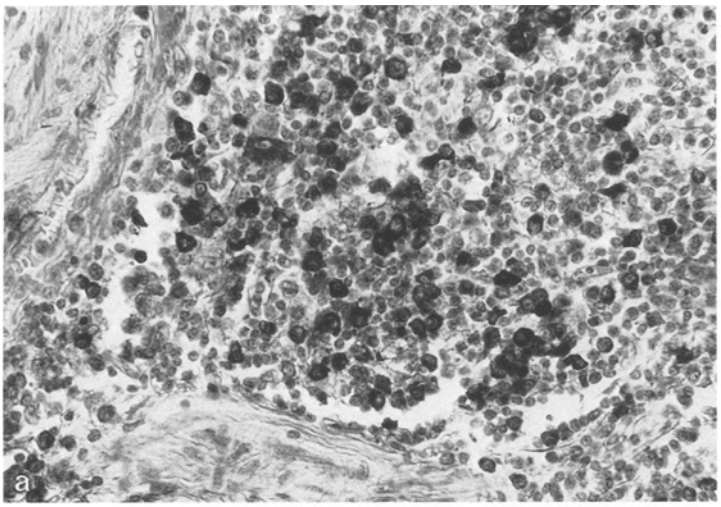

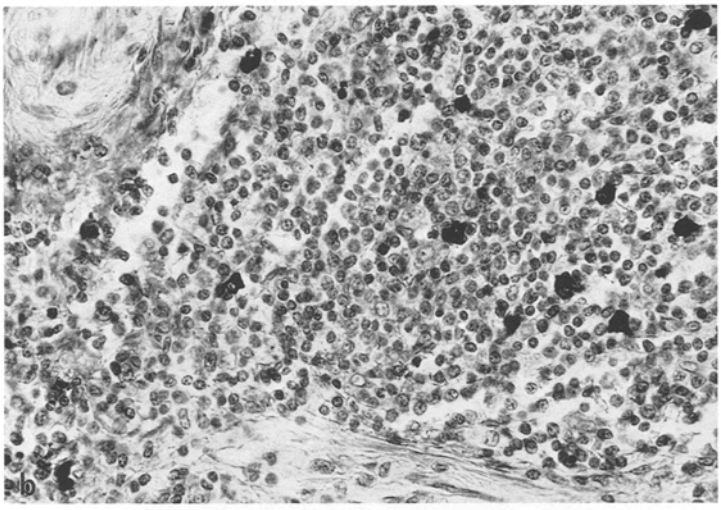

15

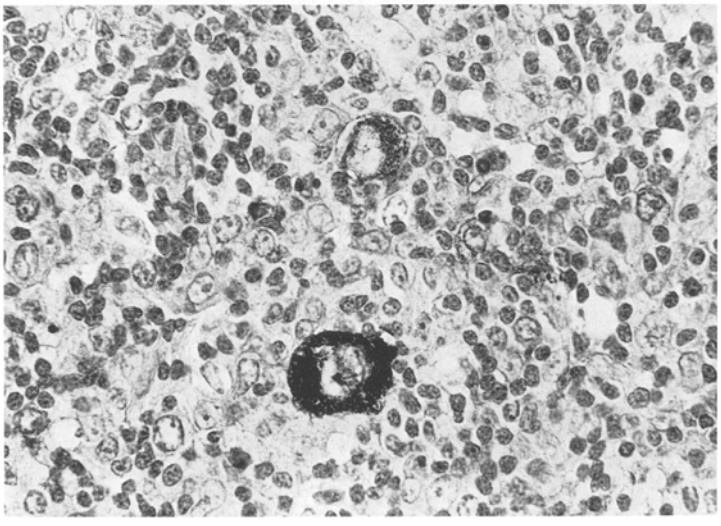

16

Table 6. Cytoplasmic immunoglobulin (CIg), J chain, and albumin staining patterns in lymph nodes of 15 patients

	Lymph node lesion			
	Reactive	Circumscribed proliferation areas	LP immunocytoma	Immunoblastic lymphoma[a]
CIg				
Polytypic	4	–	–	–
IgM/κ	–	1	4 (6)[b]	3 (5)[b]
−/κ	–	–	1	1
IgA/λ	–	–	1 (2)[b]	–
J chains[c]	2	–	2	1
Albumin	–	–	–	–

[a] Including cases of polymorphic immunocytoma with transformation into immunoblastic lymphoma

[b] A total of 20 lymph nodes were analyzed, because multiple biopsies were available from some patients. The number in parentheses is the number of nodes showing the respective pattern

[c] A total of 14 lymph nodes from 11 patients were stained for J chains

Biopsies from 14 patients showed germinal centers. In 6 of these cases, there was preponderance of cells with the same Ig pattern as in the proliferation areas. There were only a few reactive plasma cells.

Two salivary gland biopsies revealed the simultaneous occurrence of immunoblastic lymphoma with the same CIg pattern as in the confluent proliferation areas. In one of these cases, the number of Ig-positive cells in the immunoblastic lymphoma was smaller than that in the confluent proliferation areas.

Several additional salivary gland biopsies were obtained at different times from 2 patients. The CIg pattern of the immunoblasts and plasmacytoid cells remained the same.

In another patient, subsequent biopsies revealed transformation from circumscribed to confluent proliferation areas with a monotypic CIg pattern. The Ig pattern did not change.

All the "Sternberg-Reed cells" identified in 7 patients with proliferation areas with a monotypic PAP staining pattern showed a polytypic CIg pattern, which differed from that of the proliferation areas. In 3 cases, the "Sternberg-Reed cells" were positive for IgG and both κ and λ chains; in the other cases, only κ and λ chains were found. J chains or lysozyme were not demonstrable in these giant cells (Fig. 16).

Fig. 15. (a) Myoepithelial sialadenitis with confluent proliferation areas composed of lymphoplasmacytoid cells with a monotypic immunoglobulin pattern. Immunostaining for κ. ×556. **(b)** Same area as in **a** with a few reactive plasma cells. Immunostaining for λ. ×556

Fig. 16. Giant cell resembling Sternberg-Reed cell and containing IgG. The reaction for IgG is negative in the surrounding cells of the proliferation area (which showed a monotypic pattern of IgM/κ). Immunostaining for IgG. ×556

2. Lymph Nodes (Table 6)

A total of 20 lymph nodes from 15 patients were investigated. The immunohistologic findings were largely identical with those on the salivary gland biopsies.

Lymph nodes from four patients with reactive changes contained many plasma cells and a few immunoblasts with polytypic Ig patterns. The heavy chains were mostly of the IgG class. J chains were demonstrable in two cases.

One lymph node with circumscribed proliferation areas contained IgM/κ-positive immunoblasts and plasmacytoid cells, as found in the salivary gland of the same patient.

All other lymph nodes with immunocytoma or immunoblastic lymphoma showed a monotypic CIg pattern identical with that of the cells in the circumscribed or confluent proliferation areas in the salivary glands. Six cases were IgM/κ positive, 2 were $-/\kappa$ positive, and 1 was IgA/λ positive.

One immunoblastic lymphoma with plasmacytic differentiation in a patient with Sjögren's syndrome, but without histologically documented MESA, showed a monotypic pattern of IgM/κ.

Three of the 9 tumors stained for J chains showed a positive reaction.

Germinal center cells in the lymph nodes showed the same tendency to a monotypic CIg pattern as in the salivary glands.

3. Extrasalivary and Extranodal Findings

Only the malignant lymphoma (polymorphic immunocytoma with transformation into immunoblastic lymphoma) in the soft tissue of the lower leg of one patient was investigated. A few tumor cells contained IgM and κ chains.

III. Summary of Most Important Histologic and Immunohistologic Results (Table 7)

A comparsion of a few important morphologic and immunohistologic findings reveals the following noteworthy aspects:

(1) All three biopsies with MESA without proliferation areas showed a polytypic CIg pattern, did not contain epithelioid cells, intranuclear PAS-positive globules, or "Sternberg-Reed cells", and were not associated with an extrasalivary malignant lymphoma.

(2) Four of the 16 patients with MESA with circumscribed proliferation areas developed extrasalivary malignant lymphoma after an interval of 2–84 months. This was observed only in cases with a monotypic CIg pattern, and not in cases with a polytypic CIg pattern in the proliferation areas.

(3) All 26 cases of MESA with confluent proliferation areas showed monotypic CIg patterns. Extrasalivary malignant lymphoma was found at the same time in 8 patients in this group. Six patients developed extrasalivary malignant lymphoma after an interval of 10–66 months.

(4) Intranuclear PAS-positive globules were found in one case of MESA with circumscribed proliferation areas with a monotypic CIg pattern and in 17 cases of MESA with confluent proliferation areas. Epithelioid cells were seen in three cases of MESA with circumscribed proliferation areas and in 19 cases

Table 7. Important histologic and immunohistologic findings in myoepithelial sialadenitis (MESA) ($n=45$)

Type of MESA	n	Cytoplasmic immunoglobulin		Intra-nuclear PAS-positive globules	Epithelioid cells	"SR cells"[a]	Extrasalivary malignant lymphoma	
		Pattern	n				With MESA	Later
Without proliferation areas	3	Polytypic	3	0	0	0	0	0
		Monotypic	0	–	–	–	–	–
		Not studied	0	–	–	–	–	–
Circumscribed proliferation areas	16	Polytypic	4	0	0	2	0	0
		Monotypic	9	1	2	5	0	3
		Not studied	3	0	1	1	0	1
Confluent proliferation areas	26	Polytypic	0	–	–	–	–	–
		Monotypic	18	13	14	12	6	2
		Not studied	8	4	5	6	2	4

[a] "SR cells" = giant cells resembling Sternberg-Reed cells

with confluent proliferation areas. Like the PAS-positive globules, epithelioid cells did not occur in proliferation areas with a polytypic CIg pattern. "Sternberg-Reed cells" were found in 8 cases of MESA with circumscribed proliferation areas (2 of these cases showed a polytypic CIg pattern) and in 18 cases with confluent proliferation areas.

IV. Clinical Findings

The clinical findings will be related to the three types of MESA only when there are significant differences. The two patients with malignant lymphoma and only clinically demonstrated Sjögren's syndrome are included in the third group (MESA with confluent proliferation areas).

1. Age and Sex Distribution (Fig. 17)

MESA occurs most often in the 5th to 8th decades of life. The 3 patients with MESA without proliferation areas were 11, 14, and 70 years old. The median age of the patients with MESA with circumscribed proliferation areas was 61.5 years (range: 24–81), and the median age of the patients with MESA with confluent proliferation areas was 66 years (range: 43–80). There is a marked preponderance of females (male-to-female ratio 1:7).

2. Localization and Symptoms (Table 8)

Two of the patients with MESA without proliferation areas showed unilateral enlargement of the parotid gland, and the third patient showed bilateral involvement of the submandibular glands. One of these patients also had cervical lymphadenopathy.

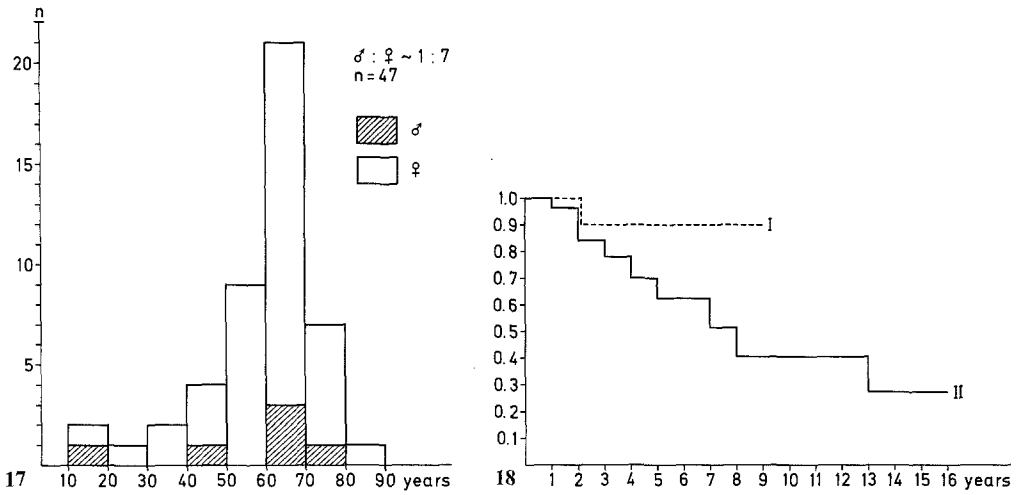

Fig. 17. Age and sex distribution of 47 patients with myoepithelial sialadenitis and/or Sjögren's syndrome

Fig. 18. Probability of survival of 42 patients with myoepithelial sialadenitis with circumscribed proliferation areas (I, $n=16$) or confluent proliferation areas (II, $n=26$)

Table 8. Localization of salivary gland enlargement and cervical lymphadenopathy ($n=47$)

Site of enlargement	Type of myoepithelial sialadenitis			Total
	Without proliferation areas	Circumscribed proliferation areas	Confluent proliferation areas[a]	
Parotid gland				
unilateral	2	5	8	15
bilateral	0	7	8	15
Submandibular gland				
unilateral	0	2	5	7
bilateral	1	1	2	4
Both parotid and submandibular glands				
unilateral	0	0	2	2
bilateral	0	1	3	4
Cervical lymph nodes	1	6	13	20

[a] The two patients with only clinical evidence of Sjögren's syndrome are included in this group

Unilateral involvement of the parotid gland was seen in 5 patients with MESA with circumscribed proliferation areas, and bilateral involvement in 7 patients. Two patients in this group showed unilateral involvement of the submandibular gland and one showed bilateral involvement. Bilateral enlargement of both salivary glands was noted in one case. Six patients had cervical lymphadenopathy. One patient also showed enlargement of a lacrimal gland.

The group of patients with MESA with confluent proliferation areas also showed a predominance of parotid involvement, with 8 cases of unilateral enlargement and 8 cases of bilateral

Table 9. Sjögren's syndrome and other types of autoimmune disease associated with myoepithelial sialadenitis ($n=47$)

	Type of myoepithelial sialadenitis			Total
	Without proliferation areas	Circumscribed proliferation areas	Confluent proliferation areas[a]	
Sjögren's syndrome	0	3	4	7
Sjögren's syndrome plus other autoimmune disease				
Rheumatoid arthritis	0	1	1	2
Necrotizing vasculitis[b]	0	0	1	1
Autoimmune disease without Sjögren's syndrome				
Rheumatoid arthritis	0	1	0	1
Lupus erythematosus	0	1	1	2
"Collagen disease"	0	0	1	1
Necrotizing vasculitis[b]	0	1	1	2

[a] The two patients with only clinical evidence of Sjögren's syndrome are included in this group
[b] It has not been proven that this is an autoimmune disease

enlargement. Unilateral involvement of the submandibular gland was seen in 5 patients, and bilateral involvement in 2 patients. Two patients showed unilateral enlargement of both salivary glands, and 3 patients showed bilateral enlargement. Cervical lymphadenopathy was seen in 13 patients, and enlargement of lacrimal glands was noted in 2 patients.

The salivary gland enlargement was characterized by slow growth and was free of pain. The patient's general condition was affected only when MESA was associated with an autoimmune disease (Table 9). Eight of the patients with MESA with confluent proliferation areas had had a "salivary gland tumor" for 2 to 20 years, which enlarged rapidly before the biopsy included in the present study.

3. Sjögren's Syndrome and Autoimmune Diseases (Table 9)

The patients with MESA without proliferation areas did not show any evidence of Sjögren's syndrome with or without associated autoimmune diseases.

Four of the patients with MESA with circumscribed proliferation areas had had typical Sjögren's syndrome for 2 to 20 years before biopsy. In one of these cases, Sjögren's syndrome was combined with rheumatoid arthritis. Another patient presented with lupus erythematosus, one with rheumatoid arthritis, and one with necrotizing vasculitis.

Six of the patients with MESA with confluent proliferation areas had shown symptoms of Sjögren's syndrome for 1.5 to 12 years before biopsy. These were associated with rheumatoid arthritis in one patient and with necrotizing vasculitis (with cryoglobulinemia) in another patient. Three patients in this group did not exhibit signs of Sjögren's syndrome, but did have an autoimmune disease: necrotizing vasculitis with cryoglobulinemia, collagen disease with recurrent pleurisy and myositis, or lupus erythematosus.

4. Laboratory Findings

With the exception of reactive inflammatory changes in the blood picture, there were no pathologic laboratory findings in the patients with MESA without proliferation areas.

Pathologic laboratory findings were noted especially in the 7 patients with Sjögren's syndrome or another autoimmune disease in the group with MESA with circumscribed proliferation areas. The erythrocyte sedimentation rate (ESR) was elevated in all 5 patients for whom data were available (with increased γ-globulin levels in 3 patients). Antibody tests (RF, CRP, Waaler-Rose) were positive in 4 patients. Immunoelectrophoresis was performed in 5 cases; 2 showed a polyclonal increase in IgG and one showed IgG+IgM. The IgG values were normal in 2 patients. Leukopenia was found in 3 of 6 patients and anemia in 4 of 6. In the other 9 patients without Sjögren's syndrome or autoimmune disease, there were only slight deviations from normal values.

Antibody tests were positive in all 6 patients with Sjögren's syndrome or autoimmune disease in the group with MESA with confluent proliferation areas. Thirteen of 14 patients showed elevated γ-globulin values. Immunoelectrophoresis was performed in 11 cases and revealed a polyclonal increase in IgA+IgG in one, IgA+IgM in one, IgM+IgG in one, IgA+IgM+IgG in two, and IgM in six patients. A monoclonal increase in IgM was demonstrated in one patient with confluent proliferation areas with a monotypic CIg pattern (IgM/κ). Ten of 17 patients showed elevated α_2-globulin values. The ESR was markedly elevated (>100 mm/h) in 13 patients (9 with and 4 without autoimmune disease). A slightly or moderately elevated ESR was noted in 11 patients. Slight anemia was seen in 19 of 23 patients, leukopenia in 11 of 21 patients, and lymphopenia in 6 of 14 patients.

5. Course and Prognosis (Fig. 18)

a) MESA without Proliferation Areas. At the time of the present study, the three patients in this group are still alive without treatment and without recurrence 1 to 12 months after biopsy.

b) MESA with Circumscribed Proliferation Areas. Four of the patients in this group developed extrasalivary malignant lymphoma 6 months to 9 years after enlargement of the salivary gland was noted. In one of these patients, the malignant lymphoma was associated with a drop in the γ-globulin level and led to death after 22 months.

The other 12 patients are alive 6 months to 9 years (median: 2.5 years) after enlargement of the salivary gland. Four patients were not treated after biopsy. One of these patients showed enlargement of a different salivary gland after 16 months. The other 3 are free of recurrence after 2 to 9 months. Two of the patients with autoimmune disease were treated with cortisone, which led to marked regression of the salivary gland enlargement. Three patients received radiotherapy after biopsy. One of these patients developed malignant lymphoma after 8 years, and another showed bilateral recurrence several times within 2.5 years after biopsy.

The probability of surviving 5 years was 0.9 for this group.

c) MESA with Confluent Proliferation Areas. Extrasalivary malignant lymphoma appeared in 14 patients. The interval between first appearance of salivary gland enlargement and diagnosis of malignant lymphoma was 2 months to 5 years, with the exception of 2 patients with Sjögren's syndrome, who developed malignant lymphoma after 12 years. In 6 patients, generalization of the lymphoma was associated with a drop in the serum γ-globulin values. Death occurred in 15 of the 26 cases in which clinical information was available. Complications caused by malignant lymphoma were the cause of death in 11 cases. These 11 patients had received the following treatment: radiotherapy in 5 cases, radiotherapy and chemotherapy in 2 cases, chemotherapy in 1 case, and no treatment in 3 cases. Of the living patients, 3 with unilateral salivary gland enlargement received surgical treatment and 1 patient with bilateral involvement was given cytostatic drugs and cortisone; these 4 patients are free of recurrence at the time of this report. Three other patients with generalized malignant lymphoma responded to chemotherapy.

The probability of surviving 5 years was 0.62, and of surviving 10 years, 0.41.

Discussion

I. Myoepithelial Sialadenitis

As confirmed by the present study, MESA occurs especially in the parotid gland of female patients (Godwin 1952; Bernier and Bhaskar 1958; Cruickshank 1965;

Leban and Stratigos 1974; Kelly et al. 1975) and may be associated clinically with Sjögren's syndrome (Sjögren 1933, 1948).

The myoepithelial complexes are considered to be pathognomonic (Seifert 1971a and b). For a long time, they were thought to be a histologic criterion of benignity (Godwin 1952; Batsakis et al. 1970). Recently, MESA has been called immunosialadenitis (Donath and Seifert 1972; Seifert and Donath 1976a and b) because it can be induced immunologically in animals (Haferkamp 1962; Sela et al. 1972), anti-salivary duct antibodies can often be demonstrated in patients with Sjögren's syndrome (Feltkamp and van Rossum 1968; Anderson et al. 1973; Cummings and Tarpley 1978; Zittoun et al. 1978b), and the lesion responds to immunosuppressive drugs (Pirsig and Donath 1972). The finding of an increased Ig content (Talal et al. 1970; Cummings et al. 1971; Anderson et al. 1972) and the demonstration of synthesis of rheumatoid factor (Anderson et al. 1971) by the infiltrating cells in lip biopsies from patients with Sjögren's syndrome also indicate that MESA is an immunologic process. Morphologic changes similar to those seen in lip biopsies from Sjögren patients (Greenspan et al. 1974; Tarpley et al. 1974) have been demonstrated in the salivary glands of NZB mice that spontaneously developed an autoimmune disease comparable to Sjögren's syndrome (Kessler 1968; Talal 1974; Carlsöö and Östberg 1978). Such changes have also been observed in salivary glands of mice with chronic graft-versus-host reactions (Gleichmann and Gleichmann 1980) and in human patients with chronic graft-versus-host reactions (Shulman et al. 1980). Myoepithelial proliferation has not been seen in the salivary ducts in graft-versus-host reactions, however. In animals, the experimental inducibility of the lesion is T cell dependent, and the type of infiltration is said to be consistent with a cell-mediated immunologic process (White 1973 and 1976).

In human immunosialadenitis, the relation between T and B cells within the lesion is particularly interesting. In lip and sublingual biopsies from patients with Sjögren's syndrome, T cells have been found in periductal and perivascular areas in addition to the predominant infiltrates of B cells (Chused et al. 1974; Talal et al. 1974; Koriyama and Arimori 1978). For this reason, and because of the shape of the nuclei of the lymphocytes, we presume that the CIg-negative lymphocytes found by one of us (K.L.) and other investigators (Donath and Seifert 1972; Kahn 1979; Lennert et al. 1979) around and within myoepithelial complexes are T cells. Sela et al. (1972) thought that the lymphocytes in contact with degenerating epithelial cells in experimental allergic sialadenitis in rats might be killer T cells.

II. Immunosialadenitis and Lymphoproliferation

1. Manifest Malignant Lymphoma

In the past 15 years, mostly extrasalivary malignant lymphomas were described in patients with Sjögren's syndrome (Talal and Bunim 1964; Talal et al. 1967; Pinkus and Dekker 1970; Anderson and Talal 1971; Bolognini and Riva 1975; Diebold et al. 1978). Recently, however, there has been an increasing number

of reports on intrasalivary lymphomas in immunosialadenitis with or without Sjögren's syndrome (Azzopardi and Evans 1971; Batsakis et al. 1975; Heckmayr et al. 1976; Hyman and Wolff 1976; Colby and Dorfman 1979). One of the reasons for this is probably that MESA was considered to be a benign lesion by definition, but caused histopathologists serious problems with the distiction between it and malignant lymphoma in differential diagnoses (Kelly et al. 1975; Colby and Dorfman 1979; Seifert 1980).

In the present study, we found proliferation areas in most cases. Such foci of immature cells have been described in the literature only occasionally (Azzopardi and Evans 1971). The similarity in cytologic composition and CIg pattern between large confluent proliferation areas and the extrasalivary malignant lymphomas in the same patients indicates that MESA with confluent proliferation areas represents a manifest malignant lymphoma. One patient showed immunoblastic lymphoma that developed in tissue involved by MESA with confluent proliferation areas and was confined to the salivary gland. Thus, these proliferation areas can be regarded as malignant lymphoma, even without involvement of lymph nodes.

If the confluent proliferation areas with a monotypic CIg pattern are considered to be manifest malignant lymphomas of the salivary gland and are grouped with the nodal lymphomas in immunosialadenitis and/or Sjögren's syndrome, then our series shows the following frequency distribution of malignant lymphoma (Table 10). All the lymphomas were LP immunocytoma or B-immunoblastic lymphoma, including cases in which transformation of LP immunocytoma into immunoblastic lymphoma could be observed. There were no cases of germinal center cell lymphoma or Hodgkin's disease. Thus, all the tumors were B-cell lymphomas, specificially lymphomas of the plasma cell series that are fundamentally capable of producing and secreting Ig (Lukes and Collins 1974; Lennert et al. 1975; Lennert 1978; Zulman et al. 1978). This is supported by the finding of J chains in 5 of 12 cases; J chains are specific, although not constant, markers of Ig-producing cells (Isaacson 1979; Stein et al. 1980).

Besides definite cases of malignant lymphoma, the literature also contains reports of angioimmunoblastic lymphadenopathy (Bisson et al. 1978a; Le Charpentier et al. 1978; Zittoun et al. 1978a; Aizawa et al. 1979; Pierce et al. 1979) and so-called pseudolymphoma (Deutsch 1967; Talal et al. 1967; Zittoun et al. 1974; Bisson et al. 1978b; Diebold et al. 1978; Kennealey et al. 1978) in patients with Sjögren's syndrome. The pseudolymphomas are frequently localized in the lung (Bunim 1964; Cummings et al. 1971; Scully et al. 1975; Strimlan et al. 1976) as well as in lymph nodes. Lymphomatoid granulomatosis (Weisbrot 1976) and "lymphoplasmacytic infiltrates" (Bonner et al. 1973) have also been found in the lungs of Sjögren patients. The term "pseudolymphoma" was introduced to describe a lesion that lies between hyperplasia and neoplasia and whose benign or malignant nature cannot be determined reliably by the evaluating pathologist (Talal et al. 1967; Anderson and Talal 1971). According to the various published descriptions, the so-called pseudolymphomas include lymphoplasmacytic infiltrates containing "reticulum cells", giant cells resembling Sternberg-Reed cells, and cells with intranuclear PAS-positive globules. The lymph node architecture is said to be preserved. Progression to a malignant process, specifically macroglobulinemia of Waldenström, has been described (Anderson and Talal 1971; Deegan 1977; Diebold et al. 1978). In our opinion, a majority of these "pseudolymphomas" were actually LP immunocytomas of the Kiel classification (Lennert et al. 1975; Lennert 1978), whose cells synthesize Ig, but do not secrete recognizable amounts of Ig into the blood. Such tumors are often not recognized until they induce the clinical

Table 10. Malignant lymphomas diagnosed on salivary gland biopsies with and without myoepithelial sialadenitis (MESA)

Type of lymphoma	With MESA ($n=26+4^b+2^c$)	Without MESA[a] ($n=25$)
Derived from plasma cell series		
LP immunocytoma		
lymphoplasmacytic subtype	4	0
lymphoplasmacytoid subtype	12	0
polymorphic subtype	7 ($+1^b+1^c$)	2
Immunoblastic lymphoma (including polymorphic immunocytoma with transformation into immunoblastic lymphoma)	3($+2^b+1^c$)	2
Low-grade malignant non-Hodgkin's lymphoma[d]	(1^b)	
Derived from germinal center cells		
Centroblastic-centrocytic lymphoma	0	15
Centroblastic lymphoma	0	2
Hodgkin's disease	0	4

[a] Data from Schmid et al. (1982)
[b] Only extrasalivary malignant lymphoma diagnosed in patient with MESA with circumscribed proliferation areas
[c] Only extrasalivary malignant lymphoma diagnosed in patient with clinical evidence of Sjögren's syndrome
[d] Infiltration of bone marrow by lymphoma that could not be classified further

syndrome (Waldenström's disease). A study by Diebold et al. (1978) provided the first indicative results concerning the development of Waldenström's disease out of pseudolymphomatous proliferation. In an immunofluorescent investigation of nodal pseudolymphomas, Diebold et al. (1978) found foci of cells with a monotypic pattern of IgM; these foci were found to be indications of development of Waldenström's disease. The findings of Diebold et al. (1978) thus correspond to the results of our study.

2. Premalignant and Early Stages of Malignant Lymphoma

In contrast to the group of cases of MESA with confluent proliferation areas ("manifest malignant lymphoma"), the group with small circumscribed proliferation areas fulfilled only the cytologic and sometimes the immunohistologic criteria for a presumptive malignant lymphoma. Histologically, however, these areas did not give the appearance of a tumor. Nevertheless, extrasalivary malignant lymphoma developed only in patients with MESA with a monotypic CIg pattern, as in the group with confluent proliferation areas. The tumors were also LP immunocytomas. They did not develop at the same time as the salivary gland lesions, but rather after a latency period. There was no evidence of malignant lymphoma in the three patients with circumscribed proliferation areas with polytypic CIg patterns during the course of our study. Malignant lymphoma also did not develop in the three patients with MESA without proliferation areas.

Based on the principle that malignant lymphomas of B-cell type show a monotypic CIg pattern in contrast to the polytypic pattern of reactive lesions (Levy et al. 1977; Seligmann and Clauvel 1977), we must distinguish MESA with circumscribed proliferation areas with a monotypic CIg pattern from that with a polytypic CIg pattern. We propose the term "early lymphoma"(or "early immunocytoma") for the group of cases of MESA with circumscribed proliferation areas with a monotypic CIg pattern, because such cases may show development of a manifest malignant lymphoma with an identical CIg pattern after a latency period. An early lymphoma may, but does not have to, lead to a manifest malignant lymphoma. It is similar in behavior to carcinoma in situ. Such early stages of malignant lymphoma can exist for years without transforming into manifest lymphoma. The results of our study do not show whether such changes can regress. An interesting finding was the quantitative predominance of immunoblasts with a monotypic CIg pattern in the early lymphomas (Table 5), which was not seen in the fully developed LP immunocytomas.

Cases with small proliferation areas with polytypic CIg patterns must be clearly distinguished from the cases of early lymphoma. It might be possible for cases with polytypic CIg patterns to show transformation into malignant lymphoma. We did not observe such a transformation in any of our cases. Thus, one could interpret such cases at most as "prelymphoma".

3. Diagnostic Problems

The conclusions drawn above have the following consequences in histologic diagnoses (Table 7). In our opinion, the confluent proliferation areas composed of immunoblasts and lymphoplasmacytoid cells in MESA are signs of manifest malignant lymphoma. In cases with circumscribed proliferation areas, an immunohistologic analysis has to be performed in order to determine whether there is a possibility of later development of lymphoma (indicated by a monotypic CIg pattern).

A few other histologic and immunohistologic criteria are useful in addition to these main criteria. Epithelioid cells were seen in many cases, especially near proliferation areas with a monotypic CIg pattern. Giant cells resembling Sternberg-Reed cells were also found in many cases, but they were not confined to proliferation areas with a monotypic CIg pattern. The CIg pattern of the giant cells (frequently IgG/$\kappa+\lambda$; J-chain negative) differed from that of the rest of the tumor and resembled the pattern of Sternberg-Reed cells in Hodgkin's disease (Isaacson 1979; Isaacson and Wright 1979; Poppema 1980). The combination of epithelioid-cell foci and giant cells has been mentioned in the literature (Azzopardi and Evans 1971; Zittoun et al. 1974; Diebold et al. 1978; Zulman et al. 1978). In a differential diagnosis, this combination indicates the possibility of epithelioid cellular lymphogranulomatosis ("Lennert's lymphoma"; Sebahoun et al. 1977; Noel et al. 1980). A monotypic CIg pattern in the lymphoplasmacytoid tumor cells, however, shows that the tumor is LP immunocytoma.

Another helpful histologic criterion is the presence of intranuclear PAS-positive globules, which were found chiefly in manifest malignant lymphomas and never in MESA without proliferation areas or MESA with proliferation areas with polytypic CIg patterns.

Germinal centers, which used to be considered to be pathognomonic of reactive changes, were found in all the lesions examined in this study. The germinal center cells frequently showed a tendency to produce the same type of CIg (monotypic) as synthesized by the cells in the proliferation areas. This indicates that there is a connection between germinal centers and the development of LP immunocytoma (Table 3).

Another indirect indication of malignant lymphoma is a reduction in the number of reactive plasma cells containing IgG. Cases with proliferation areas with a monotypic CIg pattern showed a much smaller number of reactive plasma cells than did cases of immunosialadenitis without complications. This finding agrees with the results published by Gumberz and Seifert (1980).

4. Clinicopathologic Correlation

Our study confirmed the inconstant association of MESA with Sjögren's syndrome or another type of autoimmune disease (Pinkus and Dekker 1970; Kelly et al. 1975). It is notable that the 3 patients with MESA without proliferation areas in our series did not have autoimmune disease, whereas the other two groups of MESA patients showed approximately equal frequencies of autoimmune disease.

A clinical comparison of patients with MESA with circumscribed proliferation areas and those with manifest malignant lymphoma associated with MESA is particularly interesting. The median age of the patients with intrasalivary malignant lymphoma was 5.5 years higher than that of the patients with MESA with circumscribed proliferation areas. A similar situation was described by Cryer and Kissane (1974). This might be an indication of the interval between early lymphoma and manifest malignant lymphoma. The latency period from the beginning of salivary gland enlargement to the development of malignant lymphoma in our patients varied from 1.5 to 12 years. This agrees with data in the literature, according to which the interval varies from 0.5 to 29 years (Pinkus and Dekker 1970; Anderson and Talal 1971; Haritopoulos et al. 1975; Hyman and Wolff 1976; Vasil'ev et al. 1978; Banks et al. 1979).

A notable laboratory finding was a decrease in the serum γ-globulin levels in seven patients who showed generalization of malignant lymphoma. In the literature, this phenomenon is said to be a clinical sign of development of malignant lymphoma (Talal and Bunim 1964; Anderson and Talal 1971; Heckmayr et al. 1976).

The actuarial survival curve (Fig. 18) demonstrates that there is a clear difference in prognosis between MESA with circumscribed proliferation areas and malignant lymphoma in MESA. Conclusions about the effectiveness of the various therapeutic measures cannot be drawn from the present study, because the available data were not uniform in this respect.

5. Histogenesis and Pathogenesis

A comparison of the malignant non-Hodgkin's lymphomas in the salivary glands of patients with MESA with those in patients without MESA (Table 10) reveals marked differences in the frequency of the various entities. A separate study of 25 patients without MESA (Schmid et al. 1982) showed a distribution somewhat similar to that of primary nodal lymphoma (15 cases of centroblastic-centrocytic lymphoma, 2 cases of polymorphic immunocytoma, 2 cases of centroblastic lymphoma, 2 cases of immunoblastic lymphoma, and 4 cases of Hodgkin's disease). In contrast, the patients with malignant lymphoma associated with MESA showed a completely different picture. All the tumors examined in the present study were derived from the plasma-cell series. In our opinion, this finding is a strong indication of a difference in histogenesis between the two groups of lymphoma patients. Moreover, the primary "salivary gland lymphomas" that were not associated with immunosialadenitis originated in lymph nodes in the salivary gland region, at least in most cases, whereas the malignant lymphomas in MESA apparently originated in the salivary glands themselves as a consequence of an immunologic process. The homogeneity of the histologic and immunohistologic findings in the lymphoma patients with MESA is a strong indication of a uniform pathogenesis.

Morphologic and immunologic changes similar to those seen in the present study have been found in NZB mice with a spontaneous autoimmune disease comparable to Sjögren's syndrome (Talal 1974; Taylor 1976) and in mice with experimentally induced, chronic graft-versus-host reactions (Armstrong et al. 1970; Grundmann and Hobik 1973; Gleichmann et al. 1978; Gleichmann and Gleichmann 1980). The mice showed first reactive and premalignant stages and then development of so-called reticulum cell sarcoma, in which the tumor cells contained CIg and often had plasmacytoid characteristics. According to the Kiel classification, these tumors were actually LP immunocytomas that transformed into immunoblastic lymphomas of B type (Lennert et al. 1979).

In the view of some investigators (Anderson and Talal 1971; Deegan 1977; Lennert et al. 1979), the lymphoproliferative process in autoimmune disorders is based on a disturbance in the T cell-dependent immune balance. The excessive B-cell proliferation in such cases is attributed to a disturbed balance between helper and suppressor T-cell functions (Talal 1978). The reduced hypersensitivity reaction to a contact allergen (2,4-dinitrochlorobenzene) in patients with Sjögren's syndrome is a sign of a disturbance in T-cell function (Leventhal et al. 1967; Whaley and Buchanan 1971). The T-cell reaction depends on a change within the genetically determined major histocompatibility complex. This is supported by the frequent presence of HLA-B8 antigen and two other factors similar to murine Ia antigens in patients with Sjögren's syndrome (Fye et al. 1976; Moutsopoulos et al. 1978; Talal 1978). Thus, genetically and immunologically defined factors are involved in the development of autoimmune diseases (Talal 1978). In Sjögren's syndrome, we do not yet know the prime agent responsible for the change in the major histocompatibility complex and thus for starting the T-cell reaction. The possibility of a virus-induced process has

been discussed, especially because electron microscopy revealed virus-like structures in the salivary gland, pulmonary, and renal lesions of patients with Sjögren's syndrome (Shearn et al. 1970; Albegger and Auböck 1972; Medical Staff Conference 1975; Sutinen et al. 1977).

According to Klein (1980), initiation of a tumor is based on a change in the genetic substance. Progression of the tumor, however, depends on genetic and epigenetic, or regulatory, changes. According to this concept, the initial process leads to the development of preneoplastic cells that are capable of dividing. These cells can remain in a certain stage of differentiation for a long time, but can transform later into a certain type of tumor cell. The immunoblasts with polytypic CIg patterns found in the small proliferation areas of immunosialadenitis might represent such preneoplastic cells, which turn into monotypic malignant lymphoma cells under the inflence of an epigenetic change (a disturbance of suppressor T-cell function?).

Acknowledgments. We are indebted to Prof. Dr. H. Stein (Kiel) for help with the PAP method and his evaluation of the immunostaining results in a few representative cases. We also thank Martha Soehring for preparation of the manuscript.

References

Aizawa Y, Zawadzki ZA, Micolonghi TS, McDowell JW, Neiman RS (1979) Vasculitis and Sjögren's syndrome with IgA–IgG cryoglobulinemia terminating in immunoblastic sarcoma. Am J Med 67:160–166

Albegger KW, Auböck L (1972) Elektronenmikroskopischer Nachweis "virusähnlicher Einschlußkörper" bei myoepithelialer Sialadenitis im Rahmen des „Sjögren"-Syndroms. Arch Klin Exp Ohr Nasen Kehlkopfheilkunde 203:153–165

Anderson LG, Talal N (1971) The spectrum of benign to malignant lymphoproliferation in Sjögren's syndrome. Clin Exp Immunol 9:199–221

Anderson LG, Cummings NA, Asofsky R, Hylton MB, Talal N (1971) Local rheumatoid factor (RF) synthesis by salivary gland tissue from patients with Sjögren's syndrome (SS). Arthritis Rheum 14:368

Anderson LG, Cummings NA, Asofsky R, Hylton MB, Tarpley TM, Tomasi TB, Wolf RO, Schall G, Talal N (1972) Salivary gland immunoglobulin and rheumatoid factor synthesis in Sjögren's syndrome. Am J Med 53:456–463

Anderson LG, Tarpley TM, Talal N, Cummings NA, Wolf RO, Schall GL (1973) Cellular-versus-humoral autoimmune responses to salivary gland in Sjögren's syndrome. Clin Exp Immunol 13:335–342

Armstrong MYK, Gleichmann E, Gleichmann H, Beldotti L, Andre-Schwartz J, Schwartz RS (1970) Chronic allogeneic disease. II. Development of lymphomas. J Exp Med 132:417–439

Azzopardi JA, Evans DJ (1971) Malignant lymphoma of parotid associated with Mikulicz disease (benign lymphoepithelial lesion). J Clin Pathol 24:744–752

Banks PM, Witrak GA, Conn DL (1979) Lymphoid neoplasia following connective tissue disease. Mayo Clin Proc 54:104–108

Batsakis JG, Weaver DK, McBurney T (1970) Controversial lymphoreticular lesions of the head and neck: Mikulicz's disease and syndrome, Sjögren's syndrome, benign lymphoepithelial lesion of salivary glands, and "malignant granuloma". Univ Mich Med Cfr J 36:8–13

Batsakis JG, Bernacki EG, Rice DH, Stebler ME (1975) Malignancy and the benign lymphoepithelial lesion. Laryngoscope 85:389–399

Bernier IL, Bhaskar SN (1958) Lymphoepithelial lesions of salivary glands: Histogenesis and classification based on 186 cases. Cancer 11:1156–1179

Bisson M, Massias P, Segond P, Jacquot JM, Brunand MD (1978a) Association of angioimmunoblastic lymphadenopathy and Gougerot-Sjögren syndrome (letter). Nouv Presse Med 7:2393
Bisson M, Massias P, Segond P, Jacquot M, Brunand MD (1978b) Gougerot-Sjögren's syndrome and pseudolymphoma. Rev Rhum Mal Osteoartic 45:357–360
Bolognini G, Riva G (1975) Lymphoproliferative Erkrankungen und Paraproteinämien beim Sjögren-Syndrom. Schweiz Med Wochenschr 105:1493–1505
Bonner H, Ennis RS, Geelhoed GW, Tarpley TM (1973) Lymphoid infiltration and amyloidosis of lung in Sjögren's syndrome. Arch Pathol 95:42–44
Bunim JJ (1964) Clinical, pathologic and serologic studies in Sjögren's syndrome. Ann Intern Med 61:509–530
Carlsöö B, Östberg Y (1978) Ultrastructural observations on the parotitis autoimmunica in the NZB/NZW hybrid mice. Acta Otolaryngol (Stockh) 85:298–306
Chused TM, Hardin JA, Frank MM, Green I (1974) Identification of cells infiltrating the minor salivary glands in patients with Sjögren's syndrome. J Immunol 112:641–648
Colby TV, Dorfman RF (1979) Malignant lymphomas involving the salivary glands. Pathol Annu 14:307–324
Cruickshank AH (1965) Benign lymphoepithelial salivary lesion to be distinguished from adenolymphoma. J Clin Pathol 18:391–400
Cryer PhE, Kissane J (1974) Sjögren's syndrome with lymphadenopathy. Am J Med 57:801–808
Cummings NA, Tarpley TM (1978) Detection of antisalivary duct antibody from Sjögren's syndrome by an autoradiographic method. J Immunol Methods 23:161–168
Cummings NA, Schall GL, Asofsky R, Anderson LG, Talal N (1971) Sjögren's syndrome: Newer aspects of research, diagnosis and therapy. Ann Intern Med 75:937–950
Deegan MI (1977) Immunologic diseases of the salivary glands. Otolaryngol Clin North Am 10:351–361
Deutsch HJ (1967) Sjögren's syndrome and pseudolymphoma. Ann Otol Rhinol Laryngol 76:1075–1084
Diebold J, Zittoun R, Tulliez M, Reynes M, Tricot G, Bernadou A, Audouin J (1978) Pseudolymphoma and lymphoproliferative syndromes in Gougerot-Sjögren syndrome. Sem Hop Paris 54:1033–1040
Donath K, Seifert G (1972) Ultrastruktur und Pathogenese der myoepithelialen Sialadenitis. Virchows Arch (Pathol Anat) 356:315–329
Feltkamp TEW, van Rossum AL (1968) Antibodies to salivary duct cells and other autoantibodies in patients with Sjögren's syndrome and other idiopathic autoimmune diseases. Clin Exp Immunol 3:1–16
Fye KH, Terasaki PI, Moutsopoulos H, Daniels TE, Michalski JP, Talal N (1976) Association of Sjögren's syndrome with HLA-B8. Arthritis Rheum 19:883–886
Gleichmann E, Gleichmann H (1980) Spectrum of diseases caused by alloreactive T cells, mode of sensitization to the drug diphenylhydantoin, and possible role of SLE-typed self-antigens in B-cell triggering. In: Krakauer RS, Cathcart MK, (eds) Immunoregulation and autoimmunity, Elsevier North Holland, Amsterdam, pp 73–83
Gleichmann E, Melief CIM, Gleichmann H (1978) Lymphomagenesis and autoimmunization caused by reactions of T-lymphocytes to incompatible structures of the major histocompatibility complex: A concept of pathogenesis. Cancer Res 64:292–315
Godwin T (1952) Benign lymphoepithelial lesion of the parotid gland. Cancer 5:1089–1103
Graham RC Jr, Karnovsky MJ (1966) The early stages of absorption of injected horseradish peroxidase in the proximal tubules of mouse kidney: ultrastructural cytochemistry by a new technique. J Histochem Cytochem 14:291–302
Green JA, Dawson AA, Walker W (1978) Systemic lupus erythematosus and lymphoma. Lancet II: 753–756
Greenspan IS, Daniels TE, Talal N, Sylvester RA (1974) The histopathology of Sjögren's syndrome in labial salivary gland biopsies. Oral Pathol 37:217–229
Grundmann E, Hobik HP (1973) Lymphoreticuläre Sarkome bei immunologisch geschädigten Mäusen. Z Krebsforsch 79:298–303
Gumberz C, Seifert G (1980) Immunoglobulin-containing plasma cells in chronic parotitis and malignant lymphomas of the parotid gland. Virchows Arch (Pathol Anat) 389:79–92
Haferkamp O (1962) Ein tierexperimenteller Beitrag zur Immunpathologie der Speicheldrüsen. Virchows Arch (Pathol Anat) 335:298–322

Hamperl H (1970) The myothelia (myoepithelial cells). Normal state; regressive changes; hyperplasia; tumors. Curr Top Pathol 53:161–220

Hartiopoulos NC, Delikaris PG, Karamanakos PP (1975) Reticulum cell sarcoma in the course of Sjögren's syndrome. Int Surg (Chicago) 60:423–424

Heckmayr M, Seifert G, Donath K (1976) Malignant lymphomas and immunosialadenitis. Laryngol Rhinol Otol (Stuttg) 55:593–607

Hyman GA, Wolff M (1976) Malignant lymphomas of the salivary glands. Review of the literature and report of 33 new cases, including four cases associated with the lymphoepithelial lesion. Am J Clin Pathol 65:421–438

Isaacson P (1979) Immunochemical demonstration of J chain; a marker of B cell malignancy. J Clin Pathol 32:802–807

Isaacson P, Wright DH (1979) Anomalous staining patterns in immunohistologic studies of malignant lymphoma. J Histochem Cytochem 27:1197–1199

Kahn LB (1979) Benign lymphoepithelial lesion (Mikulicz's disease) of the salivary gland: an ultrastructural study. Hum Pathol 10:99–104

Kassan SS, Thomas TL, Moutsopoulos HM, Hoover R, Kimberly RP, Budman DR, Costa J, Decker IG, Chused TM (1978) Increased risk of lymphoma in Sicca syndrome. Ann Intern Med 89:888–892

Kelly DR, Spiegel JC, Maves M (1975) Benign lymphoepithelial lesions of the salivary glands. Arch Otolaryngol 101:71–75

Kennealey GI, Kaetz HW, Smith GJW (1978) Sjögren's syndrome with pseudolymphoma 13 years after Hodgkin's disease. Arch Intern Med 138:635–636

Kessler HS (1968) A laboratory model for Sjögren's syndrome. Am J Pathol 52:671–685

Klein G (1980) Immune and non-immune control of neoplastic development: contrasting effects of host and tumor evolution. Cancer 45:2486–2499

Koriyama K, Arimori S (1978) The distribution of lymphocyte subpopulations in immune tissue. Part II. Studies on detection of lymphocyte subpopulations infiltrating in the target organs of various autoimmune disorders. Nippon Ketsueki Gakkai Zasshi 41:72–80

Lapes M, Antoniades K, Gartner W Jr, Vivacqua R (1976) Conversion of a benign lymphoepithelial salivary gland lesion to lymphocytic lymphoma during Dilantin therapy: correlation with Dilantin-induced lymphocyte transformation in vitro. Cancer 38:1318–1322

Leban SG, Stratigos GT (1974) Benign lymphoepithelial sialadenopathies. The Mikulicz/Sjögren controversy. Oral Surg 38:735–748

Le Charpentier Y, Faucher JN, Ghozlan R, Delbarre F, Louvel A, Lemaigre G, Vacher-Lavenu MC, Amor B, Abelanet R (1978) Angioimmunoblastic lymphadenopathy (AIL) rich in epithelioid cells presenting Gougerot-Sjögren-syndrome. Ann Anat Pathol (Paris) 23:201–216

Lennert K, in collaboration with Mohri N, Stein H, Kaiserling E, Müller-Hermelink HK (1978) Malignant Lymphomas Other than Hodgkin's Disease. Springer, Berlin Heidelberg New York (Handbuch der speziellen pathologischen Anatomie und Histologie, Bd 1, Teil 3B)

Lennert K, Knecht H, Burkert M (1979) Vorstadien maligner Lymphome. Verh Dtsch Ges Pathol 63:170–196

Lennert K, Stein H, Kaiserling E (1975) Cytological and functional criteria for the classification of malignant lymphomata. Br J Cancer 31, Suppl II: 29–43

Leventhal BG, Waldorf DS, Talal N (1967) Impaired lymphocyte transformation and delayed hypersensitivity in Sjögren's syndrome. J Clin Invest 46:1338–1345

Levy R, Warnke R, Dorfman RF, Haimovich J (1977) The monoclonality of human B-cell lymphomas. J Exp Med 145:1014–1028

Lukes RJ, Collins RD (1974) Immunologic characterization of human malignant lymphomas. Cancer 34, 1488–1503

Maurer R, Taylor CR, Terry R, Lukes RJ (1979) Non-Hodgkin lymphomas of the thyroid. A clinico-pathological review of 29 cases applying the Lukes-Collins-classification and an immunoperoxidase method. Virchows Arch (Pathol Anat) 383:293–317

Medical Staff Conference (1975) Recent clinical and experimental developments in Sjögren's syndrome. West J Med 122:50–58

Meiers HG, Voigtmann G, Haensch R, Hornstein OP (1974) Sjögren-Syndrom: Serumeiweißbild und Autoimmunphänomene. Hautarzt 25:118–123

Mepham BL, Frater W, Mitchell BS (1979) The use of proteolytic enzymes to improve immunoglobulin staining by the PAP technique. Histochem J 11:345–357

Miller DG (1976) The association of immune disease and malignant lymphoma. Ann Intern Med 66:507–521

Moutsopoulos HM, Chused TM, Johnson AH, Knudsen B, Mann DL (1978) B lymphocyte antigens in sicca syndrome. Science 199:1441–1442

Nime FA, Cooper HS, Eggleston JC (1976) Primary malignant lymphomas of the salivary glands. Cancer 37:906–912

Noel H, Helbron D, Lennert K (1980) Epithelioid cellular lymphogranulomatosis (lymphoepithelioid cell lymphoma): histologic and clinical observations. In: van den Tweel JG, Taylor CR, Bosman FT (eds) Malignant lymphoproliferative diseases. Martinus Nijhoff, The Hague Boston London (Boerhaave Series for Postgraduate Medical Education, Vol 17, pp 433–445)

Pierce DA, Stern R, Jaffe R, Zulman J, Talal N (1979) Immunoblastic sarcoma with features of Sjögren's syndrome and systemic lupus erythematosus in a patient with angioimmunoblastic lymphadenopathy. Arthritis Rheum 22:911–916

Pinkus GS, Dekker A (1970) Benign lymphoepithelial lesion of the parotid glands associated with reticulum cell sarcoma. Report of a case and review of the literature. Cancer 25:121–127

Pirsig W, Donath K (1972) Zur Ultrastruktur der Parotis beim Sjögren-Syndrom vor und nach immunsuppressiver Therapie. Arch Klin Exp Ohr Nasen Kehlkopfheilkunde 201:309–323

Poppema S (1980) The diversity of the immunohistological staining pattern of Sternberg-Reed cells. J Histochem Cytochem 28:788–791

Repetto E, Spotorno N, Cerrato O, Sorbi A (1974) Clinical study of the incidence of malignant neoplasms in some autoimmune diseases. Rheumatismo 26:102–108

Ryan GP, James RA, Milazzo SC (1974) Malignant lymphoma complicating Sjögren's syndrome. Aust NZ J Med 4:287–291

Schmid U, Helbron D, Lennert K (1982) Primary malignant lymphomas localized in salivary glands. Histopathology in press

Schwarze EW, Papadimitriou CS (1980) Non-Hodgkin's lymphoma of the thyroid. Pathol Res Pract 167:346–362

Scully RE, Galdabini JJ, McNeely BU (1975) Case records of the Massachusetts General Hospital. Weekly clinicopathological exercises, Case 28-1975. N Engl J Med 293:136–144

Sebahoun G, Gratecos N, Carcassonne Y (1977) Le lymphome de Lennert. A propos d'une observation compliquant un syndrome de Gougerot-Sjögren. Nouv Presse Med 6:3335

Seifert G (1971a) Klinische Pathologie der Sialdenitis und der Sialadenose. HNO 19:1–9

Seifert G (1971b) Die Pathologie der Speicheldrüsen im Rahmen der Kollagenkrankheiten. HNO 19:193–200

Seifert G (1980) Lymphoid lesions of the oral cavity. Pathol Res Pract 167:179–203

Seifert G, Donath K (1976a) Classification of the pathohistology of diseases of the salivary glands. Review of 2600 cases in the salivary gland register. Beitr Pathol 159:1–32

Seifert G, Donath K (1976b) Die Morphologie der Speicheldrüsenerkrankungen. Arch Otorhinolaryngol 213:111–208

Sela J, Ulmansky M, Dishon T, Rosenmann E, Boss JH (1972) Experimental allergic sialadenitis. I. Acute sialadenitis induced by a local immune reaction. Virchows Arch (Pathol Anat) 355:213–219

Seligmann M, Clauvel JP (1977) Current views on immunoglobulin abnormalities and B-cell proliferations. Adv. Nephrol 7:237–259

Shearn MA, Tu WH, Stephens BG, Lee JC (1970) Virus-like structures in Sjögren's syndrome. Lancet I:568–569

Shearn MA, Moutsopoulos HM, Sawada S, Gak C (1975) Sjögren's syndrome with light chain myeloma. West J Med 123:496–497

Shulman HM, Sullivan KM, Weiden PL, McDonald GB, Striker GE, Sale GE, Hackman R, Tsoi M-S, Storb R, Thomas ED (1980) Chronic graft-versus-host syndrome in man. A long-term clinicopathologic study of 20 Seattle patients. Am J Med 69:204–217

Sjögren H (1933) Zur Kenntnis der Keratokonjunctivits sicca. Acta Ophthamol [Suppl] (Copenh) 11:1–151

Sjögren H (1948) Keratoconjunctivitis sicca and chronic polyarthritis. Acta Med Scand 130:484–488

Stein H, Bonk A, Tolksdorf G, Lennert K, Rodt A, Gerdes J (1980) Immunohistologic analysis of the organization of normal lymphoid tissue and non-Hodgkin's lymphomas. J Histochem Cytochem 28:746–760

Sternberger LA, Hardy PH Jr, Cuculis JJ, Meyer HG (1970) The unlabeled antibody enzyme method of immunohistochemistry. J Histochem Cytochem 18:315–333

Strimlan CK, Rosenow E, Divertie M, Harrison EG (1976) Pulmonary manifestations of Sjögren's syndrome. Chest 70:354–361

Sutinen S, Sutinen S, Huhti E (1977) Ultrastructure of lymphoid interstitial pneumonia: virus-like particles in bronchiolar epithelium of a patient with Sjögren's syndrome. Am J Clin Pathol 67:328–333

Talal N (1974) Autoimmunity and lymphoid malignancy in New Zealand black mice. Prog Clin Immunol 2:101–120

Talal N (1978) Benign and malignant lymphoid proliferation in autoimmunity. Recent Results Cancer Res 64:288–291

Talal N, Bunim II (1964) The development of malignant lymphoma in the course of Sjögren's syndrome. Am J Med 36:529–540

Talal N, Sokoloff L, Barth WF (1967) Extrasalivary lymphoid abnormalities in Sjögren's syndrome (reticulum cell sarcoma, "pseudolymphoma", macroglobulinemia). Am J Med 43:50–65

Talal N, Asofsky R, Lightbody P (1970) Immunoglobulin synthesis by salivary gland lymphoid cells in Sjögren's syndrome. J Clin Invest 49:49–54

Talal N, Sylvester RA, Daniels TE, Greenspan JS, Williams RC (1974) T and B lymphocytes in peripheral blood and tissue lesions in Sjögren's syndromes. J Clin Invest 53:180–189

Tarpley TM, Anderson LG, White CL (1974) Minor salivary gland involvement in Sjögren's syndrome. Oral Surg 37:64–74

Taylor CR (1976) Immuno-histological observations upon the development of reticulum cell sarcoma in the mouse. J Pathol 118:201–219

Vasil'ev VI, Simonova MV, Finogenova IA, Probatova NA (1978) Lymphoproliferative disorders and Sjögren's syndrome. Ter Arkh 50:108–114

Weisbrot JM (1976) Lymphomatoid granulomatosis of the lung, associated with a long history of benign lymphoepithelial lesions of the salivary glands and lymphoid interstitial pneumonitis. Am J Clin Pathol 66:792–801

Whaley K, Buchanan WW (1971) Recent advances in Sjögren's syndrome. Mod Trends Rheumatol 2:139–157

White SC (1973) Experimental autoallergic parotitis. J Oral Pathol 2:341–343

White SC (1976) T-cell dependence of experimental autoallergic lesions of rat submandibular glands. J Dent Res 55:abstract 948

Wiljasalo M, Tallroth K, Korkola O, Valle M, Vuopio P (1977) Lymphographic diagnosis of malignant lymphoma in the course of Sjögren's syndrome. Lymphology 10:153–157

Zittoun R, Lebon P, Diebold J (1974) Sjögren's syndrome with pseudolymphoma. Ann Med Interne (Paris) 125:831–836

Zittoun R, Debain P, James JM, Bilski-Pasquier G (1978a) Hematological manifestations and complications in Sjögren's syndrome. Sem Hop Paris 54:1011–1020

Zittoun R, Diebold J, de Carbonniere C, Dauchot J, Zittoun J, Eyquem A, Schuhmann C, Bilski-Pasquier G (1978b) Méthodes de diagnostic du syndrome de Sjögren. Sem Hop Paris 54:1021–1025

Zulman J, Jaffe R, Talal N (1978) Evidence that the malignant lymphoma of Sjögren's syndrome is a monoclonal B-cell neoplasm. N Engl J Med 299:1215–1220

Accepted November 17, 1981

Virchows Arch [Pathol Anat] (1982) 395:45–58

Virchows Archiv A

Morphological Effects in Pituitary Tumours Following Radiotherapy

Matti Anniko and Jan Wersäll

Department of Otolaryngology, Karolinska Hospital, and King Gustaf V Research Institute, The Karolinska Institute, S-104 01 Stockholm, Sweden

Summary. Seven cases with different endocrinological types of pituitary tumours were subject to open surgery 6–25 years after fractionated and 2 months – 9 years after single dose irradiation. Two cases had been treated with both types of irradiation. Tumour tissue was analyzed at the light and electron microscopic levels.

Hyalinization around blood vessels occurred independent of type of irradiation but required some time to develop. This was not found in one tumour analyzed 2 months after single dose treatment. Single dose treatment (30–70 Gy) caused extensive fibrosis and few surviving cells in the primary target area. Tumours treated with fractionated dose irradiation (26–45 Gy) showed a large number of tumour cells present 6–8 years after treatment. Many of these cells revealed morphological damage.

The morphological findings of the presently avaliable material may indicate that a single dose treatment causes rapid and extensive tumour damage at the site of the primary target but that surviving tumour cells are present outside this area. Fractionated irradiation results in an initial dysfunction with persistance of more or less structurally altered cells for several years.

Key words: Pituitary tumours – Irradiation – Morphology

Introduction

Most pituitary tumours are subject to open surgery after diagnosis. Conventional radiation therapy is indicated postoperatively to reduce the rate of late recurrence. In rare cases, it can be used as primary therapy in patients inoperable for medical reasons (Sheline 1979; Wilson and Dempsey 1978). Based on the fact that the biological effect produced by a single radiation dose is greater than that produced by the same dose when fractionated (Strandquist 1944)

Offprints requests to: M. Anniko at the above address

Supported by grants from the Karolinska Institute and the Ragnar & Torsten Söderberg Foundation

0340-1227/82/0395/0045/$02.80

stereotactic radiosurgery was developed (Leksell 1951, 1971). A fundamental principle for radiosurgery is that the border of the tissue volume selected for destruction should be aligned to the steepest dose gradient. In selected cases, stereotactic radiosurgery of pituitary tumours has been used as an alternative to open surgery (Rähn et al. 1981).

The morphology of various endocrinological types of pituitary tumours is well documented (Halmi and Duello 1976; Horvath and Kovacs 1976; Kinnman 1973; Landolt 1975; Saeger 1977 and 1978). However, morphological studies documenting the effects of different types of irradiation are scarce. The present study analyzes the light and electron microscopical findings in 7 cases with pituitary tumours where recurrences occurred 2 months–25 years after external radiotherapy. Tumour tissue was obtained at open surgery.

Patient Material and Methods

Patient Material

Relevant clinical and laboratory findings are shown in Tables 1–3.

In cases nos 1 and 5–7 high serum concentrations of hormone persisted after radiotherapy. Patient no. 2 had fulminent Cushing's disease and a rapid progression of visual field deterioration. In cases nos 3 and 4 the tumours had a suprasellar extension and progressive changes were seen on repeated x-ray investigations. In addition, the patients experienced severe headache.

Table 1. Table showing age and sex, endocrinological type of tumour, serum hormone levels, clinical activity of disease (in acromegaly) and length of case history in 7 cases of pituitary tumours initially treated with radiotherapy later followed by open surgery

Case no.	Type of tumour	Age Sex	Serum hormone level			Clinical activity of disease[d]	Case history[e] (years)	Routine histopathology
			GH[a]	PRL[b]	ACTH[c]			
1	PRL	66, ♀	normal	2,000	normal		5	Chromophobe cells
2	ACTH	63, ♀	normal	normal	670		2–3	PAS negative, acidophilic cells
3	Non-secreting	58, ♂	normal	normal	normal		> 4	Chromophobe cells
4	Non-secreting	62, ♂	normal	normal	normal		15	Chromophobe cells
5	GH	55, ♂	2,200	normal	normal	++	25	In part sclerotic tissue. Often large nuclei and some mitosis. Many eosinophilic cells
6	GH c. PRL	31, ♂	1,950	130	normal	+++	15	
7	GH c. PRL	34, ♀	2,100	30	normal	++	1	In part fibrotic tissue, orange G positive cells

[a] Normal level < 433 pmol/l
[b] Normal level < 25 µg/l
[c] Normal level at 2 a.m. < 275 nmol/l
[d] Only concerning patients with acromegaly
[e] From first signs and symptoms until surgery

Table 2. Table showing the size of the tumour in the sella turcica as estimated at X-ray with regard to sellar morphology and suprasellar extension (SSE). These findings are compared with whether or not the tumour has effected vision pre- and postoperatively

Case no.	X-ray investigation of sella turcica/tumour extension				Vision pre/post-operative
	Intrasellar	Moderately enlarged	Extensive destruction (0 or +)	SSE (mm)	
1			+	10	++/0
2			+	10	+++/0
3			+	4–6	0/0
4			+	16–20	0/0
5			+	8	+/0
6			+	0	0/0
7		+		0	0/0

Table 3. Table showing type and dose of radiotherapy and the time between radiotherapy and open surgery

Case no.	Radiotherapy			Comments
	Years prior to surgery	Type of irradiation	Dose (Gy)	
1	2 months	^{60}Co	44	Stereotactically, single dose
2	$15^{1}/_{2}$ months 20 months	^{60}Co	70	Stereotactically, single dose
3	2.5	^{60}Co	30	Stereotactically, single dose
4	16 9	Gamma ^{60}Co	45 50	Fractionated dose Stereotactically, single dose
5	25 9	Gamma ^{60}Co	26 50	Fractionated dose Stereotactically, single dose
6	6	Gamma	40	Fractionated dose
7	8	Gamma?	unknown	Fractionated dose Therapy performed in Greece

Methods

Morphology. After excision the tumour was put into 3% glutaraldehyde in 0.133 M sodium phosphate buffer, postfixed in 2% osmic tetroxide, dehydrated in increasing concentrations of alcohol and embedded in Epon mixture. Light microscopic sections were stained with toluidine blue. Ultrathin sections were stained with uranyl acetate and lead citrate. From each tumour 7–12 different pieces were randomly analyzed with light microscopy. Based on these findings, specimens for electron microscopy were selected (4–10 different regions from each tumour).

Results

The material was classified into two parts depending on whether irradiation had been used as fractionated doses over a period of time or as a stereotactic single dose. However, cases nos 4 and 5 had been exposed to both forms

Table 4. Table showing a semiquantitative evaluation of morphological damage of tumour tissue after radiotherapy

Case no.	Type of tumour	Morphology (0, +, ++ or +++)				Irradiation dose (Gy)	
		Presence of cells	Damaged cells	Fibrosis	Hyalinization around blood vessels	Fractionated	Single
1	PRL	+	+	+++	0		44
2	ACTH	0/+	++	+++	++		70
3	Non-secreting	++	+	+	+++		30
4	Non-secreting	+	+	+	++	45	50
5	GH	+	+	+	++	26	50
6	GH cum PRL	+++	+++	0	+++	40	
7	GH cum PRL	+++	+++	0	+++	unknown	

(Table 3). A semi-quantitative survey of the material is presented/summarized in Table 4. Each case is, however, also described separately as follows:

Stereotactically Irradiated Tumours

Case No. 1 (PRL Secreting Tumour)

The primary target volume was mainly composed of fibrotic tissue containing scattered pleomorphic pituitary tumour cells which, by light microscopy, were devoid of signs of degeneration (Fig. 1). The fibrotic region was richly vascularized. Most endothelial cells were normal. No apparent hyalization around blood vessels occurred. At the ultrastructural level hormone granules were few, intracytoplasmic vesiculation was frequent and several aggregations, also with degenerative material surrounded by a limiting membrane, occurred in the cytoplasm (Fig. 2).

Other specimens, probably taken from tumour outside the primary target, contained a large number (>3/4) of very pleomorphic cells (Fig. 3). In several regions intercellular vacuolization or deposition of a rather amorphous substance occurred. Cells with nuclear or cytoplasmic oedema, intracytoplasmic vacuolization and other signs of morphological degeneration were observed. Electron microscopy revealed extremely pleomorphic lysosome-like structures (Fig. 4), a few myelin figures and very few hormone granules.

Case No. 2 (ACTH Secreting Tumour)

This patient was twice subject to open surgery (Table 3).

Tissue Obtained at First Operation. The primary tumour mass was completely fibrotic. In several specimens no tumour cells were identified. Other specimens showed minor islands with tumour cells. Many of these cells appeared ultrastructurally normal.

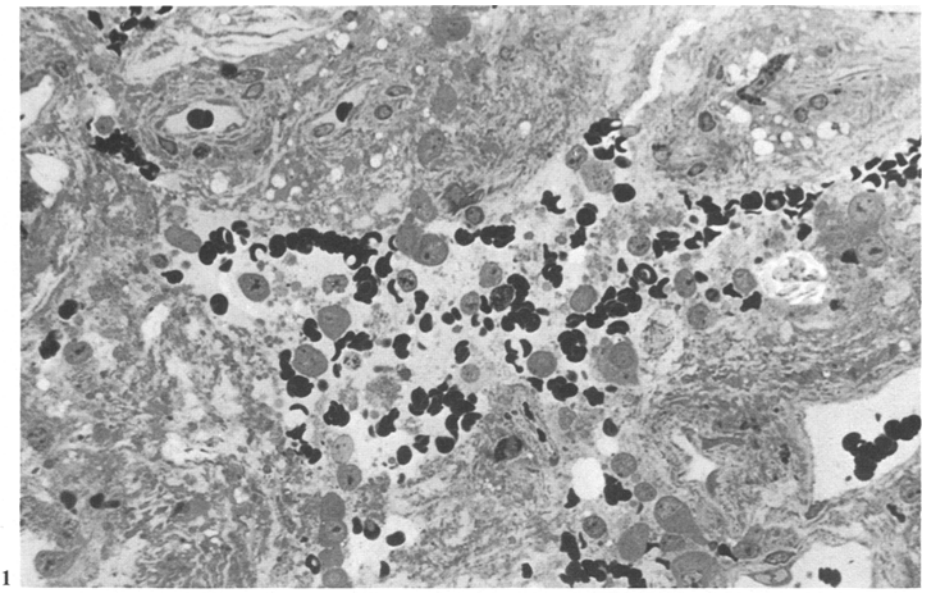

1

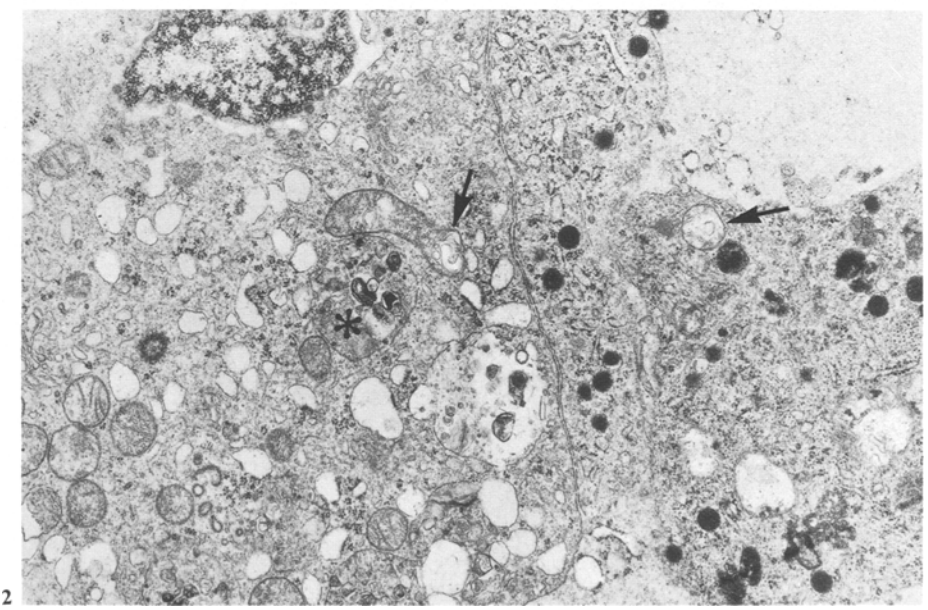

2

Fig. 1. Light microscopy (LM). Case no. 1. PRL secreting tumour. Primary target area 2 months following a single dose irradiation. Scattered pleomorphic pituitary tumour cells with prominent nucleoli. Extensive fibrosis. ×210

Fig. 2. Electron microscopy (EM). Case no. 1. Morphologically preserved cells from Fig. 1. show vesiculation of cytoplasm, damaged mitochondria (*arrows*) and aggregations with degenerating material surrounded by a limiting membrane (*asterisk*). ×8,400

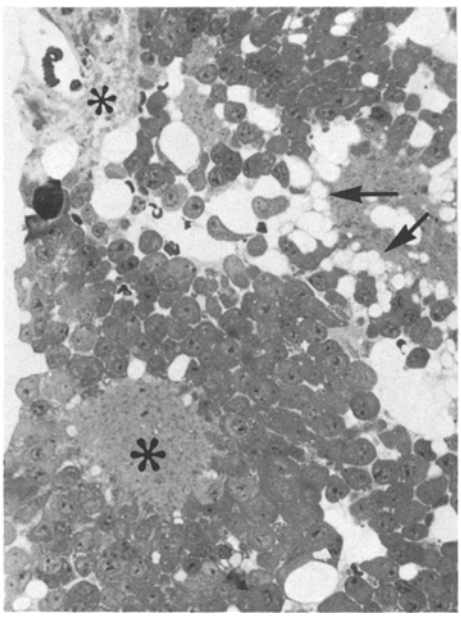

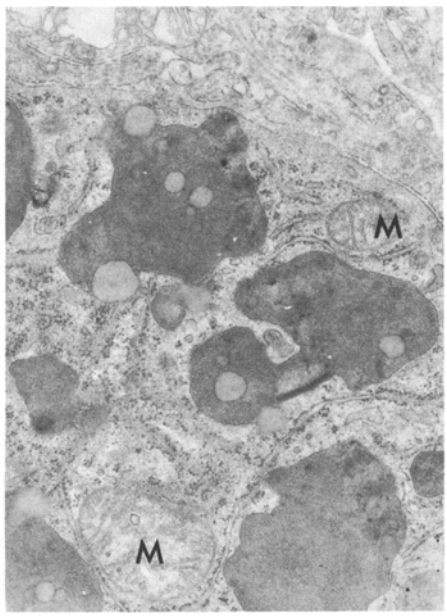

3 4

Fig. 3. LM. Case no. 1. Tumour tissue likewisely outside the primary target. A large number of pleomorphic cells. Some regions (*arrows*) are vesiculated whereas others are more fibrotic (*asterisks*). There is no hyalinization around the blood vessel (BV). ×210

Fig. 4. EM. Detail from a cell from the specimen shown in Fig. 3. Large electron optically dense accumulations in the cytoplasm but surrounded by a limiting membrane (possibly lysosomes). The cytoplasm contains both rough endoplasmic reticulum and a large number of free ribosomes. (*M*) mitochondria. ×24,800

Tissue Obtained at Second Operation. All specimens comprised both fibrous tissue and pituitary tumour cells (Fig. 5). The latter were either normal or in different stages of cell degeneration. In several specimens a border was indicated between the initial/main target of stereotactic irradiation and pituitary cells outside this area (Fig. 6). Ultrastructurally preserved tumour cells contained all characteristics as described for ACTH-secreting cells including a large number of hormone granules. Structural abnormalities of hormone granules were indicated (Fig. 7). Blood vessels showed normal morphology.

Case No. 3 (Non-Secreting Tumour)

All specimens contained a large number of pituitary tumour cells, which, however, revealed a considerable pleomorphism (Fig. 8). Blood vessels were surrounded by extensive hyalinization. Ultrastructurally hormone granules were rare. Mitochondria often showed a disintegration of their internal structure.

Tumours Exposed to Both Fractionated and Stereotactic Irradiation

Case No. 4 (Non-Secreting Tumour)

Only a small number of pituitary tumour cells was identified. Intercellular spaces were evident between rather pleomorphic cells. In this case it was neces-

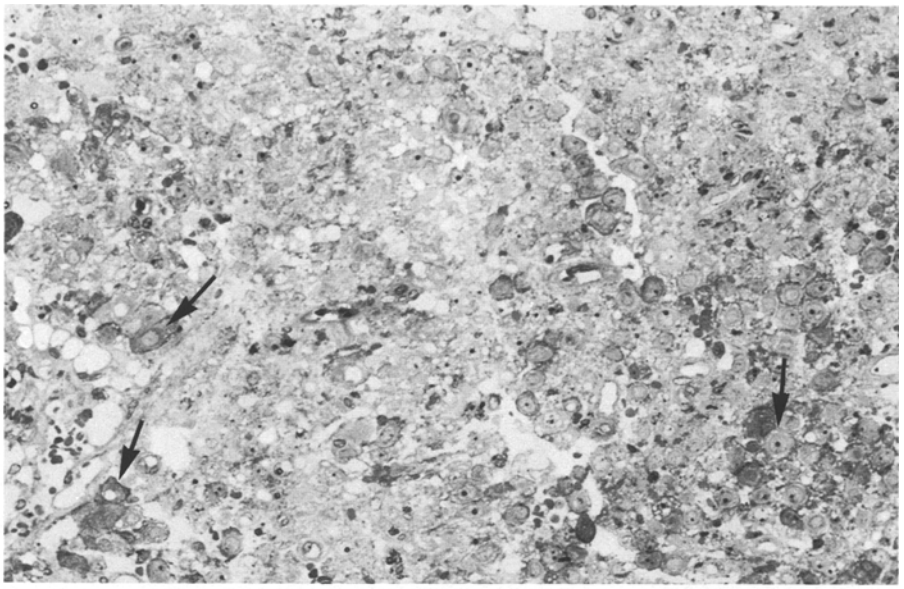

5

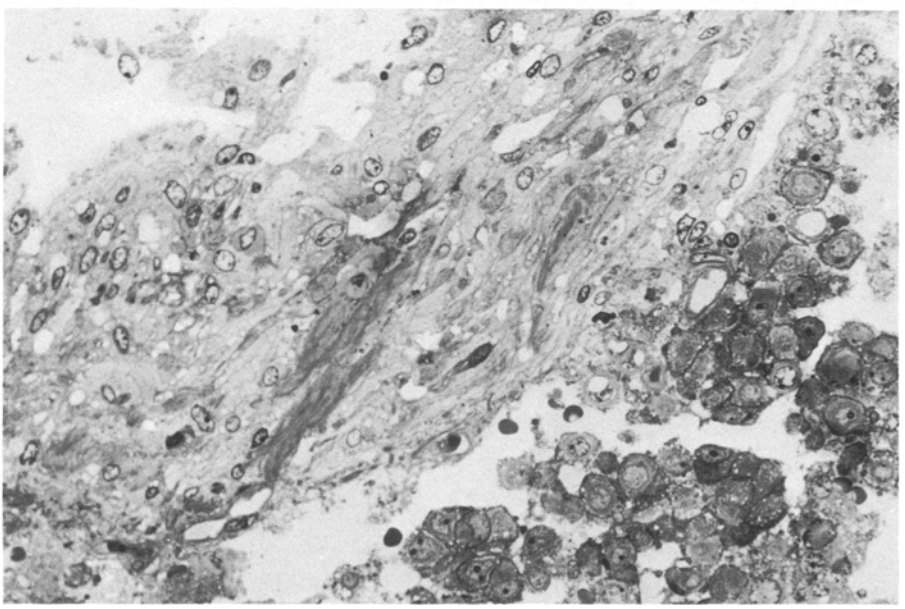

6

Fig. 5. LM. Case no. 2. Tissue obtained at the second operation 20 months after 70 Gy single dose irradiation. This specimen is likely to have been present in the outer regions of the primary target area. Scattered surviving cells but many show vesiculation (*arrows*) or pyknosis. Fibrosis is prominent. ×180

Fig. 6. LM. Case no. 2. Twenty months after 70 Gy single dose irradiation. The specimen illustrates the border between extensive fibrosis and completely degenerated pituitary tumour cells and tumour cells that have survived but appear morphologically damaged. ×240

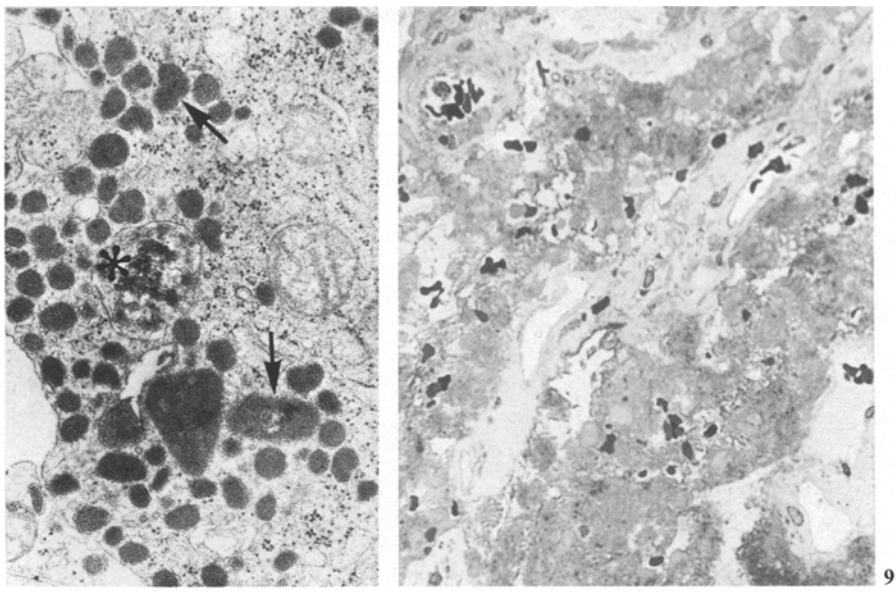

7

9

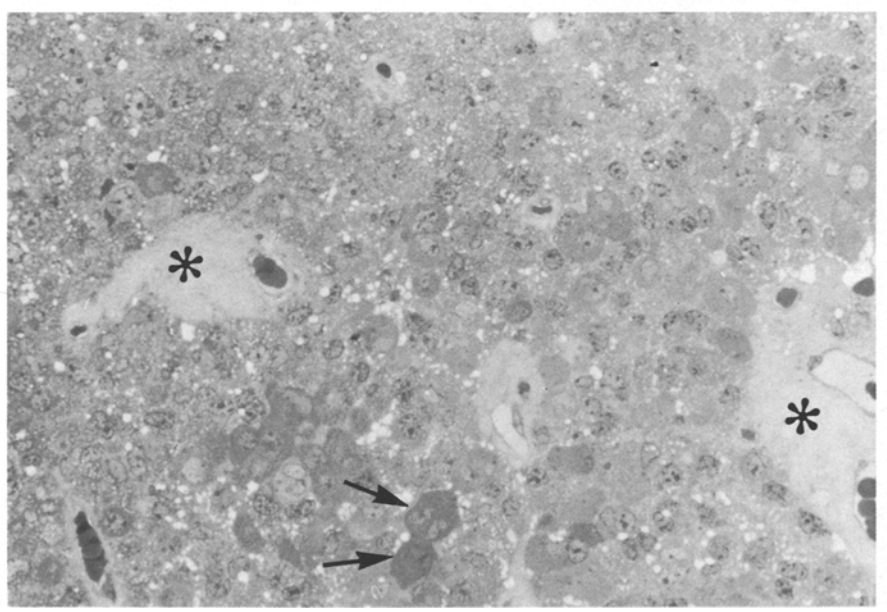

8

Fig. 7. EM. Detail from a pituitary tumour cell that had survived. Hormone granules are present but several are morphologically severely altered (*arrows*). An aggregation of degenerating material (*asterisk*) is surrounded by a limiting membrane. (*M*) mitochondria. ×14,000

Fig. 8. LM. Case no. 3. Non-secreting tumour. Exposed to 30 Gy single dose irradiation. After 2.5 years treatment. Many tumour cells are preserved and show considerable pleomorphism (*arrows*). Extensive hyalinization around blood vessels (*asterisks*). Fibrosis is scarce. ×210

Fig. 9. LM. Case no. 4. Non-secreting tumour exposed to 45 Gy fractionated and 50 Gy single dose irradiated 16 and 19 years, respectively, prior to open surgery. Extensive fibrosis and hyalinization around blood vessels. Surviving tumour cells are not identified. ×180

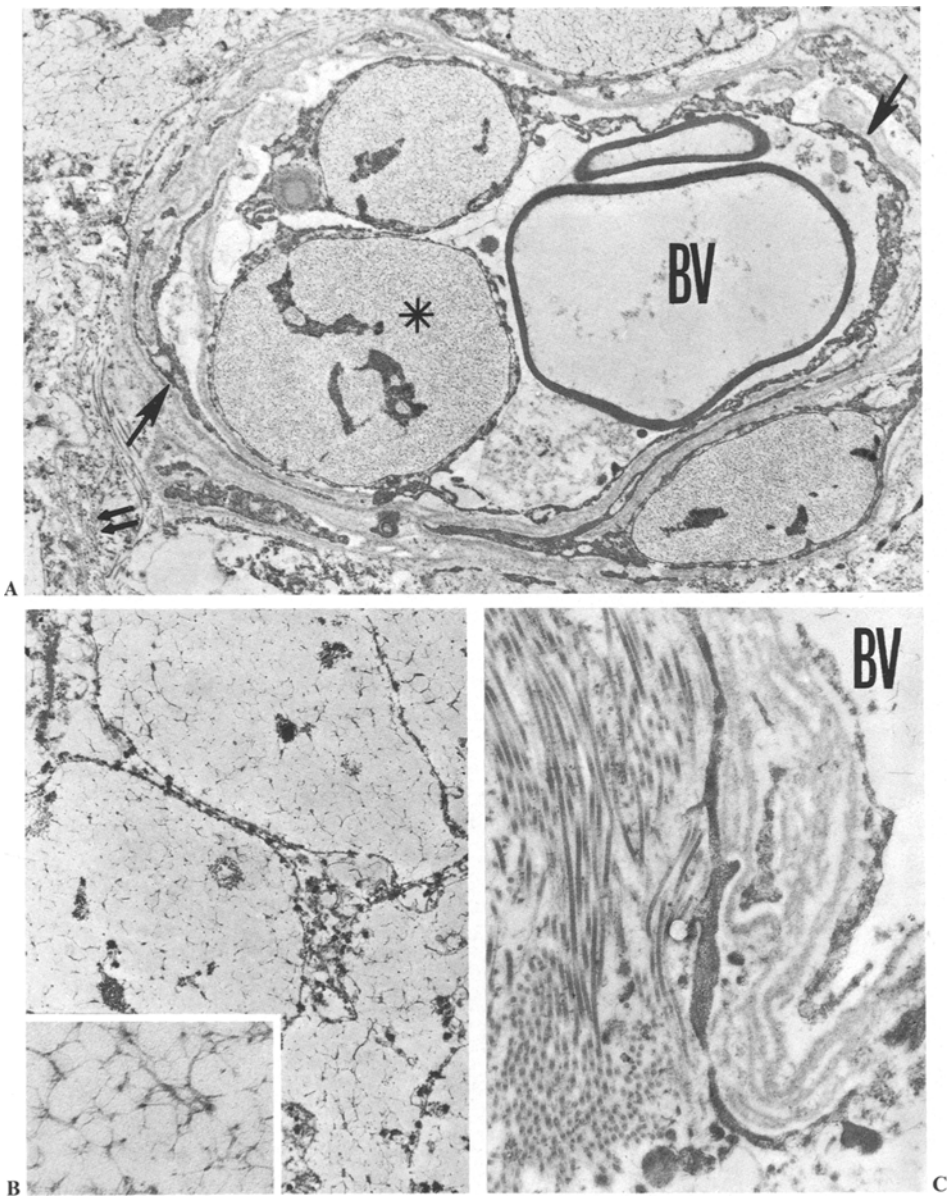

Fig. 10A–C. EM. Case no. 4. Non-secreting tumour exposed to 45 Gy fractionated and 50 Gy single dose irradiation 16 and 9 years, respectively, prior to open surgery. (**A**) Blood vessel (*BV*) which in the light microscope showed partial obliteration and hyaline degeneration. The latter (*asterisk*) consists of a loose network of extracellular material. Remnants of endothelial cells (*arrows*) occur. No pituitary tumour cells are visible adjacent to the BV. A loose fibrillar network (*double arrow*) surrounds the BV. ×4,200. (**B**) Large confluent areas of loose network which in the light microscope was identified as hyaline degeneration. ×5,900. *Inset:* ×21,000. (**C**) The blood vessel (*BV*) wall consists of remnants of endothelial cells which are morphologically severely altered and have an electron optically dense cytoplasm and lack distinct cell membranes. Several layers of basal membrane-like structures occur in the wall of the BV. Adjacent to the BV a fibrillar network occur having a cross-banded substructure (possibly collagen). ×11,000

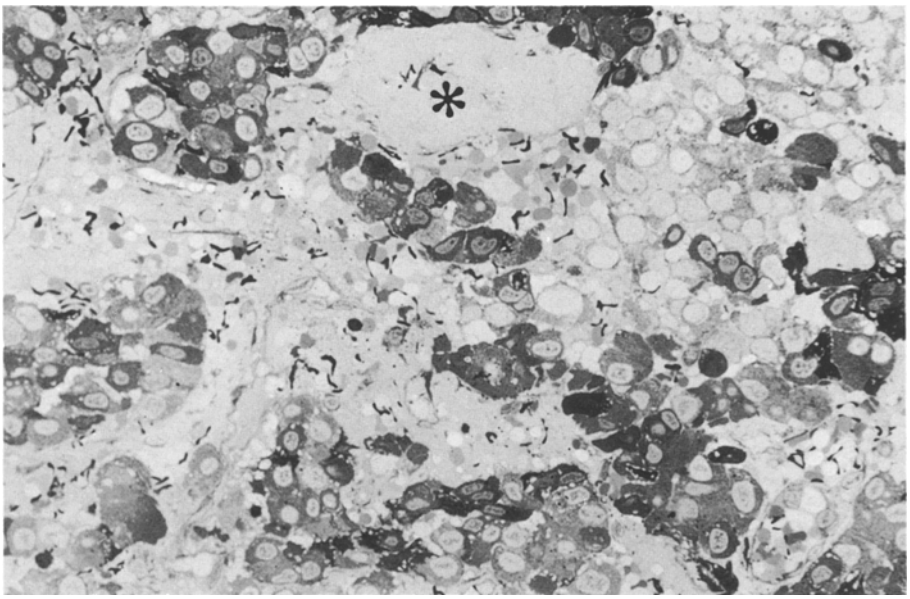

Fig. 11. LM. Case no. 6. Tumour with a concomitant secretion of GH and PRL. 40 Gy fractionated irradiation 6 years prior to open surgery. Tumour cells are present in a large number but many of them show severe morphological signs of degeneration. Many cells are pyknotic. Hyaline aggregation in the tumour (*asterisk*). ×260

sary to use the electron microscope for identifying pituitary tumour cells. In most, but not all regions of the excised tumour, blood vessels were surrounded by hyalinization (Figs. 9 and 10).

Case No. 5 (GH Secreting Tumour)

The morphology was similar to that found in case no. 4.

Tumours Irradiated with Fractionated Doses

Case No. 6 (Tumour with Concomitant Secretion of GH and PRL)

All specimens contained a large number of pituitary tumour cells many of which appeared morphologically damaged (Fig. 11). Extensive hyalinization oc-

Fig. 12. EM. Detail from Fig. 11. Severely degenerating cell between cells with well preserved ultrastructure and a large number of hormone granules. (*N*) nucleus. ×3,400

Fig. 13. EM. Detail from Fig. 11. Pyknotic, degenerating cells still contain a large number of hormone granules. Adjacent cells show varying degrees of vesiculation and several large lysosome-like structures. ×3,100

Fig. 14. EM. Detail from Fig. 11. The cytoplasm of this degenerating pituitary tumour cell is fragmented, contains lysosome-like structures (*L*) and myelin figures but still contains morphologically normal hormone granules. ×13,500

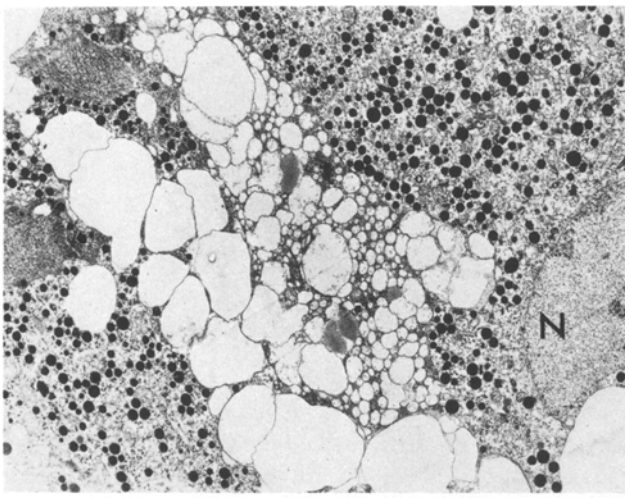

12

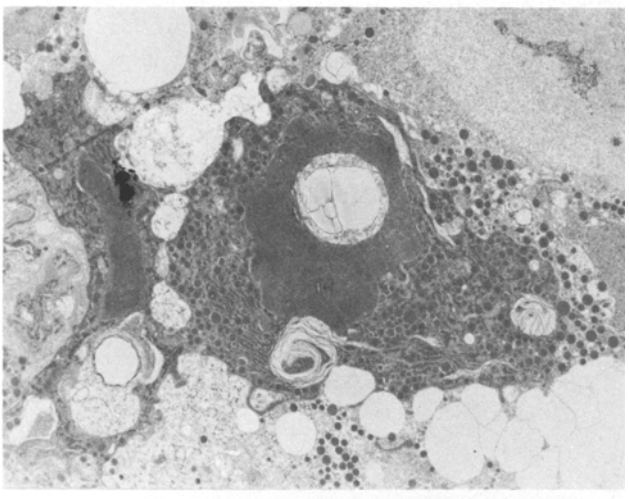

13

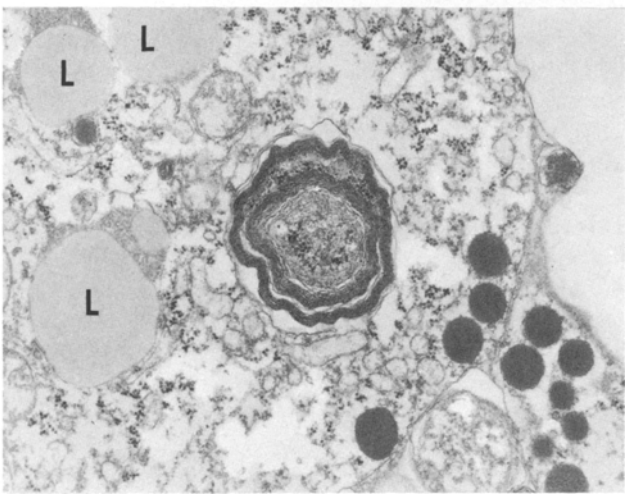

14

curred around blood vessels. Ultrastructurally normal cells were found adjacent to extensively damaged pituitary tumour cells (Fig. 12). Both intracellular and intercellular vesiculation occurred. Hormone granules were frequently found in otherwise morphologically severely damaged cells. Many tumour cells were electron dense, contained myelin figures and lysosome-like structures but often showed a considerable amount of rough endoplasmic reticulum (RER) and hormone granules (Figs. 13 and 14).

Case No. 7 (Tumour with a Concomitant Secretion of GH and PRL)

The tumour morphology was the same as described in case no. 6.

Discussion

The present study raises the question whether general morphological features can be distinguished following single dose or fractionated irradiation. In no case was treatment performed with the proton beam which is an alternative in radiosurgery (review: Kjellberg and Kliman 1980). The qualitative and quantitative differences which occur after different types of irradiation are caused by the effectiveness of the irradiation. This effectiviness depends on the volume irradiated, intensity and coefficients of absorption etc. The normal adult pituitary has been considered to be relatively radioresistant and hypopituitarism as a result of external radiation to be rare has been considered (De Schryver et al. 1973; Lederman 1961; Eastman and Roth 1979).

Except for the hyalinization around blood vessels which occurred following both types of irradiation, morphological differences occurred when irradiation was single dose or fractionated. Post-irradiation pituitary tumour cells frequently showed bizarre and atypical outlines. A single dose caused (in all three endocrinological types of tumours) extensive fibrosis with few surviving cells in the primary target area. This was found also when only a few months had passed after radiosurgery (case no. 1). These observations support recent in vitro studies on human pituitary tumours exposed to single doses of 30–150 Gy with an early morphological effect on tumour cells. In the organ culture system these effects were dose dependent. In addition, an individual response to irradiation in vitro occurred in tumours causing acromegaly (Anniko 1981; Anniko et al. 1981a). Clinically and morphologically (at the light microscopic level) individual variations in radioresistance are often experienced not only within the same type of tumours but also between the various endocrinological types (Backlund et al. 1979; Rähn and Nilsson 1980). However, there is still no definite information on differential radiosensitivities of various cell types of pituitary tumours (Emami 1980). From animal studies, differences in radioresistance between the various cell types of the normal pituitary gland are indicated (Mateyko and Charipper 1953; Van Dyke et al. 1959). Human material for morphological analysis following radiotherapy is naturally scarce. In contrast to the findings of the present study, Kinnman (1973) stated that no morphological changes were found in tumours causing acromegaly. The radiotherapeutic doses were not given however. The discrepances may reflect lower irradiation doses given to these patients.

In two cases (nos 4 and 5) the patients had a long case history and had been treated with both fractionated and single dose radiotherapy. It appears likely that the fractionated radiation did not reach an optimal level, probably allowing tumour cell proliferation. Tissue was analyzed several years after a stereotactic lesion had been given and showed a limited number of surviving cells. Many of these were morphologically altered. The single dose technique according to Leksell (1951 and 1971) limits the target volume which may explain why open surgery had to be performed later. The tissue seen macroscopically at the site of the stereotactic lesion did not contain a sufficient number of tumour cells to explain a high secretion of hormone (case no. 5) or lead to expansive growth (case no. 4).

Pituitary tumours treated with fractionated irradiation 6–8 years prior to surgery (cases nos 6 and 7) contained a large number of cells with evidence of variable morphological damage. Both tumours caused a concomitant secretion of GH and PRL. It is to be noted that fibrosis was not found in the tumours. It seems probable that the morphological effects following fractionated irradiation become manifest considerably later than after single dose treatment and effects mainly tumour proliferation.

Damage to tumour cells is reflected by low serum hormone levels. In the present two cases such a low level was not found 6–8 years after irradiation. However, a temporary decrease of hormone secretion during some months after irradiation can have occurred which then would indicate a reversible cell damage during this period of time.

Following conventional radiation therapy of different types of pituitary tumours large differences in treatment results are reported (review: Sheline 1979). It may be considered that the effects of radiation are at least in part dependent on the tumour biology of each individual case which could reflect the radioresistance. Recently Anniko et al. 1981 b–c showed that an aneuploid DNA pattern occurred in 30–40% of a consecutive series of pituitary tumours. The degree of aneuploidy was not correlated to any hormonal type of tumour but occurred in all types. In case no. 7 of the present study the pituitary tumour showed an aneuploid DNA pattern ($N=3.2$; G_1-phase – 81.4%, G_2M-phase – 3.6% and S-phase – 15%) whereas tumours nos 3 and 6 were too damaged to allow determination of DNA ploidy and proliferation rate according to the flow-cytofluorometric method. The aim of further studies is to correlate DNA ploidy with dose and type of irradiation.

References

Anniko M (1981) Early morphological changes following gamma irradiation: a comparison of human pituitary tumours and human acoustic neurinomas. Acta Pathol Microbiol Scand [A] 89:113–124

Anniko M, Arndt J, Rähn T (1981a) Gamma irradiation effects on human pituitary adenoma tissue. An analysis of histology, ultrastructure and hormone sampling in an in vitro model system. Acta Otolaryngol (Stockh) (in press)

Anniko M, Holm L-E, Werner S, Tribukait B (1981b) DNA characteristics of human pituitary tumours. Acta Otolaryngol (Stockh) Suppl. 379:5–11

Anniko M, Holm L-E, Silfverswärd C, Tribukait B (1981c) Cellular DNA content of pituitary tumours: its relationship to morphology and hormonal type of tumour. Acta Otolaryngol (Stockh) Suppl. 379:13–19

Backlund E-O, Bergstrand G, Hierton-Laurell U, Rosenborg M, Waijngot A, Werner S (1979) Tumour changes after single dose irradiation by stereotactic radiosurgery in "non-active" pituitary adenomas and prolactinomas. In: Szilka G (ed) Stereotactic cerebral irradiation. INSERM Symposium no. 12. Elsevier/North-Holland Biomedical Press, Amsterdam, pp 199–206

DeSchryver J, Ljunggren G, Båryd I (1973) Pituitary function in long-term survival after radiation therapy of nasopharyngeal tumours. Acta Radiol Ther Phys Biol 12:479–484

Eastman RC, Roth J (1979) Conventional hypervoltage irradiation is an effective treatment for acromegaly. J Clin Endocrinol Metab 48:931–940

Halmi NS, Duello T (1976) "Acidophilic" pituitary tumours. A reappraisal with different staining and immunocytochemical techniques. Arch Pathol Lab Med 100:346–351

Horvath E, Kovacs K (1976) Ultrastructural classification of pituitary adenomas. Can J Neurol Sci 3:9–21

Kinnman J (1973) Acromegaly. An ultrastructural analysis of 51 adenomas and a clinical study of 80 patients treated by transanthrosphenoidal operation. Norstedt & Söner. Stockholm

Kjellberg RN, Kliman B (1980) Radiosurgery therapy for pituitary adenoma. In: Post KD, Jackson IMD, Reichlin S (eds) The pituitary adenoma. Plenum. Medical Book Company. New York/London, pp 459–478

Landolt AM (1975) Ultrastructure of human sella tumour. Correlations of clinical findings and morphology. Acta Neuroclin [Suppl] 22:1–167

Lederman M (1961) Cancer of the nasopharynx. Its natural history and treatment. Charles C Thomas, Springfield, Ill

Leksell L (1951) The stereotaxic method and radiosurgery of the brain. Acta Chir Scand 102:316–319

Leksell L (1971) Stereotaxis and radiosurgery. An operating system. Charles C Thomas, Springfield, Ill

Mateyko GM, Charipper HA (1953) Histological effects upon the pars anterior of the rat following hypophyseal cathoderay irradiation and whole-body x-irradiation, J Morphol 93:533–559

Rähn R, Nilsson A (1980) Morphological changes in radiosurgically treated pituitaries. In: Stereotactic radiosurgery in Cushing's disease. Doctorial dissertation. Karolinska Institutet, Stockholm, pp 1–12

Rähn T, Thorén M, Hall K, Backlund E-O (1981) Stereotactic radiosurgery in Cushing's disease. Acute radiation effects. Surg Neurol (in press)

Saeger W (1977) Die Hypophysentumoren. Veröff Pathol 107:1–240

Saeger W (1978) Morphologische Klassifikation der Hypophysenadenome und ihre Bedeutung für die klinische Diagnostik. Endokrinologie 71:45–49

Sheline G-E (1979) Conventional radiation therapy in the treatment of pituitary tumours. In: Tindall GT, Collins WF (eds) Clinical management of pituitary disorders. Raven Press, New York, pp 287–314

Strandquist M (1944) Studien über die kumulative Wirkung der Röntgenstrahlen bei Fraktionierung. Acta Radiol [Suppl] 55:1–300

VanDyke DC, Simpson ME, Koneff AA, Tobias CA (1959) Long term effects of deuteron irradiation of the rat pituitary. Endocrinology 64:240–257

Wilson CB, Dempsey LC (1978) Transphenoidal microsurgical removal of 250 pituitary adenomas. J Neurosurg 48:13–22

Accepted November 23, 1981

Virchows Arch [Pathol Anat] (1982) 395:59–68

Virchows Archiv A

Adenoma of the Human Pituitary Producing Growth Hormone and Thyrotropin

A Histologic, Immunocytologic and Fine-structural Study

Kalman Kovacs[1], Eva Horvath[1], Calvin Ezrin[2], and Martin H. Weiss[3]

[1] Department of Pathology, St. Michael's Hospital, University of Toronto, 30 Bond Street, Toronto, Ontario, Canada
[2] Department of Medicine, Cedars Sinai Medical Center, UCLA Los Angeles California, USA
[3] Department of Neurosurgery, University of Southern California Los Angeles, California, USA

Summary. A pituitary adenoma removed by surgery from a 22-year-old man was studied by histology, immunocytology, transmission electron microscopy and immunoelectron microscopy. Clinically, the patient had acromegaly and euthyroidism with elevated blood GH concentrations. Blood TSH and T_4 levels were within the normal range. Histologically, the adenoma was chromophobic and exhibited no PAS, lead hematoxylin, aldehyde thionin or Grimelius silver positivity. By the immunoperoxidase technique GH, β-TSH and α-subunit but no PRL, ACTH, α-endorphin, β-FSH or β-LH were demonstrated in the adenoma cells. Electron microscopy revealed adenoma cells which were similar to TSH cells and showed no resemblance to GH cells of nontumorous pituitaries or GH-secreting tumors. Immunoelectron microscopy demonstrated GH and β-TSH in the secretory granules.

It is concluded that pituitary adenomas composed of TSH-like cells may secrete GH, resulting in acromegaly. Production of GH by adenomatous TSH cells cannot be explained on the basis of the one cell- one hormone theory. The question is raised whether bihormonal or multihormonal clones, capable of synthesizing more than one hormone, exist in the human pituitary. These cells are apparently dormant under normal conditions, but in the course of neoplastic transformation may undergo functional dedifferentiation and acquire the ability to produce two or more different hormones.

Key words: Adenohypophysis – Electron microscopy – Growth hormone – Immunocytology – Pituitary adenoma – Thyroid-stimulating hormone

Introduction

Most endocrinologically active adenomas arising in the human pituitary secrete one hormone and are classified as GH-, PRL-, ACTH-, FSH-, LH-, or TSH-

Offprints requests to K. Kovacs at the above address

0340-1227/82/0395/0059/$02.00

producing neoplasms (Horvath and Kovacs 1976; Kovacs et al. 1977). They possess distinct morphologic features; their hormone content, assessed by immunocytologic techniques, and their fine structural characteristics can be correlated with clinical findings and biochemical results (Landolt 1978; McCarty et al. 1978; Kovacs and Horvath 1979). Occasionally, pituitary adenomas produce more than one hormone. Several types of bihormonal or multihormonal adenomas have been reported, such as GH- and PRL-producing mixed GH cell-PRL cell adenomas and acidophil stem cell adenomas, FSH and LH-secreting gonadotroph cell adenomas, as well as adenomas producing GH and TSH, or PRL and TSH, or GH, PRL and ACTH, or PRL and FSH (Heitz 1979; Kovacs and Horvath 1979).

We describe here the histologic, immunocytologic and fine structural features of a GH- and TSH-producing pituitary adenoma removed by surgery from a 22-year-old man with acromegaly and euthyroidism.

Report of Case

Clinical Findings

This 22-year-old Vietnamese man had had coarsening of his features over the past few years along with marked enlargement of his hands and feet. He denied having headaches or visual problems.

On examination, he was a well-developed, well-nourished man with acromegalic features. He looked clinically euthyroid. Weight: 82 kg, height: 158 cm. The thyroid gland was not palpable. Both hands and feet were large. There was bitemporal superior quadrantic hemianopia on visual field testing. Blood pressure: 120/80 Hgmm; heart rate: 72/min.

Laboratory Results. Random blood GH at 3 p.m.: 35 ng/ml (N: 0–8 ng/ml).

Glucose Tolerance Test. Blood glucose at 0 min: 109 mg/dl; 30 min: 158 mg/dl; 60 min: 169 mg/dl; 90 min: 164 mg/dl; 120 min: 140 mg/dl. Blood GH: at 0 min: 20 ng/ml; 30 min: 20 ng/ml; 60 min: 19 ng/ml; 90 min: 18 ng/ml; 120 min: 50 ng/ml. (N: <5 ng/ml with glucose suppression). Blood PRL: 7.5 ng/ml (N: 5.5–18.0 ng/ml). Blood FSH: 4.2 mU/ml (N: 2–10 mU/ml). Blood LH: 11.4 mU/ml) (N:4–15 mU/ml). Metopirone test of ACTH reserve: within normal limits. Blood T_4: 7.3 μg/dl (N: 5–13 μg/dl). Blood TSH: 1.8 μU/ml (N: <5 μU/ml). CT scan showed a large pituitary tumor with suprasellar extension. He underwent surgery and the tumor was removed by a transsphenoidal approach. The visual field deficit was promptly resolved.

Methods

For light microscopy, pieces of tumor tissue were fixed in 10% buffered formalin and embedded in paraffin. Sections of 4–6 μm thickness were stained with hematoxylin-phloxine-saffron, PAS, lead hematoxylin, aldehyde thionin and Grimelius silver methods.

For immunostaining, the immunoperoxidase technique was used on 4–6 μm thick paraffin sections, described in detail in previous publications (Kovacs et al. 1976; Kovacs et al. 1978). The following primary antibodies were applied: anti GH (Wellcome Reagents Ltd., Beckenham, GB), anti PRL (donated by Dr. H. Friesen, Department of Physiology, University of Manitoba, Winnipeg, Manitoba, Canada), anti- (1–39) ACTH (Wellcome Reagents Ltd., Beckenham, GB), anti-α endorphin (donated by Dr. J.M. Polak, Department of Histochemistry, Postgraduate Medical School, London, GB), anti-β FSH, (donated by the National Institute of Arthritis, Metabolism and Digestive Diseases, Bethesda, MD, USA), anti-β LH (Calbiochem, La Jolla, CA, USA), anti-β TSH (donated by Bio-Red Laboratories, Richmond, CA, USA), and anti-α subunit of glycoprotein hormones (donated by Dr. I.A. Kourides, Department of Endocrinology, Sloan Kettering Institute, New York, NY, USA and by the National Institute of Arthritis, Metabolism and Digestive Diseases, Bethesda,

MD, USA). Antigen-antibody binding was demonstrated by applying the horseradish peroxidase-antihorseradish peroxidase complex (Cappel Laboratories, Downingtown, PA, USA) and 3,3′-diaminobenzidine. The specificity of immunostaining was verified by serial dilution of the primary antibodies, and by replacing them with phosphate buffered saline and normal rabbit serum and absorption of GH and β-TSH antisera with their respective antigens. For control purposes, several nontumorous pituitary glands, obtained from surgical hypophysectomies and autopsies, were also immunostained. The duration of exposure to the primary antibodies ranged from 16 to 24 h. The dilution of primary antibodies varied from 1:100 to 1:8,000; (anti-GH: 1:8,000; anti-β-TSH: 1:5,000; anti-α-subunit 1:800).

For electron microscopy, fragments of tumor were fixed in 2.5% glutaraldehyde postfixed in 1% osmium tetroxide and embedded in an Araldite-Epon mixture. Ultrathin sections were stained with uranyl acetate and lead citrate and investigated with a Philips 300 electron microscope.

For electron microscopic immunostaining the postembedding technique of Moriarty and Garner (1977) was applied. The tissue was fixed in 2.5% glutaraldehyde and embedded in Epon-Araldite without osmication. GH and β-TSH were demonstrated on consecutive ultrathin sections (antibody dilutions: GH: 1:8,000; β-TSH: 1:5,000).

Results

Gross Findings. The tumor removed in small pieces was intermingled with blood and fibrin and was not weighed. Gross inspection failed to contribute to the diagnosis.

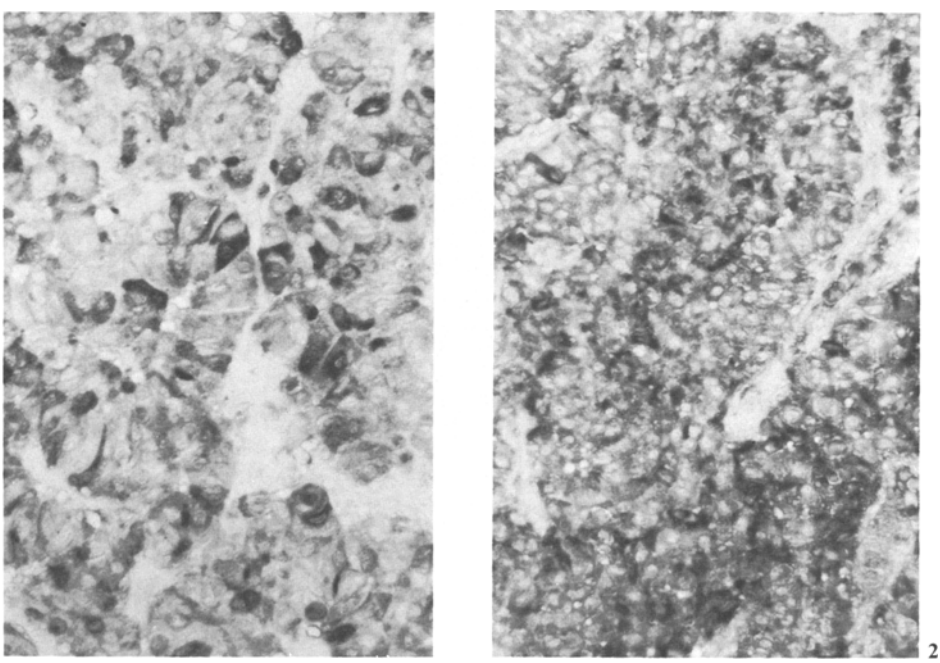

Fig. 1. Immunoreactive growth hormone is evident in the form of dark deposits in the cytoplasm of adenoma cells. Immunoperoxidase technique for growth hormone. Original magnification. ×250

Fig. 2. Immunoreactive β-TSH is clearly noticeable in the form of dark deposits in the cytoplasm of adenoma cells. Immunoperoxidase technique for β-TSH. Original magnification ×250

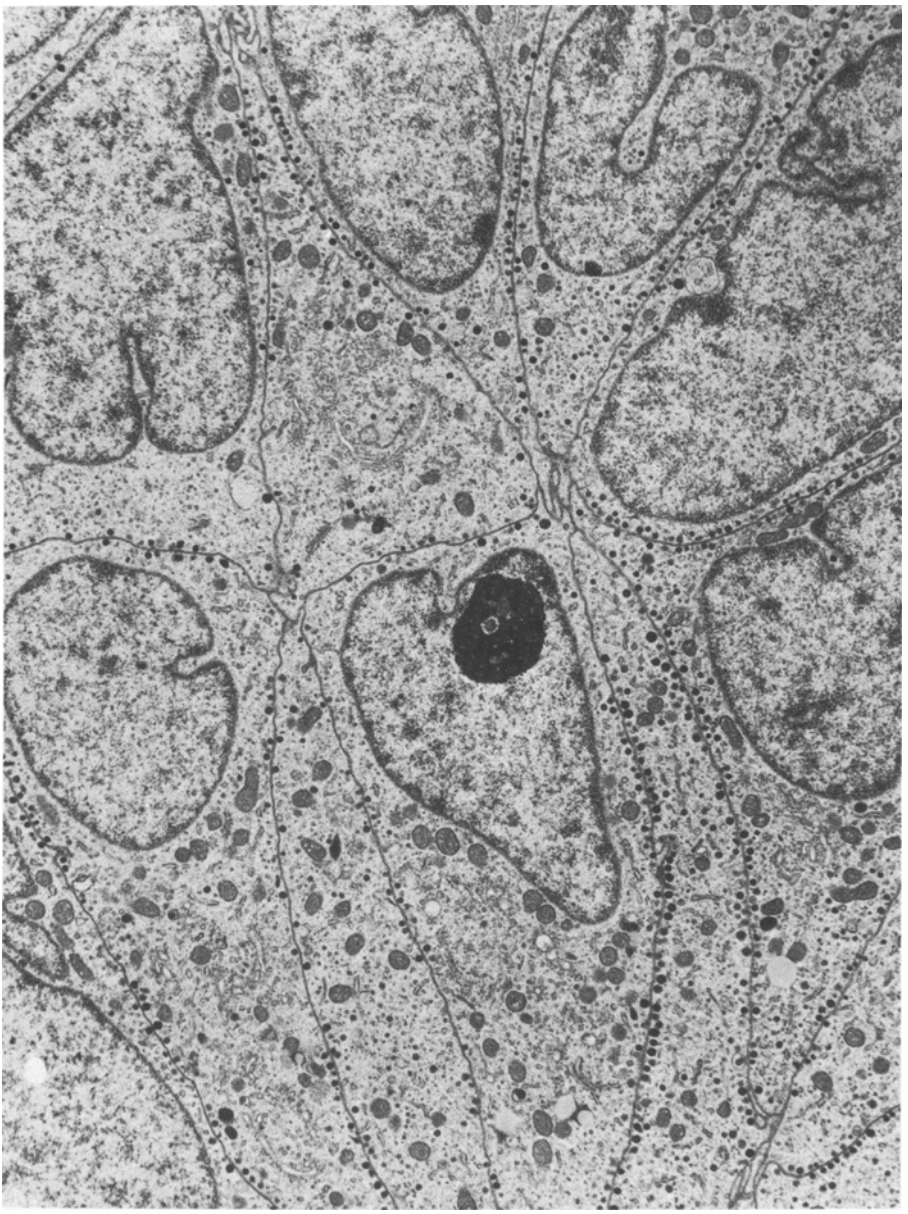

Fig. 3. Electron microscopic appearance of the adenoma, showing elongated cells with well developed Golgi complexes and small, spherical secretory granules located mainly adjacent to the plasmalemma. Magnification ×6,000

Light Microscopic Findings. The tumor was a fairly cellular and vascular chromophobic adenoma showing a sinusoidal pattern and forming pseudorosettes. The adenoma cells were relatively large and elongated, and contained a large, oval or irregular hyperchromatic nucleus and prominent nucleolus. The cytoplasm was well developed and exhibited no staining with acid or basic dyes. Staining

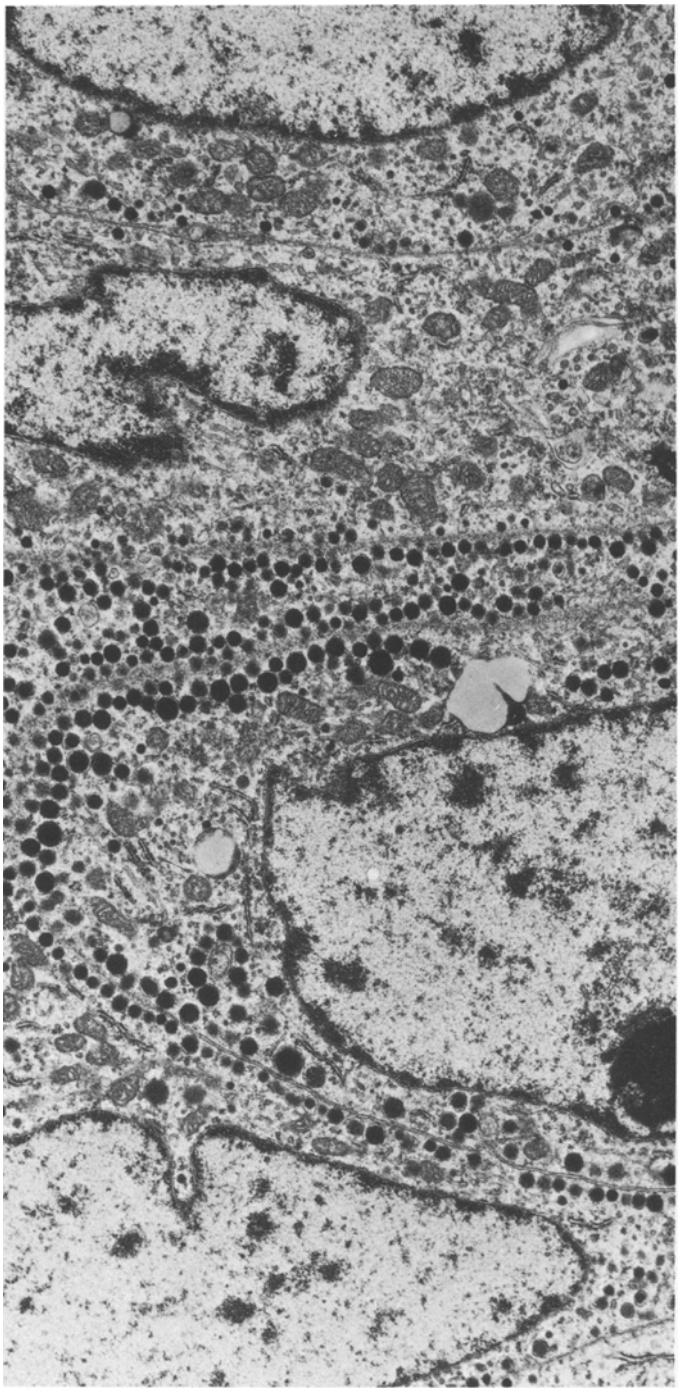

Fig. 4. Fine structural details of adenoma cells. The secretory granules line up along the plasmalemma; they vary in size as well as electron density. Magnification $\times 10{,}400$

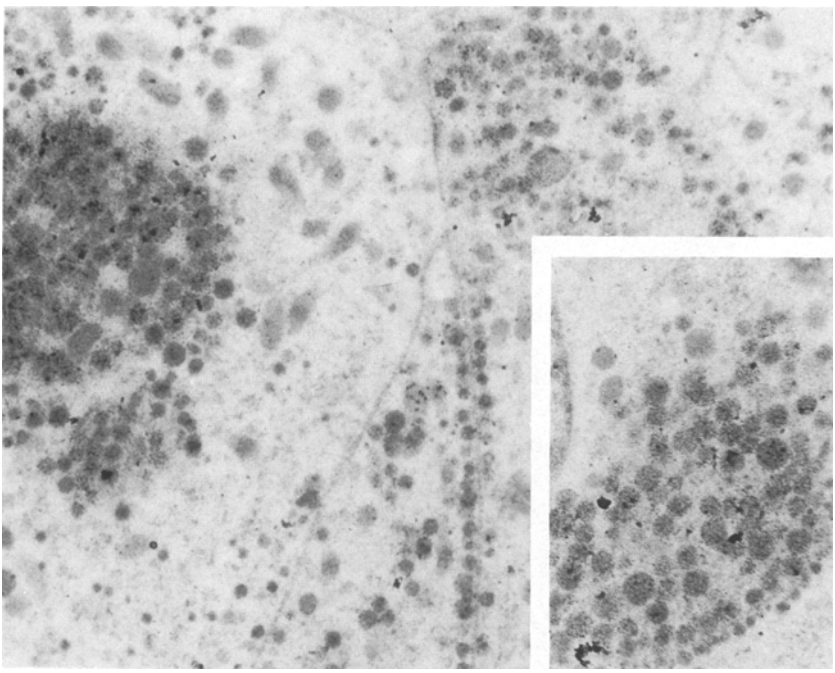

Fig. 5. Immunoelectron microscopy reveals the presence of growth hormone in the majority of secretory granules. Magnification × 13,000 *Inset* shows PAP complexes on secretory granules. Magnification × 11,000

with PAS, lead hematoxylin, aldehyde thionin and Grimelius silver yielded negative results. No pleomorphism was evident and mitotic figures were rare.

Immunocytologic Findings. The immunoperoxidase technique revealed the presence of GH in the cytoplasm of many adenoma cells (Fig. 1). Practically every adenoma cell showed positive immunostaining for β-TSH (Fig. 2) and α-subunit. No PRL, (1–39) ACTH, α-endorphin, β-FSH or β-LH were demonstrated in the adenoma cells.

Fine Structural Findings. The adenoma appeared to consist of a monomorphous cell population (Figs. 3 and 4). Unlike the predominantly spherical or oval cells of growth hormone cell adenomas, the cells of this tumor were elongated or polyhedral with long cytoplasmic processes. The nuclei were eccentric, spherical or oval and contained prominent nucleoli. The cytoplasm was moderately developed and possessed many widely scattered RER profiles, conspicuous Golgi complexes, and numerous rod-shaped mitochondria with tubular cristae and moderately electron dense matrix. The secretory granules were spherical, varied widely in size and electron density, measuring in some cells less than 150 nm, whereas in others they were 100 to 450 nm in diameter. Margination of secretory granules along the cell membranes was a prominent finding. Extrusion of secretory granules across the lateral cell surfaces was also noted in a few cells. Microtu-

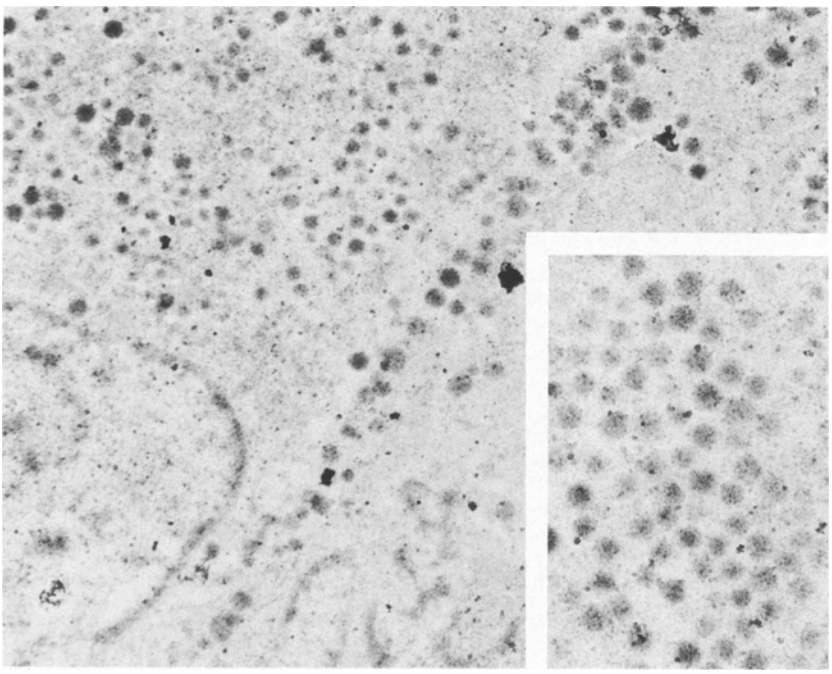

Fig. 6. Immunoelectron microscopy demonstrates the presence of β-TSH in some secretory granules. Magnification ×13,000 *Inset* shows PAP complexes on secretory granules. Magnification ×17,000

bules were numerous and a few microfilaments were detected. No lysosomal accumulation was apparent. The capillaries showed no abnormalities. In the perivascular space, a few Luse bodies composed of bands of widely-spaced collagen were observed. Based on the fine structural features, the adenoma cells were similar to TSH cells and showed no resemblance to GH cells seen in nontumorous adenohypophyses or in GH-secreting pituitary tumors.

Immunoelectron Microscopic Findings. The immunoperoxidase technique at the electron microscopic level, demonstrated GH (Fig. 5) and β-TSH (Fig. 6) in the secretory granules of adenoma cells. Some secretory granules showed no immunostaining. It was impossible to establish with certainty whether the same secretory granules showed positive immunostaining for both GH and β-TSH, or whether two separate granule populations existed.

Discussion

Although information is limited on the immunocytologic and electron microscopic features of TSH cell adenoma (Leong et al. 1976; Duello and Halmi 1977; Samaan et al. 1977; Kovacs and Horvath 1979; Waldhäusl et al. 1979), the TSH immunopositivity and the fine structural details support the interpretation that, in the present case, the pituitary tumor consisted of TSH cells.

Adenomas arising from pituitary TSH cells are assumed to be rare (Kovacs

et al. 1977; Kovacs and Horvath 1979; Gershengorn 1981). They are either preceded by long-standing primary hypothyroidism (Leong et al. 1976; Vagenakis et al. 1976; Samaan et al. 1977), and are claimed to be due to chronic overstimulation resulting from lack of negative feedback effect of thyroid hormones, or they are associated with hyperthyroidism (Hamilton et al. 1970; Faglia et al. 1972; Kourides et al. 1977; Tolis et al. 1978; Afrasiabi et al. 1979; Gershengorn 1981). In the former cases, thyroid function tests are consistent with thyroid hormone deficiency and blood TSH levels are increased; in the latter cases, elevated blood TSH levels are accompanied by high blood T_3 and T_4 concentrations. Our patient had acromegaly and high blood GH concentrations, but was euthyroid clinically and biochemically with no rise in blood TSH levels. No explanation can be offered for the apparent discrepancy between immunocytologic and electron microscopic results and clinical and biochemical findings. It may be that an abnormal TSH, which had no biologic activity and was not recognized by radioimmunoassay, was secreted by the adenoma cells. Alternatively, it is possible that intracellular TSH degradation accounted for the lack of TSH hypersecretion. Silent adenomas, composed of corticotroph cells, null cells or oncocytes and unassociated with clinical and biochemical oversecretion of adenohypophysial hormones, are known to occur in the human pituitary (Kovacs and Horvath 1973; Landolt 1975; Horvath et al. 1980; Kovacs et al. 1980).

In acromegalic subjects, simultaneous elevation of blood GH and TSH levels, hyperthyroidism, as well as various forms of goiter have been noted suggesting that GH and TSH can be secreted concomitantly by pituitary tumors (Davis 1934; Lamberg et al. 1969; Linquette et al. 1969; Hamilton and Maloof 1972; Smallridge et al. 1979). There are only two publications, to our knowledge, dealing with the morphologic features of pituitary tumors producing GH and TSH. In the case reported by Waldhäusl et al. (1979), the patient had hyperthyroidism, normal blood GH and elevated TSH levels. The tumor was composed of two separate cell types, one accounting for the production of GH, the other for that of TSH. Saeger and his associated (1980) described two patients with acromegaly and hyperthyroidism. The tumors consisted of an admixture of TSH cells showing a varying degree of differentiation.

In the pituitary tumor investigated by us, one cell type was identified. By the immunoperoxidase technique, many cells contained GH and practically every cell showed positive immunostaining for TSH. The study of consecutive and mirror sections provided evidence that GH and TSH were present in the cytoplasm of the same adenoma cells. The fine structural features of adenoma cells were similar to those of TSH cells, showing no resemblance to GH cells seen in nontumorous pituitaries and in GH-secreting tumors (Kovacs et al. 1977). Hence, in our case, one cell type, apparently the TSH cell, was capable of producing two hormones markedly different in chemical composition, immunoreactivity and biologic action.

GH- and TSH-producing pituitary adenomas were also observed by Furth et al. (1973a, b) in mice rendered hypothyroid by radiothyroidectomy. Concordant with our conclusion, they were interpreted as consisting of one cell type, since the immunoperoxidase technique revealed GH and TSH in the same area of the adenomas.

Production of GH by TSH cells is not in accordance with the view that these two hormones are produced by two separate, morphologically distinct cell types. The presence of uncommitted adenohypophysial stem cells capable of producing multiple hormones in the early phases of fetal life and their subsequent maturation into committed precursors and differentiated, monohormonal adenohypophysial cells is an intriguing possibility. Some cells, while becoming adenomatous, may undergo functional dedifferentiation and acquire the ability to synthesize more than one hormone. A similar theory was proposed by Furth et al. (1973a, b) based on investigation of adenomas of the rodent pituitary. In their view, multiple hormone production may be ascribed to derepression of the genetic code when cells undergo neoplastic transformation. It remains to be determined whether these explanations are applicable to human hypophysial tumors.

The report of our case underlines the importance of the immunoperoxidase technique and electron microscopy in the study of pituitary tumors. The question of how frequently TSH cell adenomas are overlooked in patients with acromegaly is not clear and answers can only be provided by the immunocytologic and fine structural investigation of a large number of pituitary adenomas removed from acromegalic patients. It may well be that this unusual tumor type is not as rare as previously believed.

Acknowledgement. This work was supported in part by Grant MA-6349 of the Medical Research Council of Canada and by Grant 1 RO 1 CA 21905-01 awarded by the National Cancer Institute, DHEW. The authors wish to thank Mrs. Nancy Ryan and Miss Donna McComb for their contribution in the immunocytologic and electron microscopic studies, and Mrs. Wanda Wlodarski for invaluable secretarial work

References

Afrasiabi A, Valenta L, Gwinup G (1979) A TSH secreting pituitary tumour causing hyperthyroidism: presentation of a case and review of the literature. Acta Endocrinol (Kbh) 92:448–454

Davis AC (1934) The thyroid gland in acromegaly. Proc Staff Meet Mayo Clin 9:709–714

Duello TM, Halmi NS (1977) Pituitary adenoma producing thyrotropin and prolactin. An immunocytochemical and electron microscopic study. Virchows Arch [Pathol Anat] 376:255–265

Faglia G, Ferrari C, Neri V, Beck-Peccoz P, Ambrosi B, Valentini F (1972) High plasma thyrotrophin levels in two patients with pituitary tumour. Acta Endocrinol (Kbh) 69:649–658

Furth J, Martin JM, Moy P, Ueda G (1973a) Growth hormonal activity of thyrotropic pituitary tumors. Proc Soc Exp Biol Med 142:511–515

Furth J, Moy P, Hershman JM, Ueda G (1973b) Thyrotropic tumor syndrome. A multiglandular disease induced by sustained deficiency of thyroid hormones. Arch Pathol 96:217–226

Gershengorn MC (1981) Inappropriate thyroid-stimulating hormone secretion: description and classification. In: Weintraub BD (moderator) pp 340–344. Inappropriate secretion of thyroid-stimulating hormone. Ann Intern Med 95:339–351

Hamilton CR Jr, Adams LC, Maloof F (1970) Hyperthyroidism due to thyrotropin-producing pituitary chromophobe adenoma. N Engl J Med 283:1077–1080

Hamilton CR, Jr, Maloof F (1972) Acromegaly and toxic goiter. Cure of the hyperthyroidism and acromegaly by proton-beam partial hypophysectomy. J Clin Endocrinol Metab 35:659–664

Heitz PU (1979) Multihormonal pituitary adenomas. Hormone Res 10:1–13

Horvath E, Kovacs K (1976) Ultrastructural classification of pituitary adenomas. Can J Neurol Sci 3:9–21

Horvath E, Kovacs K, Killinger DW, Smyth HS, Platts ME, Singer W (1980) Silent corticotropic adenomas of the human pituitary gland. A histologic, immunocytologic and ultrastructural study. Am J Pathol 98:617–638

Kourides IA, Ridgway EC, Weintraub BD, Bigos ST, Gershengorn MC, Maloof F (1977) Thyrotropin-induced hyperthyroidism: use of alpha and beta subunit levels to identify patients with pituitary tumors. J Clin Endocrinol Metab 45:534–543

Kovacs K, Horvath E (1973) Pituitary "chromophobe" adenoma composed of oncocytes. A light and electron microscopic study. Arch Pathol 95:235–239

Kovacs K, Horvath E (1979) Pituitary adenomas: pathologic aspects. In: Tolis G, Labrie F, Martin JB, Naftolin F (eds) Clinical neuroendocrinology. A pathophysiological approach. Raven Press, New York, pp 367–384

Kovacs K, Corenblum B, Sirek AMT, Penz G, Ezrin C (1976) Localization of prolactin in chromophobe pituitary adenomas: study of human necropsy material by immunoperoxidase technique. J Clin Pathol 29:250–258

Kovacs K, Horvath E, Ezrin C (1977) Pituitary adenomas. Pathol Annu 12 part 2:341–382

Kovacs K, Horvath E, Bayley TA, Hassaram ST, Ezrin C (1978) Silent corticotroph cell adenoma with lysosomal accumulation and crinophagy. A distinct clinicopathologic entity. Am J Med 64:492–499

Kovacs K, Horvath E, Ryan N, Ezrin C (1980) Null cell adenoma of the human pituitary. Virchows Arch [Pathol Anat] 387:165–174

Lamberg BA, Ripatti J, Gordin A, Juustila H, Sivula A, Bjorkesten G (1969) Chromophobe pituitary adenoma with acromegaly and TSH-induced hyperthyroidism associated with parathyroid adenoma. Acromegaly and parathyroid adenoma. Acta Endocrinol (Kbh) 60:157–172

Landolt AM (1975) Ultrastructure of human sella tumors. Correlations of clinical findings and morphology. Acta Neurochir [Suppl] 22:1–167

Landolt AM (1978) Progress in pituitary adenoma biology. Results of research and clinical applications. Adv Techn Standards Neurosurg 5:3–49

Leong AS, Chawla JC, Teh EC (1976) Pituitary thyrotropic tumour secondary to long-standing primary hypothyroidism. Pathol Eur 11:49–55

Linquette M, Herlant M, Fossati P, May JP, Decoulx M, Fourlinnie JG (1969) Adénome hypophysaire à cellules thyréotropes avec hyperthyroidie. Ann Endocrinol (Paris) 30:731–740

McCarty KS, Jr, Bredesen DE, Vogel FS (1978) Neoplasms of the anterior pituitary. Neurosurgery 3:96–104

Moriarty GC, Garner LL (1977) Immunocytochemical studies of cells in the rat adenohypophysis containing both ACTH and FSH. Nature 265:356–358

Saeger W, Lüdecke D, v.z. Mühlen A (1980) TSH-producing pituitary adenomas. Frequency, histology and ultrastructure. Acta Endocrinol (Kbh) [Suppl] 234:63–64

Samaan NA, Osborne BW, Mackay B, Leavens ME, Duello TM, Halmi NS (1977) Endocrine and morphologic studies of pituitary adenomas secondary to primary hypothyroidism. J Clin Endocrinol Metab 45:903–911

Smallridge RC, Wartofsky L, Dimond RC (1979) Inappropriate secretion of thyrotropin: discordance between the suppressive effects of corticosteroids and thyroid hormone. J Clin Endocrinol Metab 48:700–705

Tolis G, Bird C, Bertrand G, McKenzie JM, Ezrin C (1978) Pituitary hyperthyroidism. Case report and review of the literature. Am J Med 64:177–181

Vagenakis AG, Dole K, Braverman LE (1976) Pituitary enlargement, pituitary failure and primary hypothyroidism. Ann Int Med 85:195–198

Waldhäusl W, Bratusch-Marrain P, Nowotny P, Büchler M, Forssmann WG, Lujf A, Schuster H (1979) Secondary hyperthyroidism due to thyrotropin hypersecretion: study of pituitary tumor morphology and thyrotropin chemistry and release. J Clin Endocrinol Metab 49:879–887

Accepted November 13, 1981

Virchows Arch [Pathol Anat] (1982) 395:69–76

Virchows Archiv A

Squamous Metaplasia Following Necrosis of the Adenohypophysis and of a Chromophobe Adenoma of the Pituitary

John J. Kepes[1], Jerome Sayler[2], and Roman Hiszczynskyj[3]

[1] University of Kansas School of Medicine, Kansas City, KS 66103
[2] Central Kansas Medical Center, Great Bend, KS
[3] Stormont-Vail Medical Center, Topeka, KS, USA

Summary. Two cases of pituitary necrosis are presented, one occurring post partum in an otherwise normal gland, the other in a large chromophobe adenoma. In both cases the necrotic tissue became surrounded by squamous epithelial nests that developed through metaplasia from glandular cells of the adenohypophysis and adenoma cells respectively. The squamous elements were seen 6 days after the clinical events leading to pituitary necrosis in the first case and 20 days after pituitary apoplexy (hemorrhagic necrosis of an adenoma) in the second case. In contradistinction to the commonly found squamous nests which are usually located in the pars tuberalis and presumably develop through a slower process, the changes in the present two cases indicate that squamous metaplasia can develop quite rapidly at the margins of a necrotic process of the pituitary, either deep in the gland as in case 1 or occupying the entire circumference of a necrotic tumor as in case 2.

Key words. Pituitary adenoma – Pituitary apoplexy – Squamous metaplasia – Postpartum necrosis

Introduction

Squamous cell nests are not uncommonly found in pituitary glands. First observed by Luschka in 1860, they are most often seen in the pars tuberalis of the gland. Luse and Kernohan (1955) in an autopsy study of 1,364 pituitary glands identified squamous epithelium in 333 (24%) of them. Since none of the 78 pituitaries from patients less than ten years of age at the time of death contained squamous elements, these authors concluded that the squamous cells do not represent embryonic rests, but more likely develop through metaplasia of glandular epithelium of the adenohypophysis. This was in support of the opinion expressed earlier by Carmichael (1931), Biggart (1949), as well as Grinker and Bucy (1949) and Hunter (1955). Although Goldberg and Eshbaugh

Offprint requests to: J.J. Kepes at the above address

0340-1227/82/0395/0069/$01.60

(1960) a few years later were able to demonstrate squamous nests in the pituitaries of four newborns and one 2-month-old infant, it remains a fact that such cell nests are very rare in young individuals and their number appears to increase with age, presumably through a metaplastic process. The finding of squamous nests in otherwise normal pituitary glands sheds little light on the cause of such metaplasia and on the length of time it may take for such metaplastic process to develop. In contrast, we have recently observed two cases where extensive squamous metaplasia developed as an apparent tissue response to necrosis: in the first case ischemic necrosis of a non-neoplastic pituitary, in the second case hemorrhagic necrosis of a chromophobe adenoma (i.e., a case of "pituitary apoplexy"). In both cases the time interval between the onset of necrosis in the hypophysis and the patient's death could be deducted from the clinical history.

Case Reports

Case 1. This patient was a 35-year-old black woman with a history of five pregnancies, three deliveries and one miscarriage. Her last (fifth) pregnancy was uneventful except for episodes of documented high blood pressure, reaching at one time 150/110 mmHg. She had a normal vaginal delivery 8 days after the expected day of confinement. Because of multiparity and the history of high blood pressure, bilateral fimbriectomy was done through laparoscopy, 30 min after the completion of the delivery. During this procedure the patient developed hypotension and bradycardia with a pulse rate less than 30/min which culminated in cardiac arrest that lasted for 4 min. Resuscita-

Fig. 1. Case 1. Coagulation necrosis of anterior lobe of pituitary gland (*upper right*) with reactive squamous metaplasia at margin of necrosis (*lower left*) Hematoxylin-eosin ×90

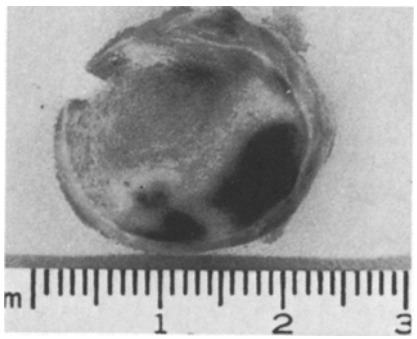

Fig. 2. Case 2. Cross section of tumor removed from greatly distended sella turcica at autopsy. The mass is encapsulated with multiple areas of grossly visible hemorrhagic necrosis

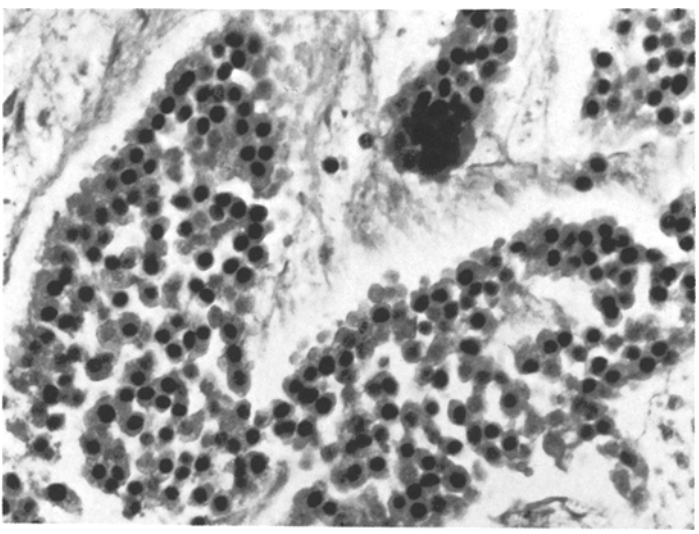

Fig. 3. One of the few non-necrotic portions of the tumor showing the typical picture of a chromophobe adenoma (H&E $\times 200$)

tion efforts were successful in the sense that heart beat and respiration were restored, but she remained unconscious and 90 min later developed generalized tonic and clonic seizures. In spite of intravenous anticonvulsant medication (Valium, Magnesium Sulfate and Phenobarbital) she suffered recurrent seizures and died on the sixth day following the cardiac arrest.

Autopsy showed generalized passive congestion of the viscera. The brain revealed hypoxic changes of gray matter in many areas, with striking anoxic necrosis of cerebellar Purkinje cells and of cerebral cortical neurons, some of them in a laminar pattern. The pituitary appeared slightly enlarged but was otherwise grossly unremarkable. Microscopically however there was evidence of recent coagulation-type necrosis in the center of the anterior lobe, involving about 35–40% of the parenchyma. Surrounding this area of necrosis and immediately contiguous to it were numerous squamous cell nests (Fig. 1). The picture was very reminiscent of squamous metaplasia seen in the prostate gland in the wake of infarction.

Case 2. This 58-year-old man, previously of apparent good health, was involved in an automobile accident on February 8, 1979 and while recuperating from a fractured hip, suddenly, for no apparent reason became comatose on March 3, 1979 and died 20 days later. At autopsy the sella turcica was distended and eroded by a globular mass, about 2.5 cm in diameter, which was rather soft

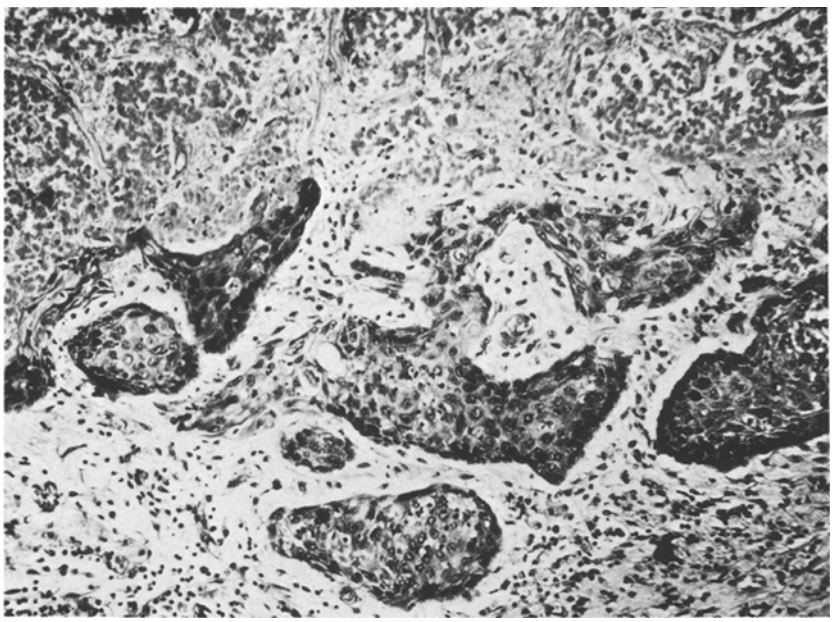

Fig. 4. The necrotic adenoma is surrounded at its periphery by nests of squamous epithelial cells (H&E ×360)

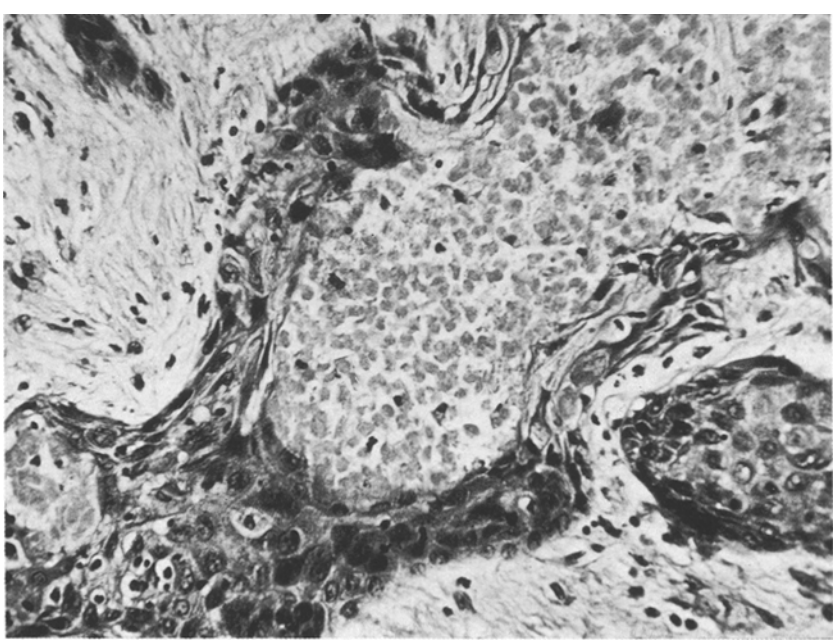

Fig. 5. Finger-like processes of squamous epithelium surround groups of necrotic adenoma cells (H&E ×360)

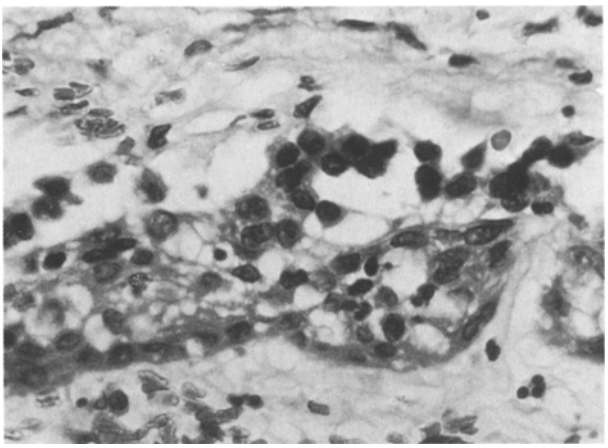

Fig. 6. In a few areas continuity between squamous cells and still viable appearing adenoma cells could be observed (H&E ×320)

and mushy and on cut surface showed areas of hemorrhagic necrosis (Fig. 2). Microscopically the mass represented a chromophobe adenoma surrounded by a fibrous capsule and some foci of non-neoplastic anterior lobe tissue. Much of the adenoma suffered hemorrhagic necrosis, but near the center of the mass there were some areas that have not totally succumbed to necrosis and they made the identification of the tumor possible (Fig. 3). In some areas necrotic debris of the tumor was engulfed by macrophages and there was also young granulation tissue present near necrotic foci. The most striking finding was the presence of irregular squamous cell nests located in a circumferential fashion between the fibrous capsule and the peripheral portions of the tumor (Fig. 4). In some areas necrotic adenoma cells were partially surrounded by arm-like extensions of squamous epithelium (Fig. 5), but in a very few areas the squamous cells appeared contiguous with remnants of non-necrotic adenoma cells (Fig. 6). The squamous cells appeared to be actively proliferating with occasional mitotic figures found among them, but there was no evidence of malignancy.

We have attempted to do immunohistochemical studies for prolactin and growth hormone on the tumor cells but did not get positive staining, partly perhaps because of advanced necrobiosis of the tumor cells. Dr. K. Kovacs (St. Michael's Hospital, Toronto) has undertaken to perform immunoperoxidase stain for keratin (Asa et al. 1981) on paraffin sections of our tumor and found the squamous component to be faintly positive. By electron microscopy the cells of the adenoma showed no discernible secretory granules, again, probably due to the necrotic process which has developed 20 days prior to the atuopsy. In contrast, squamous epithelial cells at the periphery of the tumor showed excellent preservation and had desmosomal junctions as well as cytoplasm rich in tonofilaments. They did not contain any secretory granules.

Discussion

The anterior lobe of the pituitary develops from Rathke's pouch, an evagination of the primitive stomodeum. The lining of the oral cavity that gave rise to this pouch eventually comes to be lined by stratified squamous epithelium; it is not surprising therefore that the derivates of Rathke's pouch also may differentiate into similarly constituted epithelium. Although the bulk of the lining epithelium of Rathke's pouch will develop into endocrine cells of the anterior lobe of the hypophysis, squamous cell nests have been found in the

pituitary of newborn infants (Goldberg and Eshbaugh 1960). As indicated in the introduction however, the number of squamous cells in the pituitary appear to increase with age, suggesting transformation of glandular cells of the anterior lobe into squamous elements through metaplasia (Luse and Kernohan 1955). It is not known what influence is responsible for this change which occurs predominantly in the pars tuberalis of the gland.

The develoment of squamous cell nests in our two cases had, in all probability, a pathogenesis different from the above. These nests were not found in the pars tuberalis, but immediately adjacent to necrotic tissue, in the first, non-neoplastic case, in the center of the anterior lobe; in the second case, they surrounded the necrotic adenoma in a circumferential manner. In both instances there was a strong resemblance to the arrangement of metaplastic squamous cell nests at the periphery of prostatic infarcts. Similar squamous metaplasia developing in and around infarcts of the parotid gland have also been reported by Donath (1979) who used the term necrotizing sialometaplasia to describe this phenomenon. Regressive changes associated with squamous metaplasia in salivary gland tumors, notably cystadenolymphomas of the parotid gland, have also been the focus of recent observations (Seifert et al. 1980).

All these changes from glandular epithelium to stratified squamous epithelium (whether in non-neoplastic or neoplastic conditions) in the wake of infarction or other forms of necrosis suggest that whatever groups of undifferentiated or reserve cells are present in or near the area of infarction, they proliferate to form a group of cells: squamous epithelium, that is presumably more resistant to noxious changes in the environment. The transition from a simple form of cuboidal or columnar epithelium to squamous epithelium has traditionally been regarded as a form of "progressive metaplasia" or "prosoplasia". This term is more difficult to apply if the cuboidal or columnar cells in question were in fact highly specialized glandular cells as in the case of the prostate, salivary glands or as in our cases, the anterior lobe of the pituitary. In these circumstances a change from anterior lobe cells (whether previously normal or neoplastic) to squamous cells may be regarded as a regressive form of metaplasia, particularly if one considers that squamous epithelium is characteristic of Rathke's pouch, the lining cells of which are considered as primitive predecessors of the anterior lobe cells of the hypophysis.

Squamous metaplasia of glandular cells can take place rather rapidly as commonly observed in eccrine sweat glands of the skin undergoing squamous transformation as part of wound healing. In our first case, 6 days passed between the clinically noted cardiac arrest, which in all likelihood was responsible for the infarcts in the anterior lobe of the pituitary, and the patient's death. In the second case, the patient has probably harbored his asymptomatic chromophobe adenoma for quite some time, but the clinical onset of sudden coma probably coincided with the massive hemorrhagic necrosis of the tumor (pituitary apoplexy) that created edema and pressure on surrounding tissues. In this case, 20 days passed before the patient died, allowing for squamous metaplasia to develop during that time. It should be noted that most patients who suffer this type of hemorrhagic necrosis of a pituitary tumor with a sudden increase of intracranial pressure, either die rather rapidly or are diagnosed as having

a mass in the sella and are operated by the neurosurgeon, in either case without time allowed for squamous metaplasia to take place.

As to the incidence of the changes seen in our two patients, it seems that in the non-neoplastic gland squamous metaplasia has been seen around infarcted areas by some observers (Davis 1981; Kovacs 1981). However we have not found a published report of this phenomenon. Even the detailed study of Sheehan (1965) on the repair of post-partum necrosis of the anterior lobe of the pituitary gland does not contain references to squamous metaplasia during the healing process. As far as we could determine, no similar observations have been made in cases of necrosis of a pituitary adenoma (Saeger 1977; Kovacs 1981; Rubinstein 1981).

Finally, some questions remain as to the biological character of the metaplastic squamous cells. In the first case, where they developed around a necrotic area of non-neoplastic anterior lobe, there is no reason to surmise that the squamous cells had a neoplastic nature. In the second case, however, with squamous cell nests surrounding necrotic tumor tissue, the question arises whether they developed from the remnants of surrounding non-neoplastic anterior lobe cells, or from adenoma cells? Even without preceding necrosis, squamous cell components have been occasionally seen in association with adenomas of the anterior lobe, although in such cases they are usually regarded as representing a parallel development of diverse elements of Rathke's cleft origin (which may include ciliated columnar cells also) rather than as a response to degenerative or necrotic changes (Duffy 1920; Fulstow 1928; Messimy et al. 1955; Shuangshoti et al. 1970; Kepes 1978). Nevertheless, such simultaneous occurrence attests to the potential of Rathke's pouch derivates to give rise to neoplastic endocrine as well as squamous cells in the same individual. The fact that the squamous cells in our case 2 showed some pleomorphism, hyperchromasia and a few mitotic figures, does not by itself prove their neoplastic nature since such changes are often seen in pseudoepitheliomatous hyperplasia of regenerating squamous epithelium. The fact however that squamous cells could be observed in apparent continuity with surviving adenoma cells (Fig. 6), would favor the view that they represent squamous transformation of adenoma cells in the process of "healing" within the tumor. Although true invasive squamous carcinomas arising within the pituitary (usually from preexistent epithelial cysts) have been reported (Salyer and Carter 1973), the squamous cells in our case did not show convincing evidence of being cytologically malignant.

Acknowledgements. Authors wish to thank Dr. Kalman Kovacs (St. Michael's Hospital, Toronto) and Dr. Lucien J. Rubinstein (University of Virginia Medical School) for their useful suggestions and comments, and Mrs. Donna Roembach for typing the manuscript.

References

Asa SL, Kovacs K, Bilbao JM, Penz G (1981) Immunohistochemical localization of keratin in craniopharyngiomas and squamous cell nests of the human pituitary. Acta Neuropathol (Berlin) 54:257–260

Biggart JH (1949) Pathology of the nervous system: a student's introduction. 2nd Edn, Williams and Wilkins Co., Baltimore

Carmichael HT (1931) Squamous epithelial rests in the hypophysis cerebri. Arch Neurol Psychiatr 26:966–975

Davis RL (1981) Personal Communication

Donath K (1979) Pathohistologie des Parotisinfarktes – Necrotizing sialometaplasia. Laryngol Rhinol 58:70–76

Duffy WC (1920) Hypophyseal duct tumors. Ann Surg 72:537–555 and 725–757

Fulstow M (1928) An epithelial cyst of the hypophysis. Am J Pathol 4:87–90

Goldberg GM, Eshbaugh DE (1960) Squamous cell nests of the pituitary gland as related to the origin of craniopharyngiomas. Arch Pathol 70:293–299

Grinker RP, Bucy PC (1949) Neurology. 4th Edn, Charles C. Thomas, Springfield, IL, pp 484–488

Hunter IJ (1955) Squamous metaplasia of cells of the anterior pituitary gland. J Pathol Bacteriol 69:141–145

Kepes JJ (1978) Transitional cell tumor of the pituitary gland developing from a Rathke's cleft cyst. Cancer 41: 337–343

Kovacs K (1981) Personal Communication

Luschka H (1860) Der Hirnangang und die Steissdrüse des Menschen. Georg Reimer, Berlin

Luse SA, Kernohan JW (1955) Squamous-cell nests of the pituitary gland. Cancer 8:623–628

Messimy R, Namin P, Martinez M (1955) Tumeur kystique de l'hypophyse de type vesiculaire, á revétement cilié. Troubles pigmentaries associés. Rev Neurol 235–240

Rubinstein LJ (1981) Personal Communication

Saeger W (1977) Die Hypophysentumoren. Cytologische und ultrastrukturelle Klassifikation, Pathogenese, endokrine Funktionen und Tierexperimente. Gustav Fischer Verlag, Stuttgart-New York. pp 5, 34 and 39

Salyer D, Carter D (1973) Squamous carcinoma arising in the pituitary gland. Cancer 31: 713–718

Seifert G, Bull HG, Donath K (1980) Histologic subclassification of the cystadenoma of the parotid gland. Analysis of 275 cases. Virchows Arch [Pathol Anat] 388:13–38

Sheehan HL (1965) The repair of post-partum necrosis of the anterior lobe of the pituitary gland. Acta Endocrinol 48:40–60

Shuangshoti S, Netsky MG, Nashold BS (1970) Epithelial cysts related to the sella turcica. Proposed origin from neuroepithelium. Arch Pathol 90:444–450

Accepted December 1, 1981

Virchows Arch [Pathol Anat] (1982) 395:77–85

Virchows Archiv A

Castleman's Disease in Identical Twins

C. Martin[1], M.L. Peña[1], F. Angulo[2], F. García[2], D. Vaca[2], and R. Serrano[3]

[1] Department of Pathology (Prof. Dr. A. Bullon)
[2] Department of Surgery (Prof. Dr. S. Tamames)
[3] Department of Internal Medicine (Prof. Dr. D. Espinós)
Hospital Clinico San Carlos, Facultad de Medicina, Universidad Complutense. Madrid 3, Spain

Summary. The authors present the first published case of angiofollicular lymph-node hyperplasia, observed in identical twins. In both cases the lesion had the same location, but there was a difference of two years in the time of presentation. A morphological description and discussion of pathogenesis are given.

Key Words: Castleman's disease – Giant lymphoid hamartoma – Angiofollicular lymph-node hyperplasia.

Introduction

Castleman's disease is a pathological entity of unknown aetiology, described for the first time by Symmers (1921) under the name of primary hemangiolymphoma. It was Castleman (Castleman et al. 1954; Castleman et al. 1956) who established the clinicopathological criteria for this entity, naming it lymph node hyperplasia. Later, other authors have described it as lymph nodal hamartoma (Abell 1957), benign lymphoma (Lattes and Pachter 1962), angiomatous lymphoid hamartoma (Tung and McCormack 1967), follicular lymphoreticuloma (Zettergren 1961).

The disease usually presents in people between 10 and 30 years of age (Lattes and Pachter 1962; Hochholzer et al. 1969; Llombart-Bosch and Gómez-Fayren 1978). It seems there is no sex predominance, even though some authors report that it occurs more frequently in females (Testas et al. 1980).

Two-thirds of patients have the tumor in the mediastinum (Wolfel et al. 1964; Veneziale et al. 1964; Stanford et al. 1966; Tung and McCormack 1967; Keller et al. 1972); less commonly the tumor can be found in the axillae (Zettergren 1961), cervical region (Moragas and Sala-Patau 1972), inguinal region (Enjoiji 1965), mesentery (Neerhout et al. 1969), retroperitoneal space (Lattes and Pachter 1962; Tung and McCormack 1967), muscle (Cohen 1957), lung

Offprints requests to: R. Serrano at the above address

0340-1227/82/0395/0077/$01.80

(Jamplis et al. 1961; Keller et al. 1972), and rarely in the larynx or salivary gland (Testas et al. 1980).

From the point of view of histopathology there are two varieties (Keller et al. 1972); A) The hyaline vascular type; found in 80–90% of cases, in which the lesions are clinically asymptomatic for several years, and show their presence by compression of nearby structures (Pietra 1964; Keller et al. 1972; Pérez-Peña et al. 1980); and B) The plasmacellular type, found in 10–20% of cases. The clinical features in this group are weakness, sweating, fever, retarded growth in children, elevated erythrocyte sedimentation rate, a microcytic hypochromic anemia, hypoalbuminemia, hypergammaglobulinemia and medullary plasmacytosis (Keller et al. 1972; Ballow et al. 1974; Baumann et al. 1978; Morell et al. 1979; Díaz Fernández et al. 1980).

The prognosis is usually good, and local recurrence after opperation does not occur. The best treatment is the removal of the tumor, after which all the symptoms previously mentioned disappear (Lee et al. 1965).

Clinical History

Case 1. R.T.T., a 20-year-old woman, was examined in May 1976. She had a 1-year history of a lump in the left cervical region, and had noticed another mass in the left supraclavicular fossa two months before. On physical examination, a mass (3 × 4 cm) was palpable in the left lateralcervical region; it was painless and unattached to surrounding structures. Another tumor (3 × 4 cm) was palpable in the left supraclavicular fossa. This was firm, and attached to deeper levels. Laboratory studies were within normal limits.

At operation, a mass was removed from the left lateralcervical region. It measured 3 × 4 cm, and had become partially attached to the internal jugular vein; a second mass 7 × 5 × 3 cm, found beneath the clavicle on the left side, situated under the pectoralis major muscle, surrounding the left axillary vein.

Case 2. J.T.T., 22-year-old woman and an identical twin sister of the patient in case 1, was seen in September 1978, because of a lump in the right lateralcervical region, which she had noticed two months before. During this time the patient had noticed weakness and weight loss (12 kg). On physical examination, there were two masses, one in the right lateralcervical region (3 × 4 cm) attached to the deeper levels, and the other in the right axilla unattached to surrounding structures and painless. Laboratory studies showed a raised gamma globulin (1.57 g/dl).

At operation, a mass 3 × 4 cm was found in the right lateralcervical region, attached to the jugular vein, and another mass 7 × 4 cm was situated under the right pectoralis major, closely related to the right axillary vein.

Both sisters have remained well, three and one years respectevely after operation, with no evidence of recurrence.

Pathology

Case 1. Histologic study reveals that the mass is formed by multiple lymphoid follicles, regularly distributed in a background of lymphocytes. The follicles are composed of a peripheral rim of mature lymphocytes and a central zone with large follicle center cells and histiocytes (Fig. 1).

In the germinal centers, one on more hyalinised blood vessels are seen (Fig. 2). The hyalinization often assumes a concentric arrangement around the central blood vessel. The interfollicular stroma shows a proliferation of capillaries with prominent endothelium and frequenty hyalinization of the wall. Between the vessels there are lymphocytes, plasma cells and immunoblasts (Fig. 3). Multiple

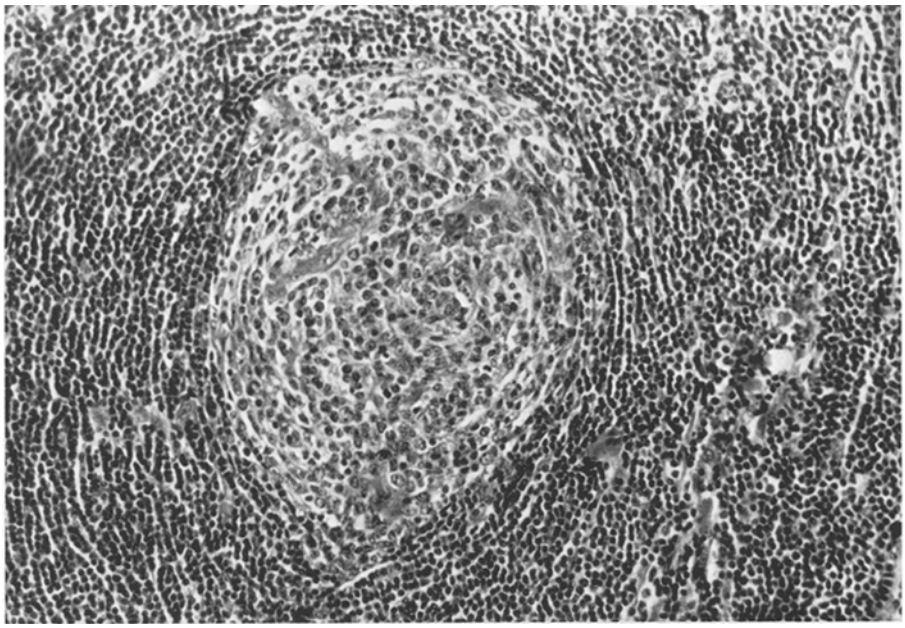

Fig. 1. The follicle-center cells consist of mature lymphocytes arranged in a concentric pattern. H&E, ×250

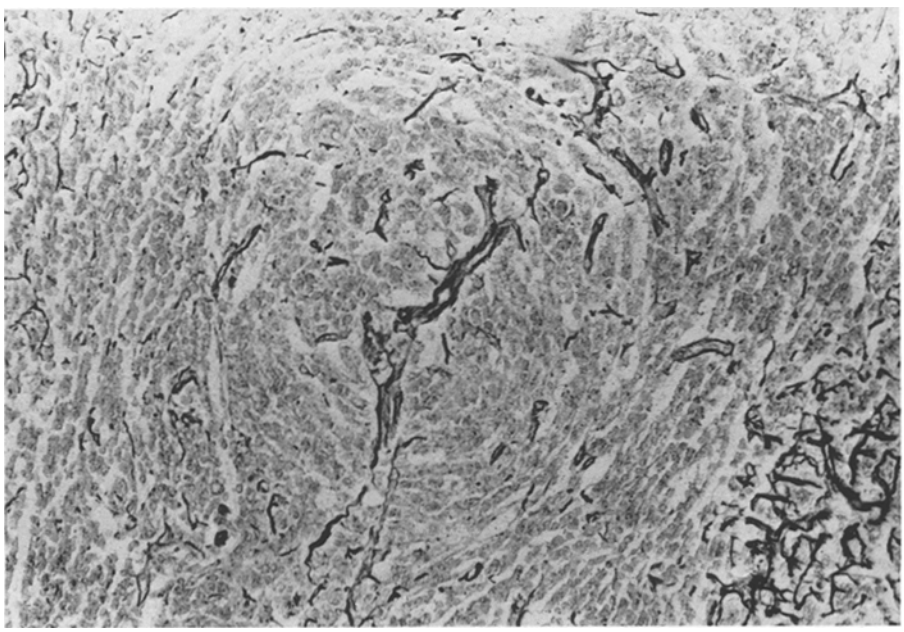

Fig. 2. Capillaries with fibrous hyalinization penetrate the small follicle center. Laidlaw stain, ×300

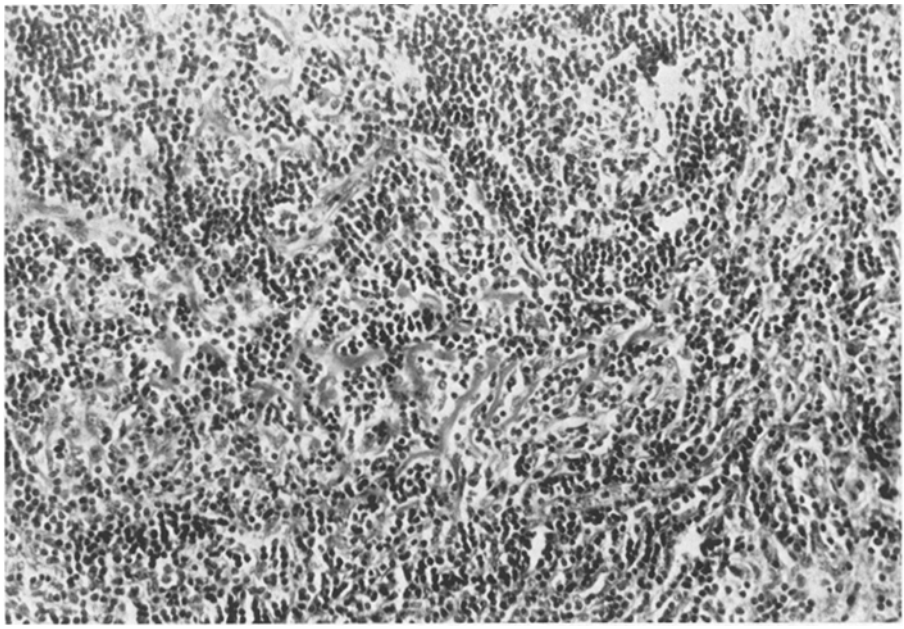

Fig. 3. The proliferated capillaries show plump endothelial cells and hyalinization. Lymphocytes and plasma cells lie between the vessels. H&E, ×166

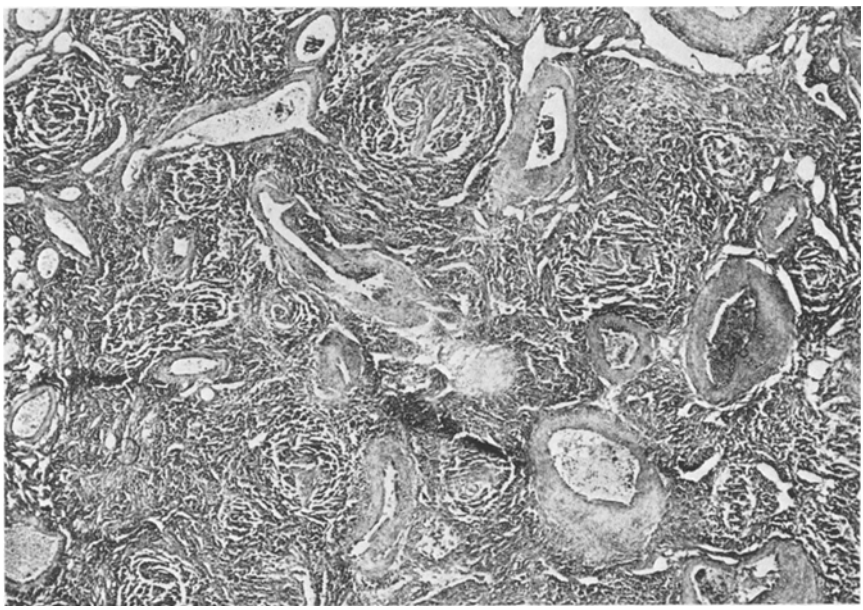

Fig. 4. Hamartomatous vessels with thick walls within the lymphoid tissue. H&E, ×166

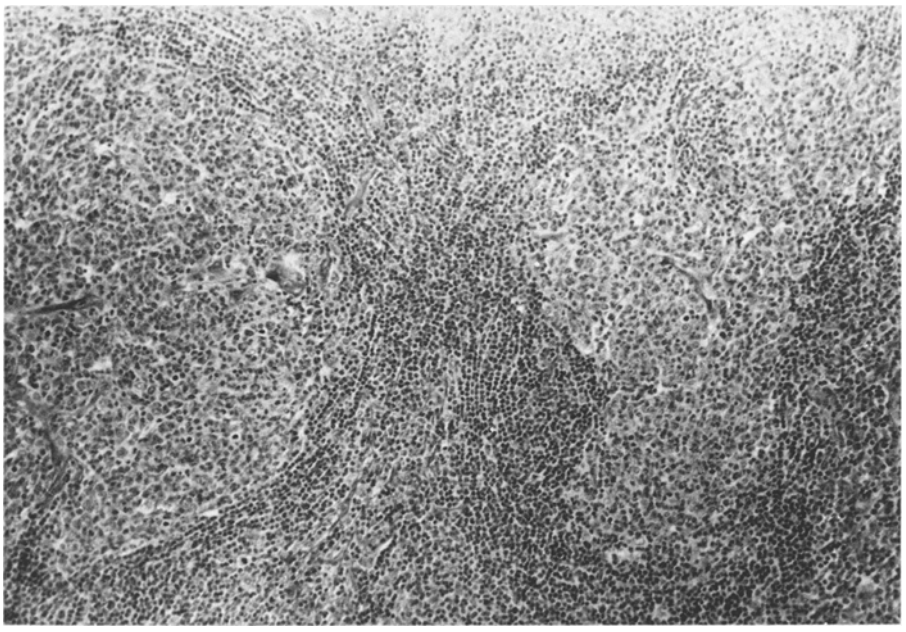

Fig. 5. The follicle center is large and cellular. The cells outside the follicle are plasma cells. H&E, ×300

tortuous vessels with wide lumina a and thickened walls are also present. Lymphoid and mature fatty tissue is seen at the margins of the lesion (Fig. 4).

A histopathologic diagnosis of "Castleman's disease, hyaline vascular type" was made.

Case 2. Histopathologic study shows larger lymphoid follicles than in the previous case. These follicles have prominent pale centers, and on irregular shape with a tendency towards hyalinization (Fig. 5). Some follicles have two on there centers. There are more plasma cells present in the interfollicular stroma that in case 1.

A histopathologic diagnosis of "Plasmacellular and Hyaline vascular type of Castleman's disease" was made.

Ultrastructure

In the interfollicular stroma we observe vessels whose endothelial cells – show projections forming arches. The lumen of the capillaries are surrounded by lymphocytes in various stages of maturity, and plasma cells (Fig. 6). The lymphocytes have abundant marginal chromatin, polarized mitochondria, ribosomes and little granular endoplasmic reticulum. In some lymphocytes the ribosomes form compact prominences around a cisterna. There are well formed venules and capillaries near pseudocavities limited by collagen bands – (Fig. 7). Collagenization is intense in some areas, surrounding groups of lymphatic cells (Fig. 8).

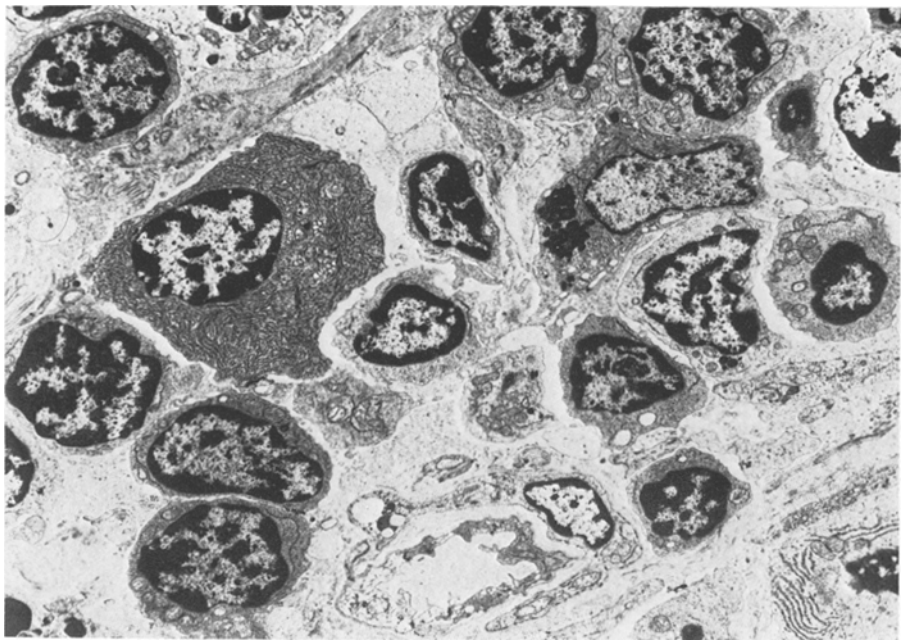

Fig. 6. Electron micrograph of interfollicular area with capillary lumen surrounded by lymphoid cells in different stages, and some plasma cells. ×8,750

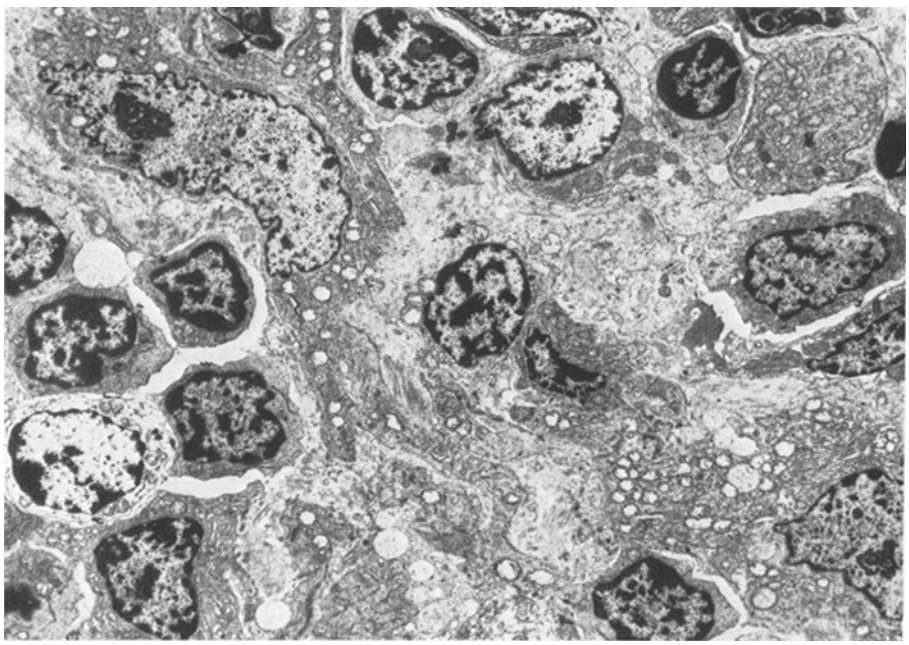

Fig. 7. Electron micrograph of sinusoid or enlarged spaces. ×7,000

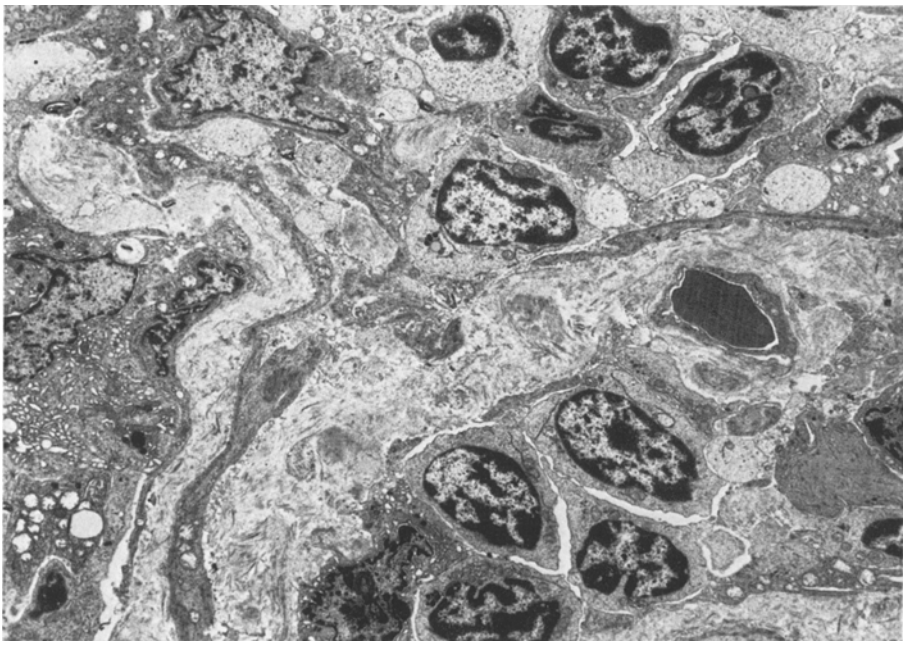

Fig. 8. Electron micrograph of collagenous tissue around areas with lymphoid cells. ×7,000

Discussion

Castleman's disease is a relatively rare entity. In 1980 there were 315 reported cases in the literature (Testas et al. 1980).

In nearly all the contributions, it is considered to be a bening disease which has a favourable course after surgical removal. We have found only two cases with a malignant course. One of them (Martin et al. 1979) corresponds to an angiofollicular hyperplasia of the hyaline-vascular type, situated in mediastinum; it was irradiated and it became a malignant lymphoma – after four years. The other case of malignant transformation was described by Laurens et al. 1973.

The true nature of this disease is controversial. There are three theories:

(A) A chronic non-specific inflamatory process as a reaction to an unknown stimulus (Castleman et al. 1956; Keller et al. 1972). This results in a nodal response consisting of a cellular infiltration of plasma cells which later changes into the hyaline-vascular type; alternatively these two forms might be two different hystological types of the same lesion, depending on the response of the host. Nevertheless, it is possible to suppose they are two different lesions caused by two closely related agents (Flendring 1969; Morell et al. 1979). The antigenic stimulus may be of an infeccious, immunological or neoplastic nature (Cohen 1957; Emson 1973).

Other authors consider the lesion to be the expression of an altered immunological response (Cabanne et al. 1965; Lennert 1964; Keller et al. 1972) manifest-

ing itself by a proliferation of germinal centres and vessels, in the course of a general activation of lymphoid tissue (probably "B" lymphocytes) (Diebold et al. 1976).

This hypothesis is the most commonly accepted. Consistent failure to show a causal agent, together with the normal appearance of nearby lymph nodes, are against this theory.

(B) Disembryonic theory. The lack of regular node structure, the absence of sinuses and the presence of neovascularization, have suggested the possibility that the lesion is a hamartoma (Abell 1957; Lattes and Pachter 1962). No evidence has been advanced that the lesions are congenital or familiar, although in the cases presented here, there is a clear genetic relationship as well as the presence of apparently hamartomatous areas. We believe these are factors in favour of this theory.

(C) Other authors think it is a benign nodal tumor (Schuman 1966). Fisher, using the electron microscope, found atypical reticular cells similar to Sternberg-Reed cell in the lesion and reached the conclusion that even though it was a apparently tumor it would have a malignant biological course (Fisher et al. 1970). We have studied one case under the electron microscope but have not found atypical cells.

References

Abell MR (1957) Lymphonodal hamartoma versus thymic choristoma of pulmonary hilium. Arch Pathol 64:584–588

Ballow M, Park BH, Dupont B, Caldwell RR, Lonsdale D, Good RA (1974) Benign giant lymphoid hyperplasia of the mediastinum with associated abnormalities of the immune system. J Pediatr 84:418–420

Baumann EP, Perrenoud JJ, Waridel D (1978) Un cas d'hyperplasie lymphoide pseudo-tumorale on maladie de Castleman. Schweiz Med Wochenschr 108:1003–1007

Cabanne F, Klepping C, Michels P, Dusserre P (1965) Pseudotumeur lymphovasculaire du mediastin. A propos d'une observation. Arch Anat Pathol 13:199–202

Castleman B, Towne VW (1954) Case records of the Massachusett's General Hospital. Case 40,001. Hyperplasia of mediastinal lymph nodes. N Engl J Med 250:26–30

Castleman B, Iverson L, Menendez VP (1956) Localized mediastinal lymphnode hyperplasie resembling thymoma. Cancer 9:822–830

Cohen H (1957) Tumor-like proliferations of lymphoid tissue. J Mt Sinai Hosp 24:750–760

Colchen A, Personne C, Audebaud G, Toty L, Hertzog P (1976) Les formes mediastinales de la tumeur de Castleman. Rev Fr Mal Respir 4:361–372

Díaz Fernández A, Ferreirós J, Lantada P, Peña ML, Martin Rodilla C (1980) Enfermedad de Castleman: Mito o realidad? Comentarios con presentación de un caso. Rev Clin Esp 156:361–363

Diebold J, Bientz M, Daussy M, Dessirier JL, Tricot G, Reynes M, Rochemaure J (1976) Hyperplasie lymphoide angiofolliculaire de localisation médias tinales. Etude en immunofluorescence directe. Rev. Fr Mal Respir 4:373–378

Emson H (1973) Extrathoracic angiofollicular lymphoid hyperplasia with coincidental myastenia gravis. Cancer 31:241–245

Enjoiji M (1965) Benign localized lymph-node hyperplasia. Acta Med Un Kagoshima 7:1–12

Fisher ER, Sieracki JC, Goldenberg DM (1970) Identity and nature of isolated lymphoid tumors (so-called nodal hyperplasia, hamartoma, and angiomatous hamartoma). Cancer 25:1286–1300

Flendring JA (1969) The benign giant lymphoma. Proefschrift Katholieke Universitiet te Nijmegen, N.V. Drukkerij "Helmond", Helmond, The Netherlands (in Dutch)

Hochholzer L, Theros EG, Rosen SH (1969) Some unusual lesions of the mediastinum: roentgenologic and pathologic features. Semin Roentgenol 4:74–90

Jamplis RW, North FS, Johnson WD (1961) Benign interlobar hyperplastic lymph node resembling thymoma. Arch Surg 83:894–897

Keller AR, Hochholzer L, Castleman B (1972) Hyaline-vascular and plasma cells types of giant lymph node hyperplasia of the mediastinum and other locations. Cancer 29:670–683

Lattes R, Pachter MR (1962) Benign lymphoid masses of probable hamartomatous nature. Cancer 15:197–214

Laurens A, Hittenbrond CH, Antoine HM, Duvosoir JL, Chomette O (1973) La maladie de Castleman: Aspects cliniques, evolutis, anatomo-pathologiques et etiopathogéniques. A propos d'une forme clinique atypique. Ann Méd Interne (Paris) 124:651–657

Lee SL, Rosner F, Rivero J, Feldman F, Hurwitz A (1965) Refractory anemia with abnormal iron metabolism, its remission after resection of hyperplastic mediastinal lymph nodes. N Engl J Med 272:761–766

Lennert K (1964) Pathologie der Halslymphknoten. Springer, Berlin Heidelberg New York

Llombart-Bosch A, Gómez-Fayren JM (1978) Tumor de Castleman: Hiperplasia angiofolicular linfoide de localización mediastínica. Un estudio de tres casos. Med Esp 77:125–137

Martin Rodilla C, Peña Mayor ML, Blanco J, Acevedo A (1979) Castleman disease. A Clinic-patological study of four cases. Pathol Res Pract 165:121

Moragas A, Sala-Patau E (1972) Hamartoma linfoide laterocervical. Med Clin 58:314–317

Morell F, Morera J, García Vandrell G (1979) Variedad plasmocelular de la enfermedad de Castleman. Arch Broncomenol 15:81–83

Neerhout RC, Larson W, Mansur P (1969) Mesenteric lymphoid hamartoma associated with chronic hypoferremia, anemia, growth failure and hyperglobulinemia. N Engl J Med 280:922–925

Pérez Peña F, Tejero J, Martin Rodilla C, Peña ML, Sanz F, Murié M, Gonzalez N, Schuller A (1980) Enfermedad de Castleman: linfoma difuso histiocitico en la evolución de la hiperplasia linfonodular hialino-vascular es una entidad benigna? Rev Clin Esp 158:83–86

Pietra G (1964) Hyalinisierende plasmazelluläre lymphknotenhyperplasie (Castleman). Schweiz Med Wochenschr 94:1755–1757

Schuman HJ (1966) Zur kenntnis der angiofollikulären lymphknotenhyperplasia (Zwiebelschalenlymphom). Zentralbl Allg Pathol 109:67–71

Stanford W, Givler R, Lawrence MS (1966) Mediastinal lymph node hyperplasia. J Thorac Cardiovasc Surg 52:303–308

Symmers D (1921) Primary hemangiopymphoma of the hemal nodes: An unusual variety of malignant tumor. Arch Intern Med 28:467–474

Testas P, Pigne A, Voinnesson A, Vieillefond A, Paillas J (1980) Les hyperplasies lymphoïdes angiofolliculaires (Maladie de Castleman). Première localisation méso-sigmoïdienne. Chirurgie 106:156–160

Tung KSK, McCormack LJ (1967) Angiomatous lymphoid hamartoma. Cancer 20:525–536

Veneziale C, Sheridan LA, Payne WS, Harrison EG Jr (1964) Angiofollicular lymphoide hyperplasia of the mediastinum. J Thorac Cardiovasc Surg 47:111–121

Wolfel SS, Antonius JJ, Cowley RA (1964) Posterior mediastinal lymph-node – hyperplasia. Am J Roentgen 91:120–124

Zettergren L (1981) Probably neoplastic proliferation of lymphoid tissue (follicular lymph-reticuloma). Acta Pathol Microbiol Scand 51:113–126

Accepted September 23, 1981

Virchows Arch [Pathol Anat] (1982) 395:87–98

Virchows Archiv A

Intracellular Keratins in Normal and Pathological Bronchial Mucosa

Immunocytochemical Studies on Biopsies and Cell Suspensions

Françoise Bejui-Thivolet[1], Jacqueline Viac[2], Jean Thivolet[2], and Michel Faure[2]

[1] Laboratoire d'Anatomie Pathologique (Pr. J.L. Vauzelle), Hôpital de la Croix-Rousse, 93, grande rue de la Croix-Rousse, 69317 Lyon Cédex 1 (France)
[2] U. 209 INSERM – ERA 788 CNRS (Pr. J. Thivolet), Laboratoire de Recherche Dermatologique, Hôpital Edouard Herriot, 69374 Lyon Cédex 2 (France)

Summary. The distribution of intracellular keratins was investigated in normal bronchial epithelium and in several morphologically distinct forms of respiratory tract carcinomas. This study was performed with two different experimentally produced antisera against normal human stratum corneum keratin and against keratin protein of MW 67000 dalton, using indirect immunofluorescence and immunoperoxidase methods on tissue sections and cell suspensions.

In *normal bronchial epithelium,* the basal cells were strongly labelled by both antisera. The ciliated columnar cells appeared devoid of cytokeratins in tissue sections but were strongly labelled with both antisera in cell suspensions. The goblet cells remained negative in every case. In *squamous metaplasia* of the bronchus, all epithelial cells were unevenly stained with both antisera.

Among *tumours,* only the squamous cell carcinomas were strongly labelled by both antisera. Primary lung adenocarcinoma appeared weakly positive, whereas metastatic lung carcinomas, undifferentiated lung carcinomas, oat cell tumours, carcinoid tumours were negative.

The immunocytochemical determination of keratins appears to be of value in the study of normal and abnormal epithelial differentiation, in the diagnosis of poorly differentiated carcinomas and in their distinction from metastatic tumours of the lung.

Key words. Bronchial mucosa – Cell suspension – Lung carcinomas – Keratin polypeptides – Immunohistochemistry

Introduction

Recent studies have demonstrated the presence of keratin proteins (K) in various kinds of epithelial tissues using antikeratin antisera and immunocytochemical

Offprint request to F. Bejui-Thivolet, at the above address

0340-1227/82/0395/0087/$02.40

testing (Franke et al. 1978; Schlegel et al. 1980b). The use of antisera that are specific for keratins represents a new tool in the determination of the epithelial origin of poorly differentiated tumours (Schlegel et al. 1980a; Sienski et al. 1981).

Specific antisera against various keratin polypeptides have been used for the study of normal and pathological keratinization (Viac et al. 1980a). It has been demonstrated that 67 K keratin polypeptide of MW 67,000 dalton (67 K) is only expressed in the suprabasal layers of human normal epidermis (Viac et al. 1980a; Loening et al. 1980) and that its expression is markedly decreased in dyskeratotic inflammatory processes such as psoriasis (Thaler et al. 1978) and altered in skin basal and squamous cell carcinomas (Thivolet et al. 1980; Viac et al. 1980b).

These findings suggest that the 67 K may be considered to be a marker of normal epithelial differentiation (Viac et al. 1980a, b).

In the present study we have investigated the distribution of the 67,000 dalton protein and of total keratin (TK) in normal bronchial mucosa and a variety of lung tumours, detected by using indirect immunofluorescence and immunoperoxidase methods performed on tissue sections and cellular suspensions.

Material and Methods

1. Mucosa Specimens and Cell Suspensions

Thirteen cell suspensions and 45 bronchial mucosa biopsies were collected from the Bronchoscopy Department of the Respiratory Clinic (Pr. Kalb, Dr. Guerin) of the Croix-Rousse Hospital (Lyon, France). Seventeen surgical specimens were obtained from the clinic of Thoracic Surgery of the Cardiovascular Hospital (Lyon, France).

Thirty-one normal mucosa or non dysplastic changes specimens and 31 tumours were studied. These tumours were 20 squamous cell carcinomas, 5 adenocarcinomas, 3 undifferentiated large cell carcinomas, 2 carcinoid tumours, 1 oat cell carcinoma.

Surgical specimens and bronchoscopic biopsies were fixed in Bouin's solution for 24 h. Prompt fixation of tissues proved to be an important factor for the optimal demonstration of cytokeratin (Schlegel et al. 1980b). The paraffin-embedded blocks were sectioned at 3.4 μm. Tissue sections were dewaxed and rehydraded in a graded alcohol series for the following immunological studies.

Table 1. Distribution of keratin polypeptides in normal bronchial cells

		TK antiserum	67 K antiserum
Tissue sections 31[a]	Basal cell	[b]	[b]
	Ciliated columnar cell	[d]	[e]
	Goblet cell	[e]	[e]
Cell suspensions 13[a]	Basal cell	[b]	[b]
	Ciliated columnar cell	[b]	[c]
	Goblet cell	[e]	[e]

[a] Number of cases
[b] Strong and diffuse intracellular labelling
[c] Moderate labelling
[d] Weak labelling
[e] No labelling

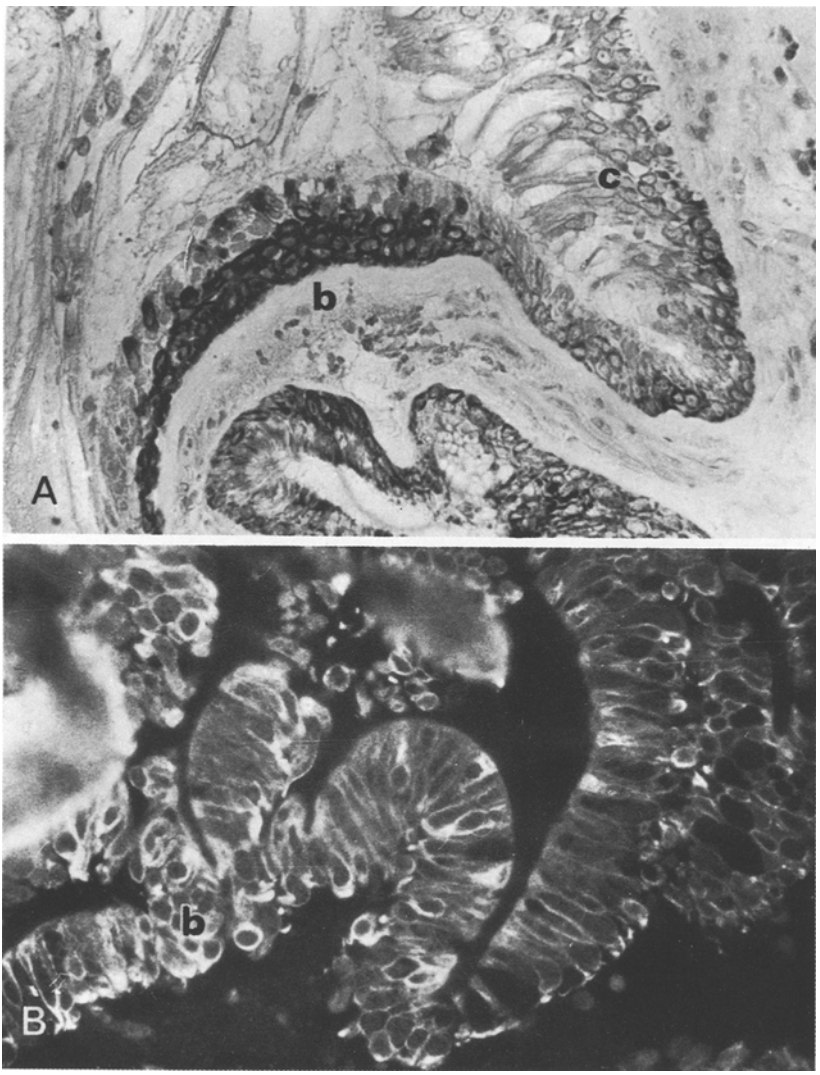

Fig. 1 A, B. Normal bronchial mucosa. Tissue sections are reacted with anti TK serum in immunoperoxidase (**A**) and immunofluorescence (**B**). Note the intense staining of basal cells (*b*) while columnar cells (*c*) are only faintly positive or negative (original magnifications respectively: $\times 300$ and $\times 400$)

Cells Suspensions. Bronchoscopic brushes were washed with phosphate buffered saline (PBS) immediately at the time when fibroscopic examination was performed. The cell suspensions were cytocentrifuged (200 g $\times$ 10 min), fixed in buffered formol acetone at $-25°$ C, washed in distilled water then directly proceded for immunological studies.

2. Extraction of Keratins

Keratins were extracted from human stratum corneum (foot callus) by TRIS buffer pH 9.0 containing 6 M urea and 0.1 m mercaptoethanol according to a technique already described (Viac et al. 1980b).

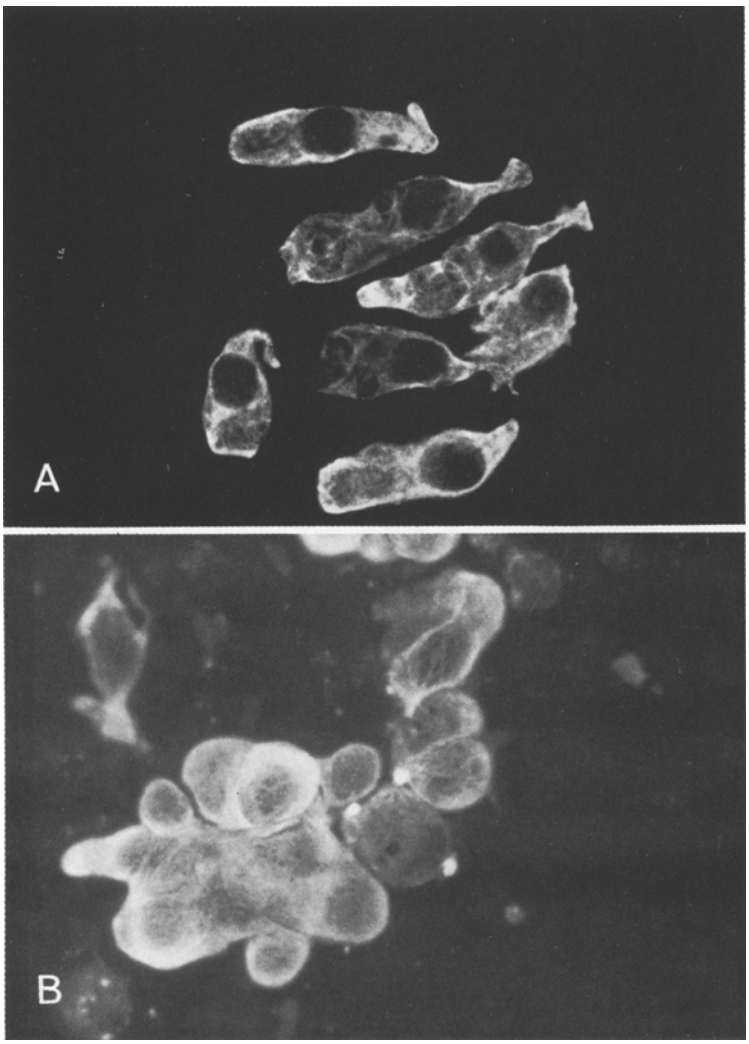

Fig. 2A, B. Immunofluorescence of ciliated (**A**) and basal cells (**B**) in suspensions reacted with anti TK serum. Only the cytoplasm is reacting while the nucleus is not (original magnification: ×400)

Fibrous proteins were then subjected to electrophoresis on 12% polyacrylamide slab gels prepared as described by Laemmli (1970) for analysis of polypeptides. The high molecular weight 67 K protein and total keratin were used for immunization.

3. Antisera

Antikeratin Antisera. 5 mg of purified keratin were emulsified in complete Freund adjuvant then injected intradermally, subcutancously and intramuscularly into rabbits. At three week intervals, the animals recieved a second and third injection of the same amount of protein. They were bled on the 7th day after the last injection (Viac et al. 1978).

Anti 67 K Antisera. Antisera to 67 K keratin polypeptides were produced in Hartley guinea pigs as previously described (Staquet et al. 1979).

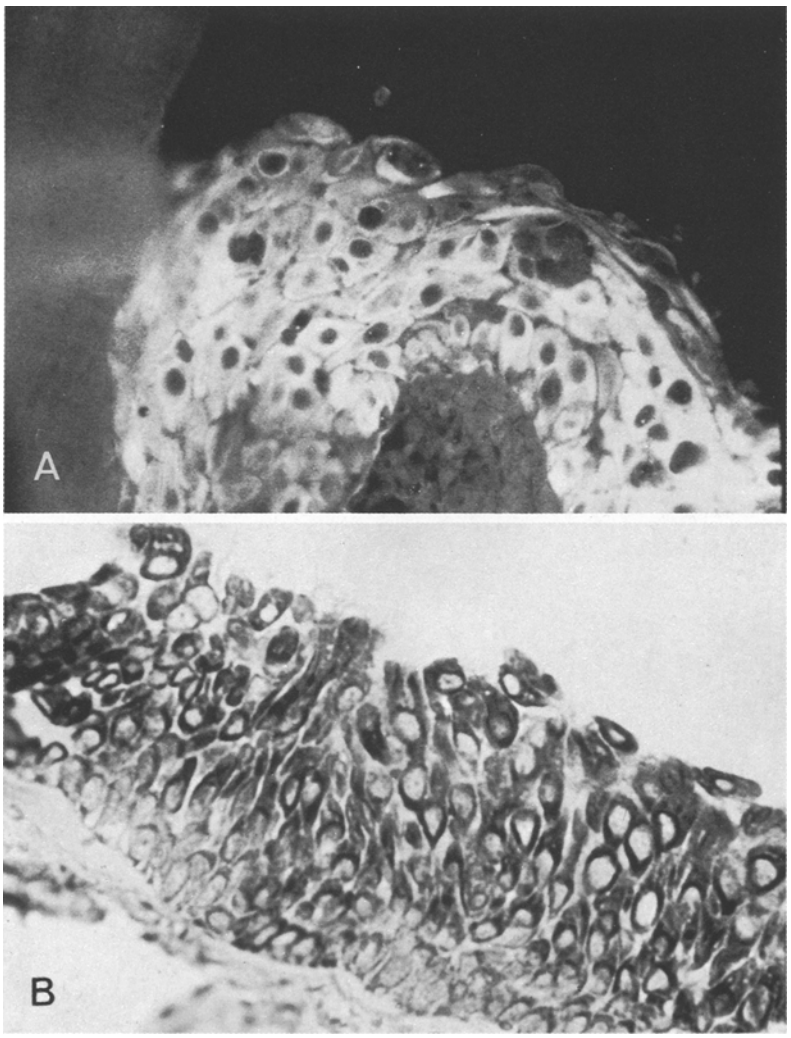

Fig. 3A, B. Squamous metaplasia. Tissue sections are reacted with anti 67 K serum in immunofluorescence (**A**) and immunoperoxidase (**B**). Diffuse staining with areas of cells that react only faintly (original magnification: ×400)

All immune sera obtained were absorbed successively with human erythrocytes and liver powder and their specificity tested by indirect immunofluorescence on normal human skin biopsies and by immunodiffusion against keratin (Thivolet et al. 1980; Viac et al. 1980a).

4. Immunofluorescence (IF) and Immunoperoxidase Stainings

These two techniques were performed on deparaffinized tissue sections and on cell suspensions.

For IF studies, commercialy available (NORDIC) fluoresceinisothiocyanate labelled goat anti guineaping IgG and swine anti rabbit IgG were used after absorption and dilution (1/50). The specificity of the IF reaction was shown by the absence of staining with sera from unimmunised animals. Indirect IF studies were performed as previously reported (Viac et al. 1980a). Slides were examined with a Leitz fluorescence microscope (epi illumination Orthoplan).

Table 2. Distribution of keratin polypeptides in bronchial squamous cell carcinomas on tissue sections

		TK antiserum	67 K antiserum
Well differentiated squamous cell carcinomas	11[a]	[b] (6)[a] [c] (5)	[b] (2)[a] [c] (5) [a] (4)
Moderately differentiated squamous cell carcinomas	7[a]	[b] (4) [c] (2) [d] (1)	[b] (1) [c] (1) [d] (2) [e] (3)
Poorly differentiated squamous carcinomas	2[a]	[c] (2)	[a] (1) [e] (1)

[a] Number of cases
[b] Diffuse and strong labelling; numerous dyskeratotic cells
[c] Moderately but diffuse labelling with some dyskeratotic cells
[d] Irregular and weak labelling with some negative cells
[e] No labelling and no dyskeratotic cells

Indirect immunoperoxidase was performed using specific sera (TK or 67 K antisera, diluted 1/50) and peroxidase conjugated specific sera (NORDIC) as described by Bustamante et al. (1978); Schmitt (1979); Thivolet et al. (1980) 3-3′ diaminobenzidine (Sigma) was used to reveal peroxidase activity (Graham and Karnovsky 1966).

In every test, normal human skin specimens (4 μm deparaffinized sections), were included as positive controls.

Results

1. Normal Bronchial Mucosa (Table 1)

As seen in Fig. 1 the basal cells exhibited a brown staining with immunoperoxidase in tissue sections (Fig. 1 A) or a bright green fluorescence of their cytoplasm in IF (Fig. 1 B) with the two antisera, while ciliated columnar cells reacted only poorly with the TK antiserum and were negative with the 67 K antiserum.

In cell suspensions columnar and basal cells were both strongly labelled with each serum (Fig. 2 A and B). An intense staining was noted on the ciliated border of the cells.

Goblet cells were negative

2. Benign Non Dysplastic Changes in Bronchial Mucosa

Basal cells from benign hyperplastic lesions reacted strongly with each antiserum on sections and cell suspensions.

Squamous metaplasia displayed a patchy but diffuse positive keratin labelling: areas of metaplasic cells were only weakly labelled (Fig. 3 A and B).

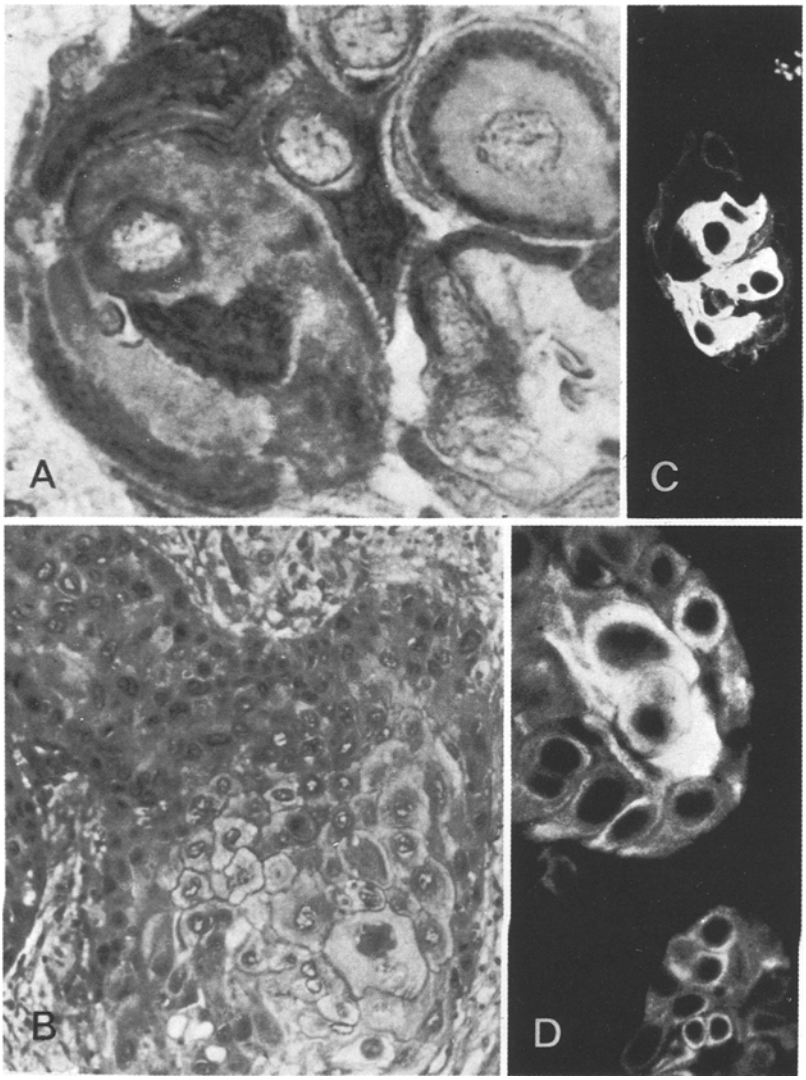

Fig. 4A-D. Well differentiated squamous cell carcinoma (**B**). Tissue sections reacted with anti TK serum in immunoperoxidase (**A**) or immunofluorescence (**C** and **D**). Dyskeratotic cells are strongly stained. Note the peripheral cytoplasmic rim (*a*) (original magnifications: **A:** × 1,250, **B C D:** × 500)

3. Lung Tumours

Squamous cell carcinomas (Table 2)

In keratinizing or highly differentiated squamous carcinomas all tumour cells were labelled. The numerous dyskeratotic cells were all strongly labelled by each antiserum (Fig. 4). As seen in Fig. 4A, TK antiserum reacted with cytoplasmic constituants which were located at the periphery of the cells along the cytoplasmic membrane.

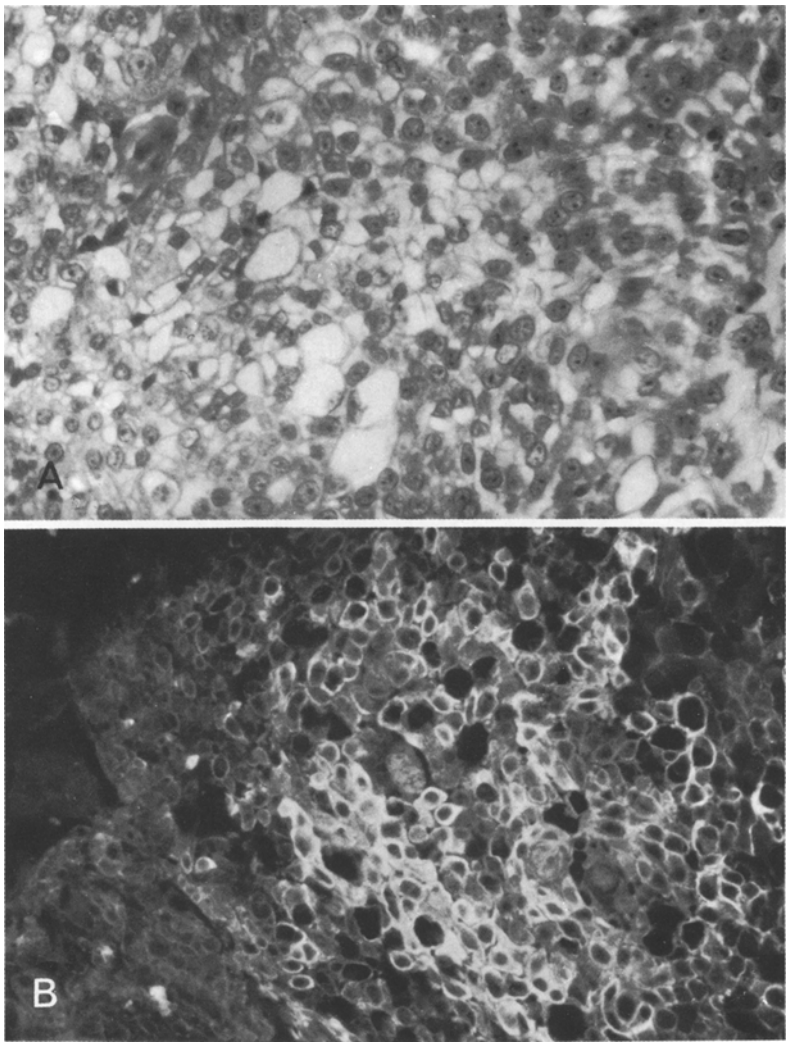

Fig. 5A, B. Clear cell carcinoma (**A**) reacted with anti TK serum (immunofluorescence) (**B**): irregular intensity of staining among the tumour (original magnification: ×250)

In moderately differentiated squamous cell carcinomas, most of the cells were strongly labelled, although some tumour cells were negative with each antiserum. In some areas, cells positive with the total keratin antiserum were negative for the presence of the 67 K protein. Clear cell carcinomas exhibited a constant but irregular fluorescence with each serum (Fig. 5 B).

In non keratinizing or poorly differentiated carcinomas, only some areas with anaplastic cells were found to react with TK antiserum (Fig. 6 B). The fluorescence was weak. Cells did not react with the 67 K antiserum.

Other Lung Tumours. From Table 3 it can be seen that in only one case of bronchogenic carcinoma, was cellular fluorescence obtained, with TK antiserum only.

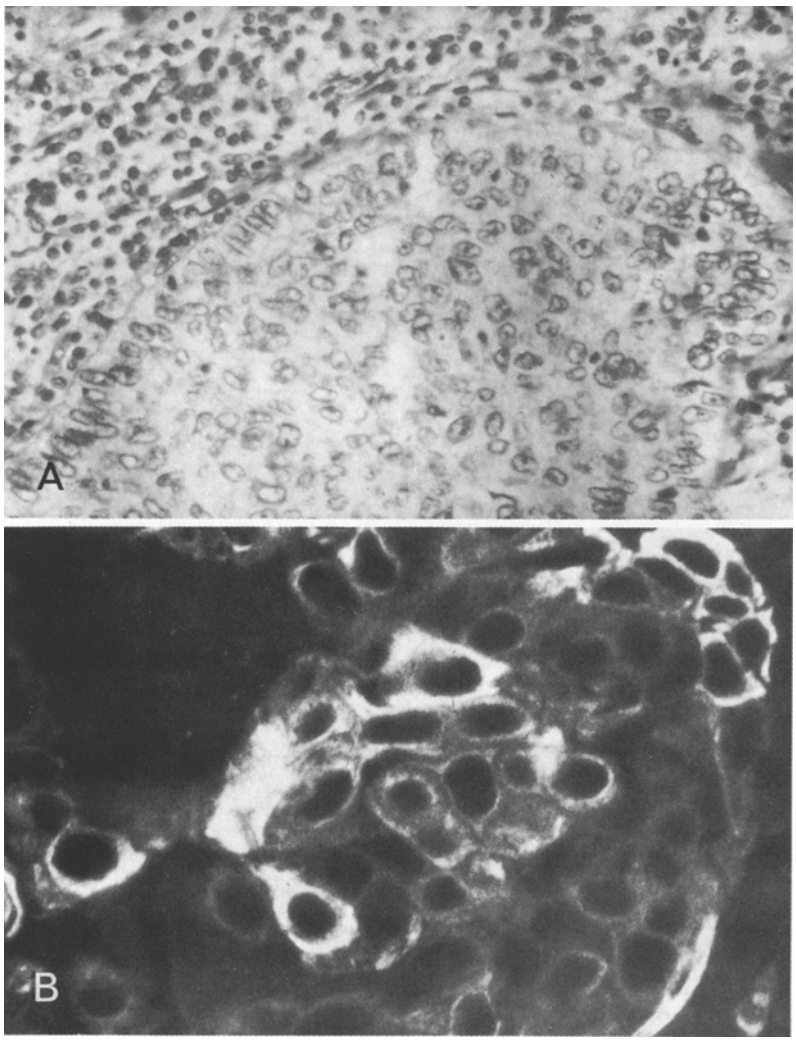

Fig. 6A, B. Poorly differentiated carcinoma (**A**) reacted with anti TK serum (immunofluorescence) (**B**): Only a few cells are stained. (original magnifications: **A**: ×250; **B**: ×500)

Table 3. Distribution of keratin polypeptides in the other respiratory tract tumours on tissue sections

		TK antiserum	67 K antiserum
Adenocarcinomas			
– bronchogenic adenocarcinoma	1[a]	[b]	[c]
– bronchoalveolar carcinoma	1	[c]	[c]
– metastatic adenocarcinoma	3	[c]	[c]
Oat cell carcinoma	1	[c]	[c]
Carcinoid tumour	2	[c]	[c]
Undifferentiated large cell carcinoma	3	[c]	[c]

[a] Number of cases
[b] Uneven and weak labelling
[c] No labelling

No staining was observed in bronchoalveolar or metastatic adenocarcinomas, in oat cell carcinoma, carcinoid tumours and undifferentiated large cell carcinomas.

Discussion

In the present study, we have investigated the expression of keratin proteins in cells from normal bronchial mucosa and from various hyperplastic and neoplastic changes. Previous studies have shown that keratin and the 67 K keratin protein may be considered to be markers of epithelial differentiation and maturation (Loening et al. 1980; Viac et al. 1980a).

The most consistent finding is the difference between normal human epidermis and ciliated pseudo-stratified bronchial mucosa in the distribution of the high molecular weight keratin protein 67 K: human epidermal basal cells do not express the 67 keratin, while only the cells from the suprabasal layers of the epidermis react with the specific 67 K antiserum (Viac et al. 1980a). Every layer of the epidermis reacts with TK antisera. Basal cells from the normal bronchial mucosa were positive when reacted under the same conditions with either 67 K antiserum or TK antiserum.

Only in cellular suspensions, did the columnar cells react strongly with K antisera. In fact, it is well known (Bergroth et al. 1980), that immunological staining of cell suspensions are able to detect very small amounts of cellular antigen or constituents that may not be detected in tissue sections. The variation in the intensity of staining between basal cells and columnar ciliated cells may be due to variation in the amounts of keratin contained in these cells. In epidermal cells, the variation of specific labelling with TK or 67 K antiserum is known to be related to the variation in the presence of cytoskeleton constituents such as tonofilaments (Spencer 1977). In cells from bronchial mucosa, the variations in staining we have observed are in agreement with previous electron microscopic observations of the cellular distribution of tonofilaments. Tonofilaments are numerous in basal cells which react strongly with each antiserum (Spencer 1977). They are only occasionally present in columnar ciliated cells (Spencer 1977); numerous tight junctions have been observed near the luminal side of the cells in cytoplasmic areas corresponding to the more strongly reacting part of the cells, in our immunocytological studies.

The intense labelling of basal cell hyperplasias may likely be related to the increased proliferation of basal cells with high keratin content.

Squamous metaplasia has been considered to be a cellular mucosal proliferative reaction to non specific stimuli, which may lead to the development of squamous cell carcinoma (Nettesheim 1981). The patchy but intense staining of the squamous metaplasia appears to be due to the focal proliferation of basal cells which are considered to be progenitor cells of the other types of bronchial epithelial cells (Spenger 1977). Other areas in squamous metaplasia stained only weakly with antisera: they probably correspond to areas with slight or moderate atypia which have been shown in electron microscopy to exhibit early atypical changes such as altered desmosome formation (Klein-Szanto et al. 1980a).

Our results indicate clearly that the expression of keratins differs in lung tumours from that seen in normal bronchial mucosa and that variations are observed according to the type of tumour and the degree in differentiation.

In squamous cell carcinoma the keratin expression is very similar to that previously observed in squamous cell carcinoma of the skin (Thivolet et al. 1980; Viac et al. 1980b) or oral mucosa (Loening et al. 1980). The expression of keratins in theses two types of squamous cell carcinomas does not depend upon the kind of epithelial tissue from which it originates (Loening et al. 1980).

In respiratory squamous cell carcinomas the degree in differentiation is usually evaluated according to morphological criteria of cellular maturation or "squamatization" (McDonald et al. 1951). The changes in the expression of keratins that we report are in good agreement with the degree of tumoural cellular differentiation, based upon cytological and histological examinations.

In every type of squamous carcinoma, labelling with the 67 K antiserum, considered to be a marker of fully differentiated epithelial cells (Loening et al. 1980) was weaker than that obtained with TK antiserum. However, well differentiated squamous carcinomas were shown to react strongly with the TK sera; intense immunoperoxidase labelling was observed at the periphery of dyskeratotic cells, where electron microscopical studies have shown the presence of numerous tonofilaments (Klein-Szanto et al. 1980a, b).

Only occasional staining was obtained in mildly or poorly differentiated carcinomas, where only reduced amounts of desmosomes are present (Klein-Szanto et al. 1980a, b). Negative areas, probably correspond to tumour areas with a defective production of cytokeratin filaments.

In clear cell carcinomas, most of the large, round, PAS positive and glycogen negative cells were positive with either TK or 67 K antiserum which indicates their epithelial origin. Moreover since metastatic carcinomas were found to be negative, keratin antisera provide an easy tool for the differentiation of clear cell carcinoma, a type of peripheral squamous carcinoma of the lung, from renal cortical carcinoma metastazing to the lung (Spencer 1977).

Regarding other respiratory tract tumours, keratin proteins appear to be expressed only in cells from bronchogenic carcinoma, as evidenced by a weak reaction with TK antiserum. This suggest the possibility of a common constitutent between these cells and epithelial squamous cells.

Furthermore, as undifferentiated large cell carcinomas may be of epithelial, glandular or endocrin origin (McDowell et al. 1981), keratin antisera should be of value in the diagnosis of the histogenic type of this kind of tumour.

Moreover, our findings that columnar cells react strongly with K antisera only in cellular suspensions, and not in tissue specimens, underline the higher sensitivity of the immunolabelling when performed on cells in suspensions. So, these techniques should appear of considerable value on bronchoscopic brushes.

The process of cell keratinization is complex, and its relation with cellular differentiation, metaplasia and dysplasia remains unclear. Further studies with monoclonal antibodies specifically directed towards the keratin constituents of normal and dyskeratotic cells will provide a new tool for the diagnosis of normal and tumoural epithelial tissues and our understanding of human abnormal keratinization.

This study was supported by grants from INSERM CRL 812045 and UER Biologie Humaine (U.C.B. Lyon).

References

Bergroth V, Reitamo S, Konttinen YT, Lalla M (1980) Sensitivity and non specific staining of various immunoperoxidase techniques. Histochemistry 68:17–22

Bustamante R, Faure M, Bejui F, Thivolet J (1978) Quantitative immunocytochemical study of plasma cells in skin tumoral stromal reaction. Eur J Cancer 14:1043–1050

Franke WW, Weber K, Osborn M, Schid E, Freudenstein C (1978) Antibody to prekeratin: decoration of tonofilament-like arrays in various cells of epithelial character. Exp Cell Res 116:429–445

Graham RC, Karnovsky MJ (1966) The early stages of absorption of injected horseradish peroxydase in the proximal tubules of mouse kindney. Ultrastructural cytochemistry by a new technique. J Histochem Cytochem 14:291–302

Klein Szanto AJP, Topping DC, Heckman CA, Nettesheim P (1980a) Ultrastructural characteristics of carcinogen-induced nondysplastic changes in tracheal epithelium. Am J Pathol 98:61–82

Kleinszanto AJP, Topping DC, Heckman CA, Nettesheim P (1980b) Ultrastructural characteristics of carcinogen induced dysplastic changes in tracheal epithelium. Am J Pathol 98:83–100

Laemmli UK (1970) Cleavage of structural proteins during the assembly of the head of bacteriophage T4. Nature 277:680–684

Loening Th, Staquet MJ, Thivolet J, Seifert G (1980) Keratin polypeptides distribution in normal and diseased human epidermis and oral mucosa. Immunohistochemical study on unaltered epithelium and inflammatory, premalignant and malignant lesions. Virchows Arch [Pathol Anat] 388:273–288

McDonald JR, McBurney RP, Carlisle JC, Patton MM (1951) The significance of cell types in bronchogenic carcinoma. J Thorac Surg 22:62–73

McDowell EM, Wilson ThS, Trump BF (1981) Atypical endocrine tumors of the lung. Arch Pathol Lab Med 105:20–28

Nettesheim P (1981) Studies of neoplastic developpement in respiratory tract epithelium. Arch Pathol Lab Med 105:1–10

Schlegel R, Banks-Schlegel S, McLeod JA, Pinkus GS (1980a) Immunoperoxidase localization of keratin in human neoplasms. Am J Pathol 101:41–47

Schlegel R, Banks-Schlegel S, Pinkus GS (1980b) Immunohistochemical localization of keratin in normal human tissues. Lab Invest 42:91–96

Schmitt D (1979) Contribution à l'étude des antigènes et des populations lymphocytaires impliqés dans les réactions immunitaires au niveau de la peau. Doctorat d'Etat ès Sciences. Thèse n° 7943 Lyon

Sienski W, Dorsett B, Iochim ML (1981) Identification of prekeratin by immunofluorescence staining in the differential diagnosis of tumors. Human Pathol 12:452–457

Spencer H (1977) Pathology of the lung. St Thomas's Hospital Medical School London. 3rd edn, Vol 1. Pergamon Press, Oxford

Staquet MJ, Viac J, Thivolet J (1979) Antigenic relationship between polypeptides derived from plantar and hand wart viruses. J Gen Virol 43:713–717

Sun TT, Green H (1978) Immunofluorescent staining of keratin fibers in cultured cells. Cell 14:469–476

Thaler MP, Fukuyama K, Inouq N, Cram DL, Epstein WL (1978) Two tris urea mercaptoethanol extractable polypeptides found uniquely in scales of patients with psoriasis. J Invest Dermatol 70:38–41

Thivolet J, Viac J, Staquet MJ, Schmitt D (1980) Utilisation des sérums anti-polypeptides de la kératine pour l'étude de la kératinisation normale et pathologique. Ann Dermatol Venereol 107:357–364

Viac J, Staquet MJ, Thivolet J (1978) Relations antigéniques entre virus des papillomes humains (VPH). Etude expérimentale chez le cobaye. Ann Immunol (Paris) 1239C, 559–570

Viac J, Schmitt D, Staquet MJ, Thivolet J, Ortonne JP, Bustamante R (1980a) Binding specificity of guinea pig anti- keratin polypeptide sera on human keratinocytes: comparison of their receptors with those of human epidermal cytoplasmic antibodies. Acta Dermatol-Venerol 60:189–196

Viac C, Staquet MJ, Goujon C, Thivolet J (1980b) Experimental production of antibodies against stratum corneum keratin polypeptides. Arch Dermatol Res 267:179–188

Accepted November 4, 1981

Virchows Arch (Pathol Anat) (1982) 395:99–107

Virchows Archiv A

Case Reports

Angiomatoid Malignant Fibrous Histiocytoma

Case Report and Electron Microscopic Findings

Hans Jörg Leu and Miroslav Makek
Institut für Pathologie der Universität, Schmelzbergstrasse 12, CH-8091 Zürich, Switzerland

Summary. A case of an angiomatoid malignant fibrous histiocytoma is presented. The electron microscopic findings demonstrate the presence of a variety of tumor cell types including smooth and striated muscle cells. This indicates that malignant fibrous histiocytoma originates from a pluripotent primitive mesenchymal cell.

Key words: Malignant fibrous histiocytoma – Angiomatoid type of malignant fibrous histiocytoma – Electron microscopic findings in angiomatoid malignant fibrous histiocytoma

Introduction

Malignant fibrous histiocytoma is today recognized as the most frequent soft tissue sarcoma (Weiss and Enzinger 1978; Angervall and Kindblom 1981; Enjoji et al. 1980). Enzinger (1977) distinguishes pleomorphic, storiform, myxoid, giant cell and inflammatory (xanthomatous) types. Recently Enzinger (1979) described an angiomatoid type as a distinct fibrohistiocytic tumor in children and young adults.

Malignant fibrous histiocytoma (MFH) occurs at any age and is more or less equally distributed among males and females (Ushigome and Hirota 1980). The tumor usually originates in musculature and deep fascia of the extremities, especially of the thigh, but also occurs in the soft tissue of the trunk and peritoneum (Weiss and Enzinger 1978; Ushigome and Hirota 1980). Sixty percent of the patients survive the first two years, the recurrence rate is 44% and the metastatic rate 42% (Weiss and Enzinger 1978). Recently we have observed a case of angiomatoid MFH with some ultrastructural aspects which have not been reported before.

Offprints requests to: H.J. Leu at the above address

0340-1227/82/0395/0099/$01.80

Case Report

In 1976 a woman 30 years old was twice operated on in a foreign country for an "old hematoma" in the posterior part of the right thigh. In 1977 she suffered from fever, loss of weight and swelling of an axillary lymph node. Biopsies from lymph node and liver were examined at our institute but revealed no signs of neoplasia. In 1978 a fast growing tumor in the posterior region of the right thigh was removed. Histology (HZ 24125/78) revealed only haemorrhages and scar tissue. In 1979 a biopsy from a local recurrence gave evidence of a malignant mesenchymal tumor in the soft tissues of the thigh. The tumor was removed as completely as possible and radiotherapy was subsequently performed. Histology showed metastatic tumor tissue in a pelvic lymph node: HZ 10336/79, 17803/79 and 20790/79. In 1980 the tumor recurred and was operated again showing the same tumor tissue as before (HZ 14327/80). In 1981 new tumor tissue was growing at the same site and was removed again (HZ 1946/81). On this occasion material was obtained for electron microscopic examination.

Histology

Light Microscope Findings. The tissue samples consist of a cell-rich tissue of varying appearance. Large areas of haemorrhage, resembling cyst are conspicuous. The cyst walls consist of multiple layers of tumor cells with an adjacent zone of inflammation. Between the cysts different tissue types can be distinguished. Haemosiderin deposits, siderophages, lymphocytes and plasma cells occur in abundance. The fibrous parts consist of spindle-shaped tumor cells with elongated chromatin-rich nuclei and occasional mitotic figures. No distinct storiform pattern is detected. Irregular reticulin fibers without definite pattern are found in the fibrous areas. The tumor cells surrounding the cysts are large, oval or roundish with large, clear nuclei with one or several prominent nucleoli. Mitotic figures occasionally occur. Some of the cysts are empty, the majority contains blood. Capillaries and larger vascular channels occur in abundant numbers, they are lined by prominent endothelial cells with large clear nuclei and marked nucleoli. These endothelial cells also show occasional mitotic figures. In some capillaries the endothelial cells appear to be multilayered and to penetrate the basal membrane. Necrotic areas are common. Occasionally there are groups of multinucleated giant cells (Figs. 1 and 2).

This histological pattern corresponds to an *angiomatoid malignant fibrous histiocytoma.*

Electron Microscope Findings. The capillaries are lined by large endothelial cells with irregularly-shaped prominent nuclei and marked nucleoli. The cytoplasm contains ribosomes, mitochondria, rough endoplasmatic reticulum and some lysosomal structures. Weibel-Palade bodies are rare and extremely small. The majority of the stromal cells are histiocyte-like with one or several irregularly-shaped large nuclei with a dense peripheral rim of heterochromatin and one or two large prominent nucleoli. The cytoplasm is filled with lipid droplets, lysosomal structures and phagosomes, it contains segments of rough-surfaced endoplasmatic reticulum, Golgi zones and occasionally mitochondria. Paracrystalline inclusions in the nuclei, as observed in MFH by Costa (1981) are not present. These cells form cytoplasmatic interdigitating projections. A minority of stromal cells are spindle-shaped with abundant rough-surfaced endoplasmatic reticulum and no lysosomal structures. They are surrounded by collagen fibers and occasionally by reticulin and elastic fibers.

Occasionally there are clusters of multinucleated giant cells with pseudopodia-like protrusions. They contain abundant numbers of mitochondria which are mostly along the cell surface. A few typical *Z*-lines are irregularly scattered throughout the cytoplasm. Lipid droplets and phagosomes with multilayered membrane material are also present within the cytoplasm. While these cells resemble primitive striated muscle cells, there are other cell groups of irregularly-shaped cells of varying size which contain myofilaments, attachment points and enlarged oval nuclei with clusters of heterochromatin along the peripheral rim and a central prominent nucleolus. The paranuclear zone contains mitochondria, a Golgi zone and some rough-surfaced endoplasmatic reticulum. These cells closely resemble smooth muscle cells.

There is massive proliferation of inflammatory cells, mostly plasma cells and lymphocytes. Some of the plasma cells appear atypical and contain two large nuclei with prominent nucleoli (Figs. 3–6).

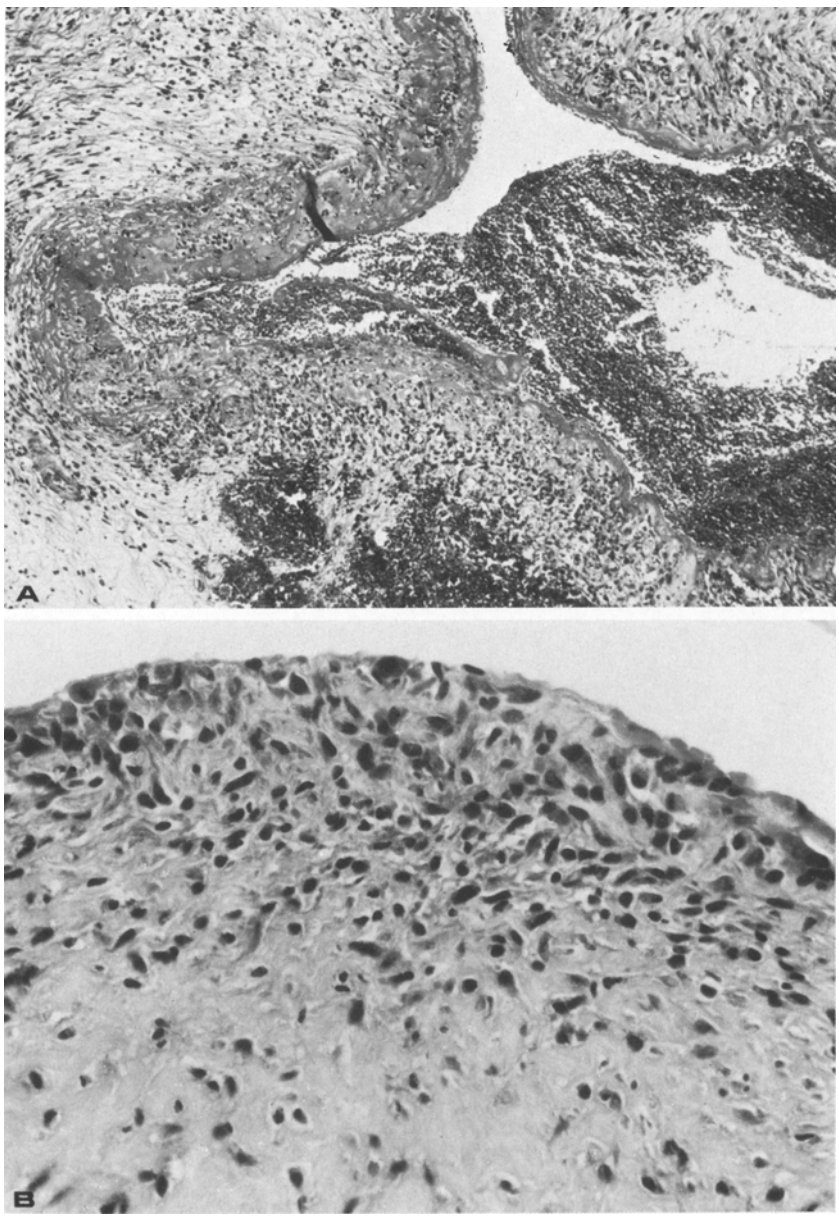

Fig. 1. A Blood-filled cyst with walls consisting of tumor tissue. HZ 1946/81, F. 69/16. Haemalaun-Eosin, ×80. **B** Cyst wall consisting of tumor tissue. HZ 1946/81, F. 70/13, Haemalaun-Eosin, ×300

Discussion

The age of the patient and the localization of the tumor are typical of an angiomatoid MFH. The tumor was ill-defined from the beginning and complete surgical removal was impossible in spite of several attempts. Recurrences followed

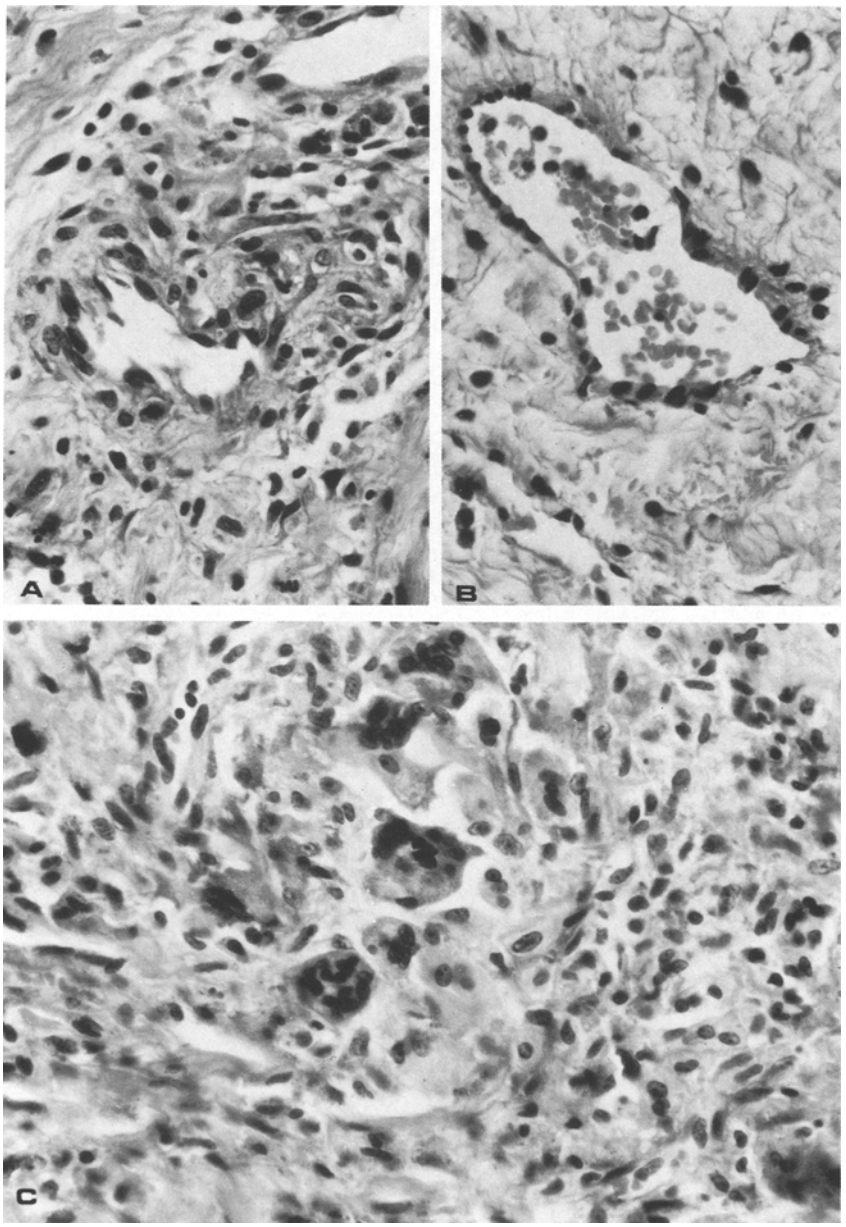

Fig. 2. A, B Proliferating capillaries with irregular endothelial lining. HZ 1946/81, F.70/6, F.70/24. Haemalaun-Eosin, ×300. **C** Multinucleated giant cells surrounded by tumor tissue. HZ 1946/81, F.70/18. Haemalaun-Eosin, ×300

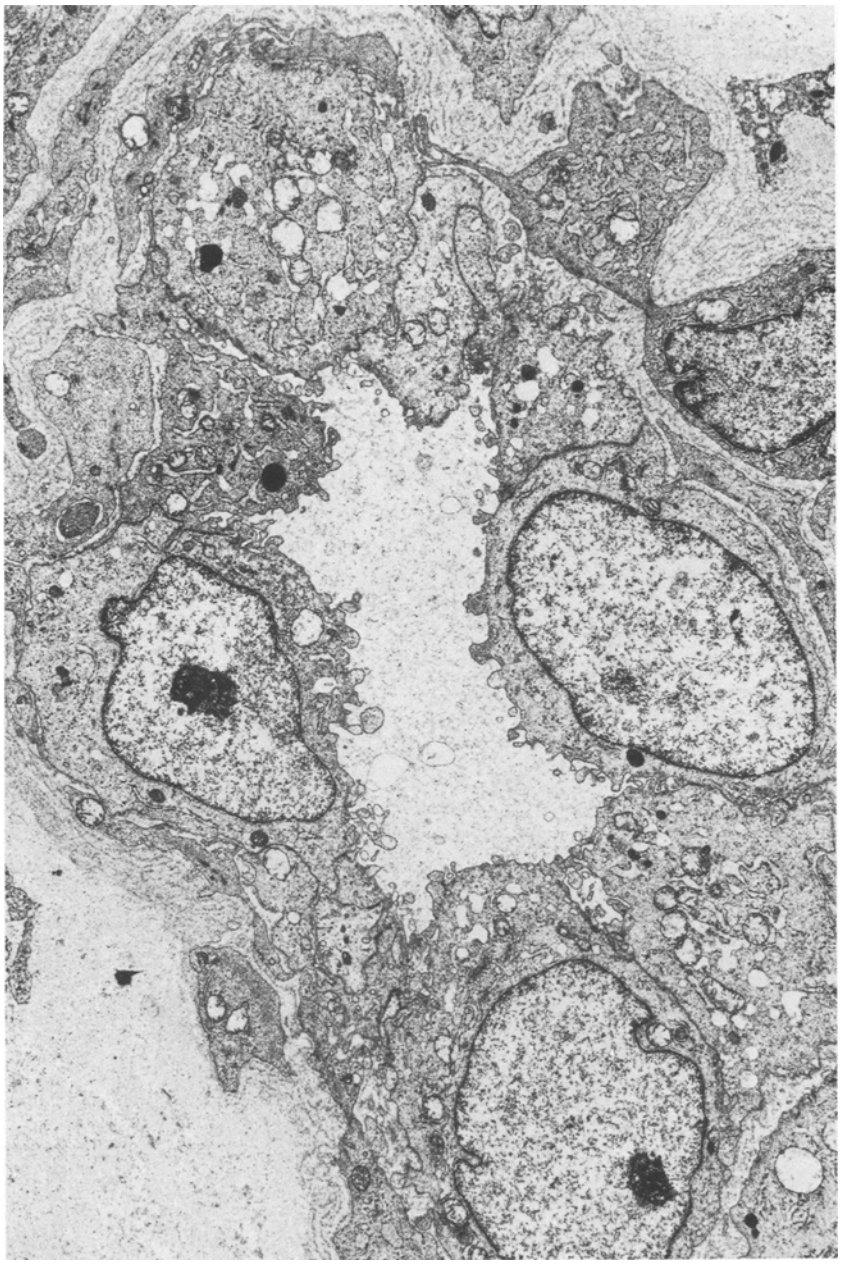

Fig. 3. Capillary with endothelial cells containing enlarged nuclei with prominent nucleoli. HZ 1946/81. Neg. 663/81. Glutaraldehyde-Cacodylate, ×5,300

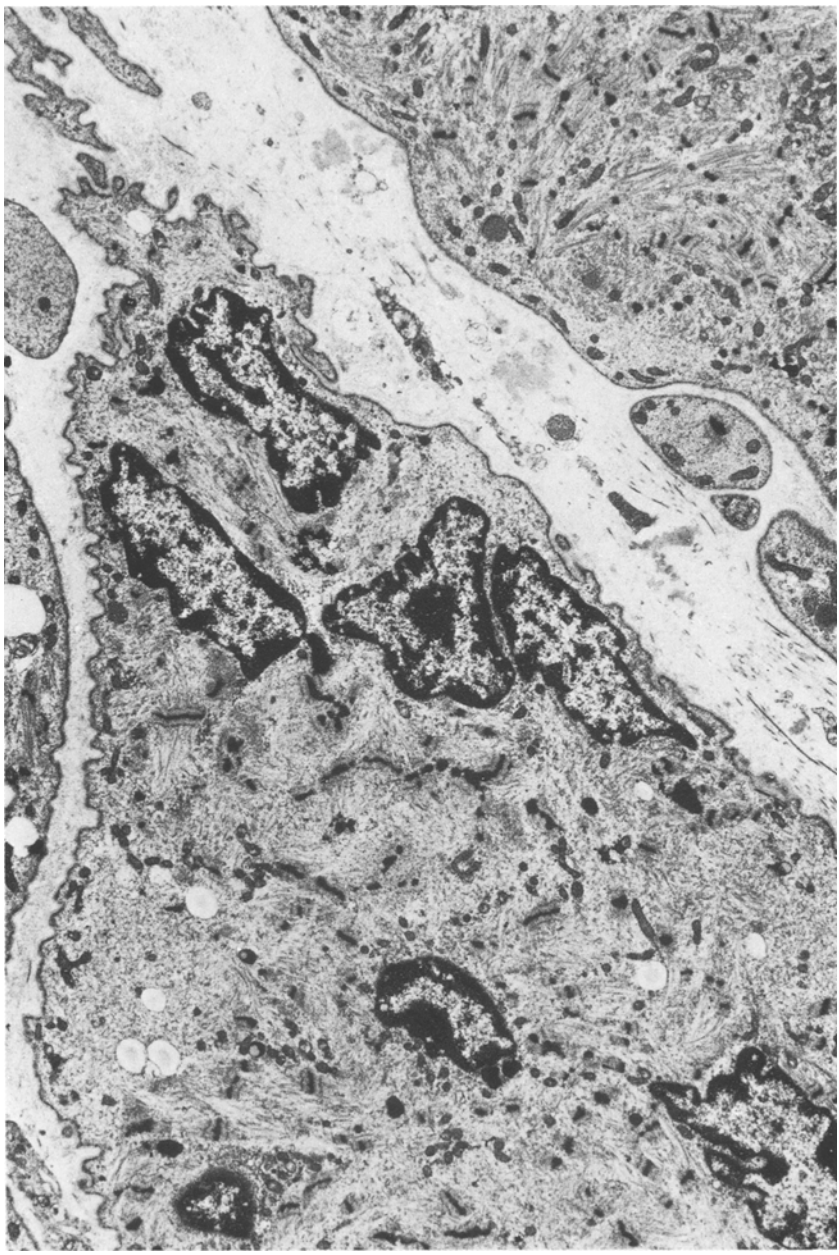

Fig. 4. Multinucleated giant cells with Z-lines. HZ 1946/81, Neg. 687/81. Glutaraldehyde-Cacodylate, × 5,300

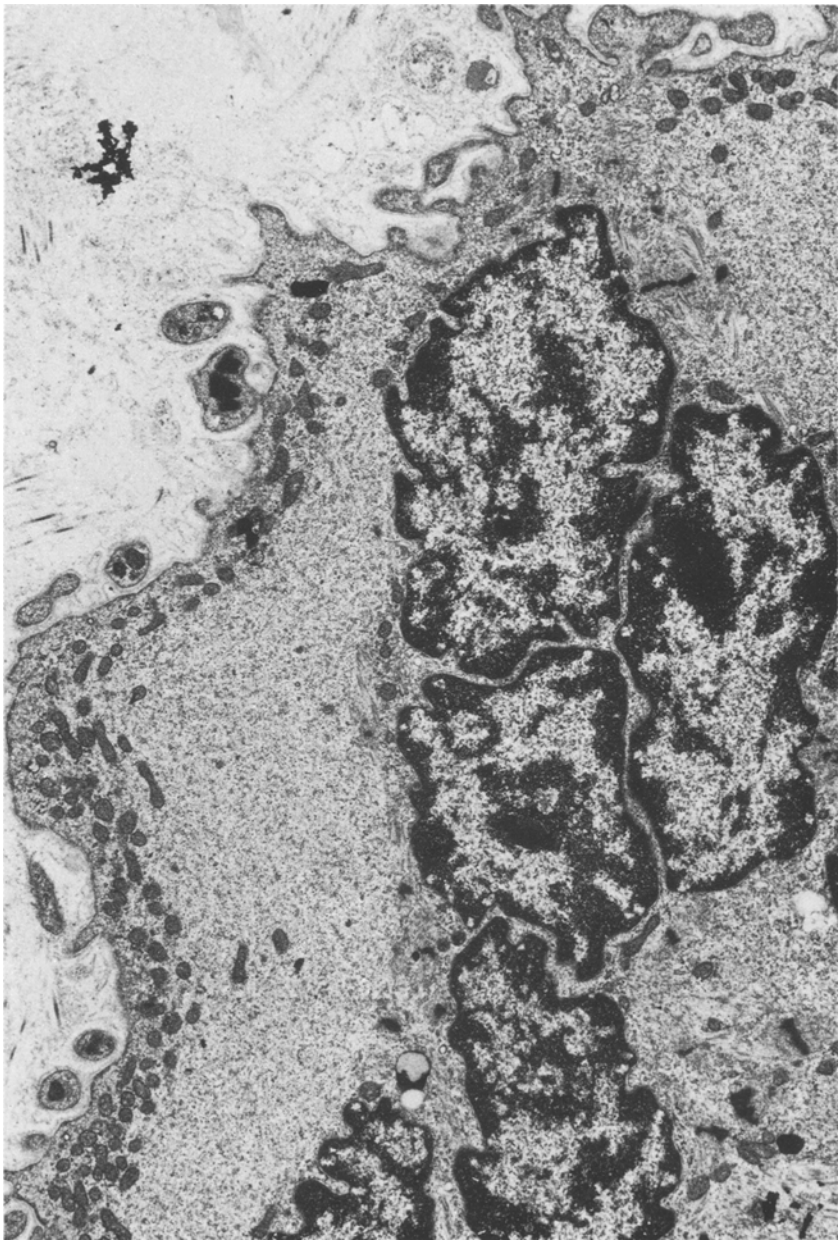

Fig. 5. Multinucleated giant cell with a few scattered *Z*-lines, pseudopodia-like protrusions and abundant mitochondria along the cell surface. NZ 1946/81, Neg. 702/81. Glutaraldehyde-Cacodylate, × 8,400

Fig. 6. Smooth muscle cells with myofilaments and attachment points. Enlarged nuclei with prominent nucleoli. HZ 1946/81, Neg. 770/81. Glutaraldehyde-Cacodylate, × 5,300

at short intervals. A metastasis in a pelvic lymph node was detected in 1979. Since then no further metastases have occurred although the local recurrences necessitated further surgical interventions and radiotherapy in addition. An enlarged lymph node from the axillary region was excised in 1978 but did not contain tumor tissue. The prognosis of this case is dubious and further metastases have to be expected.

The electron microscope findings reveal some features which have not been described before. In malignant fibrous histiocytoma Weiss and Enzinger (1979) have not observed smooth or striated muscle cells. In our case, however, there is distinct formation both of smooth and striated muscle cells in addition to the well-known two types of tumor cells (histiocyte-like and fibroblast-like cells). Furthermore the endothelial cells lining the capillaries and larger vascular channels differ from ordinary endothelial cells. They contain enlarged nuclei with a dense rim of heterochromatin and prominent nucleoli. The cytoplasm contains a very few extremely small Weibel-Palade bodies. The light microscope findings show occasionally multilayered endothelial cells which appear to penetrate the basement membrane and also reveal some mitotic figures. These findings suggest that also the endothelial cells lining the capillaries and the larger vascular channels might be part of the malignant neoplasia.

In agreement with the opinion of Weiss and Enzinger (1978) our findings indicate that MFH originates from a primitive mesenchymal cell which is pluripotent and may differentiate into a variety of mesenchymal cell types. In angiomatoid MFH this differentiation appears to be even more extensive including the formation of smooth and striated muscle cells, and possibly vascular endothelial cells.

Acknowledgement. We are very grateful to Mrs. Irmhilt Schade for her valuable technical assistance with the electron microscopic examinations.

References

Angervall L, Kindblom LG (1981) Slide seminar soft tissue tumors. VIII. European Congress of Pathology, Helsinki, Sept. 1, 1981

Costa J (1981) Paper read at the Institute of Pathology, University of Zürich, May 1981

Enjoji M, Hashimoto H, Tsuneyoshi M, Iwasaki H (1980) Malignant fibrous histiocytoma. Acta Pathol Jpn 30:727–741

Enzinger FM (1977) Recent developments in the classification of soft tissue sarcomas. In: Management of primary bone and soft tissue tumors. Year Book Medical Publishers, Inc. Chicago, London 1977, pp 226–234

Enzinger FM (1979) Angiomatoid malignant fibrous histiocytoma. A distinct fibrohistiocytic tumor of children and yound adults simulating a vascular neoplasm. Cancer 44:2147–2157

Ushigome S, Hirota T (1980) Malignant fibrous histiocytoma. With special reference to its differential diagnosis. Acta Pathol Jpn 30:799–813

Weiss SW, Enzinger FM (1978) Malignant fibrous histiocytoma. An analysis of 200 cases. Cancer 41:2250–2266

Accepted October 29, 1981

Virchows Arch [Pathol Anat] (1982) 395:109–116

Virchows Archiv A

A Case of Angioimmunoblastic Lymphadenopathy with Involvement of the Nervous System

Ralf Schober

Pathologisches Institut am St. Markus-Krankenhaus, Frankfurt a.M.
(Directors: Prof. Dr. med. D. Walther and Prof. Dr. med. H.P. Lange),
Wilhelm-Epstein-Straße 2, D-6000 Frankfurt 50, Federal Republic of Germany

Summary. A case of angioimmunoblastic lymphadenopathy with a short survival time is reported. At autopsy there was generalized lymphadenopathy with the characteristic histological pattern and widespread involvement of many organs including the meninges and the peripheral nervous system. The relation to morphologically comparable diseases of the nervous system with a suspected viral aetiology is discussed.

Key words. Angioimmunoblastic lymphadenopathy – Granulomas – Neurolymphomatosis – Peripheral nervous system

Introduction

Angioimmunoblastic lymphadenopathy is a relatively new disease entity characterized histologically by obliteration of the lymph node architecture by a pleomorphic infiltrate and extensive proliferation of venules (Frizzera et al. 1974; Lukes and Tindle 1975). Displaying great variability in its biological behaviour, the nature of the cellular proliferation which is associated with an abnormal immunological reaction remains obscure; cases with progression to monomorphous lymphomas are classified under the same clinico-pathological entity as those which resolve spontaneously (Dorfman and Warnke 1974). Depending on the clinical presentation (Radaszkiewicz and Lennert 1975) there is widespread organ involvement including spleen. liver, bone marrow, skin and lungs, but the changes here are less characteristic than those seen in the lymph nodes (Frizzera et al. 1975). Since the nervous system so far has received little attention in this disease, we report a case in which it was extensively involved.

Clinical History

The patient was a 83 year-old man with compensated cardiac and renal insufficiency. He had a cardiac pacemaker for two years. On his last admission he came in with complaints of relatively acute abdominal pain, jaundice, anorexia, postprandial vomiting, dark urine during the last week,

Offprints requests to: Dr. R. Schober at the above address

0340-1227/82/0395/0109/$01.60

and generalized pruritus for the last 10 days. Physical examination revealed hepatosplenomegaly and generalized lymph node enlargement of moderate degree. Pertinent laboratory data: Anaemia with 8.8 mg% haemoglobin and 2.7 mio. erythrocytes/mm^3. Leukocytosis of 33,500/mm^3 with a differential count of 53 segmented and 9 unsegmented neutrophils, 14 eosinophils, 15 lymphocytes, 9 plasma cells and an increased number of normoblasts. Thrombocytopenia of 170,000/mm^3. Creatinin 2.32 mg%. Bilirubin 7.4 mg%. Total protein 8 g%. On electrophoresis hypalbuminaemia with 36 rel.% and hypergammaglobulinaemia with 30 rel.%.

A right scalene lymph node biopsy gave the diagnosis of angio immunoblastic lymphadenopathy resp. lymphogranulomatosis X (Prof. Walther). The patient rapidly deteriorated despite infusions and transfusions, and after increasing sensory impairment and disorientation he died on the 13th day after admission.

Autopsy

Generalized lymphadenopathy with up to walnut-sized homogenous grey-red fleshlike nodes (Fig. 2a). Uniform grey-red bone marrow with some irregularly confirmed patches in the medullary adipose tissue of the femoral shaft and head. Splenomegaly (745 g) with a yellowish enlarged follicular pattern in the red pulp and several yellow infarcts. Splenic capsular fibrosis. Slight grey-yellowish gelatinous clouding of the leptomeninges, especially in the lateral cerebral sulcus.

Other Findings. Cardiomegaly (515 g) with hypertrophy and dilatation of both ventricles. Arteriosclerosis. Coronary sclerosis. Cardiac pacemaker. Pulmonary oedema. Pleural effusions (400 and 600 ml) and ascites (600 ml). Partial atelectasis of both lower lobes. Pulmonary emphysema. Bilateral apical pleural scars. Cholelithiasis. Small gastric leiomyoma. Small old infarct of right kidney. Moderate cerebral cortical atrophy. Small old traumatic lesions of the orbitofrontal cortex.

Histology

Lymph nodes from several regions all showed the features diagnostic of angioimmunoblastic lymphadenopathy, i.e. effacement of the normal architecture and extracapsular invasion, proliferation of venules and a mixed cellular composition of lymphocytes, large lymphoid cells (immunoblasts), and plasma cells (Fig. 1). Eosinophils were usually absent. In hilar nodes and paraaortic nodes there were, in addition, granulomas composed of rather uniform epithelioid cells with long, "cat-tongue like" nuclei and occasional giant cells of the Langhans type (Fig. 2c).

In the spleen there was hyperplasia of the white pulp, with abundant lymphocytes, histocytes and plasma cells but no germinal centers. The red pulp also showed focal infiltrates of these cells and, in addition, occasional eosinophilic leukocytes.

Similar focal and usually perivenular infiltrates of lymphocytes, histocytes and plasma cells, often with predominance of the latter, were also present in other organs. In the bone marrow they were often lying in a fibrillary mesh of increased reticulin. Interstitial infiltrates were extensive both in the heart, involving the myocardium and epicardium (Fig. 2d), and in the kidney, extend-

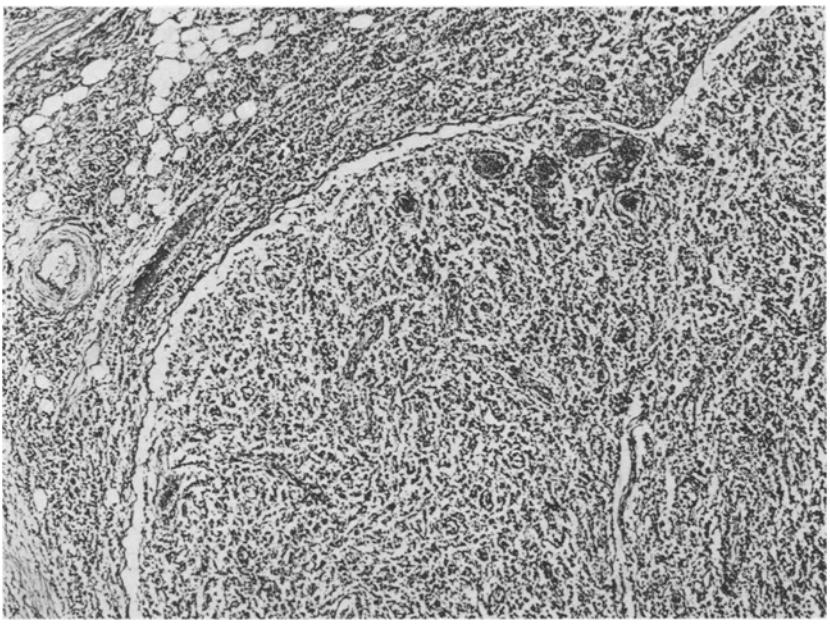

Fig. 1. Para-aortic node with features characteristic of angioimmunoblastic lymphadenopathy: effacement of the lymph node architecture, arborizing vascularity of the lymph node stroma, and patency of the subcapsular sinus despite infiltration of perinodal tissues; PAS, 45:1

ing into the perirenal adipose tissue. The myocardium showed, in addition, perivascular infiltrates with multinucleated giant cells consistent with Aschoff bodies in some areas. In the liver, the infiltrates were usually confined to the portal areas, although in places they broke through the limiting plate; in addition, there was some portal fibrosis, cholestasis and a marked Kupffer cell proliferation. The skin showed loose subepidermal and denser but patchy dermal infiltrates.

Nervous System. In contrast to the rather unremarkable macroscopical appearance, the dura showed extensive infiltrates of lymphocytes, histiocytes and plasma cells, both between its layers and on the surface (Fig. 3a). They usually lay around small veins and venules, however, in some instances they were also seen around arteries with a thickened, oedematous appearing wall. In the spinal region there were also extensive infiltrates in the epidural adipose and connective tissue.

Infiltrates in the leptomeninges were rather loose and of irregular distribution. Vasculitis was distinct with intramural infiltrates usually in veins, and in some places in arteries (Fig. 3b). In the left lateral cerebral sulcus the infiltrate was associated with homogeneous eosinophilic proteinaceous exudate.

The parenchyma of the brain and spinal cord was free of alterations apart from a moderate number of senile plaques in the cerebral cortex. The choroid plexus showed focal infiltrates, often around and also in the wall of medium-sized vessels, and scattered psammoma bodies.

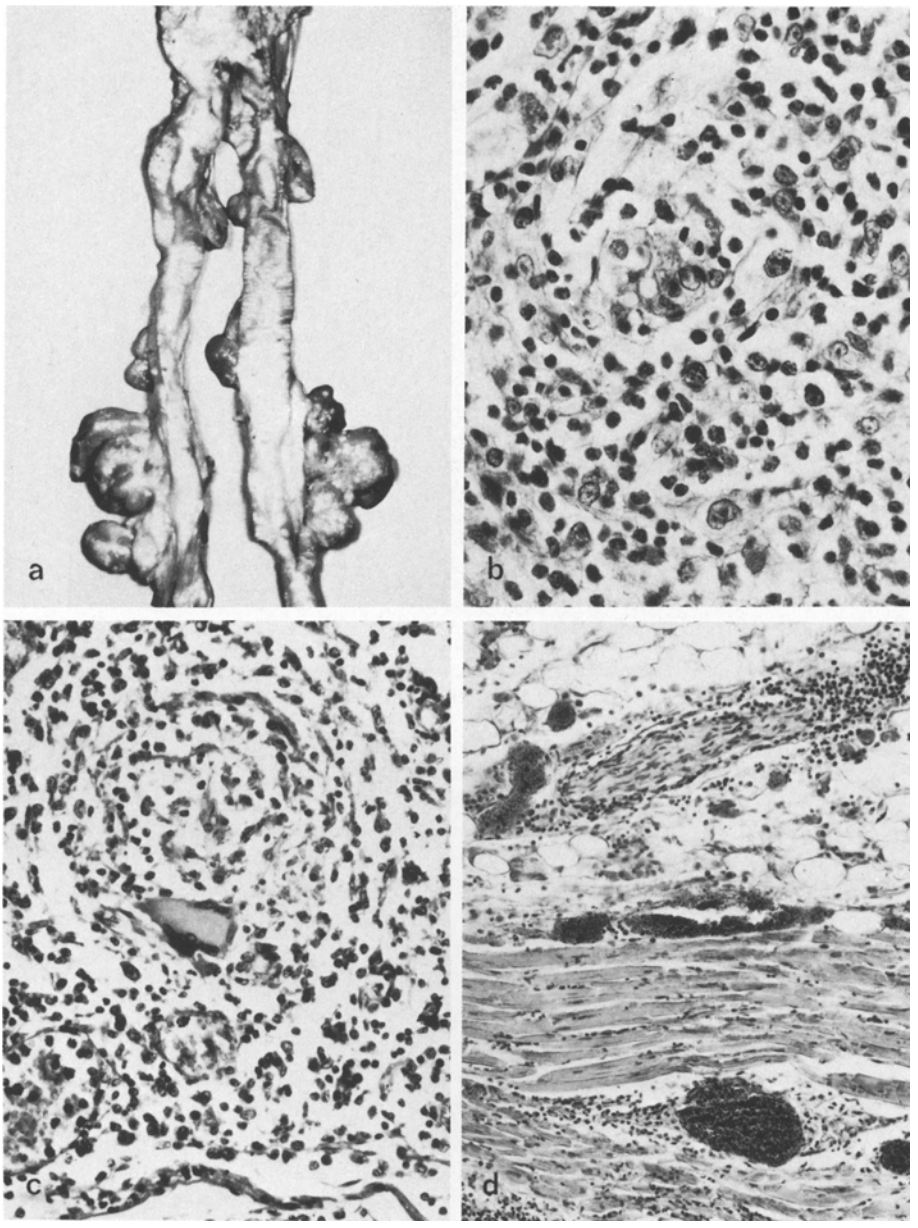

Fig. 2a. Disssection of the aortic bifurcation, iliac and femoral arteries with enlarged lymph nodes; 1:3 **b** Scalene node biopsy, showing lymphocytes and large lymphoid cells in a perivenular arrangement. One cell of the blood vessel wall is in mitosis (*center*); HE, 440:1. **c** Focal granuloma in para-aortic node; PAS, 250:1. **d** Congested left ventricle with infiltrates both of the myocardium and a small nerve in the subepicardial adipose tissue; HE, 110:1

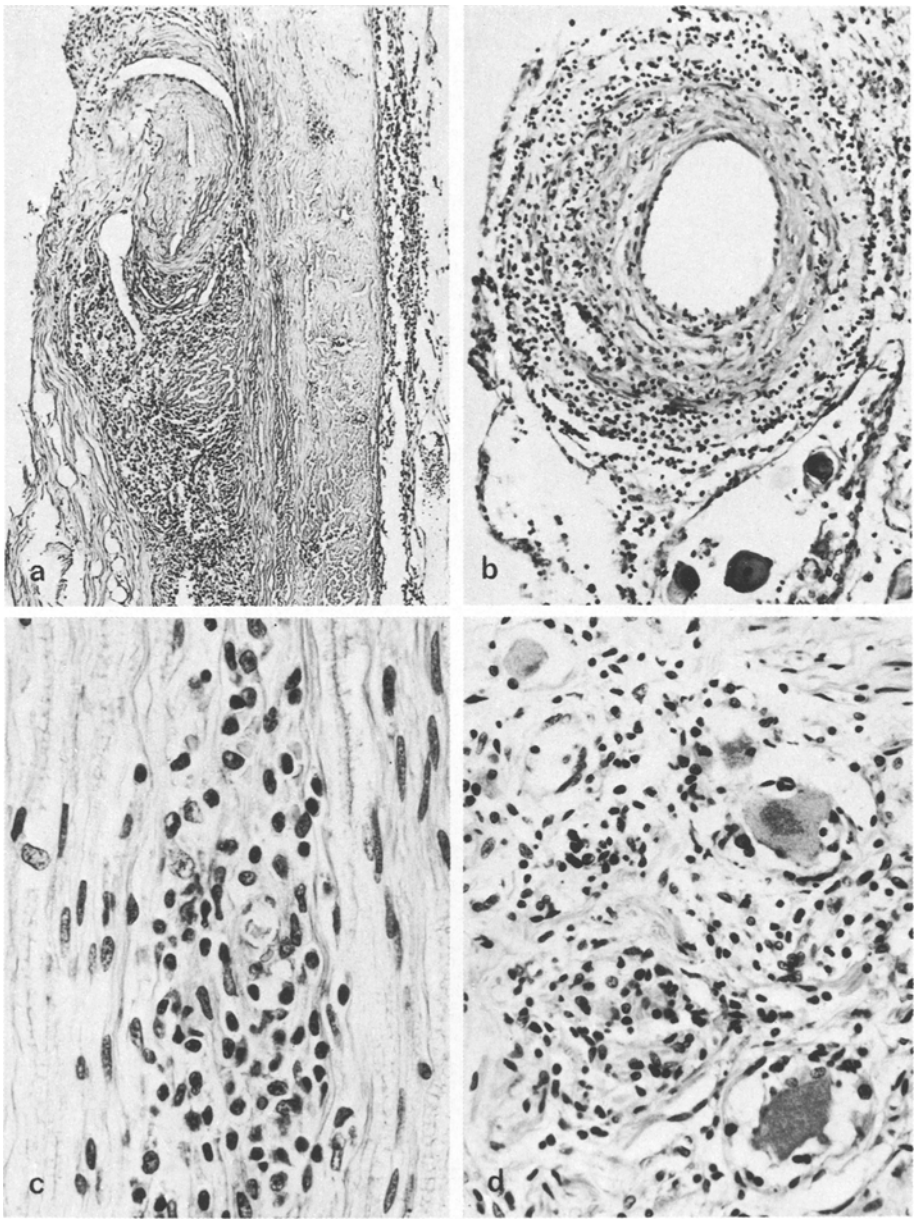

Fig. 3. a Dura with extensive interstitial perivascular and superficial infiltrates; HE, 60:1. **b** Small leptomeningeal artery with intramural and adventitial infiltrates; HE, 150:1. **c** Sciatic nerve with perivascular accumulation of lymphocytes, histiocytes, plasma cells and few erythrocytes, as well as discrete evidence of nerve fiber damage; HE, 440:1. **d** Spinal ganglion with perineuronal infiltrates and nerve cell loss; HE, 260:1

Samples taken from the peripheral nervous system showed scattered but distinct small infiltrates of lymphocytes, histiocytes and plasma cells. In the sciatic nerve they were associated with microhaemorrhages and evidence of early fiber damage (Fig. 3c). In spinal ganglia there was evidence of nerve cell damage and actual nerve cell loss, with formation of nodules of Nageotte (Fig. 3d). The infiltrates were not present, however, in all of the material examined, e.g. not in the femoral nerve, vagus nerve, or in the initial portions of the spinal nerves. Infiltrates in the spinal roots and in cranial nerves were sparse. Occasional small infiltrates were also present in the coeliac plexus, including the ganglion, and in the small vegetative nerves of the heart (Fig. 2d).

Discussion

The interest in this case lies in three features: firstly, the hyperacute clinical course; secondly, the involvement of the nervous system; and thirdly, the presence of granulomas in lymph nodes and heart.

A variable course and outcome of the disease has been stressed by most authors reporting larger series of patients and cases of less than 8 weeks duration have been included by Frizzera et al. (1975), Lukes and Tindle (1975), Moore et al. (1975), and Radaszkiewicz and Lennert (1975). The relevance of purely statistical data without reference to individual cases is, however, limited. Some of these patients may have succumbed to complications of cytostatic treatment, as was the case in the report of Kalus (1976). In our case no such treatment was given, but the advanced age of the patient may have contributed to the rapidly fatal outcome. In regard to the clinico-pathological correlations our case does not contradict the statement of Frizzera et al. (1975) that marked tissue eosinophilia is usually associated with long survival.

Changes in the nervous system have not been documented in angioimmunoblastic lymphadenopathy, although there are some cases on record with clinical evidence of involvement of the nervous system. Moore et al. (1975) listed one case with meningeal involvement. The first patient of Kalus (1976) was reported to have had the Guillain-Barré syndrome preceding immunoblastic lymphadenopathy, but he spontaneously recovered and was free of symptoms 5 years later. Spector and Miller (1977) presented two cases in which severe peripheral neuropathy developed during the course of immunoblastic lymphadenopathy. In their autopsy reports, however, data are lacking concerning the nervous system. Since the same holds true for most other reports; it remains to be seen from future investigations whether or not involvement of the nervous system in angioimmunoblastic lymphadenopathy is the exception.

Although our case undoubtedly fulfills the criteria established for angioimmunoblastic lymphadenopathy, it has many similarities with "an unusual case of acute infective polyneuritis with visceral lesions" published by Parker and Adams in 1947. In retrospect, this case may well have belonged to the nosological entity discovered 27 years later. The patient had general lymph node enlargement showing small and inactive follicles, large mononuclear cells, and extranodular plasmacellular and lymphocytic infiltrates, blood vessels not being specifically mentioned. The nervous system was affected even more extensively than in

our case. Of the infiltrates in other organs, those in the spleen and in the bone marrow are of particular interest since they were occasionally granulomatous, containing epithelioid histiocytes and giant cells of the Langhans type; in addition, there were myocardial lesions consistent with Aschoff bodies.

The similar finding of granulomatous lesions in our case of angioimmunoblastic lymphadenopathy suggests that these changes may not be merely coincidental. With regard to their pathogenesis, reactivated old tuberculosis must be considered in view of the altered immune response which develops in the disease, often leading to fatal opportunistic infections. Because of the myocardial lesions, however, this explanation appears unlikely. Secondly, these cases may fall into the epithelioid-cell subgroup of lymphogranulomatosis X as proposed by Lennert et al. (1969). A third, alternative hypothesis is that the giant cells are expression of a viral infection underlying angioimmunoblastic lymphadenopathy.

A viral aetiology for the disease has been proposed by a number of authors, and recent evidence implicating the rubella virus is cited by Lennert and Knecht (1981). An analogous search for a viral aetiologic agent exists in acute polyneuritis (Sabin and Aring 1941) and in neurolymphomatosis (Borit and Altrocchi 1971; Guberman et al. 1978), both of which are comparable to our case with regard to morphological changes in the nervous system. Furthermore, infectious mononucleosis, a systemic disease of proven viral aetiology with predominant lymph node involvment, may also be the cause of a polyneuritis (Haymayker and Kernohan 1949; Krücke 1959). It is in this context that the involvement of the nervous system in angioimmunoblastic lymphadenopathy seems of particular interest.

Acknowledgement. The clinical data were kindly provided by Dr. P.H. Greuner, St. Elisabeth-Krankenhaus, Frankfurt. Mr. E. Hepp gave preparatory assistance. The Max-Planck-Institut für Hirnforschung, Frankfurt, granted use of its photographical facilities.

References

Borit A, Altrocchi PH (1971) Recurrent polyneuropathy and neurolymphomatosis. Arch Neurol 24:40–49

Dorfman RF, Warnke R (1974) Lymphadenopathy simulating the malignant lymphomas. Human Pathol 5:519–550

Frizzera G, Moran EM, Rappaport H (1974) Angio-immunoblastic lymphadenopathy with dysproteinaemia. Lancet I:1070–1073

Frizzera G, Moran EM, Rappaport H (1975) Angio-immunoblastic lymphadenopathy. Diagnosis and clinical course. Am J Med 59:803–818

Guberman A, Rosenbaum H, Brachiale T, Schlaepfer WW (1978) Human neurolymphomatosis. J Neurol Sci 36:1–12

Haymaker W, Kernohan J (1949) The Landry-Guillain-Barré-syndrome. Medicine (Baltimore) 28:59–141

Kalus MJ (1976) Immunoblastic lymphadenopathy. A report of two cases. Arch Pathol Lab Med 100:465–468

Krücke W (1959) Histopathologie der Polyneuritis und der Polyneuropathie. Dtsch Z Nervenheilk 180:1–39

Lennert K, Knecht H (1981) Lymphogranulomatosis X. Einschließlich (angio)immunoblastische Lymphadenopathie. Dtsch Ärzteblatt 78:601–605

Lennert K, Knecht H, Burkert M (1979) Vorstadien maligner Lymphome. Verh Dtsch Ges Pathol 63:170–196

Lukes RJ, Tindle BH (1975) Immunoblastic lymphadenopathy. A hyperimmune entity resembling Hodgkin's disease. N Engl J Med 292:1–8

Moore SB, Harrison EG, Weiland LH (1976) Angioimmunoblastic lymphadenopathy. Mayo Clin Proc 51:273–280

Parker F Jr., Adams RD (1947) An unusual case of acute infective polyneuritis with visceral lesions. N Engl J Med 237:976–983

Radaszkiewicz T, Lennert K (1975) Lymphogranulomatosis X. Klinisches Bild, Therapie und Prognose. Dtsch Med Wochenschr 100:1157–1163

Sabin AB, Aring CD (1941) Visceral lesions in infectious polyneuritis (infectious neuronitis, acute polyneuritis with facial diplegia, Guillain-Barré syndrome, Landry's paralysis). Am J Pathol 17:469–482

Spector JI, Miller S (1977) Immunoblastic lymphadenopathy. A report of two cases. JAMA 238:1263–1265

Accepted November 4, 1981

Virchows Arch [Pathol Anat] (1982) 395:117–131

Virchows Archiv A

Review

Value of an Animal Model for Trisomy

Alfred Gropp
Institut für Pathologie der Medizinischen Hochschule Lübeck, D-2400 Lübeck, Federal Republic of Germany

Summary. Problems related to the developmental pathology of fetal aneuploidy are amenable to systematic investigation in a mouse model of autosomal trisomy. With a breeding design of one parent doubly heterozygous for two partially homologous Robertsonian metacentrics, some of the monosomies and all nineteen trisomies of the mouse can be studied. Monosomies are eliminated either before or shortly after implantation. Some trisomies do not survive a first critical phase of organogenesis on days 11 to 12 of fetal development, others such as Ts 12 to 14, 16, 18, and 19 have a lifespan until or beyond birth. A critical situation of long duration is caused in late development by hypoplasia of the placental labyrinth and ensuing impairment of metabolic exchange and of oxygen supply to the fetus. Model type morphogenetic analyses of anomalies (e.g. cranio-cerebral, cardio-vascular), are possible in Ts 1, 12, 14, 19, and others, and Ts 16 of the mouse is considered to be a close and natural model of human trisomy 21. The eventual breakdown and death of the aneuploid organism is inevitable. However, the introduction of monosomic or the transfer of trisomic haemopoietic stem cells to irradiated recipients is a means of rescuing the aneuploid cells and tissues with longer survival. Under these conditions isolated trisomic haemapoiesis can show almost complete and near-normal maturation, at least in trisomies 12 and 19. In other trisomies (e.g., 13 and 16) stem cell defects impair such reconstitution.

The experimental induction of mouse aneuploidy is a powerful technique which allows us to fill gaps in our existing knowledge of human trisomy, and suggests new lines of research. These are the major benefits of an experimental model.

Key words: Man – Mouse – Developmental genetics – Monosomy – Trisomy

Introduction

The value of an animal model for human disease depends on whether it is able (a) to fill gaps of clinical knowledge, (b) to elucidate mechanisms otherwise

0340-1227/82/0395/0117/$03.00

inaccessible for study in man or unclear by other reasons, and on whether (c) it can help to improve the understanding of a clinical problem by contributing a background of systematic knowledge. A further criterion of its value is its ability to provide new insights and solid guidelines for novel research.

For a systematic approach to the production of models for genetic and chromosomal disorders in man the mouse is preferred for several reasons. It is genetically the best characterized mammal apart from man since the chromosomal assignment, and in many cases the linkage and the position, of about 575 normal and mutant genes with defined phenotype are known in this species (Miller and Miller 1981; Green 1981). Normal mice, in particular mice of the conventional laboratory strains, have 40 acrocentric chromosomes (see Fig. 1, lower part) arranged in 20 pairs, 19 pairs of autosomes and 1 pair of sex chromosomes. Any two of the acrocentric autosomes can fuse at their centromeres by a mechanism called Robertsonian (Rb) translocation, to form a biarmed metacentric Rb chromosome. The availability of a great number of Rb chromosomal variants of the mouse (Gropp and Winking 1981) and the development of a breeding design (Fig. 1) for experimentally generating chromosomally unbalanced, i.e. trisomic and monosomic individuals (Gropp 1974; White et al. 1974; Gropp et al. 1975) has made the mouse a suitable model system for studying aneuploidy in mammals.

The Order of Magnitude of the Problem in Man, the Need of an Animal Model, and the Value of a Mouse Model for Trisomy and Monosomy

There is ample evidence to indicate that trisomy is the most frequent chromosome abnormality in man responsible for prenatal and early postnatal mortality.

In first trimester spontaneous abortions the observed frequency of chromosome disorders of all types is about 60%, but relatively few autosomal trisomies account together for more than half of this rate (Boue et al. 1975; Boue and Boue 1976). Other major first trimester chromosome abnormalities are triploidy and X-monosomy. On the base of a commonly accepted 15% rate of spontaneous abortions among all conceptus, the proportions of the lethal chromosome aberrations as a whole, and of autosomal trisomies in particular, extrapolated to all conceptus are 9% and 4%, respectively.

However, according to a comprehensive survey compiled by Hamerton et al. (1975), the frequency of all chromosome aberrations at birth, including numerical and structural disorders, is about 0.45%, while that of autosomal trisomies is only 0.18%. The trisomic conditions found at birth belong mainly, though not exclusively, to few selected types in which survival to or beyond term is possible, as in trisomy 21–Down's syndrome and trisomies 18 and 13.

A comparison of the rates of chromosome anomalies in newborns (Hamerton et al. 1975) and of extrapolated rates of first trimester losses is not a strictly logical procedure. It nevertheless provides an approximate notion of the developmental span of a zygote with a given type of aneuploidy (see Gropp 1981). From this premise, the comparison offers indices of a "survival chance until newborn age" such as 1 in 7.5 in G trisomy (which includes Down's syndrome), 1 in 44 in trisomy 18, 1 in 200 in trisomy D (which includes trisomy 13-Patau syndrome), and $1:\infty$ in trisomy of chromosome 16. Additional information

about the second and third trimester is needed in order to fill the gap between early abortion and birth. Some of the available data provide evidence for considerable rates of late fetal and perinatal death attributable to chromosome disorders (Milunski and Atkins 1977). Additional knowledge can be obtained from observations related to antenatal diagnosis.

The aim of clinical pathology in "chromosomal disease" is to describe the developmental profiles of individual chromosome disorders not only in terms of frequency and phenotype phenomenology, but also in terms of critical or vulnerable developmental phases. Definition of the mechanisms impairing growth and differentiation, and the display of morphogenetic processes would be of great value. The joint experience from human abortions, from cases observed in connection with antenatal diagnosis, and from late fetal or perinatal death has helped considerably, in some areas, to bring present knowledge closer to this aim, as e.g. in the case of Down's syndrome (Rehder 1981).

However, on the whole, and in the complexity of a multitude of details, very little is known in man about the direct and indirect consequences of chromosome imbalance and about the factors which produce and influence the mostly severe and highly deleterious phenotypic effects. With abortion material it is impossible to pursue studies other than static morphological or biochemical investigations, and cellular or tissular systems apart from blood cells and fibroblasts are mostly excluded from further analyses. Again in man, there is an almost complete lack of knowledge about monosomy. This is true with regard to causation, capacity for development and the ultimate fate of this condition which, after all, is expected to occur with equal frequency to trisomy.

With the mouse model discussed in this review, all aneusomic conditions possible in this species except sex chromosome disorders, i.e., all 19 autosomal trisomies and monosomies, become amenable to a systematic investigation. This is an unequivocal advantage compared with man where many types of aneuploidy cannot be studied at all, because they are too rarely (or never) observed. Moreover, the experimental system allows us to collect material in good condition for fixation, other proper pretreatment for developmental and biochemical analyses and for in vitro assessment of cells and tissues which depend on their isolation from the aneuploid organism (Gropp et al. 1981). The benefit using a mouse model for human chromosome abnormality is certainly not impaired by the fact that the phenotypes are not the same in man and in mouse. The assumption that the mechanisms by which chromosome imbalance produce developmental disorders are similar in both species is a reasonable one. Nevertheless, the mouse model of chromosome aneuploidy provides fundamental information for systematic studies of gene dosage effects, and for experimental analysis of genome phenotype relationship. Moreover, recent evidence from several sources, in particular from somatic cell hybridization studies (Francke et al. 1977), suggests that karyotype diversification of mammalian species during evolution did not completely disperse and rearrange their genomes. On the contrary, it has become clear that certain linkage groups of functionally related as well as unrelated gene loci have been conserved in close syntenic position, i.e., on sizeable homologous chromosomal segments, even in such distant species as mouse and man (Pearson and Roderick 1978).

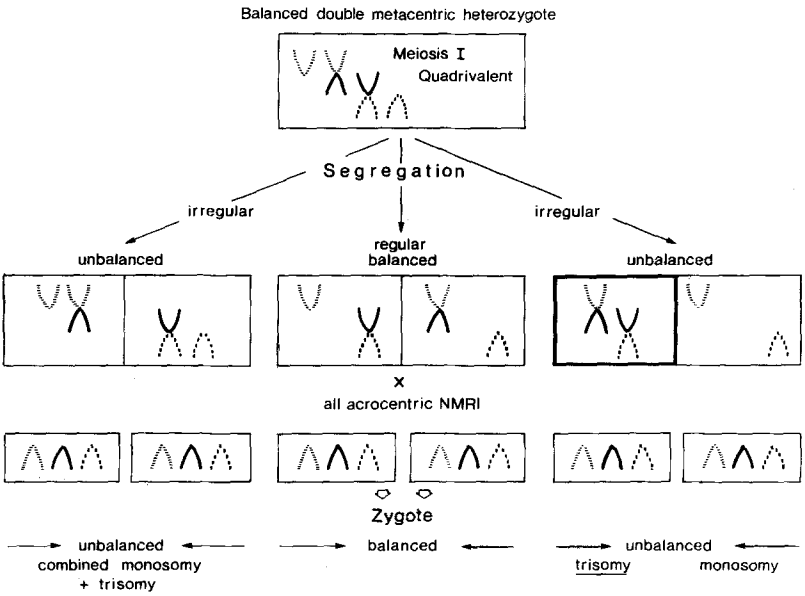

Fig. 1. Breeding design for production of aneusomy (trisomy or monosomy) in the progeny of a mouse doubly heterozygous for Robertsonian (Rb) biarmed chromosomes with partial homology (*top*). The scheme presupposes mating (x) of the heterozygous parent and a laboratory mouse (NMRI/Han) with "conventional" karyotype of acrocentric chromosomes (*below*). The unbalanced segregation products of non-disjunction with both Rb chromosomes or neither (*right*) are the desired types for trisomy (*Ts*) and monosomy (*Ms*), respectively. In this system, the autosome (Nos. 1 to 19) involved in either Ts or Ms is predetermined by selection of the doubly heterozygous Rb combination (example in Fig. 2)

Breeding Design for the Production of Whole Arm Murine Aneusomy, and Systematics of Developmental Profiles

The breeding scheme for the experimental induction of specific autosomal trisomies and monosomies (Fig. 1) is based on two premises, namely (a) the availability of a large number of chromosomally variant strains with Robertsonian (Rb) metacentric chromosomes, and (b) the controllability of meiotic non-disjunction in a Rb system of chromosome heterozygosity.

Rb metacentric (biarmed) chromosomes have been observed rarely in laboratory strains, but an almost unlimited reservoir of Rb chromosomes of varied arm composition has been detected in wild mouse populations from Southern Europe, and many of these Rb chromosomes are available for experimental research after introduction into laboratory strains by breeding procedures (Gropp et al. 1972; Gropp and Winking 1981). Animals heterozygous for two Rb's with partial homology for one of their arms (Fig. 1) are bred from homozygous lines with suitable Rb chromosomes (see example in Fig. 2). In this particular system of double Rb heterozygosity quadrivalents are formed in 1st meiotic prophase, and non-disjunction of both metacentric chromosomes occurs as a consequence of the propensity of this condition to 1st meiotic anaphase malsegregation (Gropp et al. 1975).

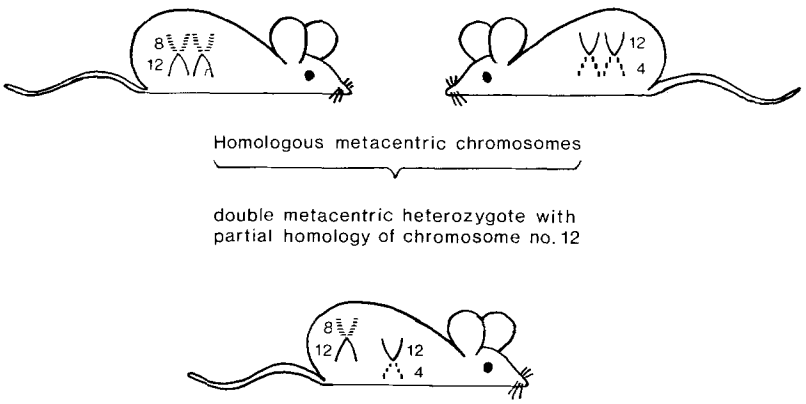

Fig. 2. Scheme for breeding double heterozygotes (*below*) with two partially homologous Rb biarmed (metacentric) chromosomes from homozygous parents. In the scheme the example suitable for production of Ts 12 is used (see Fig. 1)

It is clear from the logic of the breeding scheme (Fig. 1) that the selection of the special doubly heterozygous Rb combination in one of the parents determines the specific trisomy (Ts) or monosomy (Ms) found in the progeny. With this design, and as a result of extensive embryological studies, the systematics of the developmental profiles of each of the 19 trisomies of the mouse can be established (Fig. 3). In contrast, knowledge about the monosomies is mainly based on overall data, but some specific monosomies have been investigated.

In studies using a design of massive production of aneuploid gametes, both hypohaploid and hyperhaploid (Gropp 1971; Ford 1972), an almost equal distribution of trisomy and monosomy was noted among the preimplantation embryos on day 4 (for definition of the developmental age see note to Fig. 3). This agrees with expected figures because meiotic non-disjunction as a causative mechanism for autosomal aneuploidy produces a complementary gamete without a chromosome for every gamete carrying two copies. Yet, no monosomy was found after day 9. These results showed that the deficiency of monosomic embryos in later gestation is not due to nullisomic gametes being less able to participate in fertilization than disomic gametes. This explanation has also been excluded, for the male, by DNA measurements of spermatozoa produced by animals with extra high non-disjunction rates (Stolla and Gropp 1974). Rather, the lack of monosomic embryos is due to their impaired viability. Studies on specific monosomies have been carried out in the preimplantation period on Ms 5 and Ms 17 by Dyban and Baranov (1978), and on Ms 1, 12, 17 and 19 by Epstein and Travis (1979). It seems that Ms 19, i.e. of the smallest autosome, is the most rapidly lethal because it is no longer found by day 4.5. The other monosomies survive slightly longer, but it is not yet clear how long they are viable past implantation.

With regard to trisomies, only few survive until or beyond term, such as Ts 19 in which longest documented survival is day 13 after birth (Grohé and Gropp 1980), and Ts 16 and 18 in which viability until term is usually observed. The other trisomies result in early or later prenatal death, but viability until at least day 10 can be assumed for all trisomies. Many, such as Ts 2, 3, 4, 5, 7, 8, 9, 11, 15, and 17 are generally dead by day 12 or 13, while others, such as Ts 1, 6, and 10 survive to days 14 or 15, and still others such as Ts 12, 13 and 14 up to days 16 to 18. However, the survival profile depends

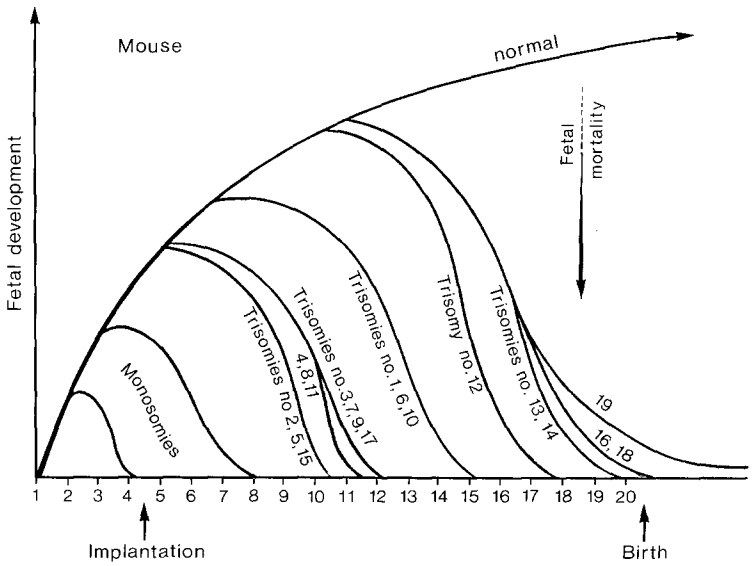

Fig. 3. Developmental profiles of mouse monosomies and trisomies. Note: Numbering of days of gestation is based on assignment of "vaginal plug day" as day 1

very much on the strain background on which the chromosome triplication had been induced. Thus, Ts 12 barely survives day 12 on C3H or certain other strains while it remains viable almost until term on the C57BL/6 genome (Gropp and Grohé 1981).

Insights Arising From the Study of Individual Trisomies of the Mouse

Some of the mouse trisomies deserve particular interest because of their suitability (a) for analysis of abnormal fetal (or neonatal) phenotypes, (b) for more "specific" models of human trisomy, and (c) for model studies on general principles of developmental errors due to chromosome abnormality.

a) Gross Phenotype Abnormality. The main abnormal features observed in all trisomies, though of variable intensity, are developmental retardation and hypoplasia. The expression of both traits is not strictly interdependent. In particular hypoplasia shows a tendency to become more prominent with progression of development. An example of marked hypoplasia without noticeable developmental retardation is shown in Fig. 4 of a Ts 19 individual on day 11 after birth compared with a normal littermate. Similar conditions are found in individual organs such as brain, lung and kidneys.

Other main developmental disorders are gross malformations. In severe manifestations of Ts 1, holoprosencephaly combined with aprosopia or cyclopia is observed (Gropp et al. 1975). Exencephaly occurs in several trisomies. It is a constant finding in Ts 12, less frequent in Ts 14, and incidental in Ts 9 and 17. The apparent non-specificity of this cranial neural tube defect is counterbalanced by the observation that it invariably includes, in Ts 12, the rhombencephalic segment of the hindbrain, while this segment is always closed in Ts 14.

Fig. 4. 11 days old Ts 19 (*left*) together with normal littermate. Main feature of trisomy is hypoplasia. (Breeding experiment by G. Grohé)

For this sort of findings the term "semispecificity" of malformations in chromosome disorders seems to be appropriate (Gropp 1978).

Support for such concept of incomplete, but restricted specificity comes also from observations of cleft palate and of cardiovascular malformations. Cleft palate is regularly associated with Ts 13 (Hongell and Gropp 1982), and frequent in Ts 18 (Gropp et al. 1981), but not found in other trisomies, at least in our own studies, whereas White et al. (1974) have reported cleft palate in some late Ts 19 fetuses. Cardiovascular malformations are frequent in several mouse trisomies (Pexieder et al. 1981). Thus, ventricular septal defect occurs in Ts 10, 12, 14, 16 and 19 with rates between 12 and 33%, and "Double outlet right ventricle" was found in Ts 13, 14, 16 and 19, thought at lower rates between 2 to 9%. Pulmonary stenosis (PS) and transposition of the great arteries (TGA) have only been observed in more specific association, namely in 22% of Ts 13 for PS, and 2.6% of Ts 14 for TGA.

Most of the developmental disorders in murine trisomies are well suited for an analysis of the morphokinetic processes, but only few such studies have been undertaken. The developmental characteristics of exencephaly in Ts 12 and the accompanying involvement of the skull base, orbita and inner ear have been investigated and compared with the malformation complex caused by the exogenous agent Vitamin A (Putz et al. 1980). It became clear from this study that descriptive morphometry is a useful tool in the analysis of

malformation. With this method it was shown that the malformation in Ts 12 affects the neural tube only, while the associated traits are determined by the effects of hypoplasia. In contrast, Vitamin A causes generalized mesenchymal and skeletal disturbances of the development of the skull base and the face apart from the exencephalic malformation. Another approach has been used by Putz and Morriss-Kay (1981) who studied the early phases of morphogenesis of exencephaly in Ts 12, in particular at day 9 when the folding of the neural plate and the closure of the neural tube take place. From these investigations it appears that submicroscopic defects of the neuroepithelial basement membrane play a role, together with other factors as cellular deficiency of the cranial mesenchyme (B. Putz, Pers. comm.).

b) Specific Models of Human Trisomy. Mouse and human trisomy may show, by morphogenetic coincidence, similar developmental disorders. The occurrence of holoprosencephaly and cyclopia in severe manifestation of murine Ts 1 and human trisomy 13 is an example of this phenomenon which reflects the fact that mammalian embryology follows similar developmental patterns in mouse and man.

A more specific relationship has been claimed for Ts 16 of the mouse and trisomy 21-Down's syndrome in man (Polani and Adinolfi 1980; Epstein et al. 1981). This assumption is based upon the conservation and synteny of at least three gene loci (SOD-1, the interferon receptor protein IFRC, and PRGS: Francke and Taggart 1979; Cox et al. 1980 and 1981) on a distal segment of the murine chromosome 16 and on the human chromosome 21. A noteworthy detail from descriptive embryology of murine Ts 16 (Miyabara et al. 1982) is the considerable role which common AV-canal plays, apart from other cardiovascular malformations, since this anomaly is a very characteristic finding in Down's syndrome. Further confirmation of genetic homology between both chromosomes should facilitate the acceptance of murine Ts 16 as a special model for human chromosomal disease, and stimulate all kinds of embryological, biochemical and immunological studies in murine Ts 16 with the aim of model analyses for human trisomy 21.

No other "homologous trisomies" in mouse and man are known at present, but the rapid progress of gene mapping may soon provide new hints. In the meantime it seems worthwhile to seek for insights into problems of human pathology by the comparatively easy access to special organs in the murine trisomic systems. The possibility of a longitudinal study of brain development in postnatally surviving Ts 19 (see Figs. 3 and 4) is of great witerest in these circumstances because of the existence of an organ-related model of human trisomy 21.

c) Use of the Mouse Model for Studying General Principles of Developmental Errors Caused by Chromosome Abnormality. There are no simple answers, neither in man nor in the mouse, to the questions of why trisomy of the zygote results in abnormal development or why early or later developmental breakdown is inevitable. But a systematic approach in the mouse model provides better clues than are available in man, permitting an analysis of the critical phases in the development of trisomic conditions.

Unlike zygotes affected by exogenous teratogens, the zygote with chromosome abnormality is a defective system from the beginning. Presumably, more or less effective regulation of growth and differentiation may be possible over variable periods of development, as long as the biochemical pathways and the morphogenetic processes are not too deeply disturbed. The functional integrity or defectiveness of a trisomic cell is determined by direct gene dosage effects as well as by indirect and secondary biochemical consequences of the triplication of a chromosome (Epstein et al. 1981).

Hypoplasia, i.e. generalized deficiency of cells, is the most common expression of such secondary cellular disorders in the developing organism (see Fig. 4), and it seems reasonable to expect, therefore, that impairment of the proliferative capacity or disturbances of the quantitative aspects of the cell cycle are a characteristic of trisomic cells. Yet, this issue is controversial. Growth impairment of in vitro cultivated fibroblast-like cells from abortions or from newborns with chromosome abnormalities has been found by some (Schneider and Epstein 1972; Paton et al. 1974) but not by others (Hoehn et al. 1980). Own experiments with Ts 12 and Ts 19 of the mouse also showed that no major differences in the cell cycle or in proliferation kinetics exist between trisomic and normal cells, at least so in monolayer cultures grown from older fetal stages (Gropp et al. 1982). However one has to realize that these findings do not exclude trisomy-dependent disorders or depression of proliferation in early stages of embryonic development by any means, and in particular we must consider that conditions in cell culture are not comparable to those present in the assembly of the intact embryonic organism (see below).

Nevertheless, despite the difficulties of assessment, impairment of growth and ensuing hypoplasia express the inherent defectiveness of a trisomic zygote and represent a basic continuum of damage of the trisomic system. On this basis, judged from the developmental profiles of monosomies and trisomies (Fig. 3), it appears meaningful to propose three main critical phases which determine the eventual downward course of these profiles (Fig. 5). A first and second critical phase of increased developmental vulnerability coincide roughly with the periods of implantation and organogenesis, respectively.

Certainly, death of the anlagen can result, in particular in early development, if cellular depletion falls short of a minimum level of cell number. Otherwise, direct dosage effects of gene triplication must be implicated during these two phases. They have been recognized in man and in the mouse (Krone and Wolf 1977; Epstein et al. 1977), and available results for the mouse on dose/effect relationships in trisomic conditions are presented in Table 1. All studied cases show an expected 3:2 ratio to normal diploids. Dosage increase of single gene controlled enzymes like the ones listed in Table 1 may not cause adverse effects, but this could well be evident if in trisomy a multitude of "ordinary" genes or a smaller number of key genes are triplicated.

Direct effects of dosage abnormality should be amenable to complementation. Supporting evidence of metabolic disorders curable by association with normal cells comes from the observation of considerable longevity (9 months) in the Ts 17 constituent in Ts 17↔normal chimeras (C.J. Epstein, Personal communication). Moreover, it has been claimed that early mortality in monosomy is caused by dosage effects rather than by the haploid expression of lethal genes. Evidence for this is provided by the observations of Magnuson et al. (1982) showing that the loss of monosomy 19 between early and late blastocyst stage occurs at similar rates in non-inbred and in inbred strains, and that viable monosomic cells were present in Ms 19↔normal chimeras on day 9. Such viability, long past the lethal period, needs an explanation like the metabolic complementation of a synthesis defect, rather than indicating cell lethality.

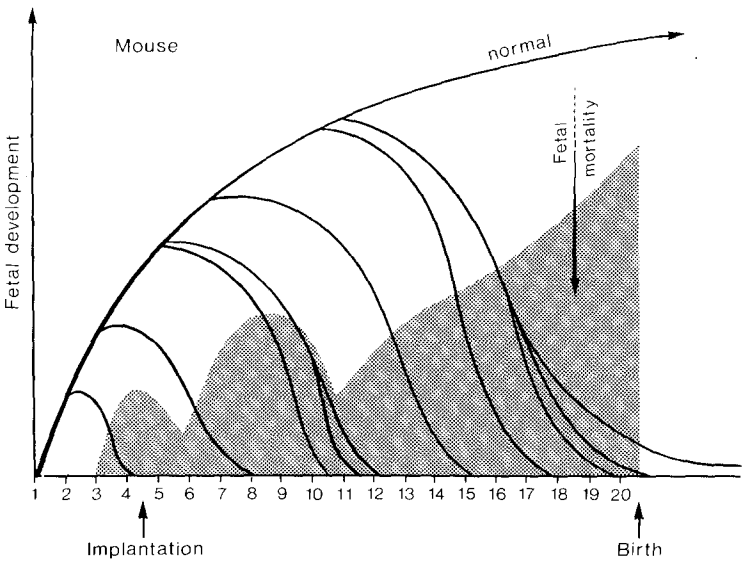

Fig. 5. Critical phases of developmental vulnerability (see Fig. 3)

A more complex pattern of gene dosage effects has become evident from a study by Klose and Putz (1982), aimed to assess protein changes in mouse trisomies (Ts 1, 12, 14, and 19). Apart from a greater number of less specific protein changes, a few seem to be specifically associated with the abnormal phenotype. It can well be argued that these latter changes concern membrane proteins, and that they provide a clue for the understanding of the membrane defects observed in the very early stages of Ts 12-dependent exencephaly (see above).

The origin of gross malformations such as neural tube defects, craniofacial anomalies and cardiovascular disorders, falls into the second critical phase (Fig. 5). Stage-, time-, and strain-specific vulnerability of blastemas involved in morphogenesis, on the one hand, and systemic hypoplasia or excessive cell deficiency in specific blastemas on the other, can explain the types and the severity of malformations as well as their semispecificity.

Evidence for a third and presumably continuous critical phase (Fig. 5) comes from the multiple observations of late fetal damage, mostly unrelated to the occurrence of malformation, but associated with severe, though sometimes transitory oedema in almost all trisomies surviving longer than day 14. Such a condition directed interest to the "oedema sydrome", described by Grabowski (1977) in chicken embryos after exposure to moderate hypoxia. It is explicable in the chicken as a consequence of generalized osmoregulatory disturbance and this seems fully applicable to the situation in the trisomic mouse fetus, where it may be caused by insufficiency of the circulation in the hypoplastic fetal part of the placenta. In fact, morphometric studies of the placenta in mouse trisomies (Ts 1, 12, and 19) have indicated the presence of hypoplasia and arrest of differentiation of the fetal vasculature commensurate to the severity of manifestation of the particular trisomies (Gropp 1981). This leads us to the conclusion that insufficiency of the fetal part of the trisomic placenta is a main critical factor causing fetal underperfusion and oxygen deficiency which, from the progressive nature of gestation, become increasingly severe with the growing metabolic needs of the fetus.

Table 1. Dose relation in triplication of autosomal genes of the mouse (observations in autosomal Ts)

Enzyme	Gene loc. on chrom. No.	Dose relation Ts: norm contr.	
ID-1	1	3:2	Epstein et al. 1977
MOD-2	7	3:2	Eicher and Coleman 1977
GPI-1	7	3:2	Eicher, E, personal communication
GOT-1	19	3:2	Fundele et al. 1981
PGAM-A2	19	3:2[a]	Fundele et al. 1981

[a] Blood, liver, brain, kidney (type AA) (Heart: Type AB – Scel. muscle: Type BB)

There is good reason to believe that each of the mechanisms discussed above are applicable to the pathology of developmental disorders in man caused by chromosome abnormalities. In particular, the "oedema syndrome" and late fetal mortality as observed in the fetal XO and several autosomal trisomy conditions in man support the assumption of an effective, long lasting epigenetic critical period during the second half of prenatal development.

Possibilities of Rescue of Trisomic Cellular Systems for Longer Survival

Developmental impairment and eventual breakdown of the trisomic organism before or shortly after birth is inevitable. Is this the consequence of defects on the cellular level or of disturbances associated with the incorporation of the cells into the organization of the developing organism? The study of cellular systems isolated from the trisomic organism can be expected to give answers to these questions, and to indicate a method for rescuing trisomic (or monosomic) cells from early death (Gropp et al. 1982). As shown in Fig. 6, several approaches to studying isolated trisomic cells at different levels of complexity are conceivable. In the following the strength of three of them is briefly checked.

As mentioned above, no important differences of growth kinetics exist between trisomic and euploid cells, at least in Ts 1, 12, and Ts 19 (Nielsen et al. 1982) using isolated fibroblast-like cells grown in vitro. The conclusion must be that the growth behaviour of cells isolated from the developing trisomic organism is not subject to the condition of limited life expectancy valid in the organized in vivo system.

The inclusion of trisomic or monosomic constituents in tetraparental chimeras (Fig. 6) produced by aneuploid↔diploid association of preimplantation embryos guarantees a considerable increase of longevity of the aneuploid part of the chimera. This has been shown for Ms 19, and for Ts 16 and 17 (Magnuson et al. 1982; Cox et al. 1982; C.J. Epstein, Personal communication). The production of association or injection chimeras with aneuploid embryos is certainly one of the main technologies for longer lasting rescue of the aneuploid (trisomic or monosomic) part, as well as for an analysis of the cell lineage, the competitive developmental capacity, and the metabolic defects or requirements of the aneuploid constituent.

Thirdly, the isolation and the transfer of trisomic haemopoietic stem cells from fetal liver to lethally irradiated adult hosts has been used for testing the capability of trisomic cells to reconstitute the haemopoietic compartments of the transplantation recipients (Herbst et al. 1981; Pluznik et al. 1981). Transplanted Ts 12 and Ts 19 stem cells are able to restore the host's haemo- and

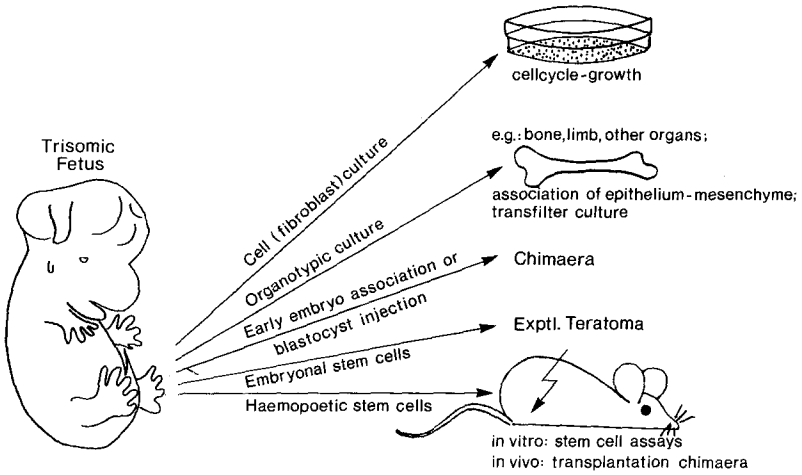

Fig. 6. Possibilities of separation of cellular systems of variable complexity from the aneuploid fetus a) for rescue of cells and tissues, and b) for stepwise analysis of the phenotype at levels between the isolated cell and the intact fetal organism

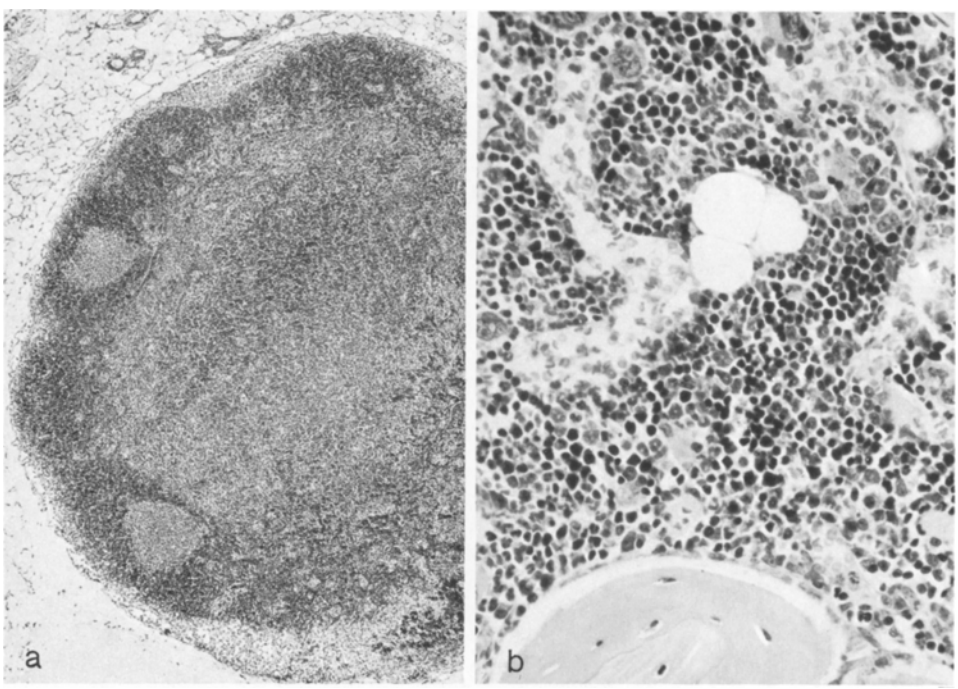

Fig. 7. a Lymph node of Ts 12 recipient ("radiation chimera") 60 days after transfer of Ts 12 fetal haemopoietic stem cells. Reconstitution and follicle formation similar to controls. **b** Bone marrow of Ts 19 recipient, 60 days after Ts 19 stem cell transfer. Full reconstitution of haemopoiesis with trisomic cells. (Transplantation experiment of Herbst et al. 1981)

lymphopoiesis successfully and permanently (Fig. 7) with longest documented survival of 270 and 180 days, respectively. Nevertheless, if Ts 12 stem cells are transplanted into a competitive (mixed cell) system with normal cells (Hongell et al. 1982), inferiority of the trisomic cells is observed.

Other trisomies of the mouse, such as Ts 13 (Hongell et al. 1982) and Ts 16 (Herbst et al. 1982), are not able to restore the haemo- and lymphopoietic systems of lethally irradiated recipients fully or permanently. In fact, present evidence from stem cell assays (CFUs and CFUc) indicates that, at least in Ts 16, the defect of the myeloid systems is located at a stage just past the pluripotent stem cell level. Reconstitution of lymphoid tissue is much below the standard of controls, or of Ts 12 and Ts 19.

Like other methods of separation of cells or tissues from an aneuploid organism (Fig. 6), the experimental strategy of isolation and transplantation of haemopoietic stem cells is a potent technique which can serve several purposes. Longer survival and, thus, better experimental accessability of trisomic (or monosomic) cellular or tissular systems to morphological and functional assays is one of the main aims. Another aim is the study of the expression of aneuploidy in vitro and in vivo in a comparative and stepwise order on different levels from the single cell up to highly organized cell complexes. The latter approach is expected to contribute substantially to knowledge of the phenotypic manifestation of aneuploidy in the organism. The methodology and the actual accumulation of such knowledge in the animal model will direct new lines of research in man. Undoubtedly, in the field of genetic and in particular, in chromosomal disease, the lessons taught by the mouse model for human pathology are not merely based on formal analogies. Their impact comes from the similarity of the fundamental mechanisms, and shown in at least some instances, from homologies of the genetic material, a subject neglected in this aspect of disease in man.

Acknowledgements. I would like to thank Drs. H. Winking, E.W. Herbst (Lübeck), C.J. Epstein (San Francisco, Calif.) and D.H. Pluznik (Ramat Gan, Israel) for continued collaborative work. This publication is based on work supported by Deutsche Forschungsgemeinschaft (Gr 71/46-50). Work on trisomy 16 and 19 of the mouse has been done in fulfilment of contract NICHD-NO1-HD-8-2858.

References

Boué JG, Boué A (1976) Chromosomal anomalies in early spontaneous abortion. In: A. Gropp, K. Benirschke (eds) Curr Top Pathol 62: Developmental Biology and Pathology. Springer, Berlin Heidelberg New York, pp 193–208

Boué JG, Boué A, Lazar P (1975) Retrospective and prospective epidemiological studies of 1500 karyotyped spontaneous human abortions. Teratology 12:11–16

Cox DR, Epstein LB, Epstein CJ (1980) Genes coding for sensitivity to interferon (IfRec) and soluble superoxide dismutase (SOD-1) are linked in mouse and man and map to mouse chromosome 16. Proc Natl Acad Sci USA 77:2168–2172

Cox DR, Goldblatt D, Epstein CJ (1981) Chromosomal assignment of mouse PRGS: Further evidence for homology between mouse chromosome 16 and human chromosome 21. Am J Num Genet 33:145A

Cox DR, Smith SA, Zamora T, Epstein LB, Epstein CJ (1982) Mouse trisomy 16 as an animal model of Down syndrome: formation of viable adult trisomy 16↔diploid chimeras. Clin. Res. 30 (In press)

Dyban AP, Baranov VS (1978) Cytogenetics of mammalian development (in Russian). Problemi Biologii Razvitija. Moskwa: Izdatelstwo "Nauka", p 216

Eicher EM, Coleman LC (1977) Influence of gene duplication and X-inactivation on mouse mitochondrial malic enzyme activity and electrophoretic patterns. Genetics 85:647–658
Epstein CJ, Travis B (1979) Preimplantation lethality of monosomy for mouse chromosome 19. Nature (Lond) 280:144–145
Epstein CJ, Tucker G, Travis B, Gropp A (1977) Gene dosage for isocitrate dehydrogenase in mouse embryos trisomic for chromosome 1. Nature (Lond) 267:615–616
Epstein CJ, Cox DR, Epstein LB (1979) Synteny of the mouse genes for soluble superoxide dismutase (*SOD-1*) and the species-specific sensitivity to interferon (*Avg*). Am J Hum Genet 31:46A
Epstein CJ, Epstein LB, Cox D, Weil J (1981) Functional implications of gene dosage effects in trisomy 21. In: GR Burgio, M Fraccaro, L Tiepolo, U Wolf (eds) Trisomy 21 Hum Genet Suppl 2. Springer, Berlin Heidelberg New York, pp 155–171
Ford CE (1972) Gross genome unbalance in mouse spermatozoa: does it influence the capacity to fertilize? In: RA Beatty, S Gluecksohn-Waelsch (eds) The genetics of the spermatozoon. Edinburgh and New York: University of Edinburgh, pp 359–369
Francke U, Taggart RT (1979) Assignment of the gene for cytoplasmic superoxide dismutase (Sod-1) to a region of chromosome 16 and of Hprt to a region of the X chromosome in the mouse. Proc Natl Acad Sci USA 76:5230–5233
Francke U, Lalley PA, Moss W, Ivy J, Minna JD (1977) Gene mapping in Mus musculus by interspecific cell hybridization: assignment of the genes for tripeptidase-1 to chromosome 10, dipeptidase-2 to chromosome 18, acid phosphatase-1 to chromosome 12, and adenylate kinase-1 to chromosome 2. Cytogenet Cell Genet 19:57–84
Fundele R, Bücher Th, Gropp A, Winking H (1981) Enzyme patterns in trisomy 19 of the mouse. Dev Gen 2:291–303
Grabowski CT (1977) Altered electrolyte and fluid balance. In: JG Wilson, FC Fraser (eds), vol. II, Handbook of teratology. Plenum Press, New York, pp 153–170
Green MC (1981) Genetic variants and strains of the laboratory mouse. G. Fischer, Stuttgart, pp 8–282
Grohé G, Gropp A (1980) Research note (on Ts 19). Mouse News Letter 63:23
Gropp A (1974) Animal model: Autosomal trisomies in fetal mice. Exencephaly in mice with trisomy 12. Am J Pathol 77:539–542
Gropp A (1981) Clinical and experimental pathology of fetal wastage. In: K Semm, L Mettler (eds) Human reproduction. Excerpta Medica, Amsterdam. ICS No 551, pp 208–216
Gropp A (1978) Relevance of phases of development for expression of abnormality. Perspectives drawn from experimentally induced chromosome aberrations. (Life Sciences Report 10) Dahlem Konferenzen, Berlin, pp 85–110
Gropp A (1971) Reproductive failure due to fetal aneuploidy in mice. VII World Congr. on Fertility and sterility, Tokyo/Kyoto. Excerpta Medica, Amsterdam. ICS No 234, pp 326–330
Gropp A, Grohé G (1981) Strain background dependence of expression of chromosome triplication in the mouse embryo. Abstract. Hereditas 94:7–8
Gropp A, Herbst EW, Nielsén K (1982) In vivo and in vitro assays of trisomic cells isolated from the fetal organism or rescued by transfer to non-trisomic hosts. In: D Neubert HJ Merker (eds), Culture techniques in prenatal toxicology. De Gruyter Berlin (In press)
Gropp A, Winking H (1981) Robertsonian translocations: Cytology, meiosis, segregation patterns and biological consequences of heterozygosity. Symp Zool Soc Lond 47:141–181
Gropp A, Winking H, Zech L, Müller HJ (1972) Robertsonian chromosomal variation and identification of metacentric chromosomes in feral mice. Chromosoma (Berlin) 39:265–288
Gropp A, Kolbus U, Giers D (1975) Systematic approach to the study of trisomy in the mouse. II. Cytogenet Cell Genet 14:42–62
Gropp D, Winking H, Gropp A (1981) Research note (on Ts 18). Mouse News Letter No 65:32
Hamerton JL, Canning N, Ray M, Smith S (1975) A cytogenetic survey of 14,069 newborn infants. Clin Genet 8:223–243
Herbst EW, Pluznik DH, Gropp A, Uthgenannt H (1981) Trisomic hemopoietic stem cells of fetal origin restore hemopoiesis in lethally irradiated mice. Science 211:1175–1177
Herbst EW, Gropp A, Nielsén K, Hoppe H, Freymann M, Pluznik DH (1982) Reduced ability of mouse trisomy 16 stem cells to restore hemopoiesis in lethally irradiated animals. In: S Baum, GD Ledney, A Khan (eds), Experimental hematology today. Karger, Basel (In press)
Hoehn H, Simpson M, Bryant EM, Rabinovitch PS, Salk D, Martin GM (1980) Effects of chromo-

some constitution on growth and longevity of human skin fibroblast cultures. Am J Med Genet 7:141–154

Hongell K, Gropp A (1982) Trisomy 13 in the mouse. Teratology (In press)

Hongell K, Herbst EW, Gropp A (1982) Transplantation of mixed trisomic and normal fetal hemopoietic stem cells of the mouse to irradiated hosts. Dev Genet (In press)

Klose J, Putz B (1982) Analysis of two-dimensional protein patterns from mouse embryos with different trisomies (developmental stages/developmental impairment). Proc Natl Acad Sci (USA) (In press)

Krone W, Wolf U (1977) Chromosome variation and gene action. Hereditas 86:31–36

Magnuson T, Smith SA Epstein CJ (1982) The development of monosomy 19 mouse embryos. J Embryol Exp Morphol (In press)

Miller DA, Miller OJ (1981) Cytogenetics. In: The mouse in biomedical research, vol I. Academic Press, New York London Toronto San Francisco, pp 241–261

Milunski A, Atkins L (1977) The frequency of chromosomal abnormalities diagnosed prenatally. In: E Hootz, IH Porter (eds) Population cytogenetics. Academic Press, New York – San Francisco – London, pp 11–25

Miyabara Sh, Gropp A, Winking H (1982) Trisomy 16 in the mouse fetus associated with generalized edema, cardiovascular and urinary tract anomalies. Teratology 25 (In press)

Nielsén K, Marcus M, Gropp A (1982) In vitro growth kinetics of mouse trisomies 12 and 19. J Cell Biol (subm)

Paton GR, Silver MF, Allison AC (1974) Comparison of cell cycle time in normal and trisomic cells. Humangenetic 23:173–182

Pearson PL, Roderick TH (1978) Report of the committee on comparative mapping. Human Gene Mapping 5. Cytogenet Cell Genet 22:150–162

Pexieder T, Miyabara Sh, Gropp A (1981) Congenital heart disease in experimental (fetal) mouse trisomies: Incidence. In: Mechanisms of cardiac morphogenesis and teratogenesis. Perspec Cardiovasc Res 5: (T Pexieder, ed), Raven Press, New York, pp 389–399

Pluznik DH, Herbst EW, Lenz R, Sellin D, Hertogs CF, Gropp A (1981) Controlled production of trisomic hematopoietic stem cells: An experimental tool in hematology and immunology. In: SJ Baum, GD Ledney, A Khan (eds), Experimental hematology today. Karger, Basel, pp 3–11

Polani PE, Adinolfi, M (1980) Annotations: Chromosome 21 of man, 22 of the great apes and 16 of the mouse. Dev Med Child Neurol 22:223–225

Putz B, Morriss-Kay G (1981) Abnormal neuralfold development in trisomy 12 and trisomy 14 mouse embryos. I. Scanning electron microscopy. J Embryol exp Morphol 66:141–158 1981

Putz B, Krause G, Garde T, Gropp A (1980) A comparison between trisomy 12 and vitamin A induced exencephaly and associated malformations in the mouse embryo. Virchows Arch (Path Anat) 368:65–80

Rehder H (1981) Pathology of trisomy 21- with particular reference to persistent common atrioventricular canal of the heart. In: GR Burgio, M Fraccaro, L Tiepolo, U Wolf (eds) Trisomy 21. Hum Genet, Suppl 2. Springer, Berlin-Heidelberg-New York, pp 57–73

Schneider EL, Epstein CJ (1972) Replication rate and lifespan of cultured fibroblasts in Down's syndrome. Proc Soc Exp Biol Med 141:1092–1094

Stolla R, Gropp A (1974) Variation of the DNA content of morphologically normal and abnormal spermatozoa in mice susceptible to irregular meiotic segregation. J Reprod Fert 38:335–346

Tettenborn U, Gropp A (1970) Meiotic non-disjunction in mice and mouse hybrids. Cytogenetics 9:272–283

White BJ, Tjio J-H, Water LC van de, Crandall C (1974a) Trisomy 19 in the laboratory mouse. I. Frequency in different crosses at specific developmental stages and relationship of trisomy to cleft palate. Cytogenet Cell Genet 13:217–231

Trisomy 19 in the laboratory mouse. II. Intra-uterine growth and histological studies of trisomics and their normal littermates. Cytogenet Cell Genet 13:232–245 (1974b)

Accepted December 7, 1981

Virchows Arch [Pathol Anat] (1982) 395:133–144

Virchows Archiv A

Endothelium and "Silver Lines"

An Electron Microscopic Study

Thomas Zand, Jean M. Underwood, John J. Nunnari, Guido Majno, and Isabelle Joris

Department of Pathology, University of Massachusetts Medical School, Worcester, Massachusetts, 01605, USA

Summary. The significance of endothelial "silver lines" was studied by TEM in rat aortas after perfusion with glutaraldehyde followed by silver nitrate. Standard TEM technique proved unsatisfactory (coarse silver granules, imprecise localization, artefacts). Exposure of the silver-treated aortas to photographic fixer markedly improved the image of the deposits leaving fine, stable, uniform "residual granules" about 100 Å in diameter. Most of these granules were localized along the intercellular junctions; they also tended to pool in the basement membrane beneath each junction. This image suggests that the Ag^+ ions pass through the junction, and react with its contents as well as with the basement membrane beyond it. A scheme is proposed to explain the reaction of Ag^+ ions with anions and negatively charged radicals within the junction. It is concluded that the "silver lines" represent not only a histochemical effect, but also the visualization of a transendothelial electrolyte pathway.

Key words: Endothelium – Permeability – Electron microscopy – Electrolytes – Silver

Introduction

To study endothelial surfaces, one of the most useful methods is also one of the oldest histological techniques: the blackening of the endothelial cell junctions by exposure to silver nitrate and then to light, producing the flagstone pattern known as "silver lines". This method (Chrzonsczewsky 1866) was inspired by von Recklinghausen's 8-line note proposing the use of silver nitrate solutions for histological studies (von Recklinghausen 1860) and by his later work on endothelia and mesothelia (von Recklinghausen 1863a, b). Julius Arnold used it extensively (Arnold 1875, 1876). It was realized from the beginning that the reaction had certain analogies with the photographic process, that

Offprint requests to: T. Zand at the above address

0340-1227/82/0395/0133/$02.40

the black deposit was metallic silver, and that the photosensitive compound formed in the tissues was probably silver chloride (Achard and Aynaud 1907; Stadtmüller 1921).

A significant step was accomplished in 1968 by Gottlob and Hoff, who tested the effect of many chemical reagents on the reaction. In their view, the prime mechanism was the binding of silver cations to macromolecules (polyanions) in the intercellular space.

With the advent of electron microscopy, there was hope that the understanding of the silver lines would be carried one step further. The results were confusing. Florey et al. (1959) did confirm that the bulk of reduced, metallic silver, which constituted the silver line, corresponded with the site of the intercellular junction. However, the correspondence was only approximate; much precipitate developed also in the cytoplasm alongside the junctions and in many other parts of the cell, in seemingly random fashion. Thus the method appeared to be far less specific than suggested by light microscopy.

To reexamine the significance of the silver lines by electron microscopy, we began by studying them in rat aortas fixed in glutaraldehyde and then prepared by the conventional technique (Florey et al. 1959). Like others before us, we found that the silver deposits in the endothelium were distributed in a disappointingly irregular fashion; furthermore, the metal grains tended to cause holes in the plastic embedding medium, possibly because they were in an unstable form. We therefore attempted to stabilize them with fixer as used in photography. The results were interesting in two respects: they demonstrated the expected specificity of the silver method with much finer detail, and they suggested a new physiologic significance for the silver line phenomenon.

Materials and Methods

Silver lines were produced in the aorta of 7 rats by perfusion as follows. Animals were male Wistar rats (Charles River Laboratories, Wilmington, MA, USA) weighing 225–250 g. Under ether anesthesia with the rat supine, a left thoracotomy was performed and the thoracic aorta was cannulated with an Angiocath 20 g (Deseret Co., Sandy, UT, USA). Solutions were then infused at 110 mmHg in the following sequence: glutaraldehyde 3% in cacodylate buffer, pH 7.4 (20 min), silver nitrate 0.05% (1 min), and bromide solution (NH_4Br 1%, + CoBr 3%, 1 min). The abdominal aorta was then excised between the iliac and renal arteries, immersed in glutaraldehyde 3% under a desk lamp (with a 60 Watt bulb) for a total fixation time of 5 h, and rinsed in cacodylate buffer.

For light microscopic control a 3–5 mm segment of aorta was cleared of loose adventitia and connective tissue, cut open with iridectomy scissors, opened flat with the endothelial face up, on a glass slide, and coverslipped. The remainder of the aorta was cut into 1 mm rings for electron microscopic study with or without photographic fixer, as described below.

Treatment with Photographic Fixer. The effect of photographic fixer on the "silvered" aortas was tested before or after osmium fixation. In either case, aortic rings were rinsed in cacodylate buffer, transferred to the solution of photographic fixer, rinsed again three times in buffer, and carried on through the routine embedding procedure. Representative rings were used for en face light microscopic control.

A stock solution of the photographic fixer (Kodak fixer, Cat. # 197–1720) was prepared according to the manufacturer's instructions, then diluted (with 0.1 M cacodylate buffer at pH 7.4), to 1:1, 1:2, 1:5, 1:10, 1:20, 1:50, 1:75, 1:100, 1:150, and 1:200. Standard exposure of the tissue to photographic fixer ranged from 1 to 30 s; longer exposures (5–10 min) were also tested.

Electron Microscopic Procedures. One mm rings of the silvered, glutaraldehyde-fixed aorta were post-fixed in 1.3% OsO_4 in 0.1 M cacodylate buffer at 4° C for 1 h, rinsed in cacodylate buffer, dehydrated in graded ethanols followed by propylene oxide, and infiltrated in either Polybed 812 (Polysciences, Inc., Warrington, PA, USA) or Epon 812 (E. Fullam, Inc., Schenectady, NY, USA). Ultrathin sections were cut with a diamond knife on a LKB III Ultrotome, picked up on 200 mesh copper grids, and viewed for silver deposits either unstained or after staining with uranyl acetate and lead citrate. All grids were carbon coated, and examined with a Philips 301 electron microscope.

Results

1. Tissues not Treated with Photographic Fixer

By light microscopy, the silver lines – examined at medium and high powers – were either narrow and dense or broader and less dense; they gave the impression of a ribbon twisting along its axis, so that it was seen at times on edge, at times flat (Fig. 1). *By electron microscopy* the electron-opaque silver deposits tended to disappear under the beam; they ranged from large, amorphous masses, to spherical bodies 500–100 Å in diameter, to very fine particles at the limit of resolution. Many of the larger grains tended to create holes in the Epon which enlarged under the beam making observation difficult (Fig. 2A and B). Some grains showed a banded crystalline structure. The heaviest deposits of grains corresponded to the intercellular junctions; at times the latter were almost obliterated by the deposit, but a part of the junction was usually recognizable

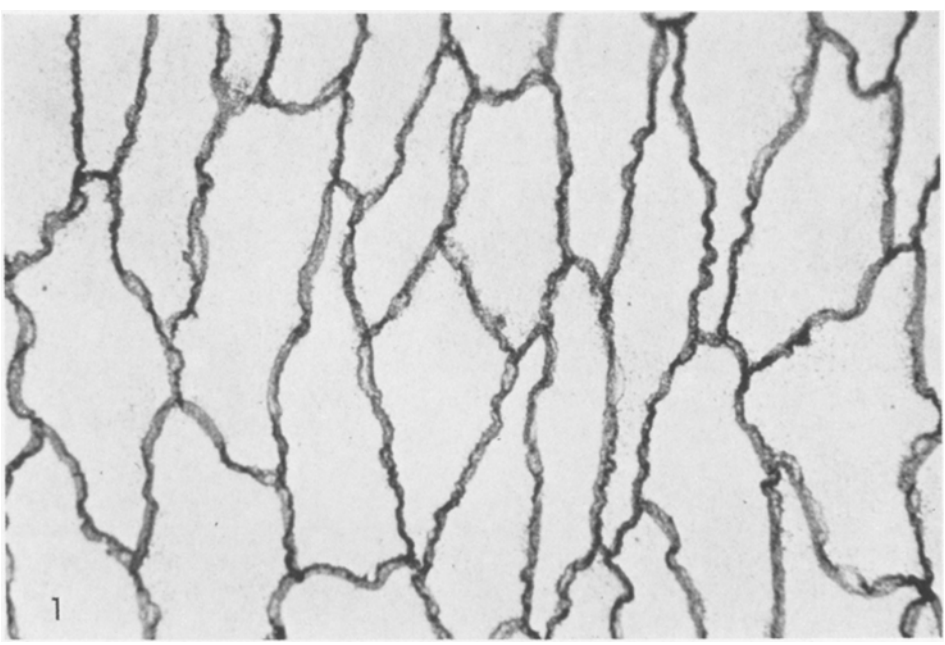

Fig. 1. Endothelium of rat aorta; appearance of the silver lines obtained by perfusion with 0.05%$AgNO_3$ after glutaraldehyde fixation. Note the "twisting ribbon" aspect of the lines. 1:925

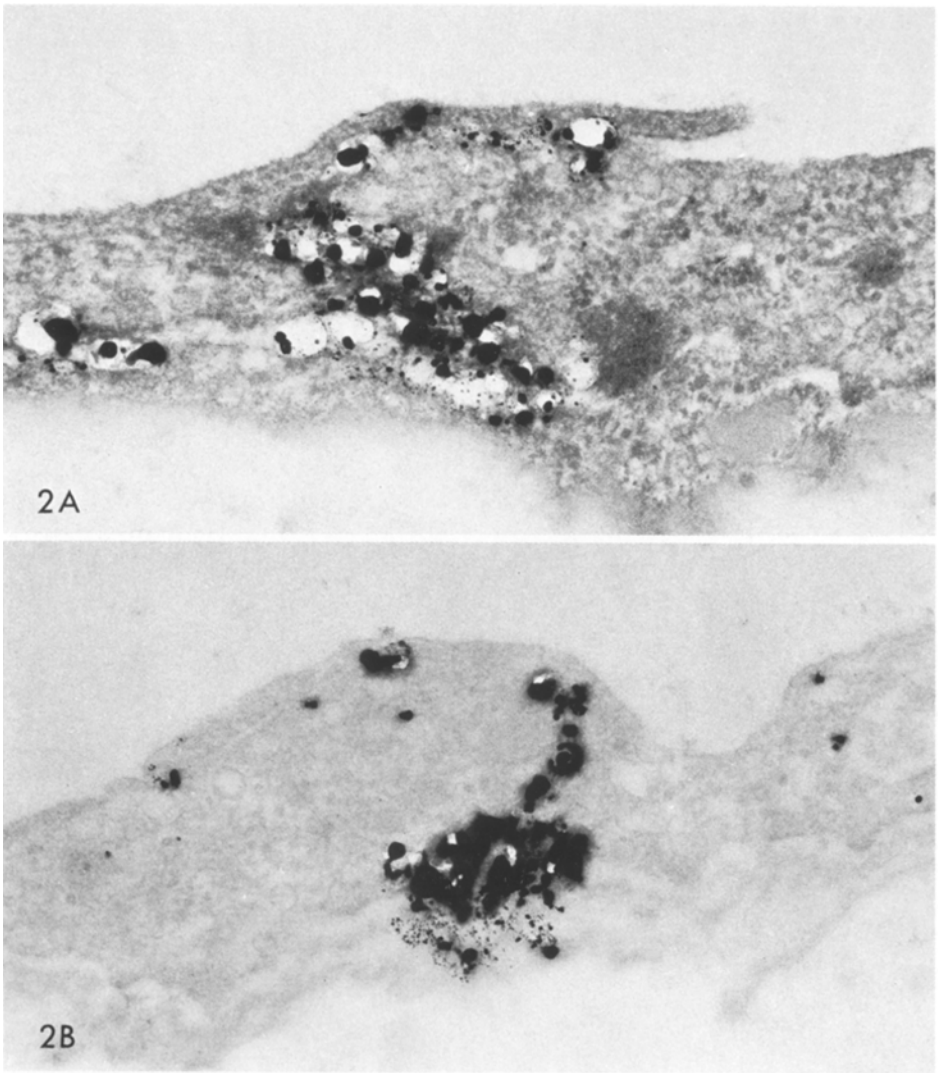

Fig. 2A, B. Appearance of a silver line in cross section, as shown by conventional TEM technique (rat aorta; 1:51,300). **A** Note coarse silver granules, poor localization and formation of holes (uranyl acetate and lead citrate). **B** Same conditions but unstained section. The silver granules are better visible, but the result is equally unsatisfactory

(Fig. 2A and B). Comparison of lead-stained and unstained sections showed that some of the silver was lost during the staining process. The luminal surface showed grains scattered at irregular intervals. Chance observation of endothelial cells cut in a grazing section showed that their free surface was peppered with many fine, dust-like granules of silver than could not be well discerned in cross sections. Granules were seen in occasional vesicles (Fig. 2B) and in the nucleus.

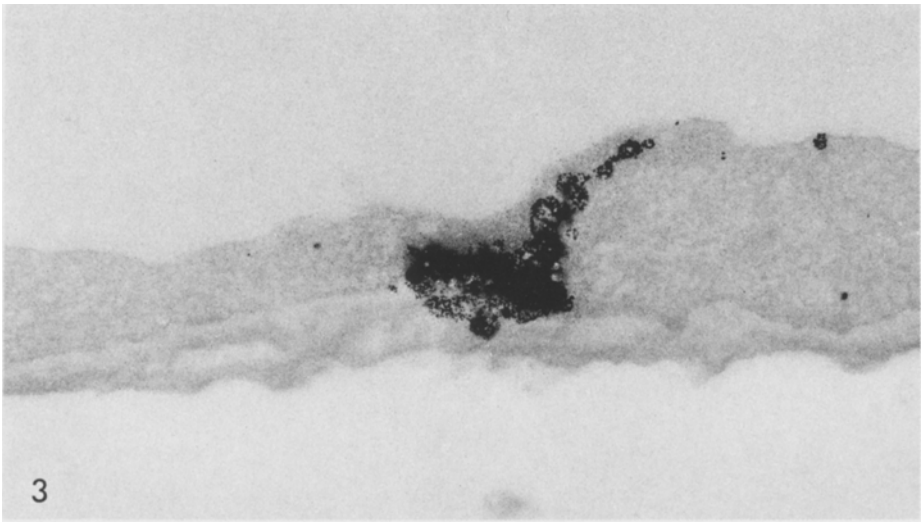

Fig. 3. Cross section of a silver line from an aorta that has been treated with dilute photographic fixer (1:50 for 1 s). Most of the coarse granules have disappeared, leaving rounded masses of smaller granules. (Unstained section; 1:40,500)

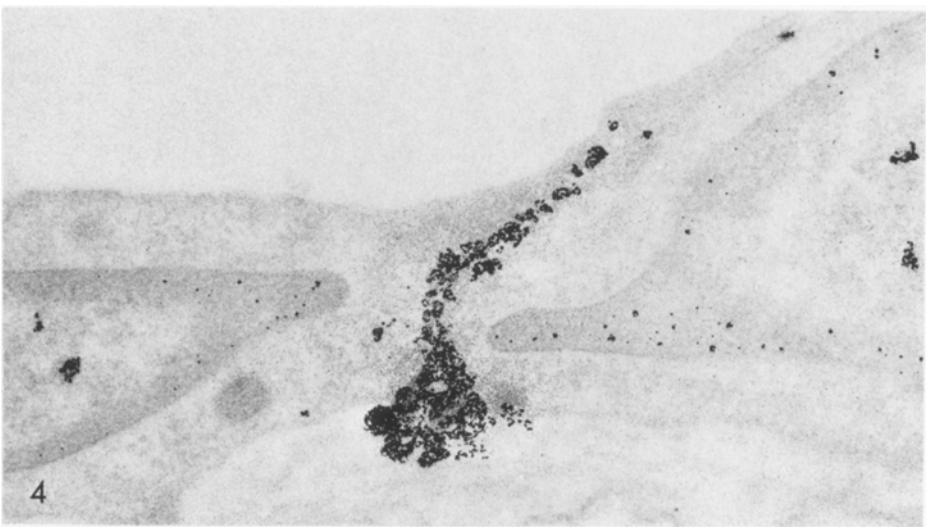

Fig. 4. Silver line from an aorta treated with more concentrated photographic fixer (1:20 for 1 s). All coarse granules have disappeared, leaving a trail of fine "residual granules" of even size. Note the pooling of granules beneath the junction in the basement membrane area. Some granules are also in the nuclei. (Unstained section; 1:40,500)

2. Tissues Treated with Photographic Fixer

During treatment with fixer no change was noticed grossly, except with tissues that had been post-fixed in osmium and then submitted to the strongest treatments with photographic fixer: a yellowish cloud emerged from these, presumably corresponding to osmium and/or silver which was being dissolved out.

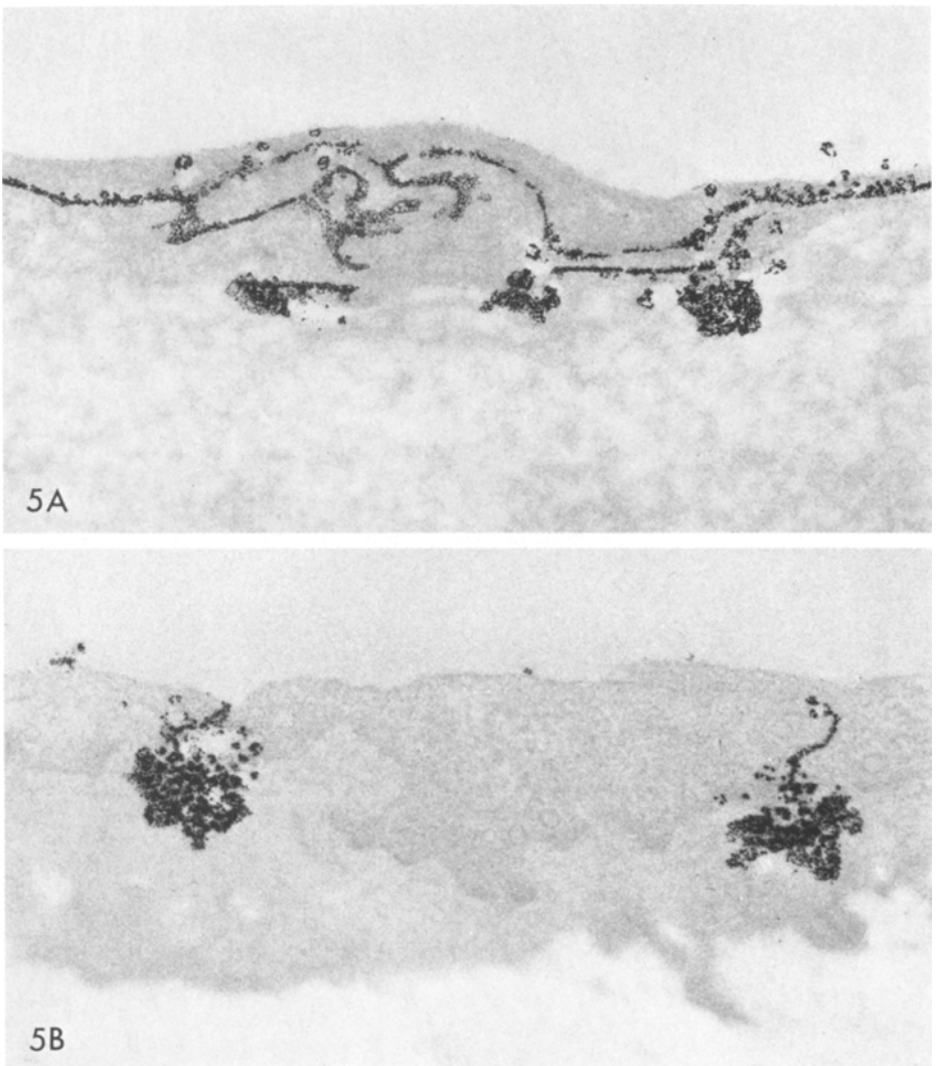

Fig. 5A, B. Silver lines after relatively strong treatment with photographic fixer (1:2 for 1 s) (unstained sections; 1:40,500). **A** The bands of residual granules represent junctions; they are broader where the junction has been cut tangentially. Note pooling of granules beneath junctions, in the basement membrane area. **B** Short junctions with abundant pooling of residual granules in the basement membrane area

By light microscopy, tissues treated with photographic fixer *before osmication* showed loss of silver; by EM results were inconsistent. When applied *after osmication*, the effect of photographic fixer was to remove the silver deposit in proportion to concentration and length of treatment. However, even with the most drastic treatments a metallic residue visible by EM always persisted (in pilot experiments, even 5 to 10 min in 1:1 dilution failed to remove this

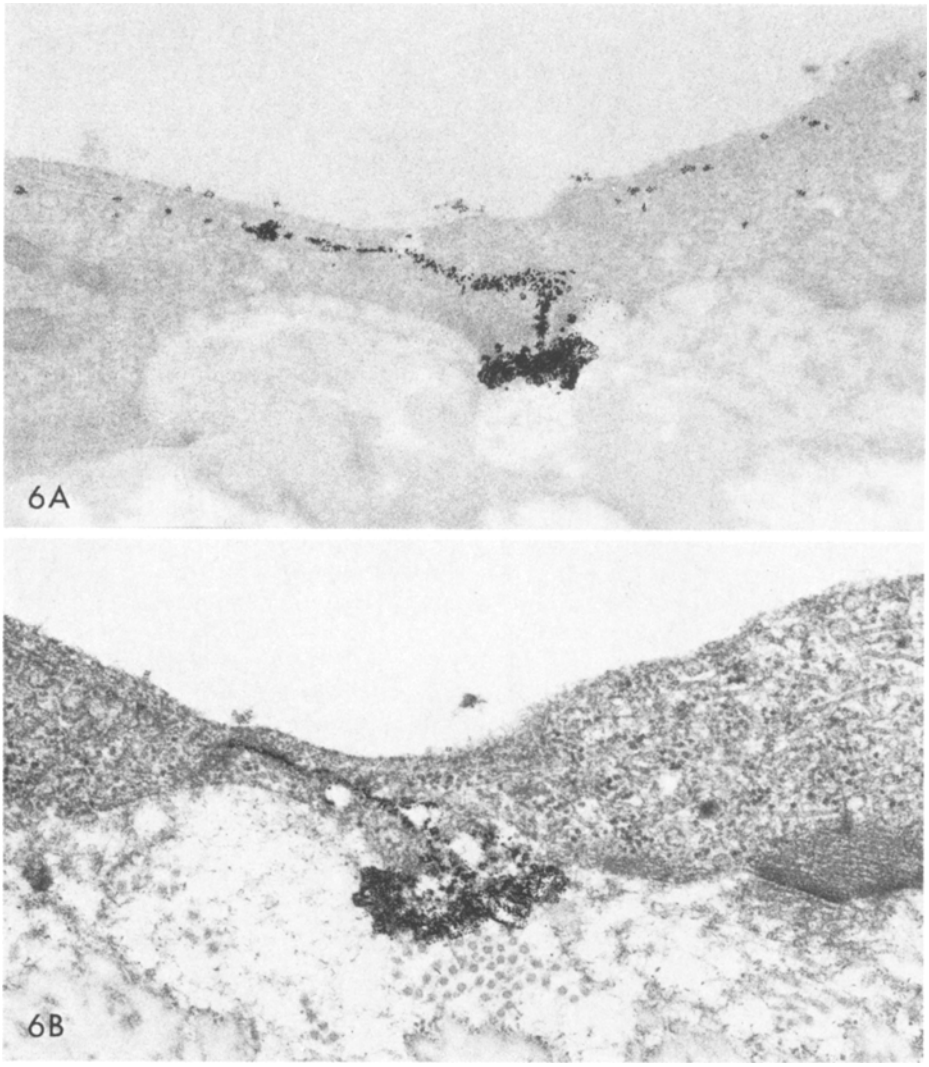

Fig. 6A, B. Adjacent sections of the same intercellular junction, from an aorta treated with 1:2 photographic fixer for 1 s (1:40,500). **A** *Unstained section.* The course of the junction is clearly visible. Note subjunctional pooling of granules. Some granules also correspond to micropinocytic vesicles. **B** *Stained section.* Silver granules in the junction are less numerous (attesting to loss of silver in the course of staining)

residue). After the mildest treatments most of the large grains were replaced by rounded masses of much smaller granules (Fig. 3). Exposure to stronger concentrations caused all the larger grains to disappear, so that the entire deposit consisted of tiny granules (*residual granules*) about 100 Å in diameter, loose or in clusters and stable under the beam (Fig. 4); the junctional deposits stood out strikingly (Fig. 5A and B). It was uncommon for one junction to be "sil-

vered" along its entire length: one or more segments usually remained free of granules. Within the junction itself, most of the granules were between the apposed cell membranes; some were just outside of these, in the cytoplasm.

A striking feature of most junctional deposits was their tendency to expand in the subendothelial layer with a cloud-like mass of granules (Figs. 4–6) that sometimes spread laterally along the basement membrane. It appeared as if the residual granules tended to pool beneath the junctions (we will refer to this phenomenon, hereafter, as *subjunctional pooling*). The ultrastructure of this zone in normal non-silvered aortas did not show any local differentiation of the basement membrane that would justify a preferential silver impregnation.

Although the amount of silver deposit decreased steadily with higher concentrations of photographic fixer, some granules always remained also on the cell surface, in the nucleus and in occasional cytoplasmic vesicles (Figs. 4 and 6A).

Discussion

Since this study combines techniques of histology and photography, it will be helpful to summarize the key steps of the photographic process.

A photographic negative is uniformly covered with photosensitive silver halide, such as bromide or chloride. When light strikes it briefly at certain points, the flash is just enough to break the link between the silver and the halogen ion, and tiny nuclei of reduced (metallic) silver are formed; these are too small to be seen and do not grow spontaneously. Developer then makes these nuclei grow by accretion; new silver ions are recruited from surrounding silver halide, to form visible black grains of metallic silver. Fixer stops the process by removing the excess (unexposed) halide; it also removes some of the secondary deposit of metallic silver. In photography as well as in the histological method the role of light is to reduce silver halide and form metallic silver. In the tissue, silver halide is present only (or primarily) at the intercellular junctions; thus light can be allowed to act intensely on the tissue as a whole, because blackening will occur primarily at one specific site. In the photographic plate, however, halide is everywhere; the action of light must be extremely brief, in order to reduce just enough silver to create a sharp image; the amount of silver reduced is so small that the image remains invisible (virtual). The process is then continued by the developer which makes sure that silver reduction – initiated by light – continues precisely at those points that have been illuminated to create a visible image.

The "twisting ribbon" aspect of the silver lines as seen by light microscopy (Fig. 1) certainly reflects the shape of the intercellular junctions; it is emphasized in our preparations because we used a very dilute concentration of $AgNO_3$, which produces finer detail.

When examined by EM, typical silver lines corresponded to coarse metallic deposits as observed by Florey et al. (1959) (Fig. 2A and B). We found that photographic fixer tended to remove the silver deposit; the disappearing grains left clear spaces indicating that their growth had somewhat disrupted the cellular structures. However, a metallic residue was always present even with the severest

exposures to fixer; this residue was qualitatively different from the deposit of the native silver lines. It consisted of very small granules of uniform size coursing along the intercellular junctions (Figs. 4–6A). The removal of silver from the tissue is entirely in accordance with the known properties of fixer; it is also known that the grains of silver corresponding to the original nucleation process are highly resistant to removal by photographic fixer (Zeiger 1938). Our evidence therefore suggests that the "residual granules" represent the original nucleation that occured during exposure to silver nitrate; the bulk of the silver, visible before exposure to photographic fixer, represents the secondary growth of these nuclei (either spontaneous [Gottlob and Hoff 1968] or induced by light). Thus we have here another parallel between the photographic and the histological process.

We can now understand the imprecise localization that puzzled Florey and collaborators; the heavy masses of silver deposited outside the junctions (in the endothelial cytoplasm) represented non-specific growth of the silver deposit, favored by an excess of $AgNO_3$ (their solution was 5 times more concentrated than ours).

In summary, our results confirm that the silver lines visible by light microscopy are the end-result of a chemical reaction with silver that starts within the intercellular junction, as was long speculated. What reacts with silver? Available data implicate chlorides and/or polyanions (Gottlob and Hoff 1968). It seems to us that chlorides could only be "held in place" by polycations; thus we propose that the interendothelial junction is filled with a material that has the properties of an ion-exchange resin endowed with anionic as well as cationic groups – possibly a glycosaminoglycan (Hayat 1975). This would explain the ability of this material to react with ions that carry a strong positive or negative charge, such as lead and other heavy metals (Sinapius 1956) as well as highly sulfated dextrans and indigo tetrasulfonate (Florey et al. 1959). We will therefore postulate – as a working hypothesis – that the silver ions interact with the junctional material as shown in Fig. 7.

Anionic groups could also be responsible for other localizations of the silver deposits on or in the endothelial cells. Although such deposits must be interpreted with caution, the grains deposited on the luminal surface were too constant to be dismissed as artefacts. Anionic groups have been demonstrated on the endothelium under a number of circumstances (Sawyer et al. 1973), using cationized ferritin or colloidal iron (Skutelsky et al. 1975; Skutelsky and Danon 1976; De Bruyn et al. 1978; Simionescu and Simionescu 1978; De Bruyn and Michelson 1979; Simionescu 1979; Pelikan et al. 1979; Cavallo et al. 1980) or dyes (Shea 1971; Behnke and Zelander 1970).

Junctional Silver: Staining Versus Passage

If we accept the notion that the residual granules represent the original silver deposits, then a very peculiar feature of these deposits must be explained: i.e. the phenomenon of subjunctional pooling. Why should silver accumulate beneath the junction? There is no special structure, in this area, that could justify a selective accumulation; nothing is present here except basement mem-

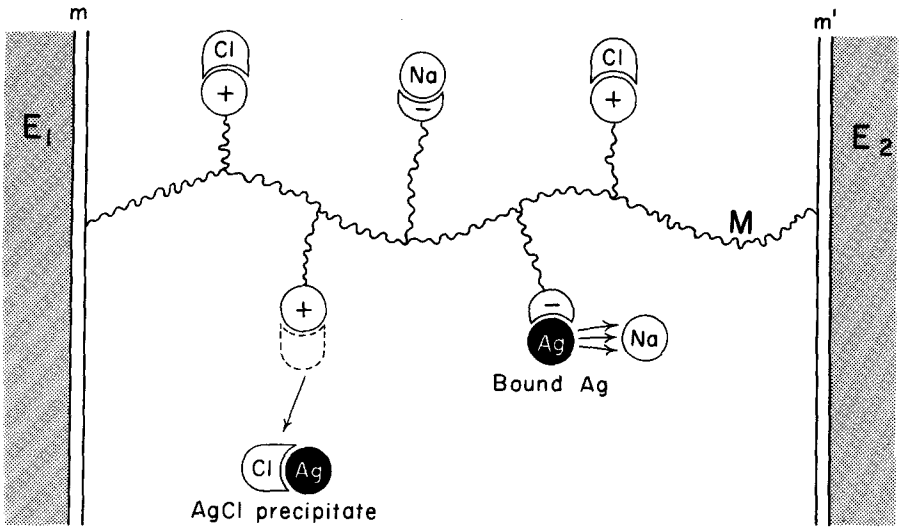

Fig. 7. Proposed scheme of the reactions of Ag^+ ions with the content of the interendothelial junction, according to the evidence available to date. E_1, E_2 endothelial cells; *m,m'* their membranes; *M* macromolecule bridging the junctional space, with side-branches bearing both positive and negative charges; these are saturated by anions and cations (represented here as Na^+ and Cl^-). In this system, *silver cations can:* 1) remove Cl^- from its binding site and form a precipitate of photosensitive AgCl; 2) displace cations attached to the macromolecule, and bind directly to the latter. Silver thus bound is said to be capable of spontaneous reduction to metallic silver even without light (Gottlob and Hoff 1968)

brane. Basement membranes in general are highly susceptible to impregnation with silver (anionic groups have been detected within them (Caufield and Farquhar 1976; Kanwar and Farquhar 1979a, b)); this is the very property underlying current histologic methods for the demonstration of basement membranes. But if we admit that we are dealing with a simple phenomenon of "silvering" of the basement membrane, the impregnation should occur everywhere beneath the endothelium, not just beneath the junctions.

We believe that the phenomenon can be explained as follows. When the solution of silver nitrate is perfused through the glutaraldehyde-fixed aorta, it finds the body of the endothelial cell relatively impermeable; a small amount of silver does permeate into it and creates some primary grains in the nucleus, but not enough to reach the basement membrane – which remains, by and large, free of silver. However, at the site of the intercellular junctions, the silver ions permeate relatively freely; be it by bulk flow, by diffusion, or by both mechanisms, silver ions reach the basement membrane in significant amounts and react with it, creating the deposits that become visible in this location as "subjunctional pooling".

We are therefore proposing that the silver is making an electrolyte pathway visible. This interpretation is entirely in line with the results of Hüttner et al. (1973) who studied the permeability of rat aortic endothelium after aldehyde fixation combined with permeation by lanthanum nitrate. The colloidal lanthanum salts formed under these conditions have an average size of 40 Å and

permeate spaces as narrow as 20 Å (Hoffstein et al. 1975). In the experiments of Hüttner et al. (1973) they penetrated along the entire length of most intercellular clefts, including the tight junctions; they were occasionally impeded by a second or third tight junction. In our experiments, the much smaller Ag^+ ion – with a diameter of 2.52 Å (West and Astle 1980) – permeated all the clefts and reached beyond them to react with the basement membrane.

Of course, we cannot offer definitive proof of a physiological electrolyte pathway by using glutaraldehyde-fixed endothelium. However, all ultrastructural and physiological correlations concerning endothelial permeability are based upon the assumption that the morphology and dimensions of the endothelial structures (junctions included) are closely preserved after glutaraldehyde fixation. If this is the case, then it should be expected that the permeability of the junction to small ions – as seen after fixation – reflects a physiological event.

Further studies are needed to test this hypothesis on living blood vessels.

Acknowledgments. This study was supported in part by Grants HL-16952 and HL-25973 from the National Institutes of Health.

We are indebted to Peter W. Healey for the photographic prints and to Jane M. Manzi for the preparation of the manuscript.

References

Achard C, Aynaud M (1907) Recherches sur l'imprégnation histologique de l'endothélium. Arch Méd Exp 19:437–458

Arnold J (1875) Über das Verhalten der Wandungen der Blutgefässe bei der Emigration weisser Blutkörper. Virchows Arch 62:587–503

Arnold J (1876) Über die Kittsubstanz der Endothelien. Virchows Arch 66:77–108

Behnke O, Zelander T (1970) Preservation of intercellular substances by the cationic dye alcian blue in preparative procedures for electron microscopy. J Ultrastruct Res 31:424–438

Caufield JP, Farquhar MG (1976) Distribution of anionic sites in glomerular basement membranes: Their possible role in filtration and attachment. Proc Natl Acad Sci USA 73:1646–1650

Cavallo T, Graves K, Granholm NA (1980) Endothelial and perivascular anionic sites during immediate transient vascular leakage. Virchows Arch [pathol Histol] 388:1–12

Chrzonsczewsky N (1866) Über die feinere Struktur der Blutcapillaren. Virchows Arch 35:169–173

De Bruyn PPH, Michelson S (1979) Changes in the random distribution of sialic acid at the surface of the myeloid sinusoidal endothelium resulting from the presence of diaphragmed fenestrae. J Cell Biol 82:708–714

De Bruyn PPH, Michelson S, Becker RP (1978) Nonrandom distribution of sialic acid over the cell surface of bristle-coated endocytic vesicles of the sinusoidal endothelium cells. J Cell Biol 78:379–389

Florey HW, Poole JCF, Meek GA (1959) Endothelial cells and "cement" lines. J Pathol Bacteriol 17:625–636

Gottlob R, Hoff HF (1968) Histochemical investigations on the nature of large blood vessel endothelial and medial argyrophilic lines and on the mechanism of silver staining. Histochemie 13:70–83

Hayat HA (1975) Positive staining for electron microscopy. Van Nostrand Reinhold Co., New York, pp 124–147

Hoffstein S, Gennaro DE, Fox AC, Hirsch J, Streuli F, Weissmann G (1975) Colloidal lanthanum as a marker for impaired plasma membrane permeability in ischemic dog myocardium. Am J Pathol 79:207–214

Hüttner I, Boutet M, More RH (1973) Studies on protein passage through arterial endothelium. I. Structural correlates on permeability in rat arterial endothelium. Lab Invest 28:672–677

Kanwar YS, Farquhar MG (1979a) Presence of heparan sulfate in the glomerular basement membrane. Proc Natl Acad Sci USA 76:1303–1307

Kanwar YS, Farquhar MG (1979b) Anionic sites in the glomerular basement membrane. In vivo and in vitro localization to the laminae rarae by cationic probes. J Cell Biol 81:137–153

Pelikan P, Gimbrone MA, Cotran RS (1979) Distribution and movement of anionic cell surface sites in cultured human vascular endothelial cells. Atherosclerosis 32:69–80

Recklinghausen F von (1860) Eine Methode, mikroskopische hohle und solide Gebilde voneinander zu unterscheiden. Virchows Arch 19:451

Recklinghausen F von (1863a) Zur Fettresorption. Virchows Arch 26:172–208

Recklinghausen F von (1863b) Zur Geschichte der Versilberungsmethode. Virchows Arch 27:419–421

Sawyer PN, Stanczewsky B, Ramsey WS, Ramasamy N, Srinivasan S (1973) Electrochemical interactions at the endothelial surface. J Supramolec Struct 1:417–436

Shea SM (1971) Lanthanum staining of the surface coat of cells. J Cell Biol 51:611–620

Simionescu N (1979) The microvascular endothelium: segmental differentiations; transcytosis; selective distribution of anionic sites. In: Weissmann G (ed) Advances in inflammation research. Vol 1. Raven Press, New York, pp 61–70

Simionescu N, Simionescu M (1978) Differential distribution of anionic sites on the capillary endothelium. J Cell Biol 79:59a

Sinapius D (1956) Über Grundlagen und Bedeutung der Vorversilberung und verwandter Methoden nach Untersuchung am Aortenendothel. Z Zellforsch 44:27–56

Skutelsky E, Danon D (1976) Redistribution of surface anionic sites on the luminal front of blood vessel endothelium after interaction with polycationic ligand. J Cell Biol 71:232–241

Skutelsky E, Rudich Z, Danon D (1975) Surface charge properties of the luminal front of blood vessel walls: An electron microscopical analysis. Thromb Res 7:623–634

Stadtmüller F (1921) Historische Darstellung zur Deutung des Wesens der Silbermethode an nicht fixierten Objekten. Anat Hefte 59:79–210

Weast RC, Astle MJ (eds) (1980) Handbook of chemistry and physics. 61st edn, CRC Press, Boca Ratón, FL, pp F-216

Zeiger K (1938) Metallimprägnationen. Vor- und Nachversilberung. In: Liesegang RE (ed). Physikochemische Grundlagen der histologischen Methodik. Wissenschaftliche Forschungsberichte, Naturwissenschaftliche Reihe, Vol 48. Verlag T Steinkopff, Dresden, Leipzig, pp 113–134

Accepted December 12, 1981

Virchow Arch [Pathol Anat] (1982) 395:145–152

Virchows Archiv A

Juvenile Milk Protein Secreting Carcinoma

Gianni Botta*, Luciano Fessia** and Bruno Ghiringhello**

* Istituto di Anatomia e Istologia Patologica, (II Cattedra, Prof. G. Bussolati), University of Turin
** Servizio di Anatomia Patologica e di Ricerche Cliniche Ospedale S. Anna, (Prim. Inc. V. Aimone), Turin, Italy

Summary. A case of juvenile secretory carcinoma of the breast is reported. The tumor occured in a 19 yr-old nulliparous woman and was treated by local resection; it recurred 7 years later. Slight infiltration of the pectoral muscle, metastatic involvement of one lymph node and multifocal areas of carcinoma were found at radical mastectomy. No further recurrence has been detected after 1 year. This case confirms the slow evolution of this neoplasm but stresses that its behaviour is not always as indolent as previously believed. We have used histochemical techniques for mucins (PAS, Alcian Blue) and immunoperoxidase methods for milk proteins (MFGM, β-Casein, α-lactalbumin), for myoepithelial cells (actin) and for oncofetal antigens (CEA). Our results suggest that:

Immunoperoxidase methods for milk proteins are a more specific and reliable marker than PAS staining in characterizing the secretory activity of juvenile carcinoma.

The absence of myoepithelial cells in infiltrative areas detected by immunoperoxidase methods for actin confirms the low degree of organization in this well differentiated carcinoma of limited aggressiveness which secretes milk proteins.

Key words: Breast neoplasms – Carcinoma – Histocytochemistry

Introduction

Juvenile secretory carcinoma is an uncommon distinctive variety of breast tumor occuring mainly in young girls or young adult females. First described by McDivitt and Stewart (1966), it is a very rare tumor of which there are no more than 50 well documented cases in the modern literature (Hartman and Magrish 1955; McDivitt and Stewart 1966; Simpson and Barson 1969; Norris and Taylor 1970; Byrne et al. 1973; Sullivan et al. 1977; Oberman 1979; Oberman 1980; Tavassoli and Norris 1980). The carcinoma is characterized by gross circumscription, a microscopic secretory growth pattern and an indolent clinical course.

Offprint requests to: G. Botta, MD, Istituto di Anatomia e Istologia Patologica, (II Cattedra) University of Turin, Via Santena 7, Torino, Italy

0340-1227/82/0395/0145/$01.60

This paper describes a juvenile secretory carcinoma, the only case in a series of 3000 primary carcinomas of the breast observed in our hospitals over a period of 12 years. This case is of interest because of certain newly detected histochemical and histopathological features and the unusual clinical behaviour.

Case Report

The patient was a 19yr old nulliparous woman when she first noticed a lump in the lower inner quadrant of her right breast. She had never taken oral contraceptives or other hormonal drugs. She also had a non-toxic goitre of moderate size. The breast lump, 2 cm in diameter, was regarded clinically as a fibroadenoma or a cyst, and was surgically explored with biopsy three months after its first detection. Histological examination, performed in another hospital, resulted in a diagnosis at that time of "atypical hyperplasia". The lesion was not completely removed according to the surgical notes, nor was the patient followed-up.

Seven years later, an area of induration was found incidentally in the previous scar. A further biopsy revealed a tumor 2 cm in diameter, gray-white and with well delineated margins. This was histologically identified as juvenile secretory carcinoma of the breast with areas of muscle infiltration; a radical mastectomy was then performed. On histological examination of the mastectomy specimen residual microscopical areas of carcinoma were observed in the lower inner quadrant, at the site of the previous excisional biopses; an additional focus of carcinoma, 1 cm in diameter, was observed in the lower outer quadrant. One of 14 axillary nodes examined contained metastatic tumor. No recurrence has been observed one year after mastectomy. The contralateral breast is clinically normal.

Since the patient complained of metrorrhagia and was found to have anovulatory cycles, her hormonal status was investigated. Hormonal determination in a presumed luteal phase showed an abnormal gonadotropin secretion characterized by low-normal FSH (4.5 mUI/ml) and high LH (18.6 mUI/ml), a high ratio of plasma oestradiol over plasma progesterone levels (Oestradiol 279 pg/ml; Progesterone 4.7 ng/ml), a high level of testosterone (2.2 ng/ml) and a normal plasma prolactin (190 mcUI/ml).

Pathological Findings

The first biopsy, originally interpreted as "atypical hyperplasia" was re-examined. This revealed the typical histology of a juvenile secretory carcinoma. The lesion is characterized by neoplastic proliferation of duct cells growing in a cribriform pattern predominantly, with the formation of rudimentary gland-like spaces (Figs. 1, 2, 3). A large amount of eosinophilic secretory material was present in extra and inter-cellular spaces.

Individual tumor cells were variably polygonal and showed only mild hyperchromatism, with variability of nuclear size and rather bland nuclear morphology. Mitoses were inconspicuous. The cytoplasm is slightly granular, stains faintly with eosin and contains droplets of secretory material. The intraductal component and the sheets and cords of tumor cells which infiltrate the stroma are morphologically indistinguishable (Fig. 1). There is a mild stromal infiltration of lymphocytes and plasma cells. Although it was grossly circumscribed, microscopically the neoplasm had irregular margins. The histological features of the second excisional biopsy specimen (apparently on the residual tumor left behind at the first operation), of the residual microscopic foci as well as of the additional gross neoplasm detected in the mastectomy specimen, all shared the same characteristics as the first biopsy.

The histology of the single node metastasis was identical to that described above: only a part of the lymph node was affected.

Histochemistry

Sections of all the biopsies were stained by means of histochemical techniques for mucins (periodic acid-Schiff, PAS, and Alcian Blue at pH 2.5) and of immunoperoxidase methods employing the indirect P.A.P. procedure (Sternberger et al. 1970) and the DAB H_2 O_2 staining (Graham and Karnovsky 1966). The following antigens have been investigated:

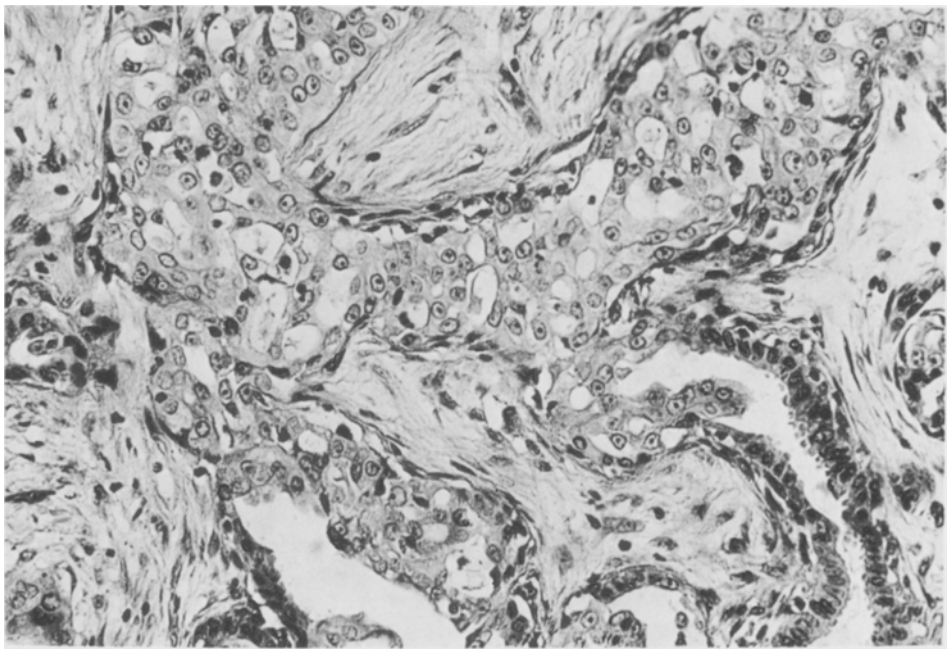

Fig. 1. In situ and invasive components of carcinoma with the typical histology of juvenile secretory carcinoma (first biopsy) (H&E, 250×)

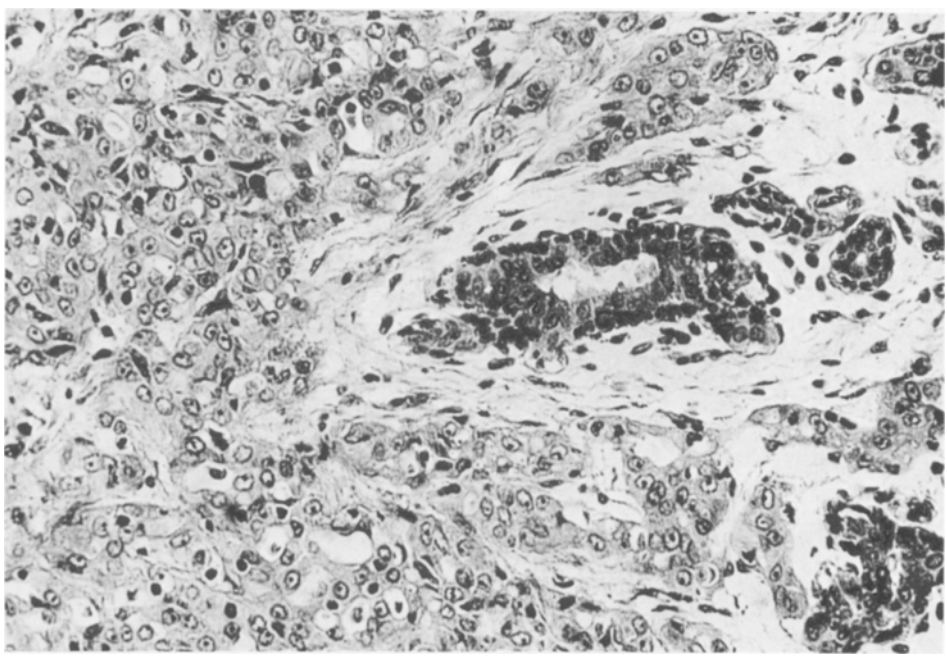

Fig. 2. Cytoplasmatic and inter-cellular vacuoles, bland vesicular nuclei and little variability of nuclear size characterize the juvenile secretory carcinoma. The nuclei of the residual duct (center right) are more hypercromatic (H&E, 250×)

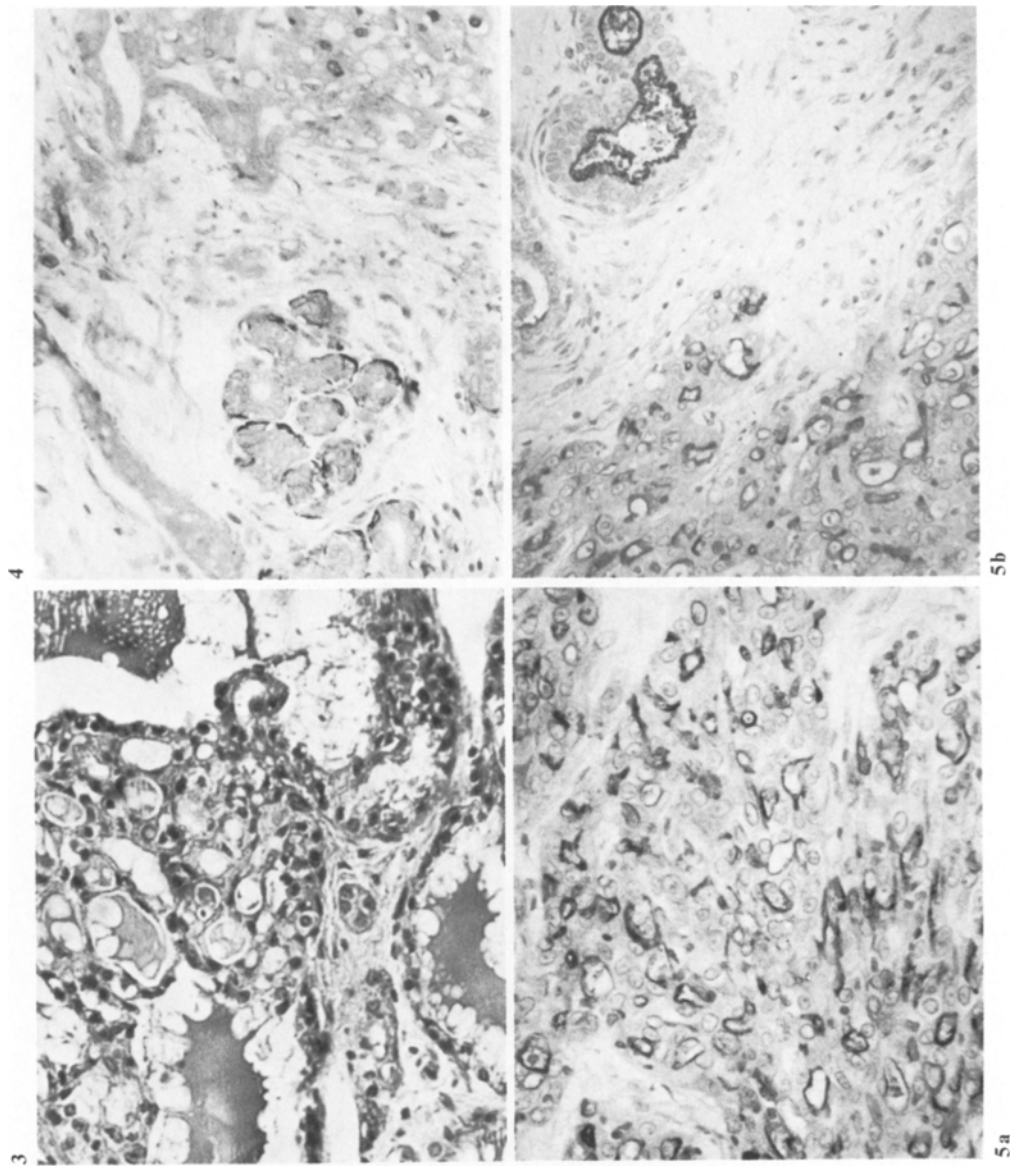

Fig. 3. Intra- and extracellular secretory material show a weak PAS positive reaction. (PAS, 250×)

Fig. 4. Immunoperoxidase staining for actin. Myoepithelial cells (dark) are located along normal ductules (center, lower) while in area of secretory carcinoma is devoid of actin-rich cells. (125×)

Fig. 5a, b. Immunoperoxidase staining for a milk protein (MFGM) Notice the intense dark staining at the cell border along inter- and intra-cellular vacuoles, similar to the staining at the apical surface of secretory cells in normal ductules (b, up on the left). (125×)

a) Anti-Milk Fat Globule Membrane (M.F.G.M.) antigen(s). Prepared according to Ceriani et al. (1977), injecting rabbits with defatted human cream.

b) Anti human β-casein was prepared in rabbits according the procedure reported elsewhere (Bussolati et al. 1975; Pich et al. 1976; Eusebi et al. 1977).

c) Anti human α-lactalbumin was prepared as reported elsewhere (Bussolati et al. 1977) in rabbits injected with lactalbumin prepared by gel chromatography.

d) Anti-carcino-embryonic Antigen (C.E.A.) was obtained from Dakopats (Copenhagen).

e) Anti-actin was generously supplied by DRS. Klaus Weber and Mary Osborn, from the Max-Planck Institute for Bio-physical Chemistry of Goettingen, (F.R.G.).

Two cases of normal lactating breast were also examined for comparison.

Results

All three biopses showed a weakly PAS positive reaction of intra- and extracellular secretory material (Fig. 3). The Alcian Blue stain was, in contrast, strongly positive in the same areas.

The immunoperoxidase methods for the detection of milk proteins (MFGM, β-casein, α-lactalbumin) were strongly positive in intra- and extracellular secretory material whether in the tumorous or in the surrounding non-neoplastic secreting breast, (Fig. 5a, b) as well as in the control lactating breast.

Neoplastic cells were intensly stained by the immunoperoxidase method for CEA.

Immunoperoxidase staining for actin showed the absence of a myoepithelial layer in the infiltrating carcinoma; the in-situ lesions showed focal areas of residual myoepithelial cells, features which have been described in situ ductal carcinomas (Bussolati et al. 1980b). By contrast, in the surrounding normal breast and in the control lactating breast the terminal ductules presented a peripheral rim of actin-rich myoepithelial cells (Fig. 4).

Discussion

Juvenile carcinoma as the name implies was originally described (McDivitt and Stewart 1966) in childhood and early adolescence. It has, however, become apparent in recent reports that tumors with the same morphology and a similarly indolent clinical behaviour are occasionally recognized in adult life (Norris and Taylor 1970; Sullivan et al. 1977; Oberman 1980; Tavassoli and Norris 1980).

The case here reported occurred in a young woman aged 19 yrs and local recurrence, after incomplete removal, developed over a time scale of 7 years. This behaviour was observed because of the erroneous original diagnosis of "atypical hyperplasia" and because of the incomplete removal of the tumor. The peculiar behaviour of this tumor, uncommonly seen with other types of breast carcinoma, confirms the opinions of other authors (McDivitt and Stewart 1966; Oberman 1979; Oberman 1980; Tavassoli and Norris 1980) on the fairly slow growth and minimally aggressive behaviour of juvenile secretory carcinoma. Our case suggests that some of the cases of juvenile secretory carcinoma which have been described in adult patients (Norris and Taylor 1970; Sullivan et al. 1977; Oberman 1980; Tavassoli and Norris 1980), might actually have originated earlier in life and shown a very slow grow rate.

The tumor here reported has the typical histological features referred to by most authors (McDivitt and Stewart 1966; Azzopardi 1979; Tavassoli and Norris 1980). This neoplasm has a distinctive pattern which includes:

an arrangement of tumor cells in acinus-like configurations
pushing infiltration of the stroma,
granular eosinophilic cytoplasm of the cells,
bland cytology with vesicular nuclei,
sparse or absent mitoses
absence of necrosis,
the presence of large amounts of intracellular and extracellular secretions.

Some authors (McDivitt and Stewart 1966; Sullivan et al. 1977; Azzopardi 1979) report that the secretory material in the neoplastic lumina is PAS and Alcian-Blue positive. In all three different biopses of our case the secretory material was only weakly positive when stained with PAS while it stained intensly with Alcian-Blue. This tumor seems therefore to secrete more acid mucosubstances than neutral ones. This indicates that the different types of mucin are not always present in equal proportion in cases of juvenile secretory carcinoma, in agreement with the observation by Tavassoli and Norris (1980): in a study of 19 cases of juvenile carcinomas none of the special histochemical stains showed uniform staining of the secretory material. A positive PAS reaction might therefore not be essential to the diagnosis, although PAS positivity is reportedly (Graumann 1964; Tobon and Salazar 1975) a distinctive histochemical pattern of the secretory mammary gland, a functional feature which the juvenile secretory carcinoma is supposed to mimic. The detection of milk proteins may provide a more specific and reliable marker of secretory activity. The presence of milk proteins in the tumor here reported was investigated with an immunoperoxidase method for MFGM antigen (s), for anti human β-casein antigen and for anti α-lactalbumin, three antigens usually present in cells showing secretory activity of the type seen in pregnancy and lactation. This case which shows a marked immunoperoxidase staining of intracellular and extracellular "secretions", confirms the special differentiation of this neoplasm in terms of a secretory function. The secretory material, observed both as droplets within the cytoplasm of the tumor cells and also in larger quantity within the rudimentary duct-like spaces formed by the tumor, is probably composed mostly of milk proteins, together with a significant amount of acid mucopolysaccarides, given the strong Alcian Blue positivity.

Some of the non-neoplastic lobules close to tumor in the first breast biopsy show focal lactational features. In these areas hypertrophic lobules are composed by ectatic acini lined by a simple to stratified epithelium which consists of cells varying in size, with ample, pale, vacuolated cytoplasm and basal nucleus. These cells show an intense apical MFGM positivity and a weak PAS staining. The reason for this lactational change is unknown. Since our patient had never been pregnant or lactating it might be related to a local abnormal response to hormones. The investigation of the hormonal status of the patient showed a high level of oestrogens. The presence in the normal breast of focal lobules with secretory features has been reported occasionally and interpreted as "focal pregnancy-like changes" (Kiaer and Andersen 1977). Kiaer and Andersen (1977)

supposed that these "changes" in a non pregnant and non lactating woman indicate a selective suscetibility of the mammary glandular tissue to oestrogen action.

The distribution of the myoepithelial cells here was also investigated with a recently developed immunoperoxidase method for actin (Bussolati et al. 1978; Bussolati et al. 1980a). The behaviour of the myoepithelial cells in juvenile secretory carcinoma confirms that in some areas the lesion was confined to extralobular ducts: in these areas the presence and distribution of the myoepithelial cells was similar to that described in the in-situ ductal carcinoma (Bussolati et al. 1980b). The absence of myoepithelial cells in the infiltrating parts of our case of juvenile secretory carcinoma (Fig. 4) confirms the ultrastructural studies of Sullivan (1977) and of Tavassoli (1980) where an absence of myoepithelial cells and of basement membrane were described.

Neoplastic cells appeared to be intensly stained by the immunoperoxidase method for CEA. These findings seem surprising in a tumor like juvenile carcinoma, characterized by an indolent clinical course. Many authors (Wahren et al. 1978; Shousha et al. 1979) report a relation between the presence of CEA in histological sections of breast carcinoma and the prognosis of the disease, CEA-positivity being described as associated with an increased incidence of lymph node metastases and decreased survival time. Immunoperoxidase staining shows that the secretory features of this carcinoma are not only a morphological marker but also correspond to specific biological behaviour.

Other special types of breast carcinoma (Gad and Azzopardi 1975; Eusebi et al. 1977; Azzopardi 1979; Eusebi et al. 1979) have recently been shown to be engaged in an active production of secretory material. Our immuno-histochemical investigation shows that the marked secretory activity of the juvenile carcinoma cannot be regarded as specific to the type of tumor, but places it in a group of carcinomas of the breast involved in milk protein production.

This case, while confirming the slow evolution of this neoplasm, also indicates that it may behave in a slightly more aggressive fashion than initially believed. (McDivitt and Stewart 1966; Oberman 1979; Oberman 1980).

The finding of many foci of tumor in the surrounding breast outside the main carcinoma, the observation of focal infiltration of the muscle and of one metastasis in a lymph node suggests that simple mastectomy with at least low axillary node dissection is probably desirable in the treatment of juvenile secretory carcinoma, especially perhaps when it involves adult patients.

The authors wish to thank: F. Ravera, MD (Primario Ostetrico-Ginecologo, Ospedale S. Lazzaro di Alba), Prof. A.P.M. Cappa and S. Coverlizza, MD (Servizio di Anatomia e Istologia Patologica dell'Istituto di Oncologia, Ospedale Maggiore di S. Giovanni Battista e della Città di Torino), C. Clemente, MD (Servizio di Anatomia e Istologia Patologica dell'Istituto Nazionale per lo Studio e la Cura dei Tumori di Milano) for having provided helpful data on the diagnosis, treatment and follow-up.

We are grateful to Prof. J.G. Azzopardi (Royal Postgraduate Medical School, University of London, Department of Histopathology) for reading the manuscript and making comments and criticisms.

Miss Elena Zigolillo provided skilful secretarial assistance.

This work was partly supported by CNR grant n° 81.01310.96

References

Azzopardi JG (1979) Problems in breast pathology. WB Saunders, London

Bussolati G, Pich A, Alfani V (1975) Immunofluorescence detection of casein in human mammary dysplastic and neoplastic tissue. Virch Arch Path Anat Histol 365:15–21

Bussolati G, Ghiringhello B, Di Carlo F, Aimone V, Voglino GF (1977) Lactalbumin synthesis in breast cancer tissue. Lancet 2:352

Bussolati G, Bonfanti S, Weber K, Osborn M (1978) Staining of myoepithelial cells in fixed and embedded tissues by immunocytochemical techniques using antibodies to actin. Riv Istochim Norm Patol 22:387–390

Bussolati G, Alfani V, Weber K, Osborn M (1980a) Immunocytochemical detection of actin on fixed and embedded tissues: its potential use in routine pathology. J Histochem Cytochem 28:169–173

Bussolati G, Botta G, Gugliotta P (1980b) Actin-rich (myoepithelial) cells in ductal carcinoma in situ of the breast. Virch B Cell Path 34:251–259

Byrne MP, Fabey MM, Gooselaw JG (1973) Breast cancer with axillary metastases in an $8^1/_2$ year old girl. Cancer 31:726–728

Ceriani RL, Thopson K, Peterson JA, Abrham S (1977) Surface differentiation antigens of human mammary epithelial cells carried on human milk fat globule. Natl Acad Sci 74:582–586

Eusebi V, Pich A, Macchiorlatti E, Bussolati G (1977) Morphofunctional differentiation in lobular carcinoma of the breast. Histopathology 1:301–314

Eusebi V, Betts Cm, Bussolati G (1979) Tubular carcinoma: a variant of secretory breast carcinoma. Histopathology 3:407–419

Gad A, Azzopardi JC (1975) Lobular carcinoma of the breast: a special variant of mucin-secreting carcinoma. J Clin Pathol 23:711–716

Graham Rc, Karnovsky MJ (1966) The early stages of adsorption of injected horseradish peroxidase in the proximal tubules of mouse kidney: ultrastructural cytochemistry by a new technique. J Histochem cytochem 14:291–302

Graumann W (1964) Ergebnisse der Polysaccharidhistochemie. Mensch und Säugetiere-Hbch. Histochemie 2/2. G Fisher, p 476 Stuttgart

Hartman Aw, Magrish P (1955) Carcinoma of the breast in children. Ann Surg 141:792–798

Kiaer HW, Andersen JA (1977) Focal pregnancy-like changes in the breast. Acta Pathol Microbiol Scand 85(6):931–941

McDivitt RW, Stewart FW (1966) Breast carcinoma in children. JAMA 195:388–390

Norris HJ, Taylor HB (1970) Carcinoma of the breast in women less than thirty year old. Cancer 26:953–959

Oberman HA (1979) Breast lesions in the Adolescente Female. Ann Pathol 195–201

Oberman HA (1980) Secretory carcinoma of the breast in adults. Am J Surg Pathol 4:465–470

Pich A, Bussolati G, Carbonara A (1976) Immunocytochemical detection of casein-like proteins in the human tissues. J Histochem Cytochem 24:940–947

Shousha S, Lyssiotis T, Godfrey VM, Scheuer PJ (1979) CEA in breast cancer tissue: a useful prognostic indicator. British Med J 1:777–779

Simpson JS, Barson AJ (1969) Breast tumors in infants and children. Canad Med Ass J 101:100–102

Sternberger LA, Hardy PHJr, Cuculis JJ, Meyer HG (1970) The Unlabelled antibody enzyme method of immunohistochemistry preparation and properties of soluble antigen-antibody complex (horseradish peroxidase anti-horseradish peroxidase) and its use in identification of spirochaets. J Histochem Cytochem 18:315–333

Sullivan JJ, Magee HR, Donald KJ (1977) Secretory (Juvenile) carcinoma of the breast. Pathol 9:341–346

Tavassoli FA, Norris HJ (1980) Secretory carcinoma of the breast. Cancer 45:2404–2413

Tobon H, Salazar H (1975) Ultrastructure of the Human Mammary Gland. II. Postpartum Lactogenesis. J Clin Endocrinol Metab 40:834–844

Wahren B, Lidbrink E, Wallgren A, Eneroth P, Zajicek J (1978) CEA and other tumor markers in tissue and serum plasma of patients with primary breast cancer. Cancer 42:1870–1878

Accepted January 12, 1982

Virchows Arch [Pathol Anat] (1982) 395:153–168

Virchows Archiv A

Immunoelectron Microscopic Study of Plasma Protein Pathways through the Different Segments of the Rat Intestinal Vasculature

Nicole Hinglais, Jeannine Grossetete, Michel Paing, and Jean Bariety

Groupe de Recherches sur la Pathologie Rénale et Vasculaire, INSERM U 28, CNRS ERA 48, Hôpital Broussais, 96 rue Didot, F-75674 Paris Cédex 14, France

Summary. Nineteen Brown-Norway (BN) rats received intravenous injections of sheep anti-peroxidase (HRP) antibodies. Four BN rats were immunized to HRP. The anti-HRP antibodies were used to trace permeability pathways of large physiological molecules across different vessels of the small intestine. This organ was chosen because of the possibility of convenient "in situ" fixation and for the diversity of vessel types it contains.

It was shown that:

1) There were no obvious transendothelial pathways in arteries with an elastic lamina.

2) The antibodies readily crossed fenestrated capillaries through the fenestrae.

3) There were two possible pathways through muscle capillaries and pericytic venules, namely transcytoplasmic vesicular "cactus-like" channels and interendothelial junctions.

4) Interendothelial permeability was a possible factor in veins with an elastic lamina.

5) Lymphatics were readily permeable through intercellular junctions and cytoplasmic vesicles.

Key Words: Immunoelectron microscopy – Plasma proteins – Transvascular pathway

Introduction

During the past decade, many electron microscope (EM) studies have addressed the question of vascular permeability using tracers of various sizes and molecular weights, most of them endowed with peroxidase enzymic activity. Fenestrated and non-fenestrated capillaries have been more thoroughly studied (Clementi and Palade 1969; Simionescu et al. 1972; Simionescu et al. 1975, 1978b; Williams and Wissig 1975; Wissig and Williams 1978) than arteries and veins (Florey and Sheppard 1970; Giacomelli et al. 1970; Hüttner et al. 1970; Schwartz

Offprint requests to: N. Hinglais at the above address

0340-1227/82/0395/0153/$03.20

and Benditt 1972; Hüttner et al. 1973a, b; Giacomelli and Wiener 1974; Giacomelli et al. 1976; Simionescu et al. 1976a, 1978b, c). There appears to be general agreement that fenestrated capillaries (Clementi and Palade 1969; Renkin 1977; Simionescu et al. 1972) and lymphatics (Dobbins and Rollins 1970; Leak 1971) are readily permeable to large macromolecules. Results are often conflicting or unclear with regard to muscle capillaries (Simionescu et al. 1975; Simionescu et al. 1978b, c; Williams and Wissig 1975; Wissig and Williams 1978), veins (Simionescu et al. 1976a, 1978c) and arteries (Florey and Sheppard 1970; Giacomelli et al. 1970; Hüttner et al. 1973b; Schwartz and Benditt 1972). All these studies have been performed with non-physiological tracers and, in particular, serum proteins have not been used in EM studies.

The aim of this work was to compare the pathways followed by an immunoglobin (IgG), easily detectable by EM (Laliberté et al. 1978; Druet et al. 1978), through different vascular structures of the same organ, namely the small intestine of the rat. The vessels studied were small arteries with an elastic lamina, fenestrated capillaries, muscle capillaries, pericytic venules, veins with an elastic lamina and lymphatics.

Materials and Methods

Animals

Twenty-five Brown Norway (BN) rats (Centre National de la Recherche Scientifique, Centre de Sélection et d'élevage des Animaux de Laboratoire (C.S.E.A.L.), Orléans, France) weighing 150–180 g were used in this study.

Nineteen rats were injected intravenously with 1 ml/100 g body weight of sheep anti-HRP antiserum and their small intestines were fixed at different times after injection of the tracer (henceforth referred to as *injected rats*) (see Table 1). Four rats were immunized against HRP and did not receive the antiserum (henceforth referred to as *immunized rats*). Two rats were neither injected nor immunized and are henceforth referred to as *control rats*.

Anti-HRP Antiserum

The anti-HRP antiserum was raised in a sheep immunized with HRP (Grade I Boehringer) as previously described (Druet et al. 1978).

The antiserum was tested with HRP by Ouchterlony's technique and by immunoelectrophoresis using a rabbit antiserum raised against whole normal sheep serum. Precipitation lines were stained after incubation with HRP. It was thus shown that the anti-HRP antibodies were IgG antibodies.

Immunizing Rats to HRP

Four BN rats were immunized by foot-pad injections of 6 mg HRP (Boehringer, grade I), mixed with complete Freund's adjuvant. The rats were boosted each month for three months by intramuscu-

Table 1.

	Time after injection							
	2 min	5 min	10 min	15 min	1.5 h	4 h	17 h	24 h
Number of injected rats	4	2	2	2	2	1	4	2

lar injections on 3 consecutive days (Laliberté et al. 1978). The amount of antibody was not measured. The serum from each of these four rats exhibited a precipitation line after testing by Ouchterlony's technique against HRP.

Experimental Procedure

Rats were anesthetized by intraperitoneal injections of 2.5 mg Nembutal per 100 g body weight (Abbot Laboratories).

In situ fixation was performed as described by Simionescu et al. (1972). A loop of small intestine was exposed by laparotomy and a ligature positioned at each end of the loop. One of the ligatures was placed around a N° 26 G 1/2 inch Terumo hypodermic needle inserted into the lumen of the intestine. The needle was used to inject the fixative into the lumen of the loop while the ligature was being tightened. The entire intestinal loop was then immersed in the fixative placed in an appropriate receptacle. In situ fixation was continued for 10 min, and the intestinal loop was then exised and left in the fixative for a total of 2 h.

Immunohistochemical Procedure

The fixative used was a 2% glutaraldehyde solution in 0.1 M phosphate buffer, pH 7.4. Specimens were washed for 48 h in several changes of phosphate 0.1 M pH 7.4 buffer at 4° C. The small intestine was first cut longitudinally with a razor blade into two halves. One of the halves was cut into transverse sections three mm wide to form strips several mm long. These strips of tissue were then cut transversally with a Smith and Farquhar tissue sectioner (Sorvall TC2) into 100 µm sections which were incubated for one hour in a 0.5 mg/ml solution of HRP (Boerhinger, grade I) in 0.1 M phosphate buffer, pH 7.4, with gentle stirring at room temperature. This was followed by 3 washes lasting 10 min each, in phosphate buffer and then an additional wash for 10 min in tris-HCl buffer 0.2 M pH 7.6. HRP was demonstrated using a two-step procedure; the sections were first incubated in a freshly prepared solution of 20 mg of 3-3′ diamino benzidine (DAB), (Sigma, grade II) in 10 ml of 0.2 M. Tris-HCl buffer, pH 7.6, for 45 min at room temperature and then incubated for 15 min in the same solution to which hydrogen peroxide had been added to a final concentration of 0.001%. The sections were washed in 0.2 M phosphate buffer, pH 7.4, and post-fixed in 2% osmic acid in 0.1 M phosphate buffer, pH 7.4, for 15 min. They were dehydrated in a graded series of alcohols and embedded in Epon 812. In four rats (three immunized and one non-immunized), an additional procedure was performed as described by Simionescu and Simionescu (1976b). After incubation in DAB-H_2O_2 medium, sections were fixed in 2% osmic acid solution in 0.2 M cacodylate buffer pH 7.4 for 15 min. Sections were then incubated in a 0.5% tannic acid solution in cacodylate buffer 0.2 M for 1 h and washed in several baths of cacodylate buffer for 18 h. Dehydration and embedding in Epon were performed in the usual manner.

Ten to fifteen semi-thin sections were obtained from each rat for examination by light microscopy (LM). Appropriate areas were then cut into thin sections. In each case, thin sections were studied with and without counterstaining using lead citrate and uranyl acetate.

The number of micrographs obtained for each type of vessels was as follows: arteries:125; fenestrated capillaries:38; muscle capillaries:176; pericytic venules:54; veins:91; lympathics:34.

Controls

The kidneys of two normal rats injected with anti-HRP antiserum were treated as above: the specimens were not incubated with HRP but only with DAB-H_2H_2, so as to test for endogenous peroxidase activity. Two other normal rats (non injected, non immunized) were processed by the complete technique to detect non specific trapping of peroxidase in fixed tissue.

Results

Controls. The following controls were negative:

1. kidneys from rats injected with anti-HRP antiserum, that were treated with DAB-H_2O_2 omitting incubation with HRP;

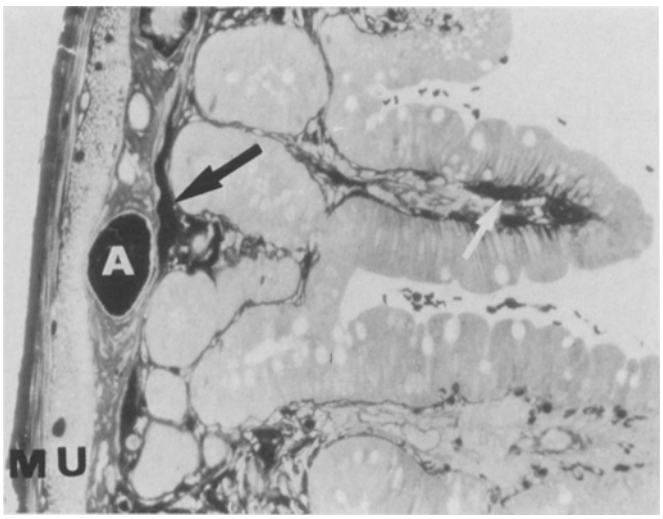

Fig. 1. Semi-thin section of the rat small intestine (15 min after injection) showing the different layers. From left to right: the muscularis with lumena of the muscle capillaries (*MU*), the submucosa with lumena of arteries (*A*) and veins with elastic lamina, the base of the villi with pericytic venules (*arrow*), and the core of the villi with the lumena of the fenestrated capillaries (*white arrow*) (×450)

2. non injected and non immunized normal rats whose kidneys were processed by the complete technique, showing no non specific trapping of peroxidase in fixed tissues.

Rats with Circulating Anti-HRP IgG. Results were identical in these two groups of rats (injected and immunized). For this reason, they are described together. Moreover, immunized rats also served as controls for the specificity of the injected anti-HRP antiserum and for determining potential undesirable pathophysiological effects resulting from the injection of heterologous antisera.

1. Semi-Thin Sections

Compartments of the intestinal wall chosen for study of the different vessels are shown on the semi-thin section in Fig. 1. All the semi-thin sections were studied for the distribution of the reaction product in the extracellular spaces. At 2 min, no diffusion was seen in the interstitial spaces. From 5 to 15 min, diffusion was very unequal from one specimen to another and from one tissue compartment to another. It was generally complete in the core of the villi. However, a diffusion gradient was observed around some venules and capillaries of the tunica muscularis. Diffusion gradients were most prominent around capillary lumina of large diameter, presumably of the venular type, as assessed by the study of 45 semi-thin sections from six injected rats. Staining by the reaction product of collagen bundles around arteries and veins with an elastic lamina was observed only when the contiguous muscle cells supplied by the capillaries were also stained.

In immunized animals, and in injected animals, from 15 min to 24 h, the reaction product generally diffused into all the interstitial spaces, though some differences were observed from one animal to another. Assessment of the extent of extravasation of the reaction product on semi-thin sections served to determine when overt permeability occured in each vascular segment. These sections were subsequently chosen for ultrastructural study since the chief aim of the present work was to determine the possible pathways of IgG across the vascular wall.

2. *Electron Microscopy*

Arteries With Elastic Lamina. The subendothelial space was generally devoid of reaction product (Fig. 2) even when the interstitial space and the basement membrane of parietal smooth muscle cells were stained. However, in some cases, reaction product was visible between smooth muscle cells and occasionnaly in the subendothelial space, though only in small quantities. Endothelial vesicles opening into the lumen were usually labeled (Fig. 2 and 3) as were a minority of intracytoplasmic vesicles. Even when the subendothelial space was apparently free of reaction product, a few labeled vesicles were observed opening on to the abluminal side of the endothelial cell (Fig. 4) or very close to the plasma membrane. Intercellular junctions were completely devoid of reaction product except in the rare instances where vesicles were seen to discharge behind a tight junction (Fig. 3).

Fenestrated Capillaries. There was no difference in staining intensity between the lumen and the basement membrane or the pericapillary space (Fig. 5). Fenestrae were freely permeable to anti-HRP IgG, even when a diaphragm was suggested by a faint line in the midst of the dense reaction product (Fig. 6). When fenestrated capillaries were situated at the base of villi, fenestrae were less conspicuous and, in some specimens, a density gradient of the reaction product was observed along the basement membrane starting from the fenestrae (Fig. 7). When the endothelial cytoplasm of these capillaries was thicker, stained vesicles were observed in the cytoplasm. No reaction product was seen in the intercellular junctions. Diffusion of the reaction product was homogeneous in the interstitial matrix of the villi, between the various cell types and collagen bundles.

Muscle Capillaries. Discrimination between arteriolar and venular capillaries was not easy in the muscular coat. The distinction was based essentially on capillary diameter: 4 μm for arteriolar capillaries and 5–6 μm for the venular end of capillaries. Staining was often denser in the smallest vessels, presumably arteriolar capillaries (Fig. 8). We did not note any obvious permeability differences between these different types of capillaries. Two unquestionable but rare qualitative features were observed. Firstly, the presence of reaction product along the entire length of some intracellular junctions (Fig. 8) and secondly, the presence of trans-cellular channels formed by superposition of labelled vesicles (Fig. 9) or opening of one labelled vesicle on both sides where the endothelial cytoplasm was very thin. In all capillaries, labelled vesicles were observed on

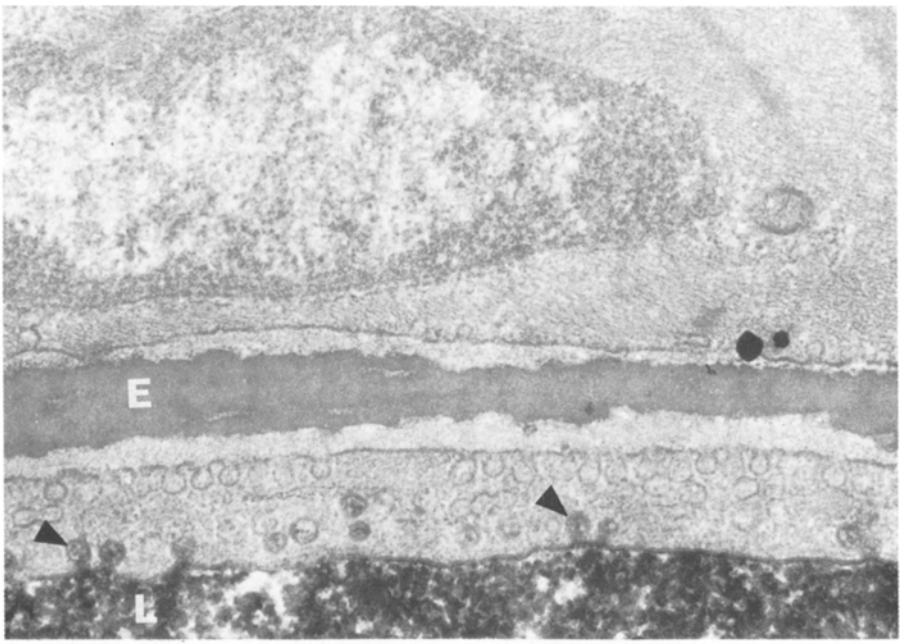

2

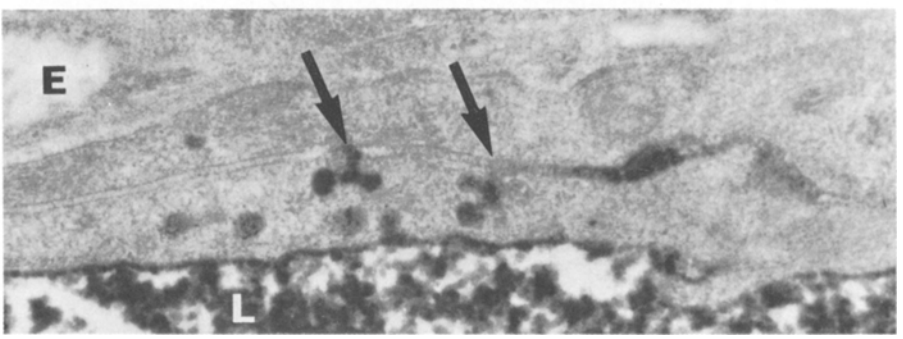

3

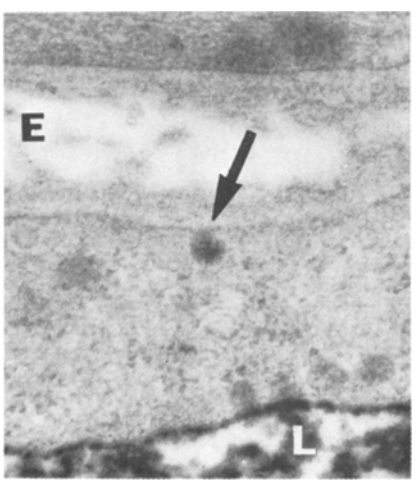

4

Fig. 2–4. Arteries with an elastic lamina (*E*)

Fig. 2. Vesicles opening into the lumen (*arrowhead*) and some apparently intra cytoplasmic vesicles are labelled. Vesicles opening into the subendothelial space are unlabeled. Tannic acid (×40,000)

Fig. 3. Two labelled cactus-like vesicles (*arrows*) opening into a partialy stained intercellular junction (×50,000)

Fig. 4. A labelled endothelial vesicle (*arrow*) opening into the non-labelled subendothelial space (×62,500)

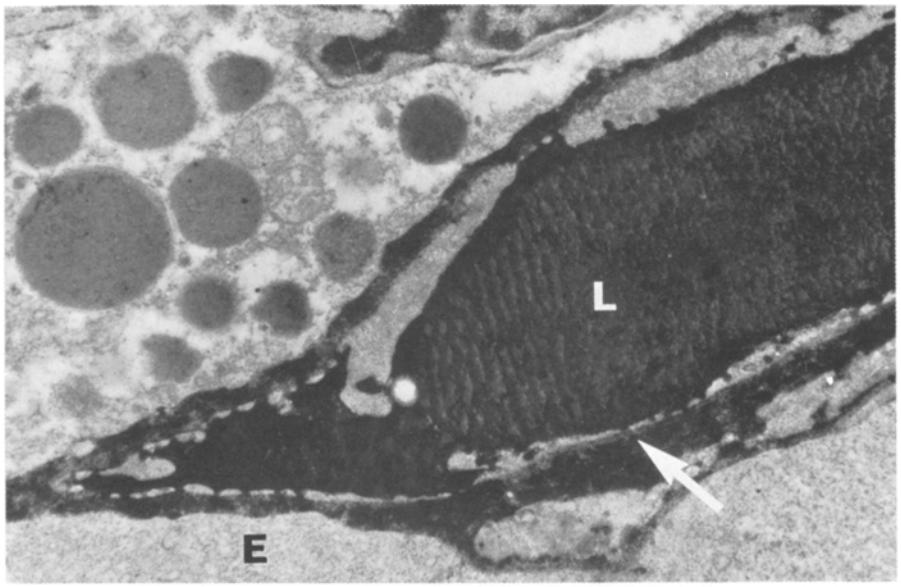

5

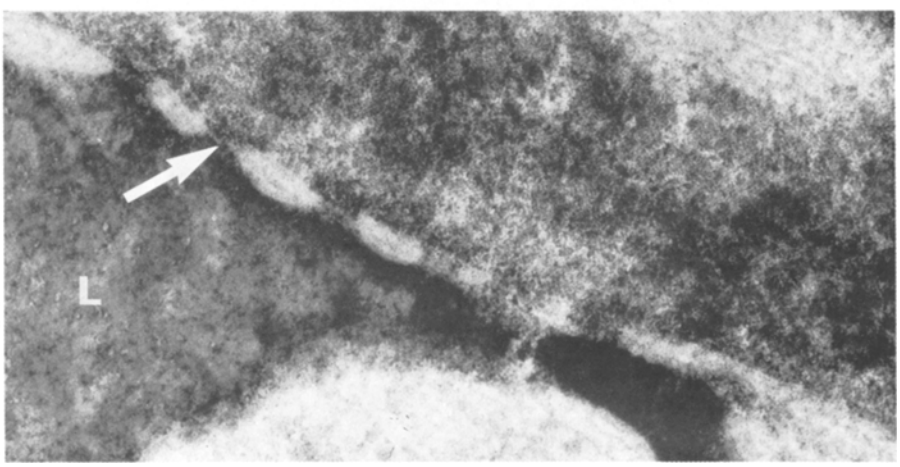

6

Fig. 5 and 6. Fenestrated capillaries along the epithelial (*E*) layer of the villi

Fig. 5. There is no difference in staining intensity between the lumen (*L*) and the interstitial space (*white arrow*) (× 16,000)

Fig. 6. Diaphragms are visible as faint lines (*white arrow*). Fenestrae are obviously permeated by the tracer (× 120,000)

the luminal or abluminal side of the cytoplasm as well as inside the cytoplasm. Unstained vesicles outnumbered stained vesicles.

Pericytic Venules. The space underlying endothelial cells was never as intensely stained by the reaction product as the capillary lumen. The endothelial basement membrane was stained to the same extent as, or less so than the external

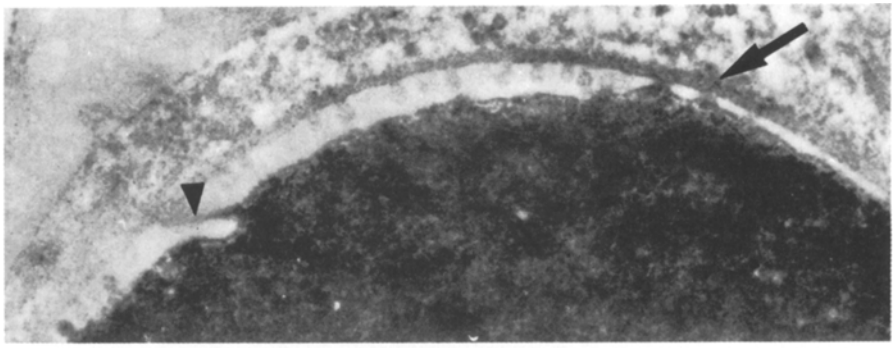

7

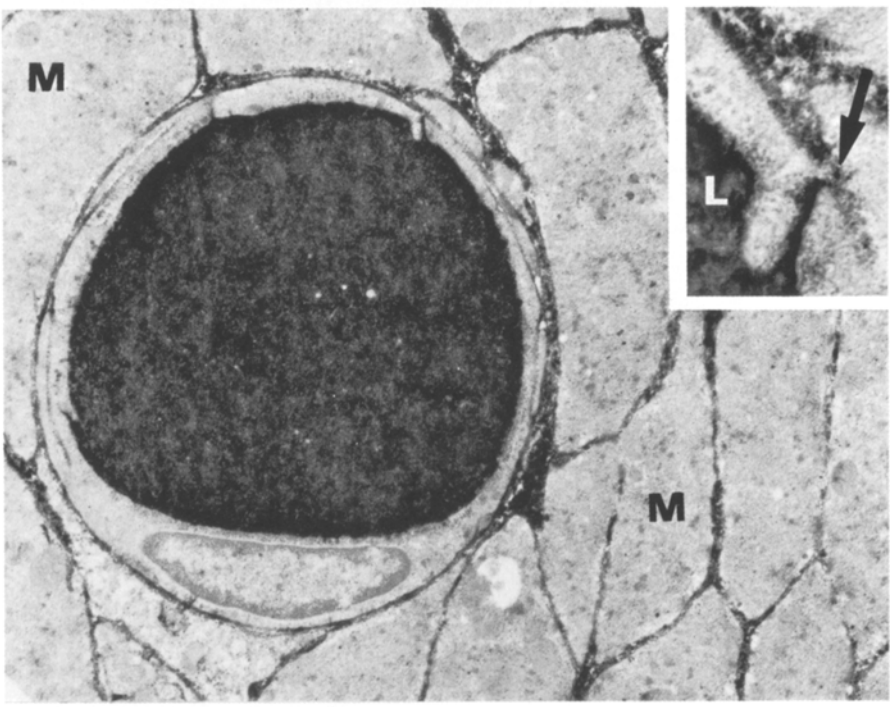

8

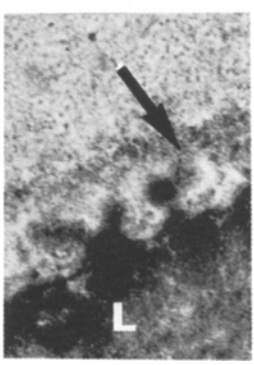

9

Fig. 7. Semi-fenestrated capillary (base of the villi). Intense staining of the basement membrane (*arrow*) in front of the two fenestrae. An unstained intercellular junction is visible on the left (*arrowhead*) (× 27,000)

Fig. 8. Muscle capillary showing extravascular diffusion of the reaction product (*M*: muscle cell) (× 10,000). *Inset*: reaction product fills up the endothelial junction and the adjacent interstitial space (*arrow*) (× 64,000)

Fig. 9. Muscle capillary showing two communicating stained vesicles opening both into the lumen (*L*) and into the stained subendothelial space (*arrow*) (× 80,000)

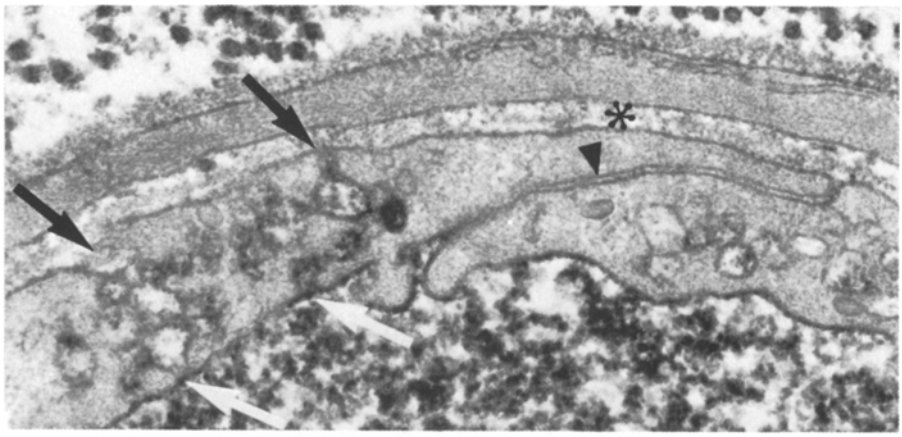

10

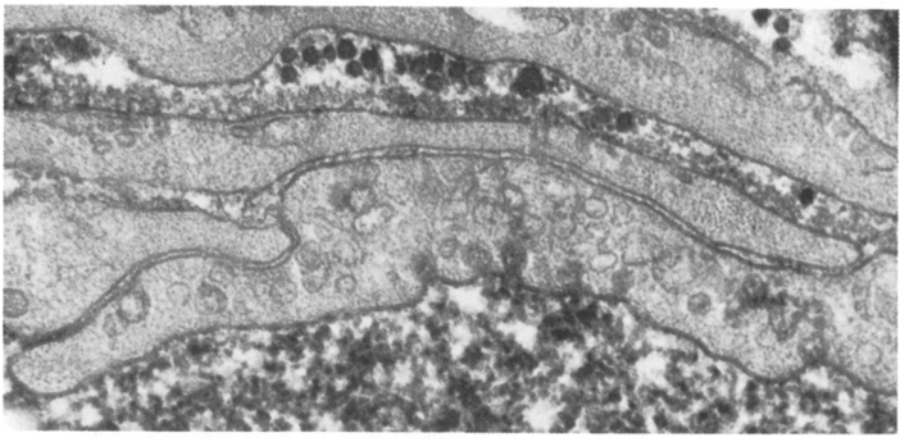

11

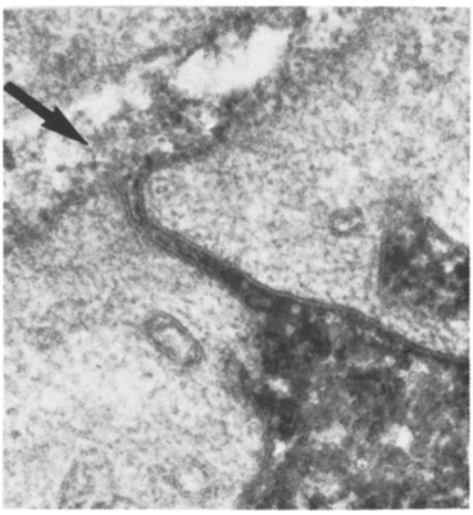

12

Fig. 10–12. Pericytic venules.

Fig. 10. A cluster of "cactus-like" stained endothelial vesicles (*arrows*) throughout the endothelial cytoplasm is presumed to open on both sides. The subendothelial space is, however, weakly stained (*asterisk*). The intercellular junction is unstained (*arrowhead*). Tannic acid (× 60,000)

Fig. 11. The arborescent vesicles of the endothelial cytoplasm are very heterogeneously stained. Tannic acid (× 60,000)

Fig. 12. This particular interendothelial junction is permeable as the reaction product is visible in the entire junction and the adjacent subendothelial space (*arrow*). Tannic acid (× 80,000)

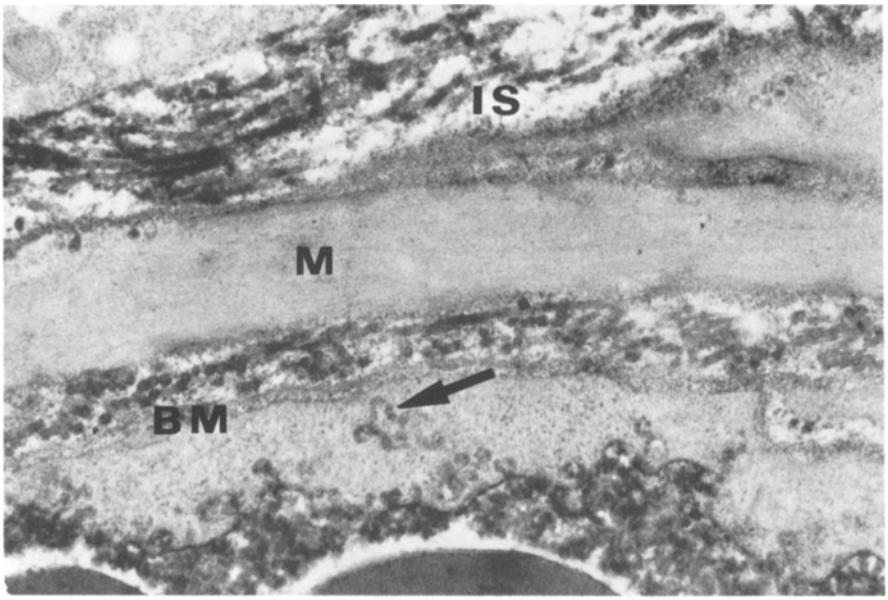

13

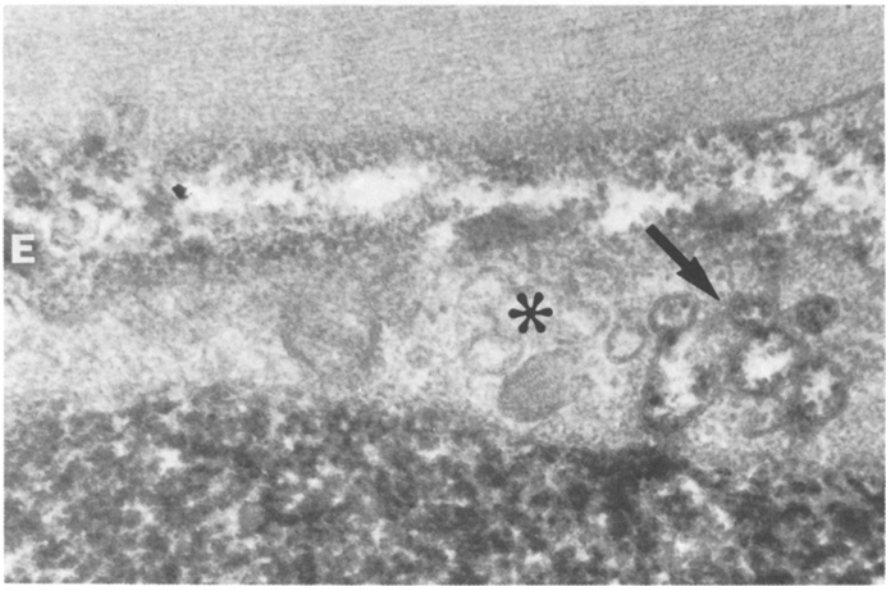

Fig. 13. Vein. Reaction product is present in the subendothelial and interstitial space (*IS*) as indicated by staining of the basement membrane (*BM*) and collagen fibrils. Stained vesicles are visible deep within the endothelial cytoplasm (*arrow*). *M* smooth muscle cell (× 37,000)

Fig. 14. Vein with an elastic lamina (*E*). A cluster of intraendothelial cactus-like stained vesicles (*arrow*) can be seen close to an unstained one (*asterisk*). Tannic acid (× 75,000)

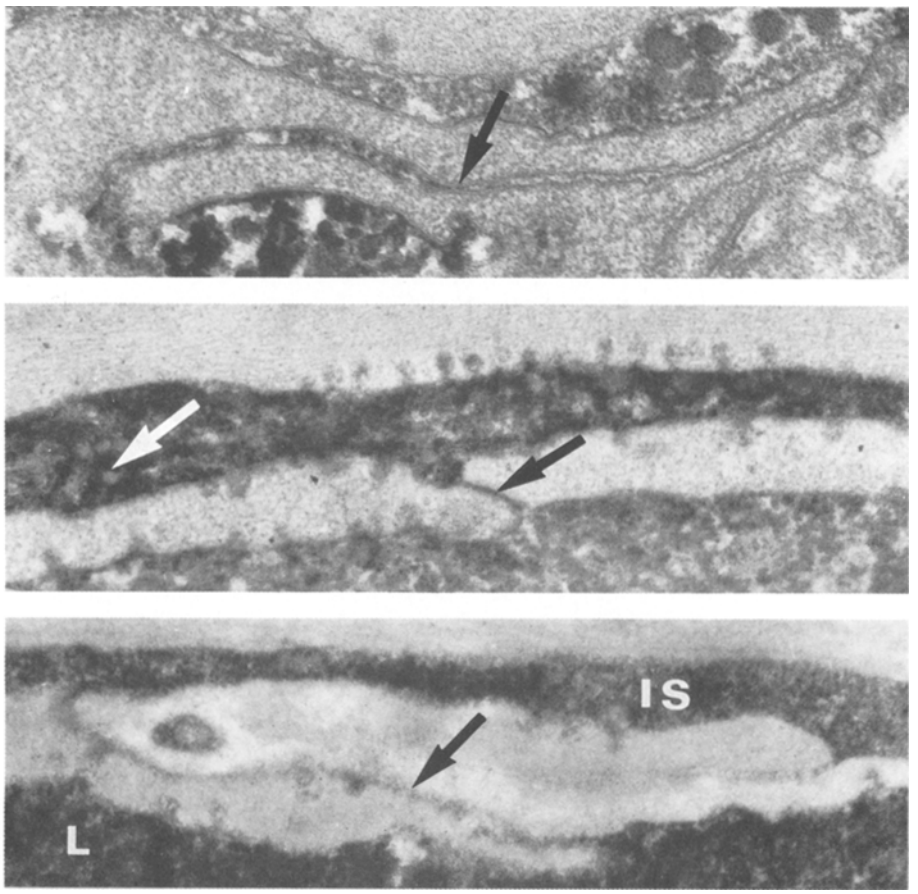

Fig. 15. Vein. Intercellular junction. Reaction product stops at the level of a unique, short, tight junction (*arrow*). Tannic acid ($\times 78{,}500$)

Fig. 16. Vein. The intercellular junction (*arrow*) is freely permeable to the tracer. There is marked accumulation of reaction product in the subendothelial space (*white arrow*) ($\times 60{,}000$)

Fig. 17. Lymphatic. The intercellular junction is outlined by reaction product (*arrow*). Staining intensity is the same in the lumen (*L*) and in the interstitial space (*IS*) ($\times 60{,}000$)

pericytic basement membrane (Fig. 10). Occasionally, reaction product trapped between both cells of the venular wall was clearly visible (Fig. 12). Intracytoplasmic vesicles were numerous but irregularly dispersed in the endothelial cytoplasm, some being stained, others unstained (Fig. 10 and 11). Stained vesicles were not more numerous on the luminal than on the abluminal side of the endothelial cytoplasm. Clusters of stained vesicles were observed forming complex "cactus-like" configurations (Fig. 10) that occasionally traversed the cell. The reaction product did not always accumulate in the subendothelial space in this situation. The simplest endothelial junctions where the cell contact area

was small without tight junctions, showed evident filling with reaction product (Fig. 12). Other types of junctions were not stained.

Veins With Elastic Lamina. The histochemical findings in veins with an elastic lamina were similar to those observed in the preceding venular segments. There was some reaction product in the subendothelial space and other intercellular spaces of the parietal wall but staining was generally of moderate intensity (Fig. 13 and 14). Groups of vesicles were dispersed throughout the cytoplasm or "cactus-like" configurations were observed inside the endothelial cells (Fig. 14). Intercellular junctions were usually free of reaction product (Fig. 15). In one case, a large vein was inordinately permeable and in situ fixation appeared to have been quite satisfactory. The subendothelial space was as intensely stained as the lumen. Most of the intercellular junctions were pervious to the tracer (Fig. 16).

The number of intracellular endothelial vesicles was no greater than in the other veins.

Lympathics. The density of the luminal reaction product was similar to that observed in the extracellular spaces (Fig. 17). Many stained vesicles were observed opening on both sides of the cytoplasm or constituting true short channels. Most of the intercellular junctions appeared to be permeable to the tracer (Fig. 17).

Discussion

The aim of this study was to compare the pathways of anti-HRP IgG, a large size probe molecule, across the walls of different types of vessels of the same tissue. To the best of our knowledge, no serum proteins such as immunoglobulins have hitheto been used as ultrastructural tracers in vascular permeability studies except in the special case of kidney glomeruli (Laliberté et al. 1978). Rat small intestine offers a diversity of vascular structures and is amenable to convenient "in situ" fixation. We used anti-HRP IgG because its detection has been shown to be more reliable than classical immunoenzymatic techniques. Circulating anti-HRP antibodies can be detected by incubating tissue sections with HRP which diffuses uniformly throughout the tissue because of its low MW. In contrast, detection of proteins by classical immunoenzymatic techniques requires incubation of tissue sections with HRP-labeled antibodies (conjugates) which diffuse heterogeneously because of their high MW. We made no attempt to quantitate our results for the aim of the study was to compare the pathways and not the leakage of IgG across the walls of different types of vessels. Immunohistochemical reactions are inappropriate for quantitating transvascular leakage.

Arteries with an elastic lamina were the least permeable vessels with little or no reaction product appearing in the subendothelial space. Intercellular junctions were devoid of reaction product. No transendothelial passage was demonstrated. Fenestrated capillaries of the villi were freely permeable to IgG antibodies which crossed the vessel wall through the fenestrae. Muscle capillaries in the muscular coat exhibited two different pathways: reaction product was

detected in some intercellular junctions and stained transcellular vesicles were seen to discharge on both sides of the endothelial cytoplasm. For pericytic venules, both transcellular and intercellular pathways were observed, whereas in veins with an elastic lamina, only the intercellular pathway was documented. It must be stressed, however, that in muscle capillaries, perycitic venules and veins with an elastic lamina, evidence for complete transcellular or intercellular pathways were very rarely observed. Lymphatic were readily permeable to IgG via a transcellular pathway as well as via intercellular junctions.

Permeability of arteries to probe molecules has been tested mainly with HRP and ferritin (Florey and Sheppard 1970; Giacomelli et al. 1970; Hüttner et al. 1973a–c); Giacomelli and Wiener 1974; Westergaard et al. 1973; Giacomelli et al. 1976), and has been shown to increase in many abnormal conditions such as for example arterial hypertension (Hüttner et al. 1970; Giacomelli et al. 1970; Giacomelli et al. 1976). The permeability of arteries in healthy individuals varies from one organ to another (Giacomelli et al. 1970; Westergaard and Brightam 1973; Giacomelli et al. 1976), and even in different parts of the same vessel (Hüttner et al. 1973b; Giacomelli and Wiener 1974). Permeability pathways have been attributed to intercellular junctions (Florey and Sheppard 1970; Hüttner et al. 1970; Hüttner et al. 1973b, c), to discharge of cytoplasmic vesicles into the junctions (Giacomelli et al. 1976) and to transcellular vesicular transport (Hüttner et al. 1970; Giacomelli et al. 1970; Hüttner et al. 1973a, b; Westergaard et al. 1973; Giacomelli et al. 1970). In our system, intestinal arteries appeared to be poorly permeable to IgG judging by the usual lack of reaction product in the intima. The layer of smooth muscle cells and the internal elastic lamina may contribute to a lack of penetration of the reagent. However, some intensely stained vesicles were observed to open into the subendothelial space. It is unlikely that these isolated vesicles were the only structures reached by the reagent. It cannot be ruled out that this phenomenon represents a very little used transcellular pathway from the lumen. Results concerning fenestrated capillaries were consistent with those of previous workers using large tracer molecules e.g. Ferritin, glycogens or dextans (Clementi and Palade 1969; Simionescu et al. 1972). In the core of the villi we saw no concentration gradient of the reaction product in the peri-capillary space centered around the fenestrae, but our observations by light and electron-microscopy, which showed no interstitial diffusion at 3 min and full diffusion around 15 min were also consistent with large size probe molecule diffusion (Simionescu et al. 1972). When full diffusion occured, all cell components and bundles of collagen fibrils were bathed in immunoglobulins. These results were more homogeneous than those found with other tracers (Simionescu et al. 1972). Permeability of muscle capillaries has been extensively studied in a number of organs by several groups (Simionescu et al. 1975; Williams and Wissig 1975; Renkin 1977; Simionescu et al. 1978a, b; Wissig and Williams 1978). Large molecules with a diameter exceeding 50 Å, such as ferritin and colloidal particles (Palade 1961) are transferred across the endothelium exclusively by vesicles. Pathways for smaller molecules such as HRP (50 Å) (Williams and Wissig 1975) are still controversial, conflicting results have been published for the same tissue capillaries and the same microperoxidase tracers (20 Å) (Simionescu et al. 1975 and 1978b; Wissig and Williams 1978). These

conflicting results may be due, in part, to problems of accurate distinction between arteriolar and venular type capillaries (Simionescu et al. 1978c). Using a larger MW probe molecules (150,000), presumed to belong to the large pore system, we found two possible pathways:

1) intercellular junctions as described for HRP (Williams and Wissig 1975) or microperoxidase (Wissig and Williams 1978);

2) transcellular channels or vesicles as described for different large or small tracers (Clementi and Palade 1969; Simionescu et al. 1975, 1978b).

The presence of this high MW molecule in the intercellular junctions of our material may be surprising in view of the large pore theory and the calculated diameter of our probe molecule (110 Å) (Bill 1977). However, it has previously been shown that MW or calculated size are not the only critical factors governing permeability and that electric charge, shape and flexibility (Rennke et al. 1978) must also be taken into account. As previously noted for the small intestine (Simionescu et al. 1978a) it is difficult to distinguish clearly on a section plane between the arteriolar and the venular end of the capillaries, the latter being more permeable (Simionescu et al. 1978c). In our specimens, morphological criteria did not allow us to identify the arteriolar and venular ends of the capillaries with certainty. Nevertheless, both pathways were encountered whatever the diameter of the lumen. These transvascular passages were rarely encountered in thin sections even when there was an obvious diffusion gradient in extra-vascular spaces with semi-thin sections. For the vesicular pathway, this is quite understandable when one considers the complex "cactus-like" branching of most of the vesicles. The question of whether this complex transcellular pathway represents a labile, dynamic event as suggested by Simionescu et al. (1975, 1978b) or a static structure, as proposed more recently by Bundgaard et al. (1979, 1980) is beyond the scope of this paper. Nevertheless, the frequent heterogeneity of the density of the reaction product between two communicating vesicles could be related to a diffusion process along static, permanent structures (Bundgaard 1980). Our results in pericytic venules and veins with an elastic lamina are in agreement with those of Simionescu et al. (1978c) in the mouse diaphragm showing that the number of permeable intercellular junctions and the extent of extravascular diffusion decreased as the M.W. of the tracer increased. These vessels were not permeable to ferritin molecules. The M.W. of our tracer could account for the observation of labeled transcellular channels without distinctly visible reaction product in the adjacent subendothelial space. These clusters of cytoplasmic vesicles and the labeled intercellular spaces, could, in some patho-physiological circumstances, be related to the "leaks" observed in LM with labeled proteins (Grotte 1956; Nakamura and Wayland 1975; Renkin 1977; Bungaard 1980). The large vein which was apparently well fixed but inordinately permeable to immunoglobulins at the level of the intercellular junctions, could be related to a superimposed inflamatory reaction due to the organ's exposure to air during experimental manipulation. The fragility of venular junctions to various pharmacological or phlogistic agents is well established (Majno and Palade 1961). Lymphatics appeared to be very permeable as nearly all the intercellular junctions were stained and the justa-interstitial space was of the same density as the lumen. This is in agreement with morphological

descriptions of these vessels (Albertine and O'Morchoe 1980; Collan and Kalima 1974) and tracer experiments (Dobbins and Rollin 1970; Leak 1971).

The methodology used in this work enabled us to study the protein pathways across the vessel walls of the same organ with a more physiological tracer than those usually employed. Our results were generally consistent with those in the literature.

References

Albertine KH, O'Morchoe CC (1980) Renal lymphatic ultrastructure and translymphatic transport. Microvas Res 19:338–351

Bill A (1977) Plasma protein dynamics Albumin and IgG capillary permeability, extravascular movement and regional blood flow in unanesthetized rabbit. Acta Physiol Scand 101:28–42

Bundgaard M (1980) Transport pathways in capillaries. In search of pores. Ann Rev Physiol 42:325–336

Bungaard M, Frøkjaer-Jensen J, Crone C (1979) Endothelial plamalemmal vesicles as elements in a system of branching invaginations from the cell surface. Proc Natl Acad Sci USA. 76:6439–6442

Clementi F, Palade GE (1969) Intestinal capillaries I. Permeability to peroxidase and ferritine. J Cell Biol 41:33–58

Collan Y, Kalima TV (1974) Topographic relations of lymphatic endothelial cells in the initial lymphatics of the intestinal villus. Lymphology 7:175–184

Dobbins WO, Rollins EL (1970) Intestinal mucosal lymphatic permeability: an electron microscopic study of endothelial vesicles and cell junctions. J Ultrastruct Res 33:29–59

Druet P, Bariety J, Laliberté F, Bellon B, Belair MF, Paing M (1978) Distribution of heterologous antiperoxidase antibodies and their fragments in the superficial renal cortex of normal Wistar – Munich rat. An ultrastructural study. Lab Invest 39:623–631

Florey L, Sheppard BL (1970) The permeability of arterial endothelium to horseradish peroxidase. Proc R Soc Lond [Biol] 174:435–443

Giacomelli F, Wiener J (1974) Regional variation in the permeability of rat thoracic aorta. Am J Pathol 75:513–528

Giacomelli F, Wiener J, Spiro D (1970) The cellular pathology of experimental hypertension V. Increased permeability of cerebral arterial vessels. Am J Pathol 59:133–160

Giacomelli F, Anversa P, Wiener J (1976) Effect of angiotensin-induced hypertension on rat coronary arteries and myocardium. Am J Pathol 84:111–138

Grotte G (1956) Passage of dextran molecules across the blood-lymph barrier. Acta Chir Scand [Suppl] 211:1–84

Hüttner I, More RH, Rona G (1970) Fine structural evidence of specific mechanism for increased endothelial permeability in experimental hypertension. Am J Pathol 61:395–412

Hüttner I, Boutet M, More RH (1973a) Studies on protein passage through arterial endothelium. I Structural correlates of permeability in rat arterial endothelium. Lab Invest 28:672–677

Hüttner I, Boutet M, More RH (1973b) Studies on protein passage through arterial endothelium. II regional differences in permeability to fine structural protein tracers in arterial endothelium of normotensive rat. Lab Invest 28:678–685

Hüttner I, Boutet M, Rona G, More RH (1973c) Studies on protein passage through arterial endothelium III. Effect of blood pressure levels on the passage of fine structural protein tracers through rat arterial endothelium. Lab Invest 29:536–546

Laliberté F, Sapin C, Belair MF, Druet Ph, Bariéty J (1978) The localization of the filtration barrier in normal rat glomeruli by ultrastructural immunoperoxidase techniques. Biol Cell 31:15–26

Leak LV (1971) Studies on the permeability of lymphatic capillaries. J Cell Biol 50:300–323

Majno G, Palade GE (1961) Studies on inflammation. I – The effect of histamine and serotonine on vascular permeability: an electron microscopic study. J Biophys Biochem Cytol 11:571–605

Nakamura Y, Wayland H (1975) Macromolecular transport in the cat mesentery. Microvasc Res 9:1–21

Palade GE (1961) Blood capillaries of the heart and other organs. Circulation 24:368–384
Renkin EM (1977) Multiple pathways of capillary permeability. Circ Res 41:735–743
Rennke HG, Patel Y, Venkatachalam MA (1978) Glomerular filtration of proteins. Clearance of anionic, neutral, and cationic horseradish peroxidase in the rat. Kidney Int 13:278–288
Schwartz SM, Benditt EP (1972) Studies on aortic intima. I – Structure and permeability of rat thoracic aortic intima. Am J Pathol 66:241–254
Simionescu N, Simionescu M, Palade GE (1972) Permeability of intestinal capillaries. Pathway followed by dextrans and glycogens. J Cell Biol 53:365–392
Simionescu N, Simionescu M, Palade GE (1975) Permeability of muscle capillaries to small heme-peptides. Evidence for the existence of patent transendothelial channels. J Cell Biol 64:586–606
Simionescu N, Simionescu M, Palade GE (1976a) Segmental differentiations of cell junctions in the vascular endothelium. Arteries and veins. J Cell Biol 68:705–723
Simionescu N, Simionescu M (1976b) Galloylglucoses of low molecular weight as mordant in electron microscopy. J Cell Biol 70:608–633
Simionescu N, Simionescu M, Palade GE (1978a) Structural basis of permeability in sequential segments of the microvasculature of the diaphragm. I – Bipolar microvascular fields. Microvas Res 15:1–16
Simionescu N, Simionescu M, Palade GE (1978b) Structural basis of permeability in sequential segments of the microvasculature of the diaphragm. II – Pathways followed by microperoxidase across the endothelium. Microvas Res 15:17–36
Simionescu N, Simionescu M, Palade GE (1978c) Open junctions in the endothelium of the post-capillary venules of the diaphragm. J Cell Biol 79:27–44
Westergaard E, Brightam MW (1973) Transport of proteins across normal cerebral arterioles. J Comp Neurol 152:17–44
Williams MC, Wissig SL (1975) Permeability of muscle capillaries to horseradish peroxidase. J Cell Biol 66:531–555
Wissig SL, Williams MC (1978) Permeability of muscle capillaries to microperoxidase. J Cell Biol 76:341–359

Accepted December 3, 1981

Virchows Arch [Pathol Anat] (1982) 395:169–179

Virchows Archiv A

Aneurysmal Bone Cyst, A Study of Ultrastructure and Malignant Transformation

Heikki J. Aho[1], Allan J. Aho[2], and Sakari Einola[2]

[1] Department of Pathology, University of Turku, Turku, Finland
[2] Department of Surgery, University Central Hospital of Turku, Kiinamyllynkatu 4–8, SF-20520 Turku 52, Finland

Summary. Four cases of aneurysmal bone cyst, of which one became malignant 7 years after irradiation, were studied by electron microscopy. The aneurysmal bone cyst was composed of four different types of stromal cells – fibroblasts, myofibroblasts, osteoblasts, and histiocytes – and osteo-clast-like multinucleated giant cells. The surface of blood spaces was devoid of specialized endothelium, which may explain the presence of large quantities of extravasated erythrocytes. Some histiocytes contained siderosomes. The malignant lesion consisted of two main types of stromal cells, of which one had electron lucent and the other electron dense cytoplasm. The stromal cells produced osteoid and the tumour was regarded as an osteosarcoma. The multinucleated giant cells resembled those observed in aneurysmal bone cysts, but the nuclei seemed to be more often spherical. It is concluded that irradiation of the aneurysmal bone cyst may cause sarcomatous transformation in a cell capable of producing osteoid.

Key words: Aneurysmal bone cyst – Malignant transformation – Osteosarcoma – Irradiation – Ultrastructure

Introduction

The aneurysmal bone cyst (Jaffe and Lichtenstein 1942; Lichtenstein 1950) is a benign non-neoplastic lesion of unknown aetiology. It usually affects vertebrae or the metaphyses of long bones and is composed of bloodfilled spaces lined by multinucleated giant-cells containing fibrous septae. The cysts are most common in the second and third decades of life, and there is a slight predominance in females (Tillman et al. 1968; Biesecker et al. 1970; Ruiter et al. 1977). Aneurysmal bone cyst may be primary or secondary, co-existing with other bone disease (Biesecker et al. 1970; Buraczewski and Debska 1971; Koskinen et al. 1976; Ruiter et al. 1977). The lesion is treated by curettage or resection en bloc with cancellous or cortical bone transplantation. Radiotherapy is sometimes used for cysts in vertebrae or other sites which are not amenable to surgical

Offprints requests to: A.J. Aho, at the above address

0340-1227/82/0395/0169/$02.20

procedures. One fifth to one third of all cases will relapse after initial treatment (Tillman et al. 1968; Ruiter et al. 1977). Sarcomas, apparently arising from irradiated aneurysmal bone cysts, have been recorded (Tillman et al. 1968) but the morphological features of this transformation are not well understood.

The present study was undertaken to see which ultrastructural characteristics separate an osteosarcoma developing after radiotherapy of an aneurysmal bone cyst from the pre-existing lesion and from other benign aneurysmal bone cysts.

Patients and Methods

Four patients suffering from the aneurysmal bone cyst were studied. The clinical data are presented in Table 1.

The aneurysmal bone cyst was associated with a fibrous defect in Case 3.

The 19-year-old patient, Case 4, sought medical help for sciatic pain. An aneurysmal bone cyst was detected in the upper part of the sacrum in May 1972. The lesion was curetted, and the treatment was completed by an X-ray radiation dose of 2000 rads. However, the cyst recurred the next year and high voltage radiation was given using a dose of 3800 rads in January 1973. Another recurrence was observed in June 1976. The lesion was curetted, but further radiotherapy was abandoned because the patient had already been given a total dose of 5,800 rads. Fifth lumbar nerve exploration was performed in January 1978. The histological picture in a new biopsy was identical with the primary lesion. Extensive growth reaching the innominate bone and malignant transformation into osteosarcoma was seen at an examination in October 1979, 7 years after radiotherapy. No response was achieved with cytotoxic drugs. The patient died in August 1980. Unfortunately no autopsy was performed. Samples for electron microscopy were taken from the cyst in June 1976 and of the malignant lesion in October 1979.

Tissues for electron microscopy were fixed in 3.0% glutaraldehyde in 0.1 M cacodylate buffer at pH 7.4 (Sabatini et al. 1963) for 24 h and postfixed in 1.0% osmium tetroxide (Millonig 1961) for 1 h. The samples were washed in buffer, dehydrated in ethanol or acetone, and embedded in Epon 812 (Luft 1961). Thin sections were stained with uranyl acetate (Watson 1958) and lead citrate (Venable and Coggeshall 1965) and studied in a Jeol JEM-100 C electron microscope. For tissue identification, semi-thin (1 μm) Epon sections were stained with alkaline toluidine blue.

Table 1. Clinical data and aneurysmal bone cysts

Case	Age and sex	Location and size	Treatment	Follow-up
1	21, F	Upper femoral head	Curettage, cancellous bone transplantation	3 years, no recurrence
2	28, F	Humeral diaphysis	Resection en bloc, autogenic fibular bone replacement, A0-osteosynthesis	6 years, no recurrence
3	31, F	Upper femoral head	Curettage, cancellous and cortical bone transplantation	4 years, no recurrence
4[a]	19, M	Sacrum	Radiotherapy (5,800 rads), curettages	8 years, recurrences, malignant change, death

[a] Detailed data given in patients and methods section

Tissues were also fixed in 10% formalin and embedded in paraffin for histological examination. Sections 5 μm thick were stained with van Gieson and with haematoxylin and eosin (HE).

Results

All cysts from cases 1–3 and that from case 4 before malignant change had similar light and electron microscopical features.

Aneurysmal Bone Cyst

a) Light Microscopy. Blood spaces of varying size were outlined by septae, which were composed of fibroblasts, multinucleated giant cells and loose collagenous ground substance. Flattened fibroblasts, often resembling endothelium, or pure collagen seemed to cover the septae (Fig. 1a). Numerous capillaries, extravasated erythrocytes, haemosiderin, histiocytes and a variety of inflammatory cells characterized the granulation tissue, which formed more solid areas. Osteoid surrounded by a line of osteoblasts and occasional osteoclastic giant cells occurred in some areas and showed signs of slight mineralization (Fig. 3a).

b) Electron Microscopy. Four kinds of stromal cells – fibroblasts, myofibroblasts, osteoblasts and histiocytes – and multinucleated giant cells were seen in ground substance composed of amorphous fine electron dense material and collagen fibres of 64 nm periodicity. Sometimes the collagen occurred in bundles.

Most cells were typical elongated fibroblasts. The nuclear membrane was irregular, and a 30–40 nm thick fibrous lamina was sometimes observed immediately beneath it. The chromatin was condensed, and the nucleolus was often prominent. The cisternae of abundant rough surfaced endoplasmic reticulum were slightly dilated, and the cytoplasm contained polyribosomes. The cells lining the cystic spaces were fibroblasts (Fig. 1). These spaces were often lined only by fibrin-covered collagen. Specialized endothelium with basement membrane and junctions between the cells were seen only in the blood vessels.

Myofibroblasts (Fig. 2) were encountered in the granulation tissue. They had the characteristic features of these cells, i.e. bundles of filaments with a diameter of 5 nm containing focal densities (Fig. 2a), pinocytotic vesicles and sometimes nuclear fibrous lamina and discontinuous basement membrane.

More prominent rough surfaced endoplasmic reticulum, abundant mitochondria, hypertrophic Golgi apparatus and less condensed chromatin distinguished the osteoblasts from the fibroblasts (Fig. 3). They were few or absent in some sections. Crystal-like electron dense hydroxy apatite needles $2–5 \times 30–70$ nm in size were attached to the collagen fibres in osteoid (Fig. 3b).

Some cells were histiocytes. They resembled fibroblasts, but contained siderosomes (Fig. 4) and both primary and other kinds of lysosomes.

The multinucleated giant cells resembled osteoclasts (Fig. 5). The cytoplasm contained numerous mitochondria and polyribosomes. The nuclei were either round or more often elongated, and the nuclear membrane was smooth or slightly serrated. They were surrounded by Golgi apparatuses. Bundles of fine filaments with a diameter of 10 nm were discernible immediately beneath the plasma membrane in some cells. The giant cells had numerous villous processi

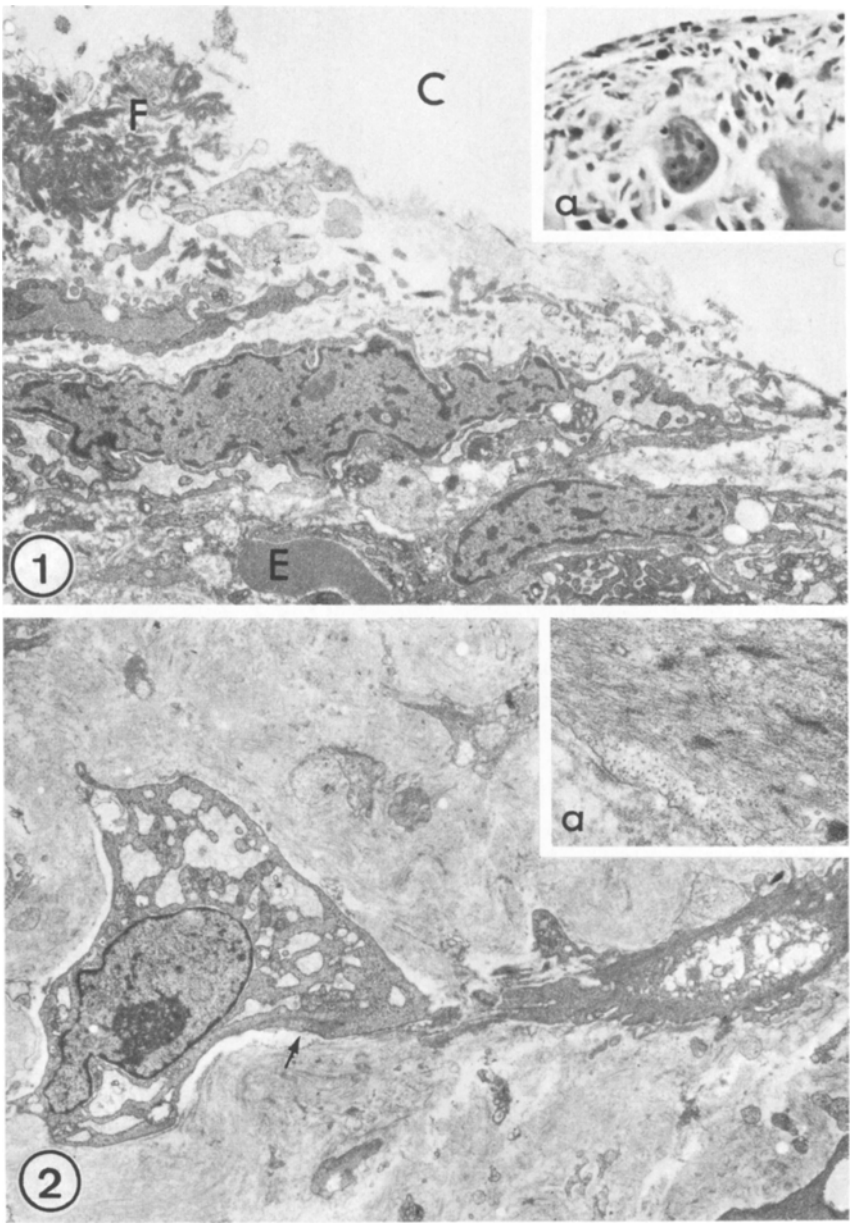

Fig. 1. Fibroblasts lining a blood filled cystic space (*C*). Fibrin (*F*), erythrocyte (*E*). Case 4. ×5,800. *Inset a.* Fibroblasts and multinucleated giant cells in fibrous septa of aneurysmal bone cyst. Case 4. HE ×240

Fig. 2. Myofibroblast with intracellular bundles of filaments discernible (*arrow*). Case 1. ×4,460. *Inset a.* Fine filaments with a diameter of 5 nm in a myofibroblast. Note the focal condensations. Case 1. ×15,000

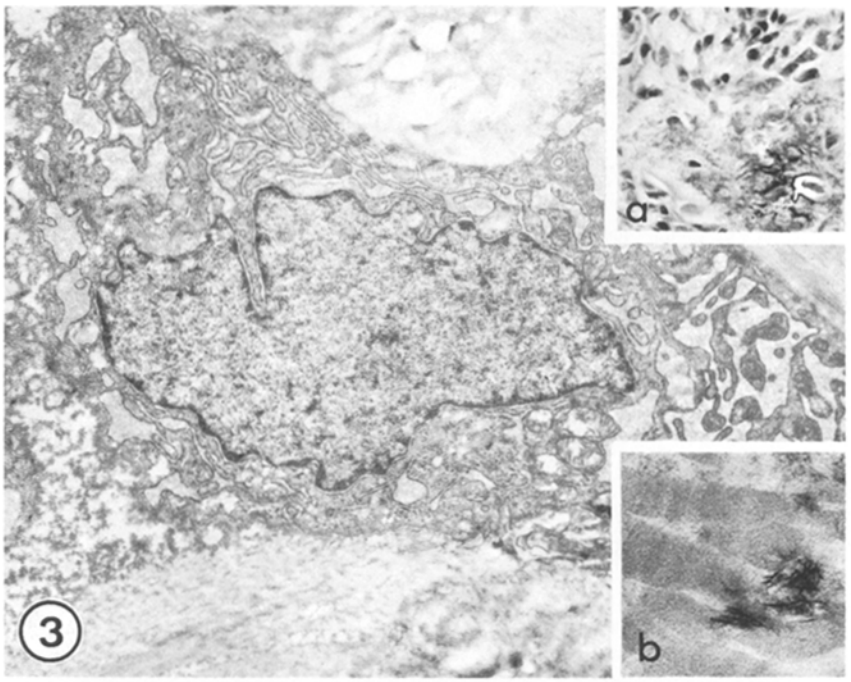

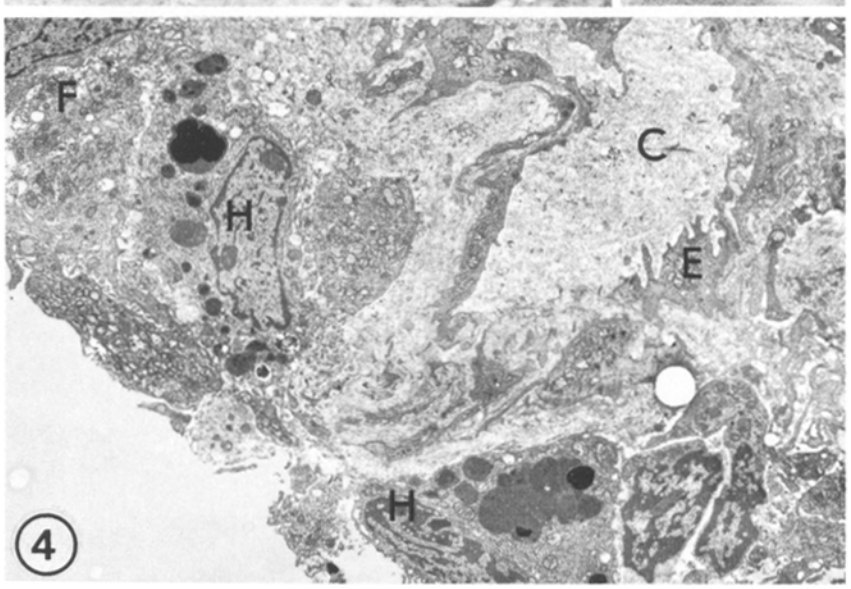

Fig. 3. Osteoblast with abundant rough surfaced endoplasmic reticulum. Case 3. ×6,320. *Inset a*. Osteoblasts lining partly mineralized osteoid. Case 4. HE ×240. *Inset b*. Collagen fibres in osteoid. Electron dense crystallike hydroxy apatite needles indicate mineralization. Case 3. ×60,000

Fig. 4. Histiocytes (*H*) laden by electron dense siderosomes. Fibroblasts (*F*), endothelium (*E*), capillary lumen (*C*). Case 4. ×3,340

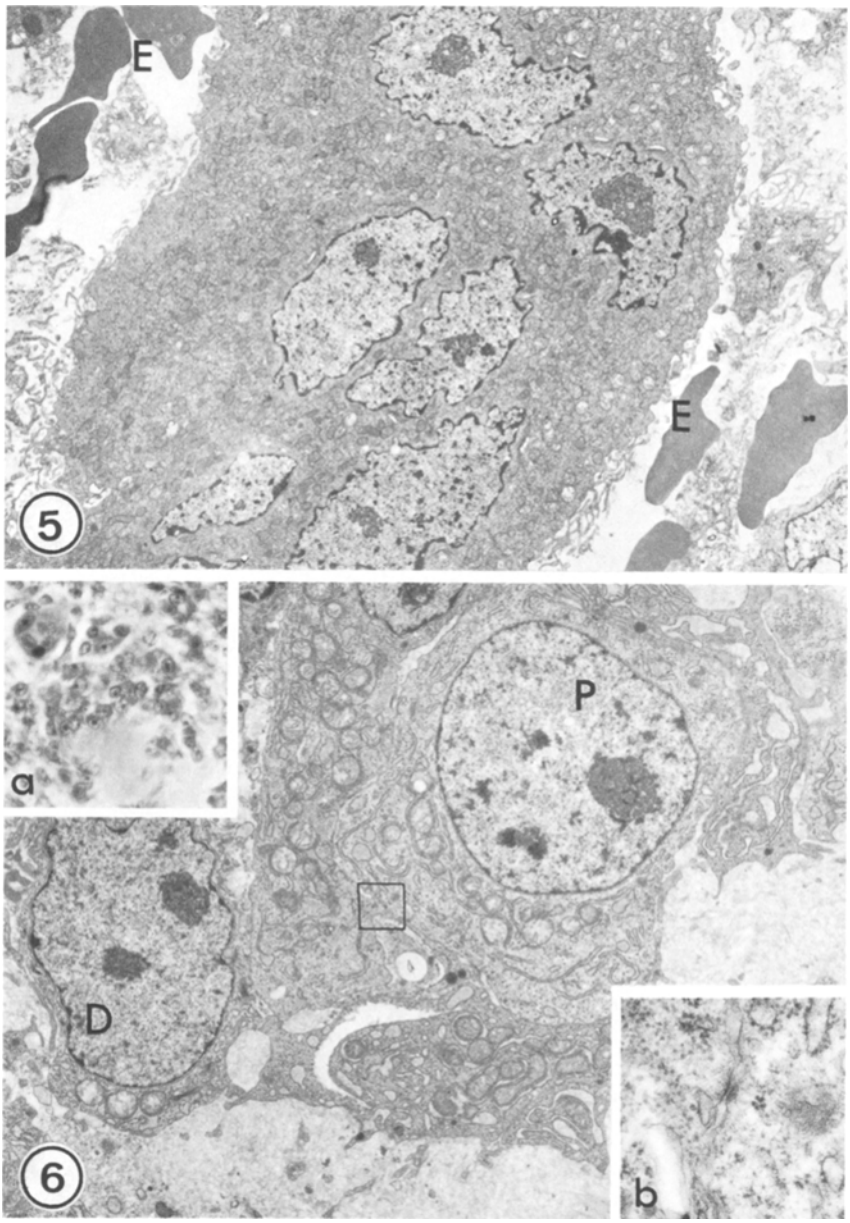

Fig. 5. Multinucleated giant cell. Note the numerous villous processes. Extravasated erythrocytes (*E*). Case 2. ×3,160

Fig. 6. Two kinds of cells surrounding osteoid areas. Cell with electron dense cytoplasm (*D*) with multiple Golgi apparatus. Junctions of zonula adherenstype connect cells with pale cytoplasm (*P*) to each other. Case 4, sarcoma. ×4,100. Inset **a**. Sarcomatous cells, multinucleated giant cells and osteoid. Case 4, sarcoma. HE ×240. Inset **b**. Intercellular junction. Encircled in Fig. 6. ×29,800

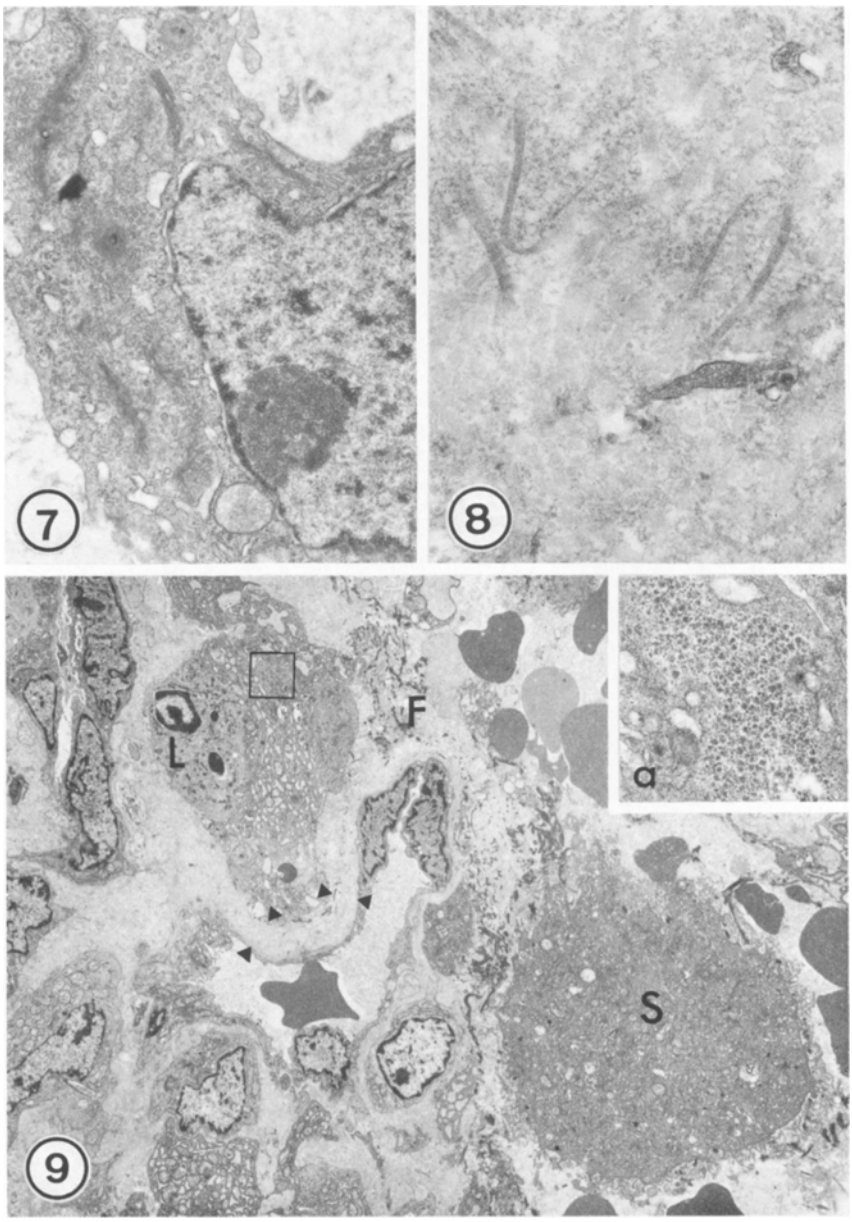

Fig. 7. Multiple Golgi apparatus in cell with electron dense cytoplasm. Case 4, sarcoma. ×14,900

Fig. 8. Osteoid, no signs of mineralization. Case 4, sarcoma. ×29,000

Fig. 9. Capillary surrounded by thick osteoid-like basement membrane (*arrow heads*). Giant cell (*S*), leukocyte (*L*), fibrin (*F*). Case 4, sarcoma. ×2,400. *Inset a.* Glycogen in a tumour cell. Encircled in Fig. 9. ×10,400

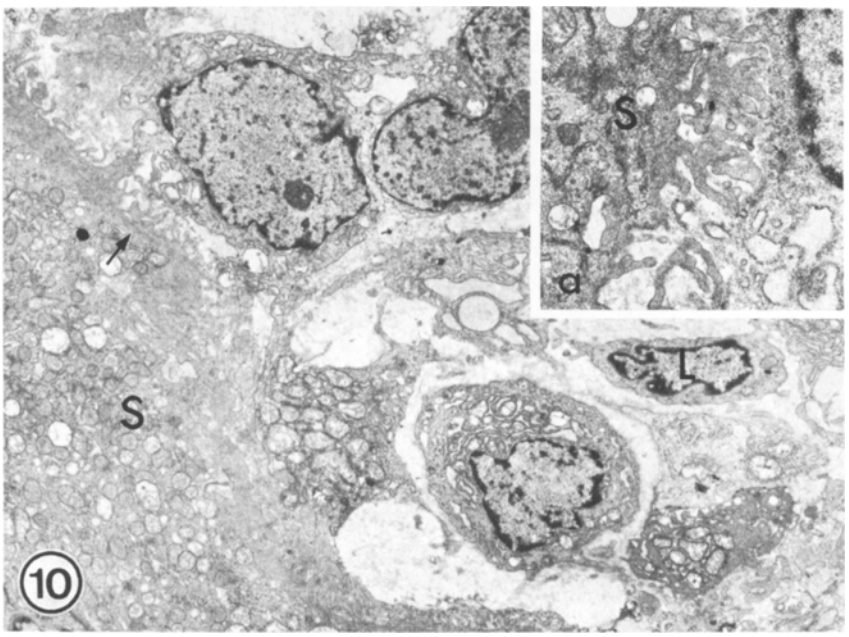

Fig. 10. Lymphocytes (*L*), mononuclear stromal cells and a multinucleated giant cell (*S*). Note subplasmalemmal zone of filaments (*arrow*). Case 4, sarcoma. ×4,100. *Inset a.* Part of a tumour cell and villous surface of a giant cell (*S*). Case 4, sarcoma. ×9,900

without a distinct internal structure. The specialized ruffled border typical of active osteoclasts was not observed, and the cells were not connected with the mineralization areas in the sections.

Macrophages, lymphocytes, leukocytes, often degenerating erythrocytes, cell debris and fibrin were seen among these five cell types.

Sarcoma. Case 4

a) Light Microscopy. The tumour was composed of solid areas with large hyperchromatic cells which were sometimes arranged in lines around often mineralized osteoid (Fig. 6a). Many cells were in mitosis. Numerous multinucleated giant cells with mainly spherical nuclei were observed between the cells surrounding the osteoid or among the other stromal cells. Septae typical of the previous aneurysmal cyst without malignant tissue were also recognizable in some sections.

b) Electron Microscopy. Two kinds of cells surrounded the osteoid. Most of them had little cytoplasm and the amount of endoplasmic reticulum was scanty (Fig. 6). Multiple Golgi complexes and several polyribosomes characterized the cells (Fig. 7). Glycogen-like rosettes were also detected (Fig. 9 inset). There were also large cells with round nuclei and pale cytoplasm, in which tubular shaped cisternae of rough surfaced endoplasmic reticulum and polyribosomes were noted (Fig. 6). Intercellular junctions of zonula adherens-type connected them to each other. The difference between the two cell types was not always clear-cut.

The osteoid was composed of collagen fibres and weakly electron dense fluffy material (Fig. 8). The basement membrane of the often large capillaries consisted of a 2–10 μm thick layer of material which was connected with large areas of osteoid (Fig. 9).

The multinucleated giant cells were similar to those observed in typical aneurysmal bone cysts, although the nuclei were largely round. They were in intimate contact with lymphocytes and mononuclear stromal cells (Fig. 10) some of which were degenerating.

Discussion

Fibroblasts, myofibroblasts, osteoblasts, histiocytes and multinucleated giant cells were seen among capillaries, extravasated erythrocytes and a variety of inflammatory cells in the septae of the aneurysmal bone cyst. These observations agree with those of Steiner and Kanter (1977). However, the large accumulations of glycogen in fibroblasts emphasized by these investigators were not shown in our study.

The character of the cells lining the large cystic spaces has been widely discussed. Histologically, they have been regarded as endothelial by some authors (Godfrey and Gresham 1959). It has also been observed, that some of the spaces may be lined by fibroblasts and bundles of collagen while others may be covered by endothelium (Koskinen et al. 1976; Ruiter et al. 1977a). Endothelium was not detected on the septae in the sections of our study. The main cell type, the fibroblast, often covered by fibrin, formed the outer layer. The observations agree with those Steiner and Kanter (1977). This absence of endothelium may explain the abundance of extravasated erythrocytes and haemosiderin in the lesions.

The sarcoma in case 4 arose 7 years after the initial radiotherapy of the aneurysmal bone cyst affecting the same location. The dose of 5,800 rads used and the latency period correspond well to those described in the literature (Huvos 1979). The tumour was classified as an osteosarcoma because the cells regularly formed osteoid, although there was some histological resemblance to malignant giant cell tumour which are considered to be capable of producing osteoid by some authors (Shuffstall and Gregory 1953).

The heterogenous cell population of most spontaneous osteosarcomas (Reddick et al. 1980; Aho and Aho) was absent in our tumour. It contained two main types of stromal cells which resembled those described by Lee et al. (1975). These workers reported a case of orbital osteosarcoma which developed 5 years after radiotherapy of a retinoblastoma in a 7-year-old boy. Small cells with electron dense cytoplasm were regarded as precursors of osteoclasts and larger ones with electron lucent cytoplasm as osteoblasts. However, some tumour cells with electron dense cytoplasm of our study contained glycogen, and the presence of this material is wellestablished in the osteoblastic tumour cells of osteosarcoma (Reddick et al. 1980) and in developing osteoblasts (Scott 1967; Scott and Glimcher 1971). Glycogen is not a feature of the osteoclast (Göthlin and Ericsson 1976; Rifkin et al. 1980). Therefore both cell types can also be regarded as primitive osteoblasts. This view is supported by the fact that many cells had features of both types, and thus classification was not possible. Intercel-

lular junctions have been reported in normal osteoblasts (Stanka 1975) and in the cells of osteosarcoma (Reddick 1980).

The osteoid often continued around blood vessels and formed a thick basement membrane-like structure in our osteosarcoma. Telangiectatic osteosarcoma, which is sometimes difficult to distinguish from the aneurysmal bone cyst (Ruiter et al. 1977b), is composed of blood-filled spaces of varying size lined by tumour cells (Matsuno et al. 1976; Farr et al. 1977; Larsson et al. 1978). The blood spaces in the sarcomatous area were, however, lined by endothelium, and therefore the tumour cannot be regarded as telangiectatic osteosarcoma.

The aetiology and pathogenesis of aneurysmal bone cyst are obscure. It has been considered to be an angiogenic neoplasm, the result of an arteriovenous communication or to be a reactive process stimulated by injury or some disease of bone, e.g. subperiosteal haemorrhage, venous thrombosis or a neoplasm (Sput et al. 1971). The reactive nature of the lesion is suggested by presence of myofibroblasts which are constantly encountered in granulation tissue (Ryan et al. 1974) and which have been regarded as participants of a host response to neoplasia (Lagacé et al. 1980). Lorenzo and Dorfman (1980) stated that the aneurysmal bone cyst and the giant cell reparative granuloma of short tubular bones represent a response to intraosseous haemorrhage. The morphology of the giant cells described by them has similarities in both lesions. Moreover, siderosomes can be found in the cells of lesions supposed to associate with extravasation of erythrocytes (Steiner 1974; Bosch et al. 1974; Ghadially et al. 1978; Bhawan et al. 1980).

In conclusion, we feel that the aneurysmal bone cyst may represent a false aneurysm-like reaction to haemorrhage probably caused by a variety of pathological conditions. Radiotherapy of the lesion may lead to sarcomatous transformation in cells capable of producing osteoid. Osteosarcomas induced by irradiation seem to have similar ultrastructural characteristics.

Acknowledgement. This study is supported by a grant from the Cancer Society of Finland.

References

Aho AJ, Aho HJ Ultrastructure of human osteosarcoma. Malignant transformation of a multipotential connective tissue cell. Pathology Res Practice (in press)

Bhawan J, Joris I, Cohen N, Majno G (1980) Microcirculatory changes in posttraumatic pigmented villonodular synovitis. Arch Pathol Lab Med 104:328–332

Biesecker JI, Marcove RC, Huvos AG, Miké V (1970) Aneurysmal bone cysts. A clinicopathologic study of 66 cases. Cancer 26:615–625

Bosch AL, Olaya AP, Fernandez AL (1974) Non-ossifying fibroma of bone. A histochemical and ultrastructural characterization. Virchows Arch [Pathol Anat] 362:13–21

Buroczewski J, Dabska M (1971) Pathogenesis of aneurysmal bone cyst. Relationship between the aneurysmal bone cyst and fibrous dysplasia of bone. Cancer 28:597–604

Farr GH, Huvos AG, Marcove RC, Higinbotham NL, Foote FW Jr (1974) Telangiectatic osteogenic sarcoma. Cancer 31:1150–1158

Ghadially FN, Lalonde J-MA, Dick CE (1979) Ultrastructure of pigmented villonodular synovitis. J Pathol 127:19–26

Godfrey LW, Gresham GA (1959) The natural history of aneurysmal bone cyst. Proc R Soc Med 52:900–905

Göthlin G, Ericsson JLE (1976) The osteoclast. Review of ultrastructure, origin, and structure-function relationship. Clin Orthop 120:201–231

Huvos AG (1979) Radiation as an oncogenic agent in sarcoma of bone. In: Bone tumors. Diagnosis, treatment and prognosis. W.B. Saunders Company, Philadelphia, London, Toronto, pp 127–138

Jaffe HL, Lichtenstein L (1942) Solitary unicameral bone cyst with emphasis on the roentgen picture, the pathologic appearance and the pathogenesis. Arch Surg 44:1004–1025

Koskinen EVS, Visuri TI, Homström T, Roukkula MA (1976) Aneurysmal bone cyst. Evaluation of resection and of curettage in 20 cases. Clin Orthop 118:136–146

Lagaće R, Schürch W, Seemayer TA (1980) Myofibroblasts in soft tissue sarcomas. Virchows Arch [Pathol Anat] 389:1–11

Larsson S-E, Lorentzon R, Boquist L (1978) Telangiectatic osteosarcoma. Acta Orthop Scand 49:589–594

Lee WR, Laurie J, Townsend AL (1975) Fine structure of a radiation-induced osteogenic sarcoma. Cancer 36:1414–1425

Lichtenstein L (1950) Aneurysmal bone cyst. A pathological entity commonly mistaken for giant-cell tumor and occasionally for hemangioma and osteogenic sarcoma. Cancer 3:279–289

Lorenzo JC, Dorfman HD (1980) Giant-cell reparative granuloma of short tubular bones of the hands and feet. Am J Surg Pathol 4:551–563

Luft JH (1961) Improvements in epoxy resin embedding methods. J Biophys Biochem Cytol 9:409–414

Matsuno T, Unni KK, McLeod RA, Dahlin DC (1976) Telangiectatic osteogenic sarcoma. Cancer 38:2538–2547

Millonig G (1961) Advantages of a phosphate buffer for OsO_4 solutions in fixation. J Appl Physiol 32:1637–1645

Reddick RL, Michelitch HJ, Levine AM, Triche TJ (1980) Osteogenic sarcoma. A study of the ultrastructure. Cancer 45:64–71

Rifkin BR, Brand JS, Cushing JE, Coleman SJ, Sanavi F (1980) Fine structure of fetal rat calvarium; provisional identification of preosteoclasts. Calcif Tissue Int 31:21–28

Ruiter DJ, Cornelisse CJ, van Rijssel ThG, van der Velde EA (1977a) Aneurysmal bone cyst and telangiectatic osteosarcoma. A histopathological and morphometric study. Virchows Arch [Pathol Anat] 373:311–325

Ruiter DJ, van Rijssel ThG, van der Velde EA (1977b) Aneurysmal bone cysts. A clinicopathological study of 105 cases. Cancer 39:2231–2239

Ryan GB, Cliff WJ, Gabbiani G, Irlé C, Montandon D, Statkov PR, Majno G (1974) Myofibroblasts in human granulation tissue. Hum Pathol 5:55–67

Sabatini DD, Bensch K, Barrnett TJ (1963) Cytochemistry and electron microscopy. The preservation of cellular ultrastructure and enzymatic activity by aldehyde fixation. J Cell Biol 17:19–58

Scott BL (1967) Thymidine – ^3H electron microscope radioautography of osteogenic cells in the fetal rat. J Cell Biol 35:115–126

Scott BL, Glimcher MJ (1971) Distribution of glycogen in osteoblasts of the fetal rat. J Ultrastruct Res 36:565–586

Shuffstall RM, Gregory JE (1953) Osteoid formation in giant cell tumors of bone. Am J Pathol 29:1123–1131

Sput HJ, Dorfman HD, Fechner RE, Ackerman LV (1971) Aneurysmal bone cyst. In: Tumors of bone and cartilage. Atlas of tumor pathology, Second Series, Fascicle 5, Armed Forces Institute of Pathology. Washington, pp 357–367

Stanka P (1975) Occurrence of cell junctions and microfilaments in osteoblasts. Cell Tissue Res 159:413–422

Steiner GC (1974) Fibrous cortical defect and nonossifying fibroma of bone. A study of the ultrastructure. Arch Pathol 97:205–210

Steiner GC, Kantor EB (1977) Ultrastructure of aneurysmal bone cyst. Cancer 40:2967–2978

Tillman BP, Dahlin DC, Lipscomb PR, Stewart JR (1968) Aneurysmal bone cyst: an analysis of ninety-five cases. Mayo Clin Proc 43:478–495

Venable JH, Coggeshall R (1965) A simplified lead citrate stain for use in electron microscopy. J Cell Biol 25:407–408

Watson ML (1958) Staining of tissue sections for electron microscopy with heavy metals. J Biophys Biochem Cytol 4:475–479

Accepted December 15, 1981

Virchows Archiv [Pathol Anat] (1982) 395:181–199

Virchows Archiv A

The Ultrastructure of Human Fibrosing Alveolitis

Jacqueline J. Coalson

Department of Pathology, The University of Texas Health Science Center at San Antonio, 7703 Floyd Curl Drive, San Antonio, Texas, 78284 USA

Summary. This report describes the ultrastructural findings in 37 patients who underwent open lung biopsy which yielded diagnoses of fibrosing alveolitis. A spectrum of lesions are categorized for the capillary endothelium and its basement membrane, the interstitial space and its fibrocellular components, and the alveolar epithelium and its basement membrane. The findings typify the different pulmonary cellular reactions to injury. Evidence for cellular regeneration and death in both epithelial and endothelial cell populations include atypical epithelial cell proliferation, capillary basement membrane multilamination, decrease in capillary lumen size and prominent pericytic ensheathment of pulmonary capillaries. Within the interstitium of the lung, proliferation of collagen and elastic fibers are documented, but in addition, abundant myofibroblasts and smooth muscle cells are present. No ultrastructural evidence of immune complex deposition was found in this study. The morphologic findings of fibrosing alveolitis further support the widespread concept that the lung responds to various injuries in a similar manner and undergoes a common reparative response regardless of etiology.

Key words: Lung disease – Electron microscopy – Interstitial pneumonia – Fibrosis

Introduction

Fibrosing alveolitis is a semantic term chosen from a multitude of others which denotes a lung disease characterized by a mixed inflammatory-fibrotic process of the distal components of the respiratory tract. The histological characteristics of fibrosing alveolitis or its multiple other designations have been described by many investigators (Crystal et al. 1976; Gaensler et al. 1972; Greenberg et al. 1974; Liebow 1975; Livingstone et al. 1964; Scadding 1974; Spencer 1967, 1968 and 1975; Winterbauer et al. 1978). A much smaller group of papers

Offprint requests to: J.J. Coalson, at the above address

0340-1227/82/0395/0181/$03.80

have included ultrastructural features of this process (Adler et al. 1981; Basset et al. 1975; Brody and Craighead 1976; Cassan et al. 1974; Davis et al. 1978; Gebbers et al. 1977; Kawanami et al. 1978 and 1979). The present report describes the ultrastructural findings in 37 patients who underwent open lung biopsy to aid in the diagnosis of diffuse pulmonary disease.

Materials and Methods

The study group consists of 37 patients seen between 1972 and 1978. All patients were evaluated by pulmonary specialists in 4 major Oklahoma City hospitals and community hospitals in surrounding Oklahoma cities. The patients underwent open lung biopsies after thorough clinical, radiologic, and pulmonary function investigations indicated progressive pulmonary interstitial disease of uncertain etiology. Due to good communication between the attending internist, pathologist and surgeon, adequate and appropriate tissue speciemens of the lung were selected at surgery and immediately processed for microbiologic, histopathologic, ultrastructural, and in many cases immunofluorescent studies.

Lung specimens were routinely put in 10% neutral buffered formalin for surgical pathology evaluation. The portions of tissue for ultrastructural study were put in 2–4% cacodylate buffered glutaraldehyde in the early years of the study and in phosphate buffered 4% formaldehyde-1% glutaraldehyde (4CF-1G) in the latter years of the study (McDowell and Trump 1976). Following primary fixation in one of these aldehyde fixatives, the tissue was postfixed in Zetterqvist's fixative, en bloc stained with uranyl acetate (last 3 years of study), dehydrated in ascending grades of ethanol, and embedded in Epon 812 or Araldite. Thick one micron sections were obtained from all blocks (15–20) and stained with either methylene blue-azure II, toluidine blue, or Paragon multiple stain. Appropriate blocks were selected for thin sectioning; thin sections were stained with uranyl acetate and lead citrate. The grids were examined with a RCA-EMU-3G or Hitachi HS-9 electron microscope.

Any tissue remaining from the electron microscopic sample was processed for routine light microscopy. In addition all slides and/or blocks from the pathology services of involved hospitals were obtained for study. Hematoxylin and eosin, Van Gieson elastica and reticulin stained preparations were available for histologic evaluation. A grading system of the histologic findings was developed. Grade 1 or mild disease was characterized by a predominantly cellular reaction within the alveolar walls and/or in the alveolar spaces. The Van Gieson elastica and reticulin stains revealed zero to minimal fibrotic proliferation in Grade 1 disease. A Grade 2 or moderate disease designation indicated a mixed fibrocellular lesion. The inflammatory inflitrate was predominantly mononuclear consisting of monocytes, lymphocytes, and plasma cells with occasional eosinophils and rare neutrophils either in the thickened alveolar walls and/or in the mural exudates undergoing organization in the alveolar spaces. Connective tissue stains in the Grade 2 category showed the presence of increased reticulin and collagen fiber deposition. Grade 3 or severe disease indicated a predominantly fibrotic response with little inflammatory cellular activity. In these lesions not only was an increase in the connective tissue fiber deposition (collagen, reticulin, and elastic) noted, but smooth muscle proliferation was present as well. Histologic examples of these three grades of fibrosing alveolitis are seen in Fig. 1a–c. The cases were graded at the time the biopsy was originally evaluated and again at the time this series was being collated for this report.

Table 1 presents the patient's age, sex, race, symptom duration if known, histologic grade, and any additional remarks concerning the patient. It should be noted that there is no information concerning clinical treatment or long term followup. Many of the hospitals involved in this study are referral centers for the state. Most of the patients were referred back to their primary physicians for long-term followup. However, to May 1979, only six of the 37 patients were known to have died of their disease (Patients 3, 5, 17, 26, 29 and 33).

The ultrastructural studies were originally performed in hopes of determining a possible etiologic agent for the progressive fibrotic process. It became obvious during the first few years that immune complexes were not present in any of the specimens examined, including patients with Grade 1 or mild disease. What was present was a spectrum of lesions which were seen in the capillary endothelium and its basement membrane, the interstitial space and its fibrocellular components,

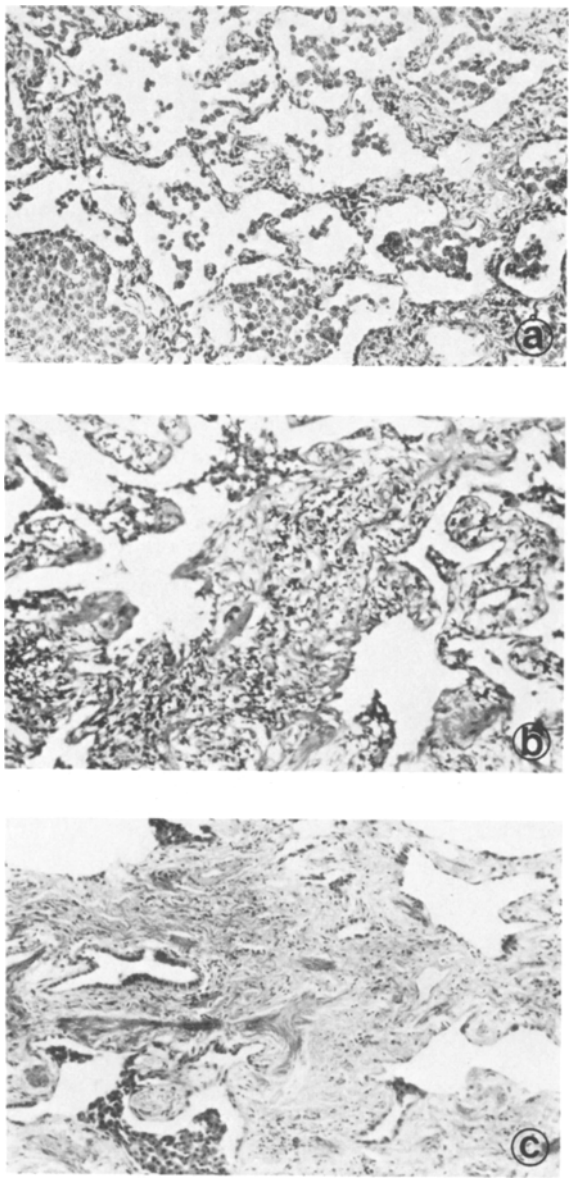

Fig. 1 a–c. Grades of fibrosing alveolitis. In 1 a, Grade 1 or mild disease is characterized by a predominantly cellular infiltrate in the interstitium and/or alveolar space, without significant reticulin, collagen, or elastic fiber deposition. In 1 b, Grade 2 or moderate disease denotes a mixed inflammatory-fibrotic lesions with some "remodeling" of alveolar walls. Abundant mononuclear inflammatory cells, smooth muscle fibers, increased collagen, reticulin and elastic fibers are seen. In 1 c, Grade 3 or severe disease, the alveoli have undergone extensive remodeling. Large bands of fibrotic tissue containing smooth muscle, collagen, elastic and reticulin fibers, but few inflammatory cells are present. Hematoxylin and eosin; ×130

Table 1. Summary of clinical-pathologic data of 37 patients with fibrosing alveolitis

Case	Age	Race and sex	Duration of symptoms prior to biopsy	Follow up duration	Histologic grade	Remarks
A. Collagen vascular disorders						
1	24	IF	5 weeks	LTF	1	RA since age 16. Wt. loss over past $1^1/_2$ years
2	26	OF	18 months	18 months	2	Mixed connective tissue disease
3	48	WF	10 years	5 months expired	2	RA, cor pulmonale, trt. with steroids & Imuran, died with opportunistic infection
4	55	WF	6 years	8 months	3	RA, Raynaud's phenomenon, anemia
5	58	BF	2 months	2 months expired	3	Sjogren's syndrome; multisystem disease for 14 years
6	66	WM	several years	LTF	3	25 yrs. hx. of RA; adult onset asthma, peripheral eosinophilia
B. Other						
7	71	WM	1 month	1 year	1	"Flu" like syndrome 1 month before study; positive ANA, unknown etiology.
8	61	BF	4 years	LTF	1	Negative workup
9	55	WM	4 months	4 months	1	Onset of symptoms following URI
10	67	WF	1 year	LTF	1	Onset of symptoms following URI 12 months earlier
11	43	WF	3 months	2 years	1	Negative workup
12	56	WM	many years	LTF	1	Repeated upper & lower respiratory infections
13	41	WM	Several months	16 months	1	Hospitalized for pneumonia 2 years before lung bx.
14	2	WF	5 months	9 months	1	Cough & tachynea for 5 months PTA
15	69	WM	5–6 years	LTF	1	Negative workup
16	51	WF	3 weeks	2 months	1	Hx. of chronic sinus problems. Superior vena caval obstruction, undetermined etiology
17	70	WM	1 year	13 months expired	2	Positive LE prep. Trt. with steroids & Cytoxan, cor pulmonale
18	68	WF	1 year	LTF	2	Positive rheumatoid factor (1:320) without arthritis
19	44	OF	0	3 years	2	Abnormal chest radiograph noted in routine exam
20	60	WM	4 years	1 year	2	Hx. of exposure to gasoline fumes & many pet birds
21	70	WF	1 month	2 years	2	Negative workup

Case	Age	Race and sex	Duration of symptoms prior to biopsy	Follow up duration	Histologic grade	Remarks
22	62	WF	1 month	1 year	2	Negative workup
23	42	WF	2 years	1 year	2	Negative workup; chest radiographs worsening during last 3 years
24	40	WF	3 years	6 months	2	Childhood asthma
25	40	WM	2 weeks	LTF	2	Negative workup
26	53	WM	9 months	2 years expired	2	Exposure to airplane fuel & fumes
27	64	WM	2–3 years	2 years	3	Occupational exposure to formaldehyde for 30 years
28	73	BM	6 months	2 months	3	Negative workup
29	69	WM	1 year	3 months expired	3	Strongyloides found in one stool specimen; peripheral eosinophilia
30	55	WM	6 months	LTF	3	Onset of symptoms following URI 6 months earlier
31	61	WM	7 months	3 years	3	Onset of symptoms following "flu" 7 months earlier
32	66	WM	1 year	3 years	3	Repeated episodes of "bronchitis" & SOB during past several years
33	67	WM	several months	10 months expired	3	Idiopathic sideroblastic anemia & in situ laryngeal ca diagnosed the same year as fibrosing alveolitis. Developed acute myeloblastic leukemia before death
34	58	WM	3 years	LTF	3	Welder by occupation
35	66	WM	3 years	LTF	3	Radiologic evidence of disease for 3 years
36	50	WM	several years	6 months	3	Negative workup
37	60	WM	3 years	LTF	3	Negative workup

RA = rheumatoid arthritis; LE = lupus erythematosis; URI = upper respiratory infection; PTA = prior to admission; SOB = shortness of breath; LTF = lost to followup;

and the alveolar epithelium and its basement membrane. The alterations sseen have been categorized in these various pulmonary compartments.

Results

The Lining Epithelium and Basement Membrane of Distal Airspaces. The lining epithelium of the airspaces in fibrosing alveolitis showed a wide spectrum of

cellular changes. Occasionally in less severely involved areas the normal epithelial type I-type II configuration was present. However, a frequent epithelial change was type II epithelial hyperplasia. Many of the hyperplastic epithelial type II cells were engorged with lamellar inclusion bodies (Fig. 2). Some of the cuboidal to columnar type II cells had a smooth cytoplasmic base and rested on their basement membrane. However, occasionally the hyperplastic II cells had prominent finger-like cytoplasmic processes which delved into the uderlying interstitium. The epithelial basement membrane underlying these cells was very attenuated or was frequently absent (Fig. 3). Wise intercellular spaces between adjacent hyperplastic type II cells were found.

An alternating dark-light cell configuration was another frequent epithelial finding (Fig. 4). Invariably these cells showed markedly attenuated cytoplasmic extensions. Within the cells, and especially the light cell, lamellar inclusion bodies were seen. Cytoplasmic organelles including rough endoplasmic reticulum, mitochondria, and occasional lamellar inclusion bodies were seen in the dark epithelial cells (Fig. 4). Beneath this attenuated lining epithelium, the basement membrane was either quite thin or was absent. These attenuated type II cells also had long finger-like extensions which dipped into the underlying interstitium.

A less frequent epithelium configuration was "bronchiolization". In Fig. 5 on one side of the thickened wall there are several alveolar type II cells which alternate in cytoplasmic density and show striking cytoplasmic extensions into the underlying septum. On the other side of the wall, ciliated epithelial cells alternate with bronchiolar-like cells which contain dense cytoplasmic granules. Infrequently, an entire remodeled airspace was lined with cells which appeared to be bronchiolar epithelial cells. Short microvilli, tight junctions and cytoplasmic granules similar to those seen in Clara cells were identified. An uncommon finding is the one depicted in Fig. 6. Two alveolar type II cells abut on each side of an intervening cell, which contains small dark cytoplasmic inclusions, rudimentary microvilli and the presence of tonofilaments within the cytoplasm. This cell is separated from the underlying interstitium by a basement membrane. Rarely a remodeled airspace contained intermixed immature type II cells and immature bronchiolar epithelial cells (Fig. 7).

Vascular Endothelium and its Basement Membrane of the Distal Airspaces. Vascular aberrations in fibrosing alveolitis were striking. In a few of the cases, foci of acute alveolar wall injury were intermixed with a proliferative reparative response. In these areas of reaction, the endothelium could show edema, intracytoplasmic blebs (Fig. 8) or abundant cytoplasmic tonofilaments. However, the more consistent vascular lesions in fibrosing alveolitis were as follows: 1) a marked decrease in the luminal size of vessels in the remodeled alveolar walls (Fig. 9); 2) alternating light and dark cell configurations (Figs. 4, 6); 3) endothelial cells with prominent quantities of cytoplasmic organelles (Fig. 10); and 4) prominent pericytes around the capillaries (Figs. 9, 10). The endothelium of the small capillaries was plump, lacking the normal attenuated configuration (Figs. 9, 10, 11). The finding of the alternating dark and light endothelial cells

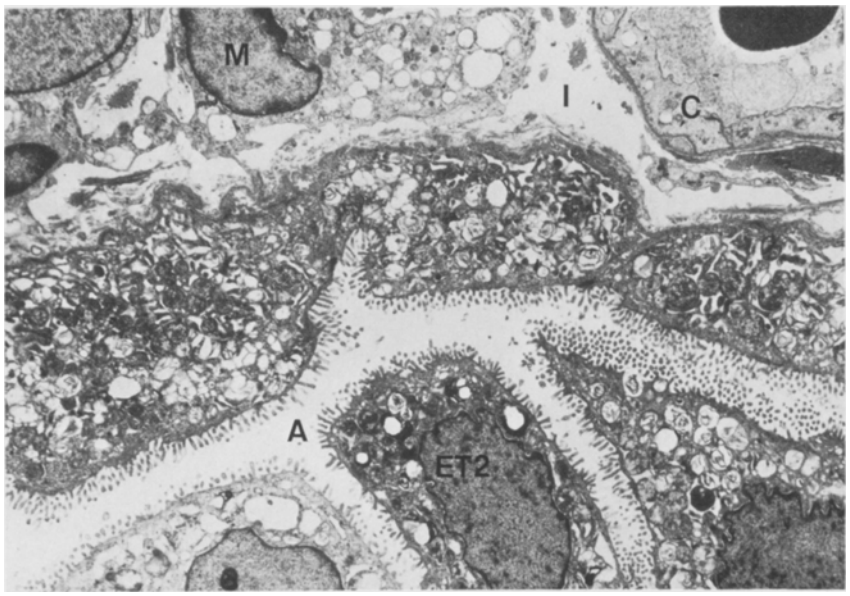

Fig. 2. The airspace *(A)* is lined by type II cells *(ET 2)*. Several cells including a macrophage (M) are seen within the interstitium *(I)*. The capillary *(C)* is lined by a slightly widened electron lucent endothelium. Uranyl acetate and lead citrate; ×3.520; case 25

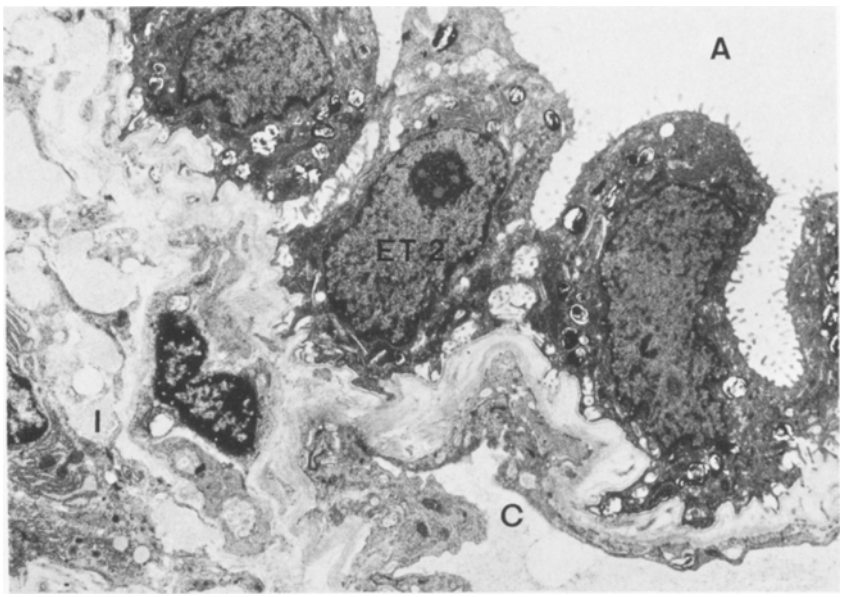

Fig. 3. Alveolar type II cells *(ET 2)* form a continuous lining for the alveolar space *(A)* but exhibit very wide intercellular spaces. Finger-like processes from the bases of type II cells penetrate into the underlying interstitium *(I)*. The epithelial basement membrane is very attenuated and is separated from the basement membrane of the capillary *(C)*. Uranyl acetate and lead citrate; ×4.800; case 2

Fig. 4. The alveolar space *(A)* is lined by an attenuated epithelium exhibiting numerous microvilli. Note that one of the attenuated epithelial cells is electron lucent whereas the other is electron dense. Lamellar bodies are seen *(arrow)* within the electron lucent cell. The capillary *(C)* shows a similar alternating pattern of dark-light endothelial cells. Increased quantities of collagen and mononuclear cells are present within the interstitium *(I)*. Uranyl acetate and lead citrate; ×6,000; case 4

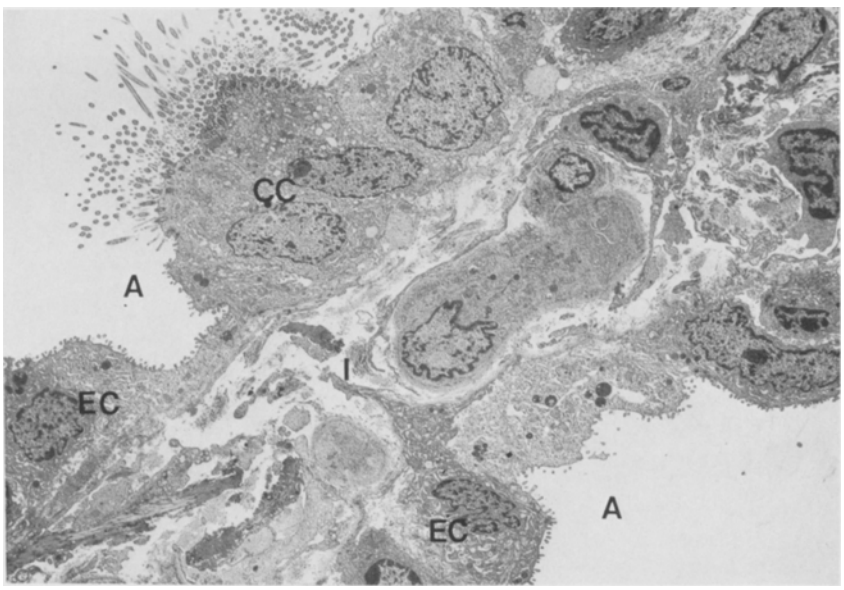

Fig. 5. An alveolar wall separates two alveolar spaces *(A)*. The upper alveolus exhibits ciliated cells *(CC)* and non-ciliated epithelial cells *(EC)* with short microvilli and dark cytoplasmic granules. The lower alveolus is lined by comparable epithelial cells, some of which resemble immature type II epithelial cells (*I*=interstitium). Uranyl acetate and lead citrate; ×1,760; case 33

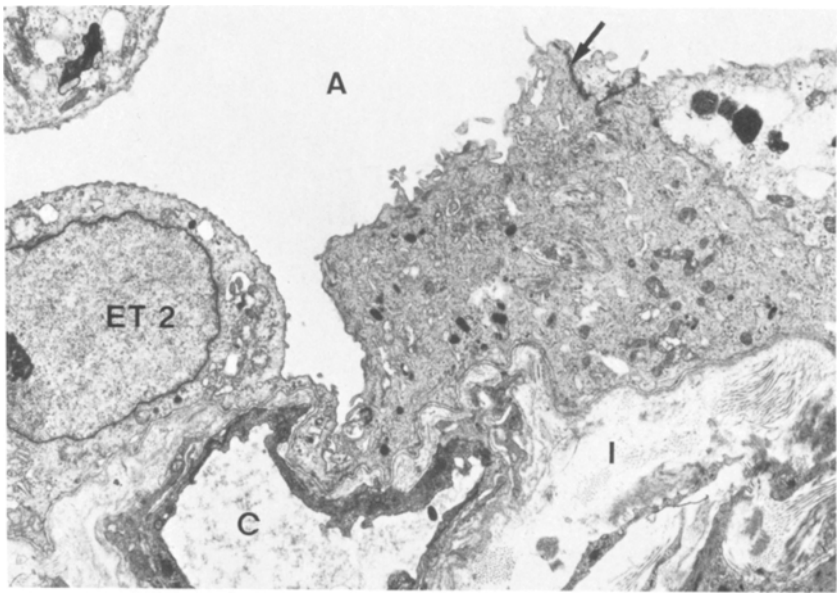

Fig. 6. Two alveolar type II's *(ET 2)* are joined by tight junctions *(arrow)* to a cell which shows small osmiophilic granules, tonofilaments and abundant rough endoplasmic reticulum. The granular configuration is more reminiscent of a bronchiolar epithelial cell than an alveolar type II cell. The interstitium *(I)* below the alveolar space *(A)* shows marked collagen deposition. (*C*=capillary). Uranyl acetate and lead citrate; ×5,840; case 2

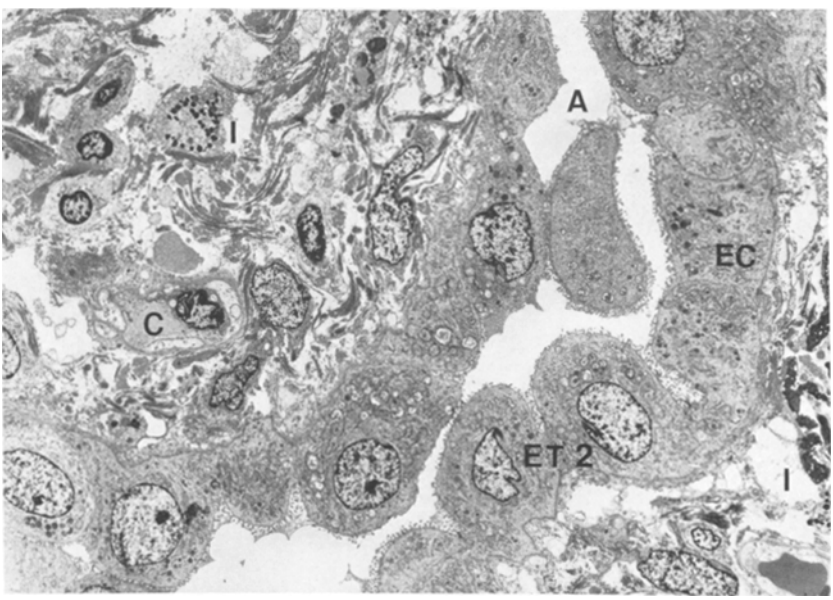

Fig. 7. The interstitium *(I)* shows a striking fibrocellular proliferation. Mononuclear cells and fibers (collagen and elastic) are well visualized. The air space *(A)* is lined by a mixture of epithelial cells, some of which contain typical lamellar inclusions *(ET 2)* while others exhibit dense osmiophilic granules reminiscent of bronchiolar epithelial cells *(EC)*. (*C*=capillary). Uranyl acetate and lead citrate; ×1,440; case 35

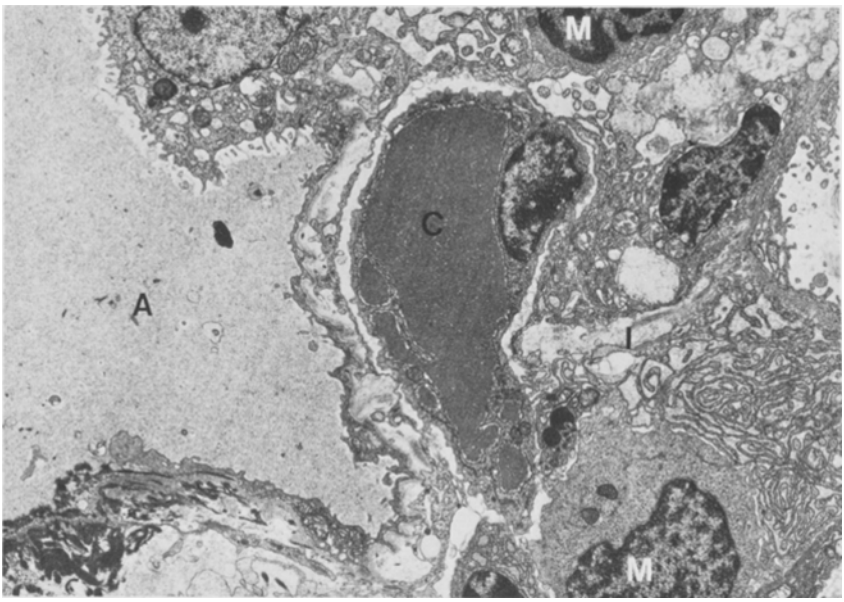

Fig. 8. The capillary *(C)* is filled with protein rich plasma. The endothelium shows intracytoplasmic blebs or vesicles. An endothelial basement membrane is not present. The interstitium *(I)* shows an influx of mononuclear cells (*M*); several show extensive arrays of rough endoplasmic reticulum. At the left, fibrin is seen both within the interstitium and over the denuded epithelial basement membrane. The alveolar space *(A)* contains edema fluid. Uranyl acetate and lead citrate; ×4,080; case 16

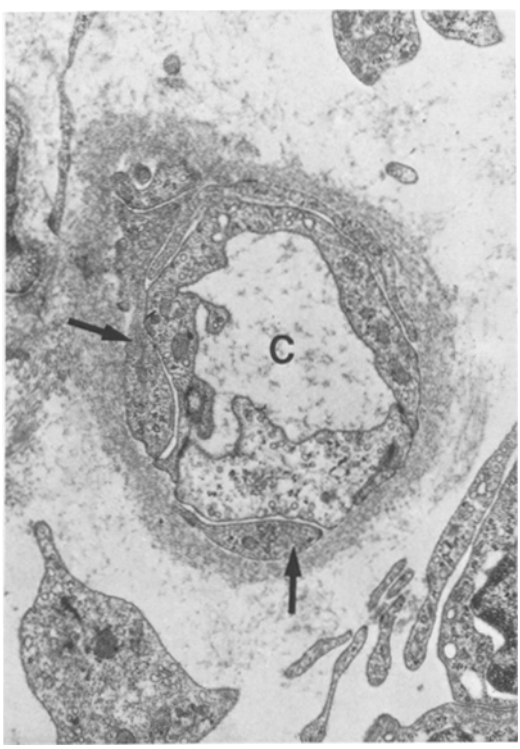

Fig. 9. The capillary *(C)* is decreased in size and is surrounded by a thick homogeneous basement membrane. Directly apposed to the concentrically plump endothelial cells are cytoplasmic extension of pericytes *(arrows)* which share cell to cell contacts with endothelial cells. One of the endothelial cells shows cytoplasmic electron lucency. Uranyl acetate and lead citrate; ×15,000; case 10

was comparable to the afore-mentioned epithelial change. In Fig. 4 condensed cytoplasmic organelles can be seen within the darkly stained cells. Occasionally dark osmiophilic cells with the characteristic location of pericytes were found beneath the endothelium.

Numerous cytoplasmic organelles were seen in the endothelium, including rough endoplasmic reticulum, abundant mitochondria, clusters of ribosomes, dense cytoplasmic granules, and microvillous cytoplasmic processes. Occasional typical Weibel-Palade bodies were evident. When the cytoplasm contained abundant organelles, a relative lack of pinocytotic vesicles was noted. In occasional capillaries in both mildly and severely diseased areas, the endothelium was noted to contain prominent bands of cytoplasmic filaments; in other sites these filaments tended to aggregate in clusters especially at the flattened tips of the nuclei.

The capillary basement membrane showed multiple changes. Often it appeared as a dense thickened homogenous structure (Fig. 9) or it could be quite tenuous and frequently discontinuous. Frequent pericytes could be observed enclosed in basement membrane material or directly encircling the endothelial cells (Figs. 9, 11). Frequently desmosomal attachments were seen between the pericytes and endothelium.

One of the most striking findings was the multilamination of the endothelial basement membrane (Figs. 10, 11). This multilamination was especially prominent in capillaries which were decreased in luminal size (Fig. 10) and in probable venular structures.

Interstitial Compartment of the Distal Airspace. Edema, cellular infiltrates and/or connective tissue deposition could be seen in the interstitium in fibrosing alveolitis. In Fig. 11, fibrin and edema are present in the interstitium. The fibrin can also be seen on the epithelial surface; the alveolar type I epithelium is absent. The accumulations of fibrin and edema were only seen in some of the Grade 1 speciemens, not in Grade 2 and 3 lesions. When the interstitium contained inflammatory cells, lymphocytes, plasma cells, eosinophils and monocytes were the predominant cell types. In many sites fibroblasts, smooth muscle cells (Fig. 12) and myofibroblasts (Fig. 13) were seen. The myofibroblasts contained lobulated nuclei with prominent peripheral chromatin. Within the cytoplasm generous quantities of rough endoplasmic reticulum, scattered mitochondria and a Golgi zone were present. In the peripheral cytoplasmic borders of the myofibroblasts, prominent bundles of fibrils comparable to those in smooth muscle, were present (Fig. 13). Occasionally these cells could be seen connecting with each other. Large increases in collagen and elastic fibers were present (Figs. 3, 7). Prominent and characteristic smooth muscle cells were present in many of the lung specimens (Fig. 12). The smooth muscle cells were invested with basement membrane material.

It is of interest to note that in none of the cases, including several patients with documented collagen vascular disease, were immune complexes seen ultrastructurally. This included specimens which were predominantly cellular and had positive immunofluorescent studies.

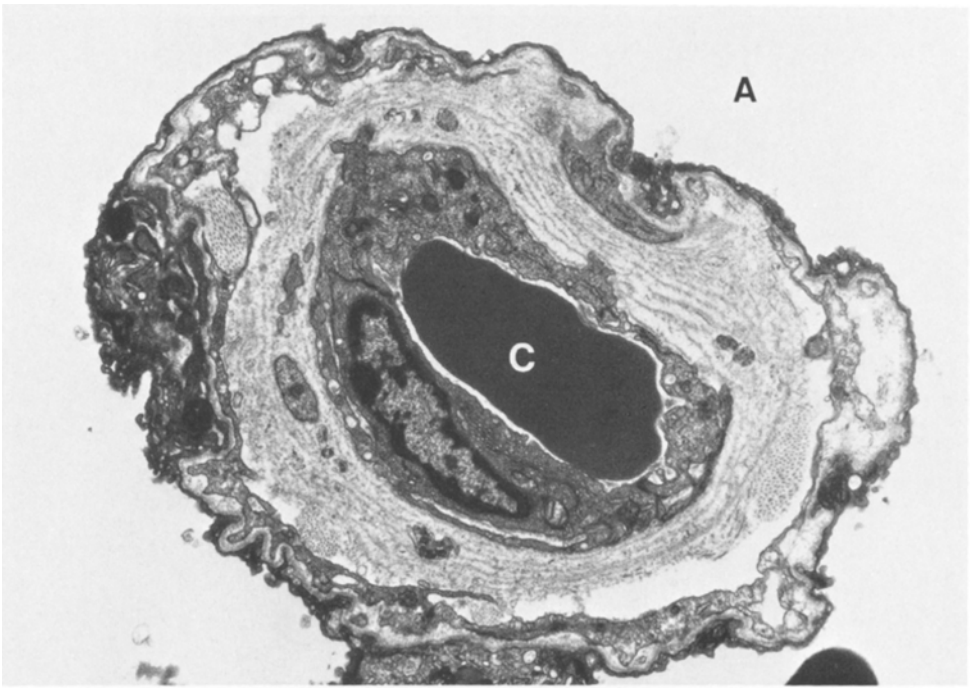

Fig. 10. The alveolus *(A)* is lined with epithelial type I and II cells. Within the interstitium, the capillaries are surrounded by multiple basement membrane laminations. The endothelial cells are plump and contain numerous cytoplasmic organelles. The small lumen of the capillary *(C)* contains a red blood cell. Uranyl acetate and lead citrate; ×8,100; case 15

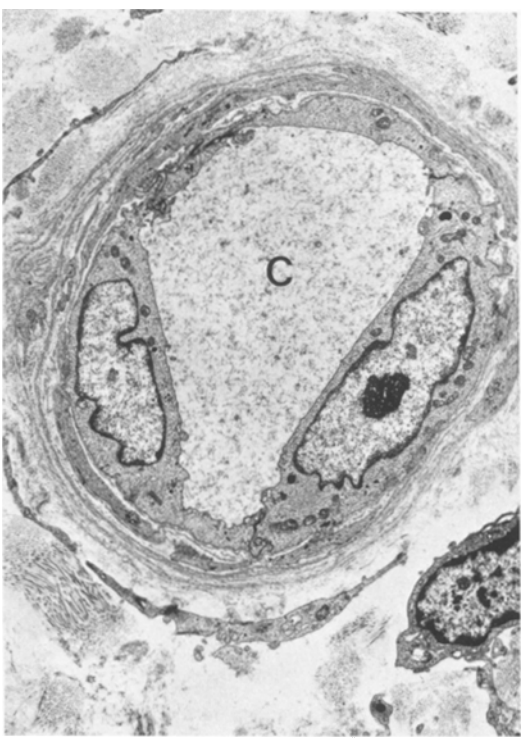

Fig. 11. This capillary *(C)* shows prominent endothelial cells with few pinocytotic vesicles but with increased mitochondria, filament aggregates, and rough endoplasmic reticulum. The capillary membrane is multilayered and contains enclosed cytoplasmic processes. Uranyl acetate and lead citrate; ×5,400; case 32

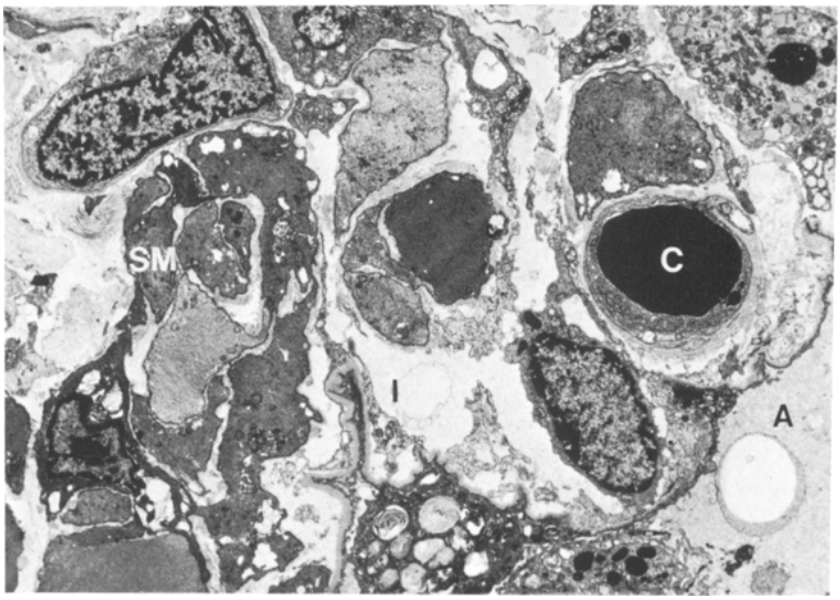

Fig. 12. The alveolar space *(A)* is lined by flattened type I epithelium; a type II cell is seen in the lower right. A small capillary *(C)* containing a red blood cell is present within the interstitium *(I)*. Additional interstitial structures include smooth muscle cells *(SM)*, fibroblasts, and other mononuclear cells. Uranyl acetate and lead citrate; ×3,200; case 15

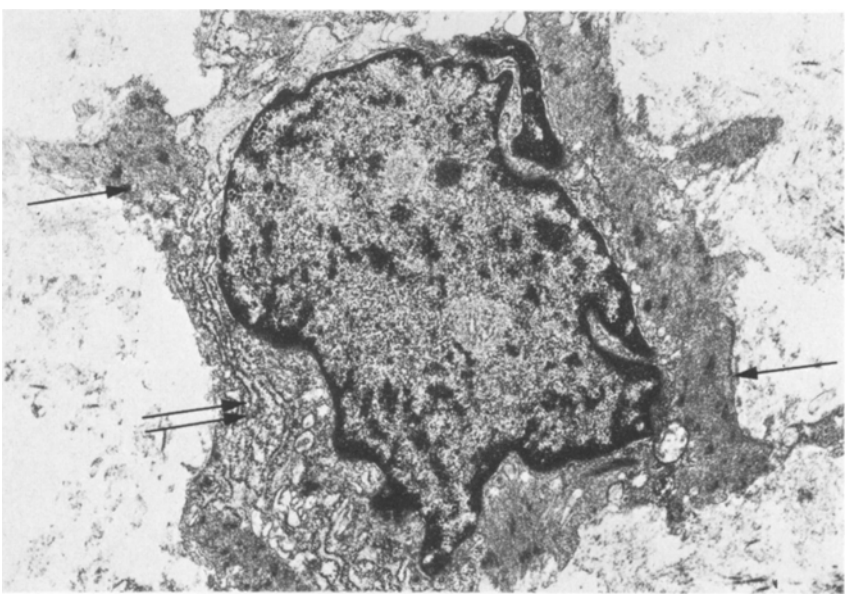

Fig. 13. A myofibroblast exhibiting extensive arrays of rough endoplasmic reticulin (*double arrows*) and bundles of filaments with dense bodies is present. Note that the filament bundles (*single arrows*) are located predominantly in the peripheral cytoplasmic areas. Uranyl acetate and lead citrate; ×12,800; case 37

Discussion

In this study some of the cases have a known or suspected etiologic agent (collagen vascular disorder); however, many of the cases fit an idiopathic fibrosing alveolitis category. Definitive pathologic patterns could not be delineated by etiologic categories, supporting the concept that this process really represents a non-specific fibrocellular reparative response of the lung to injury (Bowden and Wyatt 1970; Bachofen and Weibel 1974).

The six patients with collagen vascular disorders in the study are of interest in that one-half of them have a mixed fibrocellular or cellular designation. It was originally expected that immune complexes would be identified ultrastructurally in lung specimens designated at Grade 1 or cellular disease. However, it became evident during the early years of this study that dense deposits were not present, an experience shared by other investigators (Eisenberg et al. 1979). A multitude of reports attest to the finding of positive immunofluorescent results in patients with fibrosing alveolitis with or without an etiology of collagen vascular disorders (DeHoratius et al. 1972; Dreisen et al. 1978; Eisenberg et al. 1979; Nagaya et al. 1969; Nagaya et al. 1973; Pertschuk et al. 1977; Schwarz et al. 1978; Turner-Warwick 1966). In several electron microscopic reports, investigators have demonstrated electron dense deposits in the alveolar capillaries of patients with systemic lupus erythematosus (Churg et al. 1980; Eagen et al. 1978; Gould and Soriano 1975; Kuhn 1972). However, other than systemic lupus erythematosus, pulmonary electron dense deposits have not been described in the other collagen vascular disorders similar to the findings in this study as none of our patients had SLE.

The alveolar type II hyperplasia or cuboidalization of the lung epithelium in fibrosing alveolitis has long been appreciated as a histologic hallmark of the disease (Liebow 1975; Spencer 1967 and 1968). It is well established that the normal attenuated type I cell and the cuboidal type II cell with its characteristic lamellar inclusion bodies are derived from the undifferentiated epithelium which lines the fetal air sacs (Kikkawa et al. 1968). Multiple investigators have noted that the alveolar type II cell is the reparative cell and rapidly proliferates following injury (Evans et al. 1973; Kapanci et al. 1969; Ryan 1972; Stephens et al. 1973). Alveolar type II hyperplasia was a consistent finding in specimens of all three histologic grades in this study; however other epithelial changes were present, too. The presence of ciliated or bronchiolar cells at the alveolar level has been reported by several investigators. Nettesheim and Szakal (1972) studied mice chronically exposed to synthetic smog or CaCr04 dust and concluded that the alveolar bronchiolization represented a downgrowth of the bronchiolar cells onto the alveolar walls. Baskerville et al. (1974) concluded that the origin of the ciliate or bronchiolar cells was due to a direct alteration of intact alveolar epithelium in influenza infected mice and hamsters. More recently Adamson and Bowden (1977) have published a study on bleomycin treated mice and concluded that the bronchiolization at the alveolar level is due to abnormal epithelial repair. Our group (1981) has recently described a striking histologic finding of bronchiolization or adenomatosis in endotracheally induced bleomycin injury in baboons. An admixture of cell types including ciliated, mucus secreting and alveolar epithelial type II cells could be observed

in the sites of bronchiolization. Although bronchiolar epithelium was seen to be in continuity with some of the abnormal epithelial sites supporting the "downgrowth" concept, more frequently the cells arose directly from the airspace epithelium and shared cellular junctions with flattened type I epithelial cells. Thus, the histologic findings supported a direct alteration concept; i.e. an aberrant epithelial reparative response, and a downgrowth phenomenon. Both mechanisms strengthen the respiratory epithelium's common endodermal embryologic origin and the potential pleuripotential differentiation of this epithelium.

Brody and Craighead (1976) have described the presence of cells with fibroblast structural properties which line the air spaces in pulmonary fibrosis and lack a basement membrane. In this study, cells with prominent bundles of fibrils were occasionally seen lining the air spaces; however, though few in number, usually other epithelial cell organelles were present, i.e., lamellar bodies, secretory granules. The occasional lack of an intact epithelial basement membrane was noted in this study too.

The basement membrane of the pulmonary capillary is normally single and thin. Basement membrane thickening has been noted in multiple diseases, especially diabetes (Vracko 1970 and 1974; Vracko and Benditt 1970). As Vracko has pointed out, the basement membrane thickening seen in many organs light microscopically is frequently found electron microscopically to be multiple layers of basement membrane rather than a continuous homogeneous single layer (Vracko and Benditt 1970; Vracko 1974). However, based on his early work in lung (1974), he stated that the alveolar epithelium and septal capillaries of the lung usually did not form new layers of basement membrane but retained the old one for re-epithelialization, a statement this study would not support. Other investigators have reported both focal and extensive reduplications of basal lamina in various immunologic and non-immunologic injuries in different organ systems (Coalson et al. 1974; Dvorak et al. 1976 and 1980; McKinney and Panner 1972). There is unanimity in attributing this finding to prior episodic injuries to the endothelium indicating an accelerated rate of cell death and replacement (Coalson et al. 1974; Dvorak et al. 1976 and 1980; McKinney and Panner 1972). Vracko and Benditt (1970) noted that capillaries with thickened basement membranes had smaller lumens than capillaries with normal basement membranes, a finding seen in this study, too. Usually the lamination was found in specimens in which striking reparative processes were ongoing and was seen in material from all three histologic grades. One of our specimens (case 15) showed striking basement membrane lamination without the massive airspace remodeling usually seen in fibrosing alveolitis. The patient had no history of diabetes. The lesion is suggestive of a repeated blood-borne insult, since the overlying epithelium was usually normal.

The pulmonary capillary endothelium is of the complete, non-fenestrated type. Normally the cell body with its contained nucleus, mitochondria, scattered fragments of rough endoplasmic reticulum and small Golgi apparatus abuts to the thick or interstitial side of the alveolar wall. The thin or air portion of the endothelium contains very few pinocytotic vesicles. In this study, several ultrastructural features of the endothelial cells lend support to the suggestion that they represent regenerating endothelial cells. The cell contained increased amounts of granular endoplasmic reticulum, large mitochondria, multiple free

ribosomes and glycogen. The pinocytic vesicles were scarce in these endothelial cells. These findings are consistent with Schoefl's findings (1963) published in her treatise on growing capillaries and with Conen and Balis' observations (1969).

The constant finding of microfilaments near the junctional complexes of endothelium has been commented on by Kapanci and his coworkers (1979) and Weibel (1974). Kapanci et al. (1979) state that in normal endothelium microfilaments are scarce if not absent in other portions of the endothelial cell. However, Schoefl (1963) reported the presence of numerous fine fibrils in regenerating endothelial cells and ameboid shaped endothelial nuclei, findings supported by this ultrastructural study. Though the patterns of alternating dark and light endothelial cells has not been addressed in the literature on interstitial fibrosis, it has been noted in other diseases with a reparative component (Coalson et al. 1974; Dvorak et al. 1976 and 1980).

Weibel (1974) clearly defined the criteria for identifying pulmonary capillary pericytes and noted their similarity to systemic capillary pericytes. He also commented on the increased frequency of pericytes in the systemic circulation when compared to the pulmonary circulation. Human and dog lungs, representative of larger mammals, had more frequent capillary pericytes when compared to smaller mammals such as a rat. The ease of finding pericytes in specimens from all different histologic grades in this study of fibrosing alveolitis was striking, especially when capillaries had very small lumina and the endothelium showed obvious characteristics of regeneration. There was also evidence of pericytic necrosis in this study. The precise role of the pericyte, if any, in regenerating endothelium has not been described in the lung. In a study on development of placental vessels, Dempsey (1972) has beautifully demonstrated evidence which suggests that the pericytes serve as the principal progenitor for fetal blood vessels. This information further strengthens the thesis that the pericytic sheathed capillaries are regenerating vessels. It might also be speculated that a prominent pericytic sheath might be found in any capillary bed exposed to higher blood pressures. Certainly the relationship and role(s) of the myofibroblast, contractile interstitial cell, (Kapanci et al. 1974 and 1979), capillary pericyte (Weibel 1974) and intermediate cell (Meyrick and Reid 1979) need to be characterized in the lung.

The finding of myofibroblasts in this study was not surprising. The presence of myofibroblasts in the granulation tissue of open wounds is well described (Gabbiani et al. 1972; Ryan et al. 1974) and one might expect that in a healing, scarring lung this cell would be observed. The finding of actin containing cells in human pulmonary fibrosis has been the subject of a recent report (Adler et al. 1981). As has been recognized for years, smooth muscle cells may be greatly increased in many chronic pulmonary diseases (Liebow et al. 1953), including interstitial fibrosis (Heppleston 1956; Davies et al. 1966). However, the stimuli responsible for the proliferative response remain obscure.

It was interesting to note that no single finding such as basement membrane multilamination or alveolar cell hyperplasia was specific for any given histologic grade with the possible exception of the presence of the myofibroblasts. These cells were not found in any case designated as Grade 1 or cellular disease. Examination of the cases under each of the histologic graded categories reveal

that Grade 1 lesions were seen in 7 of the 11 patients who had had symptoms for less than 5 months, suggesting a more recent onset of the pathologic changes. Using a one year symptom period, the Grade 2 and 3 categories revealed nearly equal numbers of patients who had had symptoms for more than 1 year or more as compared to those who had had symptoms less than 1 year.

Bowden and Wyatt (1970) very capably illustrated and pointed out in their article on lung injury and repair that although the lung was injured by many different etiologic agents, its pattern of injury and its response to repair are few. The finding of diffuse alveolar damage in some of the specimens correlates very nicely with Bachofen and Weibel's study (1977) on septicemic associated respiratory insufficiency and the study of Porte et al. (1978) on acute interstitial pulmonary fibrosis of multiple etiologies. Many of the ultrastructural findings in this study document episodes of repeated cell injury and cellular regeneration, with associated basement membrane and mesenchymal cell proliferations.

In summary, this study presents the ultrastructural findings seen in human fibrosing alveolitis. The findings typify the different pulmonary cellular reactions to injury. Evidence for cellular regeneration and death in both epithelial and endothelial cell populations is illustrated. Capillary basement membrane multilamination, decrease in capillary lumen size, and prominent pericytic ensheathment of pulmonary capillaries are depicted. Within the interstitial compartment, proliferations of collagen and elastic fibers are found, but in addition, abundant myofibroblasts and smooth muscle cells are present. No evidence of immune complex deposition was found at the ultrastructural level in this study. These morphologic findings further support the notion that the lung responds to various injuries in a similar manner and undergoes a common reparative response regardless of etiology.

Acknowledgments. Special thanks go to two superb pulmonary chiefs, Clarence Guenter, MD and Robert M. Rogers, MD and all their excellent pulmonary fellows with whom I had the pleasure to know and work with at the University of Oklahoma Health Sciences Center. Appreciation for outstanding technical assistance goes to C. Kassick, G. Taylor, R. Hyde, C. Pollack, L. Manous, and Z. Blott, and for secretarial/editorial assistance to J. Noll, M. Langlinais, and L. Booth.

References

Adamson IYR, Bowden DH (1977) Origin of ciliated alveolar epithelial cells in bleomycin-induced lung injury. Am J Pathol 87:569–575

Adler KB, Craighead JE, Vallyathan NV, Evans JN (1981) Actin-containing cells in human pulmonary fibrosis. Am J Pathol 102:427–437

Bachofen M, Weibel WR (1974) Basic pattern of tissue repair in human lungs following unspecific injury. Chest 64:14S

Bachofen M, Weibel ER (1977) Alterations of the gas exchange apparatus in adult respiratory insufficiency associated with septicemia. Am Rev Respir Dis 116:589–615

Baskerville A, Thomas G, Wood M, Harris WJ (1974) Histology and ultrastructure of metaplasia of alveolar epithelium following infection of mice and hamsters with influenza virus. Br J Exp Pathol 55:130–137

Basset F, Soler P, Bernaudin JF, Turiaf J (1975) Contribution of electron microscopy to the study of interstitial pneumonias. Prog Resp Res 8:45–58

Bowden DH, Wyatt JP (1970) Lung injury and repair: A contemporary view. Pathol Annu 5:279–307

Brody AR, Craighead JE (1976) Interstitial associations of cells lining air spaces in human pulmonary fibrosis. Virchows Arch [Pathol Anat] 372:39–49

Cassan SM, Divertie MB, Brown AL (1974) Fine structural morphometry on biopsy specimens of human lung. Chest 65:275–278

Churg A, Franklin W, Chan KL, Kopp E, Carrington CB (1980) Pulmonary hemorrhage and immune-complex deposition in the lung: Complications in a patient with systemic lupus erythematosus. Arch Pathol Lab Med 104:388–391

Coalson JJ, Kastl DG, Whalen MH, Greenfield LG (1974) Allografted lungs in matched dogs with induced pulmonary hypertension. Am J Pathol 74:533–543

Collins JF, Orozco CR, McCullough B, Coalson JJ, Johanson WG (1982) Pulmonary fibrosis with small airway's disease: A model in non-human primates. Exp Lung Res (In press)

Conen PE, Balis JU (1969) Electron microscopy in study of lung development. In: Emery J (ed) The anatomy of the developing lung. William Heinemann Medical Books, Ltd. Lavenham Suffolk Great Britain, pp 18–48

Crystal RG, Fulmer JD, Roberts WC, Moss MD, Line BR, Reynolds HY (1976) Idiopathic pulmonary fibrosis. Clinical, histologic, radiographic, physiologic, scintigraphic, cytologic, and biochemical aspects. Ann Intern Med 85:769–788

Davies D, Macfarlane A, Darke CS, Dodge OG (1966) Muscular hyperplasia ("cirrhosis") of the lung and bronchial dilatations as features of chronic diffuse fibrosing alveolitis. Thorax 21:272–289

Davis GS, Brody AR, Craighead JE (1978) Analysis of airspace and interstitial mononuclear cell populations in human diffuse interstitial lung disease. Am Rev Respir Dis 118:7–16

DeHoratius RJ, Abruzzo JL, Williams RC Jr (1972) Immunofluorescent and immunologic studies of rheumatoid lung. Arch Intern Med 129:441–446

Dempsey EW (1972) The development of capillaries in the villi of early human placentas. Am J Anat 134:221–238

Dreisen RB, Schwarz MI, Theofilopoulos AN, Stanford RE (1978) Circulating immune complexes in the idiopathic interstitial pneumonia. N Engl J Med 298:353–357

Dvorak AM, Mihm MC Jr, Dvorak HF (1976) Morphology of delayed-type hypersensitivity reactions in man. II. Ultrastructural alterations affecting the microvasculature and the tissue mast cells. Lab Invest 34:179–191

Dvorak AM, Monahan RA, Osage JE, Dickersin GR (1980) Crohn's disease: Transmission electron microscopic studies. II. Immunologic inflammatory response. Alterations of mast cells, basophils, eosinophils, and the microvasculature. Hum Pathol 11:606–619

Eagen JW, Memoli VA, Roberts JL, Matthew GR, Schwartz MM, Lewis EJ (1978) Pulmonary hemorrhage in systemic lupus erythematosus. Medicine 57:545–560

Eisenberg H, Simmons DH, Barnett EV (1979) Diffuse pulmonary interstitial disease; an immunohistologic study. Chest 75:262–264

Evans MJ, Cabral LJ, Stephens RJ, Freeman G (1973) Renewal of alveolar epithelium in the rat following exposure to NO 2. Am J Pathol 70:175–198

Gabbiani G, Hirschel BJ, Ryan GB, Statkov PR, Majno G (1972) Granulation tissue as a contractile organ. A study of structure and function. J Exp Med 135:719–734

Gaensler EA, Carrington CB, Coutu RE (1972) Chronic interstitial pneumonias. Clin Notes Respir Dis 10:3–16

Gebbers JO, Seifert G, Riesner K (1977) Die fibrosierende alveolitis. Ein Beitrag zur Ultrastruktur und Pathogenese Interstitieller Lungenerkrankungen. Röntgen Bl 30:539–550

Gould DB, Soriano RZ (1975) Acute alveolar hemorrhage in lupus erythematosus. Ann Intern Med 83:836–837

Greenberg SD, O'Neal RM, Jenkins DE (1974) The pathologic findings in diffuse interstitial fibrosis of the lungs. South Med J 67:571–579

Heppleston AG (1956) The pathology of honeycomb lung. Thorax 11:77–93

Kapanci Y, Weibel ER, Kaplan HP, Robinson FR (1969) Pathogenesis and reversibility of the pulmonary lesions of oxygen toxicity in monkeys. II. Ultrastructural and morphometric studies. Lab Invest 20:101–118

Kapanci Y, Assimacopoulos A, Irle C, Zwahlen A, Gabbiani G (1974) "Contractile interstitial cells" in pulmonary alveolar septa: A possible regulator of ventilation/perfusion ratio? J Cell Biol 60:375–392

Kapanci Y, Costabella PM, Cerutti P, Assimacopoulos A (1979) Distribution and function of cytoskeletal protein in lung cells with particular reference to "contractile interstitial cells". Methods Achiev Exp Pathol 9:147–168

Kawanami O, Ferrans VJ, Roberts WC, Crystal RG, Fulmer JD (1978) Anchoring fibrils. A new connective tissue structure in fibrotic lung disease. Am J Pathol 92:389–402

Kawanami O, Ferrans VJ, Fulmer JD, Crystal RG (1979) Ultrastructure of pulmonary mast cells in patients with fibrotic lung disorders. Lab Invest 40:717–734

Kikkawa Y, Motoyama EK, Gluck L (1968) Study of the lungs of fetal and newborn rabbits. Am J Pathol 52:177–210

Kuhn C (1972) Systemic lupus erythematosus in a patient with ultrastructural lesions of the pulmonary capillaries previously reported in the Review as due to idiopathic pulmonary hemosiderosis. Am Rev Respir Dis 106:931–932

Liebow AA (1975) Definition and classification of interstitial pneumonias in human pathology. Prog Respir Res 8:1–33

Liebow AA, Loring WE, Felton WL (1953) The musculature of the lungs in chronic pulmonary disease. Am J Pathol 29:885–911

Livingstone JL, Lewis JG, Reid L, Jefferson KE (1964) Diffuse interstitial pulmonary fibrosis. A clinical, radiological, and pathological study based on 45 patients. QJ Med 129:71–103

McDowell EM, Trump BF (1976) Histologic fixatives suitable for diagnostic light and electron microscopy. Arch Pathol Lab Med 100:405–414

McKinney RV Jr, Panner BJ (1972) Regenerating capillary basement membrane in skeletal muscle wounds. Ultrastructural and histochemical study. Lab Invest 26:100–113

Meyrick B, Reid L (1979) Hypoxia and incorporation of H-thymidine by cells of the rat pulmonary arteries and alveolar walls. Am J Pathol 96:51–70

Nagaya H, Buckley CE, Sieker HO (1969) Positive antinuclear factor in patients with unexplained pulmonary fibrosis. Ann Intern Med 70:1135–1145

Nagaya H, Elmore M, Ford CD (1973) Idiopathic interstitial pulmonary fibrosis. An immune complex disease? Am Rev Respir Dis 107:826–830

Nettesheim P, Szakal AK (1972) Morphogenesis of alveolar bronchiolization. Lab Invest 26:210–219

Pertschuk LP, Morcia LF, Roscu Y, Lyons H, Marino CM, Rashford AA, Wollschlager CM (1977) Acute pulmonary complications in systemic lupus erythematosus. Immunofluorescence and light microscopic study. Am J Clin Pathol 68:553–557

Porte A, Stoeckel ME, Mantz JM, Tempe JD, Jaeger A, Batzenschlager A (1978) Acute interstitial pulmonary fibrosis. Comparative light and electron microscopic study of 19 cases. Pathogenic and therapeutic implications. Intensive Care Med 4:181–191

Ryan GB, Cliff WJ, Gabbiani G, Irle C, Montandon D, Statkov PR, Majno G (1974) Myofibroblasts in human granulation tissue. Hum Pathol 5:55–67

Ryan SF (1972) Experimental fibrosing alveolitis. Am Rev Respir Dis 105:776–791

Scadding JG (1974) Diffuse pulmonary alveolar fibrosis. Thorax 29:271–281

Schoefl GI (1963) Studies on inflammation. III. Growing capillaries: Their structure and permeability. Virchows Arch [Pathol Anat] 337:97–141

Schwarz MI, Dreisen RB, Pratt DS, Stanford RE (1978) Immunofluorescent patterns in the idiopathic interstitial pneumonias. J Clin Lab and Clin Med 91:929–938

Spencer H (1967) Interstitial pneumonia. Annu Rev Med 18:423–442

Spencer H (1968) Chapter 10: Chronic interstitial pneumonia. In: Liebow AA (ed) The lung. The Williams and Wilkins Co Baltimore, USA, pp 134–150

Spencer H (1975) Pathogenesis of interstitial fibrosis of the lung. Prog Resp Res 8:34–44

Stephens RJ, Sloan MF, Evans MJ, Freeman G (1973) Early response of lung to low levels of ozone. Am J Pathol 74:31–58

Turner-Warwick M (1966) Immuno-fluorescent studies in lung biopsies. Thorax 21:290

Vracko R (1970) Skeletal muscle capillaries in diabetics: A quantitative analysis. Circulation 41:271–283

Vracko R (1974) Basal lamina scaffold-anatomy and significance for maintenance of orderly tissue structure. Am J Pathol 77:314–338

Vracko R, Benditt EP (1970) Capillary basal lamina thickening: Its relationship to endothelial cell death and replacement. J Cell Biol 47:281–285

Weibel ER (1974) On pericytes, particularly their existence on lung capillaries. Microvasc Res 8:218–235

Winterbauer RH, Hammar SP, Hallman KO, Hays JE, Pardee NE, Morgan EH, Allen JD, Moores KD, Bush W, Walker JH (1978) Diffuse interstitial pneumonitis. Clinicopathologic correlations in 20 patients treated with prednisone/azathioprine. Am J Med 65:661–672

Accepted December 4, 1981

Virchows Arch [Cell Pathol] (1982) 395:201–206

Virchows Archiv A

Gastric Carcinomas with Argyrophil and Argentaffin Cells

C. Prokš and V. Feit

Department of Pathology (Chief: MUDr. C. Prokš, CSc.), QÚNZ-Hospital, 397 01 Písek, Czechoslovakia

Summary. In a series of 248 gastric carcinomas from surgical resections the occurence of argyrophil and argentaffin cells was studied. These cells were distinctly more frequent in diffuse than in tubular carcinomas. In all cases with both types of APUD-cells, argyrophil cells were more numerous than argentaffin cells. These tumors are considered to be a variant of current gastric carcinoma, with more pronounced APUD-differentiation of neoplastic cells. This variant stands apart from carcinoid tumors and also from those rare nasal adenocarcinomas with argentaffin cells.

Key words: Gastric carcinoma – Argyrophil cells – Argentaffin cells

Zusammenfassung. In einer Serie von 248 bioptisch untersuchten Magenkarzinomen wurde das Vorkommen von argyrophilen und argentaffinen Zellen studiert. Diese Zellen wurden bedeutend häufiger beim diffussen Karzinom nachgewiesen. Bei allen Beobachtungen, wo beide APUD-Zelltypen vorkamen, wurde eine wesentlich größere Anzahl argyrophiler als argentaffiner Zellen festgestellt. Die beschriebenen Geschwülste werden als Variante der üblichen Magenkarzinome angesehen und von karzinoiden Geschwülsten sowie dem nasalen Adenokarzinom mit argentaffinen Zellen abgegrenzt.

Introduction

The occasional occurence of argyrophil and argentaffin cells in gastric carcinomas was documented when even the nature of these cells and their presence in normal gastric mucosa were unsettled questions (Hamperl 1927). However, systematic studies are still few (Azzopardi and Pollock 1963; Kubo and Watanabe 1971) and the WHO classification of tumors (Sobin et al. 1979) does not provide separate heading for this variant of gastric carcinoma.

Material and Methods

We have reviewed all gastric carcinomas from surgical biopsies in the years from 1960 till 1979. Both authors independently reviewed paraffin sections using the Grimelius-Alcian Blue method

0340-1227/82/0395/0201/$01.20

Table 1.

Tumor type	WHO code number	Number of cases	Proportion Grimelius positive	Fontana and UV-light positive
Tubular	8211/3	153 (60%)	8 (5.3%)	4 (2.65%)
Diffuse	8430/3	63 (25%)	11 (17.4%)	11 (17.4%)
Solid	8220/3	21	1	0
Others	8010/3[a]	11	0	0
Total		248	20 (8.1%)	15 (6.03%)

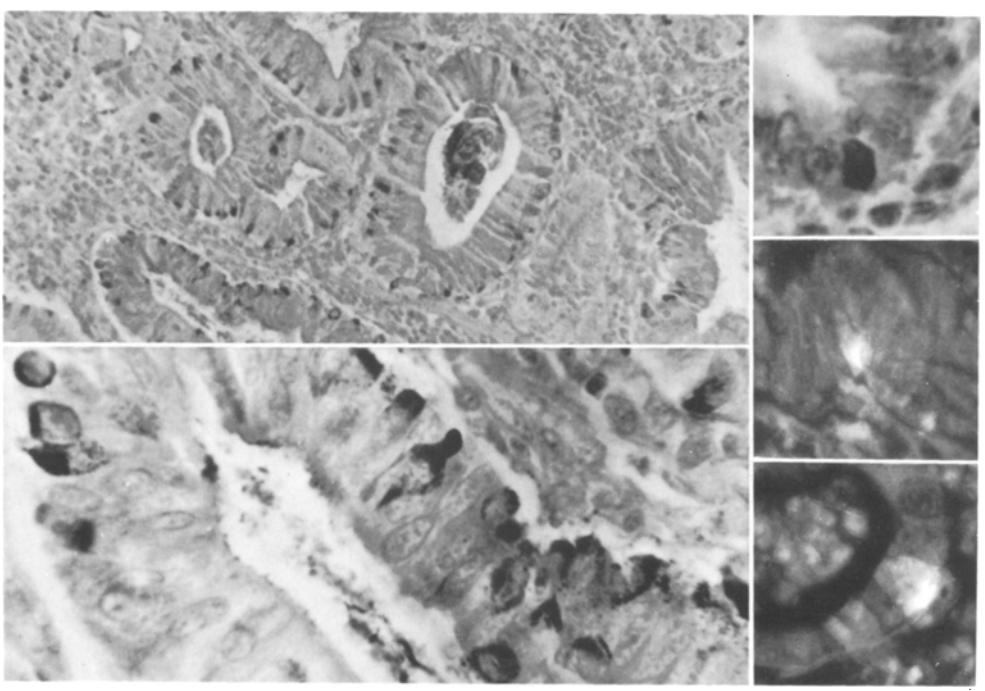

Fig. 1. *Left upper:* Tubular adenocarcinoma (Nr. 1667/64) with numerous argyrophil cells. Grimelius-Alcian Blue, ×100. *Left lower:* The same tumor and stain, ×400. *Right upper:* An argentaffin cell in the same tumor. Fontana, ×400. *Right middle and right lower:* Argentaffin cells in the same tumor. Unstained, UV-light, ×400

for staining. Three sections from every tissue block were examined. In most cases at least two blocks (marginal and central) were available, in 12 cases, however, there was only one marginal block. Tumors with easily visible argyrophil granules in the cytoplasm of some neoplastic cells were selected as positive. In these cases additional sections were stained for 24 h at room temperature with Fontana's ammonium silver (in a paraffin-coated Petri dish, the sections being downward, to avoid silver cast artifacts). Deparaffinized sections were mounted in glycerol and examined in UV-light. Further, PAS-reaction and Alcian Blue stains at pH 2.5 and pH 0.5 were examined. The results are listed in Table 3. In the Fontana method, the argentaffin cells either displayed a diffuse positivity in the cytoplasm, not seen in the nucleus or there were positively impregnated granules in the cytoplasm. Similarly, in UV-light there was either diffuse luminscence or luminescent

Table 2. Age and sex distributions of "non-argyrophil" cases

Age (years)	20–29	30–39	40–49	50–59	60–69	70–79	80–89
male	1	3	10	31	45	33	4
female	–	1	7	19	38	33	3
Total							228

Table 3. "Argyrophil cases". By ciphers 3–0 an approximate quantitative assessment is marked: 3=in most tumor cells, 2=in many cells, 1=in rare or very rare cells, 0=none found. Two ciphers express local differencies

Hist. Nr.	Hist. type	Age/years sex	Argyro-phil	Argent-affin	PAS	AB pH 2.5	AB pH 0.5
141/60	diff.	64/f	2	1	3	3	0
496/60	diff.	41/f	3–2	2–1	3	3	0
2440/61	tubul.	61/f	2	1	3	2	0
947/63	diff.	65/f	3–2	2–1	2	2	0
2235/63	diff.	62/f	2	1	3	3	0
802/64	solid.	68/f	1	0	2	2	0
1667/64	tubul.	62/f	3–2	1	2–1	2–1	0
290/66	diff.	42/m	2	1	3	3	0
715/66	diff.	52/f	2–1	1	1	1	0
755/66	tubul.	59/m	1	1	2	2–1	0
2692/66	tubul.	70/m	3–2	0	2	2	0
848/70	diff.	70/f	2–1	1	2	2	0
2243/70	tubul.	71/m	1	1	1	1	0
470/72	diff.	34/f	2–1	1	3	2	0
1602/72	tubul.	65/m	2–1	0	3	3	0
974/73	diff.	78/f	2–1	1	3–2	3–2	0
1648/73	tubul.	73/m	1	0	2	2	0
1412/76	diff.	62/f	3–2	2–1	3–2	2	0
1433/76	tubul.	72/m	2	0	3	3–2	0
2263/77	diff.	80/f	2–1	1	2	2	0

granules of the cytoplasm alone. Other methods used occasionally were the Aldehyd-fuchsin stain and Bodian and Gömöri impregnations. Normal argentaffin cells of the non-neoplastic gastric mucosa served as controls for all methods used.

Results

Table 1 shows the numbers and percentages of cases with argyrophil and argentaffin cells and general distribution of all cases in histological groups. All carcinomas in the tubular and diffuse groups were mucus-positive, although in some cases only very slightly. In the group of solid tumors three cases were mucus-negative. In the last group, 4 cases were mucus negative. In the group of tubular carcinomas there were 8 with numerous Grimelius-positive (argyrophil) cells (Fig. 1). From these, only in 4 cases were argentaffin cells (Fontana+, UV luminiscence+, Fig. 1, right side) seen. The ratio of argentaffin to argyrophil

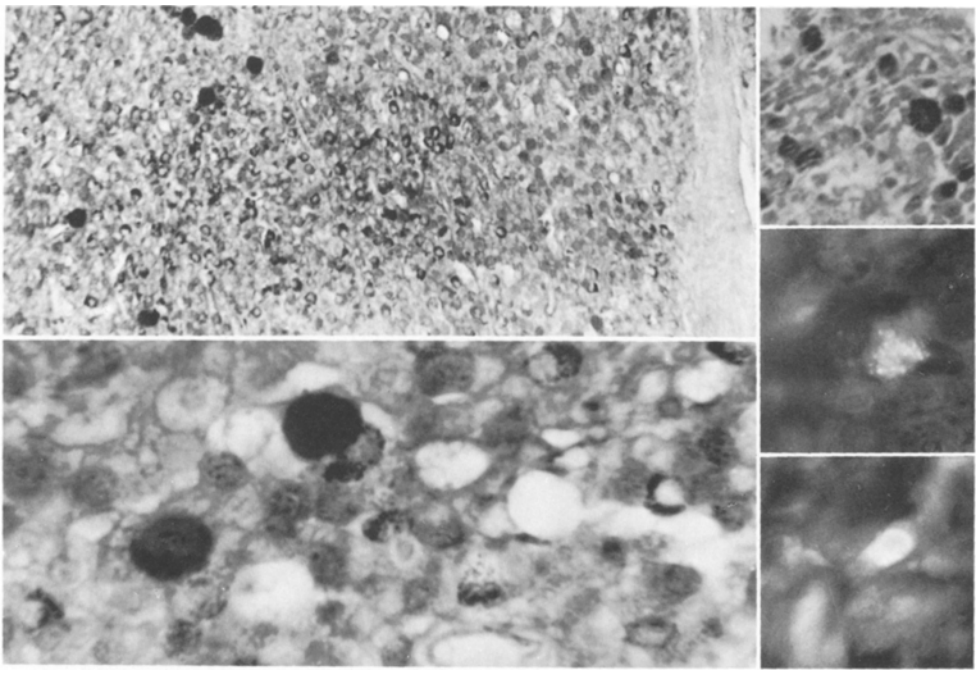

Fig. 2. *Left upper:* Diffuse carcinoma (Nr. 496/60) with numerous argyrophil cells. Grimelius-Alcian Blue, ×100. *Left lower:* The same tumor and stain, ×400. *Right upper:* Argentaffin cells in a lymph node metastasis of a diffuse carcinoma (Nr. 2235/63). Fontana, ×160. *Right middle:* Comparatively voluminous argentaffin cell with luminiscent granules in the plasma. From the same metastasis. Unstained, UV-light, ×400. *Right lower:* An argentaffin cell with a diffuse luminiscence of plasma in a metastasis of diffuse carcinoma. The same metastasis. Unstained, UV-light, ×400

cells was approximately 1:100 to 1:200. In the group of diffuse carcinomas the number of cases with both types of APUD-cells was distinctly greater. Still, argentaffin cells were fewer, their ratio to argyrophil cells being approximately 1:10 to 1:50. From 21 solid carcinomas, in only 1 case were there very few argyrophil cells and no argentaffin ones. General data for both "non-argyrophil" and "argyrophil" cases are listed separately in Tables 2 and 3. In 5 cases we had material available to study tumor tissue extending beyond the stomach. In the group of diffuse carcinomas there were 2 instances of metastatic spread to peri-gastric lymph nodes. In one of them both argyrophil and argentaffin cells were present in the lymph nodes (hist. Nr. 2235/63, Fig. 2, right upper and middle fields). The other case was negative. In another 2 cases from this group (hist. Nr. 470/72, 974/73) there were tumor infiltrates in the omentum. In one of them (Nr. 974/73) both argyrophil and argentaffin cells were found, the other was negative. In one case of tubular carcinoma (Nr. 1651/73) there were only argyrophil APUD-cells in the primary tumor while in a lymph node metastasis both argyrophil and argentaffin cells were present.

Discussion

The ratio of APUD-cell containing carcinomas in our series is in no substantial discord with other reported data. Azzopardi and Pollock 1927 used Bodian impregnation as a screening method. They clearly distinguished observations with argyrophil cells only (9 out of 13 cases) from observations with both argyrophil and argentaffin cells (4 out of 13) but with no expressed appraisal of the quantitative ratio between both types of APUD-cells. Kubo and Watanabe 1971 used the Fontana impregnation for screening and, consequently, were interested only in argentaffin cells. Their series shows lower incidence of argentaffin cell containing tumors, especially in the group of tubular carcinomas (Kubo and Watanabe 1971 0.9% – Prokš and Feit (this paper) 2.65%). This is probably due to different observation technique since we have searched intensively for argentaffin cells in doubtfull cases, even in consecutive sections.

The concept of APUD (Amine Prescursor Uptake and Decarboxylation) as a system of various disperse endocrine cells was created by Pearse in the early 1960's and later gradually amended by Pearse and others. From the beginning, it was conceptually connected with a postulate of common origin of these cells from neuroectoderm or from the neural crest. Later, three generic possibilities for APUD-cells were considered: 1) that all the cells could be derived from endodermal precursors in ducts and/or acini or 2) that all could be derived from a neuroectodermal precursor which had colonised the pancreatic anlage at an early stage of development (erlier than neural crest) or finally, 3) that some of the 5 APUD-cell types could be endodermal and some neuroectodermal in origin (Pearse 1980). Recently, however, the demonstration of a specifically neuronal enzyme (2-phospho-D-glycerate hydrolase) in some of the APUD-cell types strengthens the APUD-cell concept as a disperse system of neurocrine-programmed cells, not necessarily of common embryogenetic origin. Hence, the term Diffuse Neuroendocrine System (DNES) was suggested (Pearse 1980). This could be considered to be a third compartment of the Nervous System (I. Central, II. Autonomous, III. DNES) responsible for the control of function of the internal organs. Sidhu (1979) brought evidence that not only gastrointestinal but also bronchial APUD-cells might be of endodermal origin, with local differentiation. It seems to us that our findings clearly favor this concept to the alternative, namely that APUD-cells in carcinomas might be an accessory proliferating, non-tumor cellular clone. The occurence of APUD-cells in metastases is, in our view, hardly amenable to any other explanation than that of tumor differentiation in the direction of APUD. This might be expressed to varying extent in individual cases with variations from mere argyrophilia to full argentaffinity. The most primitive representation of such differentiation is probably the presence of electron microscopically visible secretory granules only in carcinomas, with no other demonstrable argyrophil or argentaffin cells (Soga and Hatano 1970). In this way, extreme instances of APUD differentiation in tubular gastric carcinomas may appear as "very rare cases" (Soga et al. 1971) while lesser degrees may attract no particular attention (Scully et al. 1980). The practical importance of the variants under discussion, for gastric and colonic

(Kubo and Watanabe 1971) carcinomas is probably slight. We do not think that they represent any separate diagnostic group. They apparently do not belong to the category of carcinoid tumors, but they do stand apart, in our view, from the very rare nasal adenocarcinoma with argentaffin cells (Schmid et al. 1979; Prokš 1982). These tumors consist of cylindric epithelia, "Panethoid" cells and argentaffin cells.

References

Azzopardi JG, Pollock DJ (1963) Argentaffin and argyrophil cells in gastric carcinoma. J Pathol Bacteriol 86:443–451

Hamperl H (1927) Über die „gelben (chromaffinen)" Zellen im gesunden und kranken Magen-darmschlauch. Virchows Arch 266:509–548

Kubo T, Watanabe H (1971) Neoplastic argentaffin cells in gastric and intestinal carcinomas. Cancer 27:447–454

Pearse AGE (1980) APUD – Concept, tumours, molecular markers and amyloid. Mikroskopie (Wien) 36:257–269

Prokš C (1982) (in Czech) Čs Patol (in press)

Schmid O, Auböck L, Albegger K (1979) Endocrine-amphicrine enteric carcinoma of the nasal mucosa. Virchows Arch [Pathol Anat] 383:329–343

Scully RE (1980) Case reports of the Massachussetts General Hospital. N Engl J Med 303:1049–1056

Sidhu GS (1979) The endodermal origin of digestive and respiratory tracts APUD cells. Am J Pathol 96:5–20

Sobin LH (1979) Abrégé de codification des tumeurs. Organisation Mondiale de la Santé, Geneve, l.c. p. 99

Soga J, Hatano T (1970) Argyrophil cell: Hyperplastic, pre-neoplastic and neoplastic proliferations. A preliminary observation. Acta Med Biol (Niigita) 18:1–6

Soga J (1971) Argentaffin cell adenocarcinoma of the stomach: an atypical carcinoid? Cancer 28:999–1003

Accepted December 4, 1981

Virchows Arch [Pathol Anat] (1982) 395:207–216

Virchows Archiv A

Unusual Pulmonary Vascular Lesions after Intravenous Injections of Microcrystalline Cellulose

A Complication of Pentazocine Tablet Abuse

Thomas B. Zeltner[1], Urs Nussbaumer[1], Oskar Rudin[1], and Arthur Zimmermann[2]

[1] Institute of Forensic Medicine (Prof. Eugen Läuppi) University of Berne, Bühlstrasse 20, CH-3012 Berne

[2] Institute of Pathology (Prof. Hans Cottier) of the University CH-3012 Berne, Switzerland

Summary. We present the morphological features of a case of fatal pulmonary granulomatosis from illicit intravenous injections of microcrystalline cellulose derived from pentazocine tablets. Extensive foreign body granulomas were found in the lumena and walls of pulmonary vessels and in the pulmonary interstitium. Previously unreported gaps containing foreign material were found in the walls of medium-sized muscular pulmonary arteries. This peculiar finding is discussed in the light of the possible mechanisms involved in the removal of embolized foreign material.

Key words: Cellulose – Drug abuse – Foreign body reaction – Pentazocine – Pulmonary artery

Introduction

Since 1950 at least 33 reports have documented a whole spectrum of pulmonary lesions due to the intravenous (iv.) injection of unfiltered aqueous suspensions of pharmaceutical preparations that are intended for oral use (Spain 1950; Siegel 1972; Tomashefski and Hirsch 1980). Embolized insoluble particulate material such as talc (magnesium trisilicate) cornstarch or microcrystalline cellulose, used as fillers and binders in tablets and capsules may cause pulmonary foreign body granulomatosis and angiothrombosis. After injection of abundant foreign material, vascular changes indicative of pulmonary hypertension may be seen. Talc containing preparations, known to cause these pulmonary lesions include methadone hydrochloride (Vevaina et al. 1974), propoxyphen hydrochloride (Butz 1969), methylphenidate (Hahn et al. 1969; Lewman 1972; Arnett et al. 1976) and tripelennamine hydrochloride (Wendt et al. 1964; Szwed 1970). Cornstarch is added to barbiturates (Johnston and Waisman 1971) and to pentazocine, a potent analgesic. The latter drug is manufactured in the form of tablets also containing microcrystalline cellulose (Houck et al. 1980; Tomashefski et al. 1981).

Offprints requests to: T. Zeltner at the above address

0340-1227/82/0395/0207/$01.80

In this communication we describe peculiar pulmonary lesions observed in an individual who was a known abuser of pentazocine tablet taken intravenously. To our knowledge, this is the first published case of a death related to injections of dissolved pentazocine tablets reported from a country other than the USA (Zeltner and Nussbaumer 1982).

Case Report

A 40-year-old white male nurse was found dead in the bathroom of his apartment in the vicinity of Berne, Switzerland. A syringe was discovered on the floor containing residues of pentazocine tablets. He had been suffering from back pain for several years and had been treated with pentazocine tablets for at least one year.

Six months before his death he started to complain of exertional dyspnoea and fatiguability. No medical examination was performed. About the same time pentazocine dependence was suspected, but the actual amount of drug taken is not known. An autopsy was performed.

Gross Findings

Multiple recent and old punctures were found on the left forearm and the antecubital fossa. The lungs were heavy and oedematous. The pulmonary cut surface presented a gritty texture due to the presence of numerous firm, greyish nodules measuring up to 1 mm in diameter. The heart weighed 390 g. The right atrium, ventricle and the tricuspid valve ring were dilated, but without ventricular hypertrophy. The left cardiac chambers and the endocardium were unremarkable. The liver showed signs of both acute and chronic congestion. There was no hepatitis.

The other organs showed no further important gross changes.

Histopathological Findings

In the lungs, the most impressive finding is the presence of numerous foreign body granulomas, filling up to 75% of every ten power microscopic field. About 40% of the granulomas are located in pulmonary vessels; 60% are found in the perivascular interstitium. The granulomas consist of macrophages and foreign body giant cells and often have a rim of small lymphocytes and a few plasma cells. Neutrophils are almost absent. The granulomas contain grey to green, birefringent, needle- or rod-shaped crystals that disclose the typical histochemical properties of microcrystalline cellulose:

Microcrystalline cellulose stains pale to dark violet with PAS stain and is diastase resistant. It is a deep black after staining with methenamine silver and is brilliantly orange with the Congo Red stain, showing a yellow to green birefringence in polarised light (Tomashefski et al. 1981).

No cornstarch nor other foreign material can be detected. Cellulose particles often occlude the lumena of smaller pulmonary arteries. The latter are frequently thrombosed, the thrombi being in various stages of organisation. The term "angiothrombosis" has been used for the description of these lesions (Tomashefski and Hirsch 1980). Vascular dilatation is a prominent feature of involved muscular arteries. In the dilated segments the elastic laminae are focally or totally absent and the muscular wall is often destroyed and replaced by fibrous tissue. An additional tortuosity of these vessels sometimes produces angioma-like structures. In older lesions the intravascular foreign material is laterally displaced by canalisation of the occluding thrombi. Foreign material and foreign body granulomas are found in medial layers of inflicted vessels and in perivascular locations (Fig. 1).

Perivascular foreign body granulomas are preferentially located around dilated tortous vessels with a destroyed wall (Fig. 2).

Medial hypertrophy is seen in muscular pulmonary arteries. Complete occlusion of major muscular pulmonary arteries is seldom found. In contrast, partial obstruction with foreign body granulomas or intimal hypercellularity is a frequent finding. The elastic laminae and the muscular wall beneath these lesions are often intact. However these partial occlusions often are found near the site of ramification of small arteries or arterioles that arise perpendicularly or somewhat oblique

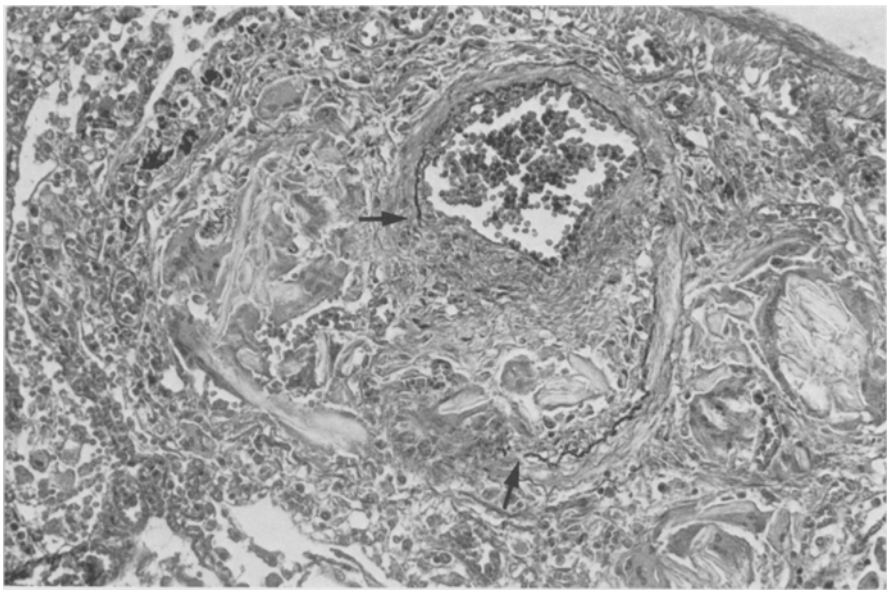

Fig. 1. Muscular pulmonary artery with excentric intimal fibrosis, focal destruction of the wall and continuous foreign body granulomas in all mural layers and in the perivascular interstitium with considerable amounts of microcrystalline cellulose particles. Note the interrupted elastic laminae (*arrows*) (Elastic-van Gieson stain, ×160)

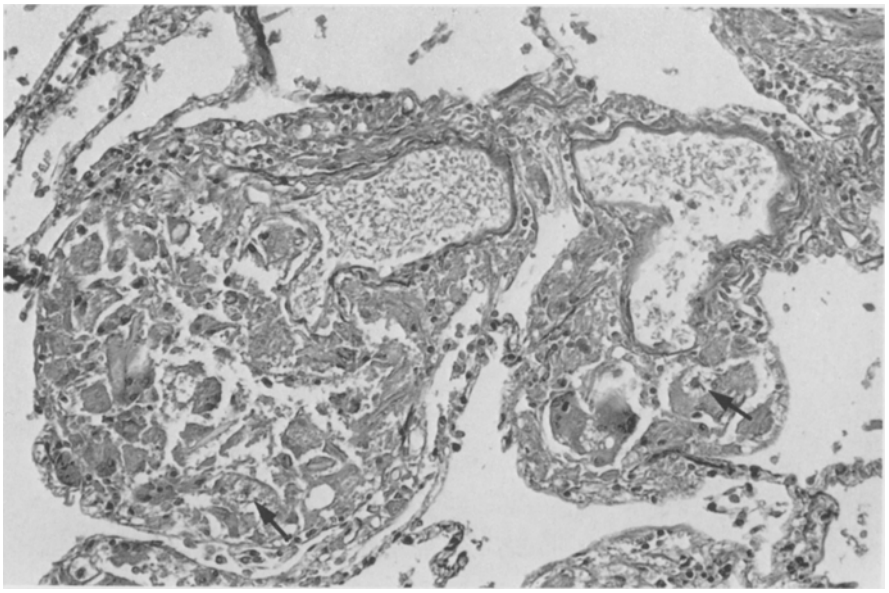

Fig. 2. Tortuous and dilated pulmonary artery with a collar of perivascular foreign body granulomas. Two giant cells contain asteroid bodies (*arrows*). (Elastic-van Gieson stain, ×160)

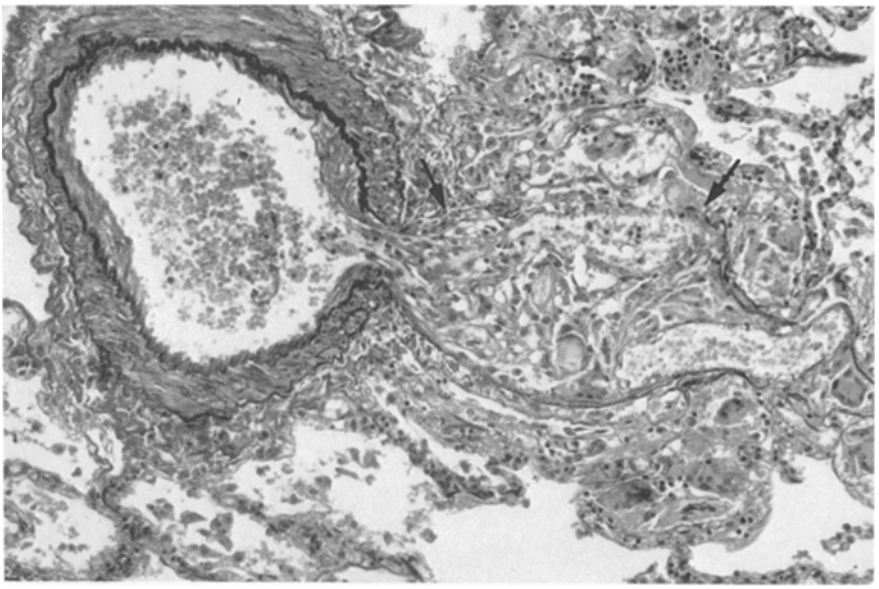

Fig. 3. Supernumerary arterial branch with saccular dilatation, intravascular foreign body granulomas and intimal hypercellularity. Note the focal destruction of the vascular wall (*arrows*). (Elastic-van Gieson stain, ×140)

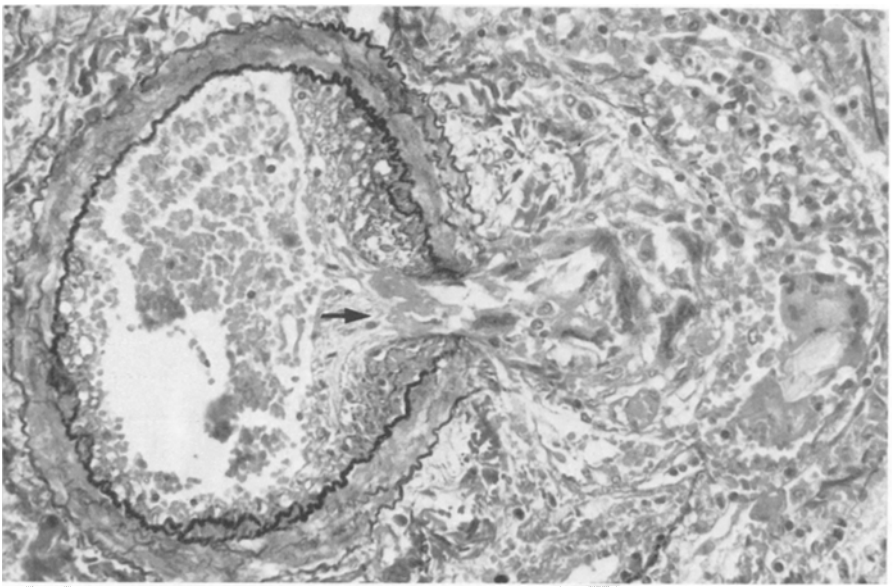

Fig. 4. Channel-like gap in the wall of a muscular pulmonary artery. Note circumjacent intimal thickening, the fibrin plug in the neck of the gap (*arrow*), the absence of a vascular wall around the advential granulomas and the marked muscular hypertrophy of the artery. (Elastic-van Gieson stain, ×200)

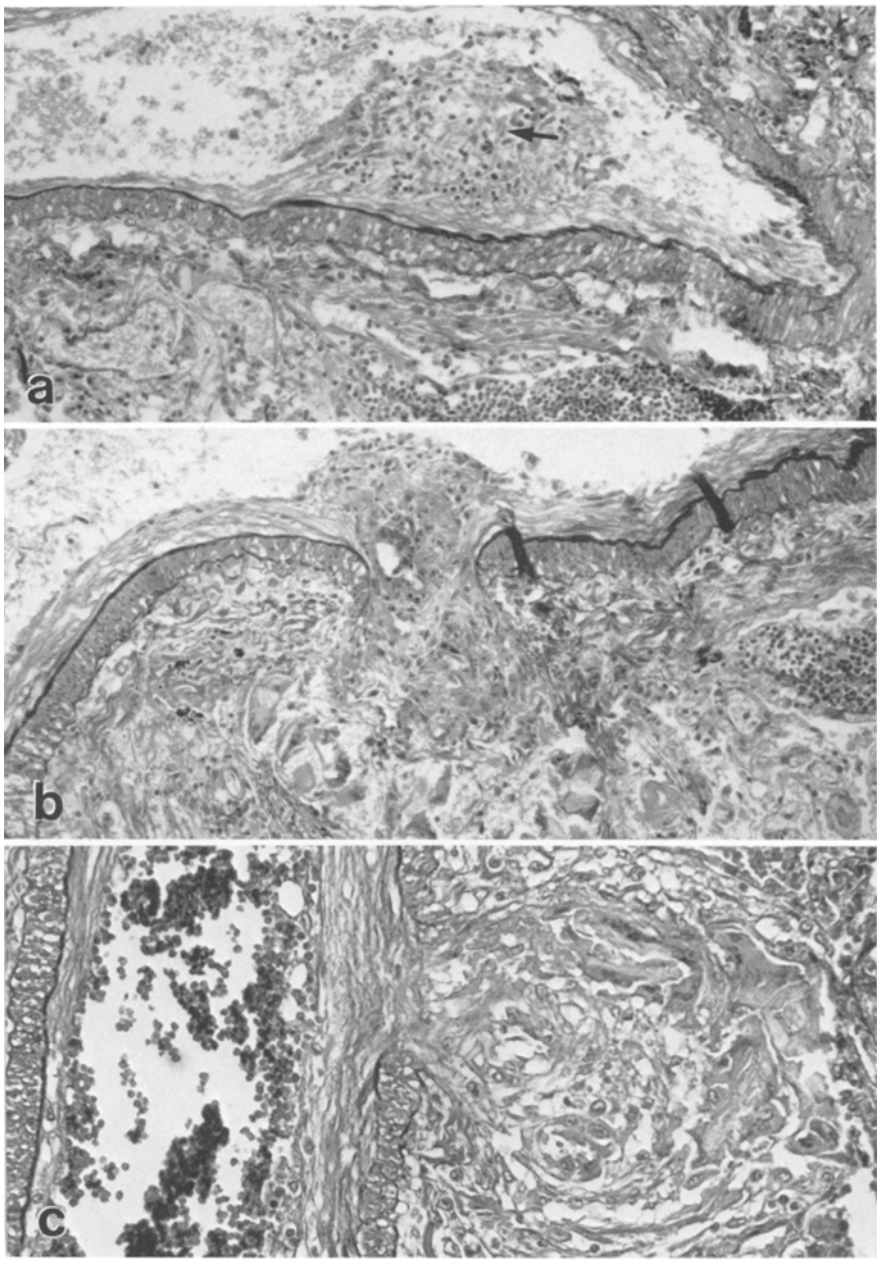

Fig. 5a–c. Histological changes in a medium-sized muscular pulmonary artery in response to microcrystalline cellulose deposition (Elastic-van Gieson stain). **a** Scanty foreign material (*arrow*) in an intimal cellular lesion. Not the presence of macrophages and few lymphocytes (×160). **b** Foreign material in a gap of the arterial wall and in the perivascular interstitium after total destruction of a supernumerary artery (×160). **c** Reconstitution of mural defect by fibrous tissue with the foreign body granulomas located in an adventitial site (×200)

from the larger muscular arteries. These arterial branches have been called supernumerary (Elliot and Reid 1965), abrupt (Robertson 1967) or monopodial (Cumming et al. 1969) arteries. In the involved vessels the proximal segments of the supernumerary arteries often are occluded by foreign body granulomas and show saccular dilatations and pronounced intimal hypercellularity. Their wall often is partially or totally destroyed (Fig. 3). In many instances the destruction of the extramural segment of the vascular wall is such that even in step sections no constituents or residues of the wall can be identified. The formerly intravascular foreign body granulomas now can be found in the perivascular interstitium. The only identifiable residue of the destroyed vessel is its intramural segment, forming a channel-like gap in the wall of the involved muscular artery. Fibrin, macrophages and foreign material fill these gaps (Fig. 4 and 5).

There is focal pulmonary oedema. Areas of recent pulmonary hemorrhages are found.

Very minute needle-shaped, birefringent crystals are detected in Kupffer cells of the liver and in splenic macrophages. No foreign material or foreign body granulomas are demonstrated in histological sections of the heart, brain or kidneys.

Toxicological Findings

Renal and hepatic tissue specimens, the gastric contents and samples of cardiac blood and bile were analysed for the presence of pentazocine after hydrolysis with hydrochloric acid and extraction in a mixture of chloroform and methanol (9:1) at pH 8.5, using a thin-layer chromatographic method; silica gel plates, a developing solution of ethylacetate-methanol-amoniumhydroxide (85:10:5) and spraying with Dragendorff reagent were used.

Pentazocine was found in the following concentrations:

	liver	kidneys	gastric contents	blood	bile
pentazocine (μg/g)	5	3	0	1	40

No other drugs or drug metabolites were detected.

The blood value obtained corresponds to the only other known data found in the literature (Tomashefski et al. 1981).

Discussion

The abuse of pentazocine, a potent analgesic, was recognised shortly after its introduction in the mid 1960'ies. At the beginning abuse was largely confined to the medical community and to patients iatrogenically addicted (Eckmann et al. 1975; Kubicki et al. 1977; King 1978). Several recent reports confirm a rising popularity of illicit iv. injection of aqueous suspensions of pentazocine tablets among "street" addicts in the USA (Showalter 1978, 1980; Poklis et al. 1978, 1980; Butch et al. 1979; Bailey 1979; Houck et al. 1980; Lahmeyer and Steingold 1980; Tomashefski et al. 1981). The drug is generally injected in combination with tripelennamine, an antihistamine.

The individual presented in this communication is the first known abuser of pentazocine tablets taken via an iv. route reported from a country other than the USA. He developed the pulmonary lesions found after the iv. injection of insoluble particulate material that is contained in pharmaceutical preparations intended for an oral use: myriads of intra- and extravascular foreign body granulomas, angiothrombosis and vascular destructions of the lung.

Puro et al. (1966) have shown that talc injected iv. into rabbits was present in the lumena of pulmonary vessels two weeks after injection, but after five

weeks could also be found in the perivascular interstitium, accompanied by foreign body granulomas.

Byers (1975) has suggested a progressive sequence of changes in small pulmonary arteries of narcotic abusers in response to foreign body emboli: initially deposition of foreign material is accompanied by acute inflammatory reaction in the innermost parts of the vessel wall with local thrombosis, further attaching it to the vascular wall. With the organisation of the thrombus a dislocation of the foreign material into medial layers of the injured vessel follows. Finally the vascular wall is reconstituted, thus excluding the foreign material from the blood stream. Other authors have confirmed this sequence of events (Tomashefski and Hirsch 1980). The morphological changes we have found in our case of iv. pentazocine tablet abuse are compatible with this concept.

We have not found a reasonable comment as to the pathogenesis of this transport of foreign material through the vascular wall. Several possible mechanisms may be proposed.

The foreign material may destroy the vascular wall locally by its own physical or chemical properties. Inflammatory response and thrombosis would be secondary events. Alternatively the foreign material could influence locally accumulated macrophages and neutrophils, leading to their activation or destruction. Liberated lysosomal enzymes might affect the vascular wall. Such an effect has been described with silica particles (Allison 1970). Furthermore, foreign material may liberate or activate endogenous factors and thus induce or sustain an inflammatory response with granulomatous reaction. In this context it has been proposed that talc could induce an inflammatory process by activating Hageman factor and initiating the formation of kinins (Ratnoff 1966; Kellermeyer and Warren 1970). Solubable components of foreign material might also act as an antigen or hapten and induce an immune reaction, leading to vascular damage and influencing granuloma formation. Finally, the hydrostatic pressure gradient in pulmonary arteries might contribute, forcing foreign particles through a damaged and thus weakend vascular wall. The presumptive pathogenetic role of these mechanisms has to be further elucidated.

However, the peculiar focal changes of pulmonary arteries found in our case and illustrated in Figs. 3–5 offer another explanation of as to how foreign material could be cleared from pulmonary arteries. We identified circumscribed gaps or channels in the wall of medium-sized muscular pulmonary arteries. These gaps represent the intramural segment of so-called supernumerary arteries or arterioles. The extramural segments of these arterial branches could sometimes still be identified and then disclosed saccular dilatations and pronounced intimal hypercellularity (Fig. 3). These dilated vascular segments showed a histological picture very similar to that of so-called plexiform lesions, as they can be found in severe cases of pulmonary hypertension (Wagenvoort and Wagenvoort 1977). It seems very likely that they are true plexiform lesions, containing foreign body granulomas. They could be compared to analogous plexiform lesions found in pulmonary Schistosomiasis that contain schistosome eggs with a granulomatous reaction (Liebow 1960).

For the most part the wall of the proximal extramural segment of the involved supernumerary arteries was totally destroyed so that the formerly intra-

vascular foreign body granulomas lay in the perivascular interstitium. The channel-like gap in the arterial wall formed thus a direct communication between the vascular lumen and the interstitium (Fig. 4). We think that foreign material is preferentially trapped in these dilated segments of supernumerary arteries and gets into the perivascular interstitium after destruction of the vascular wall (Fig. 5). The question of whether the pressure gradient between the lumen of a patent muscular artery and the perivascular space contributes to force foreign material through the gaps could not be resolved, but might be a possible contributory factor. We cannot tell, whether these lesions represent a pecularity of this case characterised by embolization of abundant microcrystalline cellulose and pulmonary hypertension, or whether they illustrate a general mechanism of pulmonary vascular foreign material disposal.

References

Allison AC (1970) On the role of macrophages in some pathological processes. In: Van Furth R (ed) Mononuclear phagocytes. Blackwell Scientific Publications, Oxford and Edinburgh, pp 422–444

Arnett EN, Battle WE, Russo JV, Roberts WC (1976) Intravenous injections of talc-containing drugs intended for oral use – a cause of pulmonary granulomatosis and pulmonary hypertension. Am J Med 60:711–718

Bailey WJ (1979) Nonmedical use of pentazocine. JAMA 242:2392

Butch AJ, Yokel RA, Sigell LT, Hanenson IB, Nelson ED (1979) Abuse and pulmonary complications of injecting pentazocine and tripelennamine tablets. Clin Toxicol 14:301–306

Butz WC (1969) Pulmonary arteriole foreign body granulomata associated with angiomatoids resulting from intravenous injection of oral medications, e.g. propoxyphene hydrochloride (Darvon). J Forensic Sci 14:317–326

Byers JM, Soin JS, Fisher RS, Hutchins GM (1975) Acute pulmonary alveolitis in narcotics abuse. Arch Pathol 99:273–277

Cumming G, Henderson R, Horsfield K, Singhal SS (1969) The functional morphology of the pulmonary circulation. In: Fishman AP and Hecht HH (eds) The pulmonary circulation and interstitial space. University of Chicago Press, Chicago and London, pp 327–340

Eckmann F, Kubicki SK, Mazaheri P (1975) Zur Frage der Pentazocin-Abhängigkeit. In: Neuhaus GA, Kubicki SK (eds) Pentazocin- ein neuer Weg. Georg Thieme Verlag, Stuttgart, pp 61–64

Elliott FM, Reid L (1965) Some new facts about the pulmonary artery and its branching pattern. Clin Radiol 16:193–198

Hahn HH, Schweid AI, Beaty HN (1969) Complications of injecting disolved methylphenidate tablets. Arch Intern Med 123:656–659

Houck RJ, Bailey GL, Daroca PJ, Brazda F, Johnson FB, Klein RC (1980) Pentazocine abuse – Report of a case with pulmonary arterial cellulose granulomas and pulmonary hypertension. Chest 77:227–230

Johnston WH, Waisman J (1971) Pulmonary cornstarch granulomas in a drug user. Arch Pathol 92:196–202

Kellermeyer RW, Warren KS (1970) The role of chemical mediators in the inflammatory response induced by foreign bodies: Comparison with the schistosome egg granuloma. J Exp Med 131:21–39

King A (1978) Abuse of pentazocine. Br Med J 2:21

Kubicki S, Lenhard-Mazaheri P, Beyer KH (1977) Pentazocin – ein Suchtproblem? Münch Med Wochenschr 119:1069–1074

Lahmeyer HW, Steingold RG (1980) Medical and psychiatric complications of pentazocine and tripelennamine abuse. J Clin Psychiatry 41:275–278

Lewman LV (1972) Fatal pulmonary hypertension from intravenous injection of methylphenidate (Ritalin) tablets. Hum Pathol 3:67–70

Liebow AA (1960) Cardiopulmonary disease. In: Gould SE (ed) Pathology of the heart. 2nd edn. Charles C Thomas, Springfield Ill., pp 940–982

Poklis A (1978) 'T's and blues'. JAMA 240:108

Poklis A, Whyatt PL (1980) Current trends in the abuse of pentazocine and tripelannamine: The metropolitan St. Louis experience. J Forensic Sci 25:72–78

Puro HE, Wolf PL, Skirgaudas J, Vazquez J (1966) Experimental production of human "Blue velvet" and "Red devil" lesions. JAMA 197:1100–1102

Robertson B (1967) The normal intrapulmonary arterial pattern in infancy and early childhood, a micro-angiographic and histological study. Acta Pathol Microbiol Scand 71:481–501

Showalter CV (1980) T's and blues – abuse of pentazocine and tripelennamine. JAMA 244:1224–1225

Showalter CV, Moore L (1978) Abuse of pentazocine and tripelennamine. JAMA 239:1610–1612

Siegel H (1972) Human pulmonary pathology associated with narcotic and other addictive drugs. Hum Pathol 3:55–66

Spain DM (1950) Patterns of pulmonary fibrosis as related to pulmonary function. Ann Int Med 33:1150–1163

Szwed JJ (1970) Pulmonary angiothrombosis caused by "Blue velvet" addiction. Ann Int Med 73:771–774

Tomashefski JF, Hirsch CS (1980) The pulmonary vascular lesions of intravenous drug abuse. Hum Pathol 11:133–145

Tomashefski JF, Hirsch CS, Jolly PN (1981) Microcrystalline cellulose pulmonary embolism and granulomatosis. Arch Pathol Lab Med 105:89–93

Vevaina JR, Civantos F, Viamonte M, Avery WG (1974) Emphysema associated with talcum granulomatosis in a drug addict. South Med J 67:113–116

Wagenvoort CA, Wagenvoort N (1977) Pathology of pulmonary hypertension. John Wiley & Sons, New York, pp 75–80

Wendt VE, Puro HE, Shapiro J, Mathews W, Wolf PL (1964) Angiothrombotic pulmonary hypertension in addicts. JAMA 188:755–757

Zeltner TB, Nussbaumer U (1982) Intravenöse Injektion von aufgelösten Pentazocin-Tabletten (Fortalgesic) – ein neuer Aspekt des Drogenmissbrauchs auch bei uns? Schweiz Med Wochenschr (in press)

Accepted January 21, 1982

Virchows Arch [Pathol Anat] (1982) 395:217–225

Virchows Archiv A

Case Reports

Disseminated Mycobacterial Histiocytosis Due to M. Fortuitum Associated with Helper T-Lymphocyte Immune Deficiency

Burkhard D. Bültmann[1], Hans D. Flad[2], Edwin Kaiserling[3], Hans K. Müller-Hermelink[3], Gernot Kratzsch[4], Jürgen Galle[1], Walter Schachenmayr[1], Hermann Heimpel[5], H. Joachim Wigger[6], and Otto Haferkamp[1]

[1] Abteilung für Pathologie (Leiter: Prof. Dr. O. Haferkamp) der Universität Ulm, Oberer Eselsberg, M23, D-7900 Ulm, Federal Republic of Germany
[2] Forschungsinstitut Borstel, Department of Immunologie und Zellbiologie (Leiter: Prof. Dr. H.D. Flad), D-2061 Borstel, Federal Republic of Germany
[3] Institut für Pathologie (Direktor: Prof. Dr. K. Lennert) der Universität Kiel, Hospitalstraße 42, D-2300 Kiel, Federal Republic of Germany
[4] Abteilung Innere Medizin I (Leiter: Prof. Dr. F.W. Pfeiffer) der Universität Ulm, D-7900 Ulm, Federal Republic of Germany
[5] Abteilung Innere Medizin III (Leiter: Prof. Dr. H. Heimpel) der Universität Ulm D-7900 Ulm, Federal Republic of Germany
[6] Department of Pathology, College of Physicians and Surgeons of Columbia University, New York, USA

Summary. Mycobacterial histiocytosis is a rare disease usually associated with haematological or immunological disorders. We report a fatal case caused by M. fortuitum infection showing the typical disseminated histiocytosis. Immunological investigations revealed impaired cellular immunity demonstrated by negative skin tests with different "recall-antigens", and in vitro an isolated defect of helper T-lymphocytes in the peripheral blood which in combination with hypergammaglobulinemia suggests a "lymphocyte mal distribution syndrome".

Key words: Mycobacterium fortuitum – Atypical mycobacteria – mycobacterial histiocytosis – Immune deficiency – Helper-T-lymphocyte defect

Introduction

Concomitant with a declining incidence of infections with Mycobacterium tuberculosis among populations of a high socioeconomic standard, there has been a rise in recognition of infections caused by atypical mycobacteria (Editorial 1978; Davidson 1979). The pathological potential of these acid-fast bacilli

Offprints requests to: B. Bültmann at the above address

0340-1227/82/0395/0217/$01.80

is reflected in local infections of cornea, lung, subcutaneous tissue, lymph nodes, joints, tendons and various other tissue (Editorial 1978; Hoffmann et al. 1978; Owens 1978; Wolinsky 1979).

Disseminated infections, however, are rare and are usually limited to immunologically compromised hosts (Cashmann et al. 1970; McCracken and Reynold 1970; Feld et al. 1976; Dibella et al. 1977; Ortbals and Marr 1978; Kaiserling et al. 1980; Weinstein et al. 1981). We present here the clinical, immunological and morphological findings of a disseminated M. fortuitum infection in a young man.

Case Report

A 21 years old soldier, who had been well prior to October 1977, initially presented with a history of ill-defined abdominal discomfort in the left upper quadrant followed by progressive weight loss. In April 1978, he developed a generalized lymphadenopathy, accompanied by fever, malaise, and diarrhoea. He was admitted to a military hospital where a bone marrow aspirate and a cervical lymph node biopsy were performed and found to contain many foam cells filled with acidfast bacteria. Cultures of lymph node, urine, faeces, and pleural effusions grew M. fortuitum. The subsequent treatment with isoniazid, cycloserine, rifampicine, and ethambutol did not result in any clinical improvement. Four months later, in October 1978, the patient was found to have a rapidly enlarging inflammatory abdominal pseudotumor with abscess cavities from which the same mycobacterium was isolated. Testing of antibiotic sensitivities led to therapy with capriomycine, protionamide and cycloserine. A presumed immune deficiency and granulocyte dysfunction were treated with leucocyte transfusions and transfer factor. These changes in therapy resulted in a transient improvement.

When the patient was transfered to the Department of Medicine of the University Hospital, Ulm, on December 4, 1978, he appeared cachectic having lost 20 kg body weight, and he had a generalized lymphadenopathy, hepatosplenomegaly and tender, palpable masses in the abdominal cavity and the abdominal wall. Small bilateral effusions were seen on chest films but the lung parenchyma was unremarkable. Contrast studies of the gut disclosed an extrinsic compression of both stomach and duodenum and a coarse mucosal pattern of small and large bowel. A lymphangiogramm showed enlarged para-aortic nodes with a coarse storage pattern. There was a moderate anaemia (Hgb 10,1 g/dl; Hct 31%), a hypalbuminaemia of 3,5 g/dl and a marked hypergammaglobulinaemia of 28.8 g/dl. The white cell count was 8,500 mm^3 with 73% neutrophils, 1% band forms, 20% lymphocytes, and 6% monocytes. The moderately hypercellular bone marrow contained normal haematopoietic elements and many foamy macrophages with masses of mycobacteria, some haemosiderin pigment and occasionally showed erythrophagocytosis.

Karyotyping of bone marrow cells failed to detect any abnormality except for a "clonal instability" (Prof. Dr. Fliedner, Department of Clinical Physiology, University of Ulm). This change was not observed in peripheral blood lymphocytes. Granulocyte function tests for chemotactic reactivity, phagocytosis, increase in oxidative metabolism during particle uptake and intracellular killing of Staph. aureus were all within normal range (for methods see: Bültmann et al. 1980).

Immunological Findings

Quantitative determinations of immunoglobulins indicated a marked increase of IgG (5,104 mg/dl), IgA (707 mg/dl), and IgM (655 mg/dl) in patient's serum. Skin reactions for testing delayed hypersensitivity were negative with Candida albicans, trichophytin, tuberculin, and streptococcal antigens. The proliferative responses of the patient's blood lymphocytes (total lymphocyte count: 1,700/mm^3) to phytohaemagglutinin, concanavalin A, pokeweed mitogen and to a pool of allogeneic, irradiated, frozen-thawed cells in mixed lymphocyte reaction were regular. Lymphocyte subpopulations in the peripheral blood were quantitated using routine techniques: the percentage of lymphocytes reacting with 5-2 aminoethyl-isothiuronium-bromidxHBr (AET)-treated sheep erythrocytes was 80% and thus in normal range (Kaplan and Clark 1974), T-lymphocytes expressing receptors with high

Table 1. Pokeweed mitogen-driven B-lymphocyte differentiation in patient and healthy human control (500 cells were counted. Numbers represent means ± SEM of 3 determinations)

Cell combination	‰ plasma cells in culture	
	Expected	Observed
Patient – MNC[a] (2×10^6)		0 ± 0
Patient – T[b]		0 ± 0
Control – MNC (2×10^6)		10 ± 1
Control – T		0 ± 0
Control "non T" + control – T (1×10^6) (1×10^6)		27 ± 2
Control "non T"		1 ± 1
Patient – MNC + control – T	0	6 ± 1
Control – MNC + patient – T	5	8 ± 2
Control "non T" + patient – T (1×10^6) (1×10^6)	27	0 ± 0

[a] Mononuclear cells (per culture); [b] T-lymphocytes

avidity for sheep erythrocytes were found to be 30% (normal range: 25–35%) (West et al. 1976). Lymphocytes with receptors for human C3 were found to be 29%, those with receptors for mouse C3 (predominantly C3d) were 21% (Ross et al. 1973). The percentage of lymphocytes bearing surface immunoglobulins was 3% (normal range 8–18%).

To investigate differentiation of B-cells into plasma cells in vitro, various cell combinations of mononuclear cells of the patient and a control person were stimulated in vitro by pokeweed mitogen. After 7 days in culture, cytocentrifuge smears were performed and the number of cells with intracellular immunoglobulins (= plasma cells) was determined by means of immunofluorescence; 500 cells were scored in each preparation. As shown in Table 1, the mononuclear cells (MNC) of the patient did not differentiate into plasma cells. When the MNC of the patient were cocultured with T-lymphocytes (isolated by rosette formation with AET-treated sheep erythrocytes) of the control person, some plasma cell differentiation was obtained. The patient's T-lymphocytes did not suppress the plasma cell differentiation of the normal donor, but they also did not cooperate with the non-T-cells of the normal donor. These data suggested that the patient's T-lymphocytes were incapable of providing help for autologous and allogeneic non-T-cells in the pokeweed mitogen driven B-cell differentiation system (helper T-lymphocyte defect).

The patient's status during this last hospitalization did not improve and he expired about 15 months after onset of his disease in sudden right heart failure from thrombosis of both main trunks of the pulmonary artery.

Autopsy Findings

The principle postmortem findings were related to the lymphatic tissues. Grossly, diffuse enlargement of cervical, mediastinal, para-gastric, portal-hilar, para-pancreatic, iliac, and inguinal lymphnodes as well as the tonsils and thymus was apparent. The moist cut surface of the lymph nodes exhibited a characteristic green-yellow-brown colour. In the enlarged spleen (1,250 g) and in mesenteric as well as retroperitoneal lymph nodes multiple, usually small foci of necrosis

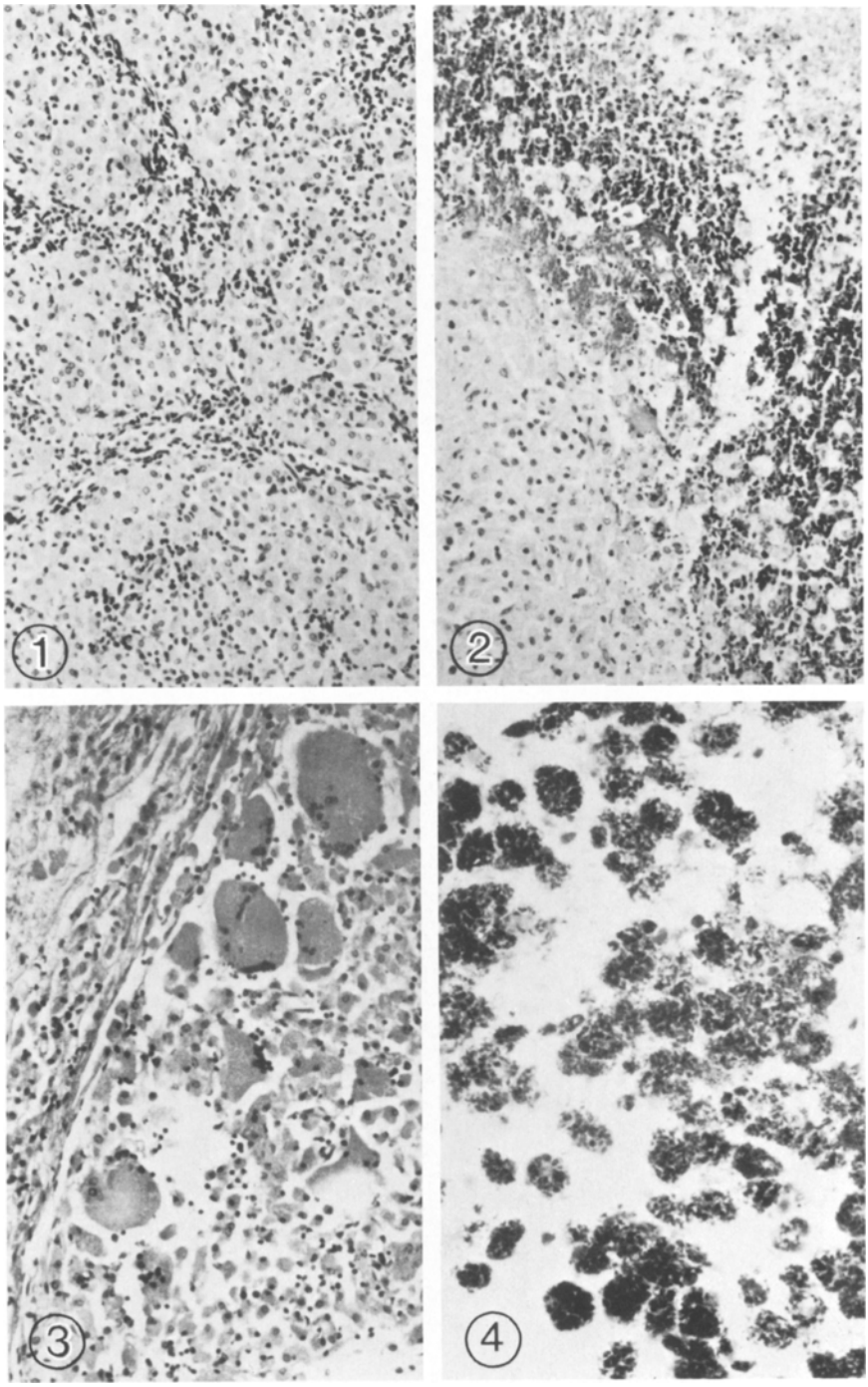

Fig. 1. Replacement of lymphatic tissue in cervical lymph node by diffuse infiltration with histiocytes (HE, ×47

Fig. 2. Circumscribed aereas of necrosis in mesenterial lymph node surrounded by a cuff of histiocytes (HE, ×47)

Fig. 3. Cortical aerea of mesenterial lymph node infiltrated by uni- and multinucleated histiocytes separated by bandlike proliferation of fibroblasts (HE, ×75)

Fig. 4. Histiocytes containing numerous acid-fast bacteria (Ziehl-Neelsen-stain, ×450)

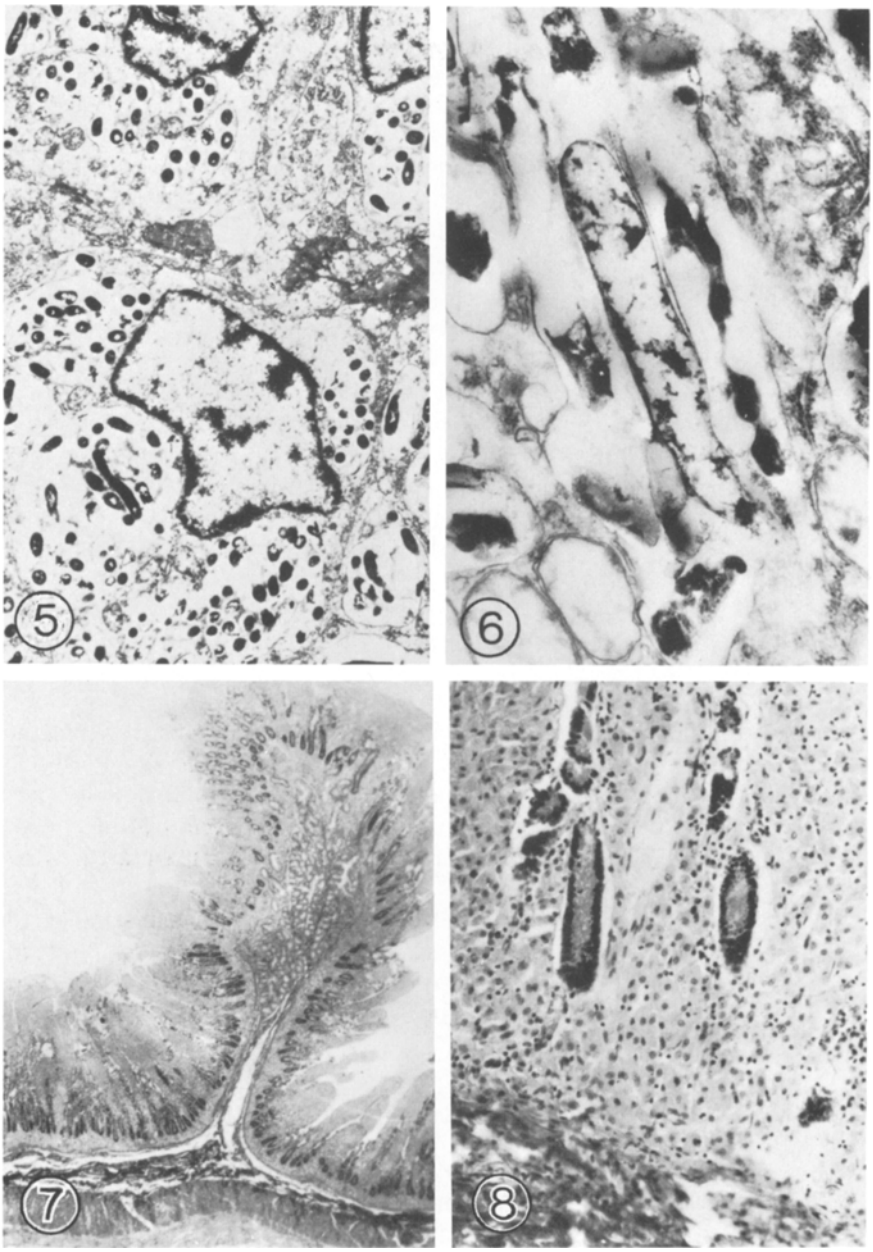

Fig. 5. Electronmicrograph of lymph node histiocytes containing myriads of well preserved mycobacteria in large phagolysosomes (Biopsy material, formalin fixation, ×6,600)

Fig. 6. Higher magnification. In the middle a rod-like microorganism with intact cell-wall and dissolved cytoplasm (Electron micrograph, ×33,700 autopsy material)

Fig. 7. Enlarged jejunal villus due to diffuse infiltration of mucosa by histiocytes (HE, ×25)

Fig. 8. Diffuse infiltration of rectal mucosa by acid-fast bacteria-containing histiocytes largely replacing lymphocytes and plasma cells (HE, ×75)

were visible in part encroaching on adjacent fat tissue with formation of multiple necrotic areas.

On microscopic examination there was a mainly diffuse, less granulomatous histiocytosis. It largely replaced the lymphatic tissue in lymph nodes (Fig. 1), tonsils, thymus and in bone marrow. Rare rudimentary Hassall's corpuscles were found in the thymus and the lobular outline of the organ was normal. A typical lesion, e.g. in mesenteric lymph node, was composed of a cuff of histiocytes and few lymphocytes and plasma cells around a small area of necrosis in which numerous nuclear fragments were present (see Fig. 2). Few epithelioid cells were observed, and multinucleated giant cells were infrequent and scattered throughout the lesion especially in marginal parts (Fig. 3). Few resembled Langhans giant cells in size and nuclear position, but most of them contained 5–50 small nuclei aggregated in central or marginal positions. The abundant cytoplasm of mono – or multinucleated histiocytes appeared finely granular in HE-sections. Ziehl-Neelsen-stains detected innumerable acid fast bacilli (Fig. 4). Electron microscopic studies of biopsy-lymph node material demonstrated the microorganisms in multiple small phagocytic vacuoles in the cytoplasm of mono- or multinucleated histiocytes (Fig. 5). The rod-shaped bacilli exhibited signs of degeneration (Fig. 6). Microbiological analysis of different organs revealed again exclusively M. fortuitum.

The liver was uniformly enlarged (2,300 g) but otherwise unremarkable. Histologically, multiple small, noncaseating histiocytic granulomata were scattered throughout the parenchyma. These histiocytes and some Kupffer cells contained acid-fast bacilli on Ziehl-Neelsen stains. The coarse mucosal pattern in both small and large bowel was due to a massive proliferation of histiocytes containing atypical mycobacteria in mucosa and submucosa sparing the other parts of bowel wall (Figs. 7 and 8).

In both lungs only few alveolar macrophages containing acid-fast bacilli were detected but neither granulomata nor caseating necrosis were observed. In other organs including cardiovascular, urogenital, and central nervous system no M. fortuitum-induced pathological lesions were detected.

Discussion

Atypical mycobacteria are organisms of low pathogenicity and rarely produce a disseminated infection but when they do, the outcome is frequently fatal. Usually the organisms have developed in patients with primary or secondary defects in host resistance (Kilbridge et al. 1967; Cashman et al. 1979; McCracken and Reynolds 1970; Feld et al. 1976). The criteria for the diagnosis of infection with these microorganisms consist of their repeated isolation in considerable numbers from the same source over a period of days or weeks and the association with the appropriate clinical picture as well as the typical histological findings (Davidson 1979). Among adults, the most suspicious constellation for these infections consists in immunosuppressive therapy or haematologic disease. Hairy cell leukaemia in particular appears to convey an unusual predisposition for infections with atypical mycobacteria (Weinstein et al. 1981). Occasionally, the infection may even precede the development of a neoplastic process as described

with cases of acute granulocytic leukemia and Hodgkin's disease. This phenomenon led to the suggestion that in the absence of an overt underlying disease, the infection may alert the clinician to the possibility of a "preneoplastic state" (Dibella et al. 1977). No evidence of an underlying disorder was found at the autopsy of our patient and the absence of any previous infections rules out most primary immune deficiencies.

The initial response to a mycobacterial infection is granulocytic; it is followed by the development of the classic granuloma frequently with caseation necrosis (Barksdale et al. 1977). Atypical mycobacteria, however, may produce lesions which are more acutely purulent and non-specific (Race 1960). Although in vitro granulocyte function had been normal in our patient as in that of McCracken et al. (1970), granulocytic infiltrates were not encountered. Giant cells are not always present, necrosis may be non-caseous and well-defined tubercles may be absent in patients with disseminated infection (Race 1960). This difference in response is largely due to the lymphopenic immune deficiency present in most of these patients. This deficiency may be primary as with thymic dysplasia and can lead to a naturally acquired infection in infancy (Cashmann et al. 1970) or to an induced infection as with BCG-immunization (Kaiserling et al. 1972). The deficiency may also be secondary, i.e. due to a malignancy or immunosuppressant chemotherapy. The preferential involvement in our patient of the lymphatic and haemopoietic system coincides with the pattern seen in patients with a lymphopenic immune deficiency. Other authors have speculated that a lack of activated lymphocytes also leads to a failure in the activation of macrophages (Kaiserling et al. 1980).

The thymus at autopsy contained rudimentary Hassall's corpuscles and had a normal lobular configuration. A complete thymic dysplasia is therefore not present, although a partial dysplasia cannot be entirely ruled out since the organ was almost completely replaced by histiocytes. Peripheral tissue lymphopenia was severe because of the same diffuse infiltrate depleting much of the lymphocytes of the spleen and virtually the entire Peyer's plaques and many of the lymphnodes. Plasma cells made up a large proportion of the remaining cells and accounted for the marked hypergammaglobulinemia of all three classes of immunoglobulins.

The finding of a defect of helper T-lymphocytes associated with hypergammaglobulinaemia is most unusual, but can be explained by a depletion of T-helper cells in the peripheral blood and a relative accumulation of these cells in the lymphoid organs. This condition has been recently termed "lymphocyte maldistribution syndrome" and has been found in patients with chronic infections (de Sousa 1981). Unfortunately, the surface phenotypes of peripheral and organ-distributed T-lymphocytes could not be determined.

There are a number of features in this case which remain obscure:

(i) With regard to the association of a helper T-cell defect and hypergammaglobulinaemia one may speculate that the selective T-cell defect is due to a disturbance in the circulation of lymphocytes trapped at the site of inflammation. T-cells that home into lymph nodes via the blood stream have been shown to penetrate the thick endothelium of post-capillary venules and from there enter the deep and midzone of the lymph node cortex (Gowand and

Knight 1964). Some such venules with hyperplastic endothelium were recognized and contained lymphocytes in their walls. Most nodes, however, failed to display this feature. The diffuse and massive infiltration of the lymphoid organs with histiocytes may have resulted in a mechanical block of the recirculation of lymphocytes.

(ii) In the presence of peripheral blood lymphocytes in the lower physiological range there is also the marked tissue lymphopenia and the replacement of the thymus with histiocytes. The end effect was a partial immune deficiency with regard to negative skin tests and helper T-cells but it is obscure with which type of defect the patient started out.

(iii) Although only a subtle T-helper defect could be demonstrated functionally the histological picture is typical of mycobacterial histiocytosis. The massive and diffuse histiocytic infiltration of the thymus, lymph nodes and intestinal mucosa and submucosa simulated a neoplastic process and is reminiscent of histiocytosis X which has now been recognized as a disorder also associated with immune deficiency (Osband et al. 1978). Thus, Lennert's characterization of the pattern of mycobacterial infection after BCG immunization in immune deficiency as mycobacterial histiocytosis may also be applied to this case (Lennert 1979).

References

Barksdale L, Kim KS (1977) Mycobacterium. Bacteriol Rev 41:217–372

Bültmann B, Geitner R, Kratzsch G, Haferkamp O (1980) Interaction of circulating immune complexes with granulocyte function in patients with rheumatoid arthritis. Klin Wochenschr 58:727–732

Cashman TM, Navin JJ, Chandor SB (1970) Thymic alymphoplasia previously reported as dysgammaglobulinemia, type I. J Pediatr 76:722–725

Davidson PT (1979) The other mycobacteria. Chest 79:110–111

Dibella NJ, Buchanan BD, Koontz CH (1977) Disseminated atypical tuberculosis antedating the clinical onset of neoplasia. Cancer 40:1276–1279

Editorial (1978) Atypical mycobacteria pose new nosocomial problems. Hosp Pract 10:38–45

Feld R, Bodey GP, Gröschel D (1976) Mycobacteriosis in patients with malignant disease. Arch Intern Med 136:57–70

Gowans JL, Knight EJ (1964) The route of recirculation of lymphocytes in the rat. Proc Royal Soc Med Biol 159:257–282

Hoffmann GS, Myers RL, Stark FR, Thoen CC (1978) Septic arthritis associated with mycobacterium avium: A case report and literature review. J Rheumatol 5:199–205

Kaiserling E, Lennert K, Nitsch K, Drescher J (1972) Ultrastruktur and Pathogenese der BCG-Histiocytose. Virchows Arch 355:333–353 [Pathol Anat]

Kaiserling E, Müller-Hermelink HK, Lennert K (1980) Zur Morphologie und Pathogenese der mycobakteriellen Histiocytose. Verhdl Dtsch Ges Pathol 64:392–396

Kaplan ME, Clark C (1974) An improved rosetting assay for detection of human T-lymphocytes. J Immunol Methods 5:131–135

Kilbridge TM, Gonella JS, Bolan JT (1967) Pancytopenia and death. Disseminated mycobacterial infections. Arch Intern Med 120:38–46

Lennert K (1979) Pseudotumoral proliferations. VII th Europ Congr Pathol Valencia, Spain 17–21 September

McCracken GH, Reynolds RC (1970) Primary lymphopenic immunologic deficiency. Disseminated M. kansassii infection. Am J Dis Child 120:143–147

Ortbals DV, Marr JJ (1978) A comparative study of tuberculous and other mycobacterial infections and their association with malignancy. Am Rev Respir Dis 117:39–45

Osband M, Lipton J, Vawter G (1978) Treatment of histiocytosis X with calf thymus extract. Am Soc Hematol Dec 1978 (abstract)
Owens DV (1978) Atypical mycobacteria. Int J Dermatol 17:180–185
Race CJ (1960) Pathological characteristica of atypical mycobacterial infections. In: Chapman JS (ed) Anonymous mycobacteria in human disease. C Thomas, Springfield, Ill, pp 37–44
Ross GD, Polley MJ, Rabellino EM, Grey HM (1973) Two different complement receptors on human lymphocytes. J Exp Med 138:798–811
de Sousa M (1981) personal communication
Weinstein RA, Golomb HM, Grumet G, Gelman E, Schechter GP (1981) Hairy cell leukemia: association with disseminated atypical mycobacterial infection. Cancer 48:380–383
West WH, Sienknecht CW, Townes AS, Herberman RB (1976) Performance of rosette assay between lymphocytes and sheep erythrocytes at elevated temperatures to study patients with cancer and other diseases. Clin Immunol Immunopathol 5:60–67
Wolinsky E (1979) Nontuberculous mycobacteria and associated diseases. Am Rev Respir Dis 119:108–159

Accepted February 3, 1982

Virchows Arch [Pathol Anat] (1982) 395:227–236

Virchows Archiv A

Cytoplasmic Inclusions in Lymphocytes of Chronic Lymphocytic Leukaemia

A Report of 10 Cases

Elisabeth Ralfkiær[1], Klaus Hou-Jensen[1], Christian Geisler[2], Torben Plesner[3], Allan Henschel[1], and Mogens Mørk Hansen[2]

[1] Departments of Pathology, [2] Medicine and [3] Clinical Chemistry
The Finsen Institute, Copenhagen, Denmark

Summary. Peripheral blood from 90 CLL patients was examined by light- and electron-microscopy for the occurrence of crystalline inclusions in lymphocytes. Inclusions were demonstrated in 10 patients (11%). In these patients the inclusions were present in 5–45% of peripheral blood lymphocytes.

In the light microscope the inclusions appeared as rectangular, unstained structures in May-Grünewald Giemsa and PAS stains. In the electron microscope the inclusions appeared as intracytoplasmic, completely partially membrane-bound bodies, which were often associated with dilated profiles of rough endoplasmic reticulum. The ultrastructure of the inclusions was granular.

In immunofluorescence staining the inclusions were found to contain immunoglobulin of the same type and class as the surface membrane-bound immunoglobulin of the neoplastic lymphocytes, most frequently IgM-lambda. The lymphocytes of one case with kappa light chains at the cell surface membrane contained inclusions of the same ultrastructural morphology as those of the other cases with lambda light chains.

The presence of inclusions was not associated with any specific clinical or prognostic features. The inclusions persisted during antileukaemic therapy. Their formation may be related to a dysfunction in the synthesis of surface membrane-bound immunoglobulins.

Key words: Intracytoplasmic crystalline inclusions – Immunoglobulin inclusions – Chronic lymphocytic leukaemia

The presence of intracytoplasmic crystalline inclusions in the lymphocytes of some patients with chronic lymphocytic leukaemia (CLL) has been known for several decades. Detailed morphological descriptions of the inclusions were presented in the early studies of Bernard et al. (1959) and de Man and Meiners

Offprint requests to: Elisabeth Ralfkiær, Dept. of Pathology, The Finsen Institute, DK-2100 Copenhagen, Denmark.

0340-1227/82/0395/0227/$02.00

(1962). Within recent years the inclusions have attracted renewed attention because of their demonstrated content of immunoglobulin (Cawley et al. 1976, Clark et al. 1973, Feremans et al. 1978, McCann et al. 1978, Roberts et al. 1979).

The largest series of CLL patients with crystalline inclusions gathered to date has consisted of four patients (Cawley et al. 1976, Clark et al. 1973). The incidence and possible clinical significance of the inclusions are thus largely uncertain. Also debated are the pathophysiological and immunological mechanisms of their formation and the consequences of their presence in terms of disease classification (Feremans et al. 1978, Hurez et al. 1972, Lennert et al. 1978).

We wish to report the morphological, immunological and clinical features of ten CLL patients with crystalline inclusions in the cytoplasm of their leukaemic lymphocytes, found by light- and electron-microscopic investigations of peripheral blood from 90 patients.

Materials and Methods

Peripheral blood from 90 CLL patients followed in the Department of Medicine during the period from January 1st 1977 to December 31st 1979 was investigated by light- and electron-microscopy for the occurrence of crystalline inclusions in peripheral blood lymphocytes.

Forty-eight of the 90 patients were newly diagnosed within the above mentioned period. In the remainder the diagnosis had been made prior to January 1st 1977, in 32 during the years 1974–76.

The criteria for the diagnosis of CLL were lymphocytosis with a lymphocyte count in peripheral blood of at least 4×10^9/l, as well as a hyperplastic bone marrow with at least 40% lymphocytes in a differential cell count (Binet et al. 1977). All patients underwent staging according to Binet's modification (1981) of Rai's staging system (1975). Serum immunoglobulin IgG, IgA and IgM was estimated by rocket-immunoelectrophoresis (Laurell 1972). M-components were demonstrated by agarose gel electrophoresis and immunofixation (Ritchie and Smith 1976).

Five patients with demonstrated inclusions were re-examined by light- and electron-microscopy after 2, 3, 10, 21 and 36 months, to study the possible persistence of the inclusions. Nine patients in whom inclusions were demonstrated were examined by immunofluorescence staining for surface membrane-bound immunoglobulins (SmIg), and five of these patients were furthermore examined for intracytoplasmic immunoglobulins (CyIg).

Light Microscopy

Methanol-fixed smear preparations of peripheral blood were examined, stained with May-Grünewald Giemsa and Periodic acid Schiff's reagent (PAS). Preparations were evaluated at 1000 × magnification and in every patient a minimum of 200 lymphocytes were examined. Attention was paid both to the presence of inclusions and to the identification of plasmocytoid features of the neoplastic lymphocytes.

Electron Microscopy

Buffy-coat preparations of lymphocytes were studied, prepared as follows: peripheral blood anticoagulated with 3.8% sodium citrate and EDTA was centrifuged at 3.000 r.p.m. for 30 minutes. After this the cell pellet was fixed with 0.2 M Karnovsky's fixative (pH 7.2) for 24 h, cut in 1 mm thin strips, washed in 0.2 M cacodylate buffer, postfixed in 2% osmium tetroxide in S-colloidine buffer (pH 7.4), stained en bloc with 1% uranyl acetate, dehydrated in graded solutions of ethanol and embedded in Epon. Sections were cut on a Reichert ultramicrotome (OM U3). Ultrathin, approximately 500 Å sections were stained with 2% uranyl acetate and Reynolds' lead citrate (Reynolds 1963). Preparations were examined in a Philips EM 301 electron microscope at 80 kV.

Immunofluorescence Staining Techniques

Mononuclear cells were isolated by gradient centrifuging on Lymphoprep® (Pharmacia Fine Chemicals) of whole blood diluted 1 plus 1 with RPMI-1640 (Gibco Biocult) containing heparin 20,000 U/l, penicillin 500,000 IU/l and streptomycin 333 mg/l. After washing three times in the same medium without heparin the cells were examined by immunofluorescence for SmIg and CyIg.

SmIg was demonstrated by examination of cell suspensions (Forni 1979, Jondal 1974) using fluorescein-or rhodamin-conjugated $F(ab')_2$-fragments (Forni 1979) of rabbit anti-human IgG, IgM, IgA, IgD, kappa and lambda (DAKO Immunoglobulins A/S, Copenhagen, Denmark). 100 µl of each antiserum in a dilution of 1 plus 9 with isotonic saline was incubated with $1–2 \times 10^7$ lymphocytes, suspended in 100 µl RPMI-1640 with sodium azide 20 mmol/l. After incubating for 30 minutes at 0° C the cells were washed three times in RPMI-1640 with sodium azide and mounted with coverslips in a glycerol phosphate buffer.

CyIg was demonstrated on ethanol-fixed, cytocentrifuge smears of isolated cells (Forni 1979). 10 µl fluorescein-or rhodamin-conjugated antisera with the above mentioned specificities was added in a dilution of 1 plus 9 to the cell pellet. After incubating for 30 minutes in a moist chamber at 4° C the preparations were washed three times in isotonic phosphate buffer (pH 7.4) and mounted as above.

The preparations were examined in a Zeiss 200 V HbO lamb epi-illumination microscope, fitted with fluorescein- and rhodamin-selective filters as well as phase-contrast optics.

Results

Light Microscopic Findings

Light microscopic studies of May-Grünewald Giemsa stained smear preparations of peripheral blood demonstrated crystalline inclusions in the neoplastic lymphocytes from seven of 90 patients examined. In these patients the inclusions were present in 5–45% of peripheral blood lymphocytes (Table 1). The inclusions

Table 1. Haematological light microscopic and immunological findings in 10 CLL patients with ultrastructurally demonstrated intracytoplasmic crystalline inclusions in peripheral blood lymphocytes

Patient No.	Peripheral blood		Serum immunoglobulins (g/l)+				Lymphocyte immunoglobulins	
	Lymphocyte count ($\times 10^9$/l)	% lymphocytes with inclusions in the light microscope	IgG	IgM	IgA	M-component	SmIg	CyIg
1	51.2	10	4.9	0.1	0.5	⁄.	IgM lambda	not ex.
2	21.6	5	6.0	0.7	0.2	⁄.	IgM kappa	not ex.
3	23.6	–	2.4	0.2	0.2	⁄.	IgM lambda	IgM lambda
4	6.4	–	9.3	1.1	0.4	⁄.	IgM lambda	not ex.
5	33.4	10	3.7	0.2	0.1	⁄.	IgM lambda	IgM lambda
6	53.4	–	5.0	0.2	0.7	⁄.	IgM lambda	IgM lambda
7	11.8	5	20.5	0.2	0.8	IgM lambda	IgM lambda	IgM lambda
8	88.9	5	2.8	0.4	0.1	⁄.	IgM lambda	IgM lambda
9	17.1	45	11.5	0.6	4.6	IgG lambda	IgG lambda	not ex.
10	316.8	20	5.0	0.2	0.7	⁄.	not ex.	not ex.

+ Normal range (g/l): *IgG* 6.8–15.7, *IgM* 0.18–1.29, *IgA* 0.56–3.30
– could not be identified, ⁄. not present, not ex, not examined

appeared as rectangular, 1–4 μ long structures, which were unstained in the May-Grünewald Giemsa as well as PAS stains (Fig. 1, inset lower left). Typically a cell contained 1–3 inclusions, though in exceptional cells as many as seven inclusions could be identified. The inclusions were demonstrated only in small characteristic CLL lymphocytes showing no plasmocytoid differentiation.

In five patients re-examined after an interim of two to 36 months, the inclusions persisted in unchanged proportions.

Electron Microscopic Findings

In electron microscopic examination of peripheral blood from 90 patients, the inclusions were demonstrated in the lymphocytes of 10 patients (11%). They could thus be demonstrated by electron microscopy in three patients in whom inclusions could not be identified by light microscopy. They were uniform with regard to ultrastructure, without significant morphological differences between the individual patients.

The inclusions were found only in the cytoplasm. They were square, rectangular or rhombic, measuring from 0.5–4.5 μ in length and from 0.2–0.7 μ in width (Fig. 1). A few had narrow interconnections (Fig. 2). They consisted of a granular, moderately electron-dense material (Figs. 2 and 3). Thus in contrast to several previously reported cases (Clark et al. 1973, Feremans et al. 1978), the inclusions in the present study showed no regularity or periodicity in structure. They were completely or partially membrane-bound and often seemed associated with dilated profiles of rough endoplasmic reticulum (Fig. 3).

Apart from the presence of inclusions, the lymphocytes of all 90 patients were alike in terms of ultrastructure. There were few organelles. The rough endoplasmic reticulum and the Golgi apparatus were poorly developed.

In five patients, re-examined after an interval of two to 36 months the inclusions had not changed in ultrastructural appearance.

Immunological Findings

The nine patients with intracytoplasmic crystalline inclusions examined for SmIg all displayed faint yet clearly monoclonal membrane fluorescence, in seven cases with IgM-lambda, in one case with IgG-lambda and in the last case with IgM-kappa (Table 1).

In five patients with crystalline inclusions examined for CyIg, the inclusions appeared as strongly and uniformly fluorescing bodies, which were sharply delimited from the surrounding, unstained cytoplasm (Fig. 1, inset lower right). The inclusions were positive only for IgM and lambda chains, whereas no fluorescence was observed for the other immunoglobulin classes. Thus in these five patients there was intimate concordance between the immunoglobulin content of the inclusions and the immunoglobulins expressed at the cell surface membrane (Table 1).

Clinical Findings

Compared to the rest of the patient material, the ten with crystalline inclusions showed no specific clinical features.

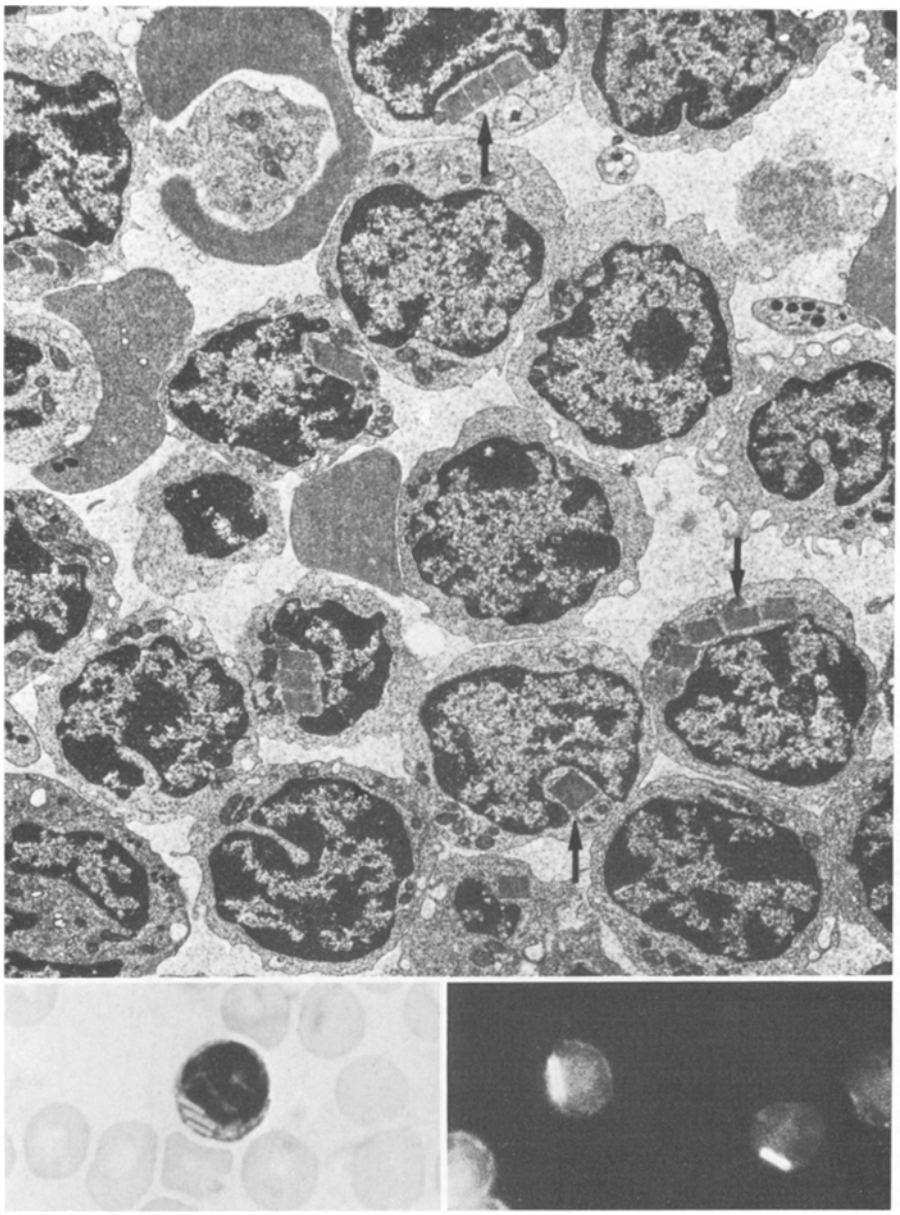

Fig. 1. Electron micrograph of buffy-coat preparation of peripheral blood from a CLL patient (×4,750). Many of the lymphocytes contain typical intracytoplasmic crystalline inclusions (arrows), which are square, rectangular or rhombic. *Inset lower left* shows the characteristic light microscopic appearance of the inclusions in May-Grünewald Giemsa stained smear preparations. The lymphocyte shown is seen to contain three rectangular unstained inclusions (×800). *Inset lower right* shows cytocentrifuge smear of CLL lymphocytes stained with fluorescein-labelled rabbit anti-human lambda light chains (×700). Uniformly fluorescing inclusions are seen in the cytoplasm

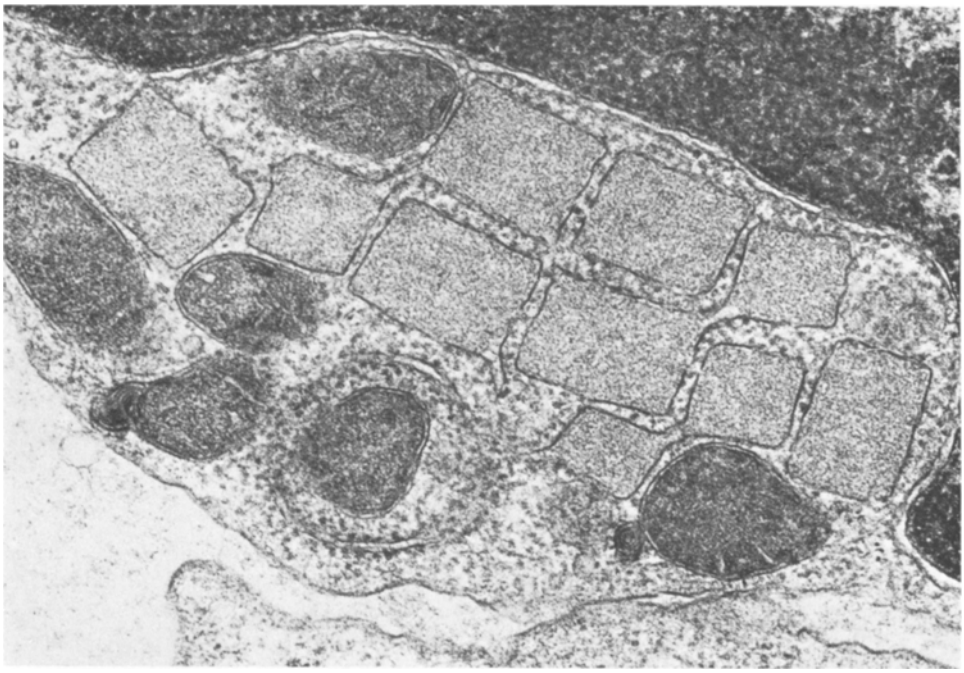

Fig. 2. Section of lymphocyte containing numerous intracytoplasmic inclusions, which are interconnected by narrow bridges. The inclusions are entirely surrounded by membrane material and consist of a granular, moderately electron-dense material (× 50,000)

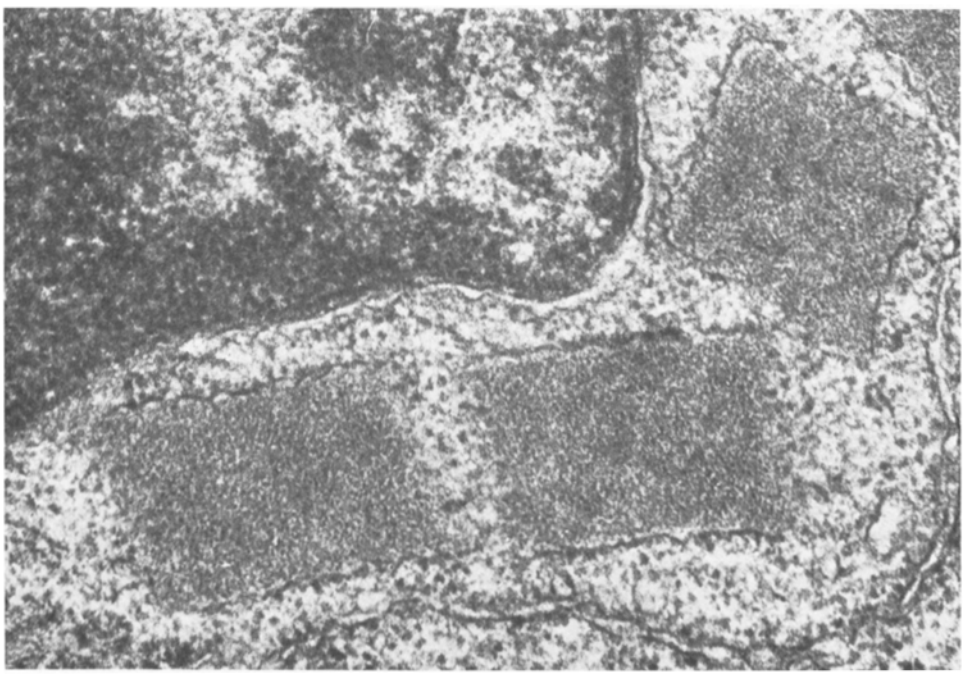

Fig. 3. Intracytoplasmic crystalline lymphocyte inclusions at high magnification (× 65,500) showing close association of the inclusions with dilated profiles of rough endoplasmic reticulum. The ultrastructure of the inclusions is granular without regularity or periodicity

There were eight men and two women. Median age was 67.5 years (range 38–84). According to the staging system of Binet et al. (1981) two patients were in stage A, six were in stage B and one was in stage C at the time of diagnosis. One patient could not be staged because of other disease (poorly differentiated squamous carcinoma of the lung). At the time of conclusion of the study the ten patients with crystalline inclusions in the cytoplasm of their neoplastic lymphocytes had been followed for 12 to 106 months (median 53).

Five of the ten patients with inclusions had been or were under treatment with alkylating drugs, corticosteroids or local high voltage irradiation at the time of blood sampling for this study. The other five patients had never received antileukaemic therapy.

Seven of the ten patients with inclusions had decreased levels of serum immunoglobulins (Table 1), compared to 52 of the 80 patients without inclusions. Two of the ten patients with inclusions had an M-component in serum of the same class and type as the SmIg and CyIg of their neoplastic lymphocytes (Table 1). Of the remaining 80 patients without crystalline inclusions, seven had serum M-components.

Discussion

The designation crystalline has been applied to different types of intracytoplasmic inclusions in various lymphocytic cells such as CLL lymphocytes (Cawley et al. 1976, Clark et al. 1973, Feremans et al. 1978), lymphocytes of malignant lymphomas (Mennemeyer et al. 1974, Vernon et al. 1979), myeloma cells (Stavem et al. 1975, Stavem and Førre 1981) and lymphocytes of inflammatory processes (Friedmann et al. 1971, Valenzuela et al. 1980). The designation thus encompasses a spectrum of inclusions which are not readily comparable.

When restricted to CLL lymphocytes however, crystalline inclusions are well-defined intracytoplasmic bodies which have shown a close concordance in morphological, cytochemical and immunological characteristics in several different studies (Bernard et al. 1959, Cawley et al. 1976, Clark et al. 1973, de Man and Meiners 1962, Feremans et al. 1978, Hurez et al. 1972, Roberts et al. 1979).

The inclusions are recognised in the light microscope as rectangular unstained structures in the May-Grünewald Giemsa as well as PAS stains. In the electron microscope they appear as intracytoplasmic membrane-bound bodies which are often associated with dilated profiles of rough endoplasmic reticulum. The inclusions have never been observed intranuclearly, but in a few reported cases they have occurred in dilated perinuclear cisterns (Cawley et al. 1976). In several prior reports they have demonstrated a regular periodic ultrastructure (Clark et al. 1973, Feremans et al. 1978, Hurez et al. 1972, Stefani et al. 1977). The granular, non-periodic ultrastructure of the present inclusions may be conditioned by the method of fixation. It has been demonstrated that the ultrastructure of inclusions in plasma cells may vary with the velocity of the fixation procedure (Bartoloni et al. 1980).

The inclusions are recognised in immunofluorescence staining as strongly and uniformly fluorescing bodies. They thus contain immunoglobulin. In this

and in several previous reports a close concordance has been found between the immunoglobulin content of the inclusions and the immunoglobulins expressed at the cell surface membrane (Cawley et al. 1976, Clark et al. 1973, Feremans et al. 1978). Compared to the usual predominance of kappa clones in lymphoproliferative disorders (Pred'homme and Seligmann 1972), there is a remarkable predominance of lambda clones in CLL patients with intracytoplasmic crystalline inclusions (Clark et al. 1973). In the present study, eight of nine patients with crystalline inclusions expressed a lambda monoclonal pattern of reaction in immunofluorescence staining for SmIg. Very few reports exist on kappa immunofluorescing crystalline inclusions (Mason et al. 1980, Preud' homme and Seligmann 1972). None of these have been studied in terms of ultrastructure. There is therefore reason to emphasize that in our patient with a kappa positive CLL clone the inclusions corresponded closely to the inclusions in the other patients with lambda light chain determinants, both in light microscopic and ultrastructural appearance. It thus appears that the crystalline inclusions are not specific for lambda light chain immunoglobulins. The predominance of lambda clones in CLL patients with crystalline immunoglobulin inclusions remains unexplained.

In the present study the inclusions could be deomonstrated in ten of 90 patients examined, corresponding to an incidence of 11%. This approximates to the incidences of 5% and 10% in two previously recorded CLL series of 72 and 30 patients, respectively (Cawley et al. 1976, Clark et al. 1973). Obviously the incidence is dependent on the screening method used, since electron microscopic examination is clearly superior to light microscopic examination in the identification of the inclusions.

In the individual patient the inclusions can be demonstrated only in a fraction of the neoplastic cell clone (Clark et al. 1973, Feremans et al. 1978). The re-examination of several of our patients demonstrates that within the individual patient the number of inclusion-containing lymphocytes tends to remain constant. It also etablishes that the inclusions are not induced by antileukaemic therapy.

The occurrence of cytoplasmic crystalline immunoglobulin inclusions thus appears to be a constant feature of roughly 10% of all CLL patients. The occurrence of inclusions is not associated with any specific clinical course. No correlation has been demonstrated between the occurrence of inclusions and the occurrence of M-components in serum or urine, either in this study or in previously reported cases (Clark et al. 1973, Feremans et al. 1978, Hurez et al. 1972).

Our patient material was selected, since both newly diagnosed patients and patients followed for a long time were included in the study. However, the median time of observation of 53 months for the ten patients with crystalline inclusions corresponds to the median time of survival in consecutive CLL series (Geisler and Hansen 1981, Hansen 1973). Thus, the occurrence of cytoplasmic crystalline inclusions in CLL lymphocytes does not seem to be significant for the survival time.

The demonstration of identical immunoglobulin type and class at the cell surface membrane and in the inclusions suggests that the inclusions represent

an intracellularly synthesized immunoglobulin product. This suggestion is supported by the demonstrated association of the inclusions with dilated profiles of rough endoplasmic reticulum. It is supposed that the crystalline inclusions are the result of a defective or imbalanced immunoglobulin production (Clark et al. 1973, Feremans et al. 1978). Currently it is not clear whether the process of crystal formation is related to the secretion of extracellular immunoglobulin or to the synthesis of surface membrane-bound immunoglobulin. In a few in vitro experiments it has been demonstrated that the secretion of heavy chains is impaired in CLL cases with crystalline immunoglobulin inclusions (Roberts et al. 1979). Since this is often the case in CLL (Roberts et al. 1979), however, it can neither explain the presence of inclusions in only 10% of CLL patients nor the occurrence of exceptional cases with pure light chain inclusions (McCann et al. 1978). The demonstration of several CLL cases with immunofluorescing crystalline inclusions but without demonstrable SmIg (Cawley et al. 1976, McCann et al. 1978, Roberts et al. 1979) might indicate that the inclusions are related to a defective synthesis or insertion of surface membrane-bound immunoglobulins. Further immunochemical investigations are needed before these theories can be properly evaluated, but it should be realized that the presence of inclusions does not necessarily reflect differentiating capability in immunological terms.

It has been suggested that CLL cases with crystalline immunoglobulin inclusions should be classified with the immunocytomas (Feremans et al. 1978). From several aspects, however, these CLL cases do not conform to conventional criteria for this designation. The negative PAS reactions, the lack of plasmocytoid differentiation and the lack of correlation between the occurrence of inclusions and the occurrence of M-components are all against the immunocytoma designation (Lennert et al. 1978).

In the present state of knowledge it thus appears that there is neither clinical, prognostic nor sufficient theoretical support for the application of specific designations in cases of CLL with crystalline immunoglobulin inclusions.

Acknowledgements. Grateful acknowledgements are due to H. Tinggaard for preparing the many blood samples, to B. Eriksen and J. Bojsen for careful typing of the manuscript and to A. Wiik for assistance in the preparation of immunofluorescence micrographs. Financial support was obtained from The Brandt Brandtved Foundation and Lundbech's Foundation for Medical Research.

References

Bartoloni C, Flamini G, Gentiloni N, Russo MA, Barone C, Gambassi G, Terranova T (1980) Immunochemical and ultrastructural study of multiple myeloma with a heavy chain protein in the serum. J Clin Pathol 33:936–945

Bernard J, Bessis M, Soulier JP, Thiéry JP (1959) Etude au microscope électronique d'une leukémie lymphoide avec cristaux intra-cytoplasmiques. Revue d'Hématologie 3:227–237

Binet JL, Leporrier M, Dighiero G, Charron D, D'Athis Ph, Vaugier G, Merle Beral H, Natali JC, Raphael M, Nizet B, Follezou JY (1977) A clinical staging system for chronic lymphocytic leukemia. Cancer 40:855–864

Binet JL, Auquier A, Dighiero G, Chastang C, Piquet H, Goasguen J, Vaugier G, Potron G, Colona P, Oberling F, Thomas M, Tchernia G, Jacquillat C, Boivin P, Lesty C, Duault MT,

Monconduit M, Belabbes S, Gremy F (1981) A new prognostic classification of chronic lymphocytic leukemia derived from a multivariate survival analysis. Cancer 48:198–206

Cawley JC, Smith J, Goldstone AH, Emmines J, Hamblin, J, Hough L (1976) IgA and IgM cytoplastic inclusions in a series of cases of chronic lymphocytic leukaemia. Clin Exp Immunol 23:78–82

Clark C, Rydell RE, Kaplan ME (1973) Frequent association of IgM λ with crystalline inclusions in chronic lymphatic leukemic lymphocytes. New Eng J Med 289:113–117

Feremans WW, Neve P, Caudron M (1978) IgM lambda cytoplasmic crystals in three cases of immunocytoma: a clinical, cytochemical and ultrastructural study. J Clin Pathol 31:250–258

Forni L (1979) Reagents for immunofluorescence and their use for studying lymphoid cell products. In: Lefkovits I, Pernis B (eds) Immunological methods. Academic Press, New York, pp 151–167

Friedmann I, Michaels L, Bird ES (1971) Crystalline structures in lymphocytes. J Pathol 105:289–293

Geisler C, Hansen MM (1981) Chronic lymphocytic leukaemia: A test of a proposed new clinical staging system. Scand J Haematol (in press)

Hansen MM (1973) Chronic lymphocytic leukaemia. Clinical studies based on 189 cases followed for a long time. Scand J Haematol (Suppl) 18:80–100

Hurez D, Flandrin G, Preud'homme JL, Seligmann M (1972) Unreleased intracellular monoclonal macroglobulin in chronic lymphocytic leukaemia. Clin Exp Immunol 10:223–234

Jondal M (1974) Surface markers on human B and T lymphocytes. IV. Distribution of surface markers on resting and blast transformed lymphocytes. Scand J Immunol 3:739–747

Laurell C-B (1972) Electronimmunoassay. Scand J Clin Lab Invest (Suppl) 124:21–37

Lennert K, Mohri N, Stein H, Kaiserling E, Müller-Hermelink HK (1978) Malignant lymphomas other than Hodgkin's disease. Springer-Verlag Berlin, Heidelberg, New York, pp 209–281

Man JCH de, Meiners WBH (1962) Crystals of protein nature in the cytoplasm of lymphocytic cells in a case of lymphoreticular malignancy. Blood 20:492–500

Mason DY, Leonard R, Laurent G, Gourdin MF (1980) Immunoperoxidase staining of surface and intracellular immunoglobulin in human neoplastic lymphoid cells. J Clin Pathol 33:609–616

McCann SR, Whelan A, Greally J (1978) Intracellular lambda light chain inclusions in chronic lymphocytic leukaemia. Br J Haematol 38:367–371

Mennemeyer R, Hammar SP, Cathey WJ (1974) Malignant lymphoma with intracytoplasmic IgM crystalline inclusions. New Engl J Med 291:960–963

Preud'homme JL, Seligmann M (1972) Surface bound immunoglobulins as a cell marker in human lymphoproliferative diseases. Blood 40:777–794

Rai KR, Sawitsky A, Cronkite EP, Chanana AD, Levy RN, Pasternack BS (1975) Clinical staging of chronic lymphocytic leukaemia. Blood 46:219–234

Reynolds EW (1963) The use of lead citrate at high pH as an electron-opaque stain in electron microscopy. J Cell Biol 17:208–213

Ritchie RF, Smith R (1976) Immunfixation I. General principles and application to agarose gel electrophoresis. Clin Chem 22:497–499

Roberts GH, Gordon J, Smith JL, Newell D, Pike R (1979) The biosynthesis and characterization of IgM λ in a case of chronic lymphocytic leukaemia with intracellular immunoglobulin inclusions. J Clin Pathol 32:272–279

Stavem P, Førre Ø (1981) The same type of crystalline inclusions in T-lymphocytes as in plasma cells and B-lymphocytes in multiple myeloma. A pathological clone originating from a common lymphocyte stem cell? Scand J Haematol 26:265–271

Stavem P, Vandvik B, Skrede S, Hovig T (1975) Needle-Like crystals in plasma cells in a patient with a plasma cell proliferative disorder. Scand J Haematol 14:24–34

Stefani S, Chandra S, Schrek R, Tonaki H, Knopse WH (1977) Endoplasmic reticulum-associated structures in lymphocytes from patients with chronic lymphocytic leukaemia. Blood 50:125–139

Valenzuela R, Deodhar SD, Braun WE (1980) Cytoplasmic crystalline structures in lymphoid cells of a human renal allograft. Human Pathology 11:84–85

Vernon S, Voet RL, Naeim F, Waisman J (1979) Nodular lymphoma with intracellular immunoglobulin. Cancer 44:1273–1279

Accepted January 12, 1982

Virchows Arch [Pathol Anat] (1982) 395:237–243

Virchows Archiv A

Lesions Characteristic of Infection or Malignant Tumor in Paleo-Eskimo Skulls

An Anatomical and Radiological Study of two Specimens

R. Lagier[1], C.A. Baud[2], G. Arnaud, S. Arnaud[3], and R. Menk[4]

Département de Pathologie (Unité Ostéoarticulaire)[1] et Institut de Morphologie[2], Faculté de Médecine, Genève, Switzerland
Centre de Recherches Archéologiques CNRS (Laboratoire de conservation, restauration et recherches)[3], Draguignan, France
Département d'Anthropologie[4], Faculté des Sciences, Genève, Switzerland

Summary. Study of two Paleo-Eskimo skulls found in a necropolis on St-Lawrence Island (Alaska), including radiography and histological examination, revealed the following features. One of the skulls showed a perforation with remodelled borders, considered to be due to trauma and secondary infection. The other showed areas of osteolysis characteristic of a malignant tumor (probably carcinomatous metastasis rather than myeloma).

These cases illustrate the advantage of using various methods of investigating bone pathology, particularly microradiography, in skeleton paleopathology.

Key words: Paleopathology – Eskimos – Frontal bone – Osteomyelitis – Bone carcinomatous metastases – Myeloma

Since skeletal changes are the primary concern of paleopathology, a thorough knowledge of bone pathology and the use of appropriate modern methodology are essential. This is illustrated in this report of two lesions observed in Paleo-Eskimo skulls.

Materials and Methods

The two cranial specimens which were of eskimoid type, were found in the Kitnepaluk necropolis in the northwest part of St-Lawrence Island (Alaska) buried in two graves that were somewhat distant from the others [Anliker-Bosshard, in press; Menk et al. in preparation]. The age of these specimens cannot be precisely determined since there is a wide range of burial dates as shown by archeological data and ^{14}C estimations; the latter indicate that the burials took place over a period beginning with the start of the Christian era and ending at about the 14th Century A.D. From its state of preservation, specimen N° 1 would seem to date from the later part of this period; it was not possible to evaluate the age of specimen N° 2.

Offprint requests to: R Lagier, Institut de Pathologie, 40 boulevard de la Cluse, CH-1211 Genève 4, Switzerland

0340-1227/82/0395/0237/$01.40

After macroscopic examination (using anthropological and anatomopathological criteria) and radiography, samples were taken from each of the two specimens and embedded in methyl methacrylate. A histological study was made of:

- 10 µm sections stained with alcoholic basic fuchsin or Harris' haematoxylin-eosin.
- 100 µm sections microradiographed according to the technique of Baud and Morgenthaler (1956).

The powder obtained from the sawing of the samples, which were of normal consistency, was submitted to various physical and chemical studies: a) X-ray diffraction for determination of the crystalline type (diagrams obtained with the Guinier camera) and crystalline parameters and the size of the crystals (diffractometric recording according to Jacquet et al. (1980); b) determination of the hydroxyproline content as an indication of collagen levels (method of Blumenkranz and Asboe-Hansen [1974]) and of the fluorine content (method of McCann [1968]).

The values were compared with those reported in the literature for normal bone and with those obtained for a control sample of skull taken at autopsy from a 78 year old man (A. 79/80, Department of Pathology, Geneva) with no history of skeletal disease.

Observations

Specimen N^0 1 (Reference 1973-K12: Seminar für Urgeschichte der Universität Bern, Switzerland)

This complete skull belonged to an adolescent of about 12 to 14 years of age and indeterminate sex. It was quite well preserved although somewhat deformed by the pressures of earth and showed some signs of superficial post-mortem abrasion. There was a perforation 15 to 20 mm in diameter on the median line of the frontal bone, 35 mm above the glabella whose free borders showed remodelling with bone overgrowth. The external table surrounding the perforation appears thickened by newly formed subperiosteal bone bearing imprints of blood vessels and extending mostly in the direction of the glabella (Fig. 1 a). On the internal table, signs of hypervascularization could be observed around the perforation. The only other lesion was a superficial star-shaped scar, 1 cm in diameter on the external table of the left parietal bone. There was no sign that would indicate human intervention with an instrument.

Radiography revealed osteosclerosis around the perforation and no other lesion (Fig. 1 b). No X-ray of the rest of the skeleton was possible since the skull was an isolated piece.

The histological examination was made on a horizontal section taken from the right side starting at the free border of the perforation (Reference Numbers: T. 11985/77, Department of Pathology, Geneva and 723, Institute of Morphology, Geneva). The sections and the microradiographs showed the bone to be well preserved, to have no signs of attack by fungi or bacteria, and to have a recognizable structure of both preexisting lamellar and newly formed woven bone (Fig. 2).

Microradiography provided a topographical view showing trabeculae of vascularized newly formed woven bone deposited on the endosteal and periosteal surfaces of the cortex. No other histological modifications were observed.

The mineral material gave an X-ray diffraction pattern typical of apatite. Crystal size and/or crystalline perfection was determined by the width of the diffraction lines at half intensity: β (31.0) = 0.457° 2θ and β (00.2) = 0.175° 2θ. The dimensions of the unit cell of the crystalline lattice were $a = 9.417$ Å and $c = 6.892$ Å.

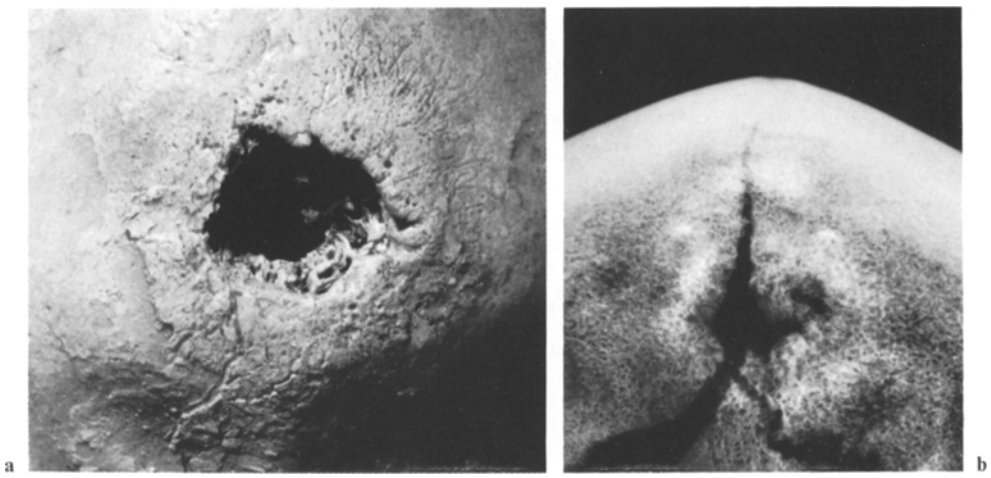

Fig. 1 a, b. Specimen N° 1. **a** Macroscopic aspect of the external orifice of the frontal perforation; overgrowth on the borders and subperiosteal thickening with imprints of blood vessels toward the lower part (×0.9 approx.) **b** X-rays AP (×0.7). The slits correspond to the superimposed lambda suture

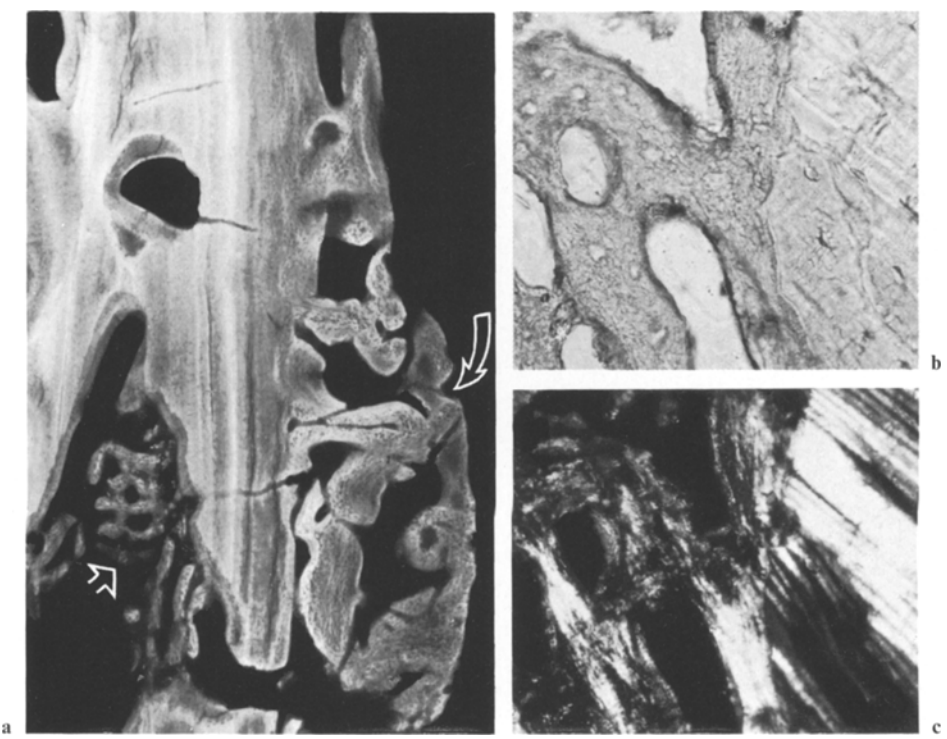

Fig. 2 a–c. Specimen N° 1. **a** Microradiography of the border of the perforation on the internal table (×30). This compact bone tissue (in the center) is flanked by a network of newly-formed bone on the endosteal (*straight arrow*) and periosteal (*curved arrow*) surfaces. **b, c** Newly-formed woven bone attached to lamellar bone trabecula (basic fuchsin stain ×75). **b** By ordinary light; **c** by polarized light

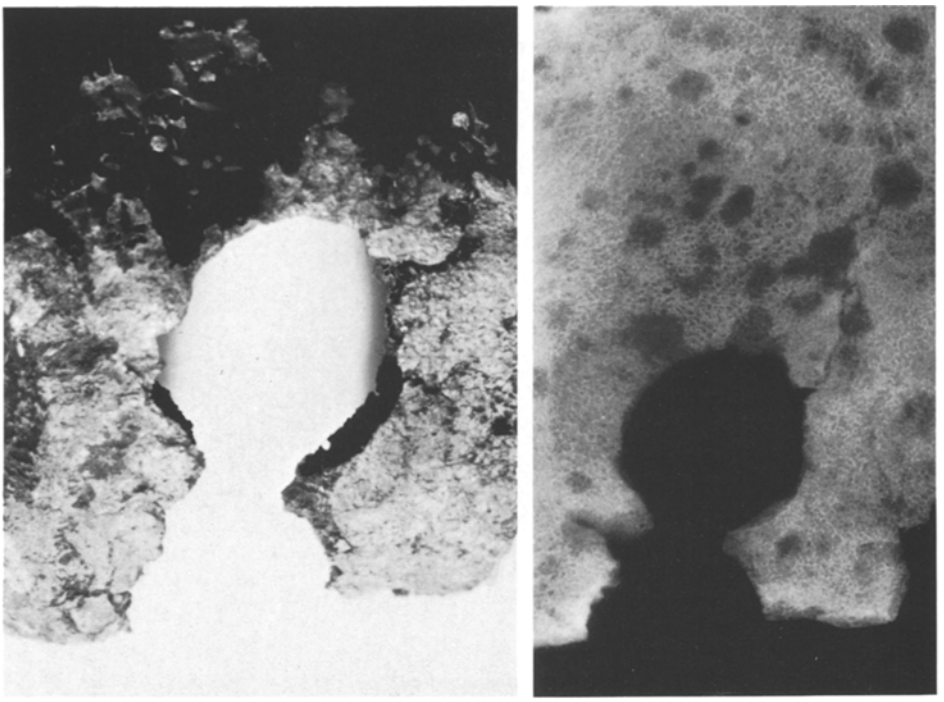

Fig. 3a, b. Specimen N° 2 (×0.9 approx.). **a** Macroscopic aspect of the principal area of bone loss. **b** X-ray of the corresponding bone fragment

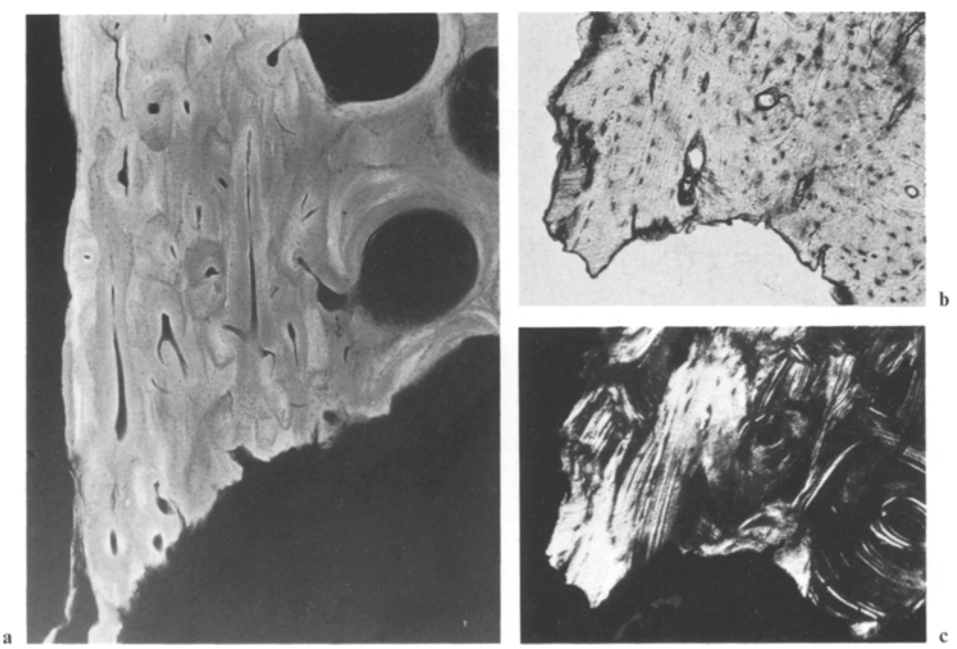

Fig. 4a–c. Specimen N° 2. **a** Microradiography of the border of the area of bone loss of Fig. 3a at the level of the external table (×30). Erosion more pronounced in the deeper part of the table. **b, c** Detail of the outer tip of the border of the eroded area showing the clear-cut erosion of the lamellar bone (basic fuchsin stain ×75). **b** By ordinary light; **c** by polarized light

Fluorine content was found to be 0.225% and hydroxyproline content 738 nmol/mg.

Specimen N° 2 (Reference 1973-K8: Seminar für Urgeschichte der Universität Bern, Switzerland)

This fragment of cranial vault measuring 13 cm × 9 cm, had the characteristics of an adult male skull. It showed a rounded well-defined area of bone loss with grooved borders (Fig. 3a). Radiography also revealed numerous smaller areas of bone loss that were not macroscopically visible (Fig. 3b). This cranial fragment was found along with some fragments of the jawbone and two segments of long bones, one of which was shown by radiography to have an area of bone loss.

A histological examination was made of a radial section of the cranial fragment, taken starting at the border of the principal area of bone loos (Reference Numbers: T. 11984/77, Department of Pathology, Geneva and 722, Institute of Morphology, Geneva). The sections and microradiographs showed the bone to be well preserved, to have no signs of attack by fungi and bacteria and to have a recognizable osteonic architecture (Fig. 4c). Microradiography showed a clear-cut erosion and no formation of new bone (Fig. 4a). This absence of new bone was confirmed by the examination of the sections by ordinary and polarized light which also showed the clear-cut erosion of the bone lamellae (Fig. 4b–c). No other histological modifications were observed.

The mineral materials gave an X-ray diffraction pattern typical of apatite. Crystal size and/or crystalline perfection was determined by the width of the diffraction lines at half intensity: 1) on the border of the eroded area β (31.0) = 0.475° 2θ and β (00.2) = 0.188° 2θ – 2) at a distance from the eroded area β (31.0) = 0.477° 2θ and β (00.2) = 0.188° 2θ. The dimensions of the unit cell of the crystalline lattice were 1) on the border of the eroded area $a = 9.419$ Å and $c = 6.892$ Å – 2) at a distance from the eroded area $a = 9.424$ Å and $c = 6.915$ Å.

Fluorine content was found to be 0.166% on the border of the eroded area and 0.065% at a distance. Hydroxyproline content was 734 nmol/mg on the border and 1,018 nmol/mg at a distance.

Discussion

The histological examination demonstrated the good state of preservation of this bone material, reflected by a normal hydroxyproline (and therefore collagen) content.

No mineral deposits from the external milieu (signs of fossilisation) were observed. The values obtained for the size and/or crystalline perfection and for the unit cell dimensions were substantially the same as those obtained for control bone tissue. The bone fluorine content (< 0.2%) found for the control subjects living in a country with low fluorine concentration in the drinking water [Baud et al. 1978] and that of the control sample of frontal bone (necropsy A. 79/80: 0.067% F) suggested that the difference in fluorine content found for the two specimens which were buried relatively close to each other

was due to individual variation rather than to post-mortem changes due to the external milieu. The fluoride ions are located inside crystal lattice, as indicated by the shortening of the a value of the unit cell proportional to the fluoride level [Bang et al. 1978]. The cristal size and/or crystalline perfection expressed as β values are the same as for the control sample of frontal bone (β (31.0) = 0.492° 2θ; β (00.2) = 0.194° 2θ).

The hydroxyproline content was also essentially the same as that of the control sample of frontal bone (966 nmol/mg).

These data indicate that both the mineral substance and the collagen organic matrix were well preserved in spite of the long period of burial in the earth. This is in contrast with observations (both for mineral substance and collagen) reported for specimens found under other conditions in direct contact with the earth [Arnaud et al. 1980]. It would seem, therefore, that the cold climate of St-Lawrence Island protected the bone tissue from the attack by fungi and bacteria which is frequently seen under other climatic conditions especially when the bone is in direct contact with the earth [Arnaud et al. 1980; Marchiafava et al. 1974; Morgenthaler and Baud 1956–1957].

In Specimen N° 1 both the macroscopic aspect (in particular the vascularized subperiosteal thickening) and the radiological and histological data indicate a chronic infectious condition. Based on the observations and data, a diagnosis of syphilis can be excluded without entering into the discussion of the existence of the disease in pre-Columbian America [Hackett 1976]. The histology of the newly-formed bone suggests pyogenic osteitis but if this were the only cause, the perforation could have been expected to be larger. More probably, it was a secondary infection of a primary lesion due to trauma, resulting not from trephining (considering the relatively small diameter of the perforation) but rather after damage by a weapon. This conclusion is in accord with the finding of Stewart and Quade [1969; cit. in Stewart 1979] that most frontal lesions observed in Indian skulls from archaeological sites appear to be of traumatic origin.

In Specimen N° 2, the radiological picture is characteristic of a malignant tumor, either a myeloma or more likely, in view of the diameter of the main area of bone loos, carcinomatous metastasis. Histological data indicate an actively erosive process with no osteogenic remodelling. The area of bone loss in a segment of long bone was shown by radiology to be compatible with these two diagnoses.

The joint study of these two specimens demonstrates the necessity of proceeding with a paleopathological study as if it were a contemporary study in pathology and considering it to be the "forensic medicine" of archaeology or history. A wide range of methods, from conventional macroscopic evaluation to biophysical, chemical and histological analyses, can be used. The choice of methods will vary according to the case and the technical and financial possibilities. In Specimen N° 1, the macroscopic and histological examinations were determinant, while in Specimen N° 2, it was radiography that provided the crucial data.

Histological examination, providing that certain precautions are taken, allows for a thorough study of the extra-cellular structures. Embedding the specimen in methyl methacrylate insures the necessary physical properties to allow for the sectioning of fragile material (especially if it has deteriorated after attack by microorganisms) while also allowing for the use of various stains. Examination by polarized light provides data concerning the bone structure. Microradiography on thick sections seems to be a particularly useful technique since it provides a topographical evaluation of a quite large surface.

Acknowledgments. We wish to thank Prof. H.G. Bandi, Director of the "Seminar für Urgeschichte", Bern, Switzerland and of the St-Lawrence Island excavation for having made the specimens available to us. The X-ray diffraction analyses, the preparation of the specimens for the histological study and the fluorine determinations were respectively performed by Dr. J.M. Very, Mrs. M. Tachon-Saban and Miss C. Demeurisse (Institut de Morphologie, Genève). The hydroxyproline determinations were performed by Miss J. Bornand (Laboratoire CEMO, Hôpital Cantonal, Genève).

We are grateful to Mrs Judith L. Noebels for her invaluable collaboration in the preparation of the English version of this paper.

References

Anliker-Bosshard E (in press) Beiträge zur Archaeologie der St-Lorenz-Insel, Alaska. Teil II. Academica Helvetica

Arnaud G et S, Baud CA, Lagier R (sous presse) Etude comparative d'os humains inhumés et immergés (en milieu marin ou lacustre). Approche histologique, chimique et cristallographique. In: Paleopathology Association, 3rd European Meeting. Caen 1980, pp 91–95

Bang S, Baud CA, Boivin G, Demeurisse C, Gössi M, Tochon-Danguy HJ, Very JM (1978) Morphometric and biophysical study of bone tissue in industrial fluorosis. In: Courvoisier B, Donath A, Baud CA (eds) Fluoride and Bone. Second Symposium CEMO, Nyon 1977. Médecine et Hygiène, Genève, p 168

Baud CA, Lagier R, Boivin G, Boillat MA (1978) Value of the bone biopsy in the diagnosis of industrial fluorosis. Virchows Arch [Pathol Anat] 380:283–297

Baud CA, Morgenthaler PW (1956) Recherches sur le degré de minéralisation de l'os humain fossile par la méthode microradiographique. Arch Suisses Anthropol Gén 21:79–86

Blumenkranz N, Asboe-Hansen G (1974) An automated procedure for quantitative determination of hydroxyproline. Clin Biochem 7:251–257

Hackett CJ (1976) Diagnostic criteria of syphilis, yaws and treponarid (treponematoses) and of some other diseases in dry bones (for use in osteoarchaeology). S.-B. Heidelberger Akad Wiss Math.-nat. Kl 4 Abh:351–470

Jacquet J, Very JM, Flack HD (1980) The 2θ determination of diffraction peaks from "poor" powder samples. Application to biological apatite. J Appl Crystal 13:380–384

Marchiafava V, Bonucci E, Ascenzi A (1974) Fungal osteoclasia: a model of dead bone resorption. Calcif Tissue Res 14:195–210

McCann HG (1968) Determination of fluoride in mineralized tissues using the fluoride ion electrode. Arch Oral Biol 13:475–477

Menk R (in preparation) Beiträge zur Anthropologie der St-Lorenz-Insel, Alaska. Academica Helvetica

Morgenthaler PW, Baud CA (1956–1957) Sur une cause d'altération des structures dans l'os humain fossile. Bull Soc Suisse Anthropol Ethnol 33:9–10

Stewart TD (1979) Patterning of skeletal pathologies and epidemiology. In: Laughlin WS, Harper AB (eds) The first americans: origins, affinities, and adaptations. Gustav Fischer, New York, Stuttgart, p 257

Stewart TD, Quade LG (1969) Lesions of the frontal bone in American Indians. Am J Phys Anthropol 30:89–110

Accepted February 23, 1982

Virchows Arch [Pathol Anat] (1982) 395:245–256

Virchows Archiv A

Veno-occlusive Disease of the Liver in Patients Receiving Immunosuppressive Therapy*

H. Weitz, J.M. Gokel, K. Loeschke, K. Possinger, and M. Eder

Pathologisches Institut, Medizinische Klinik Innenstadt und Medizinische Klinik III im Klinikum Großhadern der Universität, Thalkirchnerstraße 36, D-8000 München 2, Federal Republic of Germany

Summary. The paper presents the morphological findings and clinical data of 4 patients with veno-occlusive disease of the liver developing after immunosuppressive therapy with azathioprine and prednisolone. The pathogenesis and a possible causal relationship of hepatic veno-occlusive disease with long term azathioprine therapy are discussed.

Key words: Hepatic veno-occlusive disease – Renal transplantation – Azathioprine

The term veno-occlusive disease of the liver (VOD) was first introduced by Bras et al. (1954) to describe obliterative lesions of the centrilobular and sublobular hepatic veins seen endemically in Jamaica. The lesions differ in morphology and in aetiology from Budd-Chiari's syndrome and VOD may be caused by the ingestion of pyrrolizidine alkaloids (Stuart and Bras 1957; McLean 1970). Recently, the disease has been observed following bone marrow transplantation and cytotoxic therapy of malignancies (Woods et al. 1980; Griner et al. 1976; Berk et al. 1979; Jacobs et al. 1979; Beschorner et al. 1979; Shulman et al. 1980); these patients showed a rapid and usually lethal deterioration of hepatic function with hepatomegaly and ascites. Extending a case report by Marubbio and Danielson (1975), we here describe 4 patients with hepatic VOD seen in the last two years; these patients received an immunosuppressive therapy for chronic iridocyclitis or following renal transplantation.

* Presented in part at the XIIIth International Congress of the International Academy of Pathology, Paris, September 15–19th 1980

Offprints requests to: H. Weitz at the above address

0340-1227/82/0395/0245/$02.40

Case Reports

Case 1. A 35-year-old man had been haemodialyzed since 1973 for chronic renal insufficiency. A cadaver kidney was transplanted in April 1977 and an immunosuppressive therapy initiated with azathioprine (2–1.5 mg/kg·day) and prednisone (0.4–0.2 mg/kg·day). Eight months after the transplantation, the patient had a febrile attack (up to 39° C) with icterus (bilirubin 5.3 mg/dl) and slight hepatomegaly. The aminotransferases were normal. In the following months, the bilirubin levels varied between 2 and 3 mg/dl; in April 1978, the SGOT was increased (30 U/l; normal <20 U/l).

A few weeks later a splenomegaly was observed. In August 1978, the patient was admitted to the hospital because of severe abdominal pain, diarrhoea, rapidly increasing ascites and progressive stupor. Laboratory findings were SGOT 23 U/l, pseudocholinesterase 1,400 U/l (normal $>3,000$ U/l), alkaline phosphatase 108 (normal <180) U/l, bilirubin 3.7 mg/dl, ammonia 120 (normal <35) µmol/l, creatinine 5.5 mg/dl. HB_s antigen was absent. The patient died as a result of hepatic failure.

Autopsy revealed the patient's own kidneys to have shrunk (60 g both); the transplanted kidney showed a severe chronic vasculopathy but no signs of acute rejection. The left ventricle was hypertrophied (540g). The liver was small and firm (1,050 g), the cut surface showed an accentuated lobular structure with haemorrhagic and small necrotic areas; there was no thrombosis. Liver revealed VOD (Fig. 1 and 2). The spleen was increased in size (340 g) and consistency. There were 5 l of slightly haemorrhagic ascites.

Case 2. A 41-year-old man suffered from chronic renal failure due to chronic glomerulonephritis; for 8 months, he was treated by haemodialysis. A cadaver kidney was transplanted in August 1977. The transplant functioned well. Azathioprine (2 mg/kg·day) and methylprednisolone (0.2 mg/kg·day) were given. In January 1979 icterus developed with bilirubin levels rising from 3.5 to 7 mg/dl. After reduction of azathioprine (0.7 mg/kg·day) and, in May 1979, withdrawal, there was no improvement of cholestasis. The aminotransferases (SGOT 48–70 U/l, SGPT 41–60 U/l) and the gamma-glutamyltransferase (64 U/l, normal <30 U/l) were slightly elevated. HB_s antigen, anti-HB_s and anti-HB_c were always absent; anti HAV (IgM and IgG) was present. In the last weeks before death bilirubin increased to 17 mg/dl. The patient died 23 months after renal transplantation due to cerebral infarction and bronchopneumonia.

Autopsy showed the patient's kidneys to have shrunk with a granular surface. The transplanted kidney showed haemorrhagic infarction (2 by 2 cm) and chronic vasculopathy of moderate degree but no signs of acute rejection. The left ventricle was hypertrophied. There was an old cystic and a fresh cerebral infarction in the right and left hemisphere respectively. The liver was firm with blunted margins; the cut surface was variegated with spotted haemorrhagic and yellow areas. No thrombosis could be seen in hepatic veins. There was no hepatosplenomegaly. Microscopical examination showed VOD of the liver. There was no ascites.

Case 3. A 39-year-old man was found to have Fabry's disease in January 1976. Because of chronic renal failure he was treated by haemodialysis until February 1977 when a cadaver kidney was transplanted. Azathioprine (3 mg/kg·day) and prednisolone (0.5 to 0.1 mg/kg·day) were maintained over the following months. In May 1977, pulmonary embolism from deep femoral vein thrombosis occured, and the patient was treated with phenoprocoumon until November 1978. In May 1978, the patient became slightly icteric; he was afebrile, the liver and spleen were of normal size. Bilirubin was 2.8 mg/dl, alkaline phosphatase 472 U/l, gammaglutamyl transferase 344 U/l, SGOT 27 U/l, and SGPT 17 U/l. HB_s antigen was absent, but anti-HB_s, anti-HB_c, and anti-HAV were present in low titers although there was no history of previous hepatitis. By November 1978, the cholestatic syndrome had progressed (bilirubin 3.4 mg/dl, alkaline phosphatase 705 U/l). After a third acute rejection episode, prednisolone was maintained (0.35 mg/kg·day) while azathioprine was discontinued. However, the patient's condition deteriorated further and cholestasis became more marked. Ascites developed with a protein content of 0.9 g/dl. The liver remained small while the spleen became enlarged. Terminal laboratory data included a further increase in bilirubin (7.1 mg/dl) and alkaline phosphatase (760 U/l) with unchanged low aminotransferases, an increase in blood ammonia (132 µmol/l), and a decline in pseudocholinesterase (1,100 U/l) and serum albumin (2.1 g/dl). The patient became confused and died in February 1979 from pneumonia.

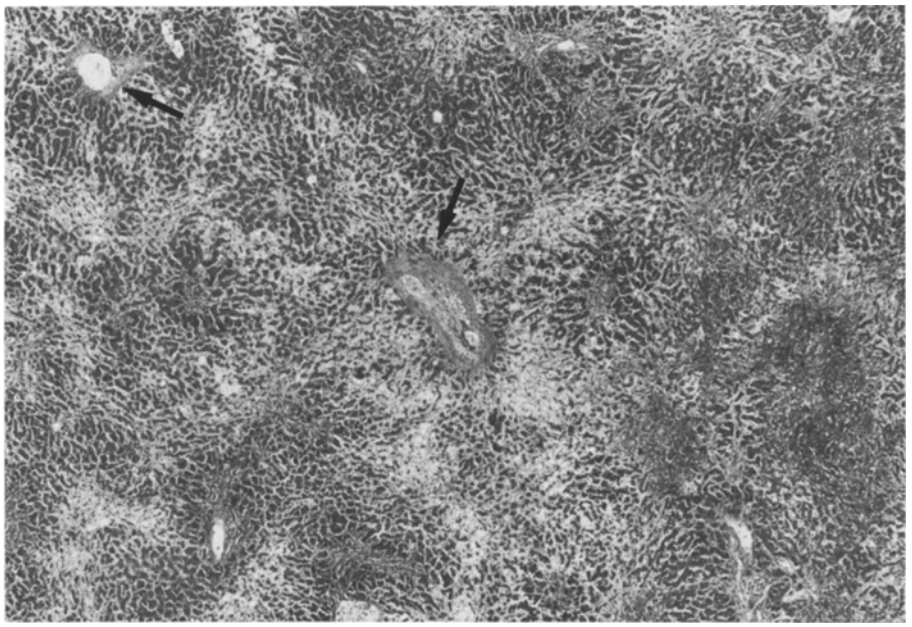

Fig. 1. Loss of hepatocytes in the centrilobular regions and hyperaemia in sinusoids; two partly occluded sublobular veins are indicated by *arrows* (case 1; H.–E., ×30)

Autopsy showed the left kidney to have shrunk (90 g). The right kidney was removed. In the transplanted kidney a slight chronic vasculopathy was observed. There was severe cardiomegaly (655 g) with PAS-positive deposits in myocardial fibers and in other organs, especially in the smooth muscle cells of blood vessels, characteristic of Fabry's disease. There was severe fungal pneumonia and encephalitis. The liver (1,550 g) was firm; the cut surface showed a nodular pattern with patchy yellowish and partly haemorrhagic areas. There was no thrombosis in the hepatic veins. Microscopically, the liver displayed typical venoocclusive changes and showed an impressive nodular regeneration of parenchyma. The spleen was increased in size (240 g) and soft. There were 1.5 l of ascites.

Case 4. In this 34-year-old man there was panuveitis of both eyes (with later development of cataracta complicata) diagnosed in 1973. Because of previously unsatisfactory response to low-dose corticosteroid medication and the progressive visual disorder, therapy was changed to azathioprine (2 mg/kg·day) and prednisolone (0.4 tapering to 0.2 mg/kg·day) in April 1977 with rapid improvement of vision. In February 1979, a slight increase in gamma-glutamyl transferase (88 U/l) was noted without other changes. In March 1979, a short febrile attack occured (40.3° C) and the patient became slightly icteric. The liver was now palpable at 2 cm below the costal border but the spleen was not enlarged. Azathioprine was discontinued and prednisolone maintained. Within the following 4 weeks, liver and spleen size increased to about 5 cm above normal and the abdomen was bloated without ascites. Roentgenograms suggested small oesophageal varices. A liver biopsy was carried out (Fig. 4). A hepatic venogram was refused by the patient. The laboratory data were bilirubin 3 mg/dl, alkaline phosphatase 673 U/l, gamma-glutamyl transferase 415 U/l, SGOT 31 U/l, SGPT 38 U/l; pseudocholinesterase, serum albumin, and prothrombin time were normal. HB_s antigen, anti-HB_s and anti-HB_c were absent while the presence of anti-HAV was compatible with previous hepatitis A. The patient was treated with heparin followed by phenprocoumon until November 1980 when there was no more hepatosplenomegaly, portal hypertension or icterus; the laboratory tests were normal except a gamma-glutamyl transferase of 118 U/l.

Histologically, the first liver biopsy showed severe hyperaemia in the centrilobular region; occlusive lesions without thrombi were detectable in a few centrilobular and in one sublobular

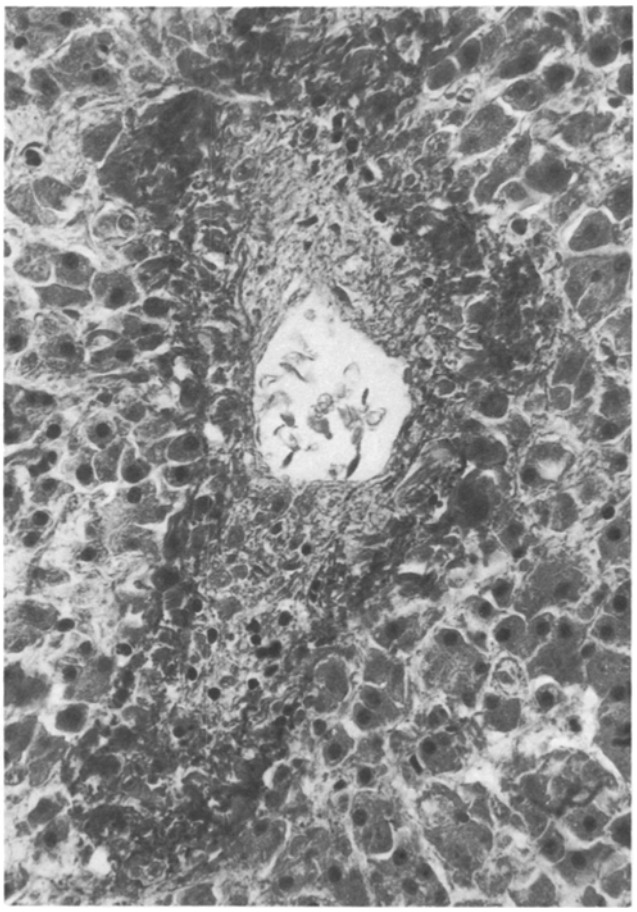

Fig. 2a–c. Subtotal or total occlusion of small hepatic veins by a fine reticular network; within the network some mononuclear cells and rare hepatocytes (**b**, →). The reticulin framework around the liver cell plates is partly collapsed (**c**). (Case 1; **a** and **b** Elastica-van Gieson, ×350; **c** silver impregnation, ×140)

vein, with moderate narrowing of the lumen; there was a subintimal oedema with very few cells (Fig. 3). Loss or necrosis of hepatocytes was not seen. In November 1980, a repeated biopsy displayed a slight perisinusoidal fibrosis but no signs of hyperemia or occlusive changes in the small hepatic veins.

Histology of the Liver

All Cases Showed Typical Veno-Occlusive Changes. The terminal (centrilobular) hepatic venules and the sublobular veins were often partly or completely obliterated by oedematous widening of the subintimal layer. Here, between the thickened collagenous venous wall and the endothelium, a fine network of reticulin fibers was detectable in silver impregnations, while in van Gieson preparations

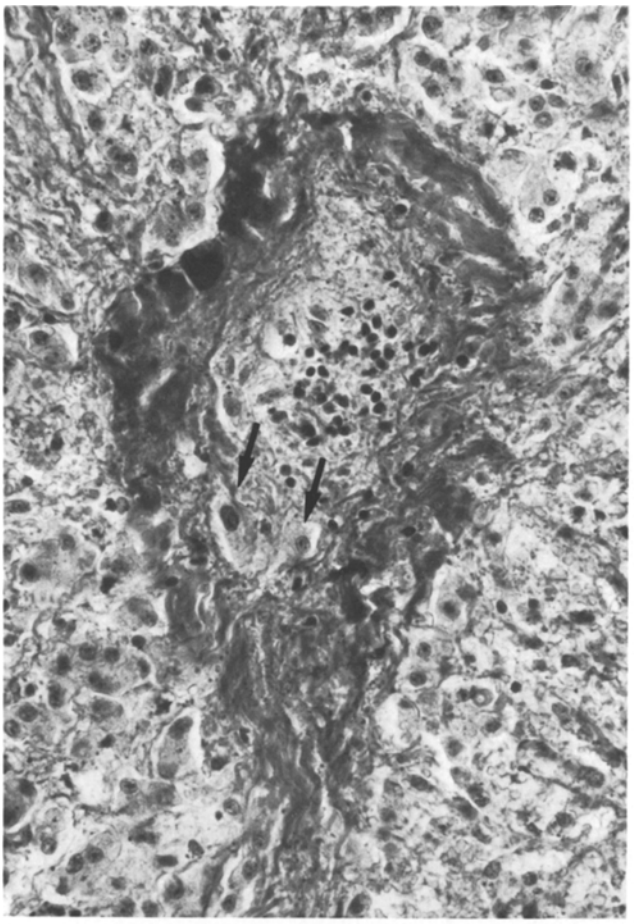

2b

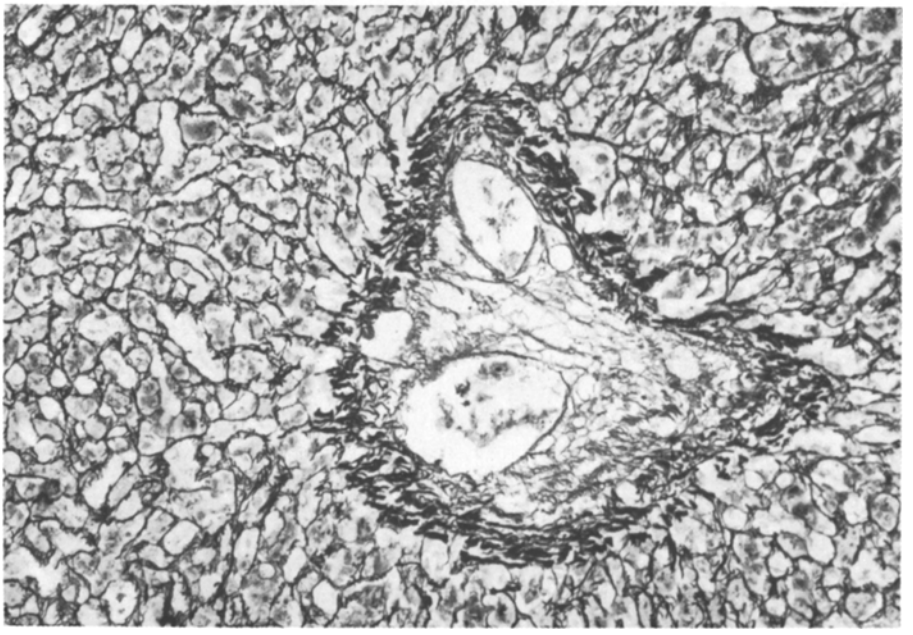

2c

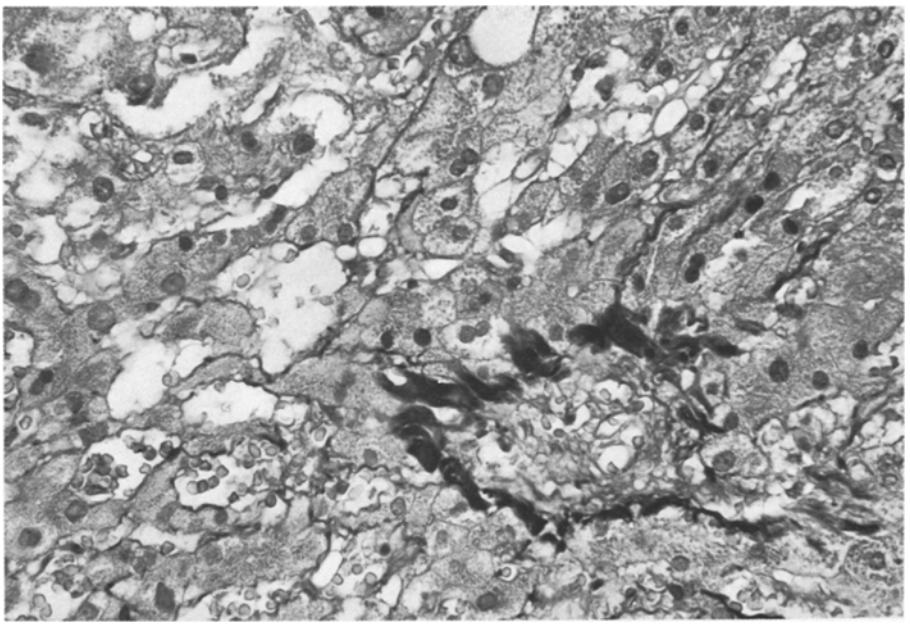

Fig. 3. Subtotal occlusion of a terminal hepatic venule with perivenular hyperaemia and dilatation of sinusoids. (Case 4; van Gieson, × 350)

only a few of these fibers were positive. Only a few cellular elements were seen in the subintimal network, predominantly lymphocytes, macrophages, fibroblasts, and occasionally erythrocytes (Fig. 2). Thrombotic material or fibrin was never demonstrated; there were small amounts of haemosiderin in the subintimal network. Around the narrowed veins and venules there was loss of hepatocytes and massive hyperaemia in sinusoids; in later stages, the reticulin framework of liver cell plates was collapsed with perisinusoidal fibrosis. Small foci of necrotic hepatocytes were occasionally observed. Sometimes, dilated blood filled spaces communicating with sinusoids were found adjacent to occluded venules compatible with peliosis hepatis (Fig. 4). In all autopsied cases, we found a variably pronounced nodular regenerative hyperplasia (Fig. 5): There was a distortion of the lobular architecture by nodules of hyperplastic hepatocytes. These nodules were smaller than the size of a hepatic lobule in case 3 and larger in cases 1 and 2. Furthermore, small clusters of hepatocytes appeared to be "prolapsed" through the collagenous venous wall (Fig. 6); some of the liver cell groups were attached to the subintimal reticular network.

Other histological liver changes were i) mild to moderate portal fibrosis with some cellular infiltration, predominantly of lymphocytes; ii) proliferation of bile ductules; iii) cholestasis, canalicular more than hepatocellular. There was no fatty change. Ground glass hepatocytes were not detectable and the orcein preparation was negative. The microscopical liver findings are summarized in Table 1.

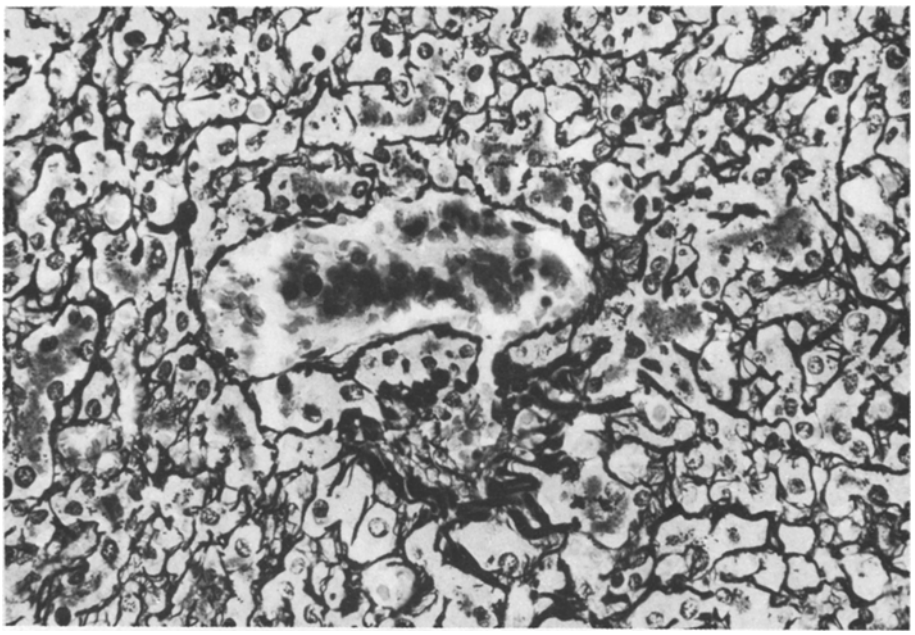

Fig. 4. Partly occluded terminal hepatic venule with an extremely widened sinusoid nearby and perivenular fibrosis. (Case 2; silver impregnation, ×440)

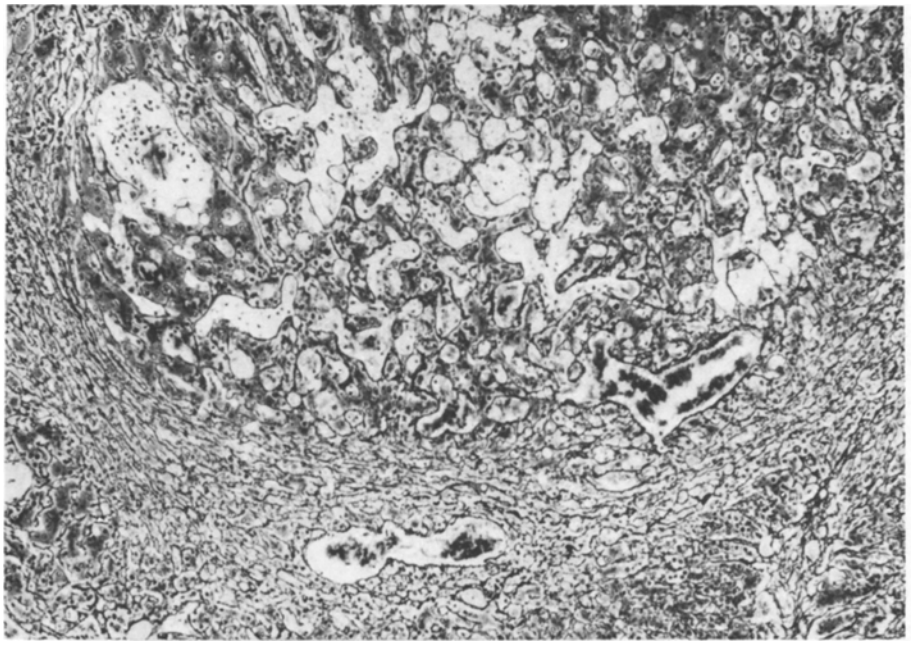

Fig. 5. Nodular regenerative hyperplasia of liver parenchyma with compression of adjacent liver cell plates. Dilated sinusoids in compressed and regenerated parenchyma. (Case 2; silver impregnation, ×87)

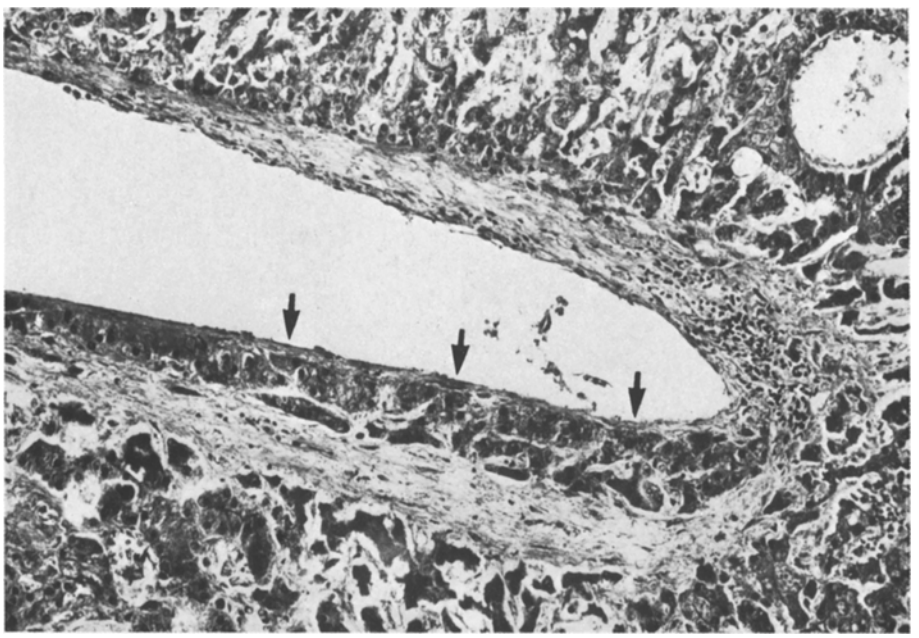

Fig. 6. "Prolapsed" hepatocytes (→) in a sublobular vein between the collagenous venous wall and the endothelial lining. In the venous wall some mononuclear cells. (Case 3; Goldner trichrome, ×140)

Table 1. Summary of the main histological findings in the liver of 4 patients under immunosuppressive therapy

	Case 1	Case 2	Case 3	Case 4
Occlusion in central venules	+++	+	++	+
Occlusion in sublobular veins	+++	(+)	++	(+)
Centrilobular necrosis/atrophy	+++	+	+++	−
Centrilobular hyperaemia	+++	++	++	+++
Nodular regenerative hyperplasia	+	(+)	+++	−
"Prolapse" of hepatocytes	+	(+)	+	−
Peliosis	(+)	(+)	−	−
Cholestasis	++	++	(+)	+
Proliferation of bile ductuli	−	++	++	−

(+)=very slight; + =mild; ++=moderate; +++=severe; − =absent

Discussion

After 8–22 months of immunosuppressive therapy with azathioprine and prednisolone, the 4 patients developed a cholestatic syndrome, improving in only one patient (case 4) after early withdrawal of azathioprine. 2–8 months following the first signs of cholestasis, all cases had morphological liver changes corresponding to the classical description of the acute to subacute form of VOD

(Bras et al. 1954). Two of the patients (cases 1 and 3) with severe obliterative lesions in hepatic venules and small veins had ascites and showed signs of hepatic failure. Case 2 had a progressive cholestatic syndrome, but died from intercurrent disease; the biopsy in case 4 revealed only slight occlusive changes which apparently subsided and were no longer seen in a control biopsy after 19 months. Unlike classical VOD (Bras et al. 1954; Stuart and Bras 1957), the VOD following renal or bone marrow transplantation is often accompanied by a cholestatic syndrome, with high bilirubin levels in most lethal cases (Woods et al. 1980; Berk et al. 1979; Jacobs et al. 1979; Shulman et al. 1980; Marubbio and Danielson 1975).

Though many late deaths after renal transplantation are attributed to liver disease (Ware et al. 1979), only rare cases of renal transplant recipients with VOD have been reported. One case comparable to our lethal cases has been seen by Marubbio and Danielson (1975). Degott et al. (1978) observed VOD-like changes in some centrilobular veins in 4 patients; however, peliosis hepatis was the predominant lesion in this series of 12 renal transplant recipients. Similar peliotic changes have also been seen in experimental VOD (McLean 1970). Hence the peliotic changes may be attributable to the VOD caused blockade of hepatic blood outflow, as was supposed by Degott et al. (1978). In 2 cases of idiopathic portal hypertension after renal transplantation Nataf et al. (1979) observed a slight perisinusoidal fibrosis which the authors suggested as a possible explanation for the portal hypertension; occlusive venous changes were not seen. Here it has to be mentioned that the diagnosis of VOD might not be made from a needle biopsy if no occluded centrilobular or sublobular vein is included (Berk et al. 1979).

A morphologically different type of obliterative disease of hepatic veins with angiomatoid proliferation of endothelium has been reported after cytotoxic therapy of leukaemia in a three month old infant (Burkhardt and Klöppel 1977).

Among the obliterative lesions of the hepatic outflow tract, Budd-Chiari's syndrome should not be confused with hepatic VOD morphologically though both present similar symptoms (predominantly hepatomegaly and ascites). Budd-Chiari's syndrome is defined as an occlusion of the main hepatic veins or their ostia and is generally the result of thrombosis. Some drugs have been associated with VOD erroneously (Asbury et al. 1980) when they are, in fact, associated with Budd-Chiari's syndrome. However, in some cases of otherwise typical Budd-Chiari's syndrome there may be obliterative non-thrombotic lesions in small hepatic veins, as Coronini and Oberson demonstrated already in 1936.

Our three autopsied cases showed a nodular hyperplasia of hepatocytes with distortion of the hepatic lobular architecture, but without cirrhosis (Fig. 5). This condition, called nodular regenerative hyperplasia by Steiner (1959) a widely accepted term, has been reported in patients with rheumatoid arthritis, Felty's syndrome, CRST syndrome (calcinosis cutis, Raynaud's phenomenon, sclerodactyly, and teleangiectasia), myeloproliferative disorders, extrahepatic neoplasms, endocrine disorders, and other diseases with immune dysfunction (Stromeyer and Ishak 1981). Some of these patients have received steroid, antineoplastic, or immunosuppressive therapy. There is one patient in the large series of Stro-

meyer and Ishak (1981) comparable to our cases 1 and 3 who had had a renal transplantation and longterm immunosuppressive therapy, and died of hepatic failure; however, veno-occlusive alterations were not observed in this case.

Another alteration in 3 of our cases, associated with nodular regenerative hyperplasia, was "prolapse" of hepatocytes into centrilobular and sublobular veins (Fig. 6). This prolapse has been reported during longterm methyltestosterone therapy (Paradinas et al. 1977); the authors assumed a relationship between foci of hyperplasia of liver cells and prolapse of hepatocytes into small veins. Another explanation might be embolization of disrupted hepatocytes into damaged central veins (Shulman et al. 1980).

Apart from pyrrolizidine – a well known causative agent – the aetiology of hepatic VOD is obscure. It has been seen after irradiation of the liver (Reed and Cox 1966; Ogata et al. 1963; Lewin and Millis 1973; Fajardo and Colby 1980), after irradiation combined with alkylating agents (Scott et al. 1962), after cytotoxic therapy of various malignancies (Meacham et al. 1952; Brodsky et al. 1961; Griner et al. 1976), in association with allo- and syngeneic bone marrow transplantation (Woods et al. 1980; Berk et al. 1979; Jacobs et al. 1979; Beschorner et al. 1979; Shulman et al. 1980), and after immunosuppressive treatment following renal transplantation (Marubbio and Danielson 1975; Degott et al. 1978). After allogeneic bone marrow transplantation, an association of VOD with graft-versus-host disease has been surmised (Berk et al. 1979), but this association has been rejected by others (Woods et al. 1980; Beschorner et al. 1979; Shulman et al. 1980). Shulman et al. (1980) observed a strong statistical correlation between VOD and chemoradiotherapy given for pretransplant conditioning, especially after dimethylbusulfan. In various case reports, urethane (Meacham et al. 1952; Brodsky et al. 1961), azathioprine (Marubbio and Danielson 1975; Degott et al. 1978), busulfan (Beschorner et al. 1979; Shulman et al. 1980), 6-thioguanine and cytosine arabinoside (Griner et al. 1976) have been incriminated. All these drugs have an antimetabolic and/or immunosuppressive effect. Our findings support the previous conjecture of Marubbio and Danielson (1975) that azathioprine might be the cause of the liver alterations in our cases while a fortuitous association of renal transplantation and VOD seems very unlikely. Most antineoplastic drugs and also azathioprine are converted in the liver to active metabolites; this is also true for pyrrolizidine alkaloids which are metabolised to pyrrol derivatives (McLean 1970). An increasing concentration of these active and obviously toxic metabolites in the pericentral sinusoids and small hepatic veins may explain the localization of damage in VOD. However, the real underlying mechanism remains unknown.

Experimental and ultrastructural studies on the pathogenesis of the venous occlusion (Allen et al. 1969; Brooks et al. 1970; McLean 1970) revealed haemorrhagic centrilobular necrosis of hepatocytes, a blockade of sinusoids by columns of red cells with extravasation, and fragmentation and necrosis of endothelium in sinusoids and small hepatic veins; recent light and electron-microscopical studies demonstrated focal fibrin deposition in central veins or centrilobular sinusoids after radiation injury of the liver (Fajardo and Colby 1980). Subsequently there was an increase in fibrous connective tissue in vein walls, eventually with recanalisation or obstruction of the veins. Obviously, in human VOD

there is often no widespread necrosis of hepatocytes in the early phase (Bras et al. 1954; Stuart and Bras 1957; Brooks et al. 1970), with only slight elevation of serum aminotransferases. Later, the liver reveals perisinusoidal fibrosis and because of the blockade of hepatic blood outflow, a gradual loss of hepatocytes occurs, predominantly in the centrilobular region. These alterations may be followed in some cases by regeneration of hepatocytes with partial nodular transformation, and by sinusoidal dilatation and peliosis hepatis.

To date, no predisposing factors are known to define those patients who are at risk of developing VOD under immunosuppressive and/or cytotoxic therapy. Abnormal liver tests before chemoradiotherapy may be significant (Shulman et al. 1980). We suggest that a liver biopsy should be done if there are signs of liver damage in these patients, especially with biochemical evidence of cholestasis, hepatomegaly, or ascites. If the microscopical examination reveals centrilobular haemorrhage and/or necrosis one should search for veno-occlusive lesions with appropriate staining (Berk et al. 1979). When the diagnosis VOD has been established the prompt discontinuation of azathioprine has to be considered. In our cases the VOD improved only in case 4 when azathioprine was discontinued one month after the first signs of cholestasis; however, in the other patients, possibly due to the more advanced stage of the disease, withdrawal of the drug no longer achieved any significant clinical or morphological improvement. A possible protective effect of anticoagulation on the development of VOD is questionable. While in case 4 the clinical improvement coincided with anticoagulation and withdrawal of azathioprine, in case 3 VOD developed despite longterm anticoagulation. In radiation hepatitis, a protective effect of anticoagulation has been suggested (Lightdale et al. 1979).

References

Allen JR, Carstens LA, Katagiri GJ (1969) Hepatic veins of monkey with veno-occlusive disease. Arch Pathol 87:279–289

Asbury RF, Rosenthal SN, Descalzi ME et al. (1980) Hepatic veno-occlusive disease due to DTIC. Cancer 45:2670–2674

Berk PD, Popper H, Krueger GRF et al. (1979) Veno-occlusive disease of the liver after allogeneic bone marrow transplantation. Ann Intern Med 90:158–164

Beschorner WE, Pino JL, Boitnott JK, Santos GW (1979) Liver pathology following bone marrow transplantation. Lab Invest 40:241 (Abstract)

Bras G, Jelliffe DB, Stuart KL (1954) Veno-occlusive disease of liver with nonportal type of cirrhosis, occuring in Jamaica. Arch Pathol 57:285–300

Brodsky I, Johnson H, Killmann S-A, Cronkite EP (1961) Fibrosis of central and hepatic veins, and perisinusoidal spaces of the liver following prolonged administration of urethane. Am J Med 30:976–980

Brooks SEH, Miller CG, McKenzie et al. (1970) Acute veno-occlusive disease of the liver. Arch Pathol 89:507–520

Burkhardt A, Klöppel G (1977) Unusual obliterative disease of the hepatic veins in an infant. Virchows Arch [Pathol Anat] 375:225–232

Coronini C, Oberson G (1936) Neue histologische Ergebnisse bei Endophlebitis obliterans hepatica. Virchows Arch [Pathol Anat] 298:251–297

Degott C, Rueff B, Kreis H et al. (1978) Peliosis hepatis in recipients of renal transplants. Gut 19:748–753

Fajardo LF, Colby TV (1980) Pathogenesis of veno-occlusive liver disease after radiation. Arch Pathol 104:584–588

Griner PF, Elbadawi A, Packman CH (1976) Veno-occlusive disease of the liver after chemotherapy of acute leukemia. Ann Intern Med 85:578–582

Jacobs P, Miller JL, Uys CJ, Dietrich BE (1979) Fatal veno-occlusive disease of the liver after chemotherapy, whole-body irradiation and bone marrow transplantation for refractory acute leukaemia. S Afr Med J 55:5–10

Lewin K, Millis RR (1973) Human radiation hepatitis. Arch Pathol 96:21–26

Lightdale CJ, Wasser J, Coleman M et al. (1979) Anticoagulation and high dose liver radiation. Cancer 43:174–181

Marubbio AT, Danielson B (1975) Hepatic veno-occlusive disease in a renal transplant patient receiving azathioprine. Gastroenterology 69:739–743

McLean EK (1970) The toxic actions of pyrrolizidine (Senecio) alkaloids. Pharmacol Rev 22:429–483

Meacham GC, Tillotson FW, Heinle RW (1952) Liver damage after prolonged urethane therapy. Am J Clin Pathol 22:22–27

Nataf C, Feldmann G, Lebrec D et al. (1979) Idiopathic portal hypertension (perisinusoidal fibrosis) after renal transplantation. Gut 20:531–537

Ogata K, Hizawa K, Yoshida M et al. (1963) Hepatic injury following irradiation – a morphologic study. Tokushima J Exp Med 9:240–251

Paradinas FJ, Bull TB, Westaby D, Murray-Lyon IM (1977) Hyperplasia and prolapse of hepatocytes into hepatic veins during longterm methyltestosterone therapy: possible relationships of these changes to the development of peliosis hepatis and liver tumours. Histopathology 1:225–246

Reed GB, Cox AJ (1966) The human liver after radiation injury. Am J Pathol 48:597–611

Scott RB, Budinger JM, Prendergast RAM, Nydick I (1962) Hepatic veno-occlusive syndrome in an American adult. Gastroenterology 42:631–636

Shulman HM, McDonald GB, Matthews D et al. (1980) An analysis of hepatic venocclusive disease and centrilobular hepatic degeneration following bone marrow transplantation. Gastroenterology 79:1178–1191

Steiner PE (1959) Nodular regenerative hyperplasia of the liver. Am J Pathol 35:943–953

Stromeyer FW, Ishak KG (1981) Nodular transformation (nodular "regenerative" hyperplasia) of the liver. Human Pathol 12:60–71

Stuart KL, Bras G (1957) Veno-occlusive disease of the liver. Q J Med 26:291–315

Ware AJ, Luby JP, Hollinger B (1979) Etiology of liver disease in renal transplant recipients. Ann Intern Med 91:364–371

Woods WG, Dehner LP, Nesbit ME et al. (1980) Fatal veno-occlusive disease of the liver following high dose chemotherapy, irradiation and bone marrow transplantation. Am J Med 68:285–290

Accepted December 18, 1981

Virchows Arch [Pathol Anat] (1982) 395:257–271

Virchows Archiv A

Histiocytic Necrotizing Lymphadenitis Without Granulocytic Infiltration*

S. Pileri**, M. Kikuchi***, Dagmar Helbron, and K. Lennert
Lymph Node Registry, Institute of Pathology, Christian Albrecht University, Hospitalstraße 42, D-2300 Kiel, Federal Republic of Germany

Summary. Twenty-seven cases of an unusual necrotizing lymphadenitis previously described only in Japan are reported as occurring in West Germany (23 cases), Iran (1 case), Italy (1 case), Korea (1 case) and Spain (1 case). The lesion frequently develops in the cervical lymph nodes of young women. It is characterized by infiltration of the cortex and/or paracortex by large collections of proliferating histiocytes and is devoid of granulocytes. Complete or, more often, incomplete necrosis of lymphoid tissue is seen in all cases. In cases with incomplete necrosis, the histiocytes are interspersed with pyknotic cells and nuclear debris. Based on the histological findings, the term "histiocytic necrotizing lymphadenitis without granulocytic infiltration" is proposed. Lesions to be considered in a differential diagnosis are malignant histiocytic neoplasms and necrotizing lymphadenitis with granulocytic infiltration, which is seen in lupus erythematosus and bacterial infections. The aetiology of histiocytic necrotizing lymphadenitis without granulocytic infiltration is still unclear. Some clinical and histological features indicate the possibility of an underlying viral infection.

Key words: Necrotizing lymphadenitis – Histiocytic lymphadenitis – Lupus erythematosus

In 1972, one of the authors (M.K.) described an unusual "lymphadenitis showing focal reticulum cell hyperplasia, with nuclear debris and phagocytes", which was usually found in cervical lymph nodes of young women and showed an excellent prognosis. At about the same time, similar lesions were reported by Fujimoto et al. (1972) as "cervical subacute necrotizing lymphadenitis". Since

* This study was supported by the Kind-Philipp-Stiftung

** Present address: Istituto di Anatomia e Istologia Patologica, Policlinico S. Orsola, Bologna, Italy

*** Present address: Department of Pathology, Fukuoka University School of Medicine, Nishiku, Nanakuma 34, Fukuoka 814-01, Japan

Offprint requests to: K. Lennert at the above address

0340-1227/82/0395/0257/$03.00

then, about 380 examples of the lesion occurring only in Japanese patients have been published under several different names, viz.: "necrotizing lymphadenitis" (Wakasa et al. 1975, 1978; Kikuchi et al. 1977), "necrotizing histiocytic lymphadenitis" (Shimamine et al. 1974), "phagocytic necrotizing lymphadenitis" (Kikuchi and Uryu 1976), "focal histiocytic necrotizing lymphadenitis" (Kikuchi 1978) and "pseudolymphomatous hyperplasia in lymph nodes" (Michaeleck 1977). According to the observers, the lesion might be a new entity, because it shows special clinicopathological features.

Clinically, the lesion often appears as lymphadenopathy in the neck; the enlarged nodes are painful. Manifestation in sites other than the cervical region and generalized lymphadenopathy are less common. Fever and leukopenia are observed frequently. The prognosis is always excellent, and many patients recover without treatment.

Histological examination of involved lymph nodes reveals partial effacement of the architecture and the presence of foci of proliferating and infiltrating cells in the cortex and/or paracortex. The foci are composed of histiocytes interspersed with small lymphocytes, immunoblasts and only a few plasma cells. Regressive changes, such as nuclear debris or marked tissue necrosis, are always observed. Neutrophils and eosinophils have not been found in any case, with very few exceptions.

The aetiology of the lesion is still unclear. It has been suggested that some cases might be due to a toxoplasmic infection (Kikuchi et al. 1977; Kikuchi 1978), but this has not been confirmed.

The aim of the present study was to determine whether the lesion occurs outside Japan. The collection of the Lymph Node Registry in Kiel (FRG) was reviewed and was found to contain 27 examples of the lesion.

Materials and Methods

In a 10-year period (1970–1979), 164 cases of necrotizing lymphadenitis and 579 cases of hyperimmune reaction had been collected at the Lymph Node Registry. These cases were reviewed and found to include 40 cases showing lesions resembling the ones described in Japan. Paraffin blocks of formalin-fixed tissue were available in all but two cases. New sections were prepared and stained with the following methods: haematoxylin and eosin (H & E), Giemsa, periodic acid Schiff (PAS), silver impregnation (Gomori), Goldner and naphthol-AS-D-chloroacetate esterase.

Immunohistological analyses were also performed with the PAP method described by Mepham et al. (1979). Briefly, after inhibition of endogenous peroxidase activity with 0.3% H_2O_2 in methanol for 30 min, dewaxed paraffin sections were pretreated with fresh 0.1% trypsin solution in 0.4% calcium chloride (pH 7.8) at 37° C for 30 min. After two 10 min washes in PBS, the sections were incubated with non-immune swine serum (diluted 1:5) for 10 min. Antisera were then applied in the following sequence: specific rabbit antiserum, swine anti-rabbit IgG serum, rabbit PAP complexes; each of these stages lasted 30 min and was followed by a wash in PBS. Peroxidase activity was demonstrated with the 3,3′-diaminobenzidine tetrahydrochloride (Fluka 32750) reaction described by Graham and Karnovsky (1966). The sections were counterstained with haemalum and mounted with Eukitt (Kindler, Freiburg, FRG). In the present investigation, the following antisera were employed: (1) rabbit anti-human κ (Dako 10-9K2), diluted 1:300 with PBS, pH 7.4, (2) rabbit anti-human λ (Dako 10-9L2), diluted 1:300 with PBS, pH 7.4, (3) rabbit anti-human lysozyme (Dako 10-099), diluted 1:100 with PBS, pH 7.4, (4) rabbit anti-human albumin (Dako 10-001), diluted 1:100 with PBS, pH 7.4, (5) swine anti-rabbit IgG (Dako 21-090), diluted 1:50 with PBS, pH 7.4, and (6) rabbit PAP complexes (Dako Z113), diluted 1:100 with PBS, pH 7.4.

Clinical data were collected by sending a questionnaire to the physician or hospital caring for each patient at the time of biopsy.

Results

Of the 743 cases reviewed, 40 cases had been diagnosed as "lymphadenitis as described by Kikuchi". These cases showed more or less extensive infiltration of the cortex and/or paracortex by histiocytes and lymphoid cells, associated with varying degrees of necrosis. Evaluation of the content of neutrophils indicated, however, that the lesions could be divided into two groups: those with and those without granulocytic infiltration. Based on the clinical findings, it was evident that only the lesions without granulocytic infiltration corresponded to the lesion described by Kikuchi (1972 and 1978; Kikuchi and Uryu 1976; Kikuchi et al. 1977); the cases with granulocytic infiltration showed completely different clinical features.

Group of Lesions Without Granulocytic Infiltration

There were 27 cases in this group. *Histologically* (Table 1), they were characterized by partial or almost complete effacement of the lymph node architecture, which was replaced by one or several large collections of infiltrating and proliferating cells, usually located in the pulp of the cortex and/or paracortex (Fig. 1). The infiltrating and proliferating cells looked gray with Giemsa staining and were mostly histiocytes (Figs. 2, 3a and b). These cells showed phagocytic activity and a strong reaction for lysozyme (Figs. 3c and 4). They were interspersed with numerous small lymphocytes, which often showed twisted nuclei. There were also medium-sized lymphoid cells with sparse gray cytoplasm (possibly so called T-associated plasma cells), a few plasma cells and a variable number of immunoblasts, which were usually negative for both κ and λ chains.

Necrotic changes were found in all cases. These mainly consisted of pyknotic, small or medium-sized cells with oxyphilic cytoplasm and nuclear debris (Fig. 3a

Table 1. Histological findings in 27 cases of histiocytic necrotizing lymphadenitis without granulocytic infiltration

Constant findings
Focal infiltration of the cortex and/or paracortex by proliferating histiocytes interspersed with small lymphocytes, medium-sized lymphoid cells and T immunoblasts
Necrotic changes, ranging from single pyknotic cells to extensive tissue necrosis
Absence of granulocytes
Marked phagocytotic activity
Low content of plasma cells and B immunoblasts
Variable number of mitotic figures
Hyperplasia of the pulp in portions spared by necrosis
Remnants of sinuses
Facultative findings
Capsulitis and pericapsulitis (96%)
Expansion of capsule (38%)
"Immature sinus histiocytosis" (30%)
Fibrin thrombi (24%)
Small collections of foamy cells (17%)
Foci of so called T-associated plasma cells (14%)
Germinal centres (7.5%)

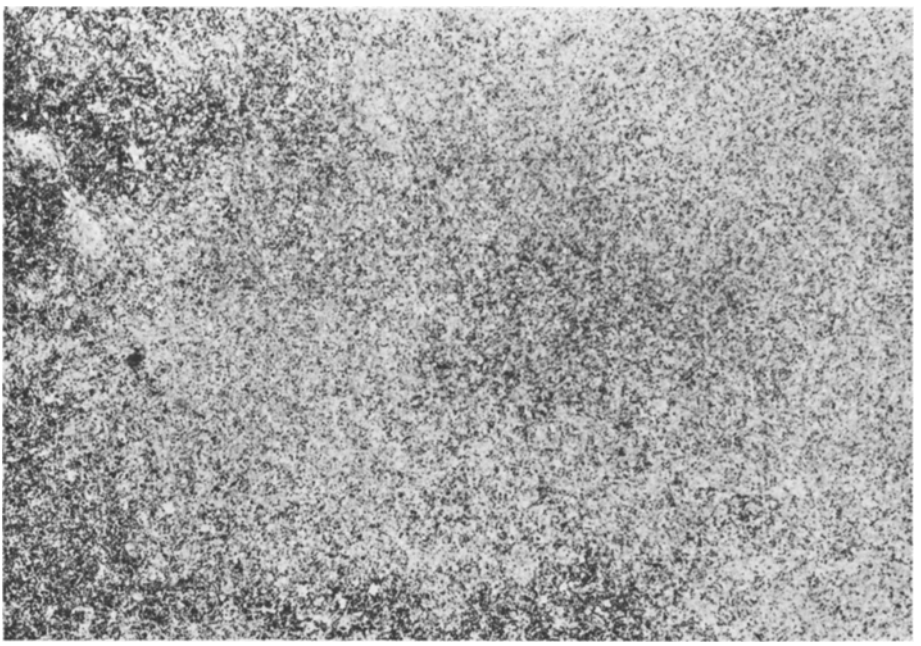

Fig. 1. Large area showing necrobiosis and many histiocytes. Giemsa × 56

and b), with or without complete tissue necrosis (Fig. 5). When examined at a low magnification, Giemsa-stained sections from the cases with more extensive tissue necrosis showed a pink area surrounded by a mass of medium-sized gray cells. In areas of incomplete necrosis, there was a marked increase in the number of small vessels and argyrophilic fibres (Fig. 6). Areas of complete necrosis contained only a few recognizable fibres. The number of mitotic figures varied from few to many; they were found mainly among the histiocytes surrounding necrotic areas, but also in parts of the pulp farther away from the necrosis. In some cases, we found occasional fibrin thrombi, rare nuclear shadows, small collections of foamy cells (Fig. 7) and foci of so-called T-associated plasma cells (Müller-Hermelink and Lennert 1978).

In portions of lymph nodes spared by necrosis, the main change was hyperplasia of the pulp, with numerous epithelioid venules and a "mottled" appearance (Fig. 8). The latter was due chiefly to the presence of numerous reticulum cells scattered among small lymphocytes. The reticulum cells were identifiable as interdigitating reticulum cells because of their negative reaction for lysozyme. Most cases showed no, or only a few residual follicles. In 2 cases, however, there were several germinal centres in the second or third phase of development (Müller-Hermelink and Lennert 1978). The sinuses were largely preserved in all cases. In eight cases, however, features of so-called immature sinus histiocytosis (Lennert 1959) could be recognized. The capsule of the lymph nodes was focally or heavily infiltrated by lymphocytes in all but one case and showed expansion in 11 cases.

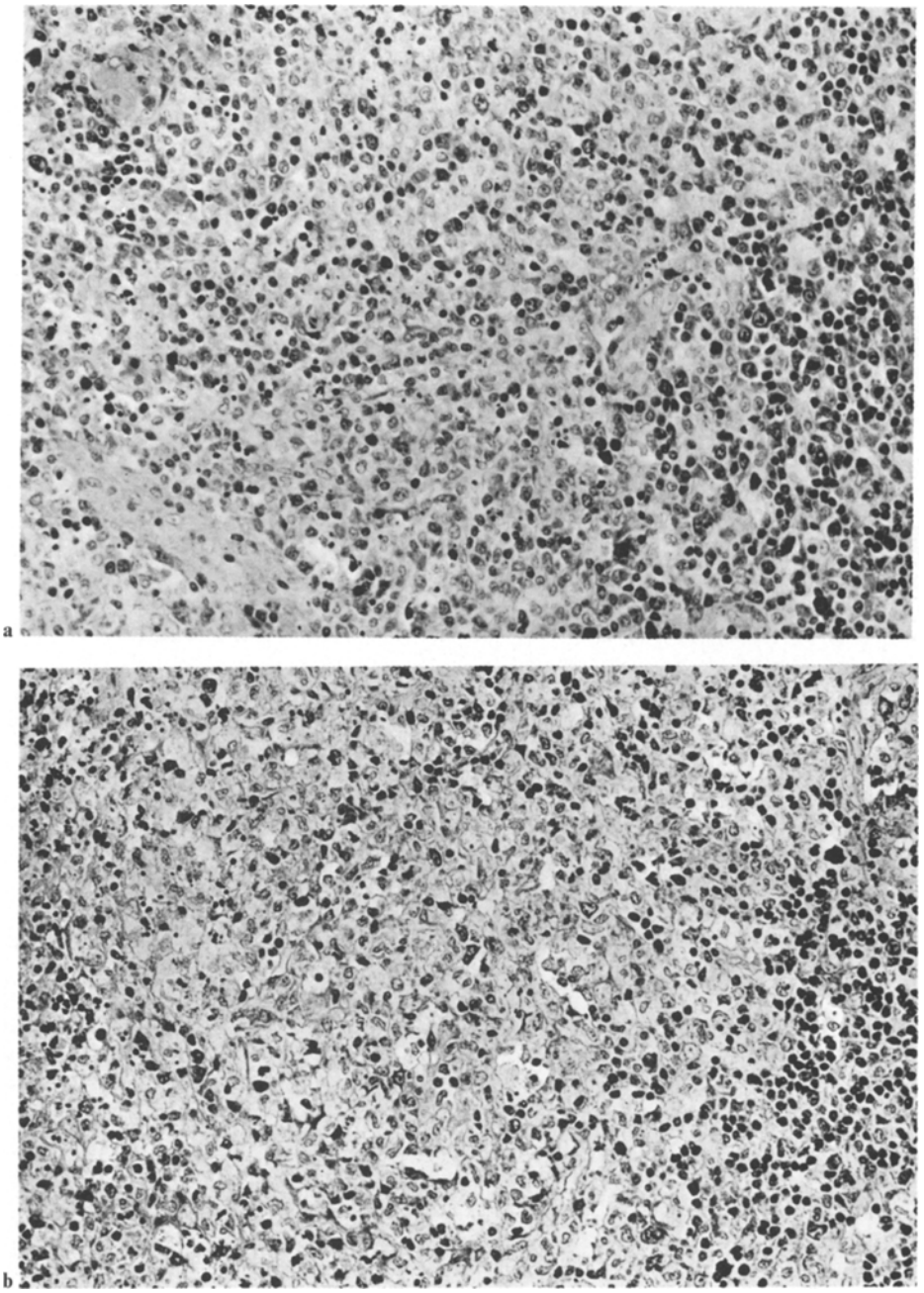

Fig. 2a, b. Two different areas of necrobiosis of the same lymph node. The adjoining lymphocyte-rich pulp is visible in the lower right corner of each photomicrograph. Giemsa ×280

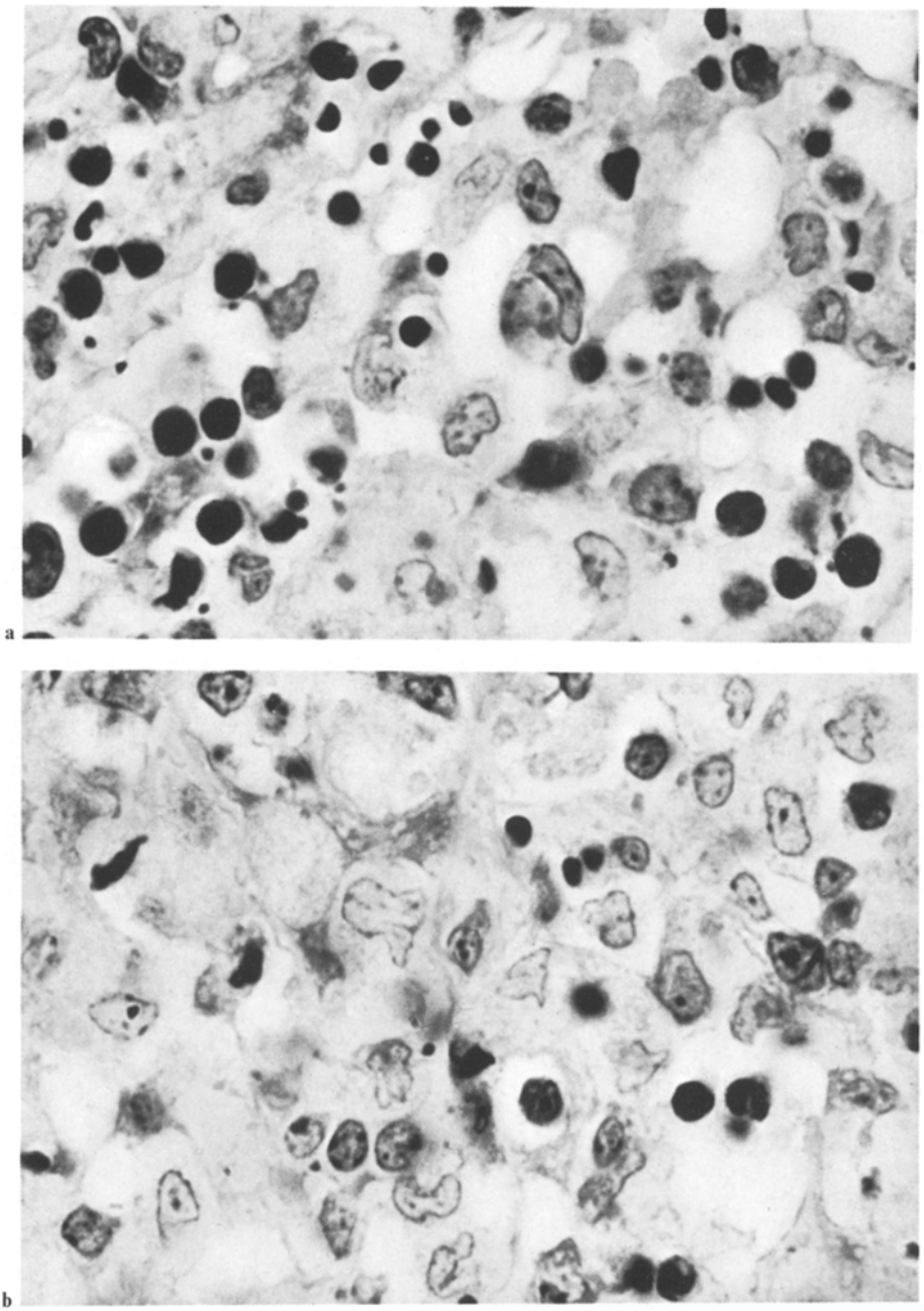

Fig. 3a–c. Three different areas of necrobiosis of the same lymph node as in Fig. 2. *a* Some histiocytes and many pyknotic cells. Giemsa ×1,350. *b* Many histiocytes and a few pyknotic cells. Giemsa ×1,350. *c* Lysozyme-positive histiocytes are intermingled with many medium-sized lymphoid cells devoid of lysozyme activity. PAP immunostaining ×1,350

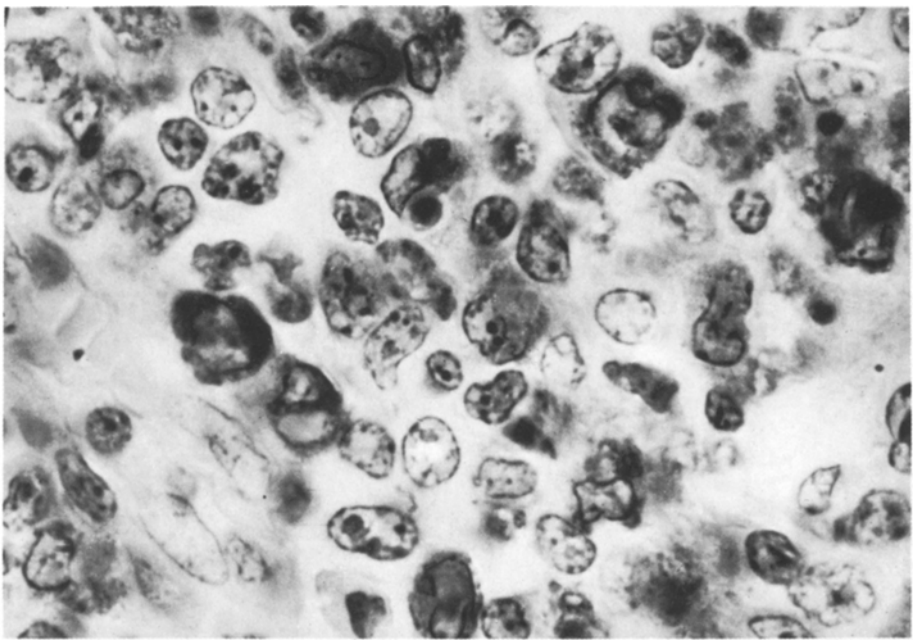

c

Fig. 3c

Clinically (Table 2), the lesion presented as lymphadenopathy, usually localized in the cervical region. Most patients were young women working in small communities (schools, kindergartens, hospitals, banks, etc.). Tonsillectomy was recorded in the past medical history of 11 patients. One patient had diabetes mellitus. In another patient, the response of peripheral lymphocytes to PHA stimulation was reduced. Twenty-three patients were born and living in West Germany, one in Iran, one in Italy, one in Korea and one in Spain. Six patients showed enlargement of solitary lymph nodes at sites other than the cervical region and six showed generalized lymphadenopathy.

The enlarged nodes were reported to vary in size (bean- to plum-sized) and consistency. On palpation, they were painful in nine of 17 patients. Fever was reported in 11 of 22 cases, hepatomegaly in four of 21 and splenomegaly in two of 21. Fifteen of 21 patients showed an elevated ESR. Leukocytosis, leukopenia and elevated α_2- or γ-globulins were less common. Serological tests for toxoplasmosis and infectious mononucleosis were negative in all cases tested.

Follow-up data were available in 14 cases. The prognosis was excellent in all cases, and a majority of the patients recovered without treatment. One patient received chemo- and radiotherapy, because "histiocytic malignant lymphoma" had been diagnosed elsewhere.

Group of Lesions With Granulocytic Infiltration

Granulocytic infiltration was found in 13 cases. The clinical data are summarized in Table 3. Clinical evidence of lupus erythematosus was reported in five cases,

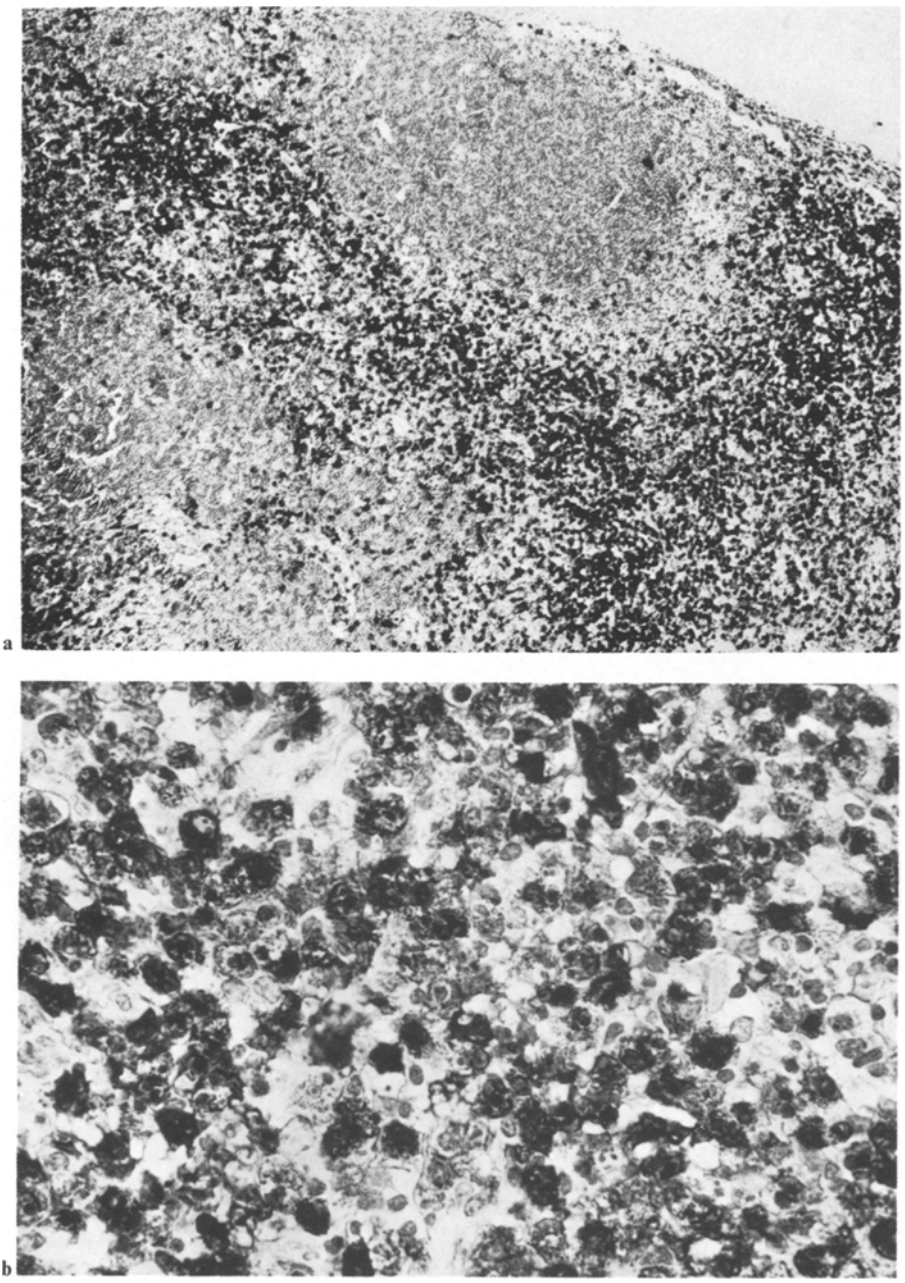

Fig. 4. **a** Large confluent areas of histiocytes in the pulp of cortex and paracortex (dark-staining cells). Remnants of the cortex and paracortex can be recognized. PAP immunostaining for lysozyme ×80. **b** Histiocytes showing a strong reaction for lysozyme. PAP immunostaining for lysozyme ×400

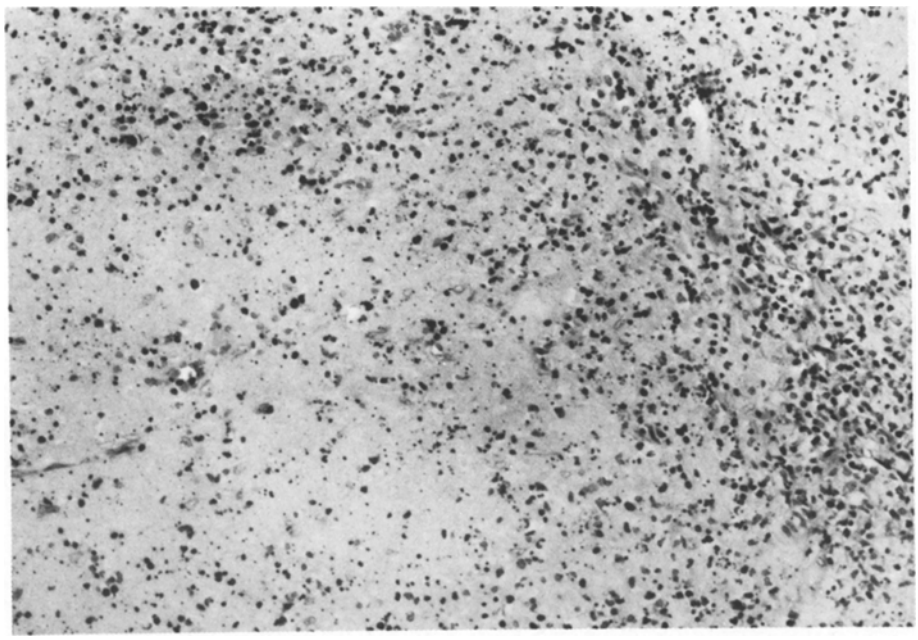

Fig. 5. Extensive tissue necrosis. Giemsa ×80

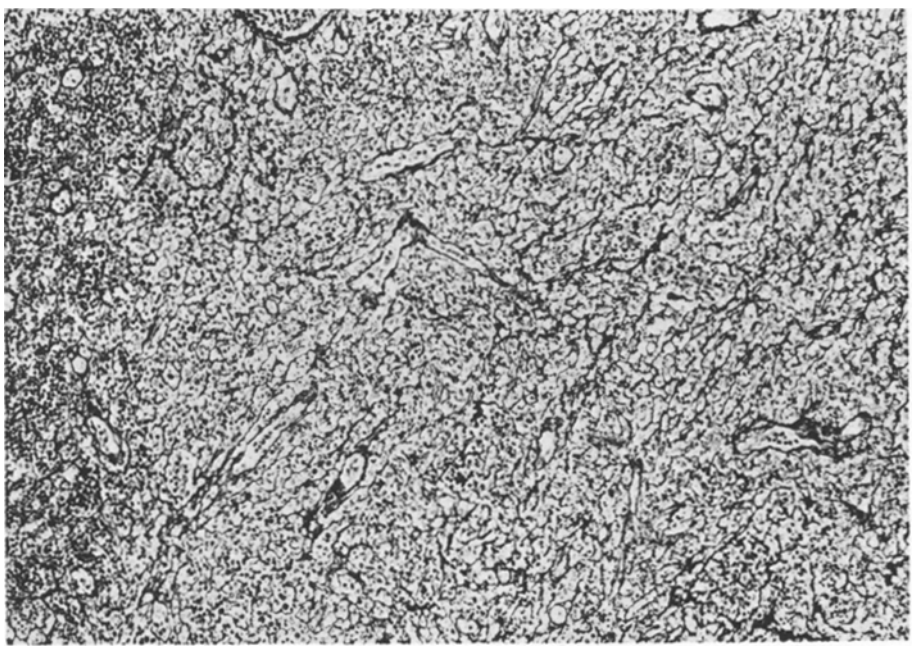

Fig. 6. The same lymph node as in Figs. 2 and 3 with silver impregnation. Many fibres and small vessels are visible. Gomori ×112

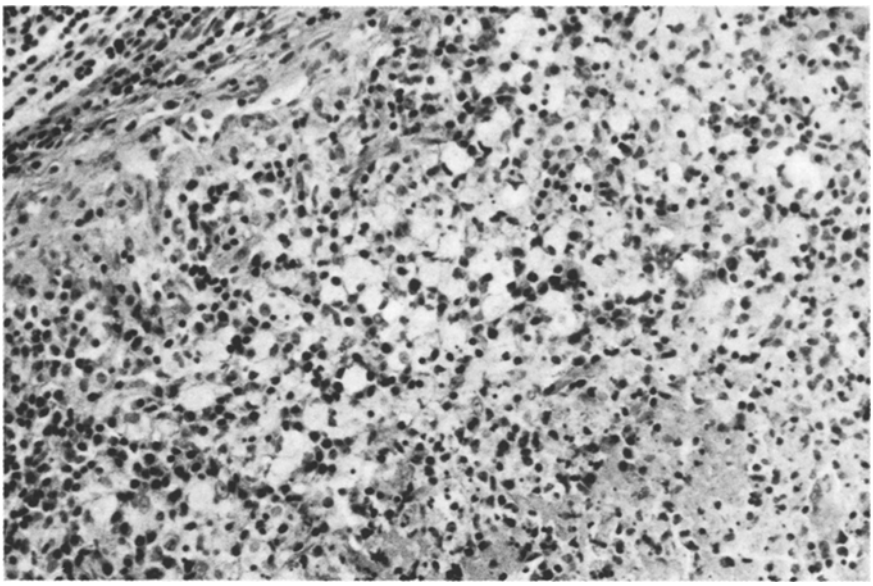

Fig. 7. Focus of foamy cells at the margin of a necrotic area. H & E ×250

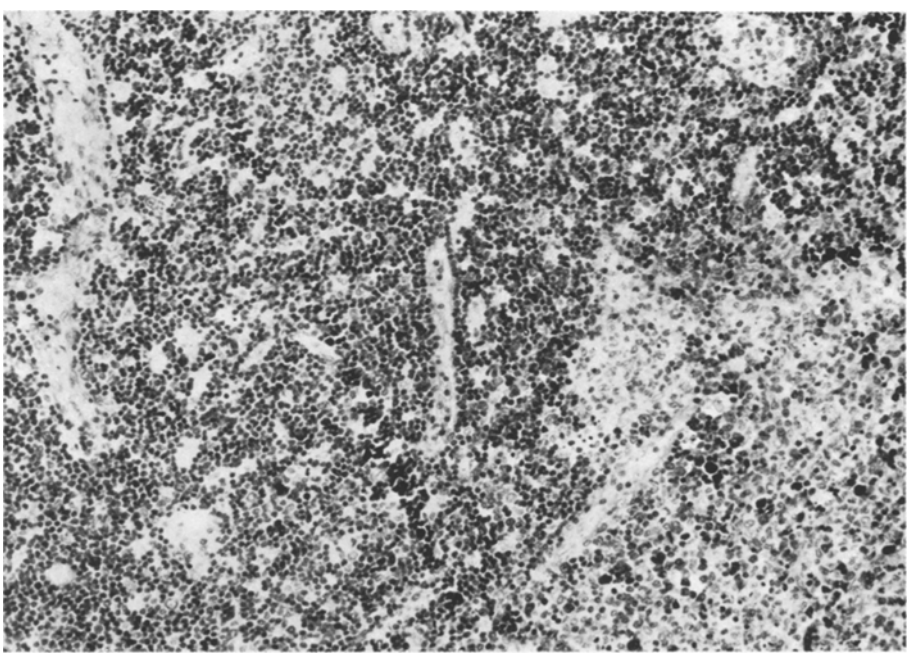

Fig. 8. The pulp next to a necrotic area shows hyperplasia with a mottled appearance and numerous epithelioid venules. The necrotic area in the lower right corner contains many histiocytes. Giemsa ×80

Table 2. Clinical findings in 27 cases of histiocytic necrotizing lymphadenitis without granulocytic infiltration

Age: range: 10–48 years, mean: 26.6 years	
Sex ratio: ♂:♀=1:2.85	
Nationality: German (23), Iranian (1), Italian (1), Korean (1), Spanish (1)	
Past medical history: Tonsillectomy was recorded in 11 cases	
Lymphadenopathy	
Site	
Cervical	10 (3 bilateral)
Axillary	3 (1 bilateral)
Inguinal	2
Cervical + axillary + supraclavicular	2
Cervical + axillary	2
Cervical + supraclavicular	1
Supraclavicular	1
Generalized	6
Size	
Bean-sized	8/21
Cherry-sized	10/21
Plum-sized	3/21
Consistency	
Hard	6/19
Medium	5/19
Soft	8/19
Pain	9/17
Signs and symptoms	
Fever	11/22
Hepatomegaly	4/21
Splenomegaly	2/21
Laboratory findings	
Leukocytosis (>10,000 WBC/μl)	1/20
Leukopenia (<4,000 WBC/μl)	5/20
ESR elevated (20–100)	15/21
α_2-Globulins elevated	6/13
γ-Globulins elevated	4/13
Serological tests	
Toxoplasmosis, negative	10/10
Mononucleosis, negative	9/10
Autoimmune disease: No evidence in any of 14 patients	
Treatment	
None	9/14
Antibiotic	4/14
Chemo- and radiotherapy	1/14
Prognosis: Data were available in 14 cases. All patients were alive and well 12–126 months after biopsy	

Table 3. Clinical findings in the group with granulocytic infiltration ($n=13$)

Case No.	Age	Sex	Site of lymphadenopathy	Other significant clinical findings
1	23	F	Generalized	Lupus erythematosus
2	24	F	Generalized	Lupus erythematosus
3	27	F	Generalized	Lupus erythematosus
4	38	M	Cervical	Lupus erythematosus
5	72	F	Axillary	Lupus erythematosus
6	22	M	Axillary	Skin abscess in the same region as lymphadenopathy
7	23	F	Generalized	Generalized bacterial disease
8	23	M	Inguinal	Skin abscess in the same region as lymphadenopathy
9	68	M	Peripancreatic	Retroperitoneal abscess 20 days after pancreatectomy
10	27	F	Axillary	High cryoglobulin titres and thrombosis of axillary vein at same site as lymphadenopathy
11	23	F	Cervical	Not available
12	26	M	Cervical	Not available
13	33	M	Generalized	Not available

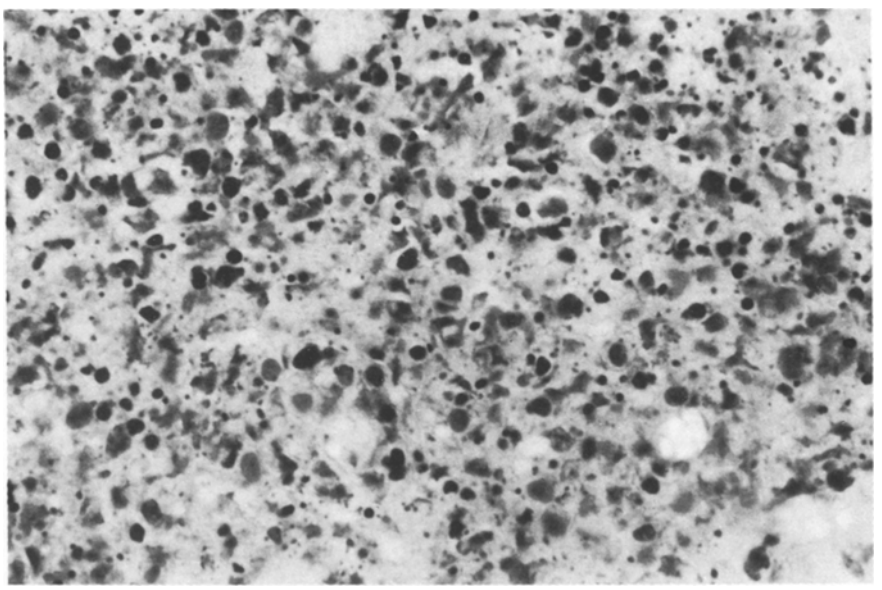

Fig. 9. Necrotizing lymphadenitis in a case with clinical evidence of lupus erythematosus. Many nuclear shadows are seen in addition to pyknotic cells and nuclear debris. Giemsa ×400

generalized or localized bacterial infections in 4 cases and venous thrombosis at the same site as lymphadenopathy in 1 case. In 3 cases, only the age, sex, and site of biopsy were known.

Histological examination revealed that the number of histiocytes and pyknotic cells and the degree of phagocytosis were much lower in these cases than in the group without granulocytic infiltration. The biopsies from the patients with lupus erythematosus showed numerous nuclear "shadows" (Fig. 9)

Table 4. Main histological criteria for differential diagnosis between histiocytic necrotizing lymphadenitis without granulocytic infiltration (HNLWG) and necrotizing lymphadenitis in lupus erythematosus and bacterial infections

	HNLWG	Lupus erythematosus	Bacterial infections
Granulocytes	−	++	++
Nuclear shadows	+/−	++	+/−
Histiocytes	++	+	+
Nuclear debris	++	+	+
Phagocytosis	++	+	+
B immunoblasts	+/−	+	++

in addition to pyknotic cells and cellular debris in the necrotic areas. The biopsies from patients with bacterial infections contained a relatively large number of immunoblasts and plasma cells, which were positive for κ and λ chains. In the case with venous thrombosis at the same site as lymphadenopathy, the lymph node biopsy revealed extensive necrosis of lymphoid tissue, capsule fibrosis, dilatation of the marginal sinus, marked sclerosis of the medullary sinus and thrombosis of the veins around the node. Two of the three cases with incomplete clinical data showed nuclear shadows like those seen in the patients with lupus erythematosus. In the third case, there was a relatively large number of B immunoblasts and plasma cells.

Discussion

Among the cases presented here, the group without granulocytic infiltration represents the first observation of the lesion described by Kikuchi (1972) outside Japan. As in the Japanese reports, a majority of the patients in the present series were young women. The lesion frequently appeared as painful lymphadenopathy in the neck. The prognosis was always excellent, and many patients recovered without treatment. It is noteworthy, however, that generalized lymphadenopathy and enlargement of solitary lymph nodes outside the cervical region were more frequent in our series than in the larger ones reported previously (Kikuchi 1978; Wakasa et al. 1978). In contrast, leukopenia and fever appeared to be somewhat less common in the present series than in Japan.

On histological examination, involved lymph nodes showed varying degrees of necrosis and infiltration by histiocytes phagocytosing necrotic cells in the cortex and/or paracortex. Neutrophils and eosinophils were not found in any case. There was only a small number of plasma cells, and reactive changes were not evident in follicles. Only 2 cases showed moderate follicular hyperplasia; we could not determine whether it was preexistent. These findings are consistent with those previously reported to be characteristic of the lesion in Japan (Fujimoto et al. 1972; Kikuchi 1972, 1978; Wakasa et al. 1975, 1978; Kikuchi and Uryu 1976; Kikuchi et al. 1977). We propose that the lesion be called "histiocytic necrotizing lymphadenitis without granulocytic infiltration", because this term meets all the prerequisites for a histological diagnosis.

The second group of lesions included in the present study demonstrates that changes similar to those observed in histiocytic necrotizing lymphadenitis without granulocytic infiltration may be found in lymph nodes of patients with other diseases, namely, lupus erythematosus and bacterial infections. In such cases, however, the differential diagnosis is easy because of the large number of granulocytes, the moderate to small number of histiocytes, the small amount of nuclear debris and the low phagocytic activity. Futhermore, in lupus erythematosus, a high number of nuclear shadows is seen and in bacterial infections, the content of B immunoblasts and plasma cells is always larger. A similar lesion was also found in a patient with venous thrombosis at the same site as lymphadenopathy. This case showed features resembling those described by Steinmann et al. (1981) in lymph nodes of rabbits after venostasis and lymphostasis. A differential diagnosis was possible, not only because of the large number of granulocytes, but also because of the presence of thrombi in the veins around the involved node, which has never been observed in histiocytic necrotizing lymphadenitis without granulocytic infiltration.

Neoplasms that must be considered in a differential diagnosis are "sarcomas of histiocytic reticulum cells" or malignant histiocytosis. In the present series, a case without granulocytic infiltration had been diagnosed elsewhere as "histiocytic malignant lymphoma". In histiocytic necrotizing lymphadenitis without granulocytic infiltration, however, the histiocytes are more polymorphic, phagocytose more cellular debris (and relatively seldom erythrocytes) and do not show any atypical features.

Definite conclusions as to the aetiology of the lesion cannot be drawn from the present study. Only 10 cases were tested serologically. Toxoplasma gondii has been suspected of being responsible for the disease (Kikuchi et al. 1977; Kikuchi 1978), but all tests for this pathogen in our present series were negative. Nevertheless, the possibility of an underlying viral infection has to be considered, because necrosis of the lymph node parenchyma, especially in the paracortical region, is not uncommon in nodes of patients with viral diseases (e.g., infectious mononucleosis, vaccinia, varicella). There have been no reports, however, of contagion of histiocytic necrotizing lymphadenitis without granulocytic infiltration from one person to another.

References

Fujimoto Y, Kojima Y, Yamaguchi K (1972) Cervical subacute necrotizing lymphadenitis. (In Japanese) Naika 30:920–927

Graham RC Jr, Karnovsky MJ (1966) The early stages of absorption of injected horseraddish peroxidase in the proximal tubules of mouse kidney: ultrastructural cytochemistry by a new technique. J Histochem Cytochem 14:291–302

Kikuchi M (1972) Lymphadenitis showing focal reticulum cell hyperplasia with nuclear debris and phagocytes: a clinico-pathological study (In Japanese). Nippon Ketsueki Gakkai Zasshi 35:379–380

Kikuchi M (1978) Lymphadenopathy due to toxoplasmic infection and anti-convulsant. Recent Adv RES Res 18:97–123

Kikuchi M, Uryu Y (1976) Phagocytic necrotizing lymphadenitis (In Japanese). Medical Bulletin of Fukuoka University 3:321–322

Kikuchi M, Yoshizumi T, Nakamura H (1977) Necrotizing lymphadenitis: possible acute toxoplasmic infection. Virchows Arch [Pathol Anat] 376:247–253

Lennert K (1959) Diagnose und Ätiologie der Piringerschen Lymphadenitis. Verh Dtsch Ges Pathol 42:203–208

Mepham BL, Frater W, Mitchell BS (1979) The use of proteolytic enzymes to improve immunoglobulin staining by the PAP technique. Histochem J 11:345–357

Michaeleck H (1977) Pseudolymphomatous hyperplasia in lymph nodes (reports of 9 cases). Trans Soc Pathol Japan 66:209–210

Müller-Hermelink HK, Lennert K (1978) The cytologic, histologic, and functional bases for a modern classification of lymphomas. In: Lennert K (Handbuch der speziellen pathologischen Anatomie und Histologie, vol 1, part 3B pp 1–71) Malignant lymphomas other than Hodgkin's disease. Springer Berlin Heidelberg New York

Shimamine T, Mori S, Itoyama S (1974) Diagnostic points on biopsied lymph node of malignant lymphoma and allied disorders. (In Japanese) Nippon Rinsho 32:1197–1202

Steinmann G, Földi-Börczsök E, Földi M, Lennert K (1981) Morphologic alterations in lymph nodes after experimental lymphostasis and venostasis. In: Weissleder H, Bartoš V, Clodius L, Málek P (eds) Progress in lymphology. Proceedings of the VIIth International Congress of Lymphology, Florence, 1979. Avicenum, Czechoslovak Medical Press, Prague, pp 79–81

Wakasa H, Kimura N, Takahashi T (1975) Necrotizing lymphadenitis. (In Japanese) Nippon Rinsho 33:1938–1943

Wakasa H, Takahashi H, Kimura N (1978) Necrotizing lymphadenitis. Recent Adv RES Res 18:85–96

Accepted February 10, 1982

Virchows Arch [Pathol Anat] (1982) 395:273–278

Virchows Archiv A

Hepatocellular Carcinoma in an Urbanised Black Community

A Changing Pattern

A.C. Paterson and C. Isaacson

Department of Pathology, Baragwanath Hospital, School of Pathology of the South African Institute for Medical Research and the University of the Witwatersrand, Johannesburg 2000, South Africa

Summary. Hepatocellular carcinoma has been extensively studied in Southern Africa, and particularly its relationship to hepatitis B virus infection. Most of this work involved rural Black populations. In this study the impact of urbanization on this relationship is investigated. The material is derived from the laboratory records at Baragwanath Hospital which serves the Black urban community of Soweto. Cases autopsied during the periods 1956–1960 and 1976–1980 have been examined with regard to age, sex, underlying cirrhosis and presence of HBsAg in the non-tumour liver. In addition, all *biopsies* from 1955 to 1980 have been analysed with respect to age and sex. There is evidence of a significant increase in overall average age and in the proportion of female cases, while the percentage of HBsAg positive cases has fallen. Possible causes for these findings are considered.

Key Words: Hepatocellular carcinoma – Hepatitis B Virus – Age – Sex

While the precise role of hepatitis B virus (HBV) in the aetiology of hepatocellular carcinoma (HCC) has still to be established, a relationship between the two has been demonstrated (Vogel et al. 1970; Tabor et al. 1976; Kew et al. 1979). Many studies of this relationship have originated from Southern Africa (Macnab et al. 1976; Kew et al 1974; Kew et al. 1979). To date, however, relatively little work has been done on the disease as it affects an urbanised population.

HCC is still a very common entity at Baragwanath Hospital which serves Soweto, a Black urban community twelve kilometers south-west of Johannesburg and with a population in excess of one million. Until recently, the absence of adequate serological records for this population precluded a detailed study of the relationship between HBsAg and HCC. Satisfactory biopsy and autopsy

Offprints requests to A.C. Paterson at the above address

0340-1227/82/0395/0273/$01.20

records are however available. Using autopsy material and histochemical techniques, it has been shown that HBsAg is present far less frequently in cases presenting at Baragwanath Hospital than in a rural series (Cohen et al. 1978; Isaacson et al. 1979; Kew et al. 1980). This paper describes the impact of urbanisation on HCC in a Black population.

Materials and Methods

Autopsied cases of HCC for the years 1956–1960 and 1976–1980 were examined. There were 43 and 47 cases respectively which were then selected for further study on the basis of the availability of adequate amounts of non-tumour liver tissue.

The formalin-fixed, paraffin embedded autopsy tissue was stained with haematoxylin and eosin, reticulin, Masson, and Perl's Prussian-blue for iron. In addition all cases were stained for HBsAG with Gomori's aldehyde fuchsin (Gomori 1950), and an immunoperoxidase technique modified from that described by Burns (1975) and Weisburg et al. (1978). The sections were counterstained with Perl's Prussian-blue to facilitate detection of positive cases in the heavily iron-overloaded livers commonly encountered in this population. Iron overload was assessed independently by two observers (A.C.P. and C.I.) on a scale of 0 to 4+ as described previously (Scheuer 1962) and for the purpose of this study a score of greater than 2+ was taken as significant.

Age, sex and tribal origin (when available) were obtained from autopsy records. In addition, the presence and type of cirrhosis reported macroscopically at autopsy were correlated with the histological pattern which was based on the criteria of Anthony et al. (1977). Further to this, the clinical details of all cases of HCC diagnosed by biopsy for the period 1955–1980 were studied. Of 603 cases, the age and sex of 517 were available for analysis.

Results

Table 1 compares the ages, male:female ratios and tissue HBsAg positivity for 2 periods, 1956–1960 and 1976–1980. It reflects an increase in average age, a rise in the proportion of female cases and a pronounced drop in HBsAg positivity over a period of 20 years.

Table 2 illustrates the incidence and type of cirrhosis associated with HCC for the two periods, as well as the percentage with significant iron overload. The tribal distribution of the autopsied cases for both periods showed no significant variation from that in the general population of Soweto.

Table 1. Average age, sex ratio and tissue HBsAg positivity of autopsy series

	1956–1960	1976–1980
Total cases	34	39
Average age	38.5 years	54.7 years
Male:Female	10:1	4:1
Tissue $HBsAg^+$	47%	15%

Table 2. Cirrhosis and iron overload in autopsy series

1956–1960		1976–1980	
Cirrhosis	=59%	Cirrhosis	=59%
	=80% Macronodular		=61% Macronodular
	=15% Micronodular		=30% Micronodular
	= 5% Mixed		= 9% Mixed
Iron overload	=32%	Iron overload	=44%

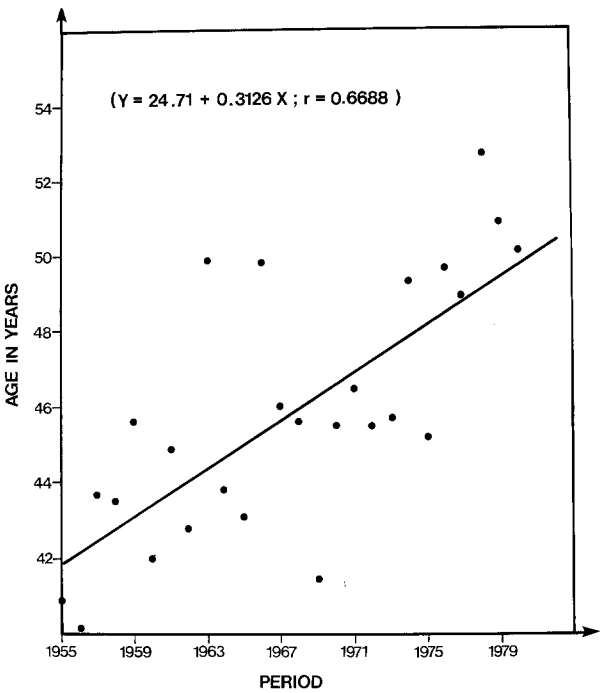

Fig. 1. Average Age of Cases of HCC 1955–1980

HCC is a sufficiently common entity at this hospital as not to present a diagnostic problem in most cases and autopsy is not routinely requested. As such, the possibility of a degree of artificial selection at the time of autopsy, influencing particularly the male/female ratio, has been considered. For this reason, the age and sex of all cases of HCC diagnosed by *biopsy* during the period 1955–1980 were analysed.

Figure 1 shows a scatter diagram of the relationship of average age to year of diagnosis. The correlation coefficient (r equals 0.6688) is statistically signficant. While the age range is somewhat narrower than that observed in the autopsy series, there has nevertheless been a significant rise over the twenty-six year period.

During this period, also, the male/female ratio changed abruptly, being 10:1 during 1955–1968 and 3.9:1 during 1969–1980. (U-test of Mann-Whitney significant at $p < 0.004$).

The possibility that the increased percentage of females could have influenced average age was considerd, but linear regression models confirmed that the rise in average age was independent of the proportion of female cases.

Discussion

The development of an urbanised Black population in the Johannesburg area has its origins in the discovery of gold in 1886. The movement of the Black population between rural and urban areas, in particular from the rural to the

urban setting, was relatively unimpeded until the late 1950's and early 1960's (Urban Foundation 1980). By 1978 the population of Soweto was estimated to be slightly in excess of one million, with the mean period of residence of the male head of house being 35.7 years (9–57 years), and that of a wife 28.8 years (1–78 years), (Shuenyane et al. 1977). This population has moved away from traditional rural diets, now consumes a partially westernised diet, and is showing a rising incidence of certain western diseases (Manning et al. 1974; Seftel 1977; Walker 1979).

With the growth of this urban population there has been an upward shift in the average age of cases of HCC, a fact also noted by Kew (1981). In the first part of the survey, the average age was similar to that in the rest of Africa during the same period (Steiner 1960) and to that in the rural communities in more recent times (Vogel et al. 1970; Kew et al. 1979). Similarly, the sex ratio of 10:1 for the earlier period reflects the well recognised male predominance in areas of high incidence. The abrupt and sustained increase in female cases probably reflects a population shift as the population of Soweto was predominantly male in the early 1950's but the male/female ratio rapidly equalised by the late 50's (Urban Foundation 1980).

The incidence of cirrhosis for both periods falls within the range reported from all areas (Szumuness 1978). The numbers in this series are too small for significance to be attached to the rise in cases of micronodular cirrhosis relative to the macronodular group, although this lesion is becoming more common (Isaacson 1978).

The fall in tissue HBsAg positivity is striking. In the absence of serological studies these findings are not intended to represent the true incidence of HBsAg positivity in cases of HCC. They probably represent an under-estimate as Kew et al. (1980) demonstrated tissue HBsAG in only 45% of cases but serum positivity in 68%. What is of interest, however, is the observation that the 47% positivity in our earlier group approximates the 45% in recent studies on tissue from rural Mozambican Blacks (Cohen et al. 1978; Kew et al. 1980). In contrast, the 15% incidence detected in our later period is much closer to that seen in low incidence areas such as Britain and the USA (Omata et al. 1978; Bassendine et al. 1979; Keshgegian and Ochs 1981). The fall in tissue HBsAg is the reverse of that described in similar studies from California (Peters et al. 1977).

The fall in HBsAg positivity could relate to the increased average age as a decline in incidence of HBsAg occurs in older patients (Kew et al. 1979, Coursaget et al. 1980). It is possible that other markers of HBV may have been present in these patients, although the significance of markers other than HBsAg in HCC has been questioned (Hadziyannis 1980).

It has been proposed that HCC has a multifactorial aetiology (Szmuness 1978; Kew et al. 1979), and that other environmental factors are of importance. While the geographic origins of the cases in this series are unknown, ongoing studies within the same community show that the majority of cases of HCC are born and reared in rural areas where there is a high incidence of HBsAg positivity, only moving to the urban environment on attaining work-seeking age (Paterson). The increasing average age may reflect some alteration in a possible co-carcinogen such as smoking, alcohol, aflatoxin and nitrosamines.

It is possible that potential cases of HCC are arriving in the urban environment, chronically infected with HBV, and encountering new carcinogens, or similar substances as in the rural areas but at lower concentrations. This may modify the carcinogenic process, enabling the patient to convert to HBsAg negativity prior to the development of his malignancy.

Satisfactory figures comparing the smoking habits of rural and urban populations are not available, but it would seem reasonable to assume that smoking, particularly cigarettes, is more prevalent in urban dwellers due to exposure to intensive advertising.

Alcohol is playing an increasingly important role in the urban Black culture. Western-type liquor first became freely available to the Black population in 1962, and with its increased consumption (Walker 1979), a changing pattern in the nature of alcoholic liver disease is evolving (Isaacson 1978). Asvat and Hodkinson (1981) have shown that alcohol is now the most common factor in cirrhotics presenting at Baragwanath Hospital. However, in our series, the predominent cirrhosis was macronodular, although there has been an increase in micronodular cirrhosis. Significant numbers of our autopsy cases, show substantial amounts of iron (Table 2), a marker of the intake of traditional home brewed beverages (Bothwell and Bradlow 1960; Bothwell and Isaacson 1962). The precise drinking habits of the urban HCC population have yet to be established.

The role of aflatoxin in the development of HCC has always been controversial, it being suggested that it acts either as a direct carcinogen or alternatively as an immunosuppressive agent resulting in an increase in HBV carriers (Peers and Linsell 1973; Lutwick 1979). The importance of aflatoxin in the urban Black community has tended to be overlooked, although autopsy studies have demonstrated traces of aflatoxin in infant livers (Isaacson and van Rensburg).

Aflatoxin has been demonstrated in the livers of patients dying with HCC (Onyemelukwe et al 1980).

Finally, the role of nitrosamines is uncertain. In Southern Africa most work was concentrated on its relationship to carcinoma of the oesophagus. To what extent nitrosamines are present in Soweto is not known, but oesophageal carcinoma is by far the most common malignant tumour in the Soweto male population.

Acknowledgements. This study is supported in part by a grant from the South African Medical Research Council to one of the authors (A.C.P.). The assistance of the Department of Biostatistics, M.R.C. (Tvl. Branch) is greatly appreciated.

References

Anthony PP, Ishak KG, Nayak NC, Poulsen HE, Scheuer PJ, Sobin LH (1977) The morphology of cirrhosis: definition, nomenclature and classification. Bull WHO. 4:521–540

Asvat MS, Hodkinson HJ (1981) Cirrhosis of the liver in Johannesburg Blacks. S Afr Med J 60:290

Bassendine MF, Chadwick RC, Lyssiotis T, Thomas HC, Sherlock S, Cohen BJ (1979) Primary liver cell cancer in Britain a viral aetiology? Br Med J:166

Bothwell TH, Bradlow BA (1960) Siderosis in the Bantu: A combined histopathological and chemical study. Arch Pathol 70:279–292

Bothwell TH, Isaacson C (1962) Siderosis in the Bantu: A comparison in incidence in males and females. Br Med J 1:522–524

Cohen C, Berson SD, Geddes EW (1978) Hepatitis B antigen in Black patients with hepatocellular carcinoma. Cancer 41:245–249

Coursaget P, Maupas P, Goudeau A, Chiron J, Drucker J, Denis F, Diop-Mar I (1980) Primary hepatocellular carcinoma in intertropical Aftrica: Relationship between age and hepatitis B virus etiology. J Natl Cancer Inst 65:687–690

Gomori G (1950) A new stain for elastic tissue. Am J Clin Pathol 20:665–666

Hadziyannis S.J. (1980) Hepatocellular carcinoma and type B hepatitis. In: Sherlock, Sed. Virus Hepatitis. Clinics in Gastroenterology, 9:117–34

Isaacson C (1978) The changing pattern of liver disease in South African Blacks. S Afr Med J 53:365–368

Isaacson C, Paterson AC, Berson SD (1979) Hepatitis B surface antigen and hepatocellular carcinoma in Southern Africa. Virchows Arch [Pathol Anat] 385:61–66

Isaacson C, van Rensburg SJ (Unpublished data)

Keshgegian AA, Ochs RH (1981) Orcein-positive hepatitis B surface antigen and liver carcinoma. Their association in an Eastern US population. Arch Pathol Lab Med 105:190–193

Kew, MC, Geddes EW, MacNab GM, Bersohn I (1974) Hepatitis-B Antigen and Cirrhosis in Bantu Patients with Primary Liver Cancer. Cancer 34:539–541

Kew MC, Desmyter J, Bradburne AF, Macnab GN (1979) Hepatitis B virus infection in Southern African Blacks with hepatocellular cancer. J Natl Cancer Inst 62:517–520

Kew MD, Ray MB, Desmet VJ, Desmyter J (1980) Hepatitis B surface antigen in tumour tissue and non-tumorous liver in Black patients with hepatocellular carcinoma. Br J Cancer 41:399–406

Kew MC (1981) Clinical, pathologic, and etiologic heterogeneity in hepatocellular carcinoma: Evidence from Southern Africa. Editorial: Hepatology 1:366–369

Macnab GM, Urbanowicz JM, Geddes EW, Kew MC (1976) Hepatitis B surface antigen and antibody in Bantu patients with primary hepatocellular cancer. Br J Cancer 33:544–548

Manning EB, Mann JI, Sophangisa E, Truswell AS (1974) Dietary patterns in urbanised Blacks. S Afr Med J 48:485–98

Omata M, Ashcavai M, Liew C-T, Peters RL (1979) Hepatocellular carcinoma in the U.S.A., etiology considerations. Localization of hepatitis B antigen. Gastroenterology 76:279–287

Onyemelukwe CG, Nirodi C, West CE (1980) Aflatoxin Bl in hepatocellular carcinoma. Trop Geogr Med 32:237–240

Paterson AC (Unpublished data)

Peers FG, Linsell CA (1973) Dietary aflatoxins and liver cancer. A population based study in Kenya. Br J Cancer 27:473–484

Peters RL, Afroudakis AP, Tatter D (1977) The changing incidence of association of hepatitis B with hepatocellular carcinoma in California. Am J Clin Pathol 68:1–7

Scheuer PJ, Williams R, Muir AR (1962) Hepatic pathology in relatives of patients with haemochromatosis. J Pathol Bacteriol 84:53–64

Seftel HC (1977) Diseases in urban and rural Black populations. S Afr Med J 45:121–125

Shuenyane E, Mashigo S, Eyberg C, Richardson BD, Buchanan N, Pettifor J, MacDougal L, Hansen JDL (1977) A socioeconomic, health and cultural survey in Soweto. S Afr Med J 51:495–500

Steiner PE (1960) Cancer of the liver and cirrhosis in trans-Saharan Africa and the United States of America. Cancer NY 13:1085–1145

Szmuness W (1978) Hepatocellular carcinoma and the hepatitis B virus: Evidence for a causal association. Prog med Virol 24:40–69

Tabor E, Gerety RJ, Vogel CL, Bayley A, Anthony P, Barker LP (1976) Hepatitis B virus infection and primary hepatocellular carcinoma. Abstract. Digestion 14:98–99

Urban Foundation (1980) Soweto–a study by the Transvaal region of the Urban Foundation. pp 3–58. Perskor Printers Doornfontein, Johannesburg

Vogel CL, Anthony PP, Mody N, Barker LF (1970) Hepatitis-associated antigen in Ugandan patients with hepatocellular carcinoma. Lancet 2:621–624

Walker ARP (1979) Changes in patterns of diet and disease in South African populations. Karger, Basel Pediat Adolesc Endocr 7:57–60

Weisburg WR, Mendelsohn G, Eddleston JC, Baylin SB (1978) Immunohistochemical localization of histaminase (diamine oxidase) in decidual cells of human placenta. Lab Invest 38:703–706

Accepted February 10, 1982

Virchows Arch [Pathol Anat] (1982) 395:279–288

Virchows Archiv A

Early (Stage A) Prostatic Cancer

VI. A Critical Look at the Follow-up

Salvatore Battaglia, Giuseppe Barbolini, Annibale R. Botticelli, Giuseppe Berri, and Evandro Nigrisoli

Istituto di Anatomia e Istologia Patologica dell'Università, di Modena e Divisione di Urologia dell'Ospedale Civile, I-41100 Modena, Italy

Summary. The 4 year follow-up of an original series of 100 patients treated by subtotal prostatectomy and analysed on histopathological grounds is presented.

87 out of 100 were traced and were in the following groups: 37/45 A_1, 27/29 A_2, 10/12 A_3, 13/14 benign prostatic hyperplasia. No therapy was performed. All three patients who died of prostatic carcinoma fitted into substage A_3, all three patients living with metastases fitted into A_1.

The progression observed is significant when related to the brief interval of time, the size of the prostatic microcarcinoma and the histological grade (well differentiated tubular carcinomas in 5 out 6 cases).

Prostatectomy with capsulectomy is strongly recommended in order to prevent progression.

Key words: Prostatic cancer–Stage A carcinoma–Follow-up

Introduction

This paper concerns the follow-up at 4 years of an original series of patients treated by subtotal prostatectomy for benign prostatic hyperplasia (BPH), previously considered on histopathological grounds by some of us (Battaglia et al. 1979). The step-section technique showed for early (stage A) prostatic carcinoma, or prostatic microcarcinoma (PMC), as a whole, a percentage rate as high as 86. Detailed figures were reported for the substaging score suggested according to the size (sum of the two main diameters measured in mm): A_1 ($\leqq 2$); A_2 ($\geqq 3 \leqq 9$); A_3 ($\geqq 10 \leqq 20$).

A reliable staging system is required for diagnosis and, at the present time, the therapy of prostatic cancer reflects uncertainties accumulated in the past. Whitmore's (A, B, C, D) staging system (1956) was the most used although

Offprint requests to: S. Battaglia, Direttore Istituto di Anatomia e Istologia Patologica dell'Università di Modena, Via Berengario 4, I-41100Modena, Italy

Supported by a Ministry of Education Grant (22/1/6/R A4, 1980/81)

0340-1227/82/0395/0279/$02.00

ill-suited to the complexity of the stages, particularly of stage A. Since it is conditioned by negative rectal palpation, it collects cancers of non homogenous size and some even larger than those subsequently assigned to stage B. In order to overcome this drawback, it was suggested by Jewett (1975) to split stage A into A_1 (focal) and A_2 (diffuse) and by other authors (Bruce and Mahan 1980; Zincke et al. 1981) to double the whole staging system from A_1, A_2 to D_1, D_2.

Other attempts to quantify the extent of prostatic cancer between stage A_1 and stage B_2 (Barnes et al. 1976; McLaughlin et al. 1976; Boxer 1977; Donohue et al. 1977; Heaney et al. 1977; Catalona and Scott 1978; Golimbu et al. 1978; Klein 1979; Sheldon et al. 1980) have not had encouraging results, failing to clarify the problem significantly. Practically speaking the essential need is to avoid the excess of understaging; simple and crude clinical criteria are not adequate for this purpose. Golimbu et al. (1978) proposed, for instance, a single (focal) stage A, followed by B_1, B_2-α (corresponding to A_2 of Jewett 1975) and B_2-β (corresponding to B_2 of Jewett, 1975). On the other hand Catalona and Scott (1978) and Sheldon et al. (1980) proposed three substages A, as follows: A_1 F (focal), A_1 (up to one lobe), A_2 (diffuse). This kind of personal staging system derives from the fact that the so-called A_2 appears more advanced in progression than B_1 as judged in terms of survival (Barnes and Ninan 1972; Schoonees et al. 1972; Gleason et al. 1974; Jewett 1975; De Vere White et al. 1977; Golimbu and Morales 1979; Guerriero et al. 1980; Sheldon et al. 1980). This anomaly of natural history relates to the fact that B is usually both palpable and circumscribed whereas A_2 may not be so.

The resort to pelvic lymphadenectomy for staging showed a number of metastases in cases otherwise considered as A_2, B_1, B_2, C and a higher metastases rate in A_2 when compared with B_1 (Rous and Mallouh 1972; Dahl et al. 1974 and 1975; McCullough et al. 1974 and 1977; Varkarakis et al. 1975; McLaughlin et al. 1976; McMillen and Wettlaufer 1976; De Vere White et al. 1977; Donohue et al. 1977; Heaney et al. 1977; Wilson et al. 1977; Golimbu et al. 1978, Golimbu and Morales 1979; Murphy et al. 1980; Sheldon et al. 1980; Zincke et al. 1981). The opportunity to move some understaged A_2 to D_1 derives from this as suggested by Bruce et al. (1977), Sadlowski et al. (1978), Klein (1979) and McCullough (1980). Consequently, it appears useless to refer simply to stage A when follow-up is in progress. Lymphadenectomy in combination with the afore-said diagnostic criteria should lead to the so-called "surgical stage" (Wilson et al. 1977; Sheldon et al. 1980) or "true stage" (Klein 1979) or "correct stage" (McCullough 1980). Lymph node aspiration for staging of prostatic carcinoma in combination with lymphography was recently claimed (Efremidis et al. 1981) to be the major advance compared with pelvic lymphadenectomy. However, in our opinion, further support is needed. Referring to the so-called focal stage A, where pelvic lymphadenectomy failed to show metastases, the use of a morphometric substaging score (A_1, A_2 and A_3, according to Battaglia et al. 1979) should lead to the evaluation of the "true stage" and fulfil the correct, even quantitative, staging system criteria, as wished for by Cantrell et al. (1981). Unfortunately, the data reported in a number of series by a number of authors are far from comparable. The same applies to the stage 0 preceding Whitmore's staging-system (Corriere et al. 1970; Dhom 1974; Dhom and Hautumm 1975;

De Vere White et al. 1977). Finally, I-IV (American Joint Comittee for Cancer Staging) and TNM (UICC) staging-systems are scarcely in use and do not seem better when applied to the so-called incidental carcinomas.

Thus, further additional modifications are needed.

Personal Series

As shown in Table 1, 87 out of 100 patients were traced for follow-up at 4 years. Distribution within single groups was reasonably homogeneous: 37/45 A_1; 27/29 A_2; 10/12 A_3; 13/14 BPH. All patients were followed in the same way by using standardized prostatic follow-up forms, medical (digital rectal examination), laboratory and radiological (skeletal radiography and radionuclide bone scan) examinations (Table 2). No therapy was performed.

This study showed that 3 patients died from prostatic carcinoma, 3 had confirmed bone metastases and 7 more had suspected bone metastases. Progression was confirmed in 6 (8.10%) and suspected in 7 (9.45%) patients.

Discussion

The 4 year follow-up data of our series are quite significant. The progression observed is considerable when related to: (1) the brief interval of time, (2) the size of PMC (mostly A_1, i.e. ≤ 2 mm), (3) the histological grade (well-differentiated tubular carcinomas in 5 out of 6 cases). All patients who died of prostatic carcinoma fitted into substage A_3, i.e. the largest and, sometimes, less differentiated tumour; all those living with metastases fitted into A_1. The size measured as the sum of the two main diameters was less than 20 mm and it disagrees with Byar and Mostofi (1972) who suggested a low aggressiveness for small cancers and with McNeal (1969) who estimated that metastases occur only with carcinomas larger than 1 cm^3.

As shown by Tables 3 and 4, the incidence of progression in the literature is quoted from 0 to over 80%. These variations in the figures recorded are possibly concerned with the different diagnostic and staging system criteria used, different sampling and often, poor sampling, as suggested by the standard deviation (Table 3 and 4). A number of papers focus on the survival rate (Bauer et al. 1960; Vickery and Kerr 1963; Cook and Watson 1968; Hanash et al. 1972; Gleason et al. 1974; Barnes et al. 1976; Golimbu et al. 1978). However, a simple survival rate without detailed data does not clarify progression at all, since the number of patients who died from/or with cancer or living with cancer and/or metastases is not known.

Some authors have pointed out that their patients had a survival rate very close to the life expectancy of the general population (Montgomery et al. 1961; Gilbertsen 1971; Byar and Vacurg 1972; Correa et al. 1974; McMillen and Wettlaufer 1976), the only rather low survival rate being that of the series of De Vere White et al. (1977): 50 and 29% at 5 and 10 years, respectively.

The complex relationship between stages, grades, survival and progression is clearly shown by Schoonees et al. (1972). When ordered according to stages, mortality increases proportionally from A (14.3%) to D (84.0%), whereas the mean survival rate, from A to D, 1.96, 4.03, 3.65, 1.72, respectively, does not. However, proportionally decreasing figures for mean survival rate are noticeable where grades (I-IV) are concerned: from 3.21 to 1.80. An inverse ratio

Table 1. Stage A prostatic cancer in patients treated by subtotal prostatectomy for BPH: four years follow-up with relationship between size (A_1, A_2, A_3 substaging score), histologic grade and mean age.

Original series			No. of cases traced (%)	Survival (%)	Deceased				Living with metastases	
Histologic grade 1, 2, 3[a]		Mean age (years)			with or from prostatic carcinoma	other neoplasia	other causes	Tot.	Confirmed	Suspected
A_1	45 (45, 0, 0)	65.51 ± 5.68	37 (82.2)	33 (89.1)	0	1	3	4 (10.8)	3	6
A_2	29 (29, 0, 0)	69.45 ± 6.63	27 (93.1)	25 (95.5)	0	0	2	2 (7.4)	0	1
A_3	12 (7, 5, 0)	70.50 ± 5.71	10 (83.3)	6 (60.0)	3	0	1	4 (40.0)	0	0
BPH	14	66.43 ± 6.00	13 (92.8)	9 (62.9)	0	1	3	4 (30.7)	0	0
	100		87	73 (83.9)	3	2	9	14 (16.1)	3	7

[a] According to Gaeta (1978)

between the histological grade and survival rate was observed by Bauer et al. (1960); Correa et al. (1974), Gleason et al. (1974); Jewett (1975); Catalona and Scott (1978) and Sheldon et al. (1980). Referring to metastases, Rous and Mallouh (1972) stated that grades I and II may be concerned with early metastases and this agrees with our findings (Table 3). When compared with other recorded figures (Table 4), the rate of progression in our series is high since it concerns A focal (PMC) only. We do not know, at the moment, if the progression observed is related to the original tumours, which were small and well-differentiated on the whole, or, whether more likely, to other remaining cancer foci. The latter hypothesis is consistent with the finding of cancer foci in the material examined after subsequent radical prostatectomy (Smith and Woodruff 1950; Hirst and Bergman 1954; Lehman et al. 1968; Blackard et al. 1971; Culp and Meyer 1973; Heaney et al. 1977; Nichols et al. 1977; Wilson et al. 1977) or TUR (McMillen and Wettlaufer 1976).

It is not correct, therefore, to state that stage A has a low aggressive potential (Greene and Simon 1955; Montgomery et al. 1961; Whitmore 1963; Correa et al. 1974; Jewett 1975; Barnes et al. 1976) and does not require therapy, as claimed by Lehman et al. (1968); Prout (1973), Barnes et al. (1976) and Heaney et al. (1977). Conservative therapy is advised for stage A by a number of authors, e.g. Wiederanders et al. (1963), Rous and Mallouh (1972); Khalifa and Jarman (1976); Donohue et al. (1977); Heaney et al. (1977); for stage A_1 only, it is supported also by Correa et al. (1974), Barnes et al. (1976) and Cantrell et al. (1981). Conservative therapy could lead to a survival rate (Bauer et al.

Table 2. Clinicopathological findings in 13 cases of PMC with detected or doubtful progression

Case Number	Biopsy Number	Age (Years)	Tumour substaging grade	Patients status	Symptoms at follow-up examination	Serum acid/ alkaline phosphatases (mu.ml)	X-ray	Bone scanning	Detected (+) or suspected (?) metastases
1	1708/77	64	$A_1/1$	Alive	Nocturia, enlarged hard nodule left behind (atypical cells)	26/202	+	−	?
2	4535/77	68	$A_1/1$	Alive	Nocturia, frequency	80/188	±	−	?
3	4758/77	74	$A_1/1$	Alive	Nocturia, Bone pain	rejects any control			?
4	8181/77	66	$A_1/1$	Alive	Frequency, hematuria (atypical cells)	88/208	±	−	?
5	9744/77	74	$A_1/1$	Alive	Frequency	88/284	+	−	?
6	11825/77	64	$A_1/1$	Alive	Frequency, bone pain	80/215	±	−	?
7	8898/77	61	$A_1/1$	Alive	Nocturia, frequency	91/395	+	+	+ (pelvic bones)
8	9991/77	76	$A_1/1$	Alive	Nocturia, frequency, bone pain, hard nodule left behind	90/320	+	+	+ (dorsal column)
9	1013/77	67	$A_1/1$	Alive	Nocturia, frequency	87/300	+	+	+ (sacrum)
10	3408/77	72	$A_2/1$	Alive	Nocturia	80/188	±	±	?
11	320/77	66	$A_3/1$	Dead	Nocturia, bone pain	434/115	+	+	+ (scattered)
12	2503/77	75	$A_3/2$	Dead	Nocturia, bone pain	−	+	+	+ (scattered)
13	11073/77	75	$A_3/2$	Dead	Nocturia, bone pain	−	+	+	+ (scattered)

Table 3. Progression of early (stage A) prostatic carcinoma

Author (year)	Follow-up (years)	Original series	Progression					
			Alive with carcinoma	(%)	Dead from or with carcinoma	(%)	Total	(%)
1. Alleman (1952)	7.5	14	0	(0.00)	3	(21.42)	3	(21.42)
2. Ballar et al. (1966)	2.8	22	0	(0.00)	0	(0.00)	0	(0.00)
3. Bauer et al. (1960)	5	52	1	(1.92)	19	(36.53)	20	(38.46)
4. Blackard et al. (1971)	5	24	21	(87.50)	0	(0.00)	21	(87.50)
		91	17	(18.68)	2	(2.19)	19	(20.87)
5. Byar and Vacurg (1972)	10	120	19	(15.80)	0	(0.00)	19	(15.80)
		148	10	(6.80)	0	(0.00)	10	(6.80)
6. Cantrell et al. (1981)	15	117	5	(4.27)	9	(7.69)	14	(11.96)
7. Correa et al. (1974)	10	37	1	(2.70)	2	(5.40)	3	(8.10)
8. Corriere et al. (1970)	5	18	0	(0.00)	1	(5.55)	1	(5.55)
9. Culp and Meyer (1973)	10	20	1	(5.00)	3	(15.00)	4	(20.00)
10. Edwards (1955)	5	23	0	(0.00)	2	(8.69)	2	(8.69)
11. Gleason et al. (1974)	5	66	0	(0.00)	0	(0.00)	0	(0.00)
12. Greene and Simon (1955)	10	82	5	(6.09)	7	(8.54)	12	(14.63)
13. Heaney et al. (1977)	10	100	16	(16.00)	8	(8.00)	24	(24.00)
14. Khalifa and Jarman (1976)	10	48	11	(22.91)	15	(31.25)	26	(54.16)
15. Labess (1952)	5	41	3	(7.31)	0	(0.00)	3	(7.31)
16. Lehman et al. (1968)	5	25	1	(4.00)	1	(4.00)	2	(8.00)
17. Miller and Seljelid (1971)	7	27	0	(0.00)	9	(33.33)	9	(33.33)
18. Montgomery et al. (1961)	10	35	0	(0.00)	0	(0.00)	0	(0.00)
19. Munsie and Foster (1968)	5	20	0	(0.00)	3	(15.00)	3	(15.00)
20. Murphy et al. (1975)	10	10	0	(0.00)	2	(20.00)	2	(20.00)
21. Myers (1937)	5	11	0	(0.00)	0	(0.00)	0	(0.00)
22. Nesbit and Baum (1951)	15	40	0	(0.00)	1	(2.50)	1	(2.50)
23. Nichols et al. (1977)	5	33	27	(81.81)	0	(0.00)	27	(81.81)
24. Puntenney and Lamson (1961)	10	11	0	(0.00)	3	(27.27)	3	(27.27)
25. Present series	4	74	3	(4.05)	3	(4.05)	6	(8.10)
Total	from 2.8 to 15	1,309	141	(10.77)	93	(7.10)	234	(17.87)
Mean (SD)	7.6 (±3.32)	48.49 (±38.20)	5.22 (±7.92)	(10.55) (±22.52)	3.44 (±4.82)	(9.50) (±11.46)	8.66 (±9.09)	(20.88) (±22.34)

Table 4. Survival and progression rates for stage A prostatic carcinoma according to various therapy of selected series

Author (year)	Number of patients with micro-carcinoma (stage A)	Therapy: hormone (h) nothing (n), X-ray (x) surgical (s)	Survival (years)		Progression	
			5	10	Alive with carcinoma	Dead from/with carcinoma
1. Bauer et al. (1960)	52	h 33, n 17, X2	(54%)	(37%)	1 (3.0%)	h 16 (48.4%), n 2 (11.7%) X1 (50.0%)
2. Blackard et al. (1971)	91	h 22, n 45, SRP 24	(>60%)		h 2 (9.09%), n 13 (28.8%) SRP 2 (8.3%)	hO, n 1 (2.2%) SRP 1 (4.1%)
3. Correa et al. (1974)	37	h 17, n 20	(>60%)	(50%)	1 (2.7%)	2 (5.4%)
4. Culp and Meyer (1973)	20	SRP 20		12 (60%)	1 (5.0%)	3 15.0%)
5. Edwards (1955)	23	SRP 23	16 (69.5%)		0 (0.0%)	2 (8.69%)
6. Gleason et al. (1974)	66	SRP 66	(69%)		0 (0.0%)	0 (0.0%)
7. Heaney et al. (1977)	100	h 67, n 33	h(>60%), n(>70%)	h(>30%), n(>50%)	16 (16.0%)	8 (8.0%)
8. Khalifa and Jarman (1976)	48	n 48	36 (75%)	17 (35.4%)	11 (22.9%)	15 (31.2%)
9. Lehman et al. (1968)	25	h+SRP 25	(>50%)		1 (4.0%)	1 (4.0%)
10. Montgomery et al. (1961)	35	h+s([a])35		11 (31.4%)	0 (0.0%)	0 (0.0%)
11. Puntenney and Lamson (1961)	11	SRP 11		6 (54.5%)	0 (0.0%)	3 (27.2%)
12. Present series	74	n 74	64 (86.48%)		3 (4.05%)	3 (4.05%)
Total of each group of therapy	h	139	(58.27%)[b]	(35.04%)[b]	(9.09%)[b]	(29.09%)[b]
	n	237	(72.15%)[b]	(42.37%)[b]	(16.16%)[b]	(25.00%)[b]
	x	2	(50.00%)[b]	–	–	(50.00%)[b]
	s	144	(52.77%)[b]	(58.06%)[b]	(2.08%)[b]	(6.25%)[b]
	h+s	60	(52.00%)[b]	(31.42%)[b]	(1.66%)[b]	(1.66%)[b]
Total	582	582	342/547 (62.52%)[b]	120/303 (39.60%)	51 (8.76%)	58 (9.96%)
Mean (SD)	48.50 (±28.60)	116.40 (±89.56)	68.40/109.40[b] (±67.74) (±96.19)[b]	30.00/75.75[b] (±18.49) (±48.28)	4.25/48.50[b] (±6.48) (±28.86)[b]	4.83/48.49[b] (±6.10) (±28.86)

RP radical prostatectomy RPP radical perineal prostatectomy

[a] Orchiectomy inclusive 4 years [b] Figures refer to data adjusted by the Authors of this paper

1960) or a life expectancy (Khalifa and Jarman 1976) equivalent to that following radical prostatectomy.

In contrast, radical prostatectomy is strongly recommended by Bauer et al. (1960, A focal excepted), Vacurg (1967); Lehman et al. (1968); Blackard et al. (1971); Byar and Vacurg (1972), Correa et al. (1974), Nichols et al. (1977); Wilson et al. (1977, A_1 excepted), Walsh and Jewett (1980, A_1 and B_2 only), Rous and Mallouh (1972) (grades I and II only). Radical prostatectomy results in both higher survival rates and minor progression, as shown by Table 4.

Therapy, in the case of progression, should be selected patient by patient, (symptoms, extension, general condition of the patient, etc.), without being a factor *a priori* either for or against surgical treatment.

The most important point is to prevent progression. Consequently, the therapeutic strategy is comparatively simple and turns on two main, parallel but alternative lines. However, it is clear that large, peripheral lateral and posterior zones are left behind by a subtotal prostatectomy. Due to the high frequency of location of PMC in these zones (Battaglia et al. 1982) it follows as mandatory that each BPH-patient should be treated by perineal prostatectomy as strongly recommended by Lilien et al. (1968), or, more appropriately, in our opinion, by prostatectomy with capsulectomy. It will then be only a remote possibility that cancer foci are left behind and progression of PMC could and should be prevented.

References

Allemann R (1952) Prostatahypertrophie und Prostatakrebs: Ein Beitrag zur Frage der okkulten Karzinome. Schweiz Med Wochenschr 82:147–154

Bailar JC III, Mellinger GT, Gleason DF (1966) Survival rates of patients with prostatic cancer, tumor stage, and differentiation. Preliminary report. Cancer Chem Rep 50:129–136

Barnes R, Hirst A, Rosenquist R (1976) Early carcinoma of the prostate: comparison of stages A and B. J Urol 115:404–405

Barnes RW, Ninan CA (1972) Carcinoma of the prostate. Biopsy and conservative therapy. J Urol 108:897–900

Battaglia S, Barbolini G, Botticelli AR (1979) Early (Stage A) prostatic cancer. IV. Methodological criteria for histopathological diagnosis. Virchows Archiv [Pathol Anat] 382:245–259

Battaglia S, Barbolini G, Botticelli AR (In press) Early (Stage A) prostatic cancer. V. Stereotopography. Appl Pathol

Bauer WC, McGavran MH, Carlin R (1960) Unsuspected carcinoma of the prostate in soprapubic prostatectomy specimens. A clinicopathological study of 55 consecutive cases. Cancer 13:370–378

Blackard CE, Mellinger GI, Gleason DF (1971) Treatment of stage I carcinoma of the prostate: a preliminary report. J Urol 106:729–733

Boxer RJ (1977) Adenocarcinoma of the prostate gland. Urol Survey 27:75–94

Bruce AW, Mahan DE (1980) Staging of adenocarcinoma of the prostate. Male Accessory Sex Glands. E. Spring-Mills, E.S.E. Hafez. (eds) Biochemical Press, Elsevier/North-Holland 23:409–425

Bruce AW, O'Cleireachain F, Morales A, Awad SA (1977) Carcinoma of the prostate: a critical look at staging. J Urol 117:319–322

Byar DP, Mostofi FK (1972) Carcinoma of the prostate: prognostic evaluation of certain pathologic features in 208 radical prostatectomies. Examined by the step-section technique. Cancer 30:5–13

Byar DP, Vacurg (1972) Survival of patients with incidentally found microscopic cancer of the prostate. Results of a clinical trial of conservative treatment. J Urol 108:908–913

Cantrell BB, De Klerk DP, Eggleston JC, Boitnott JK, Walsh PC (1981) Pathological factors that influence prognosis in stage A prostatic cancer: the influence of extent versus grade. J Urol 125:516–520

Catalona WJ, Scott WW (1978) Carcinoma of the prostate: a review. J Urol 119:1–8
Cook GB, Watson FR (1968) Twenty single nodules of prostate cancer not treated by total prostatectomy. J Urol 100:672–674
Correa RJ jr, Anderson RG, Gibbons RP, Mason JT (1974) Latent carcinoma of the prostate. Why the controversy? J Urol 111:644–646
Corriere JN, Cornog JL, Murphy JJ (1970) Prognosis in patients with carcinoma of the prostate. Cancer 25:911–918
Culp OS, Meyer JJ (1973) Radical prostatectomy in the treatment of prostatic cancer. Cancer 32:1113–1118
Dahl DS, Wilson CS, Middleton RG, Bourne HH (1974) Pelvic lymphadenectomy for staging localized prostatic cancer. J Urol 112:245–246
Dahl DS, Wilson CS, Middleton RC (1975) Staging of localized prostatic carcinoma by pelvic lymphadenectomy. Urology 5:804–807
De Vere White R, Paulson DF, Glenn JF (1977) The clinical spectrum of prostate cancer. J Urol 117:323–327
Dhom G (1974) Differentialdiagnostische Probleme des Prostatacarcinoms (Erfahrungen mit dem Prostatacarcinom-Register). Beitr Pathol 153:203–220
Dhom G, Hautumm B (1975) Die Morphologie des Klinischen Stadium O des Prostatacarcinoms (incidental carcinoma). Urologe A 14:105–111
Donohue RE, Pfister RR, Weigel JW, Stonington OG (1977) Pelvic lymphadenectomy in stage A prostatic cancer. Urology 9:273–275
Edwards C (1955) Observations on occult carcinoma of the prostate gland. Med J Aust 1:223–224
Efremidis SC, Dan SJ, Nieburgs H, Mitty HA (1981) Carcinoma of the prostate: lymph node aspiration for staging. AJR 136:489–492
Gaeta JF (1978, 1979) Quoted by Murphy, Whitmore
Gilbertsen VA (1971) Cancer of the prostate gland. Results of early diagnosis and therapy undertaken for cure of the disease. JAMA 215:81–84
Gleason DF, Mellinger GT, Vacurg (1974) Prediction of prognosis for prostatic adenocarcinoma by combined histological grading and clinical staging. J Urol 111:58–64
Golimbu M, Morales P (1979) Stage A_2 prostatic carcinoma should staging system be reclassified? Urology 13:592–596
Golimbu M, Schinella R, Morales P, Kurusu S (1978) Differences in pathological characteristics and prognosis of clinical A_2 prostatic cancer from A_1 and B disease. J Urol 119:618–622
Greene LF, Simon HB (1955) Occult carcinoma of the prostate. Clinical and therapeutic study of eighty three cases. JAMA 158:1491–1498
Guerriero WG, Carlton CE, Hudgins PT (1980) Combined interstitial and external radiotherapy in the definitive management of carcinoma of the prostate. Cancer 45:1922–1928
Hanash KA, Utz DC, Cook EN, Taylor WF, Titus JL (1972) Carcinoma of the prostate: a 15-year follow up. J Urol 107:450–453
Heaney JA, Chang HC, Daly JJ, Prout GR jr (1977) Prognosis of clinically undiagnosed prostatic carcinoma and the influence of endocrine therapy. J Urol 118:283–287
Hirst AF, Bergman RT (1954) Carcinoma of the prostate in men 80 or more years old. Cancer 7:136–141
Jewett HJ (1975) The present status of radical prostatectomy for stages A and B prostatic cancer. Urol Clin North Am 2:105–124
Khalifa NM, Jarman WD (1976) A study of 48 cases of incidental carcinoma of the prostate followed 10 years or longer. J Urol 116:329–331
Klein LA (1979) Prostatic carcinoma. N Engl J Med 300:824–833
Labess M (1952) Occult carcinoma in clinically benign hypertrophy of the prostate. J Urol 68:893–896
Lehman TH, Kirchheim D, Braun E, Moore R (1968) An evaluation of radical prostatectomy for incidentally diagnosed carcinoma of the prostate. J Urol 99:646–650
Lilien OM, Schaefer JA, Kilejian V, Andaloro V (1968) The case for perineal prostatectomy. J Urol 99:79–86
McCullough DL (1980) Surgical staging of carcinoma of the prostate. Cancer 45:1902–1905
McCullough DL, McLaughlin AP, Cittes RF (1977) Morbidity of pelvic lymphadenectomy and radical prostatectomy for prostatic cancer. J Urol 117:206–207

McCullough DL, Prout GR jr, Daly JJ (1974) Carcinoma of the prostate and lymphatic metastases. J Urol 111:65–71
McLaughlin AP, Saltzstein SL, McCullough DL, Cittes RF (1976) Prostatic carcinoma incidence and location of unsuspected lymphatic metastases. J Urol 115:89–94
McMillen SM, Wettlaufer JN (1976) The role of repeat transurethral biopsy in stage A carcinoma of the prostate. J Urol 116:759–760
McNeal JE (1969) Origin and development of carcinomas in the prostate. Cancer 23:24–34
Miller A, Seljelid R (1971) Cellular atypia in the prostate. Scand J Urol Nephrol 5:17–21
Montgomery TR, Whitlock GF, Nohlgren JE, Lewis AM (1961) What becomes of the patient with latent or occult carcinoma of the prostate? J Urol 86:655–658
Munsie WJ, Foster EA (1968) Unsuspected very small foci of carcinoma of the prostate in transurethral resection specimens. Cancer 21:692–698
Murphy GP, Saroff J, Joiner J, Gaeta JF (1975) Prostatic carcinoma treated at categorical center 1960–1969. NY State J Med 75:1663–1669
Murphy GP, Whitmore WF (1979) A report of the workshops on the current status of the histological grading of prostate cancer. Cancer 44:1490–1494
Murphy GP, Gaeta JF, Pickren J, Wajsman Z (1980) Current status of classification and staging of prostate cancer. Cancer 45:1889–1895
Meyers CM (1937) The occurence of carcinoma in clinically benign prostatic obstructions. Colorado Med 34:248–251
Nesbit RM, Baum WC (1951) Management of occult prostatic carcinoma. J Urol 65:890–894
Nichols RT, Barry JM, Hodges CV (1977) The morbidity of radical prostatectomy for multifocal stage I prostatic adenocarcinoma. J Urol 117:83–84
Prout GR (1973) Diagnosis and staging of prostatic carcinoma. Cancer 32:1096–1103
Puntenney REH, Lamson BG (1961) Cancer of the prostate gland: a clinical and pathological evaluation of patients treated by radical prostatectomy. J Urol 85:649–658
Rous SN, Mallouh C (1972) Prostatic carcinoma: the relationship between histologic grade and incidence of early metastases. J Urol 108:905–907
Sadlowski RW (1978) Early stage prostatic cancer investigated by pelvic lymph node biopsy and bone marrow acid phosphatase. J Urol 119:89–93
Schoonees R, Palma LD, Gaeta JF, Moore RM, Murphy GP (1972) Prostatic carcinoma treated at categorical center. Clinical and pathologic observations. NY State J Med 72:1021–1027
Sheldon CA, Williams RD, Fraley EE (1980) Incidental carcinoma of the prostate: a review of the literature and critical reappraisal of classification. J Urol 124:626–631
Smith GC, Woodruff LM (1950) The development of cancer of the prostate after subtotal prostatectomy. J Urol 63:1077–1080
Vacurg (1967) Carcinoma of the prostate: treatment comparisons. J Urol 98:516–522
Varkarakis MJ, Murphy GP, Nelson CMK, Chehval M, Moore RH, Flocks RH (1973) Symposium on the prostate. Lymph node involvement in prostatic carcinoma. Urol Clin North Am 2:197–212
Vickery AL Jr, Kerr WS (1963) Carcinoma of the prostate treated by radical prostatectomy. A clinicopathological survey of 187 cases followed for 5 years and 148 cases followed for 10 years. Cancer 16:1598–1608
Walsh PC, Jewett HJ (1980) Radical surgery for prostatic cancer. Cancer 45:1906–1911
Whitmore WF Jr (1956) Symposium on hormones and cancer therapy; hormone therapy in prostatic cancer. Am J Med 21:697–713
Whitmore WF (1963) The rationale and results of ablative surgery for prostatic cancer. Cancer 16:1119–1132
Wiederanders RE, Stuber RV Motta C, O'Connell D, Haslam GJ (1963) Prognostic value of grading prostatic carcinoma. J Urol 89:881–888
Wilson CS, Dahl DS, Middleton RG (1977) Pelvic lymphadenectomy for the staging of apparently localized prostatic cancer. J Urol 117:197–198
Zincke H, Fleming TR, Furlow WL, Myers RP, Utz DC (1981) Radical retropubic prostatectomy and pelvic lymphadenectomy for high-stage cancer of the prostate. Cancer 47:1901–1910

Accepted February 1, 1982

Virchows Arch (Pathol Anat) (1982) 395:289–301

Virchows Archiv A

Adenoid Cystic Carcinoma of Minor Salivary Glands. Analysis of 86 Cases

Clinico-Pathological, Histoenzymological and Ultrastructural Studies

G. Chomette[1], M. Auriol[1], P. Tranbaloc[1] and J.M. Vaillant[2]

[1] Pathology Department (Prof. G. Chomette), Hôpital de la Pitié 83, Boulevard de l'Hôpital, F-75013 Paris, France
[2] Institute of Stomatology (Prof. J.M. Vaillant) Hôpital de la Salpétrière 47, Boulevard de l'Hôpital, F-75013 Paris, France

Summary. 819 salivary gland tumors in surgical pathology files over a 25-year period were reviewed. Among 117 adenoid cystic carcinomas, 86 were located in minor salivary glands and were selected for a clinico-pathological analysis. Complementary histoenzymological investigations and electron microscopic study were performed on specimens from 7 and 13 patients respectively.

Adenoid cystic carcinoma occured in older patients (mean age of 54 years) than the other salivary neoplasms. The sex ratio was 1/1. The tumor was located more often in the palate and, to a lesser degree in the buccal floor, tongue or gums.

Histologically, epithelial nests contained characteristic cyst-like spaces (cylinders) and 3 varieties of such cylinders were described (mucoïd, muco-hyalin and hyalin). According to the predominant pattern, 3 types of tumors were shown: basaloïd, cribriform and trabecular. A comparison between histological results and clinical behaviour, available in 67 patients, demonstrated positive correlations. The basaloïd form had always a poor prognosis (numerous early recurrences and metastases, frequent lethal evolution). The cribriform type had an intermediate prognosis, better than basaloïd type and less good than trabecular group (100% of patients still alive at 8 years).

Histoenzymological studies revealed high level of acid phosphatase, alkaline phosphatase and leucine aminopeptidase activities round cylindromatous cavities. On the other hand, high oxidative enzyme activities were evenly distributed in all cell types.

Ultrastructural findings emphasized the immature characters of epithelial tumor cells. These cells contained numerous ribosomes, but few other organelles. Some more differentiated glandular or epidermoid cells were scattered in neoplastic islands. Rare myoepithelial cells lay in periphery of lobules. Cylinder-like spaces were filled with replicated basal lamellae, mucopolysaccharidic granules and fibrillar structures (microfibrils and periodic collagen fibrils).

Offprint requests to: G. Chomette at the above address

0340-1227/82/0395/0289/$02.60

In the light of these results the histogenesis of this neoplasm was discussed. Like the pleomorphic adenoma, adenoid cystic carcinoma was thought to arise from intercalated ducts. Unable to acquire any high degree of differentiation, this blastomatous tumor had a cellular component almost similar to that shown in intermediate stage of salivary gland embryogenesis.

Key words: Adenoid cystic carcinoma – Minor salivary glands – Clinico-pathological study – Enzymological study – Ultrastructural study

Of all the adenoid cystic carcinomas occuring in the head and neck, the most common are those located in minor salivary glands (Eby et al. 1972; Spiro et al. 1974). These tumors, as in other sites, have an uncertain clinical course, with risk of focal recurrences and metastases. Numerous authors have attempted to correlate the histological characteristics of these tumors with their behaviour (Eneroth et al. 1968; Eby et al. 1972; Nochomovitz and Kahn 1977; Perzin et al. 1978).

In consideration of such a question, we wish to report a great number of oral adenoid cystic carcinomas with long-term follow-up and clinico-pathological comparative studies. In addition, histoenzymological and ultrastructural findings about some cases lead us to discuss the much debated problem of histogenesis of these neoplasms.

Materials and Methods

819 salivary gland tumors in our surgical pathology files over a 25-year period (1955 to 1980) were reviewed.

Among 117 adenoid cystic carcinomas, 86 were located in minor salivary glands and were selected for further study. Sections were stained with the usual methods (Haematoxylin and eosin, Masson's trichrome stain, Wilder's technique for reticular fibers, Weigert's method for elastic fibers). They were also stained with periodic acid-Schiff reagent (PAS), alcian blue, mucicarmine for detection of mucins. In addition a semi-quantitative study of various histological components was performed in each case (measurement by examination of 10 fields at magnification 25).

The morphological features and clinical course (focal recurrences, metastases, survival data) were compared in the greatest number of patients.

In other respects, biopsy specimens were taken from 7 patients for histoenzymological investigations. These specimens were immersed in liquid nitrogen and sections were obtained using a cryostat. Enzyme activities were tested according to Pearse's methods (1972): oxidative enzyme activities (Lacticodehydrogenase-LD-, enzymes of Krebs cycle, enzymes of pentose shunt); hydrolases activities (acid phosphatase, alkaline phosphatase, ATPases); leucine aminopeptidase activity.

Biopsy specimens for electron microscopy were obtained from 11 patients. The specimens were fixed in glutaraldehyde, post-fixed in osmium tetroxyde and embedded in Epon. Thin sections, cut on LKB ultramicrotome, stained with uranyl acetate – lead citrate and Silver – methenamine (Movat's method), were examined with a Hitachi H 300 electron microscope.

Results

Statistical and Topographic Data

Among 819 salivary tumors, 478 were located in main glands and 331 in accessory glands. They included 117 adenoid cystic carcinomas (Table 1). In main

Table 1. Classification of 819 tumours of the salivary glands (1955–1980)

Type of tumour	*n*	%
Benign tumours	532	65
Pleomorphic adenomas	433	53
Cystadenolymphomas	70	8.5
Monomorphic adenomas (other types)	29	3.5
Malignant tumours	287	35
Acinic cell tumours	13	1.5
Mucoepidermoid tumours	99	12.2
Adenoid cystic carcinomas	117	14.3
Other carcinomas	58	7
Sum	819	100

Table 2. Localisation of 819 tumours of the salivary glands

Type of tumour	Major salivary glands		Minor salivary glands	
	n	%	*n*	%
Pleomorphic adenomas	301	61.8	132	40
Cystadenolymphomas	68	13.9	–	–
Monomorphic adenomas (other types)	15	3	16	4.7
Sum	384	78.7	148	44.7
Acinic cell tumours	11	2.2	2	0.6
Mucoepidermoid tumours	28	5.8	71	21.5
Adenoid cystic carcinomas	31	6.3	86	26
Other carcinomas	34	7	24	7.5
Sum	104	21.3	183	55.3

glands (Table 2), the relative frequency of adenoid cystic carcinoma is low (31 cases – 6.3% of all cases), if compared with that of parotid pleomorphic adenomas; it is not rare in submandibular and sublingual glands. In our material as in other reports (Frable and Elzay 1970; Spiro et al. 1974; Tarpley and Giansanti 1976), adenoid cystic carcinoma occurs more frequently in minor salivary glands (Table 2) (26% of tumors) and, in association with mucoepidermoïd tumors, is a major contribution to the high level of malignant neoplasms (55.3%) in this site.

The mean age (54 years) at diagnosis in the adenoid cystic carcinoma group was higher than in patients with other salivary neoplasms. The tumor was noted equally in both sexes (41 men for 45 women).

This tumor was more often located in palate and, to a lesser degree in the buccal floor, tongue or gums, whereas pleomorphic adenoma was especially found in the cheeks and lips (Table 3).

Table 3. Comparison of the localisation and frequency of pleomorphic adenomas and adenoid cystic carcinomas in minor salivary glands

Type of tumour	Palate		Tongue, buccal floor, gum		Cheek		Lip	
	n	%	*n*	%	*n*	%	*n*	%
Adenoid cystic carcinoma	64	35.3	13	23.6	9	13	4	4.8
Pleomorphic adenoma	73	40	5	10	25	46.3	25	61
Other tumours	44	24.7	37	56.4	20	40.7	12	34.2
Sum	181		55		54		41	

Histopathological Findings

Macroscopically, the size of these tumors varies from 1 to 4 cm. They are often ill-bounded. The cut surface is greyish white and firm, with some red necrotic areas.

Histologically, the typical adenoid cystic carcinoma is composed of sheets of epithelial cells with numerous cribriform mucoïd – filled spaces.

However, in the same tumor, 3 different structural types are always associated in various proportions (Evans and Cruickshanc 1970):

The basaloïd type is composed of solid epithelial islands, often necrotic in their core. Their small, cuboidal and basophilic cells are provided with chromophilic nuclei. Mitoses are fairly numerous. The cribriform spaces and mucoïd-filled cavities are scanty among these closely packed cells (Fig. 1 a).

In the *cribriform type*, the cells vary from polygonal to fusiform in shape. Their nucleus is pale and vesicular. The cell nests show numerous cribriform spaces, communicating with peripheral stroma. These (cylinders) are occupied by mucoid material which stains positively with PAS and alcian blue. Other cylinders possess a safranophilic and trichrome stained core with peripheral mucoid material. Some entirely hyalin cylinders are only stained with safran and trichrome technics (Fig. 1 b)

The *trabecular or tubular type* is related to dislocated cribriform patterns. The epithelial strands, composed of ovoid or fusiform cells, are surrounded by large areas of collagen tissue (Fig. 1 c). Some tubular lumens, lined with several layers of cuboidal cells are sometimes shown among these structures.

Some reticulin concentric fibers are demonstrated in the lumen of cylinders by Wilder's method.

According to the main histological component, the 86 cases of adenoid cystic carcinomas reported in this work fall into the categories of 24 basaloid tumors (more than 30% of baseloïd structures), 48 cribriform tumors and 15 trabecular or tubular tumors.

The *stroma*, poorly developed in basaloid type, often contains thin elastic ribbons round epithelial islands. Some endovascular tumor cells are often present. Perineural neoplastic infiltration is usually a prominent feature.

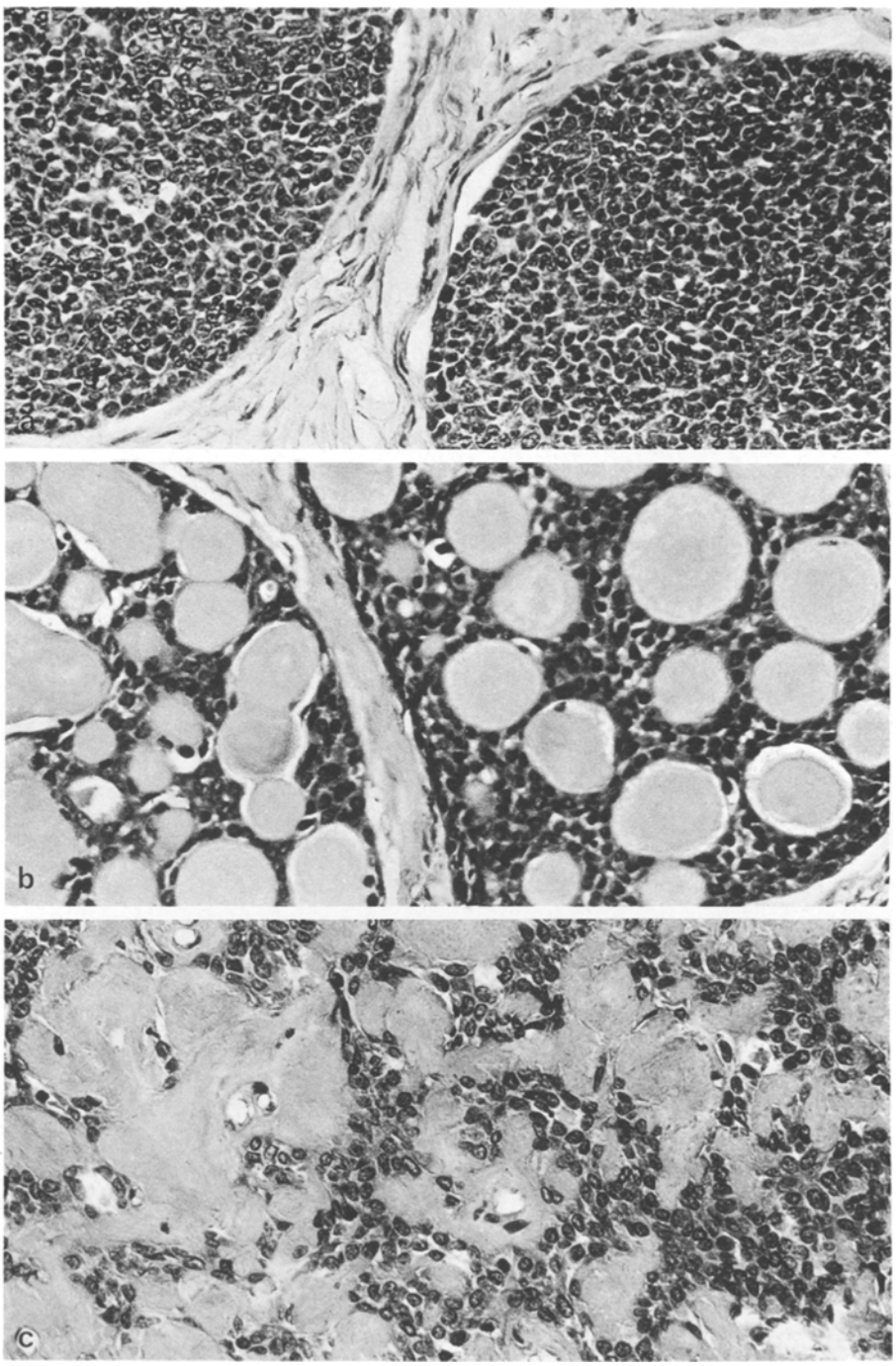

Fig. 1. Adenoid cystic carcinoma. **a** Basaloïd type. Dark epithelial islands composed of cuboidal or ovoid cells with chromophilic nuclei. Narrow areas of stromal tissue. Haematoxylin-eosin ×350. **b** Cribriform type. 2 epithelial nests containing numerous mucoïd – filled cavities. Haematoxylin-eosin ×350. **c** Trabecular type. Epithelial strands surrounded by large areas of hyalin stroma. Haematoxylin-eosin ×350

Clinico-Pathological Correlations

Some histological findings, such as poor limitation of tumor, invasion of adjacent bone structures, presence of perineural growth and neoplastic embolism may indicate a poor prognosis.

Moreover, a comparison between histological results and clinical behaviour, available in 67 patients (8 cases of trabecular type, 26 of cribriform type, 23 of basaloïd type) demonstrates positive correlations:

Recurrences and metastases (mainly in lymph nodes and lungs) are uncommon in the trabecular type (14% at 5 years, 27% at 8 years). They are more numerous in cribriform type (36% at 5 years, 50% at 8 years). In basaloïd type, they occur with a high frequency (70% at 5 years, 88% at 8 years).

Follow-up data on these 67 patients show variable survivals. All patients with trabecular tumours are alive and well at 5 and 8 years. 89% at 5 years and 67% at 8 years are still alive with the cribriform type. Only 39% of patients at 5 years and 32% at 8 years are alive with the basaloïd type.

Histoenzymological Study

A high oxidative enzyme activity (Krebs, diaphorases, lacticodehydrogenase) is evenly distributed in all cell types.

However, some enzymatic activities are enhanced round the cylinders. Thus, a high level of acid and alkaline phosphatase activity is noted in the cribriform islands, along mucoïd cylinders. In the same way, leucine aminopeptidase activity, high in basaloïd sheets, is predominant in cells surrounding cavities.

Electron Microscopic Observations

In cribriform or trabecular features, as in the solid neoplastic islands, close cohesion of epithelial cells is always present (Fig. 2a). Only few myoepithelial cells, separated from main lobules, are lying in adjacent stroma.

Most *tumor cells* are *poorly differentiated.* Polygonal or fusiform in the periphery of cyst-like spaces, these cells are attached to one another by desmosomes. Enlarged extracellular spaces filled with numerous cytoplasmic folds are seen between these junctions (Fig. 2b). Nuclei are pale, with finely dispersed chromatin and large nucleoli. The cytoplasm contains many free ribosomes but only few other organelles (Fig. 2c): some ovoïd mitochondria, ill-developed rough-surfaced endoplasmic reticulum and Golgi apparatus (Fig. 2d). However, the peripheral cells, besides these organelles contain lysosomal bodies and numerous small vesicules adjacent to the plasma membrane apparently discharging a granular product into extra-cellular spaces (Fig. 2d). Further more, some cells contain peculiar features (glycogen deposits, lipid droplets, cilia – Fig. 2e). Sometimes, malignant characteristics are evident (large irregular nuclei with several nucleoli and mitotic figures, whorls of rough endoplasmic reticulum Fig. 3a, necrosis).

Only a *few, more differentiated cells* are scattered here and there. Some *glandular cells*, closely packed by tight-junctions, have apical poles with numer-

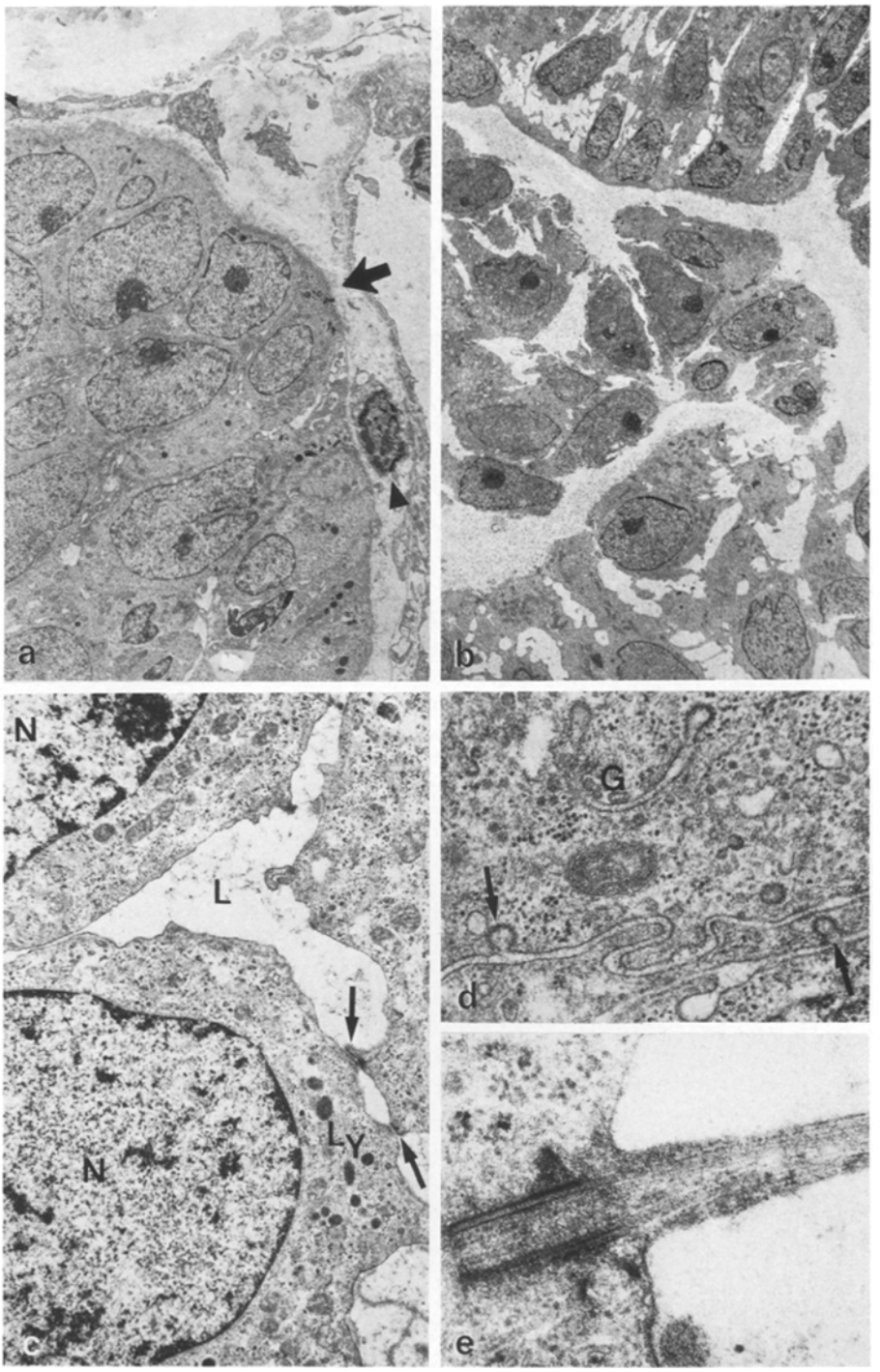

Fig. 2. **a** Epithelial islands with closely packed cells: dark cytoplasm; nuclei with finely dispersed heterochromatin and large nucleoli. Basement lamina (→) Myoepithelial cell in periphery of lobule (▶). ×4,000. **b** 2 epithelial islands. In the *upper part*, dense lobule. Another lobule is composed of dissociated cells with intercellular slits. ×2,000. **c** Dehiscence between 3 cells (*L*). Nuclei (*N*); desmosomal junctions (→); lysosomal bodies (*Ly*). ×12,500. **d** Cytoplasm of 2 tumoral cells. Golgi apparatus (*G*); microvesicules against plasmic membrane are opened in extracellular spaces (→). ×60,000. **e** Epithelial cell: cilium evaginated in extracellular space. ×80,000

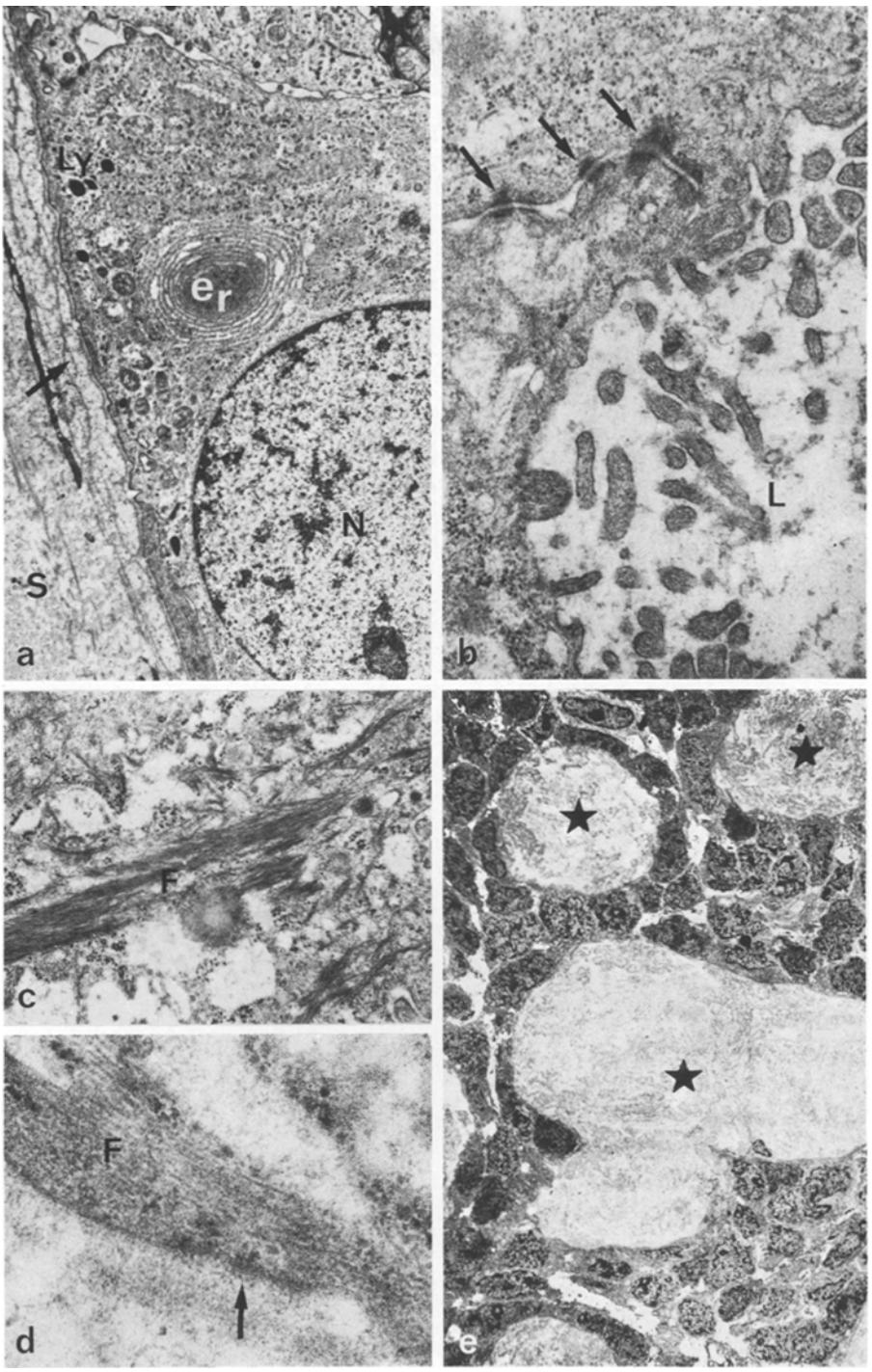

Fig. 3. a Tumoral cell. Nucleus (*N*); whorl of rough endoplasmic reticulum (*er*); lysosomal bodies (*Ly*); replicated basal lamina (→); stroma (*S*). ×10,000. **b** Differentiated glandular cells closely packed by desmosomes (→); apical poles with numerous microvilli lining a glandular lumen (*L*). ×40,000. **c** Differentiated epidermoid cell. Loosely arranged tonofilaments (*F*). ×60,000. **d** Differentiated myoepithelial cell. Parallel microfilaments (*F*); focal densities (→) against cytoplasmic membrane. ×100,000. **e** Epithelial island with cylinders (★), ×4,000

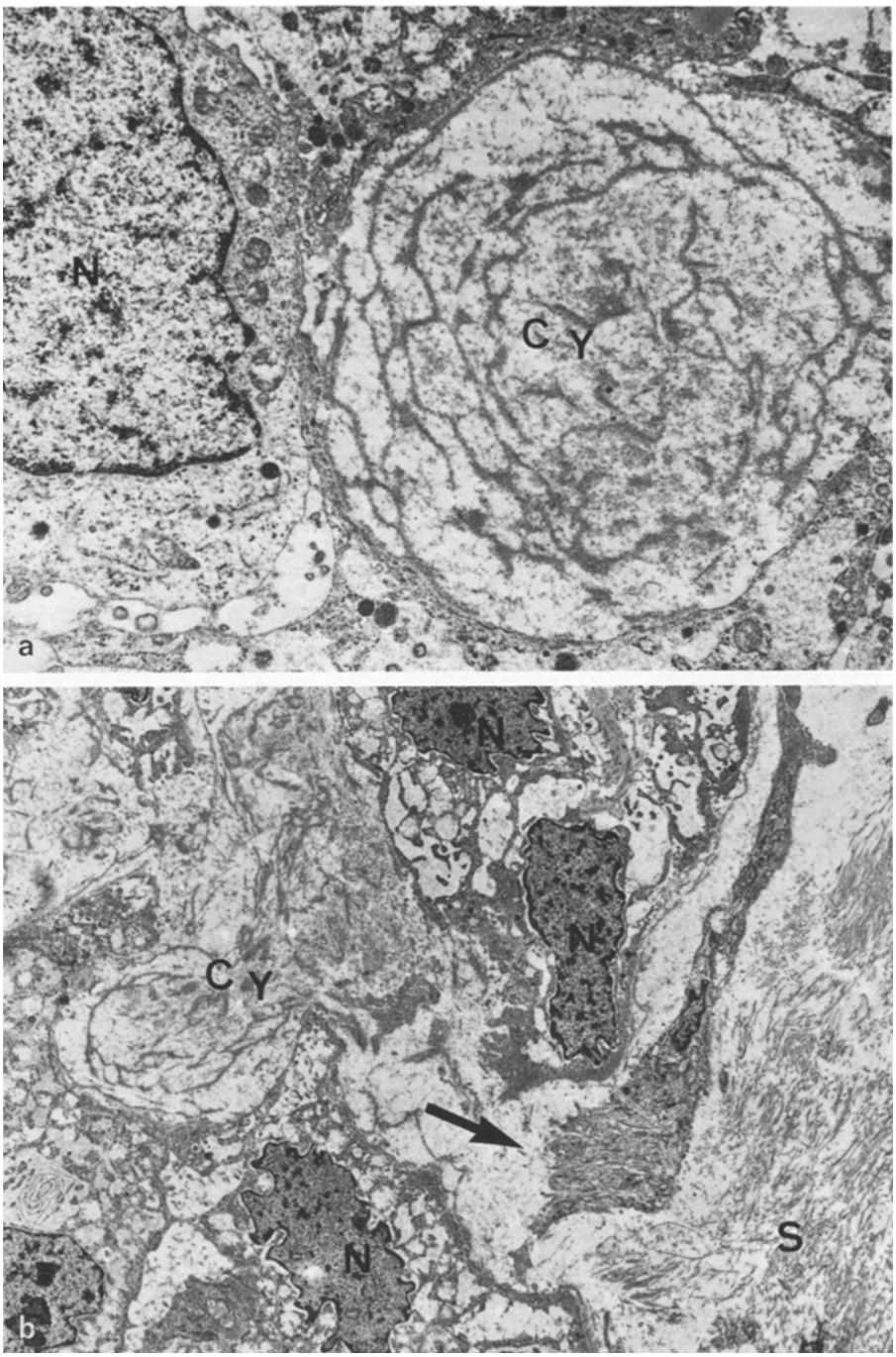

Fig. 4. a Tumor cell with nucleus (*N*) surrounding a cylinder (*Cy*) filled with a concentric network of replicated basal lamellae; mucopolysaccharidic granules between these lamellae. ×8,000. **b** Periphery of tumor island. 2 disjoined epithelial cells with nuclei (*N*). Cylinder (*Cy*), filled with basal lamellae, communicates with collagen stroma (*S*) through intercellular dehiscence (→). ×4,000

ous microvilli (Fig. 3b); they surround a lumen filled with granular epithelial mucins, positively stained with the silver-methenamine technique. Other cells, *epidermoïd*, contain few loosely arranged tonofilaments (Fig. 3c). Some myoepithelial cells, lying in periphery of lobules, contain convoluted nuclei, parallel microfilaments (100 to 200 A), focal densities and micropinocytotic vacuoles against the cytoplasmic membrane (Fig. 3d).

The *cylinder-like spaces* which characterize this tumour are of various sizes. Some narrow slits are shown between two epithelial cells. Other are wide round cavities (Fig. 3e); in the lumen of these cavities, the basal infra-epithelial lamina is replicated in concentric multilayers forming a network (Fig. 4a); lattices of tiny ovoid or stellated mucopolysaccharidic granules and fibrillar structures (microfibrils of 150 to 200 Å and periodic collagen fibrils) are present in the interstices among the network. Sometimes, cylinder-like spaces communicate through intercellular dehiscences with the adjacent stroma (Fig. 4b).

The supporting *stroma* is composed of fibroblasts, vessels and numerous collagen fibrils. It shows also young microfilament-rich elastic lamellae, located round myoepithelial cells in periphery of tumor islands and sometimes in lumen of cyst-like spaces.

Discussion

As in other reports (Frable and Elzay 1970; Spiro et al. 1974; Tarpley and Giansanti 1976), in our series of 819 salivary gland tumors 1/3 of cases are malignant and adenoïd cystic carcinoma accounts for 14,5% of the total. In fact, in accessory glands (331 cases), the percentage of malignant neoplasms is higher (53,5%) and adenoid cystic carcinoma is the more common malignant tumor in this site (26% of all cases).

The distribution of tumor types in oral cavity shows that adenoid cystic carcinoma is most often located in the palate (64 cases about 86). Other varieties of tumors are equally distributed in the palate and other parts of the oral mucosa. Pleomorphic adenoma is more often observed in the lips.

The histological picture in adenoid cystic carcinoma is varied (Evans and Cruickshanc 1970). 3 different patterns are commonly observed: the first type is basaloïd, because of its similarity to cutaneous basal cell carcinomas; it is composed of solid areas of basophilic cells, sometimes with central necrosis; careful inspection may reveal, in these solid sheets, tiny slits. The second, cribriform, is the most characteristic pattern; the clumps of epithelial cells are associated with numerous mucoïd-filled, often cystic spaces. In the third type, the cells are arranged in a reticular pattern within a great amount of stromal tissue; some tubular structures, lined with several layers of cuboidal cells are also seen.

The microscopic diagnosis of adenoid cystic carcinoma is sometimes difficult because of the great polymorphism of this neoplasm. Thus, basaloïd undifferentiated structures may suggest a basal cell adenoma (Walter et al. 1977; Seifert and Schulz 1979) but basal cell adenoma is encapsulated, without nuclear abnormalities; its ultrastructural features, which are more differentiated, are of epidermoid or glandular type (Luna and Mackay 1976). In the same way, if reticular

and tubular patterns of epithelial cells are embedded in abundant fibro-hyalin stroma, they may look like pleomorphic adenoma (Frable and Elzay 1970; Nochomovitz and Kahn 1977).

Some histological features, such as incomplete encapsulation of the neoplasm, perineural infiltration and spread of tumoral growth into adjacent bone (Thackray and Lucas 1974) may be of value in evaluation of prognosis in adenoid cystic carcinoma. In particular true histological-prognosis factors have been described by some authors (Eby et al. 1972; Nochomovitz and Kahn 1977; Perzin et al. 1978) and our findings agree with their results. All tumors in basaloïd group are of high grade malignancy: they spread largely in adjacent tissues; local recurrences soon occur; a great number of patients precociously die from distant metastases. Cribriform and trabecular tumors are of low grade malignancy: even though they might recur, slowly growing metastases are less frequent (Bakir et al. 1974) and death occurs rarely.

In our opinion, the cyst-like space or cylinder may be the characteristic structure of adenoid cystic carcinoma and may allow us to understand the histogenesis of this peculiar neoplasm.

According to other reports, our histological and histochemical studies demonstrate 3 groups of cylinders: the first one, wholly mucoïd, is stained positively with PAS and alcian blue. It contains few argyrophilic basal lamellae. The second, muco-hyalin, is partly mucoid at the periphery; its core stains positively with safran. The third is wholly hyalin, without any mucoïd material.

However, as in previous reports (Friborsky 1966; Huebner et al. 1969; Hoshino and Yamamoto 1970; Tandler 1971; Chisholm et al. 1975; Chen 1976; Nochomowitz and Kahn 1977), the ultrastructural features of these tumors are quite homogenous. Indeed, all cylinders are composed of 3 substances, each of them always located in the same part of cylinder (Friborsky 1966; Tandler 1971; Chen 1976). Basal lamellae, concentrically disposed are more numerous in periphery close to epithelial cells; they arise from excessive production and abnormal replication of infra-epithelial basal lamina. Ovoid or stellate mucopolysaccharidic granules fill spaces between an interlacing network of basal lamellae in the middle of cylinder. Microfibrils and periodic collagen fibrils, more numerous in the core of the cylinder are sometimes seen in the periphery of the cavity.

These morphological findings clearly indicate several successive stages in organization of these cylinders:

Firstly, an excessive amount of membranoid material becomes visible. It seems to play the major part in genesis of cylinder.

The material filling narrow slits gradually spreads within large cavities which dislocate tumor islands.

Filamentous structures occur later. They seem to arise from stromal collagen fibrils which invade cylinders via intercellular dehiscences (Hoshino and Yamamoto 1970). These fibrils are then depolymerizated and release their microfibrillar aperiodic component (Chen 1976).

Finally, progressive organization of mucopolysaccharidic material results in formation of thicker fibrils. These fibrils gradually take the place of membranoid material and end as hyalin substance.

The role of different varieties of differentiated cells in formation of cylinder substances is not obvious. A few glandular cells with their apical poles lining lumens are secreting PAS positive granules (Hoshino and Yamamoto 1970; Bloom et al. 1977; Nochomowitz and Kahn 1977); but this secretion is poorly developed. Other cells, of myoepithelial type, produce some elastic fibers (Azzopardi and Zayid 1972; Adkins and Daley 1974; Takeuchi et al. 1976; David and Buchner 1980), but their activity is never so marked as it is in pleomorphic adenoma. In fact, undifferentiated cells, far away the most numerous component (Tandler 1971) containing some vesicles situated near plasma membrane and few lysosomes (Fukushima 1968) seem able to produce intercellular substance in adjacent cavities (Bauer and Fox 1945; Markert 1965; Chisholm et al. 1975). This concept agrees with a high level of some enzymatic activities (acid phosphatase, alkaline phosphatase, leucine aminopeptidase, Bruce and Wertheimer 1967) within cells lining cylindromatous cavities. This immature cellular component is similar to that noted in intermediate stadium of salivary gland embryogenesis (Donath et al. 1978) and its metabolic activity induces formation of cylinders in conjunctive tissue. Thus, the degree of differentiation of this tumor is only estimated by development of cylinders. If poorly differentiated, the basaloïd islands are predominant but do not have any effects on the stroma. If more differentiated, their mesenchymatous inductive effect becomes more apparent, leading to formation of mucoid cylinders and to further hyalinization by means of interaction between stromal cells and mucoid material.

Thus adenoid cystic carcinoma may be neither epithelial nor myoepithelial (Mylius 1960) but a true embryonic tumor. Although generally believed to arise from intercalated ducts (Huebner et al. 1969; Hoshino and Yamamoto 1970; Eversole 1971) like pleomorphic adenomas it differs from them, as their totipotent cells are able to acquire a high degree of differentiation. On the other hand it is more comparable with salivary clear cell carcinoma (Donath et al. 1972), being composed of blastomatous cells, unable to express differentiation. The nature of these cells may explain, to a large extent, the morphological varieties and peculiar behaviour of this neoplasm.

The authors wish to thank M.A. Lesot and M. Tacnet for their technical assistance

References

Adkins KF, Daley TJ (1974) Elastic tissues in adenoid cystic carcinoma. Oral Surg 38:562–569

Azzopardi JG, Zayid I (1972) Elastic tissue in tumours of salivary glands. J Pathol 107:149–156

Bakir A, Vaillant JM, Brocheriou C, Laudenbach P (1974) Cylindromes des glandes salivaires. Bull Cancer 61:501–508

Bauer WH, Fox RA (1945) Adenomyoepithelioma (Cylindroma) of palatal mucous glands. Arch Pathol 40:96–102

Bloom GD, Carlsoo B, Gustafson H, Henricksson R (1977) Distribution of mucosubstances in adenoid cystic carcinoma. A light and electron microscopic study. Virchows Arch [Pathol Anat] 375:1–12

Bruce RA, Wertheimer FW (1967) Enzyme histochemistry of adenoid cystic carcinoma of minor salivary glands. Oral Surg 25:30–37

Chen SY (1976) Adenoid cystic carcinoma of minor salivary gland. Histochemical and electron microscopic studies of cystlike spaces. Oral Pathol 42:606–619

Chisholm DM, Waterhouse JP, Kraucunas E, Sciubba JJ (1975) A qualitative and quantitative electronmicroscopic study of the structure of the adenoid cystic carcinoma of human minor salivary glands. J Oral Pathol 4:103–119

David R, Buchner A (1980) Elastosis in benign and malignant salivary gland tumors. A histochemical and ultrastructural study. Cancer 45:2301–2310

Donath K, Seifert G, Schmitz R (1972) Zur Diagnose and Ultrastruktur des tubulären Speichelgangcarcinoms. Epithelial-myoepitheliales Schaltstückcarcinom. Virchows Arch [Pathol Anat], 356:16–31

Donath K, Dietrich H, Seifert G (1978) Entwicklung und ultrastrukturelle Cytodifferenzierung der Parotis des Menschen. Virchows Arch [Pathol Anat] 378:297–314

Eby LS, Johnson DS, Baker HW (1972) Adenoid cystic carcinoma of the head and neck. Cancer 29:1160–1168

Eneroth CM, Hjertman L, Moberger G, Wersall J (1968) Ultrastructural characteristics of adenoid cystic carcinoma of salivary glands. Arch Klin Exp Ohr Nas Kehlkopfheilk 192:358–367

Evans RW, Cruickshanc AH (1970) Epithelial tumors of the salivary glands. WB Saunders, Philadelphia

Eversole LR (1971) Histogenic classification of salivary tumors. Arch Pathol 92:433–443

Frable WJ, Elzay RP (1970) Tumor of minor salivary glands. A report of 73 cases. Cancer 25:932–941

Friborsky V (1966) Submicroscopical structure of adenoid cystic carcinoma of salivary glands. Acta Morphol Acad Sci Hung 14:105–116

Fukushima M (1968) An electron microscopic study of human salivary gland tumors. Pleomorphic adenoma and adenoid cystic carcinoma. Bull Tokyo Med Dent Univ 15:387–408

Hoshino N, Yamamoto I (1970) Ultrastructure of adenoid cystic carcinoma. Cancer 25:186–198

Huebner G, Kleinsasser O, Klein HJ (1969) Zur Feinstruktur und Genese der Cylindrome der Speicheldrüsen. Virch Arch [Pathol Anat] 347:296–315

Luna MA, Mackay B (1976) Basal cell adenoma of the parotid gland. Case report with ultrastructural observation. Cancer 37:1615–1621

Markert J (1965) Zur Ultrastruktur der Cylindrome. Arch Ohr Nas Kehlkopfheilk 184:496–505

Mylius EA (1960) The identification and the role of the myoepithelial cells in the salivary gland tumours. Acta Pathol Microbiol Scand 50: (Suppl) 139

Nochomovitz LE, Kahn LB (1977) Adenoid cystic carcinoma of the salivary gland and its histologic variants. A clinicopathologic study of 30 cases. Oral Surg 44:394–404

Pearse AGE (1972) Histochemistry theoretical and applied. 3rd edn Churchill Livingstone, London

Perzin KH, Gullang P, Clairmont AC (1978) Adenoid cystic carcinoma arising in salivary glands. A correlation of histologic features and clinical course. Cancer 42:265–282

Seifert G, Schulz CP (1979) Das monomorphe Speichelgangadenom. Klassifikation und Analyse von 79 Fällen. Virch Arch [Pathol Anat] 383:77–99

Spiro RH, Koss LG, Hajdu SI, Strong EW (1974) Tumors of minor salivary origin; a clinicopathologic study of 492 cases. Am J Surg 128:512–520

Takeuchi J, Sobue N, Katoh Y, Esaki T, Yoshida M, Miera K (1976) Morphologic and biologic characteristics of adenoid cystic carcinoma cells of the salivary gland. Cancer 38:2349–2356

Tandler B (1971) Ultrastructure of adenoid cystic carcinoma of salivary gland origin. Lab Invest 24:504–512

Tarpley TM, Giansanti JS (1976) Adenoid cystic carcinoma. Analysis of fifty oral cases. Oral Surg 41:484–497

Thackray AC, Lucas RB (1974) Tumors of the major salivary glands. Atlas of Tumor Pathology 2nd series Fasc. 10 Armed Forces Institute of Pathology, Washington

Walter P, Prevot M, Ludwig L (1977) Adénomes à cellules basales des glandes salivaires. Analyse de 7 observations et revue de la litterature. Etude comparative avec les cylindromes. Ann Anat Pathol 22:233–250

Accepted February 3, 1982

Virchows Arch [Pathol Anat] (1982) 395:303–318

Virchows Archiv A

Papillary Carcinoma of Choroid Plexus

Light and Electron Microscopic Study

Nobuo Nakashima, Kishiko Goto, and Jun Takeuchi
Division of Pathology, Clinical Laboratory, Nagoya University Hospital, Nagoya 466, Japan

Summary Two cases of papillary carcinoma, one in a 23-month-old girl and the other in a 25-month-old boy who both died within a relatively short time after operation, were studied histologically and electron microscopically. Both tumors originated in the right trigone of the lateral ventricle and spread widely via the cerebrospinal fluid. Histologically, the tumors consisted mostly of a differentiated papillary architecture closely resembling choroid plexus papilloma. Some carcinoma cells, showing cellular atypism, displayed a multilayer arrangement. The amount and distribution of PAS-, Alcian blue- or orcein-positive substances on the cell surface and/or in the interstitial elements of the carcinomas differed from that of choroid papillomas examined in our laboratory. Electron microscopically, the carcinoma cells in some areas showed a loss of apical-basal polarity, and the formation of both microvilli and desmosome-like structures was indistinct. Papillary carcinoma is reviewed on the basis of the literature from 1906 till 1980.

Key words: Choroid plexus carcinoma – Choroid plexus papilloma

Tumors originating from the choroid plexus are rare. The incidence of choroid plexus tumors is reported to be about 0.4 to 0.8% of all verified intracranial tumors (Cushing 1932; Norlen 1949; Grant 1956; Zülch 1965; Arai 1976); they account for 1.5 to 3.9% of tumors in children (Bodian and Sawson 1953; Matson and Crofton 1960; Sato and Sano 1975), and 1.1 to 2.0% of intracranial gliomas (Cushing 1932; Ringertz and Reymond 1949; Russell and Rubinstein 1977). The tumors occur at any age, but the majority are found in young subjects, particularly in the first decade of life (Friedman and Solomon 1936; Turner and Simon 1937; Posey 1942; Matson and Crofton 1960; Bohm and Strang 1961; Zülch 1965; Rubinstein 1970). It is generally accepted that lateral ventricle papillomas develop in children while fourth ventricle papillomas occur mostly in

Offprint requests to N. Nakashima at the above address

0340-1227/82/0395/0303/$03.20

adults (Wagenen 1930; Ringertz and Reymond 1949; Bohm and Strang 1961), and in males in particular (Tooth 1912; Kahn 1952). Most tumors of the choroid plexus are benign in character, and malignant tumors are extremely rare. Almost all malignant tumors have been reported to occur in the lateral ventricle in childhood (Russell and Rubinstein 1977. Although several choroid plexus carcinomas have been reported in adults, the diagnosis in most cases was considered to be uncertain (Lewis 1967). Zülch (1965) postulated that the few cases described as having been malignant from their very inception might well have been metastases from some primary malignancy elsewhere in the body. The basic pattern of the histological features of plexus carcinoma in children was described in detail by Lewis (1967), but more cases of the same genus would be necessary to generalize on the basis of his findings. Plexus carcinoma is a distinct clinicopathologic entity and should be distinguished from other benign or malignant neoplasms.

In our laboratory, 8 tumors originating from the choroid plexus were encountered from 1960 to 1980. They accounted for 0.8% of all verified intracranial tumors (995 cases), and 2.8% of all intracranial gliomas (287 cases). Two of them, from a 23-month-old girls and a 25-month-old boy, showed malignant features, and both cases were autopsied. The present study reports these 2 primary carcinomas of the choroid plexus which were studied histochemically and electron microscopically and compared with benign papillomas and normal choroid plexus examined in our laboratory. Also, papillary carcinoma is reviewed on the basis of the literature from 1906 till 1980.

Case Reports

Case 1. A 23-month-old Japanese girl was admitted in August 1978. She was unable to walk or stand up; her external ocular movements appeared full and without nystagmus. Babinski's and Chaddock's signs were positive on the right side. After admission her general condition became poor, and she was drowsy and inactive just before the operation. X-rays of the skull showed separation of the sutures and a CT brain scan revealed a large, well demarcated lobulated, high density mass in the right temporo-parieto-occipital area and a round high density mass in the mid-brain, with dilatation of the left lateral ventricle and third ventricle. There was a shift of the septum to the left. The right carotid arteriogram showed a large mass in the right temporo-occipital region.

On 1st September, 1978, a right temporal craniotomy was performed. A massive tumor, encountered 1 cm below the cortex, was reddish, granular, fragile and well demarcated from the brain substance. The tumor was not resectable, and small biopsy specimens were removed for light and electron microscopic examination.

On 10th September, 1978, the 2nd operation was performed for marked bulging at the site of the craniotomy. Gradual deterioration occurred along with decerebrate posture, anisocoria and dilatation of the pupils before death on 4th November, 1978. Autopsy revealed that the right hemisphere contained a lobulated, partly encapsulated tumor, 9 cm anteroposteriorly, 13 cm transversely and 7 cm vertically. It was partly gray-pink and finely granular, suggesting a papillarly structure with widespread necrosis and hemorrhage. The cerebral cortex was thin, atrophic and necrotic in part. The right thalamus and the corpus striatum were invaded by the tumor. The trigone of the right lateral ventricle was occupied completely by the tumor tissue. The anterior half and the inferior horn of the right lateral ventricle and the left lateral ventricle were generally dilated, and the third ventricle and the cerebral aqueduct were closed under pressure from the tumor. On sections through the rostral part, the pons was almost replaced by the tumor mass (Fig. 1). Sections through the pons near its caudal border showed massive tumor deposits in the subarachnoid space, and the pons was compressed from outside and atrophied. The medulla oblon-

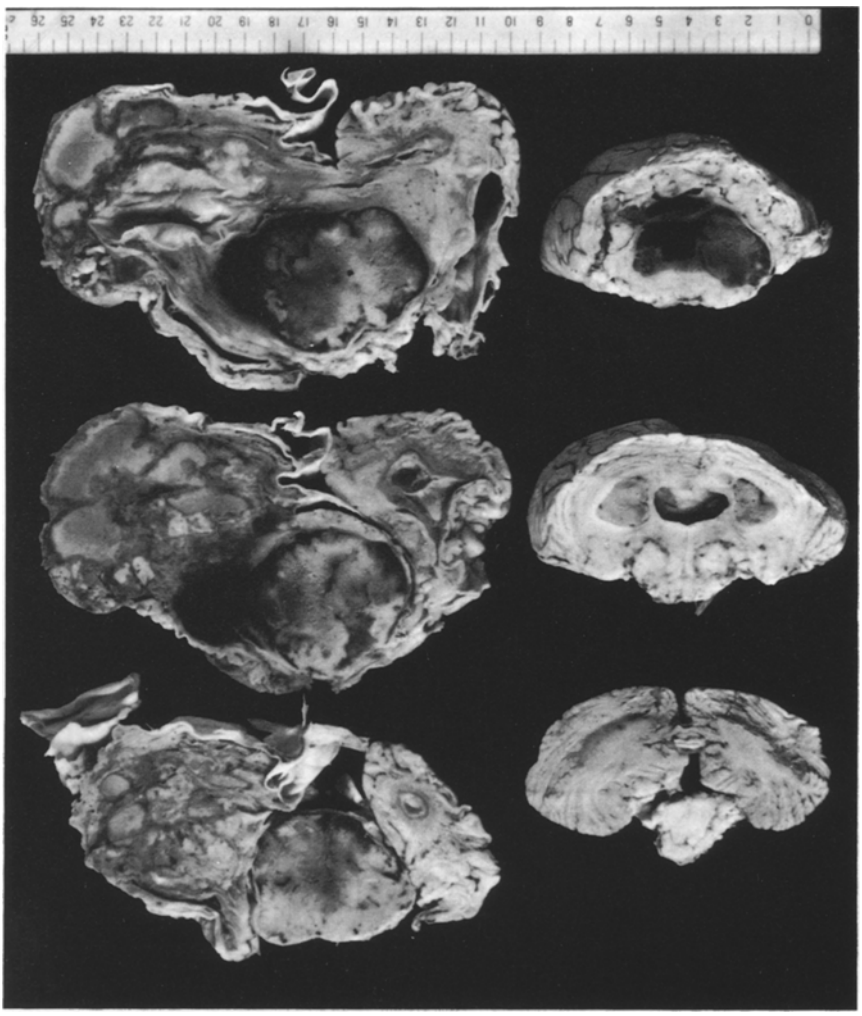

Fig. 1. Coronal sections of the brain from Case 1. Left: Cerebrum; upper, a section through corpus mammilaris; middle, a section through trigonum of the lateral ventricle; below, a section through pons. A large tumor mass occupies mostly right cerebral hemisphere. Right: Cerebellum and pons. Pons is surrounded and compressed by the tumor tissue

gata was also surrounded on every side by the tumor mass in the subarachnoid space. Many tumor deposits ranging from the size of a grain of wheat to that of a kidney bean were seen throughout the ventricular system, including each choroid plexus. In the brainstem and cerebellum, the tumor was gray-pink and finely granular without necrosis or hemorrhage. The basal ganglia on the left was greatly distorted (Fig. 1). No significant changes were found in the thoracic or abdominal viscera.

Case 2. A 25-month-old Japanese boy had a slight fever, vomited several times, and later was noticed to walk dragging the left foot and to be unable to move his left hand. After 3 months, the child was affected with a tonic or clonic convulsion each day, and about ten days later lapsed into unconsciousness, whereupon he was admitted.

On examination he was comatose; his pupils were small bilaterally with no reaction to light. The optic fundi showed bilateral advanced papilledema. A left spastic hemiplegia was present with a marked constant Babinski's sign, and clonus was easily elicited. Skull X-rays showed an enlarged cranial cavity and thinned skull bones. Ventriculography was performed through the anterior fontanel. The left ventricle was tapped but the right was not. The ventricular cerebrospinal fluid contained 180 mg of protein and 83 mg of glucose per 100 ml. The right carotid arteriogram showed a tumor stain in the site normally occupied by the right lateral ventricle.

One month after admission, a right parietal craniotomy was performed. When the dura mater was opened, the cerebral tissue herniated out. Cortical incision revealed a subcortical tumor probably filling the lateral ventricle. The tumor was partially removed in pieces weighing about 40 g.

Post operative recovery was poor, and the child remained comatose. After a while, another tumor was found subcutaneously in the right parieto-occipital region at the site of the craniotomy; it increased gradually to exceed the size of a hen's egg. A second operation was performed and later the patient was given a three-week course of radiotherapy. Gradual deterioration occurred, with anisocoria and generalised convulsions before death.

An autopsy revealed no significant changes in the thoracic and abdominal viscera. The skull was thinned and the bone flap was absent. The right cerebral hemisphere was adherent to the dura in places. At the site of the craniotomy, a hemispherical tumor ($14 \times 11 \times 6$ cm) with soft, partially fluctuating consistency, was found subcutaneously. A large cavity in the tumor was filled with yellow-brown turbid fluid (400 ml). A fist-sized tumor occupied the posterior part of the right lateral ventricle, and invaded and compressed the surrounding white matter. The tumor had spread diffusely through the cerebrospinal fluid and formed a layer on both cerebello-pontine angles. The pons and medulla were surrounded on all sides by a layer of tumor. There were innumerable small tumor deposits in the ventricular system and on each choroid plexus. There was no apparent penetration of the dura by tumor. The left lateral ventricle was dilated and filled with cerebrospinal fluid (200 ml).

Materials and Methods

The tumor tissues obtained from the surgical excisions and autopsies were fixed in buffered formalin, embedded in paraffin and sectioned. The tissue sections were stained by the following dyes: H-E, periodic acid Schiff's reagent, orcein, Alcian blue, AZAN and silver impregnation. In order to detect the glycosaminoglycan components, a digestion test was performed with chondroitinase ABC (Yamagata et al. 1968) (pH 8.0, 10 units/ml, 37° C, 1 h) or Streptomyces hyaluronate lyase (Ohya and Kaneko 1970) (pH 5.0, 100 turbidity reducing units/ml, 37° C, 1 h). Some tissues were fixed in cold 2% gultaraldehyde in 0.05 M phosphate buffer solution (pH 7.4) and post fixed in 2% Millonig's phosphate buffered osmium tetraoxide, and embedded in Epon 812. Thin sections were observed under A Hitachi electron microscope operating at 50 KV.

For comparative purposes, 6 cases of papilloma originating from choroid plexus (left lateral ventricle of a 5 year and 11-month-old boy; fourth ventricle of a 5 year and 10-month-old girl, a 26-year-old man, a 40-year-old woman, a 46-year-old man, and a 50-year-old man) were observed histochemically and electron microscopically by the same procedures as described above. A normal choroid plexus was also observed four purposes of comparison.

Results

Light Microscopy

The histological appearances of the two carcinoma cases are characteristic of choroid papillary carcinoma. As shown in Figs. 2 and 3, the majority of the tumor tissue exhibits a papillary architecture of a single layer of columnar to cuboidal cells around a slender vascular connective tissue core. In some portions, the cells are multilayered (Figs. 4 and 5), and sometimes a solid pattern can be observed (Fig. 6). The cytoplasm of the cells is scanty, and nuclei are hyperchromatic, with moderate variation in size (Figs. 4 and 7). Many mitoses

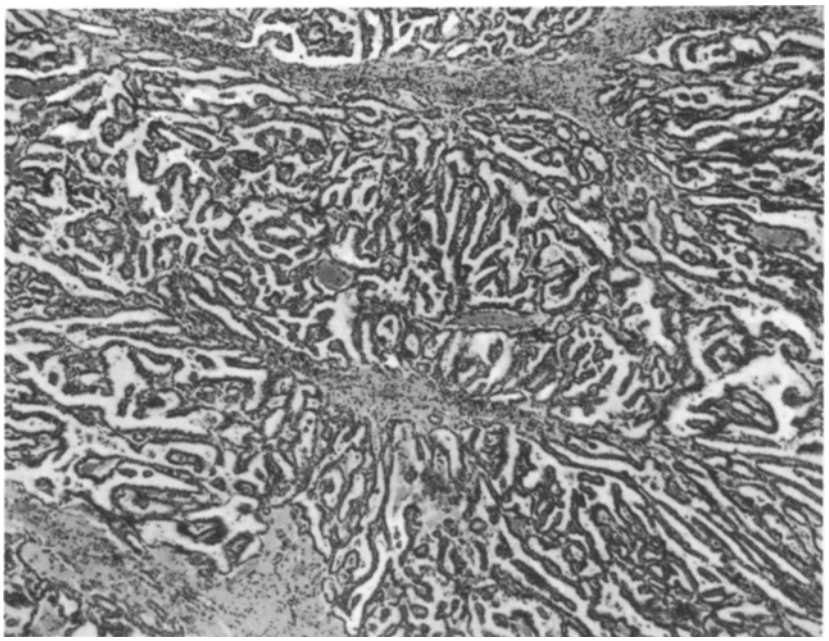

Fig. 2. Microscopic section of the carcinoma tissue from Case 1, showing a papillary architecture (HE, 100:1)

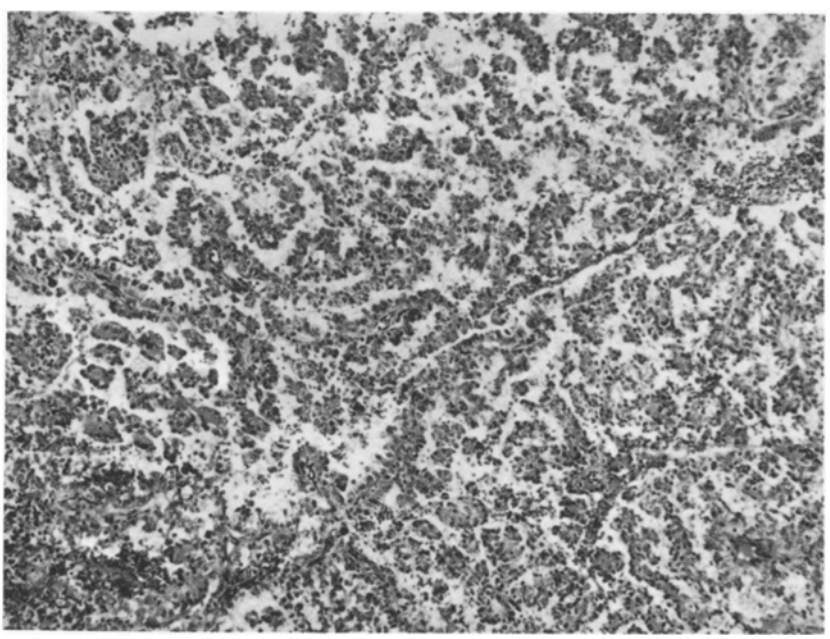

Fig. 3. Microscopic section of the carcinoma tissue from Case 2, showing a papillary pattern (HE, 100:1)

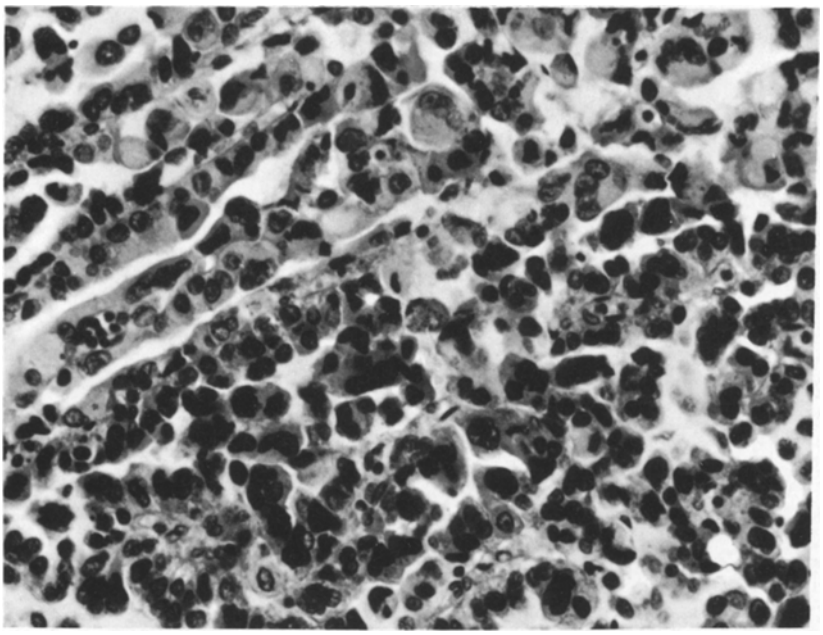

Fig. 4. Microscopic section from Case 1, showing nuclear pleomorphism of the carcinoma cells (HE, 400:1)

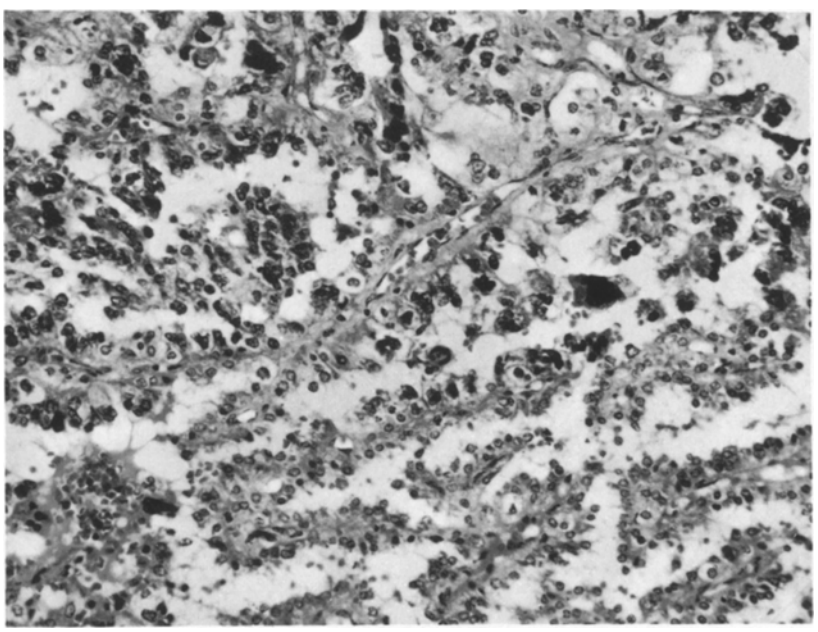

Fig. 5. Microscopic section from Case 2, showing multilayer arrangement of the carcinoma cells (HE, 200:1)

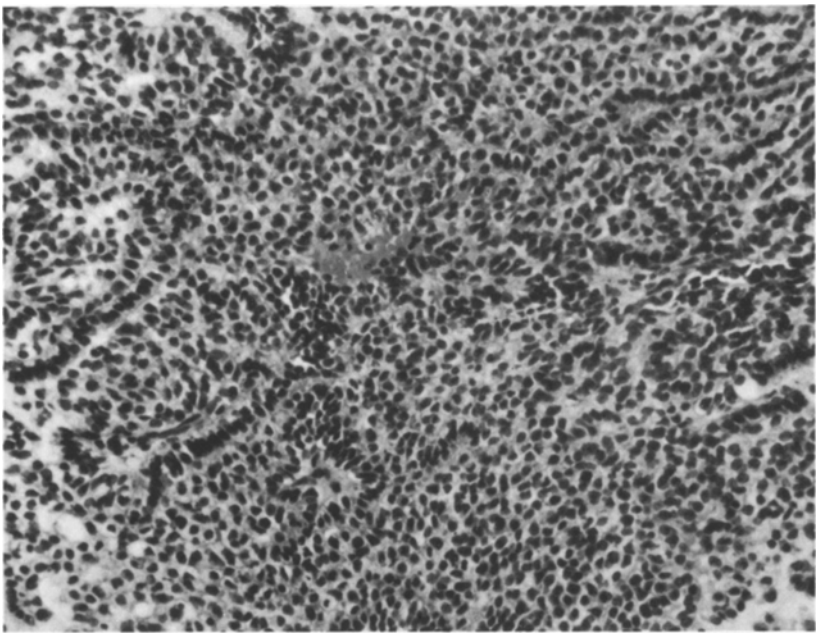

Fig. 6. Microscopic section from Case 1. A solid pattern is observed (HE, 200:1)

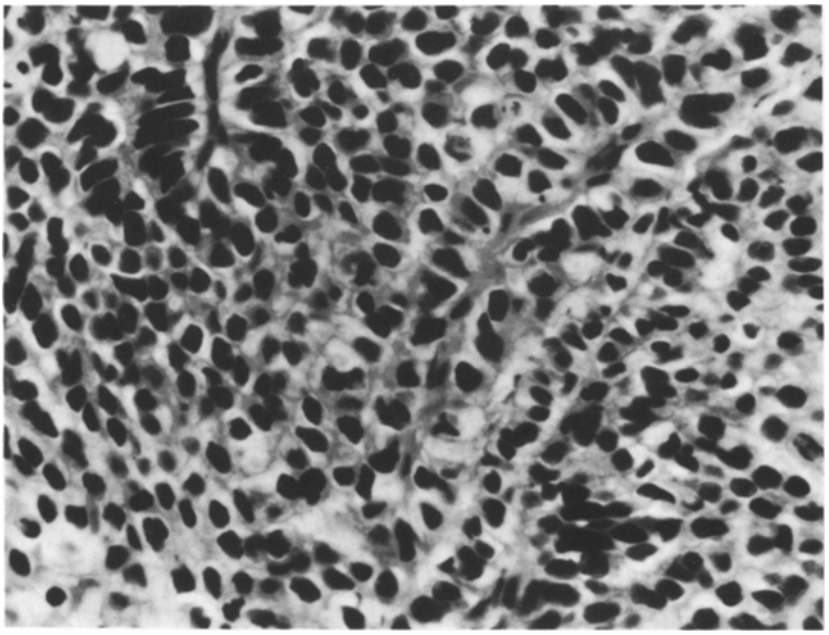

Fig. 7. Microscopic section from Case 1. The cytoplasm of the carcinoma cells is scanty, and nuclei are hyperchromatic (HE, 400:1)

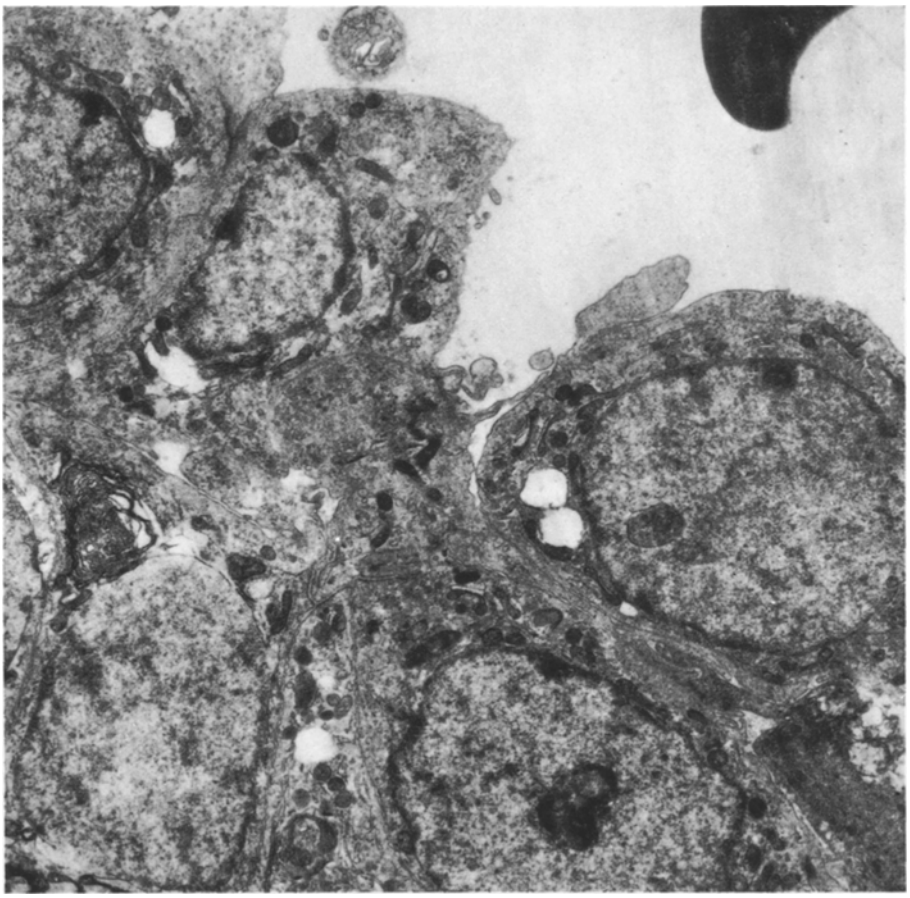

Fig. 8. Electron micrograph showing the carcinoma cells from Case 1 (700:1)

are seen. Many psammoma bodies are visible. In some parts (Fig. 4) there is marked nuclear pleomorphism with giant and multiple nuclei and abnormal mitoses. In autopsy specimens, wide areas of necrosis and hemorrhage can be observed.

PAS-stain: Deposits of PAS-positive cytoplasmic material that disappear following diastase digestion are observed. The amount of PAS-positive intracytoplasmic material is much larger in the carcinomas than in papillomas examined. PAS-positive material can also be observed on the ventricular surface of tumor cells, and its staining of the cell surface is much more intense in the cases of papilloma than in the carcinomas. Indeed, the surface material of carcinoma cells is hardly demonstrable by PAS.

Alcian blue-stain: Alcian blue-positive material is hardly observed on the ventricular surface of the carcinoma cells though intense staining with Alcian blue is seen on the papilloma cells. On the other hand, Alcian blue-positive material can be observed in the stromal components of the interstitium between the basal surface of carcinoma cells and the vascular tissue.

Alcian blue-positive material on the ventricular surface of tumor cells is not abolished by the treatment with either hyaluronidase or chondroitinase, but the staining in the interstitium is diminished by enzyme treatment. The former is considered to consist of heparan sulfate and/or glycoprotein, the latter mainly of hyaluronic acid and chrondoitin sulfate.

Orcein-stain: In the papilloma cases, a strikingly large amount of orcein-positive material, both granular and fibrillar, can be observed in the interstitium surrounded by the tumor cells. In the carcinoma cases, only a very small amount of the same material can be demonstrated.

Electron Microscopy

The carcinoma cells have nuclei of regular round or oval shape containing abundant chromatin and conspicuous nucleoli of compact type with occasional thread-like structure (Fig. 8). Mitochondria are scarce and small in size with a dense matrix. Rod-like and C-shaped mitochondria are often found. Rough endoplasmic reticulum is difficult to detect but an abundance of free polyribosomes is noted in the cytoplasm. Development of the Golgi-apparatus is normal in size and number. Glycogen particles are visible, but the deposits are few compared to the case with the papillomas.

Some of the carcinoma cells have tendency to maintain an apical-basal polarity, but the multilayered cells show a complete loss of polarity. The ventricular surfaces are irregular, but the formation of microvilli is not distinct. Only three cilia could be detected throughout. On the lateral surfaces, there are a small number of attenuated desmosome-like structures by which the carcinoma cells adhere with each other. Invagination of the basal plasma membrane is infrequent in the carcinoma cases, although many basal plasma membrane invaginations, outlined by a basal lamina, can be observed in the papilloma cases.

Discussion

In the present study the morphology of papillary carcinoma of plexus chroioideus was observed and compared with benign papillomas. The structure of the carcinoma was essentially similar to that of papillomas and the choroid plexus of infants, but the multilayered carcinoma cells with a solid pattern showed "atypia", as observed generally in malignant tumors derived from other origins; namely, loss of polarity, hyperchromatic nucleus, nuclear pleomorphism, anisocytosis, and increase in the ratio of nucleus to cytoplasm etc. Moreover, the following differences in morphology could be pointed out:

1) Both PAS- and Alcian blue-positive materials could be observed on the ventricular surface of papilloma cells, but they were difficult to detect in the carcinoma cases. Electron miccroscopically, the few microvilli on the ventricular surface of the carcinoma cells were underdeveloped. Alcian blue staining, which was not abolished by digestion with either hyaluronidase or chondroitinase, may have consisted of heparan sulfate and/or glycoprotein. In a previous study (Takeuchi et al. 1977), the present author reported that Alcian blue-positive materials, consisting mainly of heparan sulfate, could be detected on the surface of microvillous processes of the cell line MDCK which has a distinct quality

Table 1. The literature on papillary carcinoma of choroid plexus

Authors		Case No.	Age	Sex	Location	Total length of history	P	F	Mi	G	N	I	Mt	[a] [b]
Bielshowsky and Ungar	1906		43 y	F	IV	6 months	–	–	–	–	–	–	+	PC:SC
Kölpin	1909		53 y	F	Mul	4 months	–	+	–	–	+	–	+	PC:SC
Boudet and Clunet	1910	1	45 y	M	RL	2 months	–	–	–	–	–	–	–	PC:UCT
Hart	1910		50 y	F	Mul	3 months	–	–	+	–		–	+	PC:SC
Bouwdijk Bastiaanse	1914		59 y	F	Cerebellum	2 months	–	–	+	–	–	–	+	PC:SC
Körner	1919	1	42 y	M	IV	12 months	–	–	–	–	–	–	–	PC:SC
		2	9 y	M	RL		+	–	–	–	–	–	–	PC:PP
		3	7 y	M	IV	2 weeks	–	–	–	–	–	–	–	PC:EP
Kono	1924		31 y	M	LL	4 months	+	–	+	–	–	–	–	PC:SC
Davis and Cushing	1925	2	9 y	M	LL	11 months	+	+				–	–	PP:PC
		4	30 y	F	IV	17 months	+	–		–	–			PC:SC
Töppich	1926		2 y	M	IV	2 months	+	+	+	–	+	+	+	PC:PC
Esser	1926		22 y	M	IV	6 months	+	+	+	+	–	+	–	PC:PC
Glomelski	1926		50 y	F	Spin	4 months	–	–		–		–	–	PC:SC
Lehoczky	1928		27 y	F	IV	2.5 months	–	–	+	+	–	–	–	PC:SC
Schuster	1931		57 y	F	III		+	–		+	–	+	+	PC:SC
Hall and Fentress	1933		61 y	M	Cauda equina	13 months	–	–						PC:SC
Graves and Fliess	1934		9 m	M	LL	3 weeks	+	+		+	–	+	–	PC:PC
Faber	1934		29 y	M	RL	2 weeks	–	–	+	–	–	+	–	PC:SC
Omura	1936		36 y	M	RL	10 months	–	–	+	+	+	+	+	PC:SC
Zdrahal	1936		10 y	F	III	4 years	–	–	+	–	–	+	–	PC:PIN
Friedman and Solomon	1936		20 m	M	LL	3 weeks	+	+		+	+	–	–	PP:PC
Tuner and Simon	1937	1	27 y	M	III	14 months	–	–	+	+	+	–	–	PC:SC
Rand and Reeves	1940	4	21 m	F	LL	2 weeks	+	+	+					CE:PC
Berger	1942		53 y	M	IV	5 months	–	–	+	–	+	+	+	PC:SC
Globus and Kuhlenbeck	1944	8	2.5 m	M	LL	12 days	+	+	+			+	–	EP:PC
Walker and Horrax	1947		44 y	M	IV	> 163 months	–	–	–			+		PC:SC
Wilkins et al.	1948		6 y	M	LL	> 40 months	–	–	+		+	+		PC:UCT
Ringertz and Reymond	1949	10	33 y	F	III	12 months	–	–	+			+		PC:EP
Zander	1949	6	26 y	M	RL	> 15 months	+	–	+	–	–	–	–	PC:PP
Vraa-Jensen	1950		7 y	F	RL	52 months	+	+	+	+	+	+	+	PC:PC
Lindenberg	1951		41 y	M	III	6 years	–	–	+	–			–	PC:HD

Kahn and Luros	1952	2	2 y	F	RL	11 months	+	+				+		PP:PC
Tamura et al.	1954		13 y	M	III	6 months	−	−	−	+	+	−	−	PC:SC
Cardauns	1957		23 y	M	IV	52 months	+	−	−	+	−	−	−	PC:PP
Hoytema and Winckel	1957	1	10 m	M	LL	2 months	+	+	+	+			−	PC:PC
Takabatake and Iizuka	1957		54 y	M	LL	9 years	−	−	+	+	−	+	−	PC:SC
Nomura et al.	1958		5 y	F	RL	> 8 months	+	−			+	+	−	PC:PP
Dufek	1959		31 y	F	RL	5 months	−	−	+	+	+	−	−	PC:PP
Tokoro	1959		37 y	M	RL	18 months	−	−	+			+	+	PC:SC
Matson and Crofton	1960	8	20 m	F	LL	3 weeks	+	+	+	+		+		PP:PC
Fairburn	1960		15 m	F	RL	2 months	+	+						PP:PC
Watanabe	1961		11 y	F	RL	2 months	+	+	−	+	+	−	−	PP:PC
Vinken and Slooff	1965		17 m	M	LL	1.5 months	+	+	+	+	+	+	+	PC:PC
Lewis	1967	1	20 m	F	LL	2.5 years	+	+	+	+	−	+	+	PC:PC
		2	11 m	F	LL	5 months	+	+	+	+	+	+	+	PC:PC
		3	4 y	M	RL	5 months	+	+	+	+	+	+	−	PC:PC
Tham et al.	1969		66 y	F	IV	10 years	−	−	+	−	+	+	+	PC:SC
Otsuki	1970		14 y	M	RL?	4 years	−	−	+	+	−	+	−	PC:EMB
Brochu and Lefebvre	1971		53 y	M	RL	6 weeks	−	−	+	−		+	+	PC:SC
Shuangshoti and Tangchai	1971		47 y	M	RL	3 months	−	−	−	−	−	+	+	PC:SC
Dohrman and Collias	1975		55 y	F	IV	> 13 months	+	−				+		PC:PP
Kida et al.	1978		8 m	M	RL	2 weeks	+	+	+	+	+	+	+	PC:PC
Iwahara et al.	1979		5 y	M	RL	34 months	+	+	+		+		+	PC:PC
Fujiwara et al.	1979		16 m	F	RL	> 6 months	+	+	+	+				PC:PC
Hayakawa et al.	1979		2 m	F	LL	3 months	−		+				+	PC:UCT
Casentini et al.	1979		13 y	F	IV	> 71 months	+	+	+	+	−			PC:UCT
Vaquero et al	1979		26 y	F	LL	> 46 months	−	−				+	+	PC:SC
Valladares	1980		11 m	M	RL	> 9 years	+	+	+	+	−	+		PC:EP
Present cases		1	23 m	F	RL	4 months	+	+	+	+	+	+	+	
		2	25 m	M	RL	9 months	+	+	+	+	+	+	+	

[a] Diagnosis by the author reporting each case
[b] Our histological review

P=structure resembling plexus papilloma; F=fine branching of sheets of cells; Mi=Mitosis; G=giant or multinuclear cell; N=necrosis; I=invasion; Mt=metastases; y=year; m=month; RL=right ventricle; LL=left ventricle; III=third ventricle; IV=forth ventricle;; PC=choroid plexus carcinoma; SC=secondary carcinoma; UCT=uncertain, PP=choroid plexus papilloma; EP=ependymoma; PIN=ectopic pinealoma; CE=choroidoependymoma; EMB=embryonal carcinoma; HD=tumor of hypophyseal duct origin

as a kind of renal tubular epithelium, and heparan sulfate was considered to play an important role in fluid transportation. It is conceivable that the papilloma cells of the choroid plexus, forming many microvilli on which heparan sulfate may exist, have a function in fluid transportation.

2) Alcian blue-positive material was observed in the stromal components of the interstitium between the basal surface of carcinoma cells and the vascular tissue. The enzyme-digestion test showed that the material consisted mainly of glycosaminoglycans. Toole et al. (1979) postulated that glycosaminoglycan, the major component of extracellular matrices through which cells migrate during embryonic tissue development, is also concentrated in regeneration in the environment through which neoplastic cells invade local host tissues. Our previous studies (Takeuchi 1965, 1966, 1974) showed that glycosaminoglycan support the viability of tumor cells in vivo and in vitro. It is conceivable that in the papillary carcinoma under discussion here, the growth of tumor cells is facilitated by glycosaminoglycans, which were observed as the interstitial components between the basal surface and the vascular tissue.

3) Orcein-positive material was very sparse in the interstitium between the carcinoma cells and vascular tissues, whereas a strikingly large amount of granular and fibrillar material could be seen in the papilloma cases. The papilloma cells had many invaginations in the basal plasma membranes which increased the interstitial space (between epithelial and vascular tissue) where the orcein-positive material existed. Papilloma cells may have an important role in the formation of this orcein-positive material. In previous studies, Takeuchi (1975, 1976) suggested that pleomorphic adenoma and adenoid cystic carcinoma cells of the salivary gland can produce orcein-positive fibrils.

The literature on choroid carcinoma is reviewed in Table 1. Although various authors reported cases as primary carcinoma, some seemed to be secondary carcinoma, and there were probably choroid papilloma, ependymoma or teratomatous tumors (tumors of hypophyseal duct origin, ectopic pinealoma or embryonal carcinoma). A few tumors were considered to belong to the same category as the papillary carcinoma presented here (Davis and Cushing 1925; Töppich 1926; Esser 1926; Graves and Fliess 1934; Friedman and Solomon 1936; Rand and Reeves 1940; Globus and Kuhlenbeck 1944; Vraa-Jensen 1950; Kahn and Luros 1952; Hoytema and Winkel 1957; Matson and Crofton 1060; Fairburn 1960; Watanabe 1961; Vinken and Slooff 1965; Lewis 1967; Kida et al. 1978; Iwahara et al. 1979; Fujiwara et al. 1979). The ages of these 22 cases, including the two under study, ranged from 2.5 months to 22 years, the mean age being 3.6 years. The ratio of males to females was 1:0.8. The time from the onset of symptoms to death was approximately 8.6 months. Thus, the choroid carcinoma is one of the most malignant tumors. The data are essentially in accord with those of Dohrmann and Collias (1975) in children. Sixteen cases (73%) were less than 3 years of age. Choroid carcinoma is quite similar in age distribution to retinoblastoma and neuroblastoma either of which may arise from the immature cells of the same embryonal stages. In reporting a case of congenital tumor, Matson and Crofton (1970) suggested that plexus papilloma in children is frequently of congenital origin, based chiefly on the statistical data. Vinken and Sloof (1965) reported a case of plexus carcinoma

with neuroblastoma of the adrenal medulla. Twenty cases originated in the lateral ventricles, where the right and left ventricle are equally affected, and 2 cases in the fourth ventricle. It is interesting that outside Japan, 10 of 14 cases affecting the lateral ventricle were found on the left side, whereas within Japan all six cases were on the right side. Van Wagenen stated that the majority (93%) of choroid papillomas of the temporal ventricle arose from the left ventricle. On the other hand, Watanabe (1961) reported that the incidence of choroid papilloma of the right ventricle was about twice that of the left ventricle in Japan. The higher incidence of choroid papilloma of the right lateral ventricle in Japan is considered to have an intimate relation to the incidence of choroid papillary carcinoma.

Herren (1941) and Norlen (1949) postulated that tumors originating from the choroid plexus in children are much more malignant in their local growth features than those arising in adults, though they show histologically benign features. Lewis (1967) considered that the lateral ventricle is the main site of neoplasia of the choroid plexus in childhood, and that the incidence of malignant transformation in such cases is relatively high. It is conceivable that, although almost all cases of choroid carcinoma are already malignant at the beginning of their development, there are a few choroid papillomas which transform into malignant neoplasms.

The authors thank Dr. S. Nagayoshi, Dr. N. Hirabayashi and Dr. I. Asamoto, who performed the autopsies, for their permission to publish.

References

Arai H, Yamasaki K, Yamasaki E, Ueki K (1976) A statistical study of brain tumors. No To Skinkei 28:779–791

Berger M (1942) Metastasierendes Papillom des Plexus Chorioideus Ventriculi IV. Zbl Allg Path Anat 80:5–9

Bielschowsky M, Unger E (1906) Zur Kenntniss der primären Epithelgeschwülste der Adergeflechte des Gehirns. Arch Klin Chir 81 (i):61–82

Bodian M, Sawson D (1953) The intracranial neoplastic diseases of childhood. A description of their natural history based on a clinicopathological study of 129 cases. Br J Surg 40:368–392

Bohm E, Strang R (1961) Choroid plexus papillomas. J Neurosurg 18:493–500

Boudet G, Clunet J (1910) Contribution àltude des tumeurs épithéliales primitives de l'éncephale. Développées aux dépens des formation épendymaires et particuliérement des plexus choroides. Arch Méd Exp 22:397–411

Bouwdijik Bastiaanse van (1914) Primäres, metastasirendes Gehirncarcinom. Z Ges Neurol Psychiat 27:96–108

Brochu P, Lefebvre R (1971) Adénocarcinome papillaire mucipare, multicentrique des plexus choroïdes. Union Méd Can 100:1787–1789

Cardauns H (1957) Über ein malignes Plexus Papillom. Zbl Neurochir 17:349–353

Casentini L, Rigobello M, Gerosa M, Pardatscher K, Andrioli GC (1979) Choroid plexus carcinoma. Case report. Zentral Neurochir 40:239–244

Cushing H (1932) Intracranial tumors: Notes upon a series of two thousand verified cases with surgical mortality percentages pertaining thereto. Charles C Thomas, Springfield, Ill USA

Davis LE, Cuching H (1925) Papillomas of the choroid plexus with the report of six cases. Arch Neurol Psychiat 13:681–710

Dohrman GJ, Collias JC (1975) Choroid plexus carcinoma. Case report. J Neurosurg 43:225–232

Dufek H (1959) Zur Frage des primären Carcinoms des Plexus chorioideus. Zentralb Allg Pathol Anat 100:136–142

Esser A (1926) Ein Carcinom des Plexus chorioideus des 4 Ventrikels. Z ges Neurol Psychiat 106:511–517

Faber V (1934) Fall von carcinomatös entartetem Papillom des Seitenventrikels. Frankfurt Z Pathol 47:168–172

Fairburn B (1960) Choroid plexus papilloma and its relation to hydrocephalus. J Neurosurg 17:166–171

Friedman JJ, Solomon CI (1936) Tumors of the choroid plexus in childhood. Am J Dis Child 52:114–127

Fujiwara S, Kodama N, Endo T, Takahisa H, Suzuki J (1979) A case of huge choroid plexus carcinoma of a childhood. No Shinkei Geka 7:889–892

Globus JH, Kuhlenbeck H (1944) The subependymal cell plate (matrix) and its relationship to brain tumors of the ependymal type. J Neuropathol Exp Neurol 3:1–35

Grant FC (1956) A study of the results of surgical treatment in 2, 326 consecutive patients with brain tumor. J Neurosurg 13:479–488

Graves GW, Fliess MM (1934) Neoplasm of the choroid plexus. Report of a case with review of the literature. Am J Dis Child 47:97–103

Gromelski A (1926) Beitrag zu der Lehre von den primären epithelialen Geschwülsten des Zentralnervensystems. Virchow's Arch Pathol Anat 261:933–942

Hall GW, Fentress TL (1933) Papilloma choroideum with diffuse central nervous system metastases. J Neurol Psychopathol 14:108–115

Hart K (1910) Über primäre epitheliale Geschwülste des Gehirns zugleich Untersuchungen und Betrachtungen über das Ependymepithel. Arch Psychiatr Nervenkr 47:739–773

Hayakawa I, Fujiwara K, Tsuchida T, Aoki M (1979) A case of choroid plexus carcinoma. No Shinkei Geka 7:815–818

Herren RY (1941) Papilloma of the choroid plexus. Arch Surg Chicago 42:758–774

Hoytema GJ, Winckel WEF (1957) Zur des primären Plexus-karzinoms. Zentralb Neurochir 17:353–363

Iwahara T, Tashiro K, Abe H, Tsuru M (1980) An autopsy case of malignant choroid plexus papilloma. Shinkei Kenkyu No Shimpo 24:397–398

Kahn EA, Luros JT (1952) Hydrocephalus from overproduction of cerebrospinal fluid. (And experiences with other papillomas of the choroid plexus). J Neurosurg 9:59–67

Kida H, Kamishiro M, Yonekura A, Yamamoto M, Sasakuri Y (1978) Malignant choroid plexus papilloma – An autopsy case report – No To Shinkei 30:99–105

Kölpin O (1909) Multiple Papillome (Adeno-Carcinoma) des Gehirns. Arch Psychiat Nervenkr 45:595–604

Kono N (1924) Über Implantationsmetastasen in Subarachnoidalraum, zugleich ein Beitrag zur Frage der Liquorstörung. Frankfurt Z Pathol 30:92–103

Körner H (1919) Geschwülste der Adergeflechte. Zentralb f Allg Pathol 30:121–135

Lehoczky TV (1928) Zur Frage der primären Gehirncarcinome. Arch Psychiat Nervenkr 82:527–566

Lewis P (1967) Carcinoma of the choroid plexus. Brain 90:177–186

Lindenberg R (1951) Über ein Plexusepitheliom des 3 Ventrikels mit geschichtetem Plattenepithel und einer Auskleidung der Ventrikelwand mit dem gleichen Epithel. Zentralb Allg Pathol Anat 88:47–51

Matson DD, Crofton FDL (1960) Papilloma of the choroid plexus in childhood. J Neurosurg 17:1002–1027

Nomura R, Yamakawa H, Uno T, et al. (1958) Malignant papilloma of the choroid plexus. No To Shinkei 10:639–643

Norlen G (1949) Papillomas of the choroid plexus. With report of a successfully removed tumor of the left lateral ventricle in a 7 months old child. Acta Chir Scand 98:273–279

Ohya T, Kaneoko Y (1970) Novel hyaluronidase from Streptomyces. Biochim Biophys Acta 198:607–609

Omura J (1936) A case of choroid plexus carcinoma with multiple metastases. Tokyo Iji Shinshi 109:24–29

Otsuki M, Okura H, Tamaoka M, et al. (1970) A case of choroid plexus papilloma with a mosaic neuroendocrine picture. No To Shinkei 22:1071–1077

Posey LC (1942) Papilloma of the choroid plexus. Report of a case and summary of recorded cases. Arch Path 34:911–916
Rand CW, Reeves DL (1940) Choroid plexus tumors in infancy and childhood; report of four cases. Bull Los Angeles Neurol Soci 5:31–46
Ringertz N, Reymond A (1949) Ependymomas and choroid plexus papillomas. J Neuropathol Exp Neurol 8:355–380
Rubinstein LJ (1970) Atlas of Tumor Pathology. Second Series. Fascicle 6. Tumors of the Central Nervous System. Armed Forces Institute of Pathology, Washington, D.C., pp 257–267
Russell DJ, Rubinstein LJ (1977) Pathology of tumors of the nervous system. Fourth ed. Edward Arnord, London, pp 220–224
Sato O, Sano K (1975) Brain tumors of children. No To Shinkei 27:185–193
Schuster H (1931) Über diffuse Meningeal carcinomatose. (Ein Beitrag zu ihrer Entstehung) Virchows Arch 280:195–203
Shuangshoti S, Tangehai P (1971) Primary adenocarcinoma of choroid plexus. Arch Pathol 91:101–106
Takabatake N, Iizuka R (1957) Über einen Fall von Plexus papillom mit diffuser infiltrierender Piametastase. No To Shinkei 9:728–733
Takeuchi J (1965) Growth-promoting effect of chondroitin sulphate on solid Ehrlich ascites tumour. Nature 207:537–538
Takeuchi J (1966) Growth-promoting effect of acid mucopolysaccharides on Ehrlich ascites tumor. Cancer Res 26:797–802
Takeuchi J, Tchao R, Leighton J (1974) Protective action of mucopolysaccharides on dog kidney cell line MDCK in meniscus-gradient culture. Cancer Res 34:161–168
Takeuchi J, Sobue M, Yoshida M, Esaki T, Katoh Y (1975) Pleomorphic adenoma of the salivary gland. With special reference to histochemical and electron microscopic studies and biochemical analysis of glucosaminoglycans in vivo and in vitro. Cancer 36:1771–1789
Takeuchi J, Sobue M, Katoh Y, Esaki T, Yoshida M, Miura K (1976) Morphologic and biologic characteristics of adenoid cystic carcinoma cells of the salivary gland. Cancer 38:2349–2356
Takeuchi J, Sobue M, Shamoto M, Yoshida M, Sato E, Leighton J (1977) Cell surface glycosaminoglycans of cell line MDCK derived from canine kidney. Cancer Res 37:1507–1512
Tamura J, Ushijima H, Takashi M, Sakai I (1954) An autopsy case of malignant tumor of plexus chorioideus. Gann 45:333–334
Tham KT, Wen HL, Teoh TB (1969) A case of papillary adenocarcinoma of the choroid plexus. J Pathol 99:321–324
Tokoro Y (1959) Brain tumors. Igakushoin, Tokyo, pp 263–269
Toole BP, Biswas C, Gross J (1979) Hyaluronate and inovasioness of rabbit V 2 carcinoma. Proc Natl Acad Sci USA 76:6229
Tooth HH (1912) Some observations on the growth and survival period of intracranial tumors, based on the record of 500 cases, with special reference to the pathology of the gliomata. Brain 35:61–108
Töppich G (1926) Die Zottenkrebse des Adergeflechtes der Rautengrube. Frankfurt Z Pathol 33:238–247
Turner OA, Simon MA (1937) Malignant papillomas of the choroid plexus. Report of two cases with a review of the literature. Am J Cancer 30:289–297
Valladares JB, Perry RH, Ramanand MK (1980) Malignant choroid plexus papilloma with extraneural metastases. Case report. J Neurosurg 52:251–255
Vaquero J, Cabezudo J, Seunda G, Carrillo R, Uria JG (1979) Primary carcinoma of the choroid plexus with metastatic dissemination within the central nervous system. Acta Neurochir 51:105–111
Vinken PJ, Slooff ACJ (1965) A case of carcinoma of the choroid plexus in a child. Zentralb Neurochir 26:313–317
Vraa-Jensen G (1950) Papilloma of the choroid plexus with pulmonary metastases. Acta Psychiatr Neurol 25:299–306
Wagenen WP van (1930) Papillomas of the choroid plexus. Report of two cases, one with removal of tumor at operation and one with "seeding" of the tumor in the ventricular system. Arch Surg (Chicago) 20:199–231

Walker JC, Horrax G (1947) Papilloma of the choroid plexus with report of an unusual case. J Neurosurg 4:387–391

Watanabe M (1961) An autopsy case of the choroid-plexus tumor originated from the right lateral ventricle – literary review of the cases in Japan – No To Shinkei 13:211–214

Wilkins H, Smith R, Halpert B (1948) Neoplasm of the choroid plexus of the left lateral ventricle. J Neurosurg 5:406–410

Yamagata T, Saito H, Habuchi O et al. (1968) Purification and properties of bacterial chondroitinases and chondrosulfatase. J Biol Chem 243:1523–1535

Zander E (1949) 6 Fälle von Papillomen des plexus chorioideus. Psychiat Neurol 118:321–363

Zdrahal N (1936) Ein Fall von Karzinom des Plexus chorioideus mit ungewöhnlichen klinischen Erscheinungen. Arch Kinderheilk 109:24–29

Zülch KJ (1965) Brain Tumors. Their Biology and Pathology. Translated by A.B. Rothboller and J. Olszewski; 2nd American ed. Springer, New York, pp 66–70

Accepted February 19, 1982

Virchows Arch [Pathol Anat] (1982) 395:319–330

Virchows Archiv A

Giant Cell Tumor of Bone

Enzyme Histochemical, Biochemical and Tissue Culture Studies

Haruhiko Yoshida, Masahiro Akeho, and Tokichi Yumoto
Department of Pathology, Tottori University School of Medicine, Yonago, Tottori 683, Japan

Summary. Three giant cell tumors of bone (2 benign and 1 malignant) were examined enzyme-histochemically, and a tissue culture study of the malignant case was performed. Multinucleated giant cells and mononuclear round cells had similar activities of ACPase and non-specific esterase with a diffuse strong reaction. ATPase and 5′-nucleotidase reactions were strongly positive in the cytoplasm of multinucleated giant cells, and were seen not only in the cytoplasm but also on the cell membrane of round cells. The proliferating spindle cells in the malignant case were faintly positive for ACPase and non-specific esterase and were less positive for ATPase and 5′-nucleotidase on the cell membrane. The multinucleated giant cells and mononuclear round cells resembled histiocytes in the activities of 4 hydrolytic enzymes, and the multinucleated giant cells had enzyme activities similar to those of osteoclasts from new-born rat skull.

The malignant giant cell tumor and cells in its tissue culture showed ALPase activity preferentially on the cell membrane of the spindle cells, and rarely on round cells or multinucleated giant cells. ALPase was resistant to heat treatment and was found to be the type IV isoenzyme by diffusion electrophoresis. The origin of the giant cell tumor of bone and the significance of the ALPase activity are discussed.

Key words. Giant cell tumor – Tissue culture – ALPase – Osteoclast – Histiocyte

Giant cell tumor of bone is not completely characterized due to the variety of cell types present. These include multinucleated giant cells resembling osteoclasts, and mononuclear 'stromal' cells with abundant vessels. An understanding of the histogenesis of the disease requires that we resolve the correct relationships between multinucleated giant cells and the 'stromal' cells. We have used several

Offprints requests to: H. Yoshida at the above address

0340-1227/82/0395/0319/$02.40

techniques to promote a better comprehension of the subject. Electron microscopy revealed 2 types of 'stromal' cells: the fibroblast-like cell (type I cells) and the histiocyte-like cell (type II cells) (Göthlin and Erricson 1976; Aparisi et al. 1977a; Hashimoto et al. 1979). The multinucleated giant cells resemble osteoclasts cytologically, but the ultrastructural differences among them were reported to exclude a possible relationship of the multinucleated giant cells to osteoclasts (Aparisi et al. 1977a).

The enzyme-histochemical findings in giant cell tumor of bone also vary in the cases reported to date (Schajowicz 1961; Jeffree and Price 1965; Kraievski et al. 1970). ACPase and non-specific esterase activities of multinucleated giant cells were reported to resemble osteoclasts rather than osteoblasts (Kraievski et al. 1970). ALPase activity has not been recognized so far in this tumor except in 2 recently published reports which postulate a close relationship of giant cells to osteoblasts (Jeffree and Price 1965; Aparisi et al. 1978). Thus there are two controversial points: Does the multinucleated giant cell of giant cell tumor of bone resemble the osteoclast or osteogenic cell? and is the ALPase activity specific to the osteogenic cell?

In this article, 3 giant cell tumors of bone are studied histochemically, and one in tissue culture.

Materials and Methods

1. Tumor Tissues

The materials used in this study were 3 giant cell tumors of bone diagnosed histologically: From a 29-year-old male and a 65-year-old female and a 35-year-old male (Table 1). The tumor tissues excised surgically were fixed with 3 fixatives: 4% paraformaldehyde buffered at pH 7.4 for enzyme histochemistry, 3% glutaraldehyde in cacodylate buffer at pH 7.4 for electron microscopy and 10% formaldehyde for paraffin sections. The tissues for enzyme histochemistry were transferred to Holt's gum sucrose after fixation in paraformaldehyde for 5 h at 4° C, and cut at 4 μ with a cryotome (Bright) at −20° C. The enzyme activities employed in this study were as follows; alkaline phosphatase (ALPase) by Bengt et al., acid phosphatase (ACPase) by Yam and Li, β-glucuronidase by Hayashi, ATPase and 5′-nucleotidase by Müller-Hermelink and α-naphthylacetate esterase (non-specific est.) by Leder.

The material for electron microscopy was cut at 40 to 50 μ thickness with cryotome (Bright) after fixation overnight and linced with cacodylate buffer. If was then immersed in reaction mixtures of ALPase and ACPase for 45 min at room temperature, ATPase for 30 min at 37° C and 5′-nucleotidase for 120 min at 37° C. Each block, stained with reaction mixtures, was postfixed with 1% osmic acid for 1 h and processed by routine procedures.

2. Rat Osteoclasts

Imprint and short-time culture samples of osteoclasts from new-born rats were prepared for comparison with the tumor cells in enzyme activities. The frontal bones of new-born rats (2 days of

Table 1. Three giant cell tumors of bone, enzyme histochemical study

Case	Age	Sex	Site of tumor	Histology	Therapy	Recurrence
1	29	M	rt. upper arm, proximal	Grade 1	curettage	none (for 1 y. 7 m.)
2	65	F	lt. radius, proximal	Grade 1	curettage	none (for 6 m.)
3	35	M	rt. radius, distal	malignant	resection	3 times (for 5 m.)

age) were resected and the endocranial aspect used to produce imprints. The others were minced with scissors and cultivated in a short time with MEM + 5% FCS.

3. Tissue Culture

The tumor tissue diagnosed as malignant giant cell tumor of bone from a 35-year-old male, was minced aseptically with scissors and cultivated with MEM + 5% FCS. The primary culture cells were used in enzyme histochemistry, as mentioned above. Eighty mililiter of the culture medium was collected, concentrated 25 times and run on diffusion electrophoresis after divided into 3 groups: one with no treatment, one heated to 56° C for 20 min and one heated to 65° C for 10 min.

Results

I. Histological Findings

Two benign giant cell tumors of bone occurred in the right upper arm of a 29-year-old male and the left tibia of a 65-year-old female respectively, and showed similar histological features. They consisted of numerous multinucleated giant cells and mononuclear cells which were round, and scattered in the giant cells. The giant cells possessed numerous round nuclei, resembling those of round cells. The malignant giant cell tumor of bone, arising in the right radius of a 35-year-old male, recurred 3 times during 5 months. The most recent recurrence which developed at the site of excision, was of hen's egg size and also involved the dorsal subcutis of the right hand. The initial and second recurrences revealed the same histological findings as those in other 2 cases, but the last tumor showed a marked proliferation of spindle cells with a fibrosarcomatous

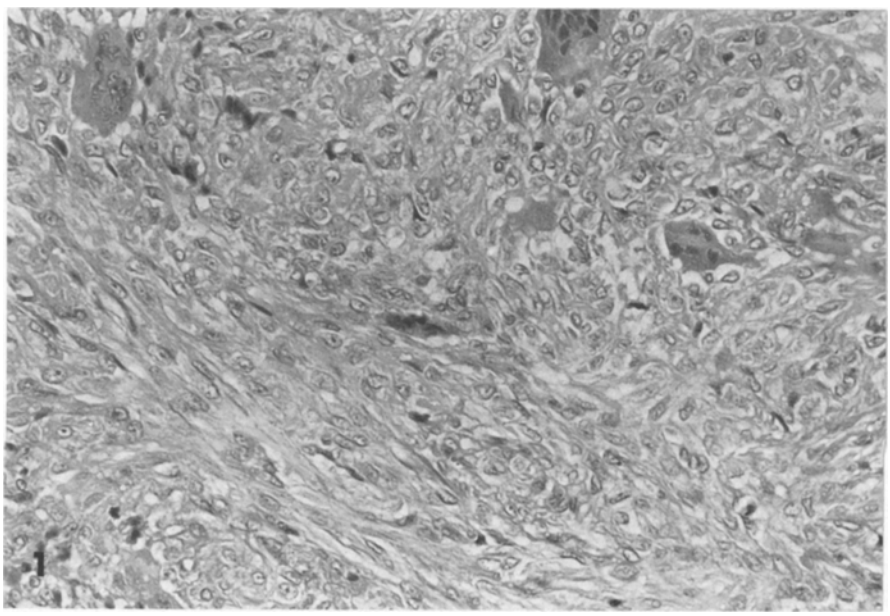

Fig. 1. Malignant giant cell tumor of bone (a 35-year-old male, rt. distal radius): The third recurrent tumor showing a proliferation of spindle cells as a fibrosarcomatous pattern. Multinucleated giant cells become smaller and less frequent.(H&E, ×80)

Table 2. Enzyme activities of giant cell tumor of bone and its tissue culture cells

	ACPase	Esterase	β-Gluc.	ALPase	ATPase	5′-Nucl.
Giant cell tumor						
Giant cell	+++	+++	−	− (+)	+++	+++
Round cell	+++	+++	−~+	− (+)	++	++
Spindle cell	+	+	+	− (++)	++	+
Tissue culture[a]						
Giant cell	+++	+++	−	−	+	++
Round cell	+++	+++	−~+	+	−~+	++
Spindle cell	−~+	+	+	+	−	−~+

( ) Malignant giant cell tumor

[a] Tissue culture cells of malignant giant cell tumor

pattern and infiltrated aggressively into the surrounding fat tissue (Fig. 1). In this area, giant cells were scanty and small. Mitotic figures were rarely observed.

II. Enzyme-histochemical Findings – Light and Electron Microscopy

The enzyme reaction was graded 0 as no reaction, + weakly positive, ++ moderately positive and +++ highly positive in accordance with the amount of the reaction product.

The cumulative result of enzyme reactions is shown in Table 2. The ACPase activity was strongly positive in the cytoplasms of the multinucleated giant cells and mononuclear round cells (Fig. 6). The enzyme reaction was present diffusely in their cytoplasm and was resistant to the addition of 5 mM tartaric acid. On the other hand, the malignant case arising in the right radius of a 35-year-old male showed less activity of ACPase following a decrease in the numbers of both multinucleated giant cells and mononuclear round cells. Proliferating spindle cells were weakly positive in the ACPase activity. This enzyme activity was located in lysosomes, small vesicles of the multinucleated giant cells and the lysosomes of round cells by electron microscope. The appearance of non-specific esterase activity was similar to that of the ACPase activity, i.e., the round cells more reactive than multinucleated giant cells (Fig. 7). The ATPase activity was highly positive in the cytoplasm of multinucleated giant cells, with a diffuse reaction. There was a considerable reaction in the cytoplasm and on the cell surface of round cells (Fig. 8). In the malignant tumor, the enzyme activity was decreased, with a weak reaction on the cell surface of spindle cells. Electron microscopy confirmed the presence of the reaction product in the lysosomes and in the small vesicles which were plentiful in multinucleated giant cells but scarce in round and spindle cells. The reaction products were also faintly precipitated on the cell membranes of multinucleated giant cells and strongly on round and spindle cells (Fig. 2). 5′-nucleotidase activity showed the same pattern as ATPase activity (Fig. 9). ALPase was positive on the vessel

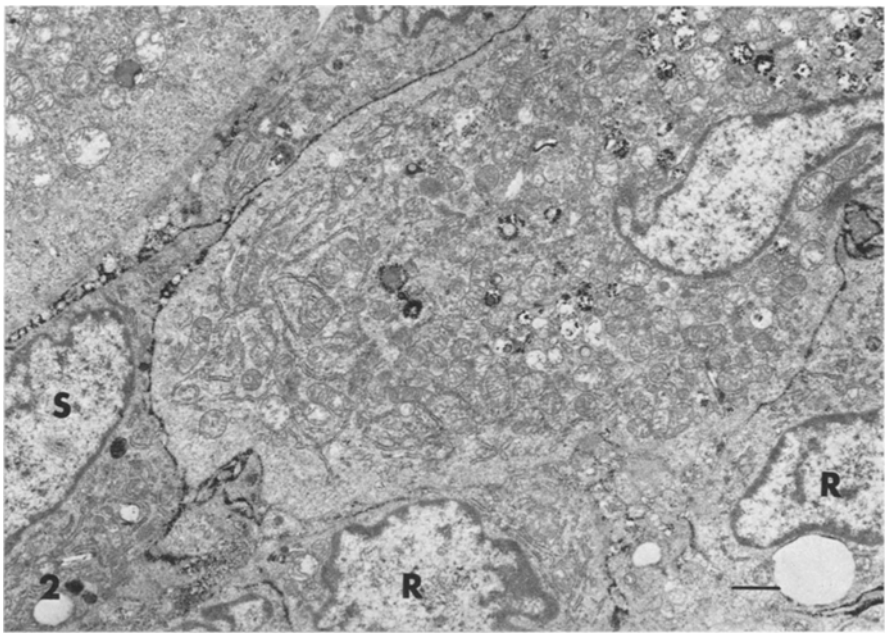

Fig. 2. ATPase reaction of the multinucleated giant cells and the 'stromal' cells (electron micrograph, case 3): The reaction products are identified in the lysosomes and on the cell membrane of the multinucleated giant cells, and the cell membranes of round cells (*R*) and spindle cells (*S*). ×8,000

walls scattered in the tumor tissue stroma but not in the tumor cells of benign giant cell tumor of bone. In the malignant case, however, the tumor cells were in the ALPase reaction to a varying degree. The most positive cells were spindle cells, proliferating vigorously. A small number of round cells and multinucleated giant cells possessed the enzyme activity faintly on their cell surfaces. To make sure of this finding, double staining was carried out with ACPase and ALPase. The result indicated that some cells were reactive to both enzymes simultaneously (Fig. 10). The reaction product was precipitated only on the cell membranes (Figs. 3 and 4).

III. Isoenzyme of ALPase

ALPase is now classified into 5 or 6 isoenzymes, according to the types of supporting materials used for diffusion electrophoresis. To clarify the type of ALPase recognized in malignant giant cell tumor of bone, it was tested after the addition of several inhibitors, and by its heat resistance. Osteosarcoma was used as a control tissue. The result is summarized in Table 3. The ALPase activity of malignant giant cell tumor of bone was resistant to heat treatment at 56° C for 30 min but inhibition was complete on addition of 5 mM L-phenylalanine, 5 mM L-leucine and 5 mM EDTA (Fig. 11 b, c and d). In contrast, the ALPase in osteosarcoma was severely inhibited by heat treatment, but resistant to the additions of 5 mM L-leucine and 5 mM EDTA.

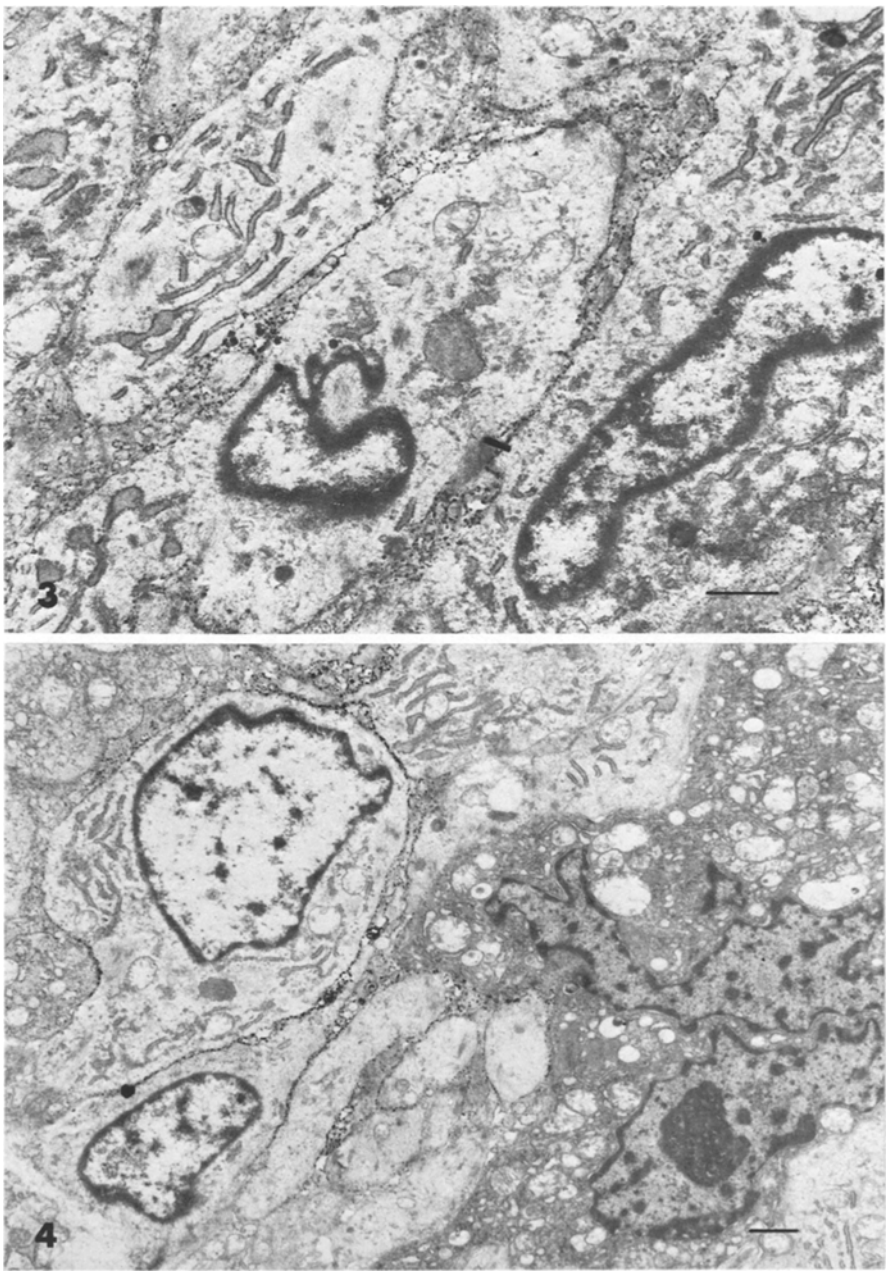

Figs. 3 and 4. ALPase reaction of malignant giant cell tumor of bone (electron micrograph). The enzyme activity is strongly positive on the cell membranes of the spindle cells (Fig. 3), and on a part of the cell membrane of the multinucleated giant cells (Fig. 4). ×12,300 of Fig. 3, and ×8,100 of Fig. 4

Table 3. ALPase activity with additions of various inhibitors and its heat resistency

	Heat	L-Phenyl.	L-Leucine	EDTA	L-Tryptophan
Giant cell tumor of bone, malignant	+++ (+++)	+ (+)	−~+ (+)	−~+ (+)	+ (+)
Osteosarcoma	−~+	+++	++	+	−

Control designated as (+++)
( ) Tissue culture cells

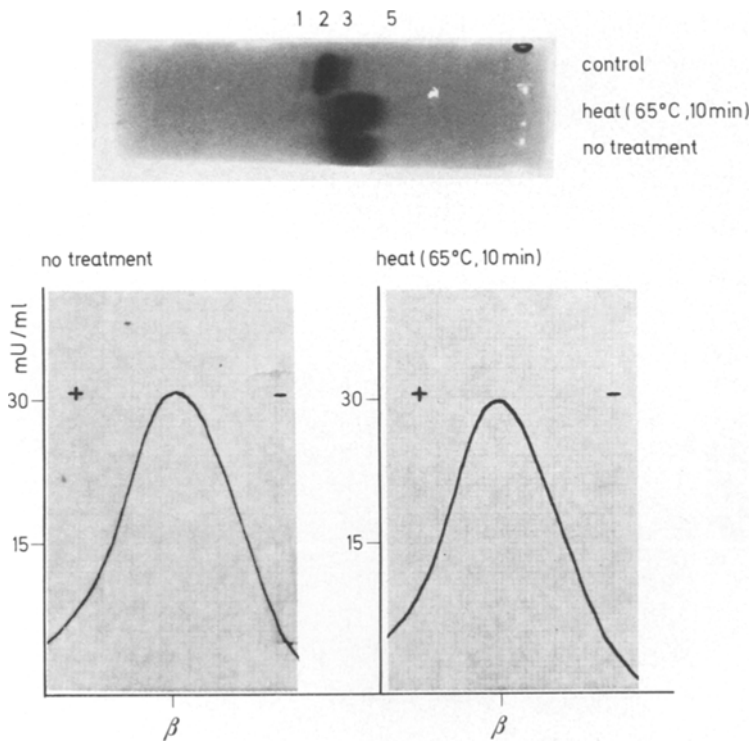

Fig. 5. Electrophoretic pattern of ALPase in tissue culture from malignant giant cell tumor of bone

IV. Enzyme Histochemistry of Cultured Cells

The tissue from the malignant giant cell tumor of bone was minced, trypsinized and cultivated in MEM with 5% FCS. Primary culture cells (1943 cells counted) showed 1.4% multinucleated giant cells, 26.5% round cells and 72.1% spindle cells. Enzyme activities of these cultured cells are shown in Table 2. All multinucleated giant cells possessed ACPase, non-specific esterase, ATPase and 5′-nucleotidase activities in the cytoplasm (Fig. 12a–d). The enzyme activities of round

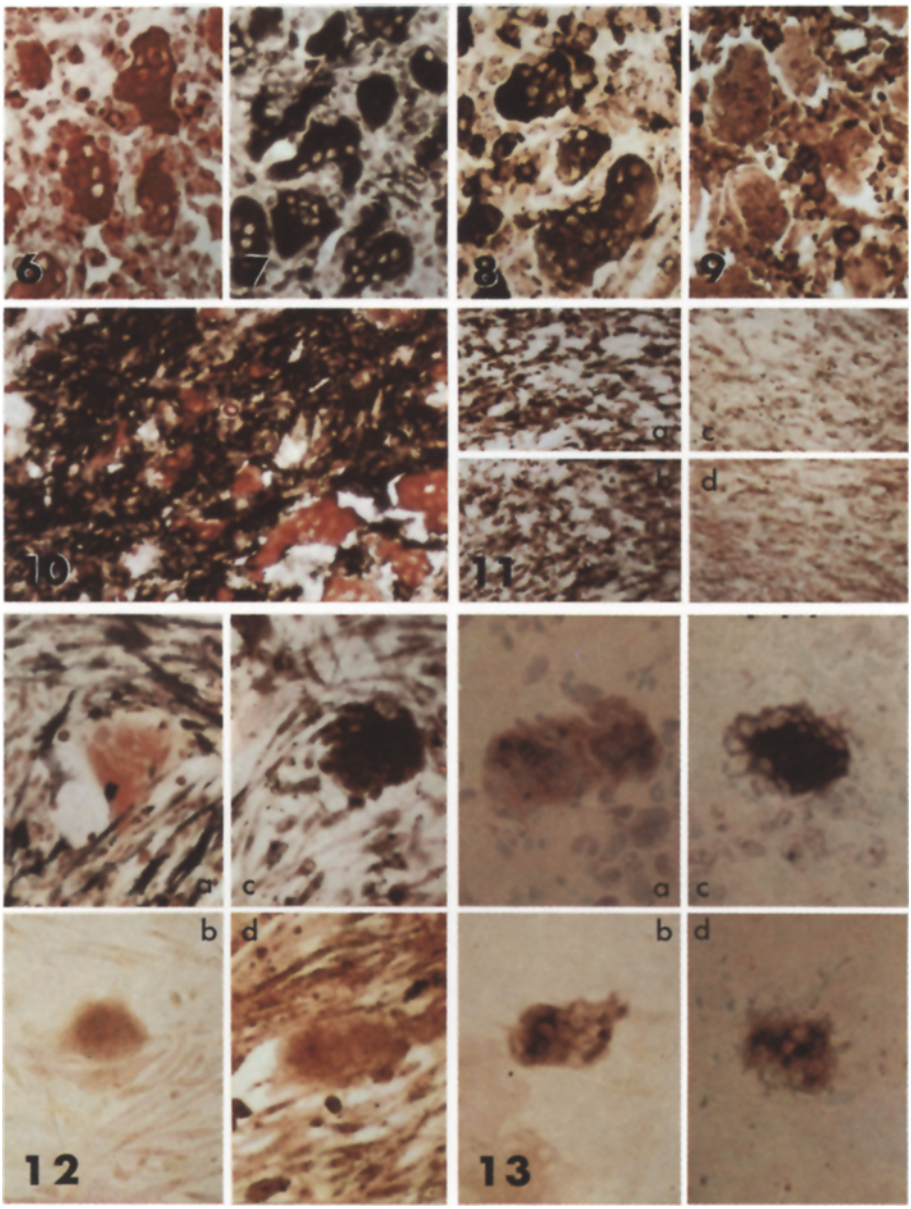

Fig. 6. ACPase reaction of giant cell tumor of bone (a 29-year-old male) and **Fig. 7.** α-Naphthylacetate esterase reaction of the same tissue. Showing strong activities in the multinucleated giant cells and mononuclear round cells with diffuse reactions

Fig. 8. ATPase reaction of giant cell tumor of bone (a 29-year-old male) and **Fig. 9.** 5′-nucleotidase reaction of the same tissue. Showing a strong activity in the cytoplasm of the multinucleated giant cells and mononuclear round cells, and on the cell surface of the mononuclear round cells. ×160 in each

Table 4. Hydrolytic enzyme activities of three types of giant cells

	ACPase	Esterase	β-Gluc.	ALPase	ATPase	5′-Nucl.
Giant cells in GCTB	+++	+++	−~+	− (+)	+++	+++
Culture cells	+++	+++	−	−	+	++
Osteoclast, rat	+++	+++	−~+	−	+++	+++
Foreign body giant cells, rabbit	+++	+++	+	−	−~+	+~++

( ) Malignant giant cell tumor
GCTB Giant cell tumor of bone

cells resembled those of multinucleated giant cells, but 20.8% of them manifested the ALPase activity simultaneously on their cell surfaces. Most spindle cells possessed the ALPase activity (Fig. 12a). Diffusion electrophoresis was performed on the culture medium collected and concentrated 25 times, and divided into 3 aliquots: an untreated one, one heated to 56° C for 20 min and one heated to 65° C for 10 min. As shown in Fig. 5, the ALPase in the culture medium made a broad band between types III and V, designated as type IV. There was no distinct difference in the enzyme activity among the three aliquots.

V. Enzyme Histochemical Findings of Rat Osteoclasts

It has been reported that there is a monolayer of a mixture of osteoclasts and osteoblasts on the endocranial aspect of the frontal bone of new-born rat (Hogg et al. 1980). An imprint of osteoclasts and short-time cultures were made from the frontal bone of 2-day-old rats. Enzyme cytochemistry was performed as mentioned above. ACPase, non-specific esterase, ATPase and 5′-nucleotidase were strongly demonstrated in the osteoclast, with a diffuse reaction (Fig 13a–d). No ALPase activity was present. In Table 4, the enzyme activities of 3 types of giant cells are summarized in comparison with multinucleated giant cells in giant cell tumor of bone, rat osteoclasts and foreign body

Fig. 10. Double staining of ALPase and ACPase reactions of malignant giant cell tumor of bone (a 35-year-old male). Showing ALPase activity in the spindle cells and part of the mononuclear round cells and on the cell surface of the multinucleated giant cells. × 160

Fig. 11a–c. ALPase resistency to heat treatment (56° C, 30 min, **b**), 5 mM L-phenylalanine (**c**) and 5 mM L-leucine (**d**). **a** Control × 160 in each

Fig. 12a–d. Enzyme activities of the tissue culture cells from the malignant giant cell tumor of bone. **a** ALPase and ACPase reactions, **b** α-Naphthylacetate esterase reaction, **c** ATPase reaction and **d** 5′-nucleotidase reaction. × 160 in each

Fig. 13a–c. Enzyme activities of the osteoclasts from new-born rat skull (2-day-old). **a** ACPase reaction, **b** α-naphthylacetate esterase reaction, **c** ATPase reaction and **d** 5′-nucleotidase reaction. × 160 in each

giant cells originating in histiocytes. They showed similar enzyme reactions for ACPase, nonspecific esterase, ATPase and 5′-nucleotidase, though the degree of the enzyme reaction varied for ATPase.

Discussion

A neoplasm is basically composed of monoclonal proliferation of tumor cells, whether benign or malignant. Giant cell tumor of bone recurs readily and invades into the surrounding tissue with a rare metastasis (Sanerkin 1980). However, it consists of a mixture of multinucleated giant cells and 'stromal' cells which vary and may be round or spindle shaped. Studies on giant cell tumor of bone have concentrated on elucidating the morphological and cytochemical characteristics of multinucleated giant cells and 'stromal' cells, in order to understand tumor histogenesis.

The electron microscopy demonstrated the similarity of multinucleated giant cells to osteoclasts, but also showed some distinction between intermediate cell types. It also showed 2 cell types of 'stromal' cell: the fibroblast-like type I cells and histiocyte-like type II cell (Göthlin and Ericcson 1976; Aparisi et al. 1977a). It is supposed that multinucleated giant cells are derived from a fusion or an amitotic division of the mononuclear 'stromal' cells (Aparisi et al. 1978). Hashimoto et al. (1979) confirmed the similarity of the cell components of giant cell tumor of bone and malignant fibrous histiocytoma of soft tissue, suggesting a derivation of giant cell tumor of bone from the histiocyte.

Many previously published reports on enzyme histochemistry suggest that the existence of ACPase and non-specific esterase activities in multinucleated giant cells indicate a similarity between these cells and osteoclasts (Schajowicz 1961; Fischman and Hay 1962; Ores et al. 1969; Hashimoto et al. 1979), but the reports on enzyme activities of 'stromal' cells vary from case to case. Aparisi et al. (1977b) reported that ACPase reaction of multinucleated giant cells and 'stromal' cells differed from that of osteoclasts in the location of the reaction product. They proposed a possible relationship of multinucleated giant cells to osteoblasts.

In this report, the 3 giant cell tumors of bone were examined enzyme-histochemically, especially for ALPase activity. The malignant case showed an aggressive growth of spindle cells of fibrosarcomatous pattern in the last recurrence although the primary tumor resembled the other 2 cases histologically. All 3 cases of giant cell tumor of bone showed high activities of ACPase and nonspecific esterase in multinucleated giant cells and mononuclear round cells. These enzyme activities were expressed in the same cells in a similar manner by double staining. The intensity and location of these enzyme reactions were identical with those of the osteoclasts of the new-born rat skull, but different from the osteoblasts. The malignant giant cell tumor of bone, however, revealed decreasing activities of both enzymes, probably due to a decrease of multinucleated giant cells and mononuclear round cells and an excessive increase of spindle cells.

For ATPase and 5′-nucleotidase activities, only a few reports have been published so far (Schajowicz 1961; Göthlin and Ericcson 1973b). Kraievski

et al. (1970) reported ATPase and 5′-nucleotidase activities in the giant cell tumor of bone at a low level. They emphasized that the ATPase related to bone resorption. Göthlin et al. (1973b) observed the reaction product of the ATPase activity at the brush border region and in lysosomes of the osteoclast in a similar manner to that of the histiocyte. In our study, both enzyme activities were recognized on the cell surface and in the cytoplasm of multinucleated giant cells, round cells and spindle cells. Electron microscopy revealed reaction products of both enzymes in the lysosomes and vesicles which were plentiful in the multinucleated giant cells and rather scarce in the round and spindle cells. The reaction products on the cell surfaces were more distinctively associated with the round and spindle cells. The tissue culture cells demonstrated the same reactions for the 4 enzymes as those of the 3 type cells of the tumor. The findings suggest that there seems to be a linear linkage among 3 types of cells (Sutton and Weiss 1966), and that the enzyme reactions of multinucleated giant cells and mononuclear round cells coincide with those of giant cells originating in histiocytes, suggesting a histiocytic origin of giant cell tumor of bone. Nevertheless, the enzyme activities of multinucleated giant cells resemble those of osteoclasts. It has been reported that there is a resemblance in biological and enzyme histochemical properties between osteoclasts and macrophages (Fischman and Hay 1962; Jee and Nolan 1963; Chambers 1979; Hogg et al. 1980). Touw et al. (1980) emphasized the possible derivation of the osteoclast from the macrophage, recognizing increasing activity of LDH following addition of calcium hydroxyapatite to macrophages, in a similar fashion to that seen with osteoclasts. Their finding supports our idea that giant cell tumor of bone should be designated as an histiocytic tumor.

ALPase reaction was not found on giant cell tumor of bone. Jeffree et al. (1965) recognized this enzyme activity only on the 'stromal' cells of malignant giant cell tumor of bone. They postulated that the enzyme activity appeared in regard to bone formation. Aparisi et al. (1978) confirmed the ALPase activity ultrastructurally on the cell membrane of multinucleated giant cells and fibroblast-like cells, and emphasized a possible relationship of multinucleated giant cells to osteoclasts. From the following 3 major reasons, however, the ALPase activity of our case seems to be independent of ALPase activity relating to bone formation. 1) The activity in our case was demonstrated only in the cell component of the malignant giant cell tumor, not in 2 benign giant cell tumors. The activity was localized to the cell membrane of spindle cells essentially and in some round cells. There was little reaction in multinucleated giant cells unrelated to bone formation. 2) According to Aparisi et al. (1978), the reaction product of ALPase was demonstrated on the plasma membrane, membranous bordering vesicles and vacuoles in multinucleated giant cells and fibroblast-like cells. The reaction product in our case was shown preferentially on the cell membranes of spindle cells and round cells, but the osteosarcoma cells possessed the ALPase activity on the cell membrane, lysosomes, vacuoles and rarely Golgi's complex. The intensity of the reaction product in osteosarcoma was much stronger when compared with that of giant cell tumor of bone. 3) The ALPase activity of malignant giant cell tumor of bone and its cultured cells were resistant to heat treatment and were proved to be type IV isoenzyme by diffusion electro-

phoresis. The appearence of type IV isoenzyme of ALPase is often recognized in association with some kinds of neoplasms and is supposed to be closely related to malignancy (Higashino 1976). Type IV isoenzyme of ALPase was manifest only in the malignant giant cell tumor in our 3 cases.

Acknowledgement. The authors are indebted to Dr. K. Matsui, Laboratory of Clinical Investigation, College of Health Science, University of the Ryukyus and Miss J. Nashiro for their technical assistance of tissue culture.

References

Aparisi T, Arborgh B, Ericcson JLE (1977a) Giant cell tumor of bone, detailed fine structural analysis of different cell components. Virchows Archiv [Pathol Anat] 376:273–298

Aparisi T, Arborgh B, Ericcson JLE (1977b) Giant cell tumor of bone, fine structural localization of acid phosphatase. Virchows Archiv [Pathol Anat] 376:299–308

Aparisi T, Arborgh B, Ericcson JLE (1978) Giant cell tumor of bone, fine structural localization of alkaline phosphatase. Virchows Archiv [Pathol Anat] 378:287–295

Chambers TJ (1979) Phagocytosis and trypsin-resistant glass adhesion by osteoclasts in culture. J Pathol 127:55–60

Fischman DA, Jay ED (1962) Origin of osteoclasts from mononuclear leukocytes in regenerating newt limbs. Anat Rec 143:329–338

Göthlin G, Ericcson JLE (1973a) Fine structural localization of acid phosphomonoesterase in the osteoblasts and osteocytes of fracture cells. Histochemie 35:81–91

Göthlin G, Ericcson JLE (1973b) Studies on the ultrastructural localization of adenosine triphosphatase activity in the fracture callus. Histochemie 35:111–126

Göthlin G, Ericcson JLE (1976) The osteoclast: Review of ultrastructure, origin and structure-function. Clin Orthop 120:201–231

Hashimoto K, Morimoto K, Akeho M, Yumoto T (1979) Electron microscopic observations of the primary malignant fibrous histiocytoma: comparison with the giant cell tumor of bone and the giant cell tumor of tendon sheath. J Clin Electron Microscopy 12:730–731

Higashino K (1976) Cancer and the alkaline phosphatase. Metabolism and disease 13:309–320 (in Japanese)

Hogg N, Shapiro IM, Jones SJ, Slusarenko M, Boyde A (1980) Lack of Fc receptors on osteoclasts. Cell Tissue Res 212:509–516

Jee WSS, Nolan PD (1963) Origin of osteoclasts from the fusion of phagocytes. Nature (London) 200:225–226

Jeffree GM, Price CHG (1965) Bone tumors and their enzymes. J Bone Joint Surg 47:120–136

Kraievski NA, Raikhlin NT, Soloviov JL (1970) Histochemical characteristics of giant cell tumor. Fol Histochem Cytochem 8:3–10

Ores R, Rosen P, Ortiz J (1969) Localization of acid phosphatase activity in a giant cell tumor of bone. Arch Pathol 88:54–57

Sanerkin NG (1980) Definition of osteosarcoma, chondrosarcoma and fibrosarcoma of bone. Cancer 46:178–185

Sanerkin NG (1980) Malignancy, aggressiveness and recurrence in giant cell tumor of bone. Cancer 46:1641–1649

Schajowicz F (1961) Giant cell tumors of bone (osteoclastoma): a pathological and histochemical study. J Bone Joint Surg 43A:1–29

Sutton JS, Weiss L (1966) Transformation of monocytes in tissue culture into macrophages, epithelioid cells and multinucleated giant cells. An electron microscope study. J Cell Biol 28:303–332

Touw JJA, Hemrika-Wagner AM, Vermeiden JPW (1980) An electron microscopic, enzyme histochemical study on the localization of lactate dehydrogenase (LDH) in osteoclasts and peritoneal macrophages of bone resorption and the origin of osteoclasts. Cell Tissue Res 209:111–116

Wood GW, Neff JR, Gollahon KA, Gourley WK (1978) Macrophages in giant cell tumor of bone. J Pathol 125:53–58

Accepted December 2, 1981

Virchows Arch [Pathol Anat] (1982) 395:331–343

Virchows Archiv A

Intrapulmonary Mesotheliomas: Their Identification by Tissue Culture

Emilio Alvarez-Fernandez and Julio Escalona-Zapata
Servicio de Anatomia Patologica, Hospital Provincial, Dr. Esquerdo nº 46, Madrid 30, Spain

Summary. Two cases of primary intrapulmonary spindle-celled sarcomas unrelated to the pleura have been studied by electron microscopy, tissue culture and histochemistry. Ultrastructurally both tumors showed some desmosomial unions. The first case showed cytoplasmic filaments, nuclear inclusions, prominent rough endoplasmic reticulum and abundant collagen in the interstitium. The second tumor showed scanty organelles and a paucity of interstitial connective tissue fibers. In spite of their spindle morphology both tumors showed a similar pattern in vitro, growing as an epithelial plaque in the same way as previously described mesotheliomas and related tumors, such as synovial sarcomas. Histochemistry of the tumor mass allowed the identification of most of the cavities which were engulfed alveoli and bronchioli.

Both neoplasm were classified as intrapulmonary mesotheliomas. Their relationship to other pulmonary lesions is discussed.

Key words: Mesothelioma – Tissue culture – Pulmonary neoplasms

Since the description by Abramhamson and Friedman, of three cases of "stromal mesotheliomas", tumors composed of spindle-celled elements resembling the typical fibrous pleural tumors, the existence of intrapulmonary mesothelial proliferations of a neoplastic or non-neoplastic nature has been suggested by some authors (Abramhamson and Friedman 1966, Costero et al. 1972), but still remains a subject of controversy.

In the absence of epithelial areas, identification of spindle cell neoplasms as being of mesothelial origin is difficult even with techniques such as electron microscopy and histochemistry. In contrast, tissue culture renders a quick and specific identification of these neoplasms, as the capability of normal mesothelium and mesotheliomas to differentiate into mesenchymal and epithelial elements

Offprint requests to: E. Alvarez-Fernandez at the above address

0340-1227/82/0395/0331/$02.60

in vitro, has been repeatedly reported (Maximow 1922; Stout and Murray 1942; Sano et al. 1960; Alvarez-Fernandez and Diez-Nau 1979).

We report here two cases of spindle-celled intrapulmonary neoplasms which showed a pattern of growth in vitro similar to that found in previously-reported monophasic mesotheliomas and synovial sarcomas (Stout and Murray 1942; Sano et al. 1960; Alvarez-Fernandez and Diez-Nau 1979, Alvarez-Fernandez and Escalona-Zapata 1981). These were classified as intrapulmonary mesotheliomas.

Material and Methods

All the specimens were sent to the laboratory quickly and under sterile conditions. Fragments for electron microscopy were cut into 1 mm^3 cubes, fixed in cold 2.5% glutaraldehyde in Milloning's phosphate buffer, osmicated, dehydrated in graded alcohols and embedded in Epon. Thick sections were stained with alkaline toluidine blue. Thin sections were obtained with an LKB III ultramicrotome, mounted on copper grids and double stained with uranyl acetate and lead citrate.

Fragments for enzyme histochemistry were deep frozen in liquid nitrogen. Cryostat sections were stained to demonstrate alkaline phosphatase (Lillie 1965), succinic dehydrogenase, diphosphopiridinnucleotide dehydrogenase, and adenosintriphosphatase (Dubowitz and Brooke 1973). For histochemical demonstration of mucosubstances fragments of tissue were fixed in 10% formalin-Cl_2Ca, and stained with PAS and Alcian blue pH 2.5.

Pieces of tissue for tissue culture were cut into 1–2 mm^3 cubes and explanted in rotating tubes following the technique of Gey modified by Kersting (Kersting 1961). Equal parts of chicken plasma and embryo extract were used. Every third day the explants were observed by phase contrast microscopy and then fixed in 10% formalin-alcohol and stained with haematoxylin and eosin. The findings were interpreted according to the criteria of Willmer (Willmer 1965). Previous cultures of normal pleural and synovial tissues as well as of pleural mesotheliomas, and a variety of soft tissue spindle cell sarcomas including monophasic and biphasic synovial sarcomas were used as controls.

Case Report

Case 1.

Clinical History. A 56-year-old male complaining of non-productive cough was found to have a round opacity in the left lower lobe and two more nodules of smaller size located in the right lobe and middle lobe. Physical, analytical and endoscopic exploration was negative. A resection of the basal segments of the left lower lobe was performed, followed by a wedge resection of the controlateral masses. The patient made an uneventful recovery and is alive and well without signs of recurrent tumor 9 months after the resection. No other tumor in the coelomic cavities or soft tissues could be found. No evidence of a previous exposure to any form of asbestos material could be obtained.

Macroscopical Appearances. The first specimen submitted included the basal segments of the left lower lobe and exhibited near the hilus a spherical mass 8 cm, in diameter without any macroscopical relationship with the pleura. It was of a rubbery consistency. The cut surface was homogeneous and whitish grey without areas of necrosis or haemorrhage. Both nodules from the contralateral lung measured 20 and 18 mm, and showed a similar appearance to the previously-described tumor. They were adherent to the visceral pleura and produced a plaque-like elevation of it.

Findings. All three nodules exhibited the same histological appearances. They were composed of spindle cells with oval normochromic nuclei joined together, forming fascicles with a well-defined storiform pattern. Mitotic figures were very rare and the cells were intermingled with abundant reticulin and collagen fibers. The neoplastic proliferation grew in a predominantly interstitial fashion,

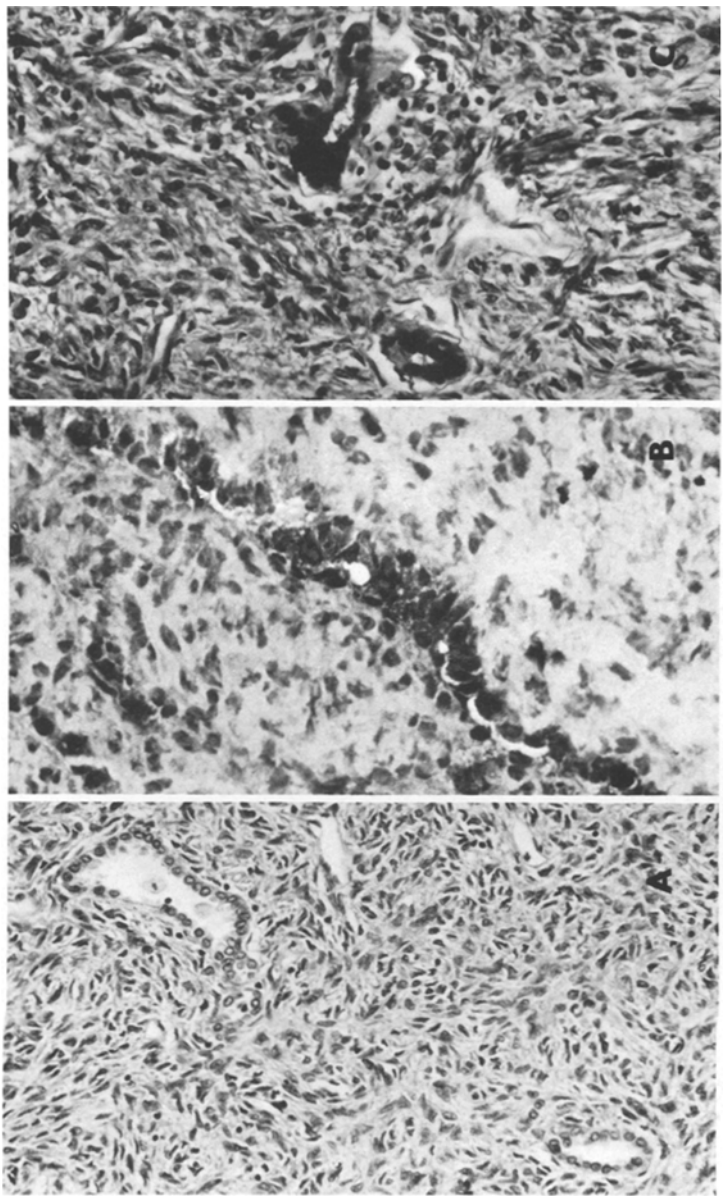

Fig. 1. (**A**) Case 1. Inside the tumor some cavities lined by cuboidal isomorphic epithelium can be seen. H.E. ×200. (**B**) Case 1. Similar field to that shown in figure to show the strong reactivity to alkaline phosphatase of the lining cells. ×400. (**C**) Case 1. Some of the cavities are lined by mucin secreting goblet cells. Alcian Blue. ×350

more evident in the peripheral part of the tumors. In places there was bronchiolar and vascular invasion shown on elastic stains. Inside the mass three different types of cavities could be seen. Some were tubular, ramified in longitudinal section, and lined by cuboidal isomorphic cells, which showed a positive reaction to alkaline phosphatase. Others were shorter and covered by cylindrical elements with mucus secretion (Fig. 1). Finally, there were numerous spherical or oval cavities, some very large, filled with PAS positive, roundish concretions and some Alcianophilic amorphous material. They were lined by cuboidal or attenuated epithelium showing degenerative phenomena with nuclear picnosis, loss of cohesion and granularity of the cytoplasm.

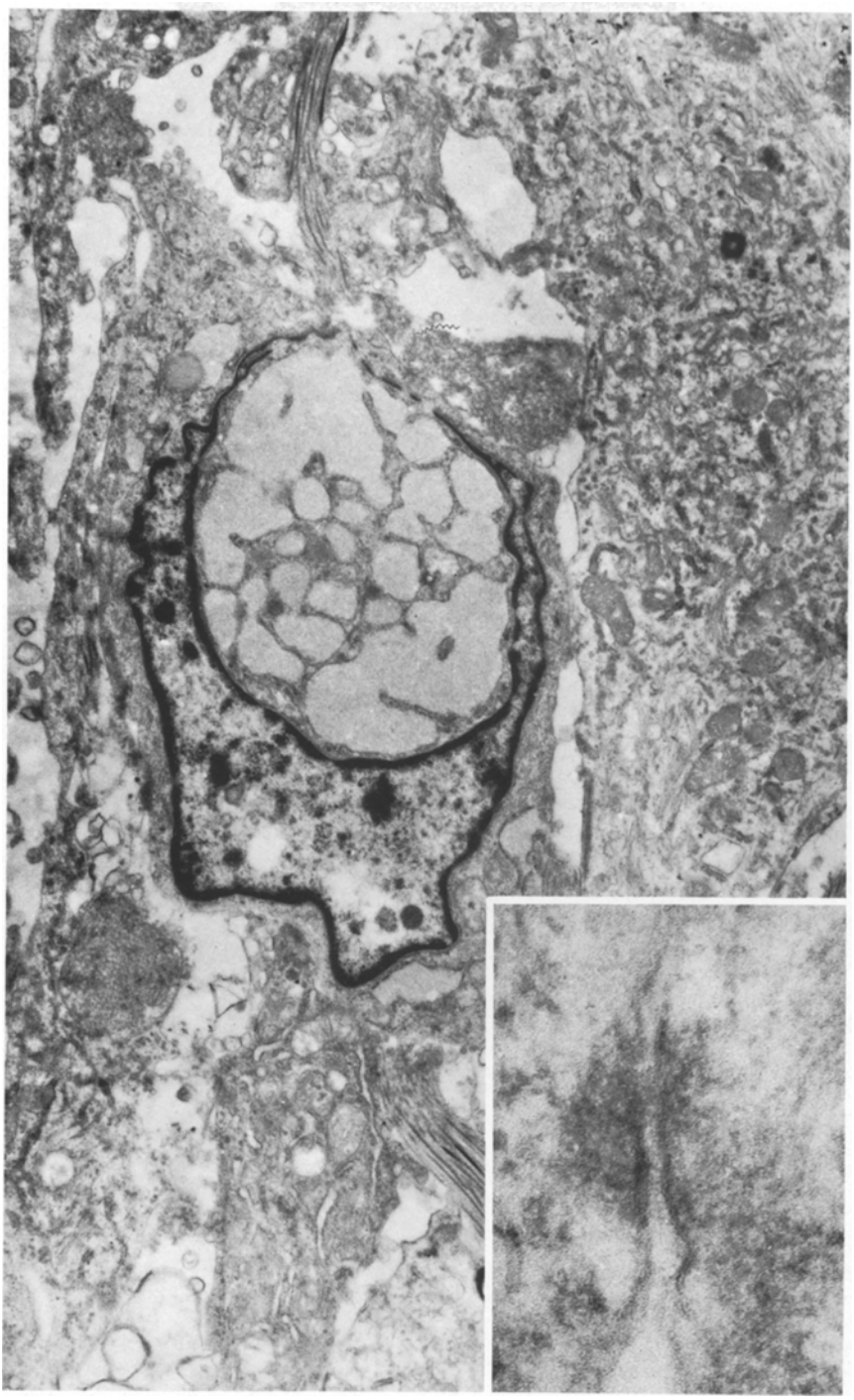

Fig. 2. Case 1. Ultrastructurally the neoplastic cells show an elongated cytoplasm with some short expansions, prominent nuclear pseudoinclusions, rough endoplasmic reticulum and some mithochondriae. Double stained ×3,000. *Insert:* Membrane condensation in the areas of close contact between adjacent cells. Double stained. ×25,000

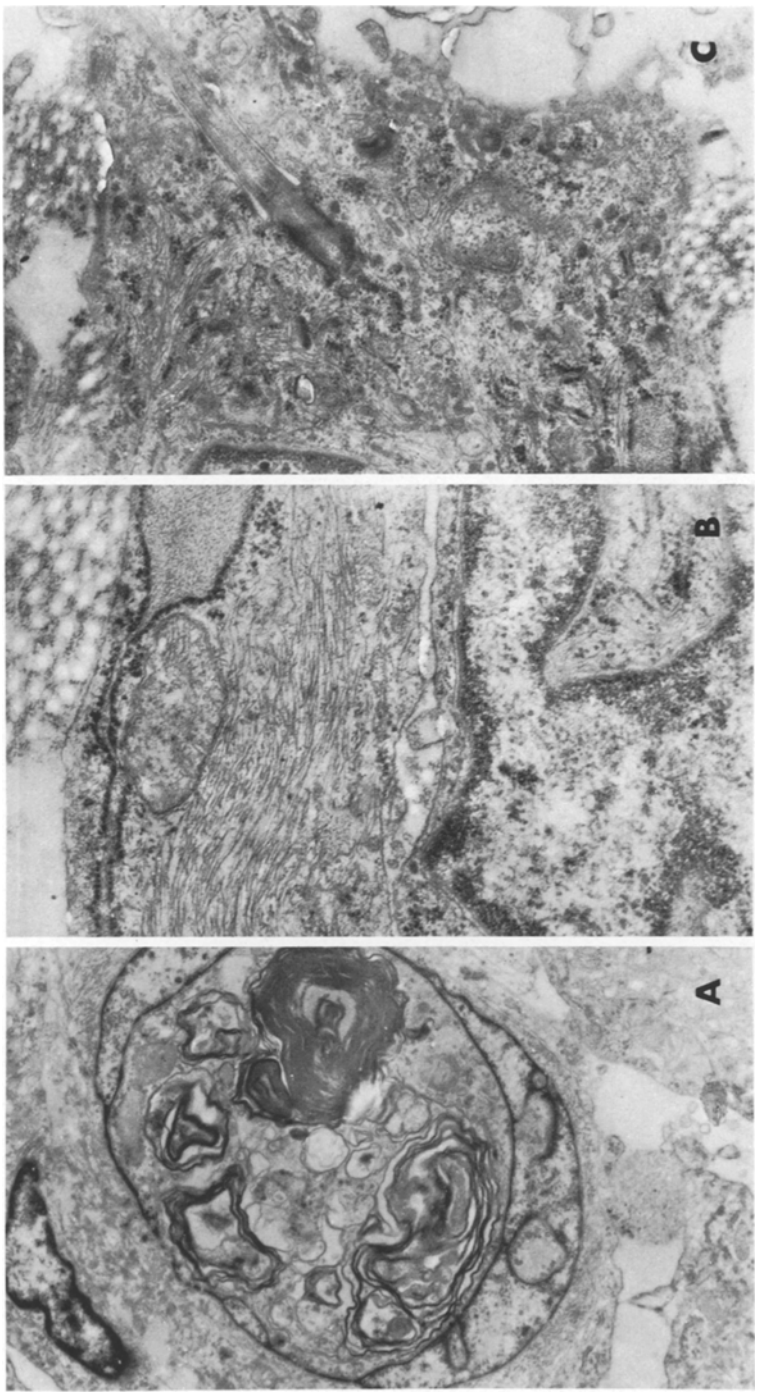

Fig. 3. (**A**) Case 1. Other variant of nuclear pseudoinclusion with abundant myelinic figures. Double stained. ×6,000. (**B**) Cytoplasm of a neoplastic cell showing abundant filaments and dilated cisternae of rough endoplastic reticulum. Double stained. ×25,000. (**C**) To show a cilium emerging to the cellular surface. Double stained. ×12,500

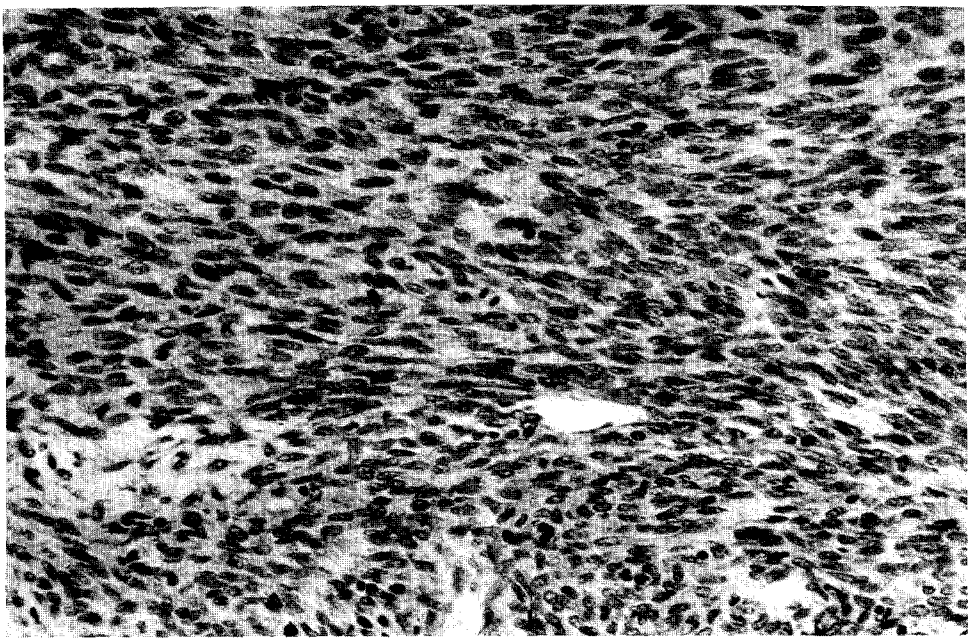

Fig. 4. Case 2. Light optical morphology of the tumor which is composed of spindle isomorphic cells with abundant mitotic figures. H.E. $\times 200$

From the ultrastructural point of view, the neoplastic cells were spindle-shaped with short cytoplasmic expansions which came in close contact with those of the neighbouring cells. At these points the plasma membrane was condensed (Fig. 2). No basal lamina was seen. The nuclei were lobulated or deeply indented, showing abundant cytoplasmic pseudoinclusions containing rough endoplasmic reticulum or myelin figures. The cytoplasm was filled with filaments, arranged in parallel bundles and without focal densities. Rough endoplasmic reticulum was very prominent and usually appeared filled with low density osmiophilic material. Mitochondria and Golgi cisternae were inconspicuous. Some abnormal cilia were seen emerging from the cell surface (Fig. 3). The interstitium showed well-structured vessels, normal-looking collagen fibers and some long-spacing collagen. The ultrastructural study of the cells lining the cavities demonstrated elements with dense osmiophilic bodies resembling Clara cells, as well as others showing features of degenerating pneumocytes.

Case 2

Clinical History. The patient was a 17-year-old female complaining of chest pain in the right hemithorax. Physical and analytical exploration demonstrated signs of collapse of the basal part of the right lung. On x-ray examination she was found to have a round opacity in the lower lobe. She was operated on and the lower lobe appeared increased in size and covered by a smooth glistening pleura. An incisional biopsy was followed by the partial ennucleation of a whitish grey encephaloid mass measuring 12×10 cm, with areas of lobulation. The mass was situated in the pulmonary parenchyma without any relationship to the visceral pleura. Frozen section was reported as spindle cell sarcoma, probably fibrosarcomatous mesothelioma. A lower lobectomy was done. The patient made an uneventful recovery. No other primary tumor either in the pleura or in the soft tissues was found. No evidence of exposure to asbestos was found.

Macroscopical Appearances. The tumor was a mass of confluent nodules of soft consistency and whitish coloration. In some places some yellowish necrotic areas with ill-defined borders were

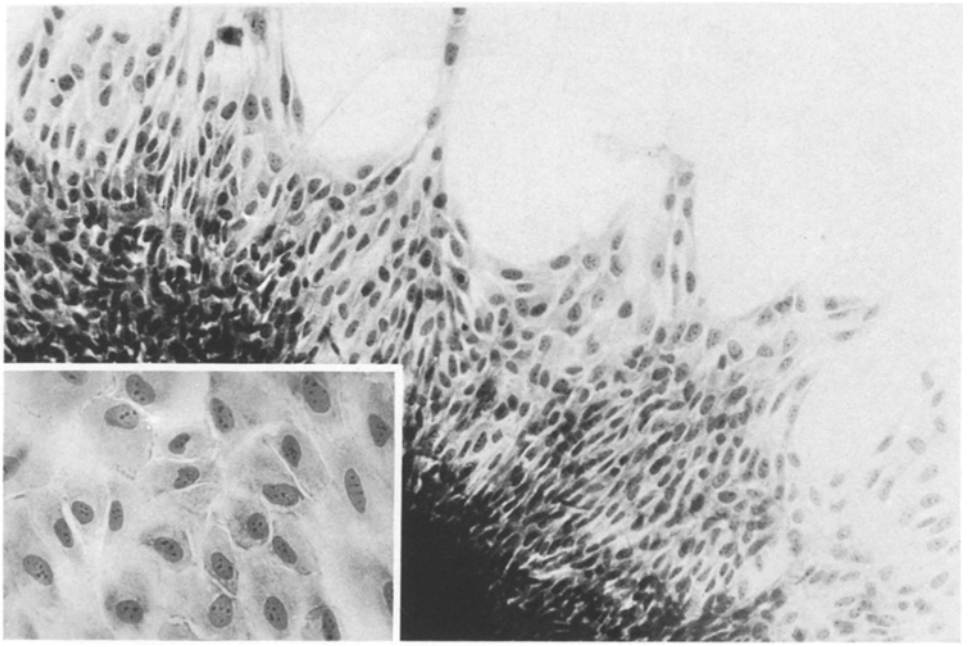

Fig. 5. Case 2. Nine day old culture. H.E. ×100. The cells emigrate from the explant as flat, polygonal elements, associated in an epithelial-like pattern. This morphology remains unvariable during the whole life of the culture. The peripheral cell association in tongues is frequent in mesothelial growths in contrast with the lineal margin of the common epithelial growths. *Insert:* A higher magnification of the same culture, showing the oval nuclei with two or three nucleoli and a flat and thin cytoplasm. The free lineal spaces among the cells are artifactual. H.E. ×400

seen. The lobectomy specimen showed an infarcted, partially-collapsed cavity measuring 8 × 9 cm, with extensive areas of haemorrhage. In the margin of the cavity some neoplastic nodules could be seen.

Microscopically, the tumor was composed of an amorphous proliferation of spindle cells with a well-defined acidophilic cytoplasm, oval isomorphic nuclei and abundant mitosis. These cells joined together in short fascicles intermingled with reticulin fibers (Fig. 4). Some areas of sclerotic and oedematous appearance were also found. Only after very diligent search and the study of multiple tissue blocks were some isolated acinar cavities, lined by cuboidal isomorphic epithelium containing glycogen, found. Alkaline phosphatase and adenosintriphosphatase clearly demonstrated the vessels, the tumor cells always being negative.

Electron microscopically the tumor was composed of polygonal or spindle cells with a rather smooth surface which defined small spaces of irregular contour. The cytoplasm showed abundant ribosomes and some profiles of rough endoplasmic reticulum, sometimes dilated and filled with amorphous material. Mitochondria, Golgi cisternae and other cytoplasmic organelles were very scanty. No filaments were seen. The nuclei showed a finely granular chromatin and a prominent nucleoli located near the nuclear membrane. In the interstitium scanty collagen fibers could be seen, the cells bein interconnected by scanty desmosomes.

Tissue Culture Findings

In spite of their light and electron microscopical differences, both tumors showed a similar growth pattern in tissue culture. From the third day of cultivation, polygonal cells joined together, forming a carpet-like structure, and emigrated

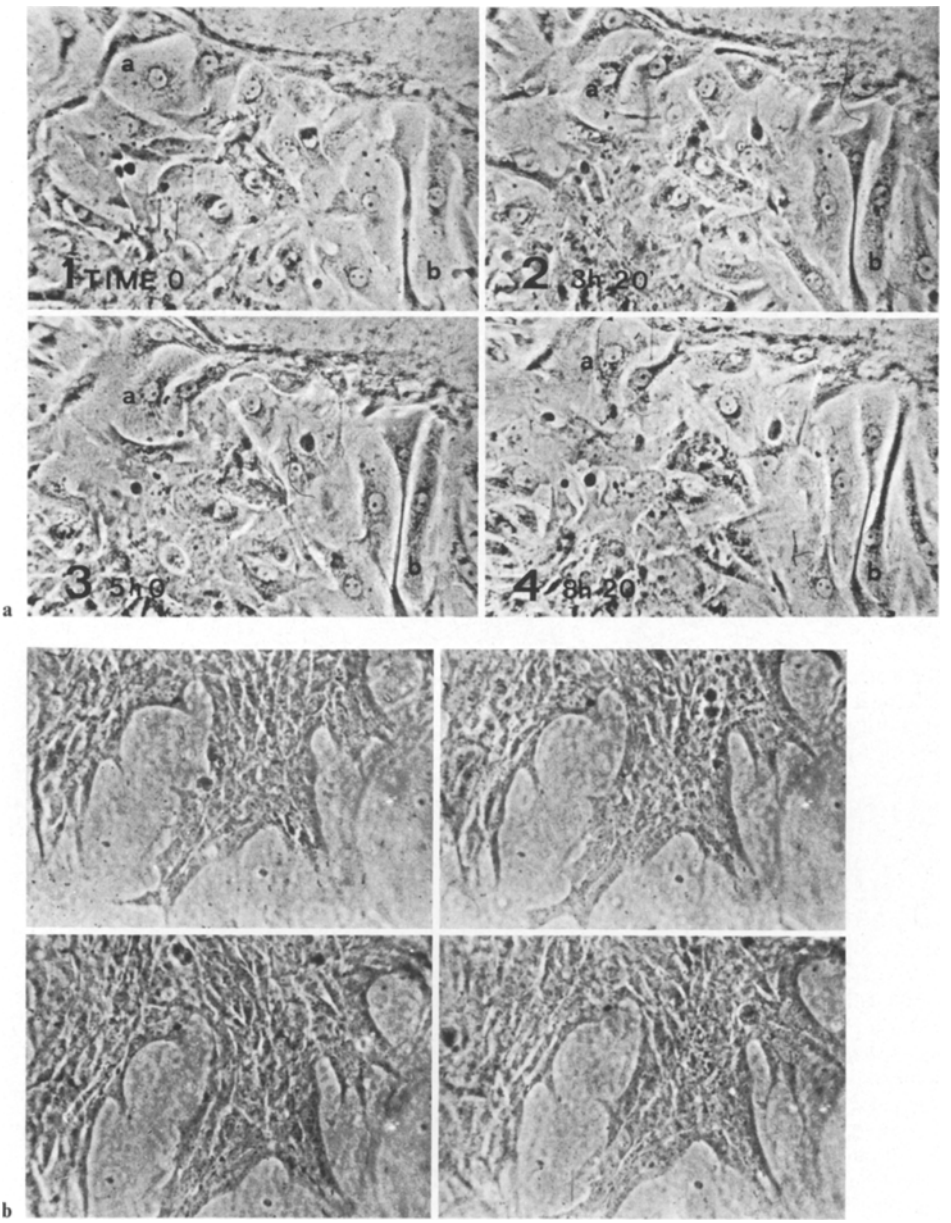

Fig. 6. (**A**) Case 1. Phase contrast. ×100. Microcinematographic time lapse sequence at 30 s per frame. The culture shows a high cohesion forming an epithelial-like carpet. During the individual movements, the cell form varies from flat, clear elements to small and dark ones cells (*a, b* and *c*). The simultaneous mass movements are more uncharacteristic and affect to larger groups of cells as those in the center of the figure. (**B**) Case 2. Nine day old culture. Phase contrast. ×100. Cinematographic time-lapse sequence at 30 s per frame. The dynamic behaviour of the case 2 differs from that of case 1 in the predominance of the whole mass movements. The individual displacement is less obvious and as a consequence the whole epithelial-like mass grows slowly far away from the explant. However, the presence of several mitotic cell divisions expresses the high proliferative rate of the cell growth

from the explant, forming a continuous sheet around it. The nuclei were round or oval, without atypia (Fig. 5). The cytoplasm was clear and eosinophilic, but no alcianophilic or PAS-positive material was found. From the 12th day of cultivation the plaques emitted some wedge-shaped groups of new cells arranged radially which quickly joined together into a continuous plaque. These characteristics persisted until the end of the observation time.

By phase contrast microscopy two types of cell can be demonstrated. The first was the most common and showed a broad, polygonal, clear cytoplasm in which only a few perinuclear refringent granules could be found. Other cells were longer and smaller with a darker cytoplasm evenly filled with granules.

Microcinematography demonstrated the following points in addition to those referred to above: 1) The cellular movements observed were very slow, as in epithelial tumors and synovial sarcomas. The cells move away from the explant sometimes as isolated elements and sometimes in groups, showing simultaneous displacement. 2) The cohesion between the cells was very high during the whole experiment. 3) Cinematography demonstrated the homogeneity of the cellular population with transitions between clear and dark cells. The clear cells seem to be a contractile phase of the dark cells. (Fig. 6).

Discussion

Demonstration by *light microscopy* of the mesothelial nature of spindle cell neoplasms can be only accomplished if plaques of epithelial-like elements or areas of acinar formation are found (Enzinger et al. 1969). In those cases in which the neoplasm grows as a pure mass of spindle cells special techniques are necessary. *Electron microscopy* has allowed the classification of some spindle-celled sarcomas arising in the soft tissues as synovial sarcomas (Mikelson et al. 1980), but for pleural mesotheliomas the results seem to be indefinite (Kannerstein et al. 1978). So while some authors have found desmosomial unions and discontinuous basal lamina in the monophasic fibrosarcomatous tumours, and have interpreted these features as evidence of mesothelial derivation (Kay and Silverberg 1971; Legrand and Pariente 1975), other reports have not demonstrated specific features of diagnostic importance (Luse and Spjut 1964; Wang 1973; Davis 1974; Klima et al. 1976; Suzuki et al. 1976). From the histochemical point of view the demonstration of hyaluronic acid synthesis by the tumor has been used as a diagnostic tool in biphasic neoplasms (Kannerstein et al. 1978; Wagner et al. 1962; Churg and Selikoff 1968; Arai et al. 1975), but the necessity for very specific enzymes (Arai et al. 1975) and the presence of this compound in the ground substance of other soft tissues sarcomas and juvenile connective tissue (Kindblom and Angervall 1975; Filipe and Mackenzie 1976), renders histochemistry an unsuitable method.

Tissue culture therefore appears to be the most reliable method by which to identify monophasic mesothelial tumors. Experimental work done by Maximow (1922) in normal pleural tissues showing biphasic growth in vitro of mesothelial cells, as "spindle fibroblast-like" and "polygonal epithelial-like" elements has been repeatedly shown to occur in explants of monophasic pleural mesotheliomas (Stout and Murray 1942; Sano et al. 1960; Alvarez-Fernandez and Diez-

Nau 1979), and also described in related tumors such as monophasic soft tissue synovial sarcomas (Alvarez-Fernandez and Escalona-Zapata 1981). This pattern of growth in vitro has been exactly the same as that shown by the present cases and so, on the basis of the tissue culture findings their mesothelial nature can be confidently claimed. Furthermore, in spite of being non-specific, the ultrastructural findings of short cytoplasmic expansions, intercellular unions, condensation of the membrane and the prominent bundes of cytoplasmic filaments are also features which support the mesothelial derivation in the first case (Stoebner et al. 1970; Davis 1974; Klima et al. 1976; Suzuki et al. 1976). In the second case the similarity between the tumor and reported cases of mesenchymal synovial sarcomas with scanty interstitial collagen and some desmosomes should be noted (Hernandez and Fernandez 1974; Mikelson et al. 1980; Alvarez-Fernandez and Escalona-Zapata 1981). Finally the similarity in the dynamic behaviour to synovial sarcoma, as shown by microcinematography, is another argument favoring a similar origin but one that in our view, needs further investigation.

The presence, inside the tumor mass, of a variety of acinar structures makes it necessary to identify their origin, in order to establish if the tumors are biphasic or monophasic. To this extent both histochemistry and electron microscopy can be of considerable help. In the first case it seems reasonable to say that the cavities lined by mucin-secreting epithelium correspond to engulfed bronchioli. The cavities lined with cylindrical non-mucin secreting and alkaline phosphatase-reactive epithelium correspond to those lined electron microscopically with cells with osmiophilic round inclusions and also are of bronchiolar origin, as alkaline phosphatase is an acceptable marker of Clara cells and granular pneumocytes (Fredricsson 1956; Sorokin 1960). Finally, most of the large-sized cavities lined with epithelium of variable morphology and non-reactive to alkaline phosphatase appear lined, electron microscopically, with degenerating granular pneumocytes and are therefore of alveolar derivation. This interpretation does not preclude the possibility that a minor proportion of the cavities could be true mesothelial slits, but this point has not been documented by the present study and so the tumor must be considered as monophasic.

In the second case, the lack of electron microscopical identification of the lining cells of the cavities precludes confident identification, but the lack of reaction to alkaline phosphatase, the presence of intracytoplasmic glycogen and the light optical morphology of the cells are arguments favoring their mesothelial origin. So, it is possible that the tumor is a biphasic one but with a marked predominance of the mesenchymal component.

In addition to the preceding arguments another requirement is necessary before being able to claim that we are dealing with true mesotheliomas. This is to exclude other biphasic pulmonary tumors or a secondary neoplasm, say metastatic mesothelioma, synovial sarcoma of soft tissues, or other biphasic neoplasms as nephroblastoma. The light microscopical appearances exclude pulmonary blastoma (Spencer 1961). The possibility of a metastasis from another mesothelioma of the peritoneum or other origin seems improbable as these tumors tend to remain localised in their territories of origin for very long periods of time before disseminating through the blood stream. Metastatic synovial sarcoma can also be excluded as usually this tumor only disseminates long

after the diagnosis of the primary mass and the development of successive local recurrences. These same facts and the age of the first patient exclude nephroblastoma.

The aggressive potential of our second case seems beyond doubt, taking into account the short clinical evolution, the size, mitotic activity and invasiveness of the tumor and its microscopical similarity to other cases with a well characterized malignant potential (Stout and Murray 1942; Sano et al. 1960; Alvarez-Fernandez and Diez-Nau 1979). The first case seems to be a more debatable one. The cells were very isomorphic with a low mitotic activity but showed a clear tendency to invade vessels. The possibility of a secondary origin of the two small nodules from the dominant mass in the contralateral lung or vice versa cannot be ruled out, but in our opinion the macroscopical protrusion of the pleura by the nodules points to a multicentric primary origin. The first case be considered to be a tumor of low malignancy and possibly of multicentric origin.

The existence of intrapulmonary mesotheliomas remains a subject of controversy. Abrahamson and Friedman (1966), described three intrapulmonary tumors composed of spindle cells without atypia or mitotic activity, joined together forming fascicles and intermingled with abundant collagen. All three tumors showed intrabronchial expansion and followed a benign course. They were considered to be "stromal mesotheliomas" similar to the common fibrous tumors arising in the pleural surface. Our cases are clearly different from these and their relationship with the case of Abrahamson and Friedman (1966) remains speculative, due to the fact that the true mesothelial nature of localized pleural mesotheliomas, although admitted by some authors (Yoshiyuki Okamura 1977; Kawai et al. 1978), has not been firmly demonstrated either by electron microscopy or tissue culture in all the cases (Maximow 1972; Hernandez and Fernandez 1974; Yoshiyuki Okamura 1977). The demonstration by Costero et al. (1972), that some of the previously considered pulmonary chemodectomas (Korn et al. 1960) show no secretory granules or nerve fibers and exhibit prominent RER and desmosomes has special importance to understanding their histogenesis, as these findings led them to hypothesize that the lesions could have a mesothelial origin. Kuhn and Askin (1975), and Churg and Warnock (1976), in later studies described other cases and reached the same conclusions, finding similarities between these lesions and meningiomas. Furthermore, embryological studies have demonstrated the possibility of mesothelial cells being entrapped during embryonic development (Hamilton et al. 1959). It can be hypothesized that intrapulmonary mesothelioma could develop both from mesenchymal cells of the pulmonary interstitium (Clarke 1915) and from misplaced mesothelial remnants. This makes the necessity to study primary intrapulmonary spindle cell tumors further especially those with an "aracnoidal pattern" (Spencer H. (personal communication 1972); Thurlbeck 1978).

References

Abrahamson JR, Friedman NB (1966) Intrapulmonary stromal mesothelioma. J Thor Cardiovasc Surg 51:300–306

Alvarez-Fernandez E, Diez-Nau MD (1979) Malignant fibrosarcomatous mesothelioma and benign pleural fibroma (localized fibrous mesothelioma) in tissue culture. A comparison of the in vitro growth pattern in relation to the cell or origin. Cancer 43:1658–1663

Alvarez-Fernandez E, Escalona-Zapata J (1981) Monophasic synovial sarcoma. Its identification by tissue culture. Cancer 47:628–635

Arai H, Endo M, Sasai Y (1975) Histochemical demonstration of hyaluronic acid in a case of pleural mesothelioma. Am Rev Respir Dis 111:699–702

Churg J, Selikoff IJ (1968) Geographic pathology of pleural mesothelioma. In: Liebow AA (ed) The lung. International academy of pathology monograph. William Wilkins, Baltimore, pp 284–297

Churg AM, Warnock ML (1976) So-called "minute pulmonary chemodectomas". A tumor not related to paragangliomas. Cancer 37:1759–1769

Clarke WC (1915/16) Experimental mesothelium. Anat Rec 10:301–306

Costero I, Barroso-Moguel R, Martinez-Palomo A (1972) Pleural origin of some of the supposed chemodectoid structures of the lung. Beitr Pathol Bb 146:351–365

Davis JMG (1974) Ultrastructure of Human mesotheliomas. J Natl Cancer Inst 52:1715–1725

Dubowitz V, Brooke MM (1973) Muscle biopsy. A modern approach. Saunders, Philadelphia, p 32

Enzinger F, Lattes R, Torloni M (1969) Tipos histologicos de tumores de los tejidos blandos. Clasificacion Internacional de tumores. Organizacion Mundial de la Salud. Ginebra

Filipe MI, Mackenzie DM (1976) Histochemical characteristics of mucosubstances in three soft tissue tumors. J Pathol 118:17–19

Fredricsson B (1956) The distribution of alkaline phosphatase in the rat lung. Acta Anat 26:246–256

Hamilton WJ, Boyd JD, Mossman HW (1959) Human embryology. H. Heflerand Sons. Cambridge. Citation: Costero et al. (1972)

Hernandez FJ, Fernandez BB (1974) Localized fibrous tumors of the pleura: A light and electron microscopic study. Cancer 34:1667–1674

Kannerstein M, Churg J, McCaughney WTE (1978) Asbestos and mesothelioma: A review In: Sommers SC, Rosen PP (eds) Pathology annual pp 81–129 Appleton Century Crofts New York

Kawai T, Mikata A, Torikata Ch, Yakumara K, Kageyama K, Shimosato Y (1978) Solitary (localized) pleural mesothelioma. A light and electron-microscopic study. Amer J Surg Pathol 2:365–375

Kay S, Silverberg SG (1971) Ultrastructural studies of a malignant fibrous mesothelioma of the pleura. Arch Pathol 92:449–455

Kersting G (1961) Die Gewebszüchtung Menschlicher Hirngeschwülste. Monographien aus dem Gesamtgebiet der Neurologie und Psychiatrie. Berlin Göttingen Heidelberg Springer

Kindblom L, Angervall L (1975) Histochemical characterization of mucosubstances in bone and soft tissue tumors. Cancer 36:985–994

Klima M, Spjut H, Seybold WD (1976) Diffuse malignant mesothelioma. Am J Clin Pathol 65:583–600

Korn D, Bensch K, Liebow AA, Castleman B (1960) Multiple minute pulmonary tumor resembling chemodectomas. Am J Pathol 37:641–672

Kuhn Ch, Askin FB (1975) The fine structure of so-called minute pulmonary chemodectomas. Human Pathol 6:681–691

Legrand M, Pariente R (1975) Diagnostic des tumeurs de la pleure par l'etude des biopsies au microscope electronique. Rev Franc Mald Resp 4:311–324

Lillie RD (1965) Histopathologic technic and practical histochemistry. 3rd. Edit p 316. Mac Graw Hill, New York

Luse SA, Spjut HJ (1964) An electron microscopic study of a solitary pleural mesothelioma. Cancer 17:1546–1554

Maximow A (1922) Über das Mesothel (Deckzellen der serösen Häute) und die Zellen der serösen Exsudate. Untersuchungen an entzündeten Gewebe und Gewebskulturen. Archiv für experimentelle Zellforschung 4:1–42

Mikelson MR, Brown GA, Mainard JA, Cooper RR, Bonfiglio M (1980) Synovial sarcoma. An electron microscopic study of monophasic and biphasic forms. Cancer 45:2109–2118

Sano ME, Weiss E, Gault ES (1960) Pleural mesothelioma. Further evidence of its histogenesis. J Thorac Surg 19:783–788

Sorokin SP (1960) Histochemical events in developing human lungs. Acta Anat 40:105–119

Spencer H (1961) Pulmonary Blastomas. J Path Bact 82:161–165

Stoebner P, Miech G, Sengel A, Witz JP (1970) Notions d'ultrastructure pleurale. II. Les Mesotheliomes. La Presse Medicale 24:1403–1408

Stout AP, Murray MR (1942) Localized pleural mesothelioma. Arch Pathol 34:951–964

Suzuki Y, Churg J, Kannerstein M (1976) Ultrastructure of human malignant diffuse mesothelioma. Am J Pathol 85:241–262

Thurlbeck WM (1978) Miscellany. In: Liebow AA (ed) The lung, structure, function and disease. International Academy of pathology monograph. Williams Wilkins Co, Baltimore, p 309

Wagner JC, Munday DE, Harington JS (1962) Histochemical demonstration of hyaluronic acid in pleural mesotheliomas. J Pathol Bacteriol 84:73–78

Wang NS (1973) Electron microscopy in the diagnosis of pleural mesotheliomas. Cancer 31:1046–1054

Willmer EN (1965) Morphological problems of cell type shape and identification. In: Willmer EN (ed) Cells and tissues in culture. Vol 1. Academic Press, London

Yoshiyuki Okamura R (1977) Ultrastructure of localized fibrous mesothelioma of the pleura: Report of a case with histogenetic considerations. Cancer 39:139–142

Accepted December 15, 1981